

# **JOURNAL OF THE MYANMAR ACADEMY OF ARTS AND SCIENCE**



## **Chemistry**

Vol. XIX, No.2A, January, 2023

**Myanmar Academy of Arts and Science**

# Journal of the Myanmar Academy of Arts and Science

Vol. XIX, No.1A

## Contents

### Section (i), Chemistry

<u>Sr. No.</u>	<u>Title</u>	<u>Page</u>
1	<b>Hnin Yu Win</b> , *Perylenequinone Derivatives from <i>Alternaria</i> sp., an Endophytic Fungus Isolated from <i>Gynura procumbens</i> (Lour.) Merr. Leaves	1
2	<b>Hnin Hnin Wai</b> , Investigation of Chemical Constituents and Some Pharmacological Properties of <i>Melicope Ptelefolia</i> (Thit- Kha) Leaf	13
3	<b>Thida Myint</b> , Biochemical Studies and Hepatoprotective Potentiality of <i>Smallanthus Sonchifolius</i> (Poepp. and Endl.) H. Robinson (Yacon) Leaves	21
4	<b>Mie Mie Aye</b> , Screening on Some Bioactivities from the Leaf of <i>Bauhinia Purpurea</i> L. (Swedaw-Ni)	29
5	<b>Soe Soe Tint</b> , Investigation of Essential Oil from the Leaf and Antioxidant Activity of Plant <i>Apium Graveolens</i> L. (Tayoke Nan-Nan)	37
6	<b>Kay Khine Nyunt</b> , Constituents of Essential Oil, Total Phenolic, Total Flavonoid Contents and Antioxidant Activity of Rhizome of <i>Curcuma Caesia</i> Roxb. (Ga Mone Tain Pyar)	51
7	<b>Aye Khaing Soe</b> , Isolation, Culture and Characterization of Lactic Acid Bacteria from Kefir Grains Fermented Milk	61
8	<b>Myint Myint Khin</b> , Study on the Anti-Arthritis Property of <i>Croton Oblongifolius</i> R. (Thetyin-Gyi) Leaves by Using Protein Denaturation Method	69
9	<b>Khin Chaw Win</b> , Investigation of $\alpha$ -Glucosidase Inhibition and Antioxidant Activities of <i>Hydrocotyle rotundifolia</i> Roxb. (Say-Myin-Khwa)	77
10	<b>Myint Myint Htay</b> , Study on Antioxidant Activity, Antimicrobial Activity and Acute Toxicity of <i>Plukenetia Volubilis</i> L. (Sacha Inchi) Leaves	85
11	<b>Kyawt Kay Khaing</b> , Repurification and Characterization of Liquid Glucose from the Sweet Potato Starch of <i>Pomoea Batatas</i> L. (Shwe-Kan-Zun-U)	93
12	<b>Thin Thin Hlaing</b> , A Study on Some Water Quality Assessment of Ngamoeyiek Creek Water Sample Near North Dagon Township and Treated with <i>Moringa Oleifera</i> L. (Dant-Da-Lun) Seeds	103
13	<b>Su Lay Yee</b> , Study on Water Quality and Treatment of Tube Well Water Samples from Shwebo Township, Sagaing Region	111
14	<b>Thin Thin Swe</b> , Removal of Calcium Ion from Water by Luffa Sponge L. <i>Aegyptiaca</i>	119
15	<b>Khin Moh Moh Hlaing</b> , Preparation of Soap in the Presence of Locally Available Natron	129

<b><u>Sr. No.</u></b>	<b><u>Title</u></b>	<b><u>Page</u></b>
16	<b>Thet Naing Soe</b> , Comparative Evaluation of the Pelletized Biomass Fuel from Different Solid Wastes	137
17	<b>Swe Sint</b> , Assessing the Application of Iron Oxide Particles for Remediation of Insecticide Contaminated Soil	145
18	<b>Myat Hnin Ei</b> , Effectiveness of Saponin on Phytoremediation of Petroleum-Contaminated Soil	153
19	<b>Lae Lae Mon Win</b> , Preparation and Characterization of Chicken Feet Collagen for Biomedical Application	163
20	<b>Nang Naunge Ying</b> , Preparation of Secreted Proteins from <i>Streptomyces</i> Sp. SIREXAA-ETO Hydrolyze CMC and Cellulose	171
21	<b>Nan Yu Nwe</b> , Applications of Modified Chitosan Composite Membranes	179
22	<b>Hnin Yu Wai</b> , Preparation and Characterization of Polymeric Material of Cellulose Acetate-Polyvinyl Alcohol Film	189
23	<b>Thwe Thwe Soe</b> , Fabrication of Areca Nut Fibre-Rubber Composites Using Taguchi Optimization	201
24	<b>Thazin Oo</b> , Preparation of Silver Colloidal Solution Coated Ceramic Filter and Its Antimicrobial Activity	213
25	<b>Theingi Win</b> , Characterization of Silica from Clay Minerals in Kyaukpadaung Township and Its Application on Lead Contaminant Waste Water	221
26	<b>Ohnmar Aye</b> , Isolation, Identification and Chromium Adsorption Behaviour of a Chromium-Resistant <i>Paecilomyces</i> sp.	233
27	<b>Yi Yi Win</b> , Some Chemical Constituents and Some Biological Activities of <i>Picrasma Javanica</i> Fruit	243
28	<b>Pann Yone</b> , Studies on Bioactivity and Structure Elucidation of Isolated Bibenzyl Derivatives from <i>Dendrobium Pulchellum</i> Root Extracts	255
29	<b>Hlaing Myint Thu</b> , Identification and Antimicrobial Activity of Selected Soil Fungus, HMF-33	267
30	<b>Mar Mar Aye</b> , Heavy Metal Tolerance and Biosorption Potential of <i>Aspergillus Niger</i> Isolated from Solid Mining Waste	279
31	<b>Khin Myo Myint Tun</b> , Nutritional Values, Total Phenolic, Total Flavonoids and Antioxidant Activity of Red and White Flower Petals of <i>Sesbania Grandiflora</i> (L.) Pers.	289
32	<b>Tha Zin Nwe Oo</b> , Investigation of Phytoconstituents and Some Bioactivities of Leaves and Barks of <i>Holoptelea Integrifolia</i> R. (Phyauk-Seik)	299
33	<b>Yu Nwe Moe</b> , Evaluation of Some Biological Activities of Tuber of <i>Gloriosa Superba</i> L. (Si-mi-dauk)	309
34	<b>Sandar Moe</b> , Isolation, Characterization and Bioactivity of Casein and Albumin from Fresh and Packed Cow Milk Samples	319

<u>Sr. No.</u>	<u>Title</u>	<u>Page</u>
35	<b>Mya Hnin Aye Khaing</b> , Preparation of Bioethanol from Sorghum Starch and Its Characterization	329
36	<b>Win Ko</b> , Study on Radon Exploration in the Building Materials by Using LR-115 Detector	337
37	<b>Zaw Oo</b> , Studies on Synthesis and Characterization of Nanocarbon from Rice Husk Char	347
38	<b>Tin Tin Sein</b> , Preparation and Application of Organic Fertilizers from Vegetable Wastes, Cow Dung, Sesame Meal Cake and Effective Microorganism Solutions	361
39	<b>Chit Chit Maw</b> , Synthesis and Characterization of Fullerene from Graphite Ore	371
40	<b>Htet Htet Than Sein</b> , Preparation and Characterization of Carboxymethyl Cellulose (CMC) from Pineapple Leaves	383
41	<b>Thandar</b> , Using Slow Sand Filtration Method with Domestic Charcoal to Treat Distillery Wastewater in Aunglan Township	393
42	<b>San San Kyu</b> , Investigation on Contamination of Heavy Metals Inroadside Soil at Kali-Tollgate and Bayintnaung-Quarter between Bago-Mawlamyine Highway	403
43	<b>Nwe Nwe Win</b> , An Investigation into the Efficacy of Graphene Oxides as an Adsorbent for the Removal of Lead from Aqueous Solution	413
44	<b>Kyawt Kyawt</b> , Preparation and Characterization of Magnetite Fe <sub>3</sub> O <sub>4</sub> Nanoparticles	423
45	<b>Ei Ei Phyo Cin</b> , Preparation of Fe <sub>3</sub> O <sub>4</sub> -Zno-CuO Nanocomposites with Different Mole Ratios and Their Characterizations	431
46	<b>Khin Mya Than Sein</b> , Synthesis and Application of Rayon Zinc Oxide Nanocompositie	441
47	<b>Thet Thet Mon</b> , Phytochemical Screening, Nutritive Values and Some Biological Activities of Seed (Kernel) of <i>Ziziphus Mauritiana</i> Lam. (Zee)	451
48	<b>Thuzar Nyein</b> , Preparation and Characterization of Silver Doped Bismuth Ferrite Nanoparticles by Co-Precipitation Method	461

# PERYLENEQUINONE DERIVATIVES FROM *ALTERNARIA* SP., AN ENDOPHYTIC FUNGUS ISOLATED FROM *GYNURA PROCUMBENS* (LOUR.) MERR. LEAVES\*

Hnin Yu Win<sup>1</sup>, Kay Thi Moh Moh Win<sup>2</sup>, Hartmut Laatsch<sup>3</sup>

## Abstract

The present study was conducted to investigate the bioactive metabolites from endophytic fungus isolated from *Gynura procumbens* (Lour.) Merr. leaves, which is locally known as Pyar-mee-ywet. A total of 17 strains were isolated from the leaf of selected medicinal plant. Among them, selection of the target fungus for further investigation was done based on chemical screening (spot pattern on TLC). From the culture broth of the selected fungus, perylenequinone derivatives, stemphytoxin II (1), alterperyleneol (2) and stemphytoxin III (3), together with common fungal metabolites, 4-hydroxy-benzaldehyde (4), adenosine (5) and uridine (6) were isolated using various chromatographic methods. The structure elucidation of the isolated compounds was performed based on NMR and mass data.

**Keywords:** endophytic fungus, *Gynura procumbens*, perylenequinone, spectroscopically

## Introduction

Endophytes play an important role in host plant. They can stimulate plant growth, increase disease resistance, improve the ability of plant to withstand environmental stresses and recycle nutrients (Sturz *et al.*, 2000). Besides these, endophytes are also known as rich sources of important bioactive metabolites. Fungal endophytes living inside the plants could also produce metabolites which possess similar or more active compounds than that of their respective hosts (Strobel *et al.*, 2003). Some of fungal metabolites include anticancer, anti-fungal, anti-diabetic and immunosuppressant compounds (Gunatilaka, 2006).

The objective of the present research work is to investigate bioactive metabolites from endophytic fungus. To achieve this aim, one important medicinal plant, *Gynura procumbens* was selected for isolation of endophytic fungus and structure elucidation of its fungal metabolites.

*G. procumbens* is a valuable medicinal plant. In Myanmar, the fresh leaves of this plant were used to treat diabetes. In Thailand, *G. procumbens* is used to treat topical inflammation, rheumatism and viral diseases of the skin. This plant can decrease blood sugar level and also induce insulin secretion. In Indonesia folk medicine, *G. procumbens* is used to treat fevers, skin rashes and as a remedy for ringworm infection.

## Materials and Methods

### General Experimental Procedures

<sup>1</sup>H NMR spectra: Varian Unity 300 (300.542 MHz), Bruker AMX 300 (300.542 MHz), Varian Inova 500 (499.8 MHz). Coupling constants (*J*) in Hz. Abbreviations: s = singlet, d=doublet, dd= doublet of doublet, t = triplet, q = quartet, quint = quintet, m = multiplet, br = broad. - <sup>13</sup>C NMR spectra: Varian Unity 300 (75.5 MHz), Varian Inova 500 (125.7 MHz). Chemical shifts were measured relatively to tetramethylsilane as internal standard. - 2D NMR spectra: H, H COSY spectra (<sup>1</sup>H, <sup>1</sup>H-Related Spectroscopy), HMBC spectra (Heteronuclear Multiple Bond Connectivity), HMQC spectra (Heteronuclear Multiple Quantum Coherence) and NOESY spectra

<sup>1</sup> Dr. rer. nat., Associate Professor, Department of Chemistry, University of Mandalay

<sup>2</sup> Dr, Lecturer, Department of Chemistry, Yenangyaung Degree College

<sup>3</sup> Professor, Institute of Organic and Biomolecular Chemistry, The University of Göttingen, Göttingen, Germany

\* Best Paper Award Winning Paper in Chemistry (2020)

(Nuclear Overhauser Effect Spectroscopy). - Mass spectra: EIMS at 70 eV with Varian MAT 731, Varian 311A, AMD-402, high resolution with perflurokerosene as standard. ESIMS with Quattro Triple Quadruple mass spectrometer Finigan MAT-Incos 50, ESIMS LCQ (Finnigan).

## Materials

Thin layer chromatography (TLC): DC-Folien Polygram SIL G/UV<sub>254</sub> (Macherey-Nagel & Co.). - Column chromatography (CC): MN silica gel 60: 0.05-0.2 mm, 70-270 mesh (Macherey-Nagel & Co). Sephadex LH-20 (Pharmacia) was used for size exclusion chromatography.

## Spray reagents

Anisaldehyde/sulphuric acid: 1 mL anisaldehyde was added to 100 mL of a stock solution containing 85 mL methanol, 14 mL acetic acid and 1 mL sulphuric acid. After spraying, the TLC cards were heated with hot air until colour development.

## Microbiological Materials

Autoclave: Fedegari Autoclavi SPA, working temperature 121 °C, working pressure 1.2 kg/cm<sup>2</sup>. - Antibiotic assay discs: 9 mm diameter, Schleicher & Schüll No. 321 261. - Culture media: glucose, yeast extract and malt extract were purchased from Merck, Darmstadt. – Petri dishes: 94 mm diameter, 16 mm height, Fa. Greiner Labortechnik, Nürtingen. – Celite: Celite France S. A., Rueil-Malmaison Cedex. - Sterile filters: Midisart 2000, 0.2 µm, PTFE-Filter, Sartorius, Göttingen. - Laminar-Flow-Box: Kojar KR-125, Reinraumtechnik GmbH, Rielasingen-Worblingen 1.

## Work Up Procedure

### Sample Collection and Isolation of Endophytic Fungi

The fresh leaves of *G.procumbens* were collected from Mandalay, Myanmar. To isolate endophytic fungi from *G. procumbens*, the fresh leaves were thoroughly washed with tap water and then the surface was sterilized by submerging them in 75% ethanol for 2 min, 5.3% NaOCl (v/v) for 1 min and thereafter dipped into 75% ethanol for 30 sec. After drying in sterile condition, small discs were cut and placed on isolation media (water agar; WA) (18 g/ L) supplemented with chloramphenicol (100 mg/ L) to suppress bacterial growth and incubated at 25°C until the outgrowth of endophytes was discerned. Individual fungal colonies were picked and transferred onto sterile water agar and periodically checked for purity.

A total of 17 fungi were isolated and each fungus was inoculated on M<sub>2</sub> medium (malt extract 10 g/L, yeast extract 4 g/L, glucose 4g/L at pH 7.8) for pre-screening. *Alternaria* sp. (fungus 1-92) was selected for further investigation due to its interesting zones on TLC both under UV and after spraying with anisaldehyde/sulphuric acid. The selected fungus was cultivated on M<sub>2</sub> medium (300 g malt extract, 120 g yeast extract and 120 g glucose in 30 L tap water pH 7.8) and transferred to 100 of 1 L Erlenmeyer flasks (300 mL each). After 14 days, the culture broth was harvested and extracted with ethyl acetate. The resulting culture extract was chromatographed to isolate the metabolites.

The culture extract (8.16 g) was chromatographed on silica gel using stepwise gradient of dichloromethane/methanol. The selected fraction I was subjected to Sephadex LH-20 using methanol only to obtain altertoxin II (1) which was isolated as red amorphous. It showed UV absorbing band at 254 nm and stained to reddish brown color with anisaldehyde/sulphuric acid on heating. After purification of fraction II on Sephadex LH-20 using methanol only, alterperyleneol (2) and stemphylltoxin III (3) were isolated as red amorphous. Both of them showed UV absorbing band at 254 nm and stained to reddish brown color with anisaldehyde/sulphuric acid on heating.

Fraction III was further chromatographed on RP-18 using the gradient of methanol and water to isolate 4-hydroxy benzaldehyde (4), adenosine (5) and uridine (6). Compound (4) was isolated as colorless solid and showed UV absorbing band at 254 nm. Compound (5) was isolated as colorless solid and showed UV absorbing band at 254 nm and turned to blue with anisaldehyde/sulphuric acid on heating. Compound (6) was isolated as yellow compound and showed UV absorbing band at 254 nm and deep green color after spraying with anisaldehyde/sulphuric acid.



**Figure 1** Selected fungus

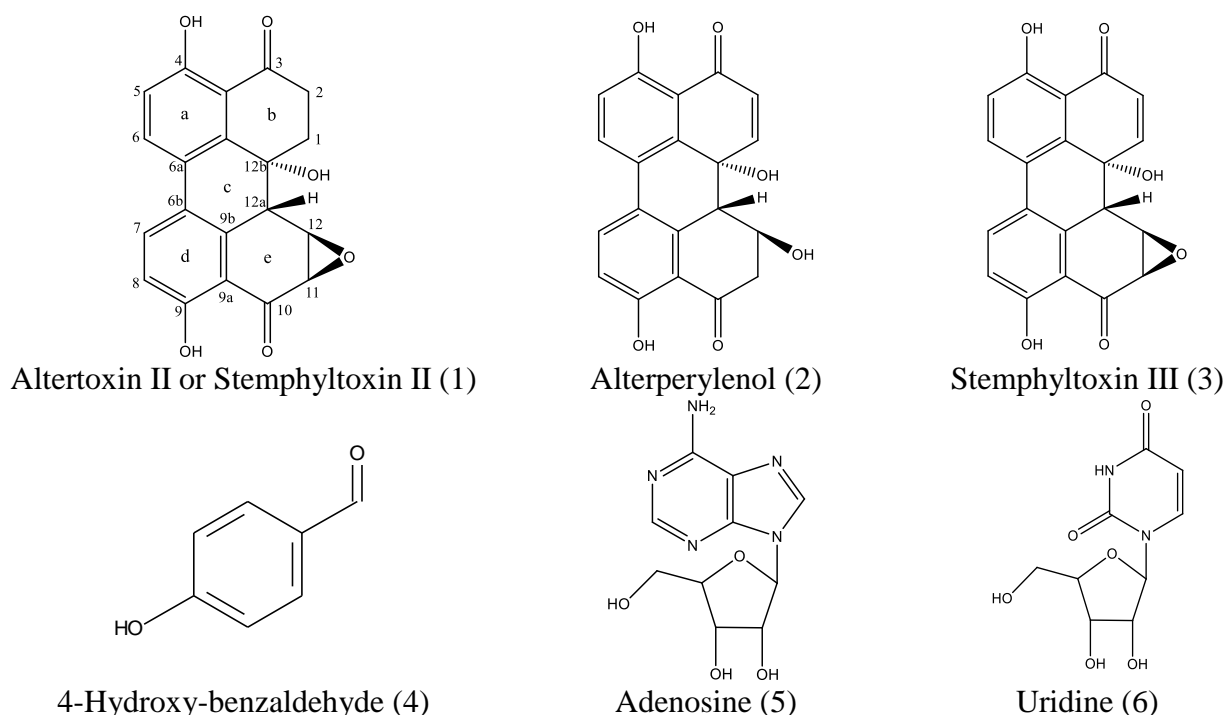


**Figure 2** Compounds isolated from *Alternaria* sp., an endophytic fungus isolated from *G. procumbens* leaves

## Results and Discussion

### Compound (1)

In the  $^1\text{H}$  NMR spectrum, Figure 7(a), two chelating OH signals at  $\delta$  12.71 and 11.88 ppm were observed. Two doublets at  $\delta$  8.16 ( $J = 8.8$  Hz) and 8.07 ppm ( $J = 8.7$  Hz) in the downfield aromatic region, and another two doublets at  $\delta$  7.07 ( $J = 8.8$  Hz) and 6.99 ppm ( $J = 8.7$  Hz) in the upfield aromatic region, with the integration of one proton in each signals were detected. In addition, there was one OH signal at  $\delta$  5.56 ppm.

In the aliphatic region, two doublets at  $\delta$  4.37 ppm (1H) and 3.76 ppm (1H) with the same coupling constant of 3.8 Hz were observed. Furthermore,  $^1\text{H}$  NMR spectrum displayed one singlet at  $\delta$  3.59 ppm (1H), two multiplets at  $\delta$  3.14 (1H) and 2.74 ppm (1H) and another multiplet at  $\delta$  2.50 ppm (2Hs). In the HMQC spectrum, Figure 7(e), the protons at  $\delta$  3.14 and 2.74 ppm

connected to the same carbon at  $\delta$  32.9 ppm and could be assigned as diastereotopic methylene protons.

According to  $^{13}\text{C}$  NMR and HMQC spectra, Figure 7(b) & 7(e), total of 20 carbon signals were observed. Whereof, those at  $\delta$  205.5 and 197.5 ppm could be assigned as carbonyl of ketone. In addition, 12 aromatic carbon signals (four methine and eight quaternary) were visible. Among them, the two  $sp^2$  quaternary carbons at  $\delta$  161.6 and 161.2 ppm were probably connected with oxygen. In the aliphatic region, one oxygenated quaternary carbon at  $\delta$  67.1 ppm, three methine signals at  $\delta$  56.2, 52.6, 44.1 ppm were observed. Moreover, there were two methylene signals at  $\delta$  32.9 and 31.9 ppm.

In COSY spectrum, Figure 7(c), doublet methine proton at  $\delta$  8.16 ppm showed ortho coupling with another doublet methine proton at  $\delta$  7.07 ppm with the coupling constant of 8.8 Hz. Similarly, one doublet methine proton at  $\delta$  8.07 ppm showed ortho coupling with another doublet methine proton at  $\delta$  6.99 ppm with coupling constant of 8.7 Hz. Therefore, two 1,2,3,4-tetrasubstituted benzene rings (a and b) could be drawn. In the HMBC spectrum, Figure 7(d), doublet methine proton at  $\delta$  8.16 ppm showed correlations to two  $sp^2$  quaternary carbons at  $\delta$  161.2 and 140.5 ppm. Another doublet methine proton at  $\delta$  7.07 ppm showed correlations to two  $sp^2$  quaternary carbons at  $\delta$  122.9 and 113.7 ppm. According to the chemical shift, the  $sp^2$  quaternary carbon at  $\delta$  161.2 ppm could be connected to oxygen. In addition, one chelating OH signal at  $\delta$  12.71 ppm showed three HMBC cross peaks to carbons at  $\delta$  161.2, 118.0 and 113.7 ppm. It confirmed the attachment of OH group on  $sp^2$  quaternary carbon at  $\delta$  161.2 ppm. According to HMBC data, the fragment (a) could be elucidated.

By analysis of the other HMBC correlations, the doublet methine proton at  $\delta$  8.07 ppm showed coupling with two  $sp^2$  quaternary carbons at  $\delta$  161.6 and 136.1 ppm. Another doublet methine proton at  $\delta$  6.99 ppm showed the HMBC correlation to two quaternary carbons at  $\delta$  124.5 and 113.9 ppm. The  $sp^2$  quaternary carbon at  $\delta$  161.6 ppm could also be connected to oxygen. As in previous fragment (a), one chelating OH signal at  $\delta$  11.88 ppm showed three HMBC cross peaks to carbons at  $\delta$  161.6, 116.1 and 113.9 ppm. According to HMBC data, the fragment (b) could be elucidated.

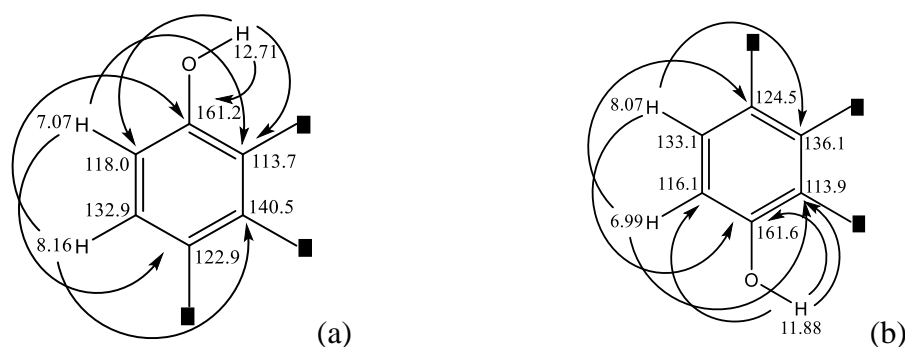


**Figure 3** HMBC correlations ( $\rightarrow$ ) in fragments (a & b)

Moreover, the methine proton at  $\delta$  8.16 ppm from fragment (a) showed HMBC correlation to one  $sp^2$  quaternary carbon at  $\delta$  124.5 ppm from fragment (b) and similarly the methine proton at  $\delta$  8.07 ppm from fragment (a) showed correlation to one  $sp^2$  quaternary carbon at  $\delta$  122.9 ppm from fragment (a). According to these correlations, the two benzene rings could be connected as shown in partial structure I.





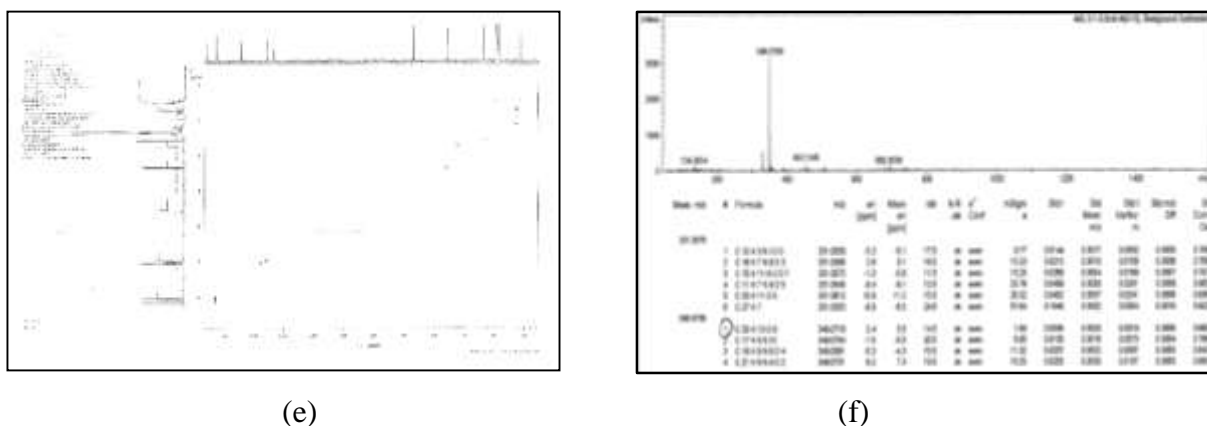


**Figure 7** (a)  $^1\text{H}$  NMR spectrum (DMSO- $d_6$ , 300 MHz), (b)  $^{13}\text{C}$  NMR spectrum (DMSO- $d_6$ , 150 MHz) (c) COSY spectrum (DMSO- $d_6$ , 600 MHz) (d) HMBC spectrum (DMSO- $d_6$ , 600 MHz) (e) HMQC spectrum of (DMSO- $d_6$ , 600 MHz) (f) (-) HRESI mass spectrum of compound (1)

The relative configuration of compound **1** was determined by analysis of splitting pattern and coupling constant as well as by comparison with literature data. H-11 and H-12 protons showed the coupling constant of 3.8 Hz, which is matched with the cis coupling constant ( $\sim 4$  Hz) of the two **vicinal** protons of the epoxide ring. So, H-11 and H-12 protons must be in the cis position. Moreover, H-12a proton showed singlet and did not show doublet as expected. Therefore, the dihedral angle between H-12 and H-12a must be approximately  $90^\circ$  with the coupling constant of zero. H-12a and OH-12b are generally trans-axial arranged for combining two cyclohexanone rings. All of the reported naturally occurring perylene derivatives have this stereochemistry for H-12a and OH-12b. Thus, the structure of compound **1** could be assigned as altertoxin II or stemphytoxin II.

### Compound (2)

Compound **2** was isolated as red amorphous powder. The molecular formula was determined as  $\text{C}_{20}\text{H}_{14}\text{O}_6$  on the basis of negative high resolution ESI mass spectrum at  $m/z$  349.0719 ( $[\text{M}-\text{H}]^-$ ) with 14 degree of unsaturation. The  $^{13}\text{C}$  NMR spectrum, Figure 8(b), revealed the presence of 20 carbon signals which include two carbonyl of ketone, 14  $sp^2$  carbons (6 methine and 8 quaternary), four  $sp^3$  carbons (one  $\text{CH}_2$  group, two CH and one  $\text{C}_q$ ). Detailed comparison of  $^1\text{H}$  NMR and  $^{13}\text{C}$  NMR spectral data of compound **2** with those of compound **1**, indicated that the structures of these two compounds are very similar, except for the two doublet methine protons of  $\alpha$ ,  $\beta$ -unsaturated carbonyl group at  $\delta$  6.31 ( $\delta_{\text{C}}$  125.9,  $J = 10.46$  Hz) and 7.87 ( $\delta_{\text{C}}$  153.3,  $J = 10.46$  Hz) in the aromatic region which were not observed in compound **1**. Moreover, in the aliphatic region of  $^1\text{H}$  NMR spectrum of compound **2**, the epoxide ring in compound **1** was replaced by methylene protons ( $\delta$  2.84 and 3.01) and one oxygenated methine proton ( $\delta$  4.75). Further analysis of 2D NMR data revealed that compound **2** was alterperyleneol. H-12 and H-12a must be trans-axial arrangement according to coupling constant of H-12 ( $J = 9.65$  Hz).

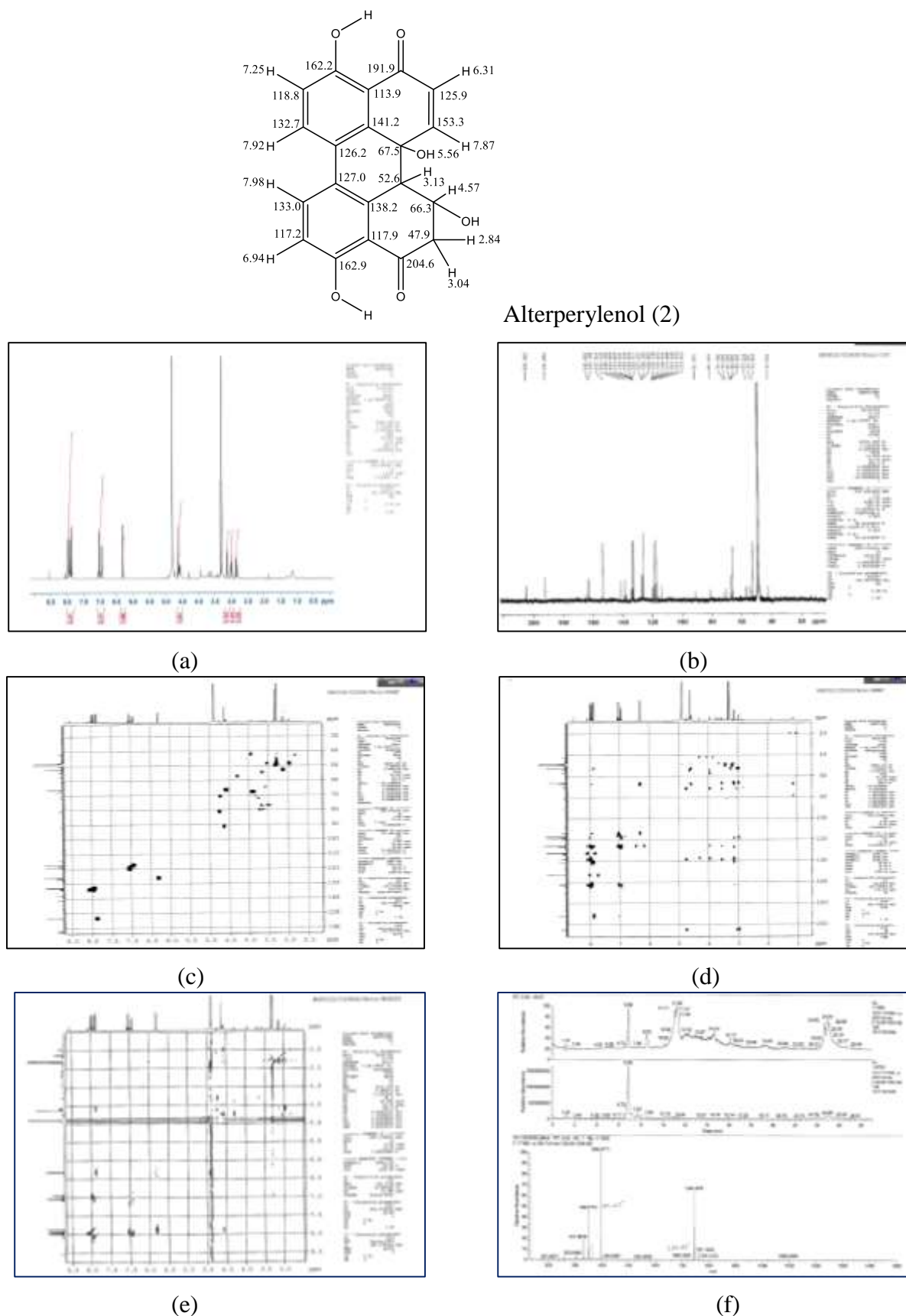


**Figure 8** (a)  $^1\text{H}$  NMR spectrum ( $\text{CD}_3\text{OD}$ , 300 MHz), (b)  $^{13}\text{C}$  NMR spectrum ( $\text{CD}_3\text{OD}$ , 150 MHz) (c) HSQC spectrum ( $\text{CD}_3\text{OD}$ , 600 MHz) (d) HMBC spectrum ( $\text{CD}_3\text{OD}$ , 600 MHz), (e) NIOSY spectrum ( $\text{CD}_3\text{OD}$ , 600 MHz) (f) (-) HR ESI mass spectrum of compound (2)

### Compound (3)

Another isolated compound is stemphytoxin III and it was isolated as red amorphous. The  $sp^2$  region of  $^1\text{H}$  NMR spectrum of compound **3** is very similar to those of compound **2**. In the  $sp^2$  region, two chelating OH, two sets of ortho-coupled protons and  $\alpha,\beta$ -unsaturated carbonyl group were detected. In the aliphatic region, two doublet methine protons (H-11 and H-12) of epoxide ring at  $\delta$  3.78 and 4.60 ppm and one singlet methine proton (H-12a) at 3.80 ppm were observed. Those signals are very similar to the pattern of ring e in compound **1**. According to EI and ESI mass spectra, the molecular mass was deduced as 348 and compound **3** could be assigned as stemphytoxin III.

The isolated perylenequinone derivatives are only soluble in DMSO and rather unstable, being quickly transformed into black insoluble products. They showed antibacterial activity *in vitro* against *Bacillus subtilis*, *Bacillus cereus*, and *Escherichia coli* (Arnone *et al.*, 1986). The presence of epoxy groups in compounds (**1**, **3**) may well support the hypothesis that they are also phytotoxic; a respective test could not be performed, as the test organism was not available.

Some metabolites of fungi and plants containing perylenequinones have been used as folk medicine for the treatment of many diseases. Perylenequinones are a type of photosensitizers pigments widespread in nature, which have been isolated from fungi, as well as other organisms (Stack *et al.*, 1986, Davis *et al.*, 1998, Xu *et al.*, 2001 and Daub *et al.*, 2005). Due to their excellent photo-sensibilizing properties, they are expected to be developed as new phototherapeutic medicines.

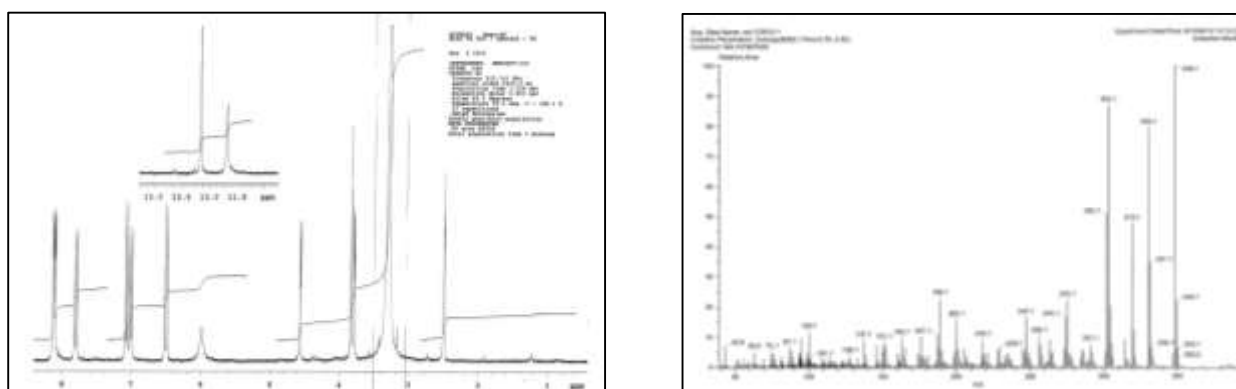


**Figure 9**  $^1\text{H}$  NMR spectrum (DMSO- $d_6$ , 600 MHz) and ESI mass spectrum of compound (**3**)

### Compound (4)

In the aromatic region of the  $^1\text{H}$  NMR spectrum, Figure 10, two doublets at  $\delta$  7.68 and 6.85 with the integration of two protons in each signal indicated the presence of 1,4-disubstituted benzene ring. Moreover, the sharp singlet signal at  $\delta$  9.75 was observed for aldehydic proton. A search in Antibase as well as comparison with authentic spectrum led to *p*-hydroxy benzaldehyde. It was isolated frequently from aquatic organisms, e.g. by Fenical and McConnel (Fenical *et al.*, 1976) from the red seaweed *Dasya pedicellata* var. *stanfordiana* and has some antimicrobial activity against *Vibrio anguillarum*, *Candida albicans* and *Staphylococcus aureus*.

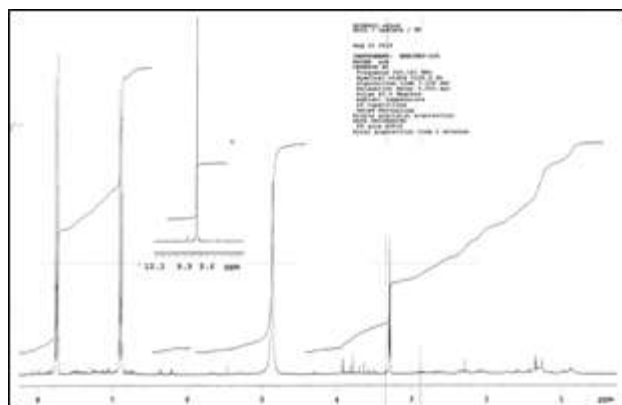
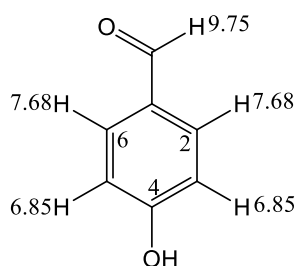


**Figure 10**  $^1\text{H}$  NMR spectrum of p-hydroxybenzaldehyde

### Compound (5)

The  $^1\text{H}$  NMR spectrum, Figure 11, showed two singlets at  $\delta$  8.38 and 8.18 for a heterocyclic aromatic ring, one anomeric proton at  $\delta$  5.90 (d) and three hydroxyl methine protons between  $\delta$  4.80 and 3.80, a diastereotopic methylene doublet of doublet at  $\delta$  3.50 and 3.70. The molecular mass 267 was deduced on the basis of negative ESI mass spectrum. According to spectroscopic data, the isolated compound could be assigned as adenosine (5). The structure was further confirmed by comparison with authentic spectra as well as literature data.

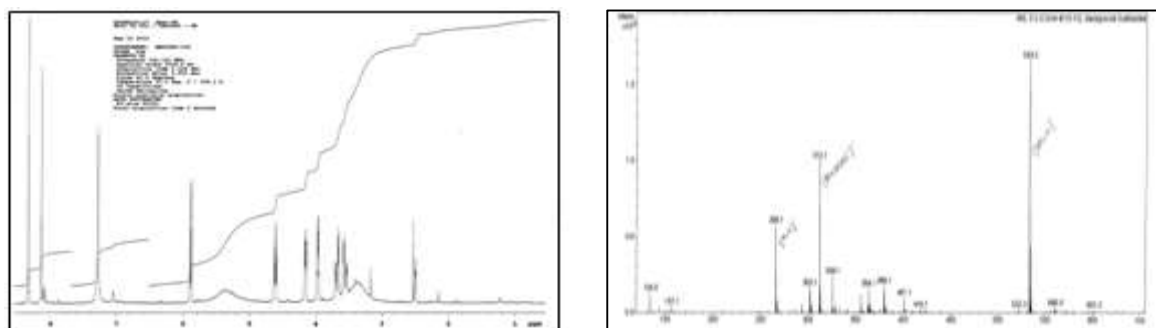


**Figure 11**  $^1\text{H}$  NMR spectrum and ESI mass spectrum of adenosine (5)

### Compound (6)

The  $^1\text{H}$  NMR spectrum of uridine exhibited two doublet peaks at  $\delta$  5.68 and 8.01 with the same coupling constant of 8.1 Hz. It indicated the presence of an  $\alpha$ ,  $\beta$ -unsaturated carbonyl group. The spectrum showed three oxymethine protons, two at  $\delta$  4.15 and third one at  $\delta$  4.01. Furthermore, one oxymethylene group was exhibited at  $\delta$  3.82 and indicated the presence of sugar moiety which was also confirmed by 1H doublet at  $\delta$  5.90 for the anomeric proton of the sugar.

The ESI mass spectrum showed a *pseudomolecular* ion peak at  $m/z$  243  $[\text{M}-\text{H}]^-$ . A search in Antibase (Laatsch, 2012) as well as comparison with the authentic spectrum afforded uridine, which is widely distributed in nature in free state or in nucleic acid and can be produced by hydrolysis (Dictionary of Natural Products on CD-ROM, Chapman & Hall Chemical Database, 2010).

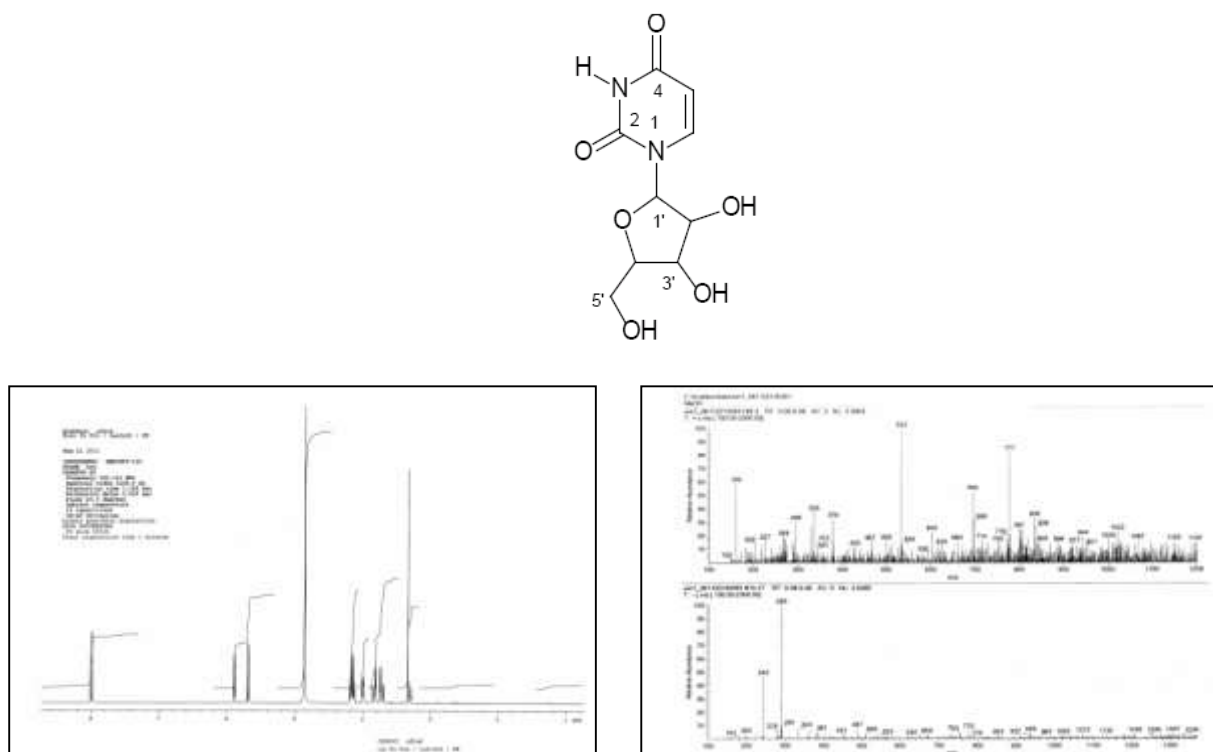


**Figure 12**  $^1\text{H}$  NMR and ESI MS spectra of uridine (6)

Altertoxin II or Stemphylytoxin II (1): red amorphous, strong UV absorbing band at 254 nm, deep green with anisaldehyde/sulphuric acid. –  $^1\text{H}$  NMR (DMSO- $d_6$ , 300 MHz)  $\delta$  12.71 (s, 1H, OH-4), 11.88 (s, 1H, OH-9), 8.16 (d,  $^3J = 8.8$  Hz, 1H, H-6), 8.07 (d,  $^3J = 8.7$  Hz, 1H, H-7), 7.07 (d,  $^3J = 8.8$  Hz, 1H, H-5), 6.99 (d,  $^3J = 8.7$  Hz, 1H, H-8), 5.56 (s, 1H, OH-12b), 4.37 (d,  $^3J = 3.76$  Hz, 1H, H-12), 3.76 (d,  $^3J = 3.76$ , 1H, H-11), 3.59 (s, 1H, H-12a), 3.14 (m, 1H, H-1), 2.74 (m, 1H, H-1), 2.50 (m, 2H, H-2). –  $^{13}\text{C}$  NMR (DMSO- $d_6$ , 125 MHz)  $\delta$  205.5 (C<sub>q</sub>-3), 197.5 (C<sub>q</sub>-10), 161.6 (C<sub>q</sub>-9), 161.2 (C<sub>q</sub>-4), 140.5 (C<sub>q</sub>-3b), 136.1 (C<sub>q</sub>-9b), 133.1 (CH-7), 132.9 (CH-6), 124.5 (C<sub>q</sub>-6b), 122.9 (C<sub>q</sub>-6a), 118.0 (CH-5), 116.1 (CH-8), 113.9 (C<sub>q</sub>-9a), 113.7 (C<sub>q</sub>-3a), 67.1 (C<sub>q</sub>-12b), 56.2 (CH-12), 52.6 (CH-11), 44.1 (CH-12a), 32.9 (CH<sub>2</sub>-1), 31.9 (CH<sub>2</sub>-2). – (-) ESIMS  $m/z$  349 ([M-H]<sup>-</sup>). – EIMS (70ev)  $m/z$  350 ([M], 100), 332 (20), 321 (35), 305 (65), 263 (25). – (-) HRESIMS  $m/z$  349.0709 [M-H]<sup>-</sup> (calcd 349.0710 for C<sub>20</sub>H<sub>13</sub>O<sub>6</sub>).

Alterperyleneol (2): red amorphous, strong UV absorbing band at 254 nm, deep green with anisaldehyde/sulphuric acid. –  $^1\text{H}$  NMR (DMSO- $d_6$ , 300 MHz)  $\delta$  7.98 (d,  $^3J = 8.7$  Hz, 1H, H-7), 7.92 (d,  $^3J = 8.8$  Hz, 1H, H-6), 7.87 (d,  $^3J = 10.5$  Hz, 1H, H-1), 7.25 (d,  $^3J = 8.8$  Hz, 1H, H-5), 6.94 (d,  $^3J = 8.7$  Hz, 1H, H-8), 6.31 (d,  $^3J = 10.5$  Hz, 1H, H-2), 4.57 (m, 1H, H-12), 3.13 (d,  $^3J = 9.7$  Hz, 1H, H-12a), 3.00 (dd,  $^3J = 4.8, 15.9$  Hz, 1H, H-11), 2.84 (dd,  $^3J = 12.3, 15.9$  Hz, 1H, H-11). –  $^{13}\text{C}$  NMR (DMSO- $d_6$ , 125 MHz)  $\delta$  204.6 (C<sub>q</sub>-10), 191.9 (C<sub>q</sub>-3), 162.9 (C<sub>q</sub>-9), 162.2 (C<sub>q</sub>-4), 153.3 (CH-1), 141.2 (C<sub>q</sub>-3b), 138.2 (C<sub>q</sub>-9b), 133.0 (CH-7), 132.7 (CH-6), 127.0 (C<sub>q</sub>-6b), 126.2 (C<sub>q</sub>-6a), 125.9 (CH-2), 118.8 (CH-5), 117.9 (C<sub>q</sub>-9a), 117.2 (CH-8), 113.9 (C<sub>q</sub>-3a), 67.5 (C<sub>q</sub>-12b), 66.3 (CH-12), 52.6 (CH-12a), 47.9 (CH<sub>2</sub>-11). – (-) HRESIMS  $m/z$  395.0771 [M-H]<sup>-</sup> (calcd 349.0719 for C<sub>20</sub>H<sub>14</sub>O<sub>6</sub>).

*p*-Hydroxy benzaldehyde (4): colourless compound,  $R_f = 0.44$  (CHCl<sub>3</sub>/10% MeOH), UV absorbing band at 254 nm, –  $^1\text{H}$  NMR (CD<sub>3</sub>OD, 300 MHz)  $\delta$  9.75 (s), 7.68 (d,  $^3J = 10.5$  Hz, 2H, H-2,6), 6.85 (d,  $^3J = 10.5$  Hz, 2H, H-3,5).

Uridine (6): yellow compound, 7.9 mg,  $R_f = 0.11$  (CHCl<sub>3</sub>/10% MeOH), UV absorbing band at 254 nm, deep green after spraying with anisaldehyde/sulphuric acid. –  $^1\text{H}$  NMR (CD<sub>3</sub>OD,

300 MHz)  $\delta$  8.01 (d,  $^3J = 8.1$  Hz, 1H, H-6), 5.90 (d,  $^3J = 6.1$  Hz, 1H, H-1'), 5.68 (d,  $^3J = 8.1$  Hz, 1H, H-5), 4.15 (m, 2H, H-2',4'), 4.01 (d,  $^3J =$  Hz, 1H, H-3'), 3.82 (m, 2H, CH<sub>2</sub>-5'). – (-)-ESIMS  $m/z$  243 ([M - H]<sup>-</sup>, 100).

### Conclusion

In this study, three perylenequinone derivatives and some common fungal metabolites were isolated and characterized. Perylenequinone derivatives are only soluble in DMSO and rather unstable, being quickly transformed into black insoluble products. They showed antibacterial activity against *Bacillus subtilis*, *Bacillus cereus* and *Escherichia coli*. Perylenequinone derivatives are photosensitizers with excellent photosensitizing properties. So, they are expected as new phototherapeutic medicines.

### Acknowledgements

The authors thank Dr H Frauendorf and R Machinek for the mass and NMR spectra, the German Academic Exchange Service (DAAD) for the financial support. HYW thanks Dr Yi Yi Myint, Professor & Head, Department of Chemistry, University of Mandalay, for her permission to submit the paper.

### References

- Arnone, A., Nasini, G., Merlini, L., and Assante G. (1986). "Secondary Mould Metabolites. Part 16. Stemphytoxins, New Reduced Perylenequinone Metabolites from *Stemphylium botryosum* var. *Lactucum*". *J. Chem. Soc. Perkin Trans*, vol. 1, pp. 525-530.
- Daub, M.E., Herrero, S., and Chung, K-R. (2005). "Photoactivated Perylenequinone Toxins in Fungal Pathogenesis of Plants". *Microbiology Letters*, vol. 252, pp. 197-206.
- Davis, V.M., and Stack, M.E. (1991). "Mutagenicity of Stemphytoxin III, a Metabolite of *Alternaria alternata*". *Appl Environ Microbiol*, vol. 57, pp. 180-182.
- Dictionary of Natural Products on CD-ROM, (2010). Chapman & Hall Chemical Database.
- Fenical, W., and O. McConnel. (1976). "Simple Antibiotics from the Red Seaweed *Dasya peicdellata* var *stanfordiana*". *Phytochemistry*, vol 15, pp. 435-436.
- Gunatilaka, A.A.L. (2006). "Natural Products from Plant Associated Microorganisms: Distribution, Structural Diversity, Bioactivity, and Implications of their Occurrence". *J Nat Prod*, vol. 69, pp. 509-526.
- Laatsch, H. *AntiBase 2012. A Data Base for Rapid Dereplication and Structure Determination of Microbial Natural Products*; Wiley VCH: Weinheim, Germany. see <http://wwwuser.gwdg.de/~hlaatsc/antibase.htm>.
- Stack, M.E., Mazzola, E.P., Page, S.W., Pohland, A.E., Hight, R.J., Tempesta, M.S., and Corley, D.G. (1986). "Mutagenic Perylenequinone Metabolites of *Alternaria alternata*: Alttoxins I, II and III". *J. Nat. Prod*, vol. 49, pp. 866-871.
- Strobel, G.A., and Daisy, B. (2003). "A Review: Natural Products from Plant Associated Endophytic Fungi". *Microbial Mol Biol Rev*, vol. 67, pp. 491-502.
- Sturz, A.V., and Nowak, J. (2000). "Endophytic Communities of Rhizobacteria and the Strategies Required to Create Yield Enhancing Associations with Crops". *J. Applied Soil Ecology*, vol. 15, pp. 183.
- Xu, S., Chen, S., Zhang, M., and Shen, T. (2011). "A Novel Method for the Preparation of Amino-substituted Hypocrellin B". *Bioorg Med Chem Lett*, vol. 11, pp. 2045-2047.

## INVESTIGATION OF CHEMICAL CONSTITUENTS AND SOME PHARMACOLOGICAL PROPERTIES OF *MELICOPE PTELEFOLIA* (THIT-KHA) LEAF

Hnin Hnin Wai<sup>1</sup>, Thiri Nandar Win<sup>2</sup>, Phyu Phyu Myint<sup>3</sup>

### Abstract

Chemical constituents of *Melicope ptelefolia* (Thit-Kha) leaf and some pharmacological properties were investigated. The preliminary phytochemical test was determined by test tube method. Dried leaf sample was found to consist of 6.39 % of moisture, 7.64 % of ash, 21.94 % of protein, 14.92 % of dietary fiber, 3.93 % of crude fat, 45.18 % of carbohydrate, and 303 kcal/100g of energy value, respectively. According to the EDXRF spectrum, the samples had relatively high Si, K and Ca. Total phenol and total flavonoid contents of *M. ptelefolia* (Thit-Kha) leaf by using Folin-Ciocalteu reagent (FCR) method and by using spectroscopic method. According to the observed data, total phenol content was very high in watery extract (273.78 µg GAE/mg) followed by ethanol extract (119.87 µg GAE/mg) and methanol extract (103.84 µg GAE/mg). In addition, the total flavonoid was also very high in watery extract (79.24 µg QE/mg) followed by ethanol extract (78.81 µg QE/mg) and methanol extract (60.09 µg QE/mg). The antioxidant activity of watery extract (IC<sub>50</sub> = 15.44 µg/mL) was found to be higher than those of ethanol extract (IC<sub>50</sub> = 59.62 µg/mL) and methanol extract (IC<sub>50</sub> = 45.79 µg/mL) determined by DPPH radical scavenging assay. Antimicrobial activity was also determined by agar well diffusion method. Ethyl acetate and methanol extracts exhibited the highest antimicrobial activities. The cytotoxicity of methanol extract was studied by MTT assay method. From the results, the concentration of methanol extract increased, the cell viability also decreased.

**Keywords:** *Melicope ptelefolis*, chemical constituents, total phenol, total flavonoid, antioxidant activity, antimicrobial activity, cytotoxicity

### Introduction

Medicinal plants are important source of valuable therapeutic agents, both in modern and in traditional medicine. Many plants, particular medicinal plants, have been extensively studied for their antioxidant activity in recent years. The study of traditional medicinal plants and their therapeutic properties play a very important role in the health care system of the country. Indigenous medicine is widely practiced in Myanmar due to its long and deep rooted tradition and also due to the trust placed by the people in its therapeutic qualities. There are many traditional plants are being used in the traditional systems of medicine in many parts of the world, especially in rural communities, for the control, management and or treatment of a variety of human and animal ailments (Kumar and Pandey, 2013). Free radicals and other reactive oxygen species are being constantly produced in the human body and they are known to be responsible for various deadly diseases such as cancer, aging, atherosclerosis, immunodeficiency, and infections. On the other hand, synthetic drugs bring about various side effects such as gastrointestinal disturbances, hypoglycemia and liver disfunction (Rang *et al.*, 2003). Free radical scavenger or antioxidant may play a major role in the prevention of a number of diseases, some forms of cancer, and may age related disorders. Among other medicinal plants, *Melicope ptelefolia* leaf was selected for this study since they are widely grown in Kayah State.

*M. ptelefolia* belonging to family Rutaceae is Thit-Kha in local name and this is the first research from the leaf of *M. ptelefolia* in Kayah State, Myanmar. Therefore, it was chosen to investigate its phytochemical constituents, nutritional values, mineral values, total phenol and total

---

<sup>1</sup> Demonstrator, Department of Chemistry, Loikaw University

<sup>2</sup> MSc. candidate, Department of Chemistry, Loikaw University

<sup>3</sup> Dr, Professor, Department of Chemistry, Loikaw University

flavonoid contents, and some bioactivities including antioxidant and antimicrobial activities, and cytotoxicity.

## Materials and Methods

### Sample Collection and Characterization

*M. ptelefolia* leaf sample (Figure 1) was collected in December, 2018 from West Padaung, Demawso Township, Kayah State. The taxonomists of the Department of Botany, Loikaw University botanically identified and authenticated the plant.



**Figure 1** Photograph of the leaf of *Melicope ptelefolia* (Thit-Kha)

### Determination of Phytochemical Constituents and Nutritional values of *M. ptelefolia* Leaf

Ethanol, petroleum ether, ninhydrin, sulphuric acid,  $\alpha$ -naphthol, Mg turning, lead acetate, ferric chloride, acetic anhydride, gelatin solution, acetic acid, sodium picrate, Benedict's solution, mercuric chloride, iodine, picric acid, acetone and sodium carbonate were used to measure phytochemical tests. The leaf extracts of *M. ptelefolia* were determined for the presence of phytochemicals such as alkaloids, carbohydrates, saponins, proteins, phenolic compounds, flavonoids and glucosides according to the common phytochemical methods described by Harbone, 1998 and Sofowora, 1994. The mineral value was also determined by using Energy Dispersive X-ray Fluorescence (EDXRF) Spectrometer. The nutritional values such as moisture, protein, fat, fiber, and carbohydrate of *M. ptelefolia* were determined at the SME Development Department, Yangon, Ministry of Industry.

### Preparation of Different Extracts

The air-dried powdered sample (20 g) was macerated with 100 mL of water in closed flask for twenty-four hours, during which they were frequently shaken six hours interval and allowed to stand for 18 h. Afterwards, they were filtered rapidly against loss of water and then 25 mL of filtrates were evaporated to dryness in a tarred flat-bottomed shallow dish. They were dried at 105 °C and weighed.

PE, MeOH, EtOAc, and EtOH extracts of leaf of *M. ptelefolia* powder sample was determined by the method given in “The British Pharmacopoeia” as described in “the preparation of water extract” by using 100 mL of respective solvents instead of water.

### Determination of Total Phenol and Total Flavonoid Content

Total phenol content (TPC) in each extract was determined using the FC method described by McDonald *et al.* (2001). The calibration curve was established using gallic acid and the TPC value was expressed as mg gallic acid equivalents per gram of dried extract. The diluted extract or gallic acid (1.6 mL) was added to 0.2 mL FC reagent and mixed thoroughly for 3 minutes. Sodium carbonate 0.2 mL was added to the mixture and the mixture was allowed to stand for 30 minutes

at room temperature. The absorbance of the mixture was measured at 760 nm using UV-Visible spectrophotometer.

The total flavonoid content (TFC) of each extract was investigated using the aluminium chloride colorimetry method described by Chang *et al.* (2002). The calibration curve was prepared by diluting quercetin (2.0 mL) was mixed with 0.1 mL of aluminium chloride solution and 0.1 mL of potassium acetate solution. The mixture was kept at room temperature for 30 min. Then the maximum absorbance of the mixture was measured at 420 nm using UV-Visible spectrophotometer. Total flavonoid content (TFC) was expressed as mg quercetin equivalent per gram of dried extract.

### Determination of Some Bioactivities of *M. ptelefolia* Leaf Extracts

The radical scavenging activity of the ethanol, methanol and watery extracts was investigated by using DPPH assay according to the spectrophotometric method. Test tubes, electric balance, magnetic stirrer, oven, water bath, glass rod, glass tube, cell (5 mL), vortex mixer, UV-Visible spectrophotometer (UV-7504), micropipette (3 mL and 5 mL) were used for the determination of antioxidant activity. In this experiment, six different concentrations (10, 20, 40, 60, 80 and 100 µg/mL) of each crude extract in ethanol solvent were used. Determination of absorbance was carried out at wavelength 517 nm using UV visible spectrophotometer. Each experiment was done triplicate (Leea, 2002).

Screening of antimicrobial activity of crude extracts namely PE, MeOH, EtOAc, EtOH, MeOH and H<sub>2</sub>O extracts from *M. ptelefolia* leaves sample was done by agar well diffusion method. In this investigation, the extracts were tested against six microorganisms: *Bacillus subtilis*, *Staphylococcus aureus*, *Pseudomonas aeruginosa*, *Bacillus pumilus*, *Candida albicans* and *E. coli* species. The measurable zone diameter, including the filter paper showed the degree of antimicrobial activity (Cruickshan *et al.*, 1960).

The cytotoxicity of methanol extract of *M. ptelefolia* (Thit-Kha) leaf was studied by MTT assay method. HepG2 hepatocellular carcinoma cell line, culture media (RPMI-1640) contains 20 mM HEPES, MTT powder, Dimethyl sulfoxide were used for the determination of cytotoxicity of crude extract. MTT powder (500 mg) was dissolved in 10 mL phosphate buffer solution. The solution was stirred by a magnetic stirrer for about 1 h in the dark. The sterilized solution was filtered by 0.22 mm filter (Millipore, Ireland) and it is stored in 10-mL aliquots (50 mg/mL) at -20 °C (van Meerloo *et al.*, 2011). The working solution (5 mg/mL) will be prepared on the day of experiment by dilution.

## Results and Discussion

### Phytochemical Constituents, Nutritional Values and Mineral Values of *M. ptelefolia* Leaf

Preliminary phytochemical investigation was carried out to know the types of phyto-organic constituents present in the leaf of *M. ptelefolia*. According to these results, *M. ptelefolia* leaf sample showed the presence of alkaloids, glycosides, α-amino acids, carbohydrates, flavonoids, phenolic compounds, saponins, steroids, and terpenoids, however, reducing sugar, starch and tannins are absent.

For quality control assessment of medicinal plant materials, some nutritional value such as moisture, fat, ash, fiber, protein, carbohydrates and energy value of *M. ptelefolia* leaf was determined. The results for these contents are summarized in Table 1. The moisture and ash content of leaf were found to be 6.39 % and 7.64 %, respectively. The protein content of leaf was found to be 21.94 %. Fiber, fat and carbohydrate contents were respectively found to be 14.92 %, 3.93 % and 45.18 %, with energy value of 303.85 kcal/ 100 g of leaf extract.

Relative abundance of elements present in different varieties of *M. ptelefolia* leaf sample was determined by EDXRF spectrometer and the result of this sample is shown in Table 2. The relative abundant of the silicon was found 1.469 % in *M. ptelefolia* leaf.

**Table 1 Some Nutritional Value of *M. ptelefolia* Leaf**

No.	Parameters	Contents
1	Moisture (%)	6.39
2.	Carbohydrates (%)	45.18
3.	Fat (%)	3.93
4.	Protein (%)	21.94
5.	Ash (%)	7.64
6.	Crude fiber (%)	14.92
7.	Energy value (kcal/100g)	303

**Table 2 Relative Abundance of Element in *M. ptelefolia* Leaf (EDXRF)**

No.	Element	Results (%)
1.	Si	1.469
2.	K	0.748
3.	Ca	0.395
4.	S	0.236
5.	Mn	0.021
6.	Fe	0.008
7.	P	0.003
8.	Cu	0.002
9.	Zn	0.001
10	Br	0.001
11.	Rb	0.000
12.	C H	97.115

### Total Phenol and Total Flavonoid Contents of *M. ptelefolia* Leaf

From the results given in Table 3, total phenol content (TPC) was expressed as microgram of gallic acid equivalent (GAE) per milligram of crude extract ( $\mu\text{g GAE/ mg}$ ). The total phenol content of watery extract ( $273.78 \pm 0.02 \mu\text{g GAE/ mg}$ ) was found to be higher than ethanol extract ( $119.87 \pm 0.01 \mu\text{g GAE/ mg}$ ) and methanol extract ( $103.84 \pm 0.01 \mu\text{g GAE/ mg}$ ). Several studies have described the antioxidant properties of medicinal plants which are rich in phenolic compounds. They possessed biological properties such as antiaging, anticarcinogen and antiinflammation, radical scavenging activity and  $\alpha$ -amylase inhibition activity (Zaino *et al.*, 2003 and Chen *et al.*, 2007).

**Table 3 Total Phenol Content ( $\mu\text{g GAE/mg}$ ) of *M. ptelefolia* Leaf Extracts**

Extracts	Total phenol content ( $\mu\text{g GAE/mg}$ )
Watery	$273.78 \pm 0.02$
Ethanol	$119.87 \pm 0.01$
Methanol	$103.84 \pm 0.01$

### Total Flavonoid Content

Total flavonoid contents (TFC) was expressed as microgram of quercetin equivalents (QE) per milligram of crude extract ( $\mu\text{g QE/ mg}$ ). The total flavonoids content of watery extract ( $79.24 \pm 0.02 \mu\text{g QE/ mg}$ ) was found to be higher than ethanol ( $78.81 \pm 0.03 \mu\text{g QE/ mg}$ ) and methanol extract ( $60.09 \pm 0.02 \mu\text{g QE/ mg}$ ) Table 4. The level of flavonoids in plants is vital for the resistance of external threats. Flavonoids rely on different phytochemicals which gives flavonoids the ability to defend the cells from oxidants.

**Table 4 Total Flavonoid Content ( $\mu\text{g QE/mg}$ ) of *M. ptelefolia* Leaf Extracts**

Extracts	Total flavonoid content ( $\mu\text{g QE/mg}$ )
Watery	$79.24 \pm 0.02$
Ethanol	$78.81 \pm 0.03$
Methanol	$60.09 \pm 0.02$

### Some Bioactivities of *M. ptelefolia* Leaf Extracts

#### Antioxidant Activity

The percent oxidative inhibition values of watery, methanol and ethanol extracts measured at different concentrations and the results are summarized in Table 5. From these experimental results, it was found that as the concentrations increased, the radical scavenging activity of crude extracts usually expressed in term of % inhibition increased. From the average values of % inhibition,  $\text{IC}_{50}$  (50 % inhibition concentration) values in  $\mu\text{g/mL}$  were calculated by linear regressive excel program.

The antioxidant activity,  $\text{IC}_{50}$  values of watery, ethanol and methanol extracts were  $15.44 \mu\text{g/mL}$ ,  $59.62 \mu\text{g/mL}$  and  $45.79 \mu\text{g/mL}$ , respectively. Therefore, the watery extract possesses higher antioxidant potency than ethanol and methanol extract. The results showed that watery exhibited the optimal solvent to extract the bioactive components from *M. ptelefolia*. This extract contained the highest level of phenolic and flavonoids. Those compounds possess powerful antioxidant activity and consequently protect the human body against oxidative damage through scavenging diverse reactive oxygen species, including hydroxyl radicals, peroxide radicals, peroxynitrite and superoxide anions (Chao, 2014).

**Table 5 Percent Oxidative Inhibition and  $\text{IC}_{50}$  Values of Watery, MeOH and EtOH Extracts from *M. ptelefolia* Leaf**

Extracts	% Inhibition (mean $\pm$ SD) in different concentrations ( $\mu\text{g/mL}$ )						$\text{IC}_{50}$ ( $\mu\text{g/mL}$ )
	10	20	40	60	80	100	
Watery	37.85 $\pm 0.93$	60.15 $\pm 0.70$	70.73 $\pm 1.86$	71.72 $\pm 1.05$	71.65 $\pm 0.58$	81.84 $\pm 0.83$	15.44
Ethanol	0.63 $\pm 8.10$	5.18 $\pm 1.31$	21.37 $\pm 2.53$	50.57 $\pm 1.53$	61.69 $\pm 1.36$	84.32 $\pm 5.95$	59.62
Methanol	6.05 $\pm 3.09$	24.59 $\pm 0.49$	43.47 $\pm 0.62$	65.97 $\pm 0.76$	63.58 $\pm 0.99$	61.02 $\pm 0.38$	45.79

#### Antimicrobial Activity

From the results given in Table 6, it was observed that EtOAc extract of *M. ptelefolia* leaves exhibit inhibition zone diameters between (12-20 mm) against *P. aeruginosa*, *B. pumilus*, *E. coli*, and *C. albicans* of Gram positive and Gram negative microorganisms tested and PE extract did not show any antimicrobial activity. MeOH extract showed inhibition zone diameters between (12-18 mm) against *S. aureus*, *B. pumilus*, *E. coli*, and *C. albicans*. EtOH extract show the activity against *S. aureus*, *B. pumilus*, *E. coli* and  $\text{CHCl}_3$  extract show the activity against *S. aureus*, *B. pumilus*, and *P. aeruginosa*. EtOAc extract showed inhibition zone diameters between (12-16 mm) against *P. aeruginosa*, *B. pumilus*, *E. coli*, and *C. albicans*. Among the extracts, MeOH extract possesses the highest antimicrobial activity.

**Table 6 Microbial Inhibition Zone Diameters of Crude Extracts from *M. ptelefolia* Leaf by Agar Well Diffusion Method (Disc diameter = 10 mm)**

No.	Microorganism	Type	Diameter of Inhibition Zone (mm)					
			PE	CHCl <sub>3</sub>	EtOAc	EtOH	H <sub>2</sub> O	MeOH
1.	<i>B. subtilis</i>	Gram(+)	-	-	-	-	-	-
2.	<i>S. aureus</i>	Gram(+)	-	15	-	16	15	12
3.	<i>P. aeruginosa</i>	Gram(-)	-	11	12	-	-	-
4.	<i>B. pumilus</i>	Gram(+)	-	11	16	14	-	14
5.	<i>E. coli</i>	Gram(+)	-	-	16	14	-	15
6.	<i>C. albicans</i>	Fungi	-	-	15	-	-	18

### Cytotoxicity

An MTT assay is a colorimetric assay based on assessing the cell metabolic activity. The sample was evaluated for cytotoxicity on human hepatoma carcinoma cell lines (HepG2), the results are shown in Table 7. In the present study, *M. ptelefolia* was found to show a potent inhibitory effect on HepG2 cell survival. Firstly, the toxicity of *M. ptelefolia* was examined on liver cancer HepG2 cells. The calculated IC<sub>50</sub> (47.22 ± 0.27 µg/mL) implied the promising inhibitory effect against these cancer cells.

**Table 7 Cytotoxicity of Different Concentration of Methanol Extract of *M. ptelefolia* Leaf against HepG2 Cell Line**

Extracts	Cell viability (mean ± SD) in different concentration (µg/mL)							IC <sub>50</sub> (µg/mL)
	3.125	6.25	12.5	25	50	100	200	
<b>MeOH</b>	0.98 ±0.25	0.73 ±0.11	0.67 ±0.05	0.66 ±0.33	0.48 ±0.22	0.42 ±0.26	0.17 ±0.03	47.22 ±0.27

### Conclusion

From the overall assessment concerning with the chemical constituents and some biological activity investigation on *M. ptelefolia* (Thit-Kha) leaf, the following inferences could be deduced. *M. ptelefolia* leaf is a good remedy for some disease due to the presence of important phytoconstituents such as phenolic compounds, flavonoids, alkaloids and steroids, etc. Moreover, Si, K and Ca were found as a major constituent in leaf samples. Higher content of carbohydrate, protein and fiber as good source of nutrients was observed in leaf sample. According to data, the amounts of total phenol and total flavonoid were very high in watery extract, than methanol and ethanol extracts. The knowledge of the phenolic compound profile, occurring in *M. ptelefolia* holds great significance from the pharmaceutical point of view. The level of flavonoids in plants is vital for the resistance of external threats and the ability to defend the cells from oxidants. The radical scavenging activity of watery extract was found to be more effective than ethanol and methanol extracts. Moreover, these are natural antioxidants, so we should use *M. ptelefolia* leaf instead of synthetic antioxidants that have shown potential health risks and toxicity. EtOAc and MeOH extracts exhibited the highest antimicrobial activities. Therefore, these extracts except PE may have mild broad spectrum activity and would be helpful in testing diseases caused by infection of these microorganisms. From the results of cytotoxic activity of methanol extract, the concentration of methanol extract increased, the cell viability also decreased. Therefore, methanol extract of

*M. ptelefolia* leaf can protect liver cancer cell. According to these experimental results, *M. ptelefolia* leaf possess the some medicinal properties and may be used as potential sources for the treatment of diseases related to oxidative stress, cytotoxic and microbial infections.

### Acknowledgements

The authors would like to express their profound gratitude to the Myanmar Academy of Arts and Science for giving permission to submit this paper.

### References

- Chang, C. C., and Yang, M. H. and Wen, H. M. (2002). "Estimation of total flavonoid content in propolis by two complementary colorimetric methods". *J. Food Drug Anal.*, vol. 10, pp. 178-182
- Chao P. Y., Lin, S. Y. and Lin, K. H. (2014). "Antioxidant Activity in Extracts of 27 Indigeneous Taiwanese Vegetables". *Nutrients*, vol. 6 (5), pp. 2115-2130
- Chen, J.C., Yeh, T. Y., Chen, P.C. and Hsu, C. K. (2007). "Phenolic Content and DPPH Radical Scavenging Activity of Yam-containing Surimi Gels Influenced by Salt and Heating". *Asian Journal of Health and Information Science*, vol. 2, pp. 1-8
- Cruickshank, R. (1960). "*Hand Book of Bacteriology*". London: 10<sup>th</sup> Edition, E. & S. Livingstone Ltd., pp. 980
- Harborne, J. B. (1998). *Phytochemical Methods. A Guide to Modern Techniques of Plant Analysis*, New York: 2<sup>nd</sup> Ed., Chapman and Hall Ltd., pp. 67-192
- Kumar, S. and Pandey, A. K. (2013). "Chemistry and Biological Activities of Flavonoids: An Overview". *The Scientific World Journal*, vol. 53 (1), pp.1-16
- Leea, E., Vitaly, I. V., Myung-Woo, L. B. and Cherl-Ho, L. (2002). "Detection of free radicals in gamma-irradiated soybean paste and model system by electron spin resonance spectroscopy". *Radiation Physics and Chemistry*, vol. 64, pp. 61-66
- McDonald S., Prenzler, P. D. and Antolovich, M. (2001). "Phenolic content and antioxidant activity of olive extracts". *Food Chem.*, vol. 73, pp. 73-84
- Rang, H. P., Dale, M. M. and Ritte, J. M. (2003). "*Pharmacology*", Melbourne: 4<sup>th</sup> Edition, Churchill Livingstone, pp. 340-385
- Sofowora, E. A. (1994). "Medicinal Plant and Traditional Medicine in Africa". Nigeria: University of Ife Press, pp. 1-23
- Van Meerloo, J., Kaspers, G. J. L. and Cloos, J. (2011). "Cell sensitivity assays: The MTT Assay". *Methods Mol. Biol.*, vol. 731, pp. 237-245
- Zaino, M. K., Abd-Hamid A., Yusof S. and Muse R. (2003). "Antioxidant Activity and Total Phenolic Compounds of Leaf, Root and Petiole of Four Accessions of *Centella asiatica* (L.)". *Food Chem.*, vol. 81, pp. 575-581

## BIOCHEMICAL STUDIES AND HEPATOPROTECTIVE POTENTIALITY OF *SMALLANTHUS SONCHIFOLIUS* (POEPP. AND ENDL.) H. ROBINSON (YACON) LEAVES

Thida Myint<sup>1</sup>, Phyu Phyu Myint<sup>2</sup>, Ni Ni Than<sup>3</sup>

### Abstract

The present work focused on the studies of chemical constituents from the leaves of *Smallanthus sonchifolius* (Poepp. and Endl.) H. Robinson (Yacon) and some biological activities. Yacon is one of the edible plants and it is collected from Ywar Ngan Township, Southern Shan State. Phytochemical investigation of Yacon leaves was performed and it was found that alkaloids,  $\alpha$ -amino acids, carbohydrates, flavonoids, glycosides, phenolic compounds, reducing sugars, saponins, steroids, tannins, terpenoids, and organic acids were present, however, cyanogenic glycosides and starch were absent. Nutritional values were observed to compose by moisture (14.35 %), fiber (11.67 %), protein (11.43 %), ash (9.09 %), fat (5.31 %), carbohydrate (40.7 %) and energy value is 313.55 kcal/100 g of Yacon leaves were found to be determined by using the respective methods. In addition, the elements such as K (0.908 %), Ca (0.801 %), S (0.120 %), Fe (0.028 %), Ba (0.008 %), Mn (0.006 %), P (0.002 %), Cu (0.002 %), Zn (0.001 %) were examined by ED XRF method. The antioxidant activities of watery and ethanol extracts of the leaves sample were determined by DPPH assay method. The IC<sub>50</sub> value of watery and ethanol extracts were found to be 786.56 and 466.92  $\mu$ g/mL, respectively. The ethanol extract is more effective than the watery extract. However, the two extracts show the mild activity when compared to the standard antioxidant ascorbic acid (IC<sub>50</sub> = 4.57  $\mu$ g/mL). *In vitro* screening of antimicrobial activity was examined by nutrient agar well diffusion method on eight different microorganisms (*Bacillus subtilis*, *Staphylococcus aureus*, *Pseudomonas aeruginosa*, *Bacillus pumilus*, *Candida albicans*, *Escherichia coli*, *Aspergillus flavus* and *Aspergillus niger*). Ethyl acetate and 95 % ethanol extracts of Yacon leaves showed antimicrobial activity on eight strains of microorganisms (inhibition zone diameter 12 mm to 30 mm). Watery extract against other strains except *A. flavus* (inhibition zone diameter 13 mm to 20 mm). In addition, petroleum ether and methanol extracts against other strains except *P. aeruginosa* (inhibition zone diameter 11 mm to 30 mm). The cytotoxicity of methanol extract from Yacon leaf against hepatoma liver cancer cell HepG2 was evaluated by MTT assay. The IC<sub>50</sub> value of methanol extract was found to be 53.68  $\mu$ g/mL for 24 h treated time. The results of this study scientifically validate the traditional use of Yacon leaves for the treatment of liver diseases.

**Keywords:** *Smallanthus sonchifolius*, phytochemical, nutritional values, antioxidant activity, antimicrobial activity, cytotoxicity, MTT assay

### Introduction

Plant is an important source of medicine and plays a key role in world health. Medicinal plants may be defined as those plants that are commonly used in treating and preventing specific ailments and diseases and that are generally considered to be harmful to humans (Schulz *et.al.*, 2001). Medicinal plants have provided mankind a large variety of potent drugs to alleviate or eradicate infections and suffering from diseases in spite of advancement in synthetic drugs, some of the plant-derived drugs still retained their importance and relevance. The use of plant-based drugs all over world is increasing. Modern medicines and herbal medicines are complementarily being used in areas for health care program in several developing countries such as countries in Africa, Asia and some part of Europe. Due to different outcomes on herbal plants, plants products surfaces all over the world due to the belief that many herbal medicines are known to be free from health and environmental effects (Angell and Kassirer, 1998). The world health organization

<sup>1</sup> Lecturer, Department of Chemistry, Dagon University

<sup>2</sup> Dr, Professor, Department of Chemistry, Loikaw University

<sup>3</sup> Dr, Professor (Head), Department of Chemistry, University of Yangon

estimates that the plant extracts or their active constituents are used as folk medicine in traditional therapies of 80 % of the world's population (Baker *et.al.*, 2005).

*Smallanthus sonchifolius* (Poepp. and Endl.) H. Robinson. (Yacon) is a tuber plant that is native to the Andean region. Yacon has been consumed commonly by diabetics and persons suffering from digestive disorders. Yacon also possesses the properties to treat kidney complaints and skin-rejuvenating activity. Fructooligosaccharides are the products recognized and used as food ingredients and prebiotics (Pedreschi *et al.*, 2002). Dried yacon leaves were used to prepare a medicinal infusion or mixed with common tea leaves in Japan (Aybar *et al.*, 2001). In the present work, *S. sonchifolius* (Yacon) leaves were selected to investigate phytochemical constituents and some biological activities.

## Materials and Methods

### Collection and Preparation of Sample

The leaves sample of *S. sonchifolius* (Yacon) was collected from Ywar Ngan Township, Southern Shan State. After collection, the botanical name of the sample was identified and confirmed as *S. sonchifolius* (Yacon) leaves at Botany Department, Dagon University. The collected fresh sample was cleaned by washing thoroughly with water and air dried. After drying, the leaf sample was cut into small pieces and ground using grinding machine. And then this powdered sample was kept in the sealed air-tight container to prevent moisture changes and other contamination. It was then used without further purification or refining.

### Phytochemical investigation

The dried powdered samples were used to chemical tests for the determination if the presence or absence of the major types of phytochemical constituents such as alkaloids,  $\alpha$ amino acids, carbohydrates, flavonoids, glycosides, phenolic compounds, reducing sugars, starch, saponins, steroids, tannins, terpenoids, organic acids, cyanogenic glycosides using standard procedure (Finar, 1968; M-Tin Wa, 1972; Marini *et al.*, 1981; Robinson, 1983; Shriner *et al.*, 1980).

### Determination of Nutritional Values

Some nutritional values such as moisture, ash, protein, fiber, fat and energy values were quantitatively determined according to AOAC methods (AOAC, 2000) and total carbohydrate contents were also quantitatively determined by phenol-sulphuric acid method (Neeru *et al.*, 2015).

### Elemental Analysis of Leaves Sample by ED XRF

In order to determine the heavy toxic metals and micronutrient elements in leaves sample, elemental contents in the leaves of *S. sonchifolius* were determined by ED XRF method at the Universities' Research Center, Yangon. The major advantage of X-ray spectrometry is that it offers a satisfactory compromise among economy, speed and ease of operation (Ertel, 1991).

### Determination of Antioxidant Activity

DPPH (1, 1-diphenyl-2-picryl-hydrazyl) radical scavenging assay was chosen to assess the antioxidant activity of plant materials. This assay has been widely used of plant materials to evaluate the free radical scavenging effectiveness of various flavonoids and polyphenols in food system (Leea *et al.*, 2002). In this experiment, the antioxidant activity was studied on 95 % ethanol and aqueous extract from selected leaf sample by DPPH free radical scavenging assay. DPPH

(7 mg) was thoroughly dissolved in 100 mL of 95 % ethanol. This 180  $\mu$ M DPPH solution was freshly prepared in the brown coloured bottle.

The control solution was prepared by mixing the 1.5 mL of 180  $\mu$ M DPPH solution and 1.5 mL of 95 % ethanol in brown bottle. Blank solution was prepared by mixing the 1.5 mL of test sample solution with 1.5 mL of 95 % ethanol. Each respective H<sub>2</sub>O and ethanol extracts (30 mg) and 30 mL of 95 % ethanol were thoroughly mixed by shaker. The mixture solution was filtered and stock solution was obtained. Desired concentration 1000  $\mu$ g/mL, 800  $\mu$ g/mL, 600  $\mu$ g/mL, 400  $\mu$ g/mL, 200  $\mu$ g/mL and 100  $\mu$ g/mL of each solutions were prepared from this stock solution by dilution with appropriate amount of 95 % ethanol.

4 mg of standard ascorbic acid was dissolved in 20 mL of 95 % ethanol to get the 200  $\mu$ g/mL stock solution. Desired concentrations of 100  $\mu$ g/mL, 50  $\mu$ g/mL, 25  $\mu$ g/mL, 12.5  $\mu$ g/mL, 6.25  $\mu$ g/mL and 3.125  $\mu$ g/mL solution were prepared by two-fold serially diluted with ethanol. These bottles were incubated at room temperature and were shaken on shaker for 30 min. After 30 min, the absorbance of these solution was measures at 517 nm by using spectrophotometer (UV-KWF, China). Absorbance measurements were done in triplicate for each solution and the mean values obtained were used to calculate % inhibition of oxidation. Then IC<sub>50</sub> (50 % inhibitory concentration) values were also calculated by linear regressive excel program.

### Antimicrobial Activity Screening by Agar Well Diffusion Method

Antimicrobial activity of different crude extracts such as (pet ether, ethyl acetate, ethanol, methanol, water extracts) of leaves were screened in *in vitro* by agar well diffusion method (Dorman and Deans, 2000). Test microorganisms are *Bacillus subtilis*, *Staphylococcus aureus*, *Pseudomonas aeruginosa*, *Bacillus pumilus*, *Candida albican*, *Escherichia coli*, *Aspergillus flavus* and *Aspergillus niger* species. This experiment was carried out at Pharmaceutical Research Department (PRD), Ministry of Industry, Yangon.

### Examination of *in vitro* Cytotoxic Activity by MTT Reduction Assay method

The cytotoxicity of methanol extract of the sample was examined by using MTT reduction assay method. HepG2 cells were seeded in a 96 well flat-bottomed microliter plate at a density of 1 $\times$ 10<sup>4</sup> cells/ well and allowed to adhere for 24 h at 37 °C in a CO<sub>2</sub> incubator. After 24 h the cell were then treated with 40 to 100  $\mu$ g/mL of methanol extract for 24 h at 37 °C in a CO<sub>2</sub> incubator. Subsequently, 10  $\mu$ L of MTT solution (5 mg/mL in phosphate buffer solution) were added to each well and incubated for 4 h at 37 °C. The culture medium was discarded, and 100  $\mu$ L of DMSO solution was added into each well and mixed by gently shaking for 10min. Absorbance (the interesting of the dissolved formazan crystal (purple color) was quantified using the ELISA plate (microplate reader) at 595 nm (Padhya et al., 2013). Cell viability was calculated from the mean values of the data from three wells and cytotoxic activity was expressed as the IC<sub>50</sub> (50 % inhibitory concentration) value.

$$(\%) \text{ Cell viability} = 100 \times \frac{A_{bs}(\text{test sample}) - A_{bs}(\text{Blank})}{A_{bs}(\text{control}) - A_{bs}(\text{Blank})}$$

## Results and Discussion

### Phytochemical Profile of Yacon Leaves

According to the phytochemical test results,  $\alpha$ -amino acids, alkaloids, carbohydrates, flavonoids, glycosides, phenolic compounds, reducing sugars, saponins, steroids, tannins, terpenoids and organic acids are present in the sample but cyanogenic glycosides and starch are absent. Alkaloids, as reported by Elekwa *et al.*, 2008, have been seen to interfere with cell division which makes them an important plant part to possibly be used as remedy in the treatment of cancer. Saponins and glycosides have been reported to have hypertensive and cardiac depressive properties (Trease and Evans, 1985). The primary role of carbohydrate is to provide energy to all cells (Slavin and Carlson, 2014). Flavonoids and many other phenolic components have been reported on their effective antioxidants, anticancer, antibacteria, cardioprotective agents, anti-inflammation, immune system promoting, skin protection from UV radiation (Dzialo *et al.*, 2016).

### Some Nutritional Values and Elemental Analysis of Yacon Leaves

The determination of some nutritional values such as moisture, ash, protein, fat, fiber, carbohydrates and energy value contents were determined by reported methods. The moisture content of sample was determined by oven dried method and was found 14.35 %. The fat content was determined by the soxhlet extraction method and 5.31 % was obtained. In addition, the sample was also studied for fiber content by acid alkali treatment, protein content by AOAC method and ash content by using muffle furnace. The total ash in the sample is the inorganic residue remaining after the organic matter has been burnt away. The fiber, protein, ash, carbohydrates contents and energy value for Yacon leaves were found to be 11.67 %, 11.43 %, 9.09 % and 40.7 % and 313.55 kcal/100 g, respectively. The results are shown in Table 1.

X-ray spectrometer permits simultaneous analysis of light element to heavy metal. Shimadzu EDX-720 spectrometer can analyze the elements from  $_{11}\text{Na}$  and  $_{92}\text{U}$  under vacuum condition. The ED XRF spectrum of the sample results was reported in Table 2. It can be seen that essential minerals for human health such as potassium and calcium in leaves were the most predominant. The primary functions of potassium in the body include regulating fluid balance and controlling the electrical activity of the heart and other muscle strength. Calcium is key for the health of bone and teeth, but it also affects muscles, hormones and nerve function. According to ED XRF, no toxic element was found in leaves sample.

### Antioxidant Activity of crude extracts from leaves of yacon

DPPH (1, 1-diphenyl-2-picryl-hydrazyl) method is the most widely reported method for screening of antioxidant activity on many plant drugs. This method is based on the reduction of colored free radical DPPH in 95 % ethanol solution by different concentration of the samples. The antioxidant activity was expressed as 50 % oxidative inhibitory concentration ( $\text{IC}_{50}$ ). The percent oxidative inhibition values of crude extracts measured at different concentration and the results are summarized in Table 3. From these experimental results, it was found that as the concentrations increased, the absorbance values decreased i.e. increase in radical scavenging activity of crude extracts usually expressed in term of % inhibition. From the average values of % inhibition,  $\text{IC}_{50}$  (50 % inhibition concentration) values in  $\mu\text{g/mL}$  were calculated by linear regressive excel program.

From these results, it can be clearly seen that  $\text{IC}_{50}$  values were found to be 466.92  $\mu\text{g/mL}$  for ethanol extract and 786.56  $\mu\text{g/mL}$  for water extract. The lower the  $\text{IC}_{50}$  showed the higher the free radical scavenging activity. Ethanol extract was found to be more effective than watery extract in free radical scavenging activity. However, it was observed that all of these extracts have the lower antioxidant activity than standard ascorbic acid ( $\text{IC}_{50} = 4.57 \mu\text{g/mL}$ ).

**Table 1 Some Nutritional Value of Yacon Leaf**

No. Parameters	Contents
Moisture (%)	11.43
2. Carbohydrates (%)	14.35
3. Fat (%)	5.31
4. Protein (%)	11.67
5. Ash (%)	9.09
6. Crude fiber (%)	40.7
7. Energy value (kcal/100 g)	313.55

**Table 2 Relative Abundance of Element in Yacon Leaf**

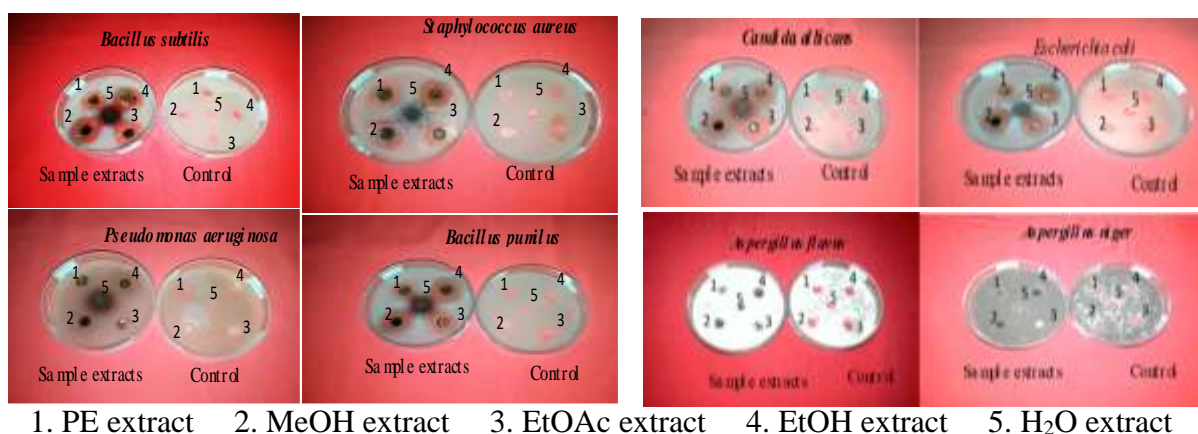
No.	Element	Relative abundance (%)
1	K	0.908
2	Ca	0.801
3	S	0.120
4	Fe	0.028
5	Ba	0.008
6	Mn	0.006
7	P	0.002
8	Cu	0.002
9	Zn	0.001
10	C H	98.122

**Table 3 Percent Oxidative Inhibition and IC<sub>50</sub> Values of 95 % Ethanol and Watery Extracts of Yacon Leaves**

Extracts	% Inhibition (mean $\pm$ SD) in different concentrations ( $\mu$ g/mL)						IC <sub>50</sub> ( $\mu$ g/mL)
	100	200	400	600	800	1000	
Watery	16.78 $\pm$ 3.78	22.72 $\pm$ 0.88	29.89 $\pm$ 0.43	41.04 $\pm$ 1.37	51.17 $\pm$ 0.85	67.62 $\pm$ 3.18	786.56
Ethanol	11.396 $\pm$ 1.79	22.61 $\pm$ 1.27	37.94 $\pm$ 4.63	73.91 $\pm$ 2.47	82.598 $\pm$ 0.609	85.48 $\pm$ 0.618	466.92

### Screening of Antimicrobial Activity

Five crude extracts (PE, MeOH, EtOAc, EtOH and H<sub>2</sub>O) were screened for antimicrobial activity against eight different microorganisms using agar well diffusion method. Larger the zone diameter, the more activity is on the test bacteria. According to the results in the Table 4. *In vitro* screening of antimicrobial activity was examined by nutrient agar well diffusion method on eight different microorganisms (*B. subtilis*, *S. aureus*, *P. aeruginosa*, *B. pumilus*, *C. albicans*, *E. coli*, *A. flavus* and *A. niger*). EtOAc and 95 % EtOH extracts of Yacon leaves showed antimicrobial activity on eight strains of microorganisms (inhibition zone diameter 12 mm to 30 mm). H<sub>2</sub>O extract against other strains except *A. flavus* (inhibition zone diameter 13 mm to 20 mm). In addition, PE and MeOH extracts against other strains except *P. aeruginosa* (inhibition zone diameter 11 mm to 30 mm). *In vitro* antimicrobial assays showed appreciable antibacterial activity against eight microorganisms. These results indicate that it can significantly decrease their representative diseases (such as, food poisoning, dizziness, head ache, stomach cramps, skin infections, respiratory infection, failure of heart, kidney and liver, pneumonia, diabetes, abdominal pain, fever, vomiting fatigue, joint pain, liver cancer).



1. PE extract 2. MeOH extract 3. EtOAc extract 4. EtOH extract 5. H<sub>2</sub>O extract

**Figure 1** Inhibition zone of various crude extracts of yacon leaves againsts *B. subtilis*, *S. aureus*, *P. aeruginosa*, *B. pumilus*, *C. albicans*, *E. coli*, *A. flavus*, *A. niger*

**Table 4** Inhibition Zone Diameters of Various Crude Extracts against Eight Microorganisms by Agar Well Diffusion Method

Samples	Inhibition Zone Diameters (mm) of Crude Extracts					
	Pet-ether	MeOH	EtOAc	EtOH	H <sub>2</sub> O	Control
<i>B. subtilis</i>	23 (+++)	30 (+++)	30 (+++)	30 (+++)	20 (++)	-
<i>S. aureus</i>	24 (+++)	30 (+++)	30 (+++)	30 (+++)	20 (++)	-
<i>P. aeruginosa</i>	-	-	15 (+)	15 (+)	17 (++)	-
<i>B. pumilus</i>	20 (++)	25 (+++)	25 (+++)	30 (+++)	20 (++)	-
<i>C. albicans</i>	20 (++)	30 (+++)	25 (+++)	28 (+++)	20 (++)	-
<i>E. coli</i>	15 (+)	25 (+++)	24 (++)	20 (++)	15 (+)	-
<i>A. flavus</i>	11 (+)	12 (+)	13 (+)	13 (+)	-	-
<i>A. niger</i>	11 (+)	13 (+)	12 (+)	13 (+)	13 (+)	-

#### Acceptance Criteria

Susceptible	Intermediate	Resistant
Disc Diffusion (mm) $\geq$ 21 (+++)	17 to 20 (++)	$\leq$ 16 (+)

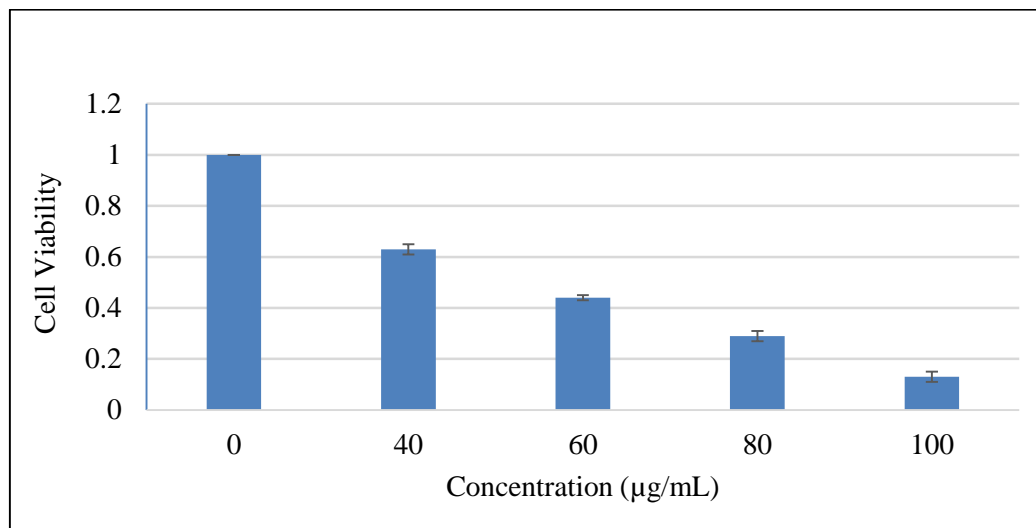
#### Cytotoxicity of Methanol Extract of yacon leaf

The cytotoxicity of methanol extract of Yacon leaf was evaluated by MTT assay. The cytotoxicity of methanol extract was expressed in terms of mean  $\pm$  SD standard deviation and IC<sub>50</sub> (50 % Inhibitory Concentration) and the results are shown in Table 5 and Figure 2. There are many plants extracts have been used as anticancer agents even vegetables and fruits many help reduce the risk of cancer in humans. Some Thai plants namely *Glochidion daltonii*, *Cladogynos orientalis*, *Catimbium speciosum*, *Acorus tatarinowii*, *Amomum villosum* and *Pinus kesiya* were also reported against the human hepatocarcinoma (HepG2) cell line (Machana *et al.*, 2011).

In this study, the local plant Yacon leaves showed IC<sub>50</sub> (53.68  $\mu$ g/mL) for cytotoxicity against HepG2 cell line.

**Table 5 Viability of HepG2 Cell by MeOH Extract of Yacon Leaves Using MTT Assay**

Extract	Cell Viability (mean $\pm$ SD) in different concentrations ( $\mu\text{g/mL}$ )					IC <sub>50</sub> ( $\mu\text{g/mL}$ )
	0	40	60	80	100	
MeOH	1.0	0.63	0.44	0.29	0.13	53.68
	$\pm 0.00$	$\pm 0.02$	$\pm 0.01$	$\pm 0.2$	$\pm 0.02$	

**Figure 2** A bar graph of cell viability for 24 h treated by MeOH extract

### Conclusion

From the overall assessments of the present work concerning with the phytochemical constituents and some biological activities of yacon leaves, the following inference could be deduced. The preliminary phytochemical investigation of yacon leaves were performed and it was found that alkaloids,  $\alpha$ -amino acids, carbohydrates, flavonoids, glycosides, phenolic compounds, reducing sugars, saponins, steroids, tannins, terpenoids, and organic acids were present, however, cyanogenic glycosides and starch were absent. Nutritional values were observed to compose by moisture. The nutritional values for yacon leaves were found to be good source of fiber, protein and carbohydrate. Qualitative elemental analysis of plant sample by ED XRF method showed that K and Ca were the highest amount of elements in the sample. The primary functions of potassium in the body include regulating fluid balance and controlling the electrical activity of the heart and other muscles. Calcium is one of the most important minerals for the human body. It helps form and maintain healthy teeth and bones. The radical scavenging activity of ethanol extract was found to be more effective than watery extract by DPPH assay. Antimicrobial activity showed significantly decreases population of pathogenic bacteria eight different microorganisms (*B. subtilis*, *S. aureus*, *P. aeruginosa*, *B. pumilus*, *C. albicans*, *E. coli*, *A. flavus* and *A. niger*). The IC<sub>50</sub> value of MeOH extract against human liver cancer line (Hep G2) was observed 53.68  $\mu\text{g/mL}$ . According to these observation, yacon leaves could be applied not only nutrition but also for therapy.

## Acknowledgements

The authors would like to acknowledge to Dr Cho Cho Win (Professor & Head), and Professor Dr Khin Than Win, Department of Chemistry, Dagon University for generously and kindly providing to do this research work. And the authors would like to express our gratitude to the Department of Higher Education, Ministry of Education, Myanmar, for their permission to do this research and also to the Myanmar Academy of Arts and Science for allowing to read this paper.

## References

- Angell, M. and Kassirer, J.P. (1998). "Alternative Medicine-The Risks of Untested and Unregular Remedies". *N Engl J Med.*, vol. 339(12), pp. 839-841
- Aybar, M.J., Riera, A.N.S., Grau, A. and Sanche, S.S. (2001). "Hypoglycemic Effect of the Water of *Smallanthus sonchifolius* (Yacon) Leaves in Normal and Diabetic rats". *J.Ethnopharmacol.*, vol. 74(2), pp.113-123
- AOAC (2000). *Methods in Food Analysis*. Pearson's Chemical Analysis of Food. *Association of Official Chemists*. America: 17<sup>th</sup> Edn., Food Science and Technology
- Baker, J.T., Boris, R.P. and Carte, B. (2005). "Natural Product Drug Discovery and Development". *New perceptive on international collaboration*, vol. 58, pp. 1325-1325
- Dorman, H. J. and Deans, S. G. (2000). "Antimicrobial Agents from Plants and Antibacterial Activity of Plants Volatile Oils". *J., Applied Microbial*, vol. 88, pp. 308-316
- Dzialo, M., Mierziak, J., Korzun, U., Preisner, M., Szopa, J., and Kulma, A. (2016). "The potential of plant phenolics in prevention and therapy of skin disorders" *Int. J. Mol. Sci.*, vol.17, pp.160
- Elekwa, I., Okereke, S.C. and Ekpo, B.O. (2008), Preliminary phytochemical and antimicrobial investigations of the stem bark and leaves of *Psidium guajaya L*, *Journal of Medicinal Plant Research*, vol.3 (1), pp. 045-048
- Ertel, D. (1991). *X-ray Fluorescence Analysis*. Karlsruhe, Germany: Nuclear Research Centre, pp. 234-237
- Finar, I. L. (1968). *Organic Experiment*. New York: 4<sup>th</sup> Ed., D-C Health and Company, p. 132
- Leea, E., Vitaly, I. V. Myung, W. B. and Cherl, H. (2002). "Detection of free radicals in Gamma-irradiated Soybean Paste and Model System by Electron Spin Resonance Spectroscopy". *Radiation Physics and Chemistry.*, vol. 64, pp. 61-64
- M-Tin Wa. (1972). "Phytochemical Screening Methods and Procedures". *Phytochemical Bulletin of Botanical Society of America Inc.*, vol. 5 (3), pp. 4-10
- Marini, G. B., Bettolo Nicoletti, M., Patomia, M., Galeffi, C. and Messona, I. (1981). "Plant Screening by Chemical and Chromatographic Procedures Under Field Conditions". *J. Chromate.* vol. 46(2), pp. 359-363
- Machana, S., Weerapreeyakul, N., Barusrux, S., Nonpunya, A., Sripanidkulchai, B. and Thitimetharoch, T. (2011). "Cytotoxic and Apoptotic Effects of Six Herbal Plants against the Human Hepatocarcinoma (HepG2) cell line", *Chin Med.*, vol. 6, pp. 39-46
- Neeru, A., K. M. Divya and R. Khushboo. (2015). "Estimation of Total Carbohydrate Present in Dry Fruits". *Journal of Environmental Science, Toxicology and Food Technology*, Vol.1(6), pp. 24-27
- Padhya. K.T., Marrero, J. A. and Singal, A.G. (2013). "Recent advances in the treatment of hepatocellular carcinoma". *Curr Opin Gastroenterol*, vol.29, pp. 285-292
- Pedreschi, R., Campos, D., Noratto, G., Chirinos, R. and Cisneros Zevallos, L.A. (2002). *Fermentation of fructooligosaccharides from yacon (Smallanthus sonchifolia poepp. End.)*. Food ExpoAnaheim, California, pp. 84-89
- Robinson, T. (1983). *The Organic Constituents of Higher Plants*. North Amberst: 5<sup>th</sup> Ed., Cordus Press, pp. 285-286
- Schulz, V., Hansel, R., and Tyler, Ve., (2001). *Rational Phytotherapy*. A Physician's Guide to Herbal Medicine: 4<sup>th</sup> Ed, Berlin: Springer Verlag, pp. 306
- Shriner, R.L., Fuson, R.C., Curtin D.Y. and Morrill, T.C. (1980). *The Systematic Identification of Organic Compounds, A Laboratory Manual* New York: 6<sup>th</sup> Ed, John Wiley and Sons, pp. 34-38
- Slavin, J. and J. Carlson. (2014). "Carbohydrate", *Advance in Nutrition*, vol. 5 (6), pp. 760-761
- Trease, G.E. and Evans, W.C. (1985). *Pharmacognosy*. London: 12<sup>th</sup> Ed., English Language Books Society, Bailliere Tindall, p. 394

## SCREENING ON SOME BIOACTIVITIES FROM THE LEAF OF *BAUHINIA PURPUREA* L. (SWEDAW-NI)

Mie Mie Aye\*

### Abstract

In the present study, the leaf of *Bauhinia purpurea* L., locally known as “Swedaw-ni” was selected to screen some bioactivities. Firstly, the phytochemical constituents were investigated by the reported chemical methods. The qualitative elemental analysis was done by EDXRF technique. The crude extracts were prepared by the solvent extraction method. Total phenolic content in ethanol and watery extracts was carried out spectrophotometrically using Folin-Ciocalteu reagent. Ethanol extract (32.58 µg GAE/mg of extract) showed higher phenolic content than watery extract (21.73 µg GAE/mg of extract). In the study of the antioxidant activity, ethanol and watery extracts were screened by DPPH radical scavenging assay. The ethanol extract (IC<sub>50</sub> = 5.75 µg/mL) was found to be more potent than the watery extract (IC<sub>50</sub> = 8.51 µg/mL) in the antioxidant activity. The antimicrobial activity of both extracts was investigated against *Bacillus subtilis*, *Staphylococcus aureus*, *Pseudomonas aeruginosa*, *Bacillus pumilus*, *Candida albicans* and *E. coli*. The results showed that all tested microorganisms were susceptible to both ethanol and watery extracts of *B. purpurea* leaf. In addition, acute toxicity of ethanol extract was investigated with the dosage of 300 mg/kg, 2000 mg/kg and 5000 mg/kg body weight on albino mice and no lethality was observed up to fourteen days after administration. The Chemical nature for not been studied yet, however, the leaf of *B. purpurea* is likely to have potent biological activities to use as ingredient in preventive medicine.

**Keywords:** *Bauhinia purpurea* L., EDXRF, total phenolic content, antioxidant activity, antimicrobial activity, acute toxicity

### Introduction

Nature has provided a complete storehouse of remedies to cure ailment of mankind. Herbal medicine, as the major remedy in traditional medical systems, has been used in medical practice for thousands of years and has made a great contribution to maintaining human health. A majority of the world’s population in developing countries still relies on herbal medicine to meet its health needs (Kumar *et al.*, 2008). *Bauhinia purpurea* L (swedaw-ni in Myanmar) is belonging to the family leguminosae and it is a small to medium-sized deciduous tree. It is native to Southern and Southeastern Asia. It has been planted as an ornamental in many tropical and subtropical regions of the world. The plant is widely distributed throughout Myanmar. It contains major class of secondary metabolites which are flavonoids, glycosides, saponins, triterpenoids, phenolic compounds, oxepins, fatty acids and phytosterols (Kumar and Chandrashekar, 2011). The research has focused on screening of some bioactivities from the leaf of *B. purpurea* (Swedaw-ni). The plant *B. purpurea* is used in several ways for the treatment of skin diseases, wounds, ulcers, cough, dysentery, snakebite, tumors, flatulence, indigestion, piles and also lots of other ailments (Gupta *et al.*, 2012). It reported to exhibit various pharmacological activities such as antioxidant activity, hepatoprotective activity, hypoglycaemic activity and antiproliferative activity (Shajiselvin *et al.*, 2011). The leaves are used for the treatment of catarrh, infection of children, boil, glandular and swelling (Avinash *et al.*, 2011). Its flowers are used to reduce fever. The bark of the plant is used as an astringent and its decoctions are recommended for ulcers as a useful wash solution. The decoction of stem bark orally twice a day is very effective in asthma and other respiratory disorder as an anti-inflammatory agent (Patil *et al.*, 2008). The whole plant is used in dropsy, pain, rheumatism, convulsions, delirium and septicemia. The medicinal activities of *B. purpurea* are of great potential and it can be used as drugs of choices. The photographs of leaves and flowers of *B. purpurea* are described in Figure 1.

---

\* Dr, Associate Professor, Department of Chemistry, East Yangon University



**Figure 1** Photographs of *B. purpurea* (a) leaves (b) flowers

### **Materials and Methods**

The chemicals used in this research were obtained from British Drug House (BDH) and the reagents used were analar grade. The instruments used were EDXRF (Shimadzu EDX-7000 spectrometer) and UV - visible Spectrophotometer (Shimadzu UV-240).

#### **Collection and Identification of Plant Material**

The fresh leaf of the *B. purpurea* (Swedaw-ni) was collected from the area of Mingalardon Township, Yangon Region, in January 2019. After collection, the sample was identified at Botany Department, Taungoo University. The sample was washed with water to remove adhering dirt and then cut into small pieces, dried at room temperature for one week. The dried sample was ground into powder form with help of a grinding machine and stored in airtight container for further use.

#### **Phytochemical Screening of Leaf of *B. purpurea***

In order to find out the types of phytoconstituents present in sample, phytochemical investigation was carried out by chemical methods (Harborne, 1984; Robinson, 1983).

#### **Qualitative Elemental Analysis of Leaf of *B. purpurea***

For this measurement, pellet of the sample was first made. Energy disperse X-ray fluorescence spectrometer (Shimadzu EDX-7000) can analyze the elements from Na to U under vacuum condition. The individual element in sample is detected by using semiconductor that permits multi-elements, simultaneous analysis. In this way, EDX-7000 spectrometer determines elements that are present in the sample. The elemental contents in *B. purpurea* leaf were determined by EDXRF spectrometer at Taungoo University.

#### **Preparation of Crude Extracts of Leaf of *B. purpurea***

Ethanol crude extract was prepared from 100 g of dried powdered sample mixed with 400 mL of ethanol and kept for three days. The mixture was then filtered and evaporated to dryness under reduce pressure using a rotatory evaporator to produce the yield.

Watery crude extract was also prepared from 100 g of dried powdered sample mixed with 400 mL of distilled water and boiled for 2 h. The mixture was then filtered and evaporated to dryness on water bath to produce the yield. Each extract was stored in a desiccator containing dry silica gel prior using in each experiment.

### Determination of Total Phenolic Content of Leaf of *B. purpurea*

The total phenolic content in ethanol and watery extracts of *B. purpurea* leaf was determined by using Folin-Ciocalteu colourimetric method described by Kim *et al.*, (2003).

In this procedure, 1 mL of tested sample solution (1000 µg/mL) was added to 5 mL of 10 % FC reagent and incubated at room temperature for 30 min. Then, 4 mL of 1 M sodium carbonate solution was added to the mixture and the tubes were kept at room temperature for 15 min. The absorbance of reaction mixture was measured at  $\lambda_{\max}$  765 nm using UV-visible spectrophotometer. The standard calibration curve was constructed by plotting the absorbance vs different concentrations (100, 50, 25, 12.5, 6.25 and 3.125 µg/mL) of gallic acid. Total phenolic content was expressed as microgram of gallic acid equivalent per milligram of crude extract (µg GAE/mg of extract).

### Screening of some Bioactivities of Leaf of *B. purpurea*

#### Antioxidant activity screening

The antioxidant activity of ethanol and watery extracts of *B. purpurea* leaf was determined by DPPH (1,1-diphenyl-2-picryl-hydrazyl) radical scavenging assay using UV-visible spectrophotometer (Jain *et al.*, 2008). In this procedure, 1.5 mL of tested sample solution with six different concentrations (50, 25, 12.5, 6.25, 3.125 and 1.5625 µg/mL) was mixed with 1.5 mL of DPPH solution (60 µM). The absorbance values of these solutions were measured by UV-visible spectrophotometer at 517 nm at 30 min intervals against a blank solution. Absorbance was measured in triplicate for each solution and the mean values so obtained were used to calculate the percent inhibition of oxidation by the following equation:

$$\% \text{ inhibition} = \frac{\text{Control} - (\text{Sample} - \text{Blank})}{\text{Control}} \times 100$$

Control = the absorbance of DPPH in EtOH solution

Sample = the absorbance of sample and DPPH solution

Blank = the absorbance of sample and EtOH solution

Then, IC<sub>50</sub> (50 % oxidative inhibitory concentration) values were calculated by linear regressive excel program.

#### Antimicrobial activity screening

The antimicrobial activity of ethanol and watery extracts of *B. purpurea* leaf was investigated by agar well diffusion method at Development Centre of Pharmaceutical and Food Technology (DCPFT). The microorganisms used in this study included five bacterial strains such as *Bacillus subtilis*, *Staphylococcus aureus*, *Pseudomonas aeruginosa*, *Bacillus pumilus*, *E. coli* and one fungal species, *Candida albicans*.

#### Acute toxicity study

The acute toxicity activity of ethanol extract of *B. purpurea* leaf was done according to the Organization for Economic Cooperation and Development (OECD) guide line 423 (2001). According to the test description, total number of 18 adult female albino mice, weighing (25-30 g) were selected and divided into three groups (six in each group). Each group was treated with ethanol extract in different concentrations (300, 2000, 5000 mg/kg body weight) by using a stomach tube. After administration of the test agent orally, the sign of toxicity or lethality was observed on the test animals. At the end of the test (i.e., 14 days), surviving animals were weighed.

## Results and Discussion

### Phytochemicals Present in Leaf of *B. purpurea*

In order to find out the types of phytochemical constituents present in *B. purpurea* leaf, phytochemical investigation was carried out by chemical methods. Phytochemical investigation of plant material was done by based on the results of colour changes or precipitation, which indicates that the presence of classes of organic constituents containing in it. According to these results,  $\alpha$ -amino acids, flavonoids, glycosides, phenolic compounds, saponins, tannins, steroids and terpenoids were present in sample. However, alkaloids, carbohydrates, cyanogenic glycosides, reducing sugars and starch were not detected.

### Some Elements Present in Leaf of *B. purpurea*

The relative abundance of elements present in leaf of *B. purpurea* was determined by EDXRF spectrometer. The EDXRF spectrum is described in Figure 2 and the relative abundance of some elements present in *B. purpurea* leaf is shown in Table 1. It was observed that Ca was found to be the principal element and K, Fe, Sr, Mn, Zn, Cu, Rb and Br were present as trace elements in the sample. Ca is the mineral that human requires in the greatest amounts. It is an essential for the development, growth and maintenance of bone. It helps regulate muscle contraction. K is an important for muscle function, including relaxing the walls of the blood vessels. This lowers blood pressure and protects against muscle cramping. Fe is a mineral vital to the proper function of hemoglobin, a protein needed to transport oxygen in the blood. Therefore, *B. purpurea* leaf contained many necessary elements and it could be a good supplement for some nutrients.

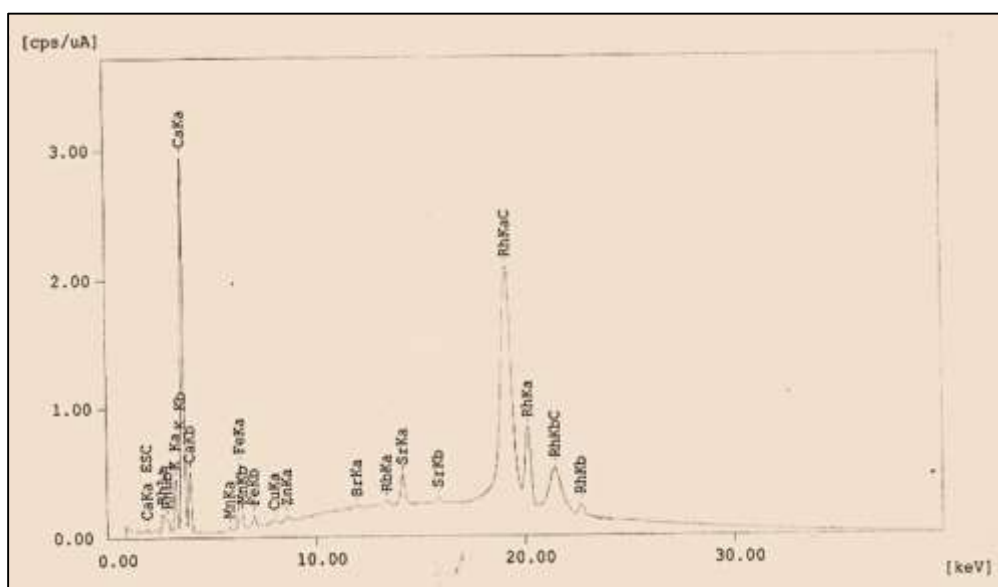


**Figure 2** EDXRF spectrum of leaf of *B. purpurea*

**Table 1** Some Elements Present in Leaf of *B. purpurea* (EDXRF)

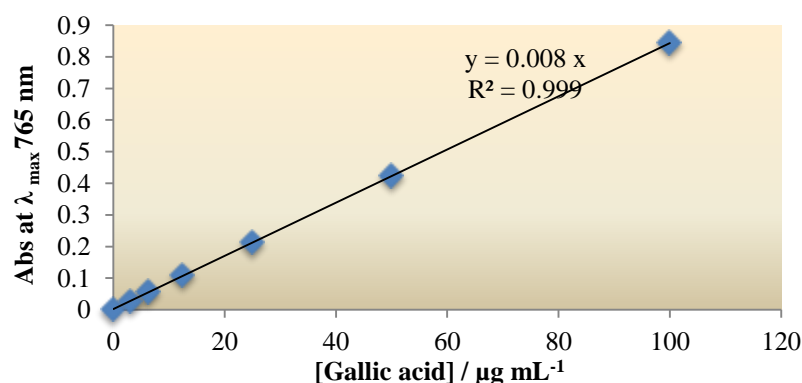
No.	Elements	Relative Abundance (%)
1	Ca	0.818
2	K	0.104
3	Fe	0.059
4	Sr	0.007
5	Mn	0.004
6	Zn	0.003
7	Cu	0.002
8	Rb	0.001
9	Br	0.001

### Soluble Matter Contents of Leaf of *B. purpurea*

In this research work, the soluble matter contents of leaf of *B. purpurea* were determined by solvent extraction method. Ethanol and watery crude extracts were prepared and the yield percent of crude extract was derived from the weight of dried and ground plant material. According to the results, it was observed that the yield of ethanol extract (15.93 %) was higher than that of watery extract (12.58 %). It can be concluded that the amount of active constituents contained in ethanol extract was higher than watery extract.

### Total Phenolic Content of Leaf of *B. purpurea*

Phenolic compounds are very important plant constituents because of their scavenging ability due to their hydroxyl groups. They may contribute directly to antioxidative action. The total phenolic contents in ethanol and watery extracts of leaf of *B. purpurea* were determined by using Folin-Ciocalteu colourimetric method. Gallic acid was used as a standard compound. The absorbance values obtained at different concentrations of gallic acid were used for the construction of calibration curve as described in Figure 3. The total phenolic content of crude extracts of *B. purpurea* leaf is shown in Table 2. This method is based on the transfer of electrons in alkaline medium from phenolic compounds to phosphomolybdenic / phosphotungstic acid complexes to form blue coloured complexes that are determined spectrophotometrically at 765 nm. Total phenolic content of each crude extract was calculated from the regression equation of calibration curve ( $y = 0.008 x$ ,  $R^2 = 0.999$ ) and expressed as microgram gallic acid equivalent per milligram of crude extract ( $\mu\text{g GAE}/\text{mg}$  of extract). In this study, ethanol extract (32.58  $\mu\text{g GAE}/\text{mg}$  of extract) showed higher total phenolic content than watery extract (21.73  $\mu\text{g GAE}/\text{mg}$  of extract). This means that ethanol extract of *B. purpurea* leaf is a source phenolic compound which may be a good source of antioxidant for the food system.

**Figure 3** Standard calibration curve of gallic acid

**Table 2 Total Phenolic Content of Crude Extracts of *B. purpurea* Leaf**

Extracts	Total Phenolic Content ( $\mu\text{g GAE/mg of extract}$ )
ethanol	32.58
watery	21.73

**Antioxidant Activity of Leaf of *B. purpurea***

The effect of antioxidants on DPPH radical scavenging is thought to be due to their hydrogen or electron donating abilities. DPPH is a stable free radical. In its radical form, DPPH has been disappeared on reduction by an antioxidant compound or a radical species to become a stable diamagnetic molecule resulting the colour changes from violet to yellow, which could be taken as an indication of the hydrogen donating ability of the tested sample.

The antioxidant activity of ethanol and watery extracts of leaf of *B. purpurea* was investigated by DPPH assay. In this study, six different concentrations (50, 25, 12.5, 6.25, 3.125 and 1.5625  $\mu\text{g/mL}$ ) of each crude extract were prepared by serial dilution method. Ascorbic acid was used as standard to be compared with the sample and ethanol without sample was employed as control. After mixing with the DPPH solution, the absorbance of each solution was measured at 517 nm using UV-visible spectrophotometer. On the basis of absorbance values, % inhibition of each sample in different concentrations was calculated and  $\text{IC}_{50}$  value was determined by linear regressive excel program. The results of % inhibition and  $\text{IC}_{50}$  values were shown in Table 3.  $\text{IC}_{50}$  value of standard ascorbic acid was 1.97  $\mu\text{g/mL}$ . According to the results, it was observed that ethanol extract ( $\text{IC}_{50} = 5.75 \mu\text{g/mL}$ ) of leaf of *B. purpurea* contained higher antioxidant activity than watery extract ( $\text{IC}_{50} = 8.51 \mu\text{g/mL}$ ), due to the lower value of  $\text{IC}_{50}$ . The ethanol extract contains a high quantity of bioactive compounds able to capture free radicals like DPPH. From these findings, it can be concluded that total phenolic content was correlated with radical scavenging activity. The ethanol extract containing the higher total phenolic content showed significant free radical scavenging activity in this study. Therefore, *B. purpurea* leaf could be employed as an additive in the food industry providing good production against oxidative damage.

**Table 3 Percent Inhibition and  $\text{IC}_{50}$  Values of Crude Extracts of *B. purpurea* Leaf and Standard Ascorbic acid**

Sample	% inhibition in various concentrations ( $\mu\text{g/mL}$ )						$\text{IC}_{50}$ ( $\mu\text{g/mL}$ )
	1.5625	3.125	6.25	12.5	25	50	
ethanol extract	23.76	32.18	53.42	71.56	89.34	92.42	5.75
watery extract	19.02	24.87	40.93	65.98	82.76	87.43	8.51
ascorbic acid	44.56	65.32	74.42	85.96	93.21	97.12	1.97

**Antimicrobial Activity of Leaf of *B. purpurea***

The antimicrobial activity of ethanol and watery extracts of *B. purpurea* leaf was investigated by agar well diffusion method on *B. subtilis*, *S. aureus*, *P. aeruginosa*, *B. pumilus*, *C. albicans* and *E. coli* as shown in Figure 4. The zone of inhibition was taken as a measure of antimicrobial activity. The larger the inhibition zone diameter, the higher the antimicrobial activity. All tested microorganisms in this study were found to be sensitive to both of the ethanol and watery

extracts of *B. purpurea* leaf. *B. subtilis* showed the highest susceptibility to both extracts with the clear zone of inhibition ranging from 18-20 mm while the rest tested microorganisms were sensitive in the inhibition zone ranging from 14-18 mm as shown in Table 4. The results indicated that the leaf of *B. purpurea* has antimicrobial activity and may be applied in local therapies in the treatment of diseases caused by the microorganisms tested.

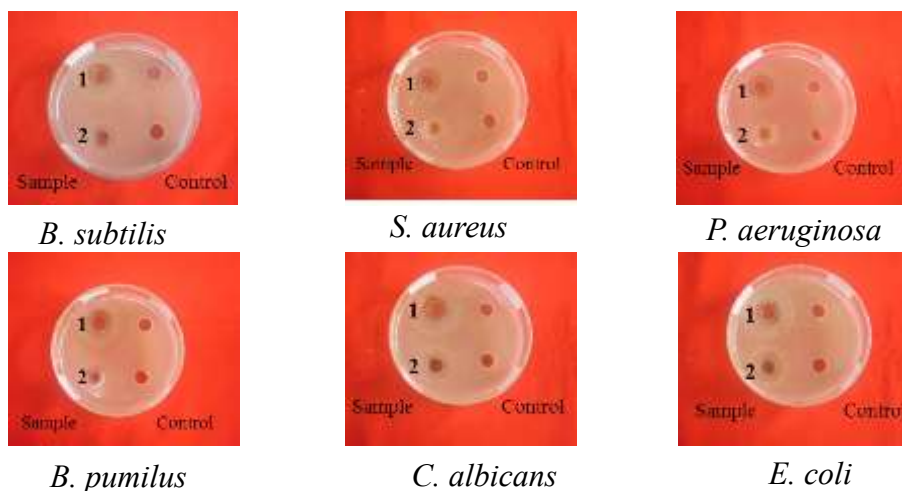


**Figure 4** Antimicrobial activity of crude extracts of *B. purpurea* leaf on six microorganisms  
 (1) = ethanol extract  
 (2) = watery extract

**Table 4** Inhibition Zone Diameters of Crude Extracts of *B. purpurea* Leaf

Extracts	Microorganisms					
	<i>B. subtilis</i>	<i>S. aureus</i>	<i>P. aeruginosa</i>	<i>B. pumilus</i>	<i>C. albicans</i>	<i>E. coli</i>
ethanol	20 mm (+++)	18 mm (++)	18 mm (++)	18 mm (++)	18 mm (++)	17 mm (++)
watery	18 mm (++)	16 mm (++)	17 mm (++)	14 mm (+)	16 mm (++)	15 mm (++)

Agar well diameter 10 mm-14 mm (+)  
 15 mm-19 mm (++)  
 20 mm above (+++)

**Acute Toxicity Study of Leaf of *B. purpurea***

The acute toxicity study of ethanol extract was done according to the OECD 423 guide line. In this study, no toxic sign and lethality were found during the observation period of 14 days with the dose of 300 mg/kg, 2000 mg/kg and also at the maximum dose of 5000 mg/kg. Therefore, the LD<sub>50</sub> value was expected to be more than 5000 mg/kg and ethanol extract leaf of *B. purpurea* is assumed to be safe. The results of acute toxicity activity of ethanol extract of leaf *B. purpurea* were shown in Table 5.

**Table 5 Acute Toxicity Activity of Ethanol Extract of *B. purpurea* Leaf**

Extract	Dose (mg/kg)	Number of mice tested	Observed period (days)	Death/tested
Ethanol	300	6	14	0/6
	2000	6	14	0/6
	5000	6	14	0/6

### Conclusion

This study showed that there is a relationship between, the total phenolic content of ethanol and watery extracts of leaf of *B. purpurea* with antioxidant activity indicating that *B. purpurea* leaf has potent antioxidant, antimicrobial and no acute toxicity activities and provides scientific evidence for its use in traditional medicine. Though the chemical nature were not identified yet, however, the leaf of *B. purpurea* may be used for the treatment of diseases caused by oxidative stress and infected by the microorganisms.

### Acknowledgements

The author would like to express sincere gratitude to Dr Kyaw Kyaw Khaung (Rector) and Dr Min Min Yee (Pro-rector), East Yangon University, for their permission to present this research paper. Special thanks are extended to Dr Tin May San (Professor and Head) and Dr Myo Myo Myat (professor), Department of Chemistry, East Yangon University, for their valuable suggestions and allowing to submit this research paper. Finally, I am deeply grateful to all my colleagues from Department of Chemistry, East Yangon University.

### References

- Avinash, P., Attitalia, I. H., Ramgopal, M. and Balaji, M. (2011). "In vitro Antimicrobial and Antioxidant Activities of Bark Extracts of *Bauhinia purpurea* Linn". *African Journal of Biotechnology*, vol. 10(45), pp. 9160-9164
- Gupta, D. C., Richard, L. and Gupta, N. (2012). "In vitro Antidiabetic Activity of Stem Bark of *Bauhinia purpurea* Linn". *Scholars Research Library Der Pharmacia Lettre*, vol. 4(2), pp. 614-619
- Harborne, J. B. (1984). *Phytochemical Methods; A Guide to Modern Techniques of Plant Analysis*. New York: 2<sup>nd</sup> Ed., Chapman and Hall Ltd., p. 154
- Jain, A., Soni, M. and Krishna, K. (2008). "Antioxidant and Hepatoprotective Activity of Ethanolic and Aqueous Extracts of *Momordica dioca* Roxb. Leaves". *J. of Ethnopharmacol*, vol. 115(1), pp. 61-66
- Kim, D. O., Jeong, S. W. and Lee, C. Y. (2003). "Antioxidant Capacity of Phenolic Phytochemicals from Various Cultivars of Plums". *Food Chemistry*, vol. 81, pp. 321-326
- Kumar, P. S., Sucheta, S. and Latha, S. (2008). "Antioxidant Activity in the some Selected Indian Medicinal Plants". *African Journal of Biotechnology*, vol. 7, pp. 1826-1828
- Kumar, T. and Chandrashekar, K. S.. (2011). "*Bauhinia purpurea* Linn.: A Review of its Enthobotany, Phytochemical and Pharmacological Profile". *Research Journal of Med. Plant*, vol. 5(4), pp. 420-431
- OECD 423 (2001). "Guideline for Testing of Chemical: Acute Oral Toxicity". *Acute Toxic Class Method 423*, pp.1-14
- Patil, G. G., Mali, P. Y. and Bhadane, V. V. (2008). "Folk Remedies Used against Respiratory Disorders in Jalgaon District, Maharaashtra". *Nat. Prod. Radiance*, vol. 7, pp. 354-358
- Robinson, T. (1983). *The Organic Constituents of Higher Plants*. North America: 5<sup>th</sup> Ed., Cordus Press, pp. 63-68
- Shajiselvin, C. D., Muthu, A. and Kottai, A. (2011). "Antioxidant Activity of Various Extracts from Whole Plants of *Bauhinia purpurea* Linn". *Journal of Advanced Pharmaceutical Research*, vol. 2(1), pp. 31-37

## INVESTIGATION OF ESSENTIAL OIL FROM THE LEAF AND ANTIOXIDANT ACTIVITY OF PLANT *APIUM GRAVEOLENS* L. (TAYOKE NAN-NAN)

Soe Soe Tint<sup>1,2</sup>, Saw Hla Myint<sup>3</sup>, Ni Ni Than<sup>4</sup>

### Abstract

Tayoke Nan-nan is known to be rich in essential oil and phenolic compounds. GC-MS analysis of the essential oil steam distilled from the dry leaf (yield 0.02 %) of *Apium graveolens* L. indicates nine compounds, mostly mono and sesquiterpenes, phthalide derivatives, and a few other compounds. Similar analysis of the essential oil from the fresh leaf (yield 0.07 %) showed fourteen compounds, mostly mono and sesquiterpenes, the phthalide derivatives and a few other compounds. Phthalides are the most abundant constituents in both essential oils. In the determination of antioxidant activity by ferric reducing antioxidant power (FRAP) method, EC<sub>50</sub> values of the ethanolic extracts of the leaf, stalk and root were 2186, 984 and 2316 µg/mL against 112 µg/mL of ascorbic acid standard. The presence of phthalides and phenolic compounds in the plant, Tayoke nan-nan may be useful as a medicinal drug in certain minor diseases.

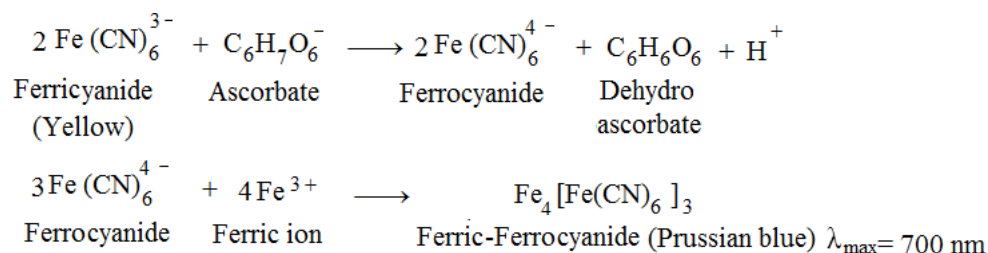
**Keywords:** *Apium graveolens* L., leaf, essential oil, phthalide derivatives, FRAP method

### Introduction

All parts of celery (*Apium graveolens* L.) plant yield high proportion of essential oil. This is pale yellow and very fluid, with a strong celery aroma consisted of phthalide derivatives (lactone sedanolide), palmitic acid, hydrocarbons such as limonene (Rožek *et al.*, 2016 and Sellami, *et al.*, 2012). Traditional processes for extracting essential oils, hydrodistillation and steam distillation, are relatively simple (Sahraoui and Boutekedjiret, 2015 and Božović *et al.*, 2017). The chemical composition of the oil was investigated by GC-MS that combines the separation power of gas-liquid chromatography with the detection feature of mass spectrometry to identify different substances within a test sample (Chauhan *et al.*, 2014).

The major bioactive compounds in the celery include phenolic compounds, flavonoids and phenols are the most important groups of secondary metabolites and bioactive compounds in plants such as *Apium* plants are good sources of natural antioxidants in human diets (Saxena *et al.*, 2012). Spectrophotometric SET-based assays measure the capacity of an antioxidant in the reduction of an oxidant, which changes colour when reduced. Like the antioxidant activity, the reducing power of celery, ethanol extract increases with increasing concentration. In ferric reducing antioxidant power (FRAP) assay, there is an increase in absorbance at a prespecified wavelength as the antioxidant reacts with the chromogenic reagent (Moharram and Youssef, 2014).

The reactions in the FRAP method (Canabady-Rochelle *et al.*, 2015) as follow:



<sup>1</sup> Lecturer, Department of Chemistry, Dagon University

<sup>2</sup> PhD Student, Department of Chemistry, University of Yangon

<sup>3</sup> Dr, Professor and Head, (Part Time Professor), Department of Chemistry, University of Yangon

<sup>4</sup> Dr, Professor and Head, Department of Chemistry, University of Yangon

The aim of the present research is to investigate the constituents of essential oils from the dry and fresh leaves of celery and to determine the antioxidant activity by FRAP method of different parts of celery (*A. graveolens*) plant.

## Materials and Methods

### Plant Material

The plant material (*A. graveolens*, Tayoke Nan-nan) used for this study was collected from Kalaw, Shan state, Myanmar. The leaf samples were dried. Fresh and dry leaf samples were used to extract the essential oil. For the antioxidant activity by FRAP method, dry leaf, stalk and root samples were used.

### Experimental Setup

Steam distillation method was used to extract essential oil (Sahraoui and Boutekedjiret, 2015). The schematic diagram of experimental setup is shown in Figure 1. The experiment was conducted in a Clevenger's Apparatus.



1. Boiling flask
2. Biomass flask
3. Connecting distillation adapter
4. Glass stopper
5. Condenser
6. Oil separator apparatus
7. Heating mantle
8. Lab support stand
9. Finger clamp

### Experimental Procedure

Dry leaf sample 25 g or fresh leaf sample 100-150 g were filled in the biomass flask and extracted with steam generated from 350 mL water in the boiling flask until oil distillation ceased after 5-6 h. The essential oil in the distillate was separated by partitioning with *n*-hexane, the extract dried over anhydrous Na<sub>2</sub>SO<sub>4</sub> and filtered and kept in the freezer after evaporation of the solvent.

**Figure 1** Essential oil steam distillation kit

### Yield of Essential Oils

The yield of essential oil of celery leaf was expressed in gram relative to 100 g of raw sample; it was calculated according to following equation:

$$\text{Yield (\%)} = \frac{\text{Amount of extracted oil (g)}}{\text{Amount of raw sample (g)}} \times 100$$

### Determination of Composition of Essential Oil by GC-MS

The chemical composition of essential oil was determined by GC-MS analysis on a PerkinElmer system consisting of a Clarus 680 GC model and a Clarus 600 MS model at National Analytical Laboratory, Department of Research and Innovation, Yangon, Myanmar. An Elite5 MS GC column with 5 % diphenyl 95 % dimethyl polysiloxane stationary phase and dimension 30 m (L), 0.25 mm (ID) and 0.25 μm (thickness) was used. The GC settings were as follows: the source temperature was 190 °C and the inlet temperature was 209 °C.



**Figure 2** GC-MS instrument

The initial oven temperature was held at 80 °C for 3 min and then heated from 100 to 140 °C at a rate of 2 °C /min, held for 1 min, and then heated to 240 °C at 10 °C /min and held for 3 min. The injector temperature was maintained at 250 °C. The sample in hexane (1 µL) was injected, with a split ratio of 1: 20. The carrier gas was helium at flow rate of 1.0 mL/min.

### **Determination of the Functional Groups Present Using FT IR**

The FT IR spectrum of the essential oil was measured at National Analytical Laboratory, Department of Research and Innovation, Yangon, Myanmar. The FT IR spectra were reported in % transmittance. The wavenumber region for the analysis was 4000-400 cm<sup>-1</sup> (in the mid-infrared range).

### **Determination of Antioxidant Activity by FRAP Method**

The 95 % ethanol extracts of dry leaf, stalk and root were used for ferric reducing antioxidant power content (Bhalodia *et al.*, 2013).

#### **Preparation of plant extract**

The leaf, stalk and root samples (5 g) of celery (*A. graveolens*) were extracted with 95 % ethanol (100 mL).

#### **Preparation of standard solutions**

Ascorbic acid (0.01 g) was dissolved in 10 mL distilled water (1000 µg/mL). This solution was serially diluted with distilled water to give solutions of 5, 10, 25, 50, 75 and 100 µg/mL serially concentrations.

#### **Preparation of test sample solutions**

Preparation of test sample stock solutions of samples were prepared by dissolving 0.02 g of each extract in 1 mL of ethanol and diluted with distilled water to make 20 mL solution (2000 µg/mL). Then sample concentrations of 125, 250, 500, 1000 and 2000 µg/mL were prepared.

#### **Protocol for reducing power**

According to this method, 1.0 mL aliquots of each solution in deionized water various concentrations of the standard (5 to 100 µg/mL) and test sample extracts (125 to 2000 µg/mL) were separately mixed with 2.5 mL of phosphate buffer (pH 6.6) and 2.5 mL of (1 %) potassium ferricyanide. The mixture was incubated at 50 °C in water bath for 20 min after cooling. Trichloroacetic acid (10 %) solution 2.5 mL was added to each mixture, which was then centrifuged at 3000 rpm for 10 min. The upper layer of solution 2.5 mL each was mixed with 2.5 mL distilled water and a freshly prepared 0.5 mL of (0.1 %) ferric chloride solution. Increase in absorbance of the reaction mixture indicates increase in reducing power. All experiments were repeated three times.

## Results and Discussion

### Yield of Essential Oils from Celery Dry and Fresh leaf

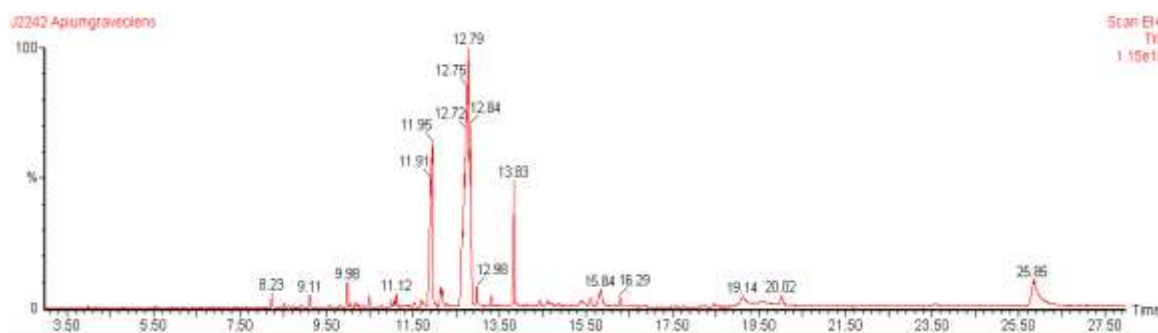
The essential oils of dry and fresh leaf of celery (*A. graveolens*) were extracted by steam distillation method. The amount of essential oils obtained were 0.02 % from dry leaf and 0.07 % from fresh sample. Both samples of essential oils have light yellow colour and pleasant aromas. Because of its high volatility, it was stored in an air tight container protected from light in cool place. The essential oil was insoluble in water but miscible in alcohol.

### Composition of Essential Oil by GC- MS Analysis

In GC-MS analysis, the obtained essential oil was dissolved in *n*-hexane. Nine volatile compounds in dry leaf and fourteen compounds in fresh leaf essential oils observed are shown in Tables 1 and 2. A high proportion of the essential oils consisted butyl phthalide derivatives (butylphthalide, senkyunolide and sedanolide) and D-limonene and carveol were also contained in the oils of both samples (Figures 3 and 4). Molecular structures of essential oil compounds in dry and fresh leaf are shown in Figure 5. GC-MS analysis of d-limonene and carveol, butylphthalide, senkyunolide and sedanolide of the both essential oils is expressed in Figure 6.

**Table 1** Chemical Composition of Essential Oil from Dry leaf sample

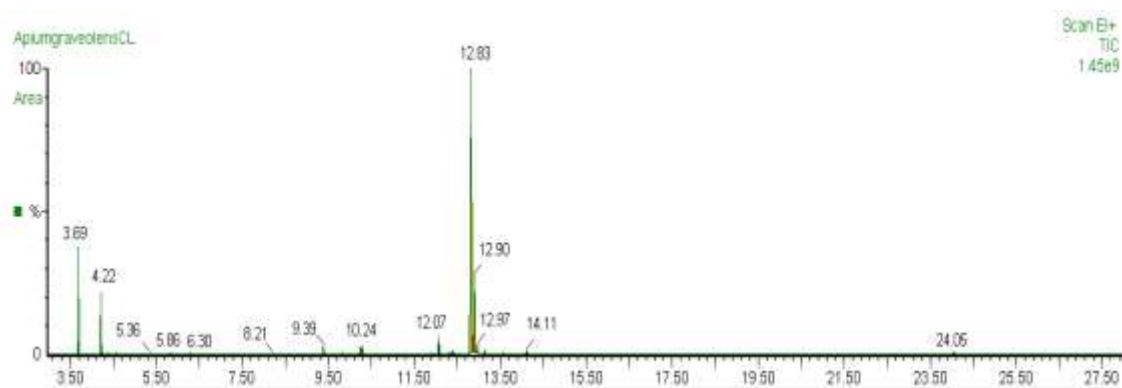
Sr. No.	Compound Name		Molecular Formula	Molecular weight	Retention time (min)
1	D- limonene	( <u>2</u> )	C <sub>10</sub> H <sub>16</sub>	136	3.970
2	Carveol	( <u>6</u> )	C <sub>10</sub> H <sub>16</sub> O	152	5.535
3	1-Pentanone 1- phenyl	( <u>7</u> )	C <sub>11</sub> H <sub>14</sub> O	162	8.231
4	Alloaromadendrene	( <u>9</u> )	C <sub>15</sub> H <sub>24</sub>	204	9.980
5	Butylphthalide	( <u>13</u> )	C <sub>12</sub> H <sub>14</sub> O <sub>2</sub>	190	11.951
6	Senkyunolide	( <u>14</u> )	C <sub>12</sub> H <sub>16</sub> O <sub>2</sub>	192	12.791
7	Sedanolide	( <u>15</u> )	C <sub>12</sub> H <sub>18</sub> O <sub>2</sub>	194	12.837
8	Palmitic acid	( <u>16</u> )	C <sub>16</sub> H <sub>32</sub> O <sub>2</sub>	256	15.840
9	6-Octa decenoic acid	( <u>17</u> )	C <sub>18</sub> H <sub>34</sub> O <sub>2</sub>	282	20.021



**Figure 3** Total ion chromatogram (TIC) of essential oil from dry leaf of *A. graveolens* at retention times 3 -28 min

**Table 2** Chemical Composition of Essential Oil from Fresh Leaf Sample

Sr. No.	Compound Name		Molecular Formula	Molecular weight	Retention time (min)
1	$\alpha$ - Pinene	( <u>1</u> )	C <sub>10</sub> H <sub>16</sub>	136	3.690
2	D- limonene	( <u>2</u> )	C <sub>10</sub> H <sub>16</sub>	136	4.219
3	$\beta$ - Ocimene	( <u>3</u> )	C <sub>10</sub> H <sub>16</sub>	136	4.353
4	3- Carene	( <u>4</u> )	C <sub>10</sub> H <sub>16</sub>	136	4.557
5	Naphthalene	( <u>5</u> )	C <sub>10</sub> H <sub>8</sub>	128	6.298
6	Carveol	( <u>6</u> )	C <sub>10</sub> H <sub>16</sub> O	152	8.208
7	Caryophyllene	( <u>8</u> )	C <sub>15</sub> H <sub>24</sub>	204	9.389
8	Humulene	( <u>10</u> )	C <sub>15</sub> H <sub>24</sub>	204	9.830
9	Naphthalene, decahydro-4A- methyl- 1-methylene - 7(1-methylethe)	( <u>11</u> )	C <sub>15</sub> H <sub>24</sub>	204	10.245
10	Butylated Hydroxytoluene	( <u>12</u> )	C <sub>15</sub> H <sub>24</sub> O	220	10.298
11	Butylphthalide	( <u>13</u> )	C <sub>12</sub> H <sub>14</sub> O <sub>2</sub>	190	12.074
12	Senkyunolide	( <u>14</u> )	C <sub>12</sub> H <sub>16</sub> O <sub>2</sub>	192	12.830
13	Sedanolid	( <u>15</u> )	C <sub>12</sub> H <sub>18</sub> O <sub>2</sub>	194	12.899
14	Phenol, 2, 2'- methylenebis [6-(1, 1- dimethylethyl)-4- methyl)	( <u>18</u> )	C <sub>23</sub> H <sub>32</sub> O <sub>2</sub>	340	24.048

**Figure 4** Total ion chromatogram (TIC) of essential oil from fresh leaf of *A. graveolens* at retention times 3 -28 min

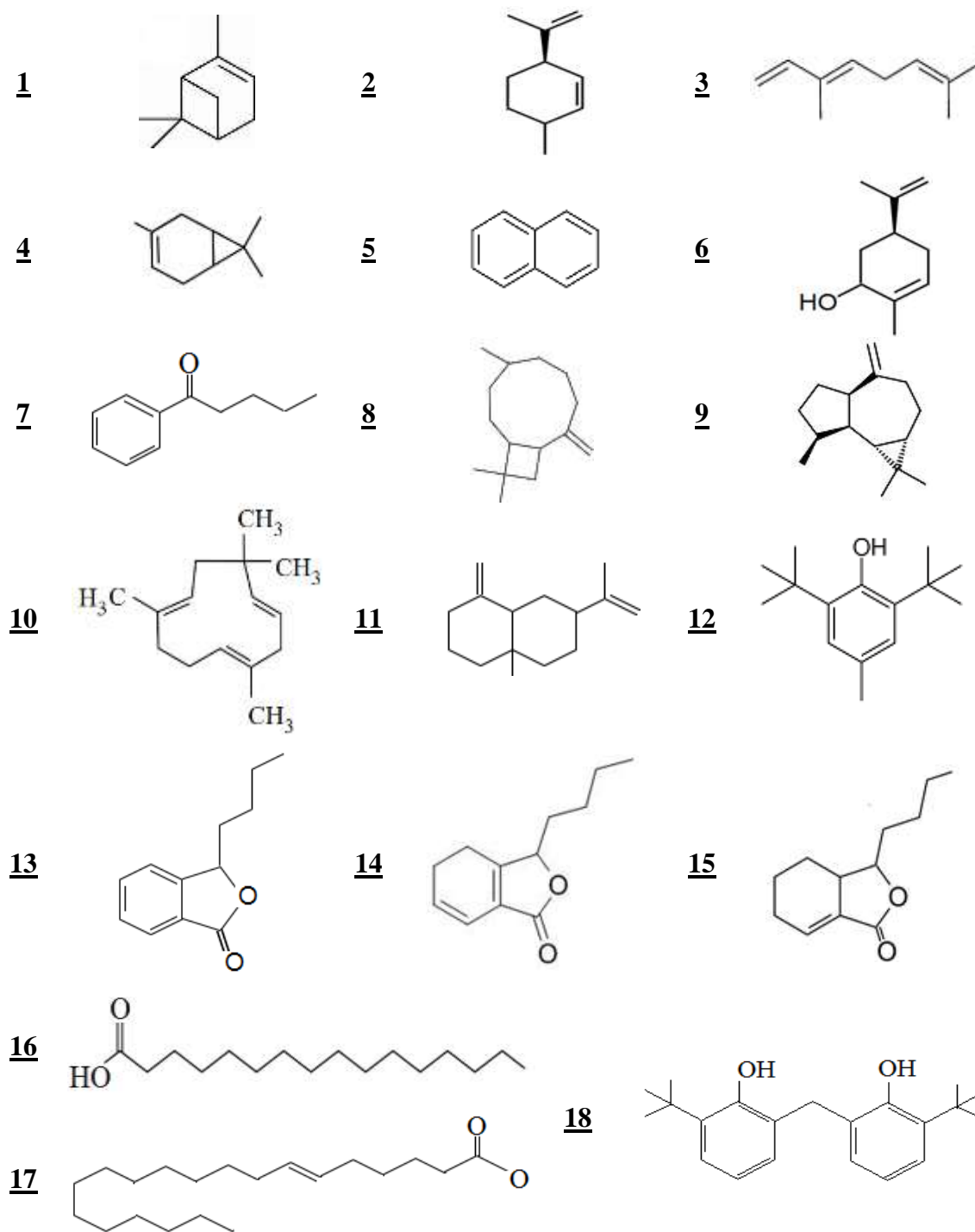


**Figure 5** Molecular structures of essential oil compounds from dry and fresh leaves

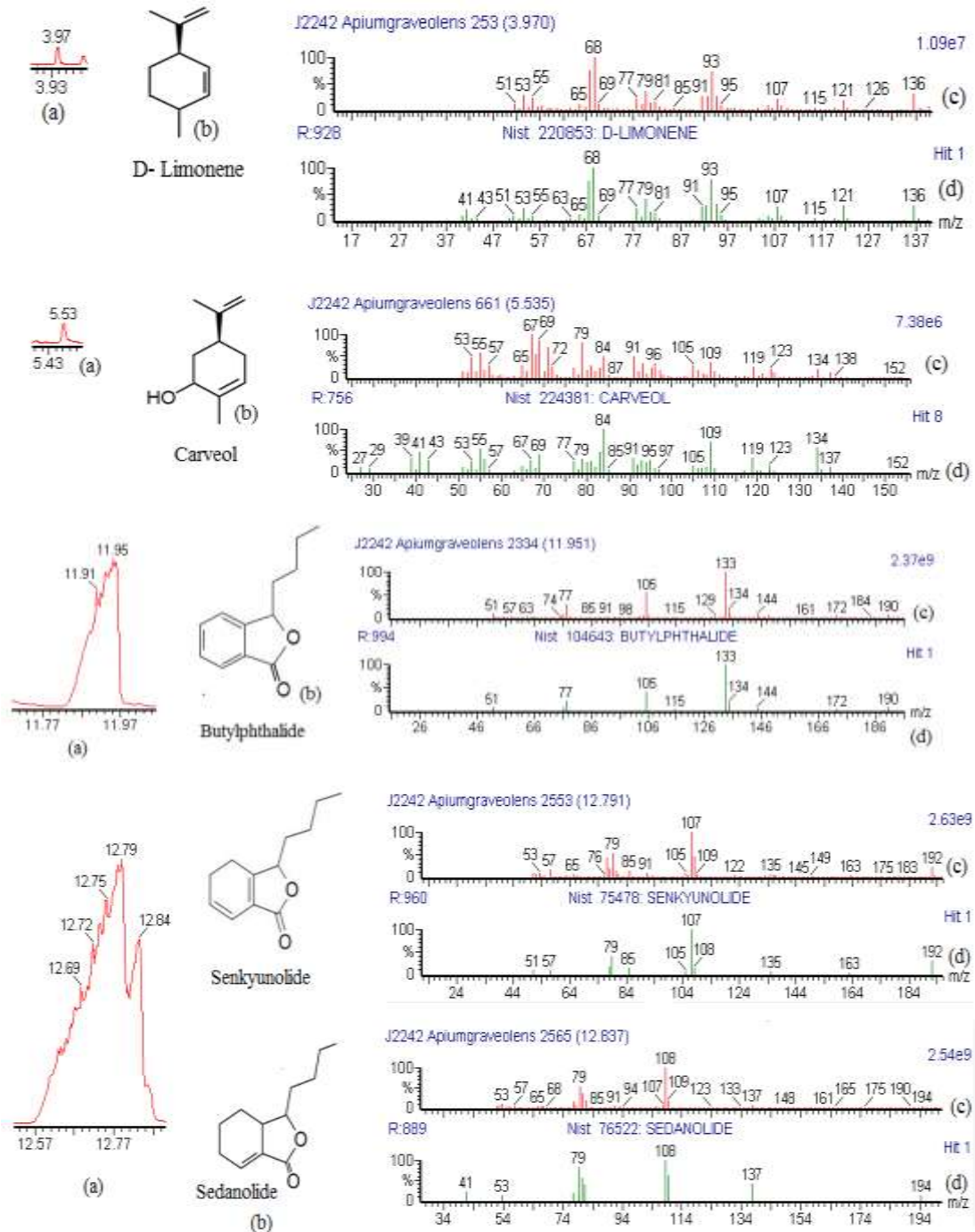


**Figure 6** GC-MS analysis of d-limonene, carveol, butylphthalide, senkyunolide and sedanolide present in the essential oil (a) TIC (b) molecular structures (c) mass spectra (recorded) (d) mass spectra (library)

### Functional groups present in the essential oil using FT IR

The functional groups present in the essential oil were determined from the wavenumbers of the sample in FT IR the spectrum (Figure 7). The FT IR absorption spectrum of essential oil obtained from dry leaf celery (*A. graveolens*) was measured in the wavelength range 4000- 400  $\text{cm}^{-1}$ .

The vibrational band given by C=O bond of ester or five members ring lactone occurs at  $1751\text{ cm}^{-1}$ , and the C–O stretching of ester, alcohol, ether leads to bands at  $1284\text{ cm}^{-1}$ ,  $1225\text{ cm}^{-1}$ ,  $1184\text{ cm}^{-1}$ ,  $1043\text{ cm}^{-1}$  (Figure 7 and Table 3).

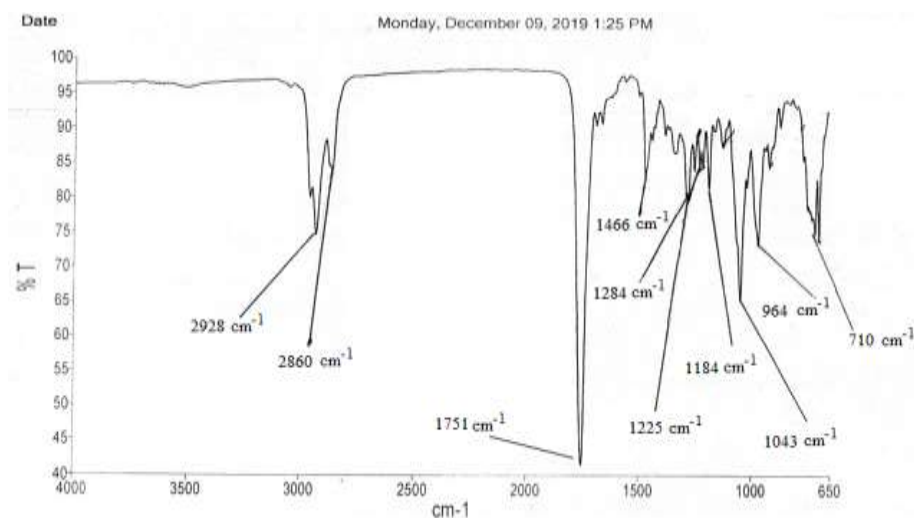


**Figure 7** FT IR spectrum of dry leaf essential oil from *A. graveolens*

**Table 3** FT IR Spectral Data of Essential Oil from Dry *A. graveolens* Leaf

Wavenumber ( $\text{cm}^{-1}$ )	Vibrational mode	Functional group
3080	= C-H stretching	Olefin, aromatic compound
2928, 2860	C-H stretching	- $\text{CH}_3 > \text{CH}_2 > \text{CH}$ -
1751	C= O stretching	Ester, 5 members ring lactone
1466	C-H bending	- $\text{CH}_3 > \text{CH}_2 > \text{CH}$ -
1284, 1225, 1184, 1043	C - O stretching	Ester, alcohol, ether
964	= C-H out of plane bending	Trans olefin
710	= C-H out of plane bending	Cis olefin

(silverstein *et al.*, 1991)

#### Activity (Reducing Power Assay)

Celery is valued for the distinctive aroma which it owes to the presence of phthalide- rich essential oil. Moreover, it is known for its antioxidant properties due to the compounds such as phenolic and flavonoid compounds as determined in the previous work (Table 4) (Soe Soe Tint *et al.*, 2020).

Reducing power assay method is based on the principle that substances, which have reduction potential, react with potassium ferricyanide ( $\text{Fe}^{3+}$ ) to form potassium ferrocyanide ( $\text{Fe}^{2+}$ ), which then reacts with ferric chloride to form ferric-ferrous complex that has an absorption maximum at 700 nm. The reducing power of the 95 % ethanol extracts and standard increases with the increase in amount of sample and standard concentrations (Tables 5, 6, 7 and 8). The plot of reducing power shows good linearity in standard ( $R^2 = 0.9181$ ) and all sample extracts (leaf, stalk and root) are  $R^2 = 0.983$ ,  $0.9553$  and  $0.9891$  respectively for leaf, stalk and root (Figures 12, 13, 14 and 15).  $\text{EC}_{50}$  values of the ethanolic extracts of leaf, stalk and root were 2186, 984 and 2316  $\mu\text{g/mL}$  against 112  $\mu\text{g/mL}$  of ascorbic acid standard (Table 9 and Figure 16).

**Table 4** Flavonoid Content, Phenolic Content and Antioxidant Activity of Celery

	Flavonoid content (mg QE/g dry or fresh weight)	Phenolic content (mg GAE/g dry or fresh weight)	Antioxidant activity of ethanol extract IC <sub>50</sub> value (µg/mL)
Dry leaf	263.453	290.119	99.646
Fresh leaf	29.757	32.769	
Dry stalk	28.743	51.338	45.219
Fresh stalk	3.425	6.117	
Dry root	37.886	53.987	125.342
Fresh root	4.018	5.726	

(Soe Soe Tint *et al.*, 2020)

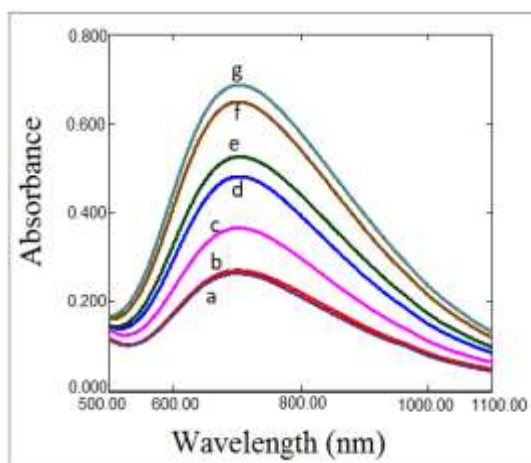


**Table 5** Variation of Absorbance with Concentrations of Standard Ascorbic Acid at 700 nm

Conc. (µg/mL)	Abs	Net Abs	EC <sub>50</sub> (µg/mL)
0, (Blank)	0.264		112
5	0.271	0.007	
10	0.366	0.102	
25	0.481	0.217	
50	0.525	0.261	
75	0.648	0.384	
100	0.686	0.422	

**Figure 8** Zero-order overlaid spectra of ferric-ferrocyanide for (a) blank solution (b) 5 µg/mL (c) 10 µg/mL (d) 25 µg/mL (e) 50 µg/mL (f) 75 µg/mL (g) 100 µg/mL standard ascorbic acid solutions

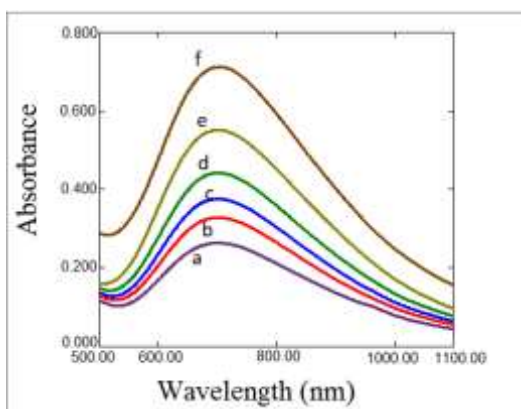


**Table 6** Variation of Absorbance with Concentrations of Leaf Extract Solution at 700 nm

Conc. (µg/mL)	Abs	Net Abs	EC <sub>50</sub> (µg/mL)
0, (Blank)	0.264		2186
125	0.328	0.064	
250	0.375	0.111	
500	0.442	0.178	
1000	0.551	0.287	
2000	0.712	0.448	

**Figure 9** Zero-order overlaid spectra of ferric-ferrocyanide for (a) blank solution (b) 125 µg/mL (c) 250 µg/mL (d) 500 µg/mL (e) 1000 µg/mL (f) 2000 µg/mL celery leaf ethanol extract solutions

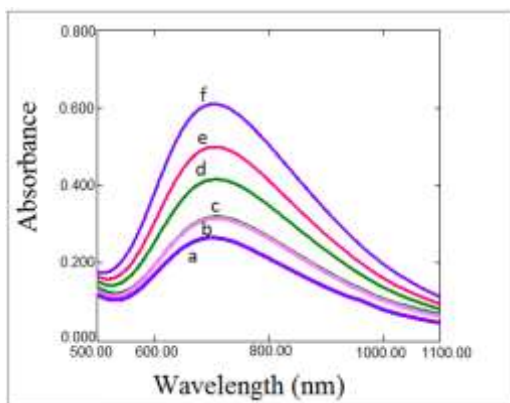
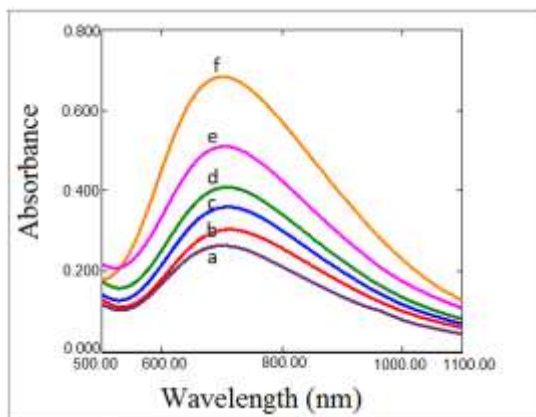


**Table 7** Variation of Absorbance with Concentrations of Stalk Extract Solution at 700 nm

Conc. (µg/mL)	Abs	Net Abs	EC <sub>50</sub> (µg/mL)
0, (Blank)	0.264		984
125	0.313	0.049	
250	0.316	0.052	
500	0.408	0.144	
1000	0.498	0.234	
2000	0.609	0.345	

**Figure 10** Zero-order overlaid spectra of ferric-ferrocyanide for (a) blank solution (b) 125 µg/mL (c) 250 µg/mL (d) 500 µg/mL (e) 1000 µg/mL (f) 2000 µg/mL celery stalk ethanol extract solutions

**Table 8** Variation of Absorbance with Concentrations of Root Extract Solution at 700 nm



Conc. (µg/mL)	Abs	Net Abs	EC <sub>50</sub> (µg/mL)
0, (Blank)	0.264		2316
125	0.302	0.038	
250	0.359	0.095	
500	0.408	0.144	
1000	0.51	0.246	
2000	0.683	0.419	

**Figure 11** Zero-order overlaid spectra of ferric-ferrocyanide for (a) blank solution (b) 125 µg/mL (c) 250 µg/mL (d) 500 µg/mL (e) 1000 µg/mL (f) 2000 µg/mL celery root ethanol extract solutions

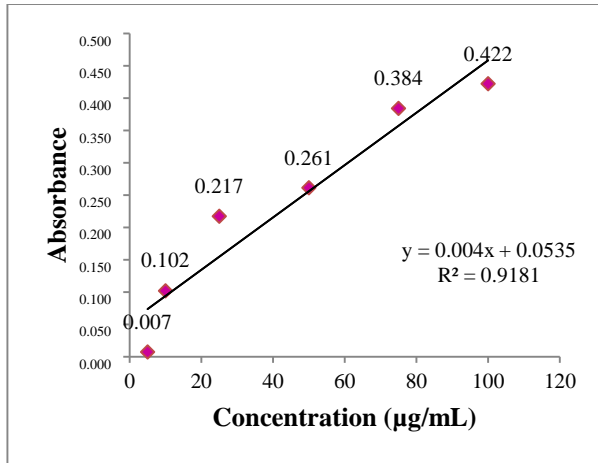


**Figure 12** Ferric reducing power determination of standard ascorbic acid

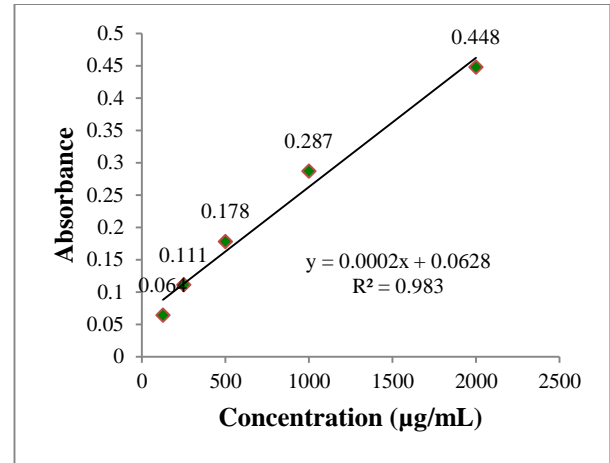


**Figure 13** Ferric reducing power determination of celery leaf extract solutions

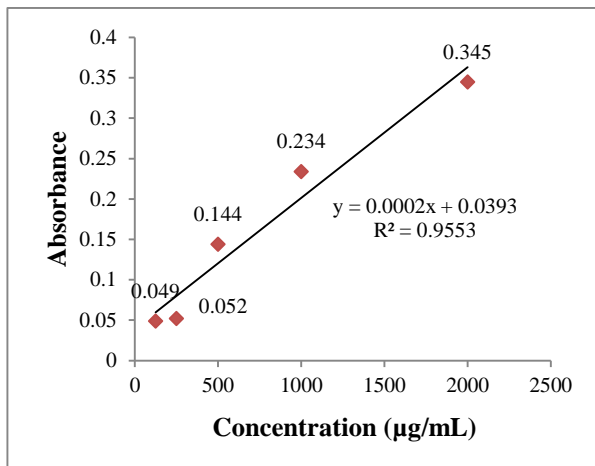


**Figure 14** Ferric reducing power determination of celery stalk extract solutions

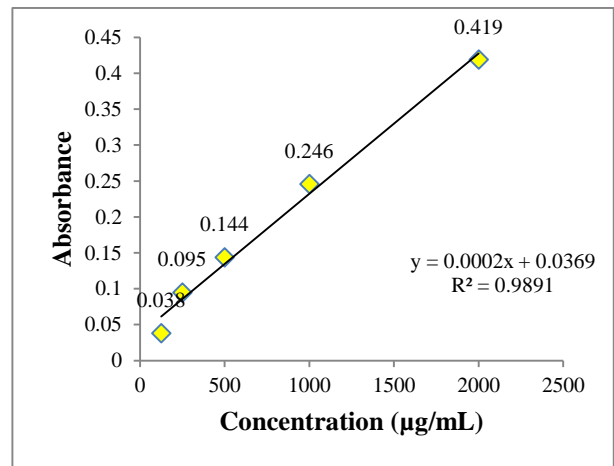


**Figure 15** Ferric reducing power determination of celery root extract solutions

**Table 9** EC<sub>50</sub> Values of Ferric Reducing Power for Ascorbic acid and Ethanol Extract of Celery Leaf, Stalk and Root

EC <sub>50</sub> (µg/ mL)			
Ascorbic Acid	Celery Leaf	Celery Stalk	Celery Root
112	2186	984	2316

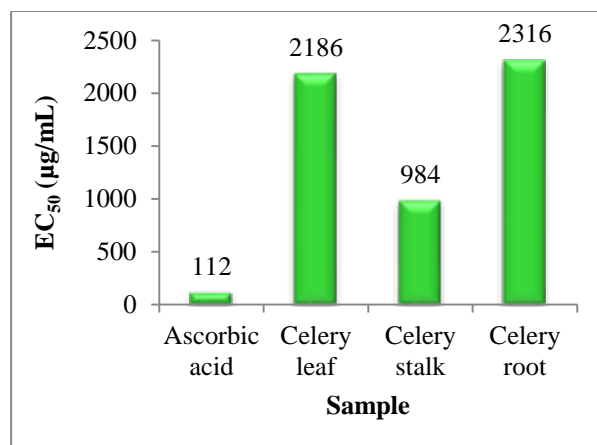


**Figure 16** A bar graph of EC<sub>50</sub> values of ascorbic acid and ethanol crude extracts of leaf, stalk and root of celery from Kalaw, Shan State, Myanmar

### Conclusion

The GC-MS analysis of essential oil of dry leaf of *Apium graveolens* L. (Celery, Tayoke Nan-nan) provides nine volatile compounds and fourteen compounds in fresh leaf. Butyl phthalide derivative compounds are most abundant in dry and fresh leaf essential oils. Senkyunolide as the main compound among them.

FT IR spectroscopy is an extremely effective method for determination of presence or absence of a wide variety of functional groups in a molecule. In this study, the absorption frequencies (cm<sup>-1</sup>) express a variety of functional groups in the essential oil. The prominent peak at 1751 cm<sup>-1</sup> for C = O stretching of five member ring ester or lactone agrees with the major component phthalides in the oil.

The leaf, stalk and root ethanol extracts of *A. graveolens* (Celery, Tayoke Nan-nan) show antioxidant activity by ferric reducing power (FRAP) in the decreasing order, stalk, leaf, root, which is the same order given by DPPH method. The reducing power shows good linear relation in standard ( $R^2 = 0.9181$ ) and all sample extracts (leaf, stalk and root).

The Presence of phthalides and phenolic compounds in the plant, Tayoke nan-nan may be useful as a medicinal drug in certain miner diseases.

### Acknowledgements

The authors would like to express our gratitude to the Department of Higher Education, Ministry of Education, Myanmar, for their permission to do this research and also to the Myanmar Academy of Arts and Science for allowing the present this paper.

### References

- Bhalodia, N. R., Nariya, P. R., Acharyal, R. N. and Shukal, V. J. (2013). "In Vitro Antioxidant Activity of Hydro Alcoholic Extract from the Fruit Pulp of *Cassia fistula* Linn. *Pharmacological Study*, vol. 34 (2), pp. 209-214
- Božović, M., Navarra, A., Garzoli, S., Pepi, F. and Ragno, R. (2017). "Essential Oils Extraction: a 24-hour Steam Distillation Systematic Methodology". *Natural Product Research*, vol. 31 (20), pp. 2387-2396
- Canabady-Rochelle L. L. S., Harscoat-Schiavo, C., Kessler, V., Aymes, A., Fournier, F. and Girardet, J-M. (2015). "Determination of Reducing Power and Metal Chelating Ability of Antioxidant Peptides: Revisited Mmethods". *Food Chemistry*, vol. 183, pp. 129- 135

- Chauhan, A., Goyal, M. K. and Chauhan, P. (2014). "GC-MS Technique and its Analytical Applications in Science and Technology. *J Anal Bioanal Tech*, vol. 5 (6), pp. 1-5
- Moharram, H. A. and Youssef, M. M. (2014). "Methods for Determining the Antioxidant Activity: A Review". *Alex. J. Fd. Sci. & Technol.*, vol. 11 (1), pp. 31-42
- Rożek, E., Nurzyńska-Wierdak, R., Sałata, A., Gumiela, P. (2016). "The Chemical Composition of The Essential Oil of Leaf Celery (*Apium graveolens* L.VAR *Secalinum* ALEF.) under the Plants' Irrigation and Harvesting Method". *Acta. Sci. Pol. Hortorum Cultus*, vol. 15 (1), pp. 147-157
- Sahraoui, N. and Boutekedjiret, C. (2015). "Innovative Process of Essential Oil Extraction: Steam Distillation Assisted by Microwave". *Progress in Clean Energy*, vol. 1, pp. 830-841
- Saxena M., Saxena, J. and Pradhan, A. (2012). "Flavonoids and Phenolic Acids as Antioxidants in Plants and Human Health". *Int. J. Pharm. Sci. Rev. Res.*, vol. 16 (2), pp. 130- 134
- Sellami, I. H., Bettaieb, I., Bourgou, S., Dahmani, R., Limam, F. and Marzouk, B. (2012). "Essential Oil and Aroma Composition of Leaves, Stalks and Roots of Celery (*Apium graveolens* var. *dulce*) from Tunisia". *The Journal of Essential Oil Research*, vol. 6, pp. 513- 521
- Soe Soe Tint, Saw Hla Myint and Ni Ni Than. (2020). "Antioxidant Activity and Nitrate, Flavonoid and Phenol Contents of Leaf, Stalk and Root of *Apium graveolens* L. (Tayoke Nan-Nan)". *J. Myanmar Acad. Arts Sci.*, vol. 18 (1A), pp. 337-361
- Silverstein R. M., G. C. Bassler and T. C. Morrill. (1991). *Spectrometric Identification of Organic Compounds*. New York: 5<sup>th</sup> Ed., John Wiley and Sons, pp. 102- 120

## CONSTITUENTS OF ESSENTIAL OIL, TOTAL PHENOLIC, TOTAL FLAVONOID CONTENTS AND ANTIOXIDANT ACTIVITY OF RHIZOME OF *CURCUMA CAESIA* ROXB. (GA MONE TAIN PYAR)

Kay Khine Nyunt<sup>1</sup>, Theingi Wint Thu<sup>2</sup>, Ni Ni Than<sup>3</sup>

### Abstract

The preliminary phytochemical screening of *Curcuma caesia* Roxb. revealed the presence of alkaloids,  $\alpha$ -amino acids, carbohydrates, flavonoids, glycosides, phenolic compounds, saponins, starch, tannins, steroids and terpenoids and the absence of cyanogenic glycosides and reducing sugars. The higher total phenol content ( $\mu\text{g GAE/mg}$ ) was detected in watery extract (234  $\mu\text{g GAE/mg}$ ) than ethanol extract (164  $\mu\text{g GAE/mg}$ ) of the rhizome of *C. caesia*. The higher total flavonoid content ( $\mu\text{g QE/mg}$ ) was detected in ethanol extract (58.3  $\mu\text{g QE/mg}$ ) than watery extract (136.1  $\mu\text{g QE/mg}$ ) of the rhizome of *C. caesia*. The rhizome of *C. caesia* was found to have antioxidant activity.  $\text{IC}_{50}$  values of ethanol and watery extracts are 10.31  $\mu\text{g/mL}$  and 56.85  $\mu\text{g/mL}$  respectively. Antioxidant potency of ethanol and watery extracts were concluded to be mild if compare with the potency of standard butylated hydroxytoluene ( $\text{IC}_{50} = 6.85 \mu\text{g/mL}$ ). The essential oil from the rhizome of *C. caesia* was extracted by steam distillation method. The components of essential oil were characterized by GC-MS. From resulting data, ten components were observed in the essential oil of *C. caesia*, namely eucalyptol, camphor, *p*-menth-2-en-9-ol, L- $\alpha$ -terpineol,  $\alpha$ -bulnesene, iso-caryophyllene,  $\gamma$ -muurolene, (5R, 6R)-3, 6-dimethyl-5-(prop-1-en-2-yl)-6-vinyl-4,5,6,7-tetrahydrobenzofuran,  $\beta$ -elemene [1-ethenyl-1-methyl-2,4 bis (prop-1-en-2-yl) cyclohexane] and  $\beta$ -elemenone.

**Keywords:** *Curcuma caesia* Roxb., antioxidant activity, essential oil, total phenol content, total flavonoid content

### Introduction

*Curcuma caesia* Roxb. (Ga Mone Tain Pyar) is a kind of turmeric with bluish-black rhizome belonging to Zingiberaceae (Ginger) famil. *C. caesia* is a perennial herb with bluish-black rhizome native to Northeast, Central India and Myanmar. The plant grows only in the rainy season but it dries in other season. However, it can grow in any type of soil like light, well drained, moist, loamy soil, and light to heavy black soil.

The rhizomes of the plant are aromatic in nature. The inner part of the rhizome is bluish-black in colour and emits a characteristics sweet smell due to presence of essential oil (Pandey, 2003). The plants are rich source of secondary metabolites such as flavonoids, phenolics, carotenoids, coumarins, anthraquinones, tannins, terpenoids, saponins that play a prominent role in inhibiting human carcinogenesis and repair the cell mutations (Ruan, 1989). The part of fresh rhizome is applied in case of snake and scorpion bite. It is recognized as a medicinal herb to possess with various properties such as anti-fungal activity, smooth muscle relaxant and anti-asthmatic activity, bronchodilating activity, antioxidant activity, anxiolytic and CNS depressant activity, locomotor depressant, anti-convulsant, anthelmintic activity, anti-bacterial activity, anti-ulcer activity (Kagyung *et al.*, 2010).

---

<sup>1</sup> Dr, Lecturer, Department of Chemistry, Yangon University

<sup>2</sup> MSc. Candidate, Department of Chemistry, Yangon University

<sup>3</sup> Professor and Head, Department of Chemistry, Yangon University

### Botanical Aspects of *Curcuma caesia* Roxb. (Ga Mone Tain Pyar)

Family	: Zingiberaceae
Genus	: <i>Curcuma</i>
Species	: <i>caesia</i>
Botanical Name	: <i>Curcuma caesia</i> Roxb.
Myanmar Name	: Ga Mone Tain Pyar
English Name	: Black Turmeric
Part used	: Rhizome



**Figure 1** Plant and rhizome of *C.caesia*

### Medicinal Uses of *C. caesia*

Leaves and rhizomes of *C. caesia* are used in traditional medicine. It contains more amounts of flavonoids and terpenoids which are responsible for the main pharmacological activities like antioxidant, anti-inflammatory, anti-fungal, etc. (Sasikala, 2012).

The rhizome of the plant is aromatic, contains essential oil and used for a variety of purposes in pharmaceutical and cosmetic industries. The essential oils of *C. caesia* were also reported to have more potent antimicrobial, antioxidant, anticancer, and anti-inflammatory activities than the solvent extract counterparts (Xiang *et al.*, 2018).

## Materials and Methods

### Sample Collection and Preparation

Several samples of *C. caesia* collected from Yangon Region, the soil was removed from the rhizome. The rhizome was carved into very small pieces and allowed to dry well. The dried pieces were made into powder by using grinding machine. The powdered sample was stored in air-tight container to prevent moisture changes and other contaminations.

### Preliminary Phytochemical Investigation of *C. caesia*

Phytochemical tests for rhizome of *C. caesia* was carried out according to the reported methods to investigate the presence and absence of phytochemical constituents (M-Tin Wa, 1972).

### Determination of Total Phenol Content

One of the antioxidative factors, total phenolic content was measured spectrophotometrically according to the Folin-Ciocalteu method (Marinova, 2005).

The total phenolic content in each sample was estimated by Folin-Ciocalteu method according to the procedure described by Marinova (2005). First, 0.5 mL of prepared extract solution was mixed with 0.5 mL of methanol. Then, 5 mL of FCR reagent (1:10) was added to the mixture and incubated for 5 min. 4 mL of 1 M sodium carbonate solution was added to each tube and the tubes were kept at room temperature for 120 min and the UV absorbance of reaction mixture was read at  $\lambda_{\max}$  765 nm. The blank solution was prepared as the above procedure by using

distilled water instead of sample solution. Total phenolic content was estimated as milligram gallic acid equivalents per gram of different extract ( $\mu\text{g GAE/ mg}$ ).

### **Determination of Total Flavonoid Content**

Total flavonoid content was measured spectrophotometrically according to the  $\text{AlCl}_3$  colorimetric method (Marinova, 2005).

Each extracts solution 0.5 mL was mixed with 1.5 mL of methanol, 0.1 mL of 1 %  $\text{AlCl}_3$  solution and 2.8 mL of distilled water. The absorbance of reaction mixture was read at  $\lambda\text{-max}$  415 nm. The blank solution was prepared as the above procedure by using distilled water instead of sample solution. Total flavonoid content was estimated as milligram quercetin acid equivalent per gram ( $\mu\text{g QE/mg}$ ) of extract.

### **Determination of Antioxidant Activity of *C. caesia***

The antioxidant activity of crude extracts *C. caesia* was measured by using DPPH free radical scavenging assay (Marinova, 2011).

DPPH free radical scavenging activity of ethanol and water extracts of rhizome of *C. caesia* was determined by UV-Visible spectrophotometer (Marinova, 2011). The control solution was prepared by mixing 1.5 mL of 0.002 % DPPH solution and 1.5 mL of ethanol in the brown bottle. The sample solution was also prepared by mixing 1.5 mL of 0.002 % DPPH solution and 1.5 mL of test sample solution. These bottles were incubated at room temperature and were shaken on shaker for 30 min. After 30 min, the absorbance of different concentrations (6.25, 12.5, 25, 50, 100 and 200  $\mu\text{g/mL}$ ) of tested sample was measured at 517 nm using UV-7420 spectrophotometer. Absorbance measurements were done in three times for each concentration and the mean value so obtained were used to calculate percentage of radical scavenging activity (% RSA).

### **Extraction of Essential Oil from the Rhizome of *C. caesia***

The sample of the fresh rhizome of *C. caesia* (100 g) was placed in the glass jacket. The glass jacket is filled with distilled water. The glass jacket was fitted to set which was joined to water condenser. When the glass jacket was heated, the condensed oil and water coming out from condenser will collected in the receiver flask. The oil was extracted with n-hexane in a separating funnel. The n-hexane was evaporated at 60-70  $^\circ\text{C}$  to get the essential oil which was then weighed until to be constant weight and kept in air tight bottle (Srivastava, 2003).

### **Organic Compounds in Essential Oil from the Rhizome of *C. caesia***

Organic constituents in essential oil from the rhizome of *C. caesia* were detected by GC-MS Spectroscopic Method at National Analytical Laboratory, Department of Research and Innovation.

## **Results and Discussion**

### **Phytochemical Constituents of *C. caesia***

The phytochemical tests were done on the rhizome with a view to determine the presence or absence of phytochemical constituents in *C. caesia*. From the result, alkaloids,  $\alpha$ -amino acids, carbohydrates, flavonoids, glycosides, phenolic compounds, saponins, starch, tannins, steroids and terpenoids are present but cyanogenic glycosides and reducing sugars are absence.

### Total Phenol Content of Crude Extracts of *C. caesia*

The determination of the quantity of phenolic compound was very important in order to determine the antioxidant capacity of sample. Ethanol and watery extracts of *C. caesia* contained large quantities of essential oil contents. The highest content of essential oil can be found on the detection of total phenol content of the sample. The total phenol content of ethanol and watery extracts of rhizome of *C. caesia* are shown in Table 1. According to the results, the total phenolic content of watery extract (234  $\mu\text{g GAE/mg}$ ) was higher than ethanol extract (164  $\mu\text{g GAE/mg}$ ) of *C. caesia*. Comparison of TPC in ethanol and watery extracts of rhizome of *C. caesia* are represented by a bar graph in Figure 2.

**Table 1** Total Phenolic Contents of Ethanol and Watery Extracts of *C. caesia*

Tested samples	Total phenol content ( $\mu\text{g GAE/mg}$ of extract)
Ethanol extract	164
Watery extract	234

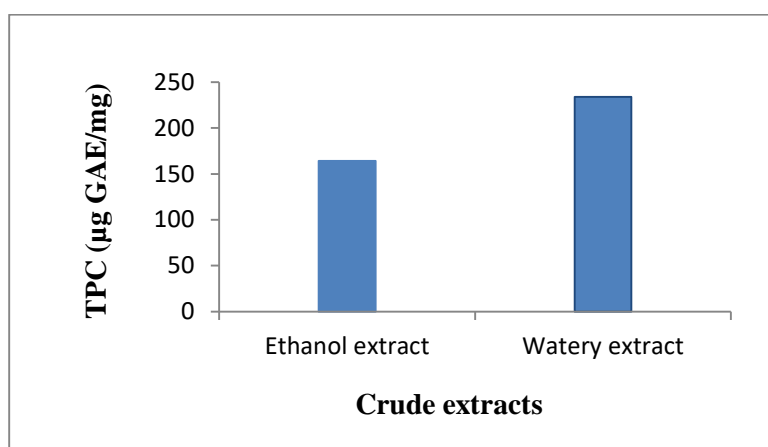


**Figure 2** Total phenol contents of the crude extracts of *C. caesia*

### Total Flavonoid Contents of Crude Extracts of *C. caesia*

In this study, high flavonoid contents have been found to exert high antioxidant potential. The total flavonoid contents of ethanol and watery extracts of rhizome of *C. caesia* are shown in Table 2. The higher TFC ( $\mu\text{g QE/mg}$ ) was detected in ethanol (136.1  $\mu\text{g QE/mg}$ ) than water (58.3  $\mu\text{g QE/mg}$ ) extracts of rhizome of *C. caesia*. According to result, flavonoid compounds were more soluble in ethanol. The different structures and substitutions of flavonoid influence the phenoxyl radical stability, thereby affecting the antioxidant properties of the flavonoids. Comparison of total flavonoid content in ethanol and watery extracts of rhizome of *C. caesia* are represented by a bar graph in Figure 3.

**Table 2** Total Flavonoid Contents of Ethanol and Watery Extracts of *C. caesia*

Tested samples	Total flavonoid content ( $\mu\text{g QE/mg}$ of extract)
Ethanol extract	136.1
Watery extract	58.3

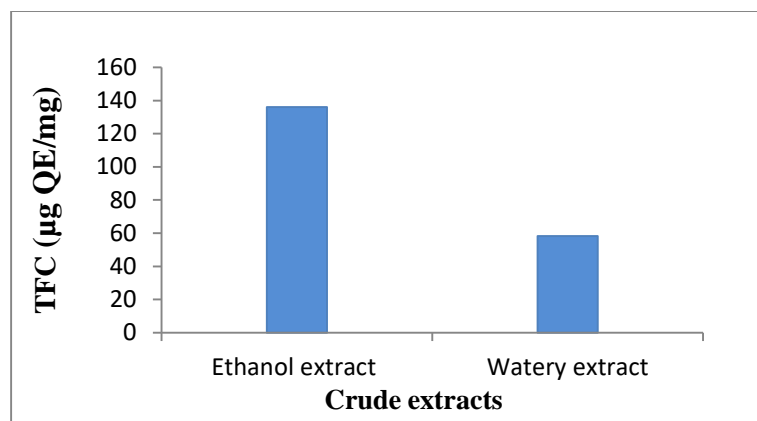


**Figure 3** Total flavonoid contents of the crude extracts of *C. caesia*

### Antioxidant Activity of *C. caesia*

From the antioxidant activity results, rhizome of *C. caesia* was found to have radical scavenging activity.  $IC_{50}$  values of ethanol and watery extracts are 10.31 and 56.85  $\mu\text{g/mL}$ , respectively. So, watery extract has less antioxidant activity than the ethanol extract. All extracts showed lower antioxidant activity when compared to the standard butylated hydroxytoluene ( $IC_{50} = 6.85 \mu\text{g/mL}$ ). The  $IC_{50}$  values of ethanol and watery extracts of rhizome of *C. caesia* and standard butylated hydroxytoluene (BHT) are shown in Table 3 and Figure 4.

**Table 3**  $IC_{50}$  Values of Crude Extracts from Rhizome of *C. caesia* and Standard BHT

Samples	$IC_{50}$ ( $\mu\text{g/mL}$ )
Ethanol	10.31
Watery	56.24
BHT	6.85

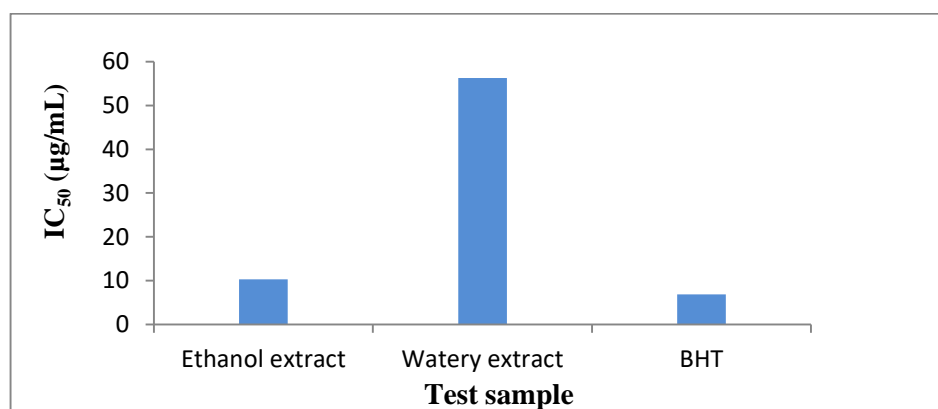


**Figure 4**  $IC_{50}$  values of the crude extracts of *C. caesia* and standard BHT

### Composition of Essential Oil of *C. caesia*

Gas chromatographic-mass spectrometry (GC-MS) is the single most important tool or identification of unknown organic compounds by matching with reference spectra. The GC-MS chromatogram of essential oil from the rhizome of *C. caesia* is showed in Figure 5, Figure 6. Retention indices of the detected compounds were calculated and characterized based on their peaks comparison with reference literature values were shown in Table 1.

According to GC-MS chromatogram, ten compounds were identified from the *C. caesia*. The compounds identified are eucalyptol, C<sub>10</sub>H<sub>18</sub>O (m/z 154), camphor C<sub>10</sub>H<sub>16</sub>O (m/z 152), *p*-menth-2-en-9-ol, C<sub>10</sub>H<sub>18</sub>O (m/z 154), L- $\alpha$ -terpineol, C<sub>10</sub>H<sub>18</sub>O (m/z 154),  $\alpha$ -bulnesene, C<sub>15</sub>H<sub>24</sub> (m/z 204), *iso*-caryophyllene, C<sub>15</sub>H<sub>24</sub> (m/z 204),  $\gamma$ -muurolene, C<sub>15</sub>H<sub>24</sub> (m/z 204), (5R,6R)3,6-dimethyl-5-(prop-1-en-2-yl)-6-vinyl-4,5,6,7-tetrahydrobenzofuran, C<sub>15</sub>H<sub>20</sub>O (m/z 216),  $\beta$ -elemene [1-ethenyl-1-methyl-2,4bis( prop-1-en-2-yl) cyclohexane], C<sub>15</sub>H<sub>24</sub>, (m/z 204) and  $\beta$ -elemenone, C<sub>15</sub>H<sub>20</sub>O, (m/z 218).

The following compounds such as eucalyptol, camphor, L- $\alpha$ -terpineol,  $\alpha$ -bulnesene, *iso*-caryophyllene,  $\gamma$ -muurolene, (5R,6R)3,6-dimethyl-5-(prop-1-en-2-yl)-6-vinyl-4,5,6,7 tetrahydrobenzofuran,  $\beta$ -elemenone, are in agreement with the reported data whereas, *p*-menth-2-en-9-ol and  $\beta$ -elemene [1-ethenyl-1-methyl-2,4bis( prop-1-en-2-yl) cyclohexane] were absent. This could be due to their geographical variations and the related environmental factors in Myanmar.

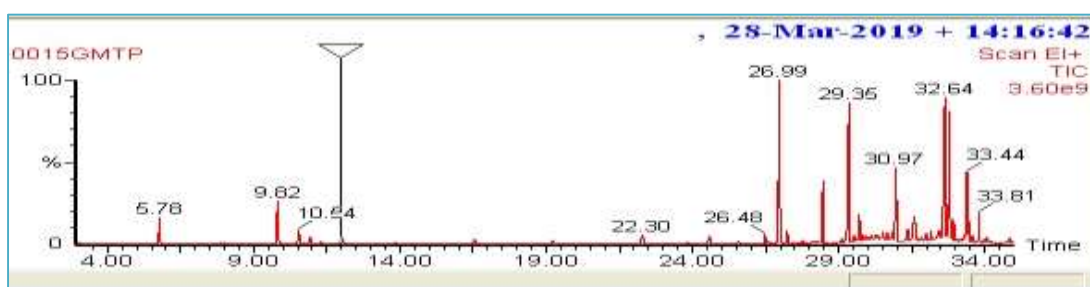
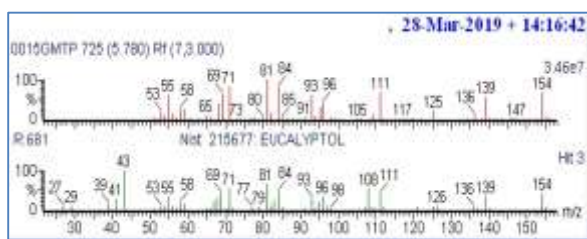


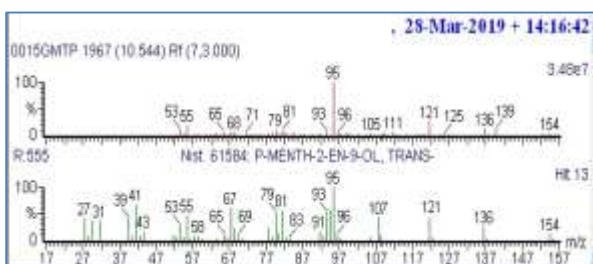
**Figure 5** Total ion chromatogram of essential oil from *C. caesia*



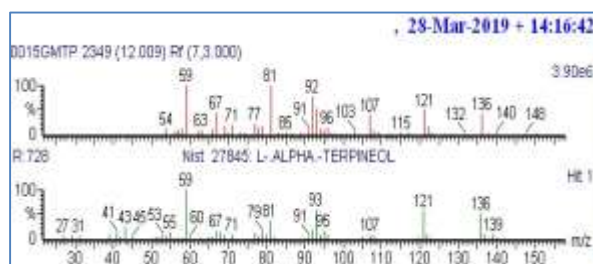
(i) Eucalyptol



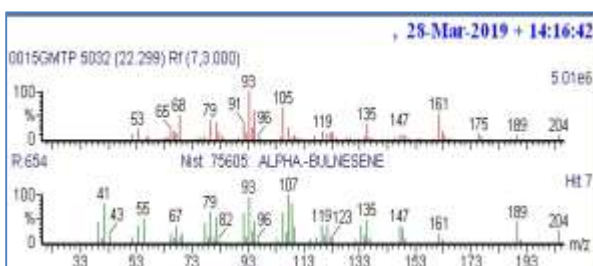
(ii) Camphor



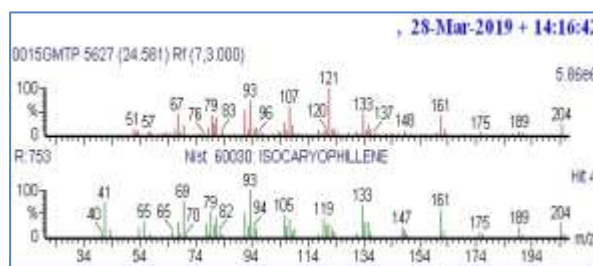
(ii) *p*-Menth-2-en-9-ol



(iv) L- $\alpha$ -terpineol



(v)  $\alpha$ -bulnesene



(vi) *iso*-caryophyllene

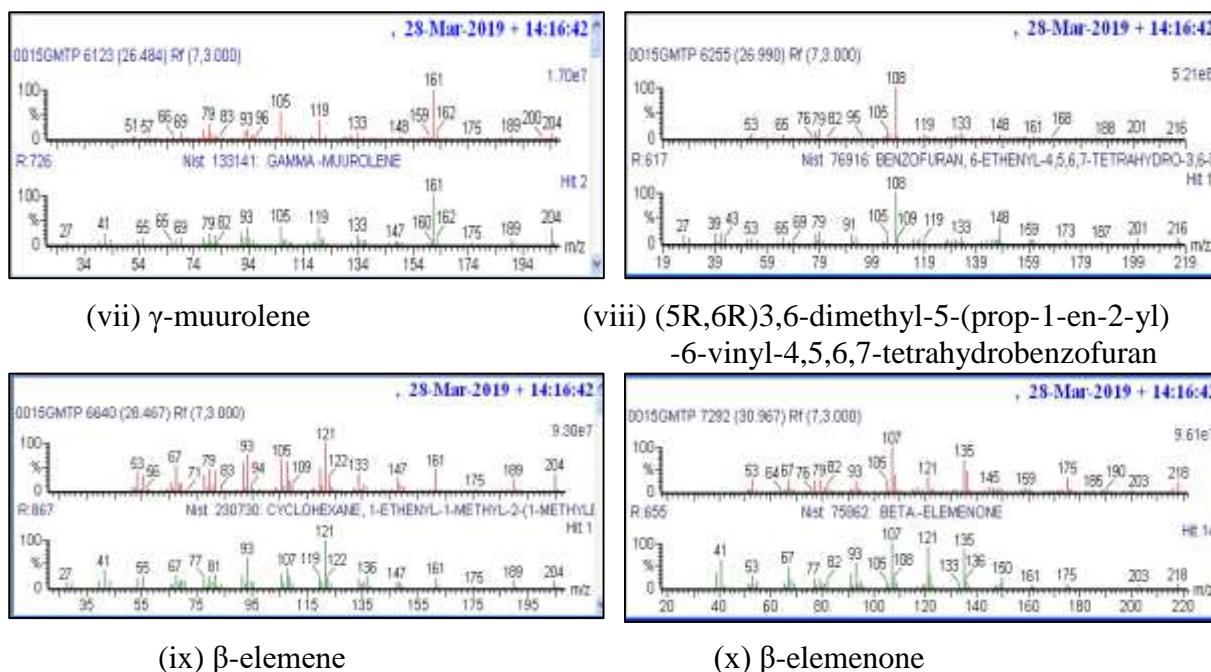


**Figure 6** Comparison of the EI mass spectra of compounds and databank from essential oil of *C. caesia*

**Table 4** Chemical Compositions of Essential Oil from the Rhizome of *C. caesia*

No.	Compounds from <i>C.caesia</i>	Compounds from <i>Curcuma</i> Species *	Molecular Weight	Retention Time (min)
1	Eucalyptol	Eucalyptol	154	5.78
2	Camphor	Camphor	152	9.82
3	<i>p</i> -Menth-2-en-9-ol		154	10.54
4	L- $\alpha$ -terpineol	L- $\alpha$ -terpineol	154	12
5	$\alpha$ - bulnesene	$\alpha$ -bulnesene	204	22.29
6	iso-caryophyllene	iso-caryophyllene	204	24.58
7	$\gamma$ -muurolene	$\gamma$ -muurolene	204	26.48
8	(5R,6R)3,6-dimethyl-5-(prop-1-en-2-yl)-6-vinyl-4,5,6,7-tetrahydrobenzofuran,	(5R,6R)3,6-dimethyl-5-(prop-1-en-2-yl)-6-vinyl-4,5,6,7-tetrahydrobenzofuran,	216	26.99
9	$\beta$ -elemene [1-ethenyl-1-methyl-2,4 bis ( prop-1-en-2-yl) cyclohexane]		204	28.46
10	$\beta$ -elemenone	$\beta$ -elemenone	218	30.97

MW=Molecular Weight\* Dosoky, 2018

### Conclusion

In this study, investigation of phytochemical constituents, total phenolic content, total flavonoid content and organic compounds from essential oil of the rhizome of *C. caesia* were reported.

The result of preliminary phytochemical screening of different crude extracts of *C. caesia*

revealed the presence of alkaloids, amino acids, carbohydrates, flavonoids, glycosides, organic acids, phenolic compounds, saponin, starch, tannins, steroids and terpenoids and the absence of cyanogenic glycosides and reducing sugars.

The higher TPC was detected in watery extract (234 µg GAE/mg) than ethanol extract (164 µg GAE/mg) of the rhizome of *C. caesia*. From the result data, phenolic compounds of *C. caesia* were more soluble in water.

The higher TFC was detected in ethanol extract (136.1 µg QE/mg) than watery extract (58.3 µg QE/mg) of the rhizome of *C. caesia*. From the experimental data, flavonoid compounds were more soluble in ethanol.

The rhizome of *C.caesia*. is found to have antioxidant activity. IC<sub>50</sub> values of ethanol and watery extracts are 10.31 µg/mL and 56.24 µg/mL, respectively. Antioxidant potency of ethanol extract significantly higher than watery extract of *C.caesia*. Radical scavenging activity both extracts were concluded to be mild if compare with the potency of standard butylated hydroxytoluene (IC<sub>50</sub> = 6.85 µg/mL).

The components of essential oil from *C.caesia*. are analyzed by GC-MS. From resulted data, ten components namely eucalyptol, camphor, *p*-menth-2-en-9-ol, L- $\alpha$ -terpineol,  $\alpha$ -bulnesene, iso-caryophyllene,  $\gamma$ - muurolene, (5R,6R)3,6-dimethyl-5-(prop-1-en-2-yl)-6-vinyl-4,5,6,7-tetrahydrobenzofuran,  $\beta$ -elemene [1-ethenyl-1-methyl-2,4bis(prop-1-en-2-yl) cyclohexane] and  $\beta$ -elemenone were identified from essential oil of *C. caesia*.

From the research data, rhizome of *C. caesia*. possess antioxidant activity and may probably derived from compounds such as flavonoids and phenols. Organic compounds from essential oil should be useful in the formulation of traditional medicine. This primary information will help in conducting further studies for identification of chemical constituent, medicinal uses of essential oil components and their effectiveness in medicine.

### Acknowledgements

The authors would like to thank Myanmar Academy of Art and Science, Ministry of Education, Myanmar, for giving us the opportunity to present this research paper. We also would like to thank to the Department of Higher Education (Lower Myanmar), Ministry of Education, Myanmar for providing us the research facilities during this research.

### References

- Dosoky, N.S. and Setzer, W.N. (2018). "Chemical Composition and Biological Activities of Essential Oils of *Curuma* Species". *J. Nutri.*, vol. 3(1), pp. 1-42
- Kagyung, R. (2010). "Ethnomedicinal Plant used for Gastrointestinal Disease by Aditribeof Dehang-Debang Biosphere Reserve in Arunochal Pradesh". *J. Trad. Know.*, vol. 9 (3), pp. 496-501
- M-Tin Wa. (1972). "Screening Methods and Procedures". *Phytochemical Bulletin of Botanical Society of America*, vol. 5(3), pp. 4 -10
- Marinova, D., Ribarova, F. and Atanassova, M. (2005). "Total phenolic and total flavonoids in Bulgarian fruits and vegetables". *Journal of the University of Chemical Technology and Metallurgy*, vol. 40 (3), pp. 255-260
- Marinova, G. and Batchvarov, V. (2011). "Evaluation of the Methods for Determination of the Free Radical Scavenging Activity by DPPH". *Bulg. J. Agric. Sci.*, vol. 17, pp. 11-24
- Pandey, A.K. and Chowdhury, A.R. (2003). "Volatile Constituents of Rhizome Oil of *Curcuma caesia* Roxb. from Central India". *J. Flavour. Frag.*, vol. 18, pp. 436-440
- Robert, M.S. and Webster, F.X. (1998). *Spectrometric Identification of Organic Compounds*. New York : 6<sup>th</sup> Ed., John Wiley & Sons, pp. 367-370

- Ruan, C. (1989). "Antimutagenic Effect of Foods and Chemoprevention of Cancer". *Acta Guangxi Med. Coll.*, vol. 1, pp. 68-71
- Sasikala, M., Gowthomi, C.L., Nithya, S. and Jamuna, K.M. (2012). "Extraction, Isolation, Characterization of Phytoconstituents from *Curuma caesia* Roxb. by various analytical methods". *Int. J. Res. Pharmaceutical and Nano Sci.*, vol. 1(2), pp. 257-268
- Srivastava, A.K., Srivastava, S.K. and Syamsudar, K.V. (2003). "Bud and Leaf Essential Oil Composition of *Syzygium aromaticum* from India and Madagascar". *Flav. Fra. J.*, vol. 20 (1), pp. 51-53
- Xiang, H., Zhang, L., Xi, L., Yang, Y., Wang, X., Lei, D., Zheng, X. and Liu, X. (2018). "Phytochemical profiles and bioactivities of essential oils extracted from seven *Curcuma* herbs". *J. Ind. Crops. Prod.*, vol.111, pp. 298-305

## ISOLATION, CULTURE AND CHARACTERIZATION OF LACTIC ACID BACTERIA FROM KEFIR GRAINS FERMENTED MILK

Aye Khaing Soe<sup>1</sup>, Phyu Phyu Win<sup>2</sup>, Saw Hla Myint<sup>3</sup>

### Abstract

Kefir or kephir is a fermented milk drink similar to a thin yogurt that is made from kefir grains, a specific type of mesophilic symbiotic culture. Home-made kefir has been improved using various natural substrates such as milk, coconut water, and fruits such as grape, apple and dragon fruits. The present study includes isolation, culture and characterization of lactic acid bacteria from milk kefir. The isolated bacteria strain was characterized by gram staining and biochemical tests. The observed background color of the selected isolated bacteria strain is violet for gram staining, the isolated bacteria strain may be gram positive. From direct isolation from milk kefir, the isolated bacteria were negative for motility, indole, gelatin, citrate utilization, catalase, Voges-Proskauer, nitrate reduction, urease, starch hydrolysis tests, sugar fermentation test and methyl red test. For the result obtained, the most of biochemical tests for all bacteria slants were agree with reported literature data for lactic acid bacteria.

**Keywords:** kefir, lactic acid bacteria, fermentation, milk, biochemical tests

### Introduction

Microorganisms play an essential role in the food fermentations. *Lactobacillus* is also formed in some fermented foods like yogurt and in dietary supplements. Fermentation is one of the oldest and most economical method used in food preservation. The properties of fermented milks (curd, yoghurt, kefir, Kumis, etc.) with their nutritional values have driven a considerable interest (Lim *et al.*, 2007).

Kefir is an alcoholic, fermented milk beverage produced by the fermentation of kefir grains, which contain lactic acid bacteria, acetic acid bacteria, and yeasts. It originated from Caucasus mountain in former Soviet Union, central Asia. Milk Kefir is made with cow milk, goat milk, or coconut milk. Starter culture is prepared from kefir grains, *Lactobacillus kefirianofaciens*, and species of the genera *Leuconostoc*, *Lactococcus*, and *Acetobacter* growing in a strong specific relationship. Kefir has a tart, creamy flavor, and it is loaded with probiotic health benefits. It is safe for most people to consume, and a single serving is full of vitamins and probiotics. It is safe to consume daily, and it may help create and maintain a healthy balance of good bacteria in multiple systems within the body (Farnworth, 2005).

Probiotic bacteria found in kefir products include: *Lactobacillus acidophilus*, *Bifidobacterium bifidum*, *Streptococcus thermophilus*, *Lactobacillus delbrueckii subsp. bulgaricus*, *Lactobacillus helveticus*, *Lactobacillus kefirianofaciens*, *Lactococcus lactis*, and *Leuconostoc* species. Lactobacilli in kefir may exist in concentrations varying from approximately 1 million to 1 billion colony-forming units per milliliter, and are the bacteria responsible for the synthesis of the polysaccharide *kefiran* (Oliveira *et al.*, 2013).

Lactic acid bacteria comprise a group of bacteria that are united by a constellation of morphological, metabolic and physiological characteristics. The genera *Lactobacillus*, *Lactococcus*, *Leuconostoc*, *Pediococcus*, and *Streptococcus* are important members of this group (Batt, 2000). Lactic acid bacteria are an order of gram-positive, either rod-shaped (bacilli) or spherical (cocci) bacteria that share common metabolic and physiological characteristics. These bacteria, usually found in decomposing plants and milk products, produce lactic acid as the major

---

<sup>1</sup> 3PhD Candidate, Department of Chemistry, University of Yangon

<sup>2</sup> Dr, Associate Professor, Department of Chemistry, Dawei University

<sup>3</sup> Dr, Professor (Retd.), Department of Chemistry, University of Yangon

metabolic end product of carbohydrate fermentation. The lactic acid bacteria are found in foods (dairy products, fermented meat, sour dough, fermented vegetables, beverages- including wine and kefir). Health benefits of lactic acid bacteria are known to give positive influence in the gastrointestinal of humans (Chen *et al.*, 2010).

In the present research work, the lactic acid bacteria were isolated from milk kefir by direct isolation method and isolated bacteria strains were identified by gram staining method and biochemical tests (Breed *et al.*, 1957).

### Materials and Methods

Firstly, sampling of milk kefir grains and processing of milk kefir were performed. Then, the lactic acid bacteria were culture by serial dilution and isolated after fermentation. The isolated bacteria were characterized by gram staining method and biochemical test. In this study, microbiological work was conducted in the Fermentation Department, Pharmaceutical Research Department, Ministry of Industry 1, Yangon Region.

#### Sample Collection

Milk kefir grains (Figure 1) was purchased from the NIHON KEFIA Co., Ltd, Japan.



**Figure 1** Milk kefir grains

#### Processing of Milk Kefir

Milk kefir grains (ca. 4 g) were added in a jar and then fresh milk (250 mL) was added. The glass jar was sealed with clean clothes and allowed to culture for 12 to 48 h at room temperature, then the kefir grains were removed, resulting the milk kefir recipes (Figure 2).



**Figure 2** Preparation of milk kefir recipes

#### Tomato juice medium

About 2 g of agar, 1 g of yeast extract, 1 g of dextrose, 0.05 g of dipotassium phosphate, 0.02 g of monopotassium phosphate, 0.02 g of magnesium sulphate, 0.001 g of manganese sulphate, 0.001 g of ferrous sulphate, 0.001 g of sodium chloride, 2 mL of tomato juice were mixed with 100 mL of distilled water (pH 6.7). The mixture was boiled on hot plate, sterilized in sterilizer (121°C), cooled and transferred 20 mL to each petridish (Atlas, 1993).

### **Isolation of *Lactobacillus* Species by Serial Dilution Method and Streaking Method**

One gram of sample was added into a conical flask containing 99 mL of sterile distilled water to make a dilution ratio of 1:100. The mixture was shaken for about 5 min. 1 mL of each serially diluted solution was added to 9 mL of sterilized distilled water for each sample to conduct bacteriological analysis. After four serial dilutions, 1 mL of each dilution level was inoculated immediately on to sterile petri dishes containing 25 mL of Rogosa and tomato juice agar media inside a clean bench under laminar flow. Each dilution was prepared in two sets, one for heterotrophic viable count and another for isolation and identification. The inoculated plates were isolated in clockwise and anti-clockwise directions to distribute the inoculums on the surface the medium and incubated at 37 °C for 24-72 h. The colonies that developed on the inoculated plates were observed under microscope and streaked selectively as pure strain to new set of petri dishes containing the same Rogosa and tomato juice agar media and, incubated at 37 °C for 24-72 h, bacteria slant cultures were obtained. From these culture slants, MK-1 and MK-2 were selected. (Collin *et al.*, 1995; Dubey and Maheshwari, 2002).

### **Identification of the Isolated *Lactobacillus* Species**

Identification of each isolate (MK-1 and MK-2) of bacteria up to genus level was carried by the gram staining method and biochemical tests.

### **Determination of Staining Characteristics by Gram's Stain**

Preparations for staining were made on microscopic slides, which were cleaned by immersion in chromic acid and then washing with water. The clean slide was held with a pair of forceps and dried by passing through the flame of spirit burner. A drop of sterile distilled water was placed on the perfectly clean slide. A loopful of pure isolated colony from plate was taken with a sterile inoculating loop and mixed with sterile distilled water on the slide. Subsequently the slide was dried by passing quickly through the flame of a spirit burner. The slide was then flooded with crystal violet solution for 1 min, washed thoroughly under tap water, and then smeared with iodine solution for 1 min. It was then decolorized with acetone/alcohol and washed with water. Counter staining with safranin was done for about 20-30 s and washed with water and dried by blotting paper and examined under a compound microscope for cell morphology.

### **Biochemical Tests**

#### **Motility test**

Motility stab agar was prepared and inoculated with isolated bacteria for 2 days at room temperature. If the tube was turbid, this indicated that isolated bacteria were motile (Atlas, 1993).

#### **Citrate utilization test**

A loopful of isolated bacteria was inoculated into the surface of citrate slant medium by even spreading and incubated at 27 °C for 5 days. After this period, the appearance of a blue colour on the citrate slant agar medium indicated a positive citrate utilization test (Cruickshank *et al.*, 1968).

#### **Indole test**

The isolated bacteria were inoculated in the peptone water medium and incubated at room temperature for 48 h. After this period for the occurrence of indole reaction, 0.5 mL of Kovac's reagent was added to the test tubes and was shaken gently. If the pink layer could occur within a few seconds in the alcoholic layer, the indole test was positive and a yellow layer develop and the indole test was taken as negative one.

### **Nitrate reduction test**

A loopful of isolated bacteria was inoculated into the nitrate medium and incubated for 96 h at 27 °C. After incubation, one drop each of the test reagent was added to the test culture. A red colour developing within a few min was indicative of a positive nitrate reduction test (Cowan, 1974).

### **Methyl red test**

Glucose phosphate peptone broth medium was inoculated and incubated at room temperature for 48 h. It is detecting on organisms that does not convert acidic products to neutral products and produces final pH lower than that of organisms producing neutral products. Because of lower pH, the addition of methyl red indicator changes to a red colour as positive reaction (Bisen and Verma, 1998).

### **Voges-Proskauer test**

After autoclaving, the solution was cooled and 5 mL of sterile glucose solution added quickly to it near the flame of a spirit burner to get glucose phosphate peptone-water medium. The medium was distributed to each of the sterile test tubes in 5 mL amounts. A loopful of isolated bacteria was inoculated into the glucose phosphate peptone-water medium and incubated at 24 °C for 48 h. After incubation for Voges-Proskauer reaction, 1 mL of 40 % potassium hydroxide solution and 3 mL of 5 %  $\alpha$ -naphthol in absolute ethanol solution were added to the test culture and shaken quickly. The development of a pink colour in 2 to 5 min was indicative of a positive VP test (Cruickshank *et al.*, 1968).

### **Gelatin liquefaction test**

A loopful of bacteria was inoculated into gelatin agar medium and incubated at 27 °C for 72 h. Then, they were stored in refrigerator for 30 min. If the medium was liquid, they would be positive in gelatin liquefaction.

### **Catalase test**

A few drops of 3 % hydrogen peroxide (H<sub>2</sub>O<sub>2</sub>) solution was added onto each slide containing strain and watched for immediate signs of bubbling, which represented positive test; absence of bubbles indicated a negative test (Salle, 1948).

### **Urease test**

The broth medium is inoculated with a loopful of a pure culture of the test organism and incubated the test tube at 37 °C for 48 h. The phenol red indicator will turn to pink due to alkaline nature of the medium because of ammonia production (Dubey and Maheshwari, 2002).

### **Starch hydrolysis test**

Isolated bacteria were streaked on starch agar medium and allowed it to grow at 37 °C for 48 h. Iodine solution was poured on the plates. If the area around streaked culture remains clear it indicated the degradation of starch had occurred due to production of amylase (Dubey and Masheshwari, 2002).

### **Sugar fermentation test**

Fermentation medium (10 mL) containing 1 % each of sugars such as glucose, lactose, maltose and sucrose were separately added into the test tubes and each with an inverted Durham

tube. The medium was sterilized at 121 °C for 15 min, which were then inoculated with isolated bacteria and incubated for 48 h. (Cruickshank *et al.*, 1968).

### Results and Discussion

The results and discussion consist of two parts. The first part concerned with isolation of *Lactobacillus* species from milk kefir sample by serial dilution method. The second part includes the identification of *Lactobacillus* species from milk kefir sample by gram staining method and biochemical tests.

#### Isolation and Identification of *Lactobacillus* Species from Milk Kefir Sample

##### Isolation of *Lactobacillus* species from milk kefir sample

In the dilution method contained in the procedure, single colonies of isolated bacteria appeared on each of the four tomato juice agar plates with different dilution after incubation for 4 days (Figure 4). The colony from each dilution (plate) was transferred to each tomato juice agar slant for culture.



**Figure 3** Photograph showing the isolation and culture of *Lactobacillus* species from mil kefir

- (i) Streaking for isolation of *Lactobacillus* species colony
- (ii) Slant culture of isolated *Lactobacillus* species

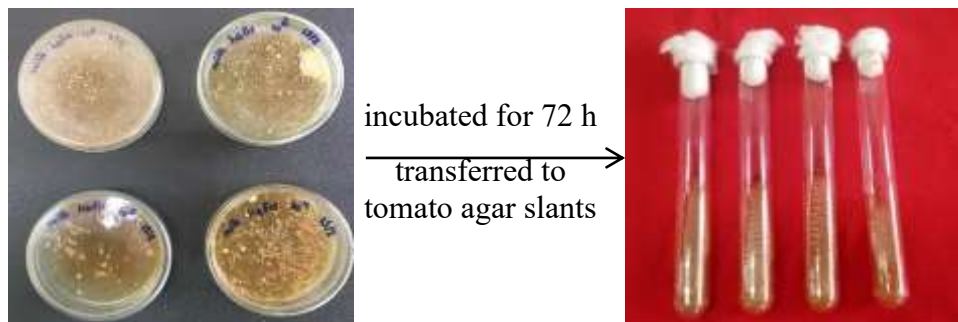


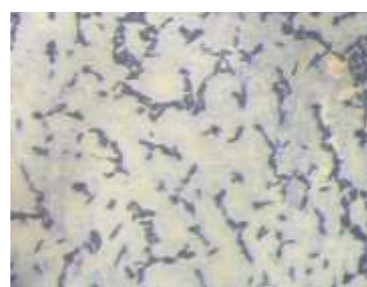
**Figure 4** Photograph showing the single colony of isolated bacteria from milk kefir by dilution method

## Identification of *Lactobacillus* species from milk kefir sample

### Gram staining



Isolate MK-1



Isolate MK-2

**Figure 5** Gram staining for bacteria strain isolated from milk kefir sample

The isolation and identification of *Lactobacillus* species from milk kefir were conducted. Two bacterial strains (MK-1 and MK-2) from 24 h incubation period was isolated, purified and identified. The colony character of isolates (MK-1) was cream colour, circular shape and MK-2 was creamish-white color and irregular shape.

The observed background colour is violet for gram staining for bacteria strain isolated from MK-1 and MK-2 sample. Therefore, the isolated bacteria were gram positive bacteria.

### Biochemical characteristics of *Lactobacillus* species from milk kefir sample

The identification of genus level, two isolated bacteria were carried out by biochemical tests. All isolated *Lactobacillus* species from milk kefir were negative results in motility test, indole test, methyl red test, gelatin liquefaction test, citrate utilization test, nitrate reduction test, catalase test, Voges-Proskauer test, urease test and starch hydrolysis test. These results were in accordance with those revealed in Bergey's Manual of Determinative Bacteriology (Breed *et al.*, 1957). From the result of biochemical tests, the most of biochemical tests for all bacteria slants were agree with the reported literature data for lactic acid bacteria.

These results are shown in Table 1.

**Table 1** Biochemical Characteristics of *Lactobacillus* Species from Milk Kefir Samples

Bacteria strain	Biochemical Tests								
	Motility	Indole	Methyl red	Gelatin Liquefaction	Citrate utilization	Catalase	Voges-Proskauer	Urease	Starch hydrolysis
MK - 1	-	-	-	-	-	-	-	-	-
MK - 2	-	-	-	-	-	-	-	-	-

+ = positive reaction, - = negative reaction

In the sugar fermentation test (glucose, lactose, maltose and sucrose) were used. All isolate showed negative results. These results were also similar to the result showed in Bergey's Manual of Determinative Bacteriology (Breed *et al.*, 1957). The results of sugar fermentation test are presented in Table 2.

**Table 2 Sugar Fermentation Tests of *Lactobacillus* Species from Milk Kefir Samples**

Bacteria strain	Sugar test			
	Glucose	Maltose	Lactose	Sucrose
MK-1	-	-	-	-
MK-2	-	-	-	-

### Conclusion

In the present study, the selected bacteria strains were isolated by using tomato juice agar medium from milk kefir samples. These strains were identified by biochemical characteristics using Bergey's Manual of Determinative Bacteriology (Breed *et al.*, 1957). From the study of identification of isolated bacteria, the observed background color of selected isolated bacteria strain is violet for gram staining reaction showed the isolated bacteria is gram positive bacteria.

From the biochemical tests, all isolated *Lactobacillus* species provided negative results in motility test, indole test, methyl red test, gelatin liquefaction test, citrate utilization test, nitrate reduction test, catalase test, Voges-Proskauer test, urease test and starch hydrolysis test. From the result of biochemical tests, the most of biochemical tests for all bacteria slants were agree with reported literature data for lactic acid bacteria.

In the results of sugar fermentation tests in milk kefir samples, all isolates were found to ferment glucose, lactose, maltose and sucrose. According to the gram staining and biochemical tests, the isolated bacteria is lactic acid bacteria.

### Acknowledgements

The authors would like to express their profound gratitude to the Department of Higher Education (Lower Myanmar), Ministry of Education, Yangon, Myanmar, for provision of opportunity to do this research and Myanmar Academy of Arts and Science for allowing to present this paper and Dr Ni Ni Than, Head of Department of Chemistry, University of Yangon, for allowing me to use the research facilities. I sincerely and gratefully express my appreciation to Dr.Khin Khin Htwe, Director, Pharmaceutical Research Department, Ministry of Industry 1, for providing all the research facilities. Thanks are also due to Daw Myint Myint Lwin, Daw Cherry Aung and all staff members of the Fermentation Department, Pharmaceutical Research Department, Ministry of Industry 1, for their cooperation and help during the present research.

### References

- Atlas, R. M. (1993). *Handbook of Microbiological Media*. The United States of America: 1<sup>st</sup> Ed., CRC Press, Inc.
- Batt, C. A. (2000). *Encyclopedia of Food microbiology*. The United States of America: 1<sup>st</sup> Ed., A Harcourt Science and Technology Company
- Bisen, P. S. and Verma, K. (1998). *Handbook of Microbiology*. New Delhi: C. B. S publishers and Distributors
- Breed, R. S., Murry, E. G. D. and Smith, N. R. (1957). "Bergey's Manual of Determinative Bacteriology". Baltimore: 7<sup>th</sup> Ed., the Willians and Wilkins Company, vol. 12, pp. 505-552
- Chen, Y. S., Wu, H. C. and Yanagida, D. F. (2010). "Isolation and Characteristics of Lactic Acid Bacteria Isolated from Ripe Mulberries in Taiwan. Brazilian". *J. Microbiol*, vol. 41, pp. 916-921
- Collins, C. H., Lyne P. M. and Grange J. M. (1995). *Microbiological Methods*. London: Butterworth-Heinemann Ltd.
- Cowan, S. T. (1974). *Cowan and Steel's Manual for the Identification of Medical Bacterial*. Cambridge: 2<sup>nd</sup> Ed., Cambridge University Press.
- Cruickshank R., Guguid, J. P. and Swain, R. H. A. (1968). *Medical Microbiology*. London: 11<sup>th</sup> Ed, The English Language Book Society and F. and S. Livingstone Ltd.

- Dubey, R. C. and Maheshwari, D. K. (2002). *Practical Microbiology*. New Delhi: 1<sup>st</sup> Ed., S. Chand and Co. Ltd.
- Farnworth, E. R. (2005). "Kefir – a complex probiotic". *Food Science and Technology Bulletin: Functional Foods*. vol. 2(1), pp. 1–17
- Lim, C. H., Rahim, R. A., Ho, Y. W. and Arbakariya, B. A. (2007). "Optimization of Growth Medium for Efficient Cultivation of *Lactobacillus Salivarius* i 24 Using Response Surface Method". *Malaysian J. Microbiol.* vol. 3(2), pp. 41-47
- Oliveira, L. A. M., Miguel, M. A., Peixoto, R.S., Rosado, A. S., Silva, J. T., Paschoalin, V. M. (2013). "Microbiological, Technological and Therapeutic Properties of Kefir: A Natural Probiotic Beverage". *Brazilian J. Microbiol.* vol. 44(2), pp. 341-349
- Salle, L. (1948). *Fundamental Principles of Bacteriology*. New York: 2<sup>nd</sup> Ed., Mc. Graw Hill Book, Co., Inc.

## STUDY ON THE ANTI-ARTHRITIS PROPERTY OF *CROTON OBLONGIFOLIUS* R. (THETYIN-GYI) LEAVES BY USING PROTEIN DENATURATION METHOD

Myint Myint Khin<sup>1</sup>, Eaint Thet Myo<sup>2</sup>, May Lay Nge<sup>3</sup>, Daw Hla Ngwe<sup>4</sup>

### Abstract

Leaves of *Croton oblongifolius* R. (Thetyin-gyi) have been known to use in Myanmar traditional medicine concerning antioxidant, anti-arthritis and antimicrobial activities. Therefore, locally grown *C. oblongifolius* has been chosen for this study. This research aimed to investigate the anti-arthritis activities of the leaves of *C. oblongifolius* (Thetyin-gyi). In the present work, anti-arthritis activity and cytotoxicity of the Thetyin-gyi leaves have been determined. The sample was collected from the campus of Inya hostel in Yangon University. The cytotoxicity of watery and ethanol extracts evaluated by brine shrimp cytotoxicity bioassay gave LD<sub>50</sub> values as 921 µg/mL and 884.5 µg/mL, respectively. The LD<sub>50</sub> value of K<sub>2</sub>Cr<sub>2</sub>O<sub>7</sub> was 1.5 µg/mL and its cytotoxicity values were between 1 and 10 µg/mL. *In vitro* anti-arthritic activity of ethanol and watery extracts of leaves of Thetyin-gyi was investigated by protein denaturation method by using bovine serum albumin and egg albumin. In both methods, the ethanol extract has shown significant activity at the concentrations of 500 µg/mL and the effects were compared with the standard drug diclofenac potassium. So, the ethanol extract of *C. oblongifolius* have higher anti-arthritic activity than watery extract.

**Keywords:** *C. oblongifolius*, cytotoxicity, anti-arthritic activity and diclofenac potassium

### Introduction

*C. oblongifolius* (Euphorbiaceae) is a tree available in most places in our country. Traditionally, this plant is employed as wound healing drug in Asia. In Myanmar, the utilization of different parts of several medicinal plants to cure specific ailments has been in vogue from ancient times. These systems of drug cater to the requirement of nearly seventy percent of our population residing in the villages. In Homeopathy system, 70 % of the medicines are synthesized from the plants. Extracts of plants from 157 families have been reported to be active against microorganisms. *C. oblongifolius* is extensively used in herbal medicine in South- East Asia. It may be an important herbal drug with some important marker useful to treat some challenging diseases to marking in future life (Mandal and Bose, 2011). The present work is to study the effect of anti-arthritis property of *C. oblongifolius* leaves by protein denaturation method by using bovine serum albumin and egg albumin.

### Description and Distribution of *C. Oblongifolius*

*C. oblongifolius* is a medium sized tree, deciduous, bark brownish, branches lepidote while young. Leaves are alternate, crowded towards the ends of the branchlets (Saleem and Nawaz, 1989). Croton is a genus of Euphorbiaceae comprising around 1300 species, wide spread in tropical regions. Several species have an extended role in traditional medicine in Africa, Asia and South America. *C. oblongifolius* popularly known as 'Thetyin-gyi' in Myanmar and 'Chucka' in Hindi is middle-sized tree belonging to the family Euphorbiaceae. It grows widely in India (Bahar *et al.*, 2002).

---

<sup>1</sup> Dr, Lecturer, Department of Chemistry, University of Yangon

<sup>2,3</sup> MSc Candidates, Department of Chemistry, University of Yangon

<sup>4</sup> Dr, Professor & Head (Retd), Department of Chemistry, Yangon University

**Botanical Aspect of *C. oblongifolius* (Thetyin-gyi)**

Family	-	Euphorbiaceae
Genus	-	<i>Croton</i>
Species	-	<i>oblongifolius</i>
Botanical name	-	<i>Croton oblongifolius</i> R.
Myanmar name	-	Thetyin-gyi
Common name	-	Chucka
Part used	-	Leaves



**Figure 1** Photograph of Plant of *C. oblongifolius* (Thetyin-gyi)

**Medicinal Uses and Chemical Constituents of *C. oblongifolius* (Thetyin-gyi)**

*C. oblongifolius* is extensively used in herbal medicine in South-East Asia. *C. oblongifolius* is used to cure liver diseases, sprains, snake bites and as a purgative, insanity, convulsions, asthma, tumors, rheumatism as documented in the Indian Ayurveda medicine system. Bark is used in reducing chronic enlargement of the liver and in remittent fever. It is applied externally to the hepatic region in chronic hepatitis (Julius and Patrick, 1976).

Cembranoid diterpenes, namely crotomembraneic acid, neocrotocembraneic acid, poilaneic acid and their synthetic derivatives including methyl crotocembraneate, crotocembranol, crotocembranol, neocrotocembranal, methyl poilaneate, poilaneol and poilanal were isolated from *C. oblongifolius*. They are approximately 4-fold more active than caffeine which is a known central nervous stimulating agent (Bhowmik *et al.*, 2013).

**Materials and Methods****Sample Collection and Preparation of *C. oblongifolius* (Thetyin-gyi)**

Leaves of *C. oblongifolius* (Thetyin-gyi) were collected from the campus of Inya hostel in Yangon University. Then, the sample was identified at the Department of Botany, University of Yangon. The sample was cleaned by washing with water and air-dried at room temperature. The sample were cut into small pieces and ground into powder by using motor. The powdered samples were stored in air-tight containers.

### **Preliminary Phytochemical Investigation of Leaves of *C. oblongifolius* R. (Thetyin-gyi).**

Phytochemical tests for leaves of *Croton oblongifolius* Roxb. (Thetyin-gyi) was carried out according to the reported methods to investigate the presence and absence of phytochemical constituents such as alkaloids,  $\alpha$ -amino acids, carbohydrates, cyanogenic glycosides, organic acids, flavonoids, glycosides, organic acids, phenolic compounds, reducing sugars, saponins, starch, steroids, tannins and terpenoids.

### **Preparation of Ethanol and Watery Extracts from *C. oblongifolius* R.**

#### **(Thetyin-gyi)**

The dried powder sample (100 g) was percolated with 95 % ethanol (500 mL) for one week and filtered. This procedure was repeated for three times. The combined filtrate containing plant constituents were evaporated under reduced pressure by means of a rotary evaporator. Consequently, 95 % ethanol soluble extract was obtained. Watery extract was prepared by boiling 100 g of sample with 500 mL of distilled water for 6 h and filtered. It was repeated three times and the filtrates were combined followed by heating on water bath and sand bath to give watery extract. Each extract was stored in refrigerator for screening of biological activities.

### **Determination of Cytotoxicity by Brine Shrimp Lethality Bioassay of *C. oblongifolius* (Thetyin-gyi)**

Artificial sea water (9 mL), (1 mL) of different concentrations of samples and standard solutions were added to each chamber of ice tray. Alive brine shrimp (10 nauplii) were taken with pasteur pipette and placed into each chamber. They were incubated at room temperature about 24 h. After 24 h, the number of dead or survive brine shrimp was counted and 50 % of lethality dose (LD<sub>50</sub>) was calculated (Sahagal *et al.*, 2010).

### **Investigation of Anti-arthritis Activity of Leaves of *C. oblongifolius* (Thetyin-gyi) by Protein Denaturation Method**

The *in vitro* anti-arthritis activity was studied by protein denaturation method using Bovine Serum Albumin and Egg Albumin (Rahman *et al.*, 2012). Test solution 0.05 mL of different concentrations (500, 250 and 125  $\mu$ g/mL) and standard drug diclofenac potassium 0.05 mL of different concentrations (500, 250 and 125  $\mu$ g/mL) were mixed with (0.5 % v/v) aqueous solution of BSA (0.45 mL). Then, the samples were incubated at 37 °C for 30 min followed by incubation at 57 °C for 3 min. 2.5 mL of phosphate buffer (pH 6.3) was added to all the above samples after cooling. UV-visible spectrophotometer was used to measure the absorbance at 660 nm. The control represents 100 % protein denaturation. The percentage inhibition of protein denaturation was calculated by the following formula:

$$\text{Percent inhibition} = \frac{\text{Abs}_{\text{Control}} - \text{Abs}_{\text{Treated}}}{\text{Abs}_{\text{Control}}} \times 100 \%$$

The reaction mixture (5 mL) consisted of 0.2 mL of egg albumin, 2.8 mL of phosphate buffered saline (pH 6.4) and test solution of different concentrations (500, 250 and 125  $\mu$ g/mL) or standard drug diclofenac potassium 0.05 mL of different concentrations (500, 250 and 125  $\mu$ g/mL) were mixed to form a reaction mixture of 5 mL. Double distilled water of same volume served as control. The samples were incubated at 37 $\pm$ 2 °C in an incubator for 15 min followed by heating at 70 °C for 5 min. UV-Visible spectrophotometer was used to measure the absorbance at 660 nm. The percentage inhibition of protein denaturation was calculated by the following formula:

$$\text{Percent inhibition} = \frac{\text{Abs}_{\text{Control}} - \text{Abs}_{\text{Treated}}}{\text{Abs}_{\text{Control}}} \times 100 \%$$

## Results and Discussion

### Preliminary Phytochemical Tests on the Leaves of *Croton oblongifolius* R. (Thetyin-gyi)

A literature survey indicated that a more systematic work needs to be carried out on the preliminary phytochemical studies of the leaves of *Croton oblongifolius* R. (Thetyin-gyi). The results of the preliminary phytochemical screening revealed the presence of alkaloids,  $\alpha$ -amino acids, flavonoids, glycosides, phenolic compounds, reducing sugars, saponins, starches, steroids, tannins and terpenoids supporting the reason of its biological activities.

### Cytotoxicity of Watery and Ethanol Extracts of Leaves of *C. oblongifolius* (Thetyin-gyi)

The cytotoxicity of watery and ethanol extracts of leaves of *C. oblongifolius* (Thetyin-gyi) was evaluated by brine shrimp cytotoxicity bioassay. This assay is a simple, high throughput cytotoxicity test of bioactive chemicals. It is based on the killing ability of test sample on a simple zoological organism-brine shrimp (*Artemiasalina*). It is a preliminary toxicity screen for further experiments on mammalian animal models. The cytotoxicity of crude extracts was expressed in terms of mean  $\pm$  SEM (standard error mean) and LD<sub>50</sub> (50 % Lethality Dose) and the results are shown in Table 1.

In this experiment, potassium dichromate (K<sub>2</sub>Cr<sub>2</sub>O<sub>7</sub>) and caffeine were used as standard. Potassium dichromate is generally used as the positive control for this brine shrimp bioassay and caffeine, a natural product, DMSO and artificial sea water, as negative control. The nauplii were counted against a lighted background after 24 h initiation of test. From these results, LD<sub>50</sub> values of watery and ethanol extracts of Thetyin-gyi were 921  $\mu$ g/mL and 884.5  $\mu$ g/mL respectively. Standard caffeine did not show cytotoxicity until 1000  $\mu$ g/mL concentration whereas LD<sub>50</sub> of standard K<sub>2</sub>Cr<sub>2</sub>O<sub>7</sub> was 1.5  $\mu$ g/mL.

**Table 1 Cytotoxicity of Different Doses of Watery and Ethanol Extracts of the Leaves of *C. oblongifolius* (Thetyin-gyi)**

Sample	Percent Survival of Brine Shrimp (Mean $\pm$ SEM) at Various Concentrations ( $\mu$ g/mL)				LD <sub>50</sub> ( $\mu$ g/mL)
	1	10	100	1000	
watery	26.03 $\pm$ 12.33	29.47 $\pm$ 6.694	31.11 $\pm$ 1.925	51.85 $\pm$ 10.5	921
ethanol	27.3 $\pm$ 6.757	28.97 $\pm$ 3.806	32.82 $\pm$ 4.885	53.33 $\pm$ 5.774	884.5
*K <sub>2</sub> Cr <sub>2</sub> O <sub>7</sub>	48.63 $\pm$ 19.19	73.13 $\pm$ 4.076	74.67 $\pm$ 11.8	100 $\pm$ 0	1.5
**Caffeine	0 $\pm$ 0	0 $\pm$ 0	9.582 $\pm$ 0.917	12.73 $\pm$ 4.103	>1000

\* = Standard for positive control

\*\* = Standard for negative control

### *In Vitro* Anti-arthritic Activity of Leaves of *C. oblongifolius* (Thetyin-gyi)

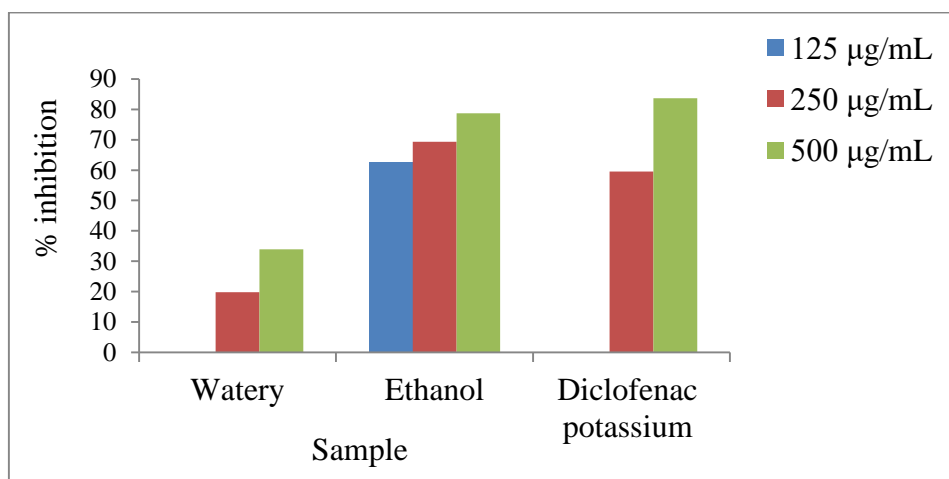
Arthritis is a type of joint disorder that involves inflammation of one or more joints, accountable for pain, swelling, stiffness, loss of function in joint. One of the main reasons of the arthritis is denaturation of protein. In certain arthritic diseases, auto antigen is produced due to the denaturation of protein. The mechanism of denaturation is probably involved in the alteration of electrostatic hydrogen, hydrophobic and disulphide bonding. In the present study, protein denaturation method (using bovine serum albumin and egg albumin) were selected for *in vitro* assessment of anti-arthritic activity of watery and ethanol extracts of leaves of *C. oblongifolius* (Thetyin-gyi). The standard anti-arthritic activity drug; diclofenac potassium was used for these tests. The absorbance at different concentrations (500, 250 and 125  $\mu$ g/mL) of tested samples was measured at 660 nm on a UV-visible spectrophotometer.

The *in vitro* anti-arthritic activity of watery and ethanol extracts of *C. oblongifolius* by protein denaturation method using bovine serum albumin was shown in Table 2 and Figure 2. The watery and ethanol extracts of *C. oblongifolius* and diclofenac potassium was tested at different concentrations for anti-arthritic activity and found significant percentage inhibition in protein denaturation. The maximum anti-arthritic activity was observed at the concentration of 500 µg/mL while the minimum activity was observed in the concentration of 125 µg/mL. According to the result, the percentage of arthritic protection was found to be 78.71 % in ethanol, 33.91 % in watery extracts and 83.66 % in diclofenac potassium at the concentration of 500 µg/mL in bovine serum albumin denaturation method. Both extracts exhibited dose dependent response. Similar type of results was observed in the protein denaturation method using egg albumin is shown in Table 3 and Figure 3. According to the result, the inhibition percentage of protein denaturation of egg albumin was found to be 53.02 % in ethanol, 36.12 % in watery extracts and 87.41 % in diclofenac potassium at the concentration of 500 µg/mL.

From this result, it can be stated that these extracts are capable of controlling the production of auto antigen to inhibit the denaturation of protein. The percent inhibition of protein denaturation of leaves of *Thetyin-gyi* and reference drug with respect to control indicated the stabilization of albumin protein. This anti-denaturation effect was further supported by the change in viscosities. It has been reported that the viscosities of protein solutions increase on denaturation.

**Table 2 Anti-arthritic Activity of Watery and Ethanol Extracts of Leaves of *C. oblongifolius* (*Thetyin-gyi*) by Protein Denaturation Method (Using Bovine Serum Albumin)**

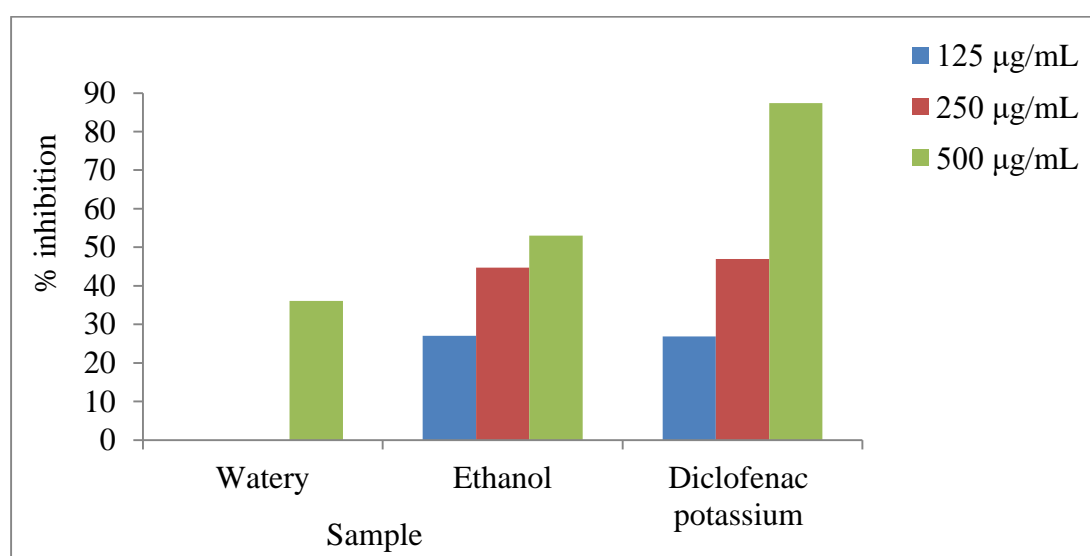
Extracts	Concentration (µg/mL)	Absorbance at 660 nm	% Inhibition
Control		0.202	
Watery	125	-	-
	250	0.16	19.8
	500	0.13	33.91
Ethanol	125	0.07	62.62
	250	0.06	69.30
	500	0.04	78.71
Diclofenac potassium	125	-	-
	250	0.08	59.57
	500	0.03	83.66



**Figure 2** % Inhibition of protein denaturation of leaf extracts and standard diclofenac potassium by using bovine serum albumin

**Table 3** Anti-arthritic Activity of Watery and Ethanol Extracts of Leaves of *C. oblongifolius* (Thetyin-gyi) by Protein Denaturation Method (Using Egg Albumin)

Extracts	Concentration ( $\mu\text{g/mL}$ )	Absorbance at 660 nm	% Inhibition
Control	-	0.596	
Watery	125	-	-
	250	-	-
	500	0.13	36.12
Ethanol	125	0.43	27.01
	250	0.32	44.71
	500	0.28	53.02
Diclofenac potassium	125	0.43	26.84
	250	0.31	46.97
	500	0.07	87.41

**Figure 3** % Inhibition of protein denaturation of leave extracts and standard diclofenac potassium by using egg albumin

### Conclusion

The result of preliminary phytochemical screening of different crude extracts of leaves of *C. oblongifolius* R. (Thetyin-gyi) revealed the presence of alkaloids,  $\alpha$ -amino acid, glycosides, phenolic compounds, saponins, steroids, tannins, terpenoids and flavonoids supporting the reason of its biological activities. The cytotoxicity of watery and ethanol extracts of leaves of Thetyin-gyi evaluated by brine shrimp cytotoxicity bioassay gave  $\text{LD}_{50}$  values as 921  $\mu\text{g/mL}$  and 884.5  $\mu\text{g/mL}$ , respectively. The  $\text{LD}_{50}$  value of  $\text{K}_2\text{Cr}_2\text{O}_7$  was 1.5  $\mu\text{g/mL}$  between 1 and 10  $\mu\text{g/mL}$ . Caffeine was not cytotoxic to brine shrimp up to the maximum dose of 1000  $\mu\text{g/mL}$ . Therefore, watery extract showed lower cytotoxicity effect than the ethanol extract. *In vitro* anti-arthritic activity, ethanol and watery extracts of leaves of Thetyin-gyi were investigated by protein denaturation method using bovine serum albumin and egg albumin. In both methods, the ethanol extract showed significant activity at the concentrations of 500  $\mu\text{g/mL}$  and the effects were comparable with the standard drug diclofenac potassium. So, the ethanol extract of *C. oblongifolius* have higher anti-arthritic activity than watery extract

## Acknowledgements

The authors would like to thank the Department of Higher Education, Ministry of Education, Yangon, Myanmar, for the permission of doing this research and also to the Myanmar Academy of Arts and Science for allowing the present of this paper.

## References

- Bahar, A., Tanveer, A., Manoj, V. and Shah, A. K. (2002). "Hepatoprotective Activity of Two Plants Belonging to the Apiaceae and the Euphorbiaceae Family". *Journal of Ethanopharmacology*, vol. 79, pp. 313-316
- Bhowmik, S., Datta, B. K., Sunrit, B. S. and Mandal, N. C. (2013). "Contribution to the Less Known Ethnomedicinal Plants Used by Munda and Sental Community of India with Their Ethnomedicinal Justification". *World Applied Sciences Journal*, vol. 23 (10), pp. 1408-1417
- Dudonne, S., Vitrac, X., Coutiere, P., Woillez, M. and Merillon, J. M. (2009). "Comparative Study of Antioxidant Properties and Total Phenolic Contents of 30 Plant Extracts of Industrial Interest Using DPPH, ABTS, FRAP, SOD and ORAC Assays". *J. Agric. Food Chem*, vol. 57, pp. 1768-1770
- Julius, T. M. and Patrick, V. D. (2011). "Why do Euphorbiaceae Tick as Medicinal Plants? A review of Euphorbiaceae Family and its Medicinal Features". *Journal of medicinal Research*, vol. 5 (5), pp. 652-662
- Maizura, M., Aminah, A. and Aida, W. M. W. (2011). "Total Phenolic content and Antioxidant activity of Kesum (*Polygonum Minus*), (*Zingiber Officinale*) and turmeric (*Curcuma longa*) Extract". *International Food Research Journal*, vol. 18 (2), pp. 529-534
- Mandal, L. and Bose, S. (2011). "Pharmacognostic Standardization and Quantitative Estimation of some Isolated Phytoconstituents from *Croton oblongifolius* Roxb.". *Journal of Pharmasci Tech.*, vol. 1(1), pp. 10-15
- Rahman, H., Eswaraiah, M. C. and Dutta, A. M. (2015). "In Vitro Anti-inflammatory and Anti-arthritis Activity of *Oryza sativa* Var. Joha Rice (An Aromatic Rice of Assam)". *American-Eurasian J. Agric. And Environ*, vol. 15(1), pp. 115-121
- Manaf, Y. N. A., Marikkar, J. M. N., Long, K. and Ghazali, H. M. (2013). "Physico-Chemical Characterization of the Fat from Red-Skin Rambutan (*Nephelium Lappaceum* L.) Seed", *Journal of Oleo Science*, vol. 62 (6), pp. 335-343
- Mandal, A. and Reddy, P. J. M. (2016). "In vitro Alpha Amylase Inhibitory Activity of Ethanol and Hot Water Extracts of Polyherbal Formulation". *World Journal Pharmaceutical Research*, vol. 5 (1), pp. 968-971
- Sahagal, G., Ramanathan, S., Sasidharan, S., Mordic, S. M. S., Ismailu, S. (2010). "A Cute Oral Toxicity Studies on *Swietenia Mahagoni* (Linn). Jacq. Seed Methanolic Extract", *Pharmacognosy Res.*, vol. 2, pp. 215-220
- Saleem, R. B. and Nawaz, R., (1989). "Preliminary Phytochemical Screening of Four Common Plants of Family Caesalpimaceae". *Pakistan Journal of Pharmaceutical Sciences*, vol. 2(1), pp. 55-57
- Saxena, M., Saxena, J., Nema, R., Singh, D. and Gupta, A. (2013). "Phytochemical of Medicinal Plants". *Journal of Pharmacognosy and Phytochemistry*, vol. 1(6), pp. 168-172

## INVESTIGATION OF $\alpha$ -GLUCOSIDASE INHIBITON AND ANTIOXIDANT ACTIVITIES OF *HYDROCOTYLE ROTUNDIFOLIA* ROXB. (SAY-MYIN-KHWA)

Khin Chaw Win<sup>1</sup>, Yin Thein<sup>2</sup>, Ni Ni Than<sup>3</sup>, Daw Hla Ngwe<sup>4</sup>

### Abstract

This research is focused on the evaluation of  $\alpha$ -glucosidase inhibitory effect from Myanmar Traditional Medicinal Plants *Hydrocotyle rotundifolia* Roxb. (Say-myin- khwa). The medicinal plant has been reported to possess the antidiabetic potential. According to the preliminary phytochemical tests indicated the presence of alkaloids,  $\alpha$ -amino acids, carbohydrates, flavonoids, glycosides, phenolic compounds, steroids, terpenoids, tannins, reducing sugars, and saponins were present while starch was not detected in this sample. The  $\alpha$ -glucosidase inhibitory effect of watery and ethanol extracts on production of glucose from sucrose was determined by using UV-Visible spectroscopy. The 50 % inhibitory concentrations ( $IC_{50}$ ) of watery and ethanol extracts on  $\alpha$ -glucosidase activity were found to be 0.73 and 0.61  $\mu\text{g/mL}$ . From this experiment, it was found that ethanol extract showed higher potency than water extract. However, all of these extracts showed lower potency than that of standard drugs Voglibose ( $IC_{50} = 0.32 \mu\text{g/mL}$  in  $\alpha$ -glucosidase inhibitory effect. The antioxidant activity of ethanol and watery crude extracts was investigated by DPPH free radical scavenging assay. The  $IC_{50}$  values of watery and ethanol crude extracts were 12.34  $\mu\text{g/mL}$  and 9.33  $\mu\text{g/mL}$ . Since the lower  $IC_{50}$  value, the higher antioxidant activity of the samples occurs. Thus, the ethanol extract showed higher antioxidant activity than that water extract.

**Keywords:** *Hydrocotyle rotundifolia* Roxb.,  $\alpha$ -glucosidase inhibitory effect, antioxidant activity

### Introduction

The systematic name of  $\alpha$ -glucosidase glucohydrolase, (E.C 3.2.1.20), hydrolytic enzymes splitting both  $\alpha$ -1, 4 and  $\alpha$ -1, 6-glucosidic linkages are usually termed  $\alpha$ -glucosidase. Mammalian  $\alpha$ -glucosidase located in the brush-border surface membrane of intestinal cells is the key enzyme catalyzing the final step in the digestive processes of carbohydrate. Hence,  $\alpha$ -glucosidase inhibitors can retard the liberation of D-glucose from dietary complex carbohydrates and delay glucose absorption, resulting in reduced postprandial plasma glucose level and suppression of postprandial hyperglycemia. To control or to manage postprandial hyperglycemia,  $\alpha$ -glucosidase inhibitors are used  $\alpha$ -glucosidase inhibitor, a class of anti-diabetic drugs is known as “starch blocker”. Taken with the first bite of a meal  $\alpha$ -glucosidase inhibitors are especially well suited to treat postprandial hyperglycemia (a sharp rise in blood sugar after meals) a common and serious problem faced by many people with type 2-diabetes. Acarbose, miglitol, voglibose and emiglitate have been approved to use as antidiabetes drugs. Because the drug prevents the immediate breakdown of starches into monosaccharides or simple sugars, which would be absorbed into the blood stream quickly, more of the carbohydrate consumed at meal gets absorbed further “downstream” in the gastrointestinal tract, towards the end of the small intestine or the colon. Slowing the absorption of carbohydrate gives the beta-cells in the pancreases more time to secrete adequate insulin to cover the meal.  $\alpha$ -Glucosidase enzyme are widely distributed in microorganism, plants and animals (Hong *et al.*, 2008). From this point of view, many efforts have been made searching for effective and safe  $\alpha$ -glucosidase inhibitors from natural materials in order to develop a physiological functional food for use against antidiabetes. In this study, traditional medicinal

---

<sup>1</sup> Dr, Lecturer, Department of Chemistry, University of Yangon

<sup>2</sup> Student, MSc (2010-11), Department of Chemistry, University of Yangon

<sup>3</sup> Dr, Professor (Head), Department of Chemistry, University of Yangon

<sup>4</sup> Dr, Professor and Head, (Retd.), Department of Chemistry, University of Yangon

plant (Figure 1) *H. rotundifolia* Roxb. (Say-myin-khwa) was chosen for the investigation of some phytochemical composition and some biological activities of its ethanol and watery extracts.



Scientific name - *H. rotundifolia* Roxb.  
 Family - Umbelliferae  
 English name - Lawn Pennyword  
 Myanmar name - Say-myin-khwa  
 Part uses - Whole plant  
 (Sultana & Khatun, 2010)

**Figure 1** Plant of *H. rotundifolia*

## Materials and Methods

### Collection and Preparation of Sample

The sample of *H. rotundifolia* Roxb. (Say-myin-khwa) plant was collected from Hmawbi Township, Yangon Region in October, 2011. The plant was identified by the authorized botanist, at Botany Department, Yangon University. The collected plants samples were cleaned by washing thoroughly with water and air-dried at room temperature. The dried samples were cut into small pieces and ground into powder by a grinding machine. The dried powdered samples were stored in air-tight containers.

### Phytochemical Investigation

The dried powdered samples were used for the chemical tests on the phytochemicals by using standard procedure (Harborne, 1984; M-Tin Wa, 1972; Marini-Bettolo *et al.*, 1981; Robinson, 1983; Shriner *et al.*, 1980; Trease and Evans, 1980; Vogel, 1966).

### Isolation and Identification of $\alpha$ -Glucosidase Enzyme from Flint Corn Seeds

Ingeminated seeds of flint corn (100 g) were powdered by using a blender. The powder obtained was then suspended with 140 mL of 0.1 M acetate buffer (pH 5). After the suspended had been stirred with magnetic stirrer for 5 h at room temperature, it was filtered by using thin cloth and 817 mL of pale yellow crude extract was obtained. About 204.3 g of solid ammonium sulphate were added to the crude extract under stirring. The resulting precipitate was removed by centrifuging at 10,000 rpm for 20 min. The supernatant was obtained as first filtrate. Subsequently, 188 g of solid ammonium sulphate were slowly added to the supernatant. The resulting precipitate was collected by the centrifuge at 12,000 rpm for 15 min and dried at room temperature. The crude enzyme precipitate was obtained. The supernatant is called second filtrate which was discarded. The extracted  $\alpha$ -glucosidase enzyme was identified as follows. 1 mL of starch and 1 mL of distilled water were added into the first test tube and allowed to stand for 30 min. Then 1 mL of iodine was added and deep blue colour was observed. In the second test tube, 1 mL of starch and 1 mL of enzyme were mixed and allowed to stand for 30 min. Then 1 mL of iodine was added. No colour was observed (Aung Myint, 1997).

### Screening of $\alpha$ -Glucosidase Inhibitory Effect of Plant Extracts

The enzyme inhibition assay is based on the breakdown of substrate to produce a colour product, followed by measuring the absorbance over a period of time. In this experiment, the  $\alpha$ -glucosidase inhibition activity of 95 % ethanol and watery extracts from selected plant was

studied by determining the  $\alpha$ -glucosidase inhibitory effect on the production of glucose from sucrose at 505 nm wavelength. This experiment was done in triplicate for each sample solution. Absorbance values obtained were used to calculate % inhibition and 50 % inhibitory concentrations (Astumi *et al.*, 1990; Cannel *et al.*, 1987; Kurihara *et al.*, 1994; Xiao and Rongli, 2005).

### Preparation of test sample solution

2 mg of each extract or each isolated compound and 10 mL of distilled water were thoroughly mixed by vortex mixer. The mixture solution was filtered and the stock solution was obtained.

### Procedure

Firstly, the control solution was prepared by mixing 1 mL of sucrose, 1 mL of enzyme and 1 mL of DMSO with vortex mixer and incubated for 30 min at 37 °C followed by addition of glucose oxidase reagent (0.5 mL). After the incubation of the above mixture at 37 °C for 30 min, the reaction was stopped by immersing the test tube into a boiling water bath for 10 min and allowed to cool to room temperature. Secondly, the background solution was prepared by mixing 1 mL of sucrose 1 mL of 6 % DMSO with vortex mixer according to the above procedure. Finally, the test solution was prepared by mixing 1 mL of sucrose, 1 mL of sample solution and 1 mL of 6 % DMSO with vortex mixer and incubated for 30 min at 37 °C followed by addition of 1 ml of enzyme. After the incubation of the above mixture at 37 °C for 30 min, glucose oxidase reagent (0.5 mL) was added. After the incubation of the above mixture at 37 °C for 30 min, the reaction was stopped by immersing the test tube into a boiling water bath for 10 min and allowed to cool to room temperature. The different concentrations (0.125, 0.25, 0.5, 1.0, 2.0  $\mu\text{g}/\text{mL}$ ) of the sample solution were used. Absorbance of all solutions was measured by using a UV-7504 spectrophotometer at 505 nm. Voglibose is an  $\alpha$ -glucosidase inhibitor used for lowering postprandial blood glucose levels in people with diabetes mellitus was used as a reference.

Absorbance measurements were done in triplicate for each of the sample solutions. From the mean absorbance values, percent inhibition of the sample on  $\alpha$ -glucosidase enzyme activity and average percent inhibition on  $\alpha$ -glucosidase enzyme activity were calculated by using following equations (Yuhao, 2004):

$$\% \text{ inhibition} = \frac{A_c - A - A_b}{A_c} \times 100$$

where,

% Inhibition = percent inhibition of test sample on  $\alpha$ -glucosidase enzyme activity

$A_c$  = absorbance of control solution

$A_b$  = absorbance of background solution

A = absorbance of test sample solution

The  $IC_{50}$ , 50 % inhibitory concentration of the sample on  $\alpha$ -glucosidase enzyme activity was calculated by Linear Regressive Excel Program.

### Determination of Antioxidant Activity by DPPH Radical Scavenging Assay

The antioxidant activity of ethanol and water extracts of plant material was assayed according to a published method with slight modification (Marinova and Batchvarov, 2011). The commercially available DPPH (2, 2-diphenyl picrylhydrazyl) is a stable free radical, which is purple in colour. The antioxidant molecule presents in the test extracts, when incubated react with DPPH and convert it into di-phenyl hydrazine, which is yellow in colour. For the preparation of

the coloured reaction, the sample extract with the concentration of 1000 µg/mL was prepared by dissolving 20 mg of the extract in ethanol or water and the final volume was made up to 20 mL (the preparation was used as a stock solution). Then different concentrations like 5 µg/mL, 10 µg/mL, 20 µg/mL, 40 µg/mL and 80 µg/mL were prepared by dilution with ethanol or water from the stock solution. The control solution was prepared by mixing 1.5 mL of 0.002 % DPPH solution and 1.5 mL of ethanol in the brown bottle. The sample solution was prepared by mixing 1.5 mL of 0.002 % DPPH solution and 1.5 mL of test sample solution. These bottles were incubated at room temperature and were shaken on a shaker for 30 min.

The absorbance for the degree of discoloration of purple to yellow was measured at 517 nm against ethanol as blank. Ascorbic acid was used as a standard. Each experiment was done triplicate. The DPPH radical scavenging activity of the plant extracts were calculated by the following formula:

$$\% \text{ RSA} = [ \{ (A_{\text{DPPH}} - A_{\text{sample}}) - A_{\text{blank}} \} / A_{\text{DPPH}} ] \times 100$$

where,

% RSA = % radical scavenging activity of test sample

$A_{\text{DPPH}}$  = absorbance of DPPH in EtOH solution

$A_{\text{Sample}}$  = absorbance of sample + DPPH solution

$A_{\text{blank}}$  = absorbance of sample + EtOH solution

IC<sub>50</sub> is defined as the concentration of substrate that causes 50 % loss of DPPH activity (colour).

## Results and Discussion

### Phytochemical Constituents Present in *H. rotundifolia*

According to the experiments, alkaloids, α-amino acids, carbohydrates, flavonoids, glycosides, phenolic compounds, steroids, tannins, terpenoids, reducing sugars, saponins and organic acids were found to be present while starch was not detected. In addition, alkaloids, α-amino acids, carbohydrates, flavonoids, glycosides, steroids, terpenoids, reducing sugar and organic acids were found to be present in larger amount in this sample.

### *In Vitro* α-Glucosidase Inhibitory Effect of Crude Extracts of *H. rotundifolia*

*In vitro* α-glucosidase inhibitory effects of watery and 95 % ethanol extracts from *H. rotundifolia* plants were determined by using α-glucosidase inhibition assay. In this method, α-glucosidase enzyme can produce the glucose and fructose from sucrose by enzymatic hydrolysis. Therefore, the presence or absence of α-glucosidase enzyme inhibition effect of a sample can be demonstrated by the enzyme inhibition effect of a sample can be demonstrated by the enzymatic production of glucose from the substrate sucrose.

If glucose is not produced from sucrose by α-glucosidase in the presence of the herbal extracts, it can be inferred that the sample has the α-glucosidase inhibitory effect, i.e., it is an enzyme inhibitor. If the glucose is still formed from the sucrose by α-glucosidase enzyme in the presence of the herbal extracts, the herbal may not possess the α-glucosidase inhibitory effect. The formation of glucose can be quantitatively determined by using UV-Visible spectrophotometric technique. If the glucose amount increases, the absorbance of the red pigment will be increased. Hence, the lower the absorbance value, the lower the glucose content. The absorbance of the red pigment formed from the glucose that produced from sucrose by α-glucosidase enzymatic hydrolysis, was found to be higher than that for the glucose produced from sucrose by α-glucosidase enzymatic hydrolysis in the presence of plant extracts. This observation showed that the extracts inhibited the α-glucosidase enzyme activity. From the mean

absorbance values, the percent inhibition of the crude extracts and reference drug (Voglibose) in various concentration: 0.125, 0.25, 0.5, 1.0, 2.0  $\mu\text{g/mL}$  on  $\alpha$ -glucosidase enzyme activity were calculated and it was found that the % inhibition of the samples on  $\alpha$ -glucosidase enzyme activity increased with increasing the concentrations. From the % inhibition, the respective  $\text{IC}_{50}$  values of the plants extracts were calculated and the results are respectively tabulated in Table 1.

According to the results shown in Table 1, it can be seen that the 50 % inhibition concentration ( $\text{IC}_{50}$ ) values for the ethanol extract (0.61  $\mu\text{g/mL}$ ) and watery extract (0.73  $\mu\text{g/mL}$ ) from Say-myin-khwa plant. Since the lower the  $\text{IC}_{50}$  values indicate the higher the  $\alpha$ -glucosidase inhibitory effect of the samples. Alpha-glucosidase inhibitory effect of ethanol extract showed higher potency than that of watery extract. But it was observed that the watery and ethanol extracts of plant samples showed lower potency than standard drug Voglibose ( $\text{IC}_{50} = 0.32 \mu\text{g/mL}$ ) in  $\alpha$ -glucosidase inhibitory effect. These observations are depicted with a bar graph in Figure 2.

**Table 1 % Inhibition of Various Concentrations and  $\text{IC}_{50}$  Values of Different Crude Extracts from *H. rotundifolia* and Standard Voglibose on  $\alpha$ -Glucosidase Enzyme Activity**

Tested Sample	% inhibition of different concentrations ( $\mu\text{g/mL}$ )					$\text{IC}_{50}$ ( $\mu\text{g/mL}$ )
	0.125	0.25	0.5	1.0	2.0	
Water extract	41.77	45.68	47.04	53.37	61.71	0.73
	$\pm$	$\pm$	$\pm$	$\pm$	$\pm$	
	0.02	0.11	0.03	0.21	0.01	
Ethanol extract	39.87	47.46	49.57	51.47	65.66	0.61
	$\pm$	$\pm$	$\pm$	$\pm$	$\pm$	
	0.35	0.12	0.03	0.01	0.05	
Standard Voglibose	31.06	48.22	55.41	58.33	64.39	0.32
	$\pm$	$\pm$	$\pm$	$\pm$	$\pm$	
	0.01	0.02	0.01	0.03	0.02	

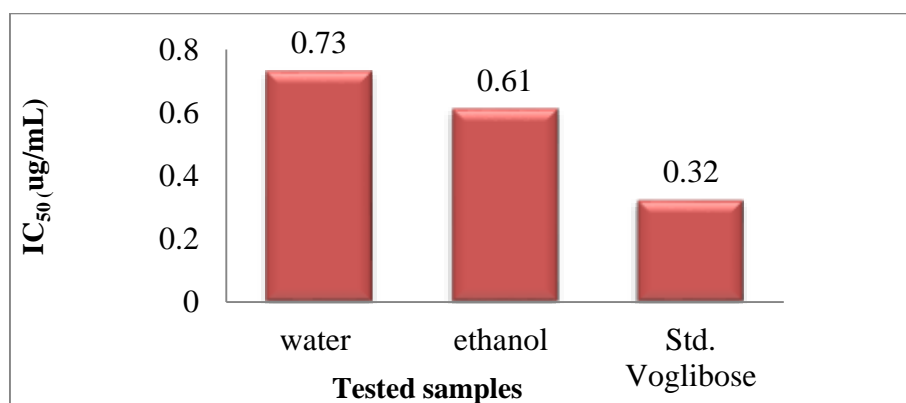


**Figure 2**  $\text{IC}_{50}$  values of water and ethanol extracts from compared with standard voglibose on  $\alpha$ -glucosidase enzyme activity

### Antioxidant Activity of Crude Extracts of *H. rotundifolia* by DPPH Free Radical Scavenging Assay

The antioxidant activity was studied on the watery and 95 % ethanol extracts from two selected plant samples by DPPH free radical scavenging assay method. DPPH (2, 2 – diphenyl -1- picryl hydrazyl) method is most widely reported method for screening of antioxidant activity of many plant drugs. This method is based on the reduction of ethanolic solution of

coloured free radical DPPH by free radical scavenger. Determination of radical scavenging activity by DPPH method bases on the change in absorbance of sample solution in various concentrations. The activity was expressed as 50 % inhibitory concentration ( $IC_{50}$ ).

The present study was carried out to investigate the radical scavenging activity of two crude extract such as ethanol, water from plant of *H. rotundifolia* by using DPPH according to the spectrophotometric method. In this experiment, five kind of different concentrations for each crude extract were prepared with ethanol solvent. The percent inhibition values and  $IC_{50}$  values of crude extracts were measured at different concentrations and the results were summarized in Table 2. And also the  $IC_{50}$  values was shown in Figure 3. From these experimental results, for all extracts, it was found that as the concentrations increased, the absorbance values decreased, i.e., increase in concentration, increase in radical scavenging activity of crude extracts usually expressed in term of % inhibition. Form the average values of % inhibition,  $IC_{50}$  (50 % inhibition concentration) values in  $\mu\text{g/mL}$  were calculated by linear regressive excel program.

From these results, it can be clearly seen that  $IC_{50}$  values were 12.34  $\mu\text{g/mL}$  for water extract and 9.33  $\mu\text{g/mL}$  for ethanol extract. Among these extracts, radical scavenging activity of ethanol extract was found to be the higher than water extract and it was also found to be lower than that of standard ascorbic acid ( $IC_{50} = 5.94 \mu\text{g/mL}$ ).

**Table 3 Radical Scavenging Activity (% RSA) and  $IC_{50}$  Values of Crude extracts of from *H. rotundifolia* and Standard Ascorbic acid**

Tested Sample	% inhibition of different concentrations ( $\mu\text{g/mL}$ )					$IC_{50}$ ( $\mu\text{g/mL}$ )
	5	10	20	40	80	
Water extract	39.77	48.68	54.32	62.32	68.35	12.34
	$\pm$ 0.52	$\pm$ 0.31	$\pm$ 0.23	$\pm$ 0.12	$\pm$ 0.21	
Ethanol extract	42.06	51.22	67.35	72.43	78.34	9.33
	$\pm$ 0.11	$\pm$ 0.32	$\pm$ 0.30	$\pm$ 0.21	$\pm$ 0.11	
Std. Ascorbic acid	48.32	57.23	55.41	58.33	62.78	5.94
	$\pm$ 0.25	$\pm$ 0.02	$\pm$ 0.51	$\pm$ 0.43	$\pm$ 0.12	

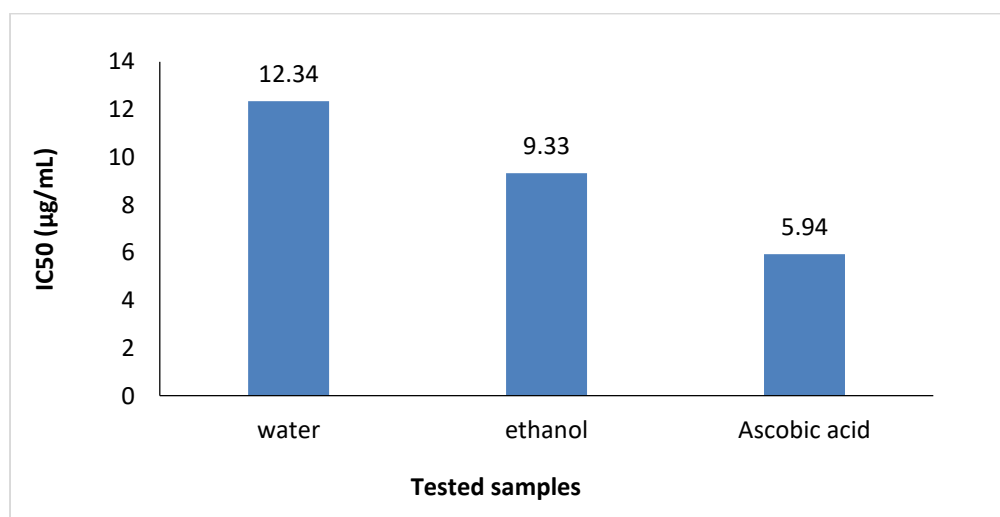


**Figure 3**  $IC_{50}$  values of water and ethanol extracts compared with standard ascorbic acid in antioxidant activity

## Conclusion

From these observations it can be suggested that selected medicinal plants was generally found to possess  $\alpha$ -glucosidase inhibitory effect. Therefore, *H. rotundifolia* plant may be used as  $\alpha$ -glucosidase inhibitor in control or managements of the postprandial hyperglycemia, Type 2 diabetes. The findings from the present work will contribute to the scientific development of Myanmar traditional medicine, specifically in the areas concerned with diabetes mellitus,  $\alpha$ -glucosidase inhibitory effect, the diseases related to oxidative stress.

## Acknowledgements

The authors would like to express profound gratitude to the Department of Higher Education (Lower Myanmar), Ministry of Education, Yangon, Myanmar, for provision of opportunity to do this research and Myanmar Academy of Arts and Science for giving permission to submit this paper.

## References

- Astumi, S.K., Umezawa, H. and Iinuma, H. (1990). "Production, Isolation and Structure Determination of a Novel  $\beta$ -Glucosidase Inhibitor, Cyclophellitol". *Phellinussp J. Antibiot.*, vol. 43(1), pp. 49-53
- Aung Myint, (1997). "Study on Flint Corn  $\alpha$ -Glucosidase", MSc Thesis, Department of Chemistry, Yangon University, pp. 31-58
- Cannel, R.T, Kellam, S.J. and Owsianka, A.M. (1987). "Microalgae and Cyanobacteria as a Source of Glycosidase Inhibitor". *J. Gen Microbiol.*, vol. 133, pp. 1701-1705
- Harborne, J.B. (1989). *Phytochemical Methods, A Guide to Modern Techniques of Plant Analysis*. New York: 2<sup>nd</sup> Ed., Chapman and Hall, pp. 120-160
- Hong, G., Hung, Y.N., Gao, B. and Kawabata, J. (2008). "Chebulagic Acids is a Potent  $\alpha$ -glucosidase Inhibitor". *Biotechno. Biochem*, vol. 72(2), pp. 601–603
- Kurihara, H., Sasaki, M. and Hatano, M. (1994). "A New Screening Method for Glucosidase Inhibitors and its Application to Algal Extracts". *Fisheries Science*, vol. 60(6), pp. 759-761
- Marini-Bettolo, G.B., Nicoletti, M., Patamia, M., Galeffi, C. and Messana, I. (1981). "Plant Screening by Chemical and Chromatography Procedure under Field Conditions." *Journal of Chromatography*, vol. 231 (1), pp. 113-127
- Marinova, G. and Batchvaros, V. (2011). "Evaluation of the Methods for Determination of the Free Radical Scavenging Activity by DPPH". *Bulgarian Journal of Agricultural Science*, vol. 17(1), pp. 11-24
- M-Tin Wa. (1972). "Phytochemical Screening, Methods and Procedures". *Phytochemical Bulletin of Botanical Society of America*, vol. 5(3), pp. 4-10
- Robinson, T. (1983). *The Organic Constituents of Higher Plants*. North America: 5<sup>th</sup> Ed., Cordus Press, pp. 63-68
- Shriner, R.L., Fuson, R.C., Curtin, D.Y. and Morrill, T.C. (1980). *The Systematic Identification of Organic Compounds-A Laboratory Manual*. New York: John Willey and Sons Inc., vol. 4, pp. 113-121
- Sultana, S.S. and Khatun, B.M.R. (2012). "*Hydrocotyle verticillata* Thunb. (Apiaceae)- New Angiospermic Record for Bangladesh". *Bangladesh J. Plant Taxon*, vol. 17(1), pp. 105-108
- Trease, G.E. and Evans, W.C. (1980). *Pharmacognosy*. London: 1<sup>st</sup> Ed., Spottis woode Ballantyne Ltd., pp. 108, 529
- Vogel, A.I. (1966). *A Text Book of Practical Organic chemistry*. London: 3rd Ed., Longmans, Green & Co. Ltd., pp. 112
- Xiao, F. and Rongli, N. (2005). "Macroalage as a source of  $\alpha$ -glucosidase inhibitors". *Chinese Journal of Oceanology and Limnology*, vol. 23(3), pp. 354-356
- Yuhao, L. (2004). "Effect of *Salacia oblonga* root and *Punica granatun* flower on  $\alpha$ -glucosidase activity". Herbal Medicine Practical, University of Sydney, pp.1-5

## STUDY ON ANTIOXIDANT ACTIVITY, ANTIMICROBIAL ACTIVITY AND ACUTE TOXICITY OF PLUKENETIA VOLUBILIS L. (SACHA INCHI) LEAVES

Myint Myint Htay<sup>1</sup>, Theingi Win<sup>2</sup>, Ni Ni Aung<sup>3</sup>

### Abstract

This research focused on the investigation of phytochemical constituent, mineral content, antioxidant, antimicrobial activities and acute toxicity of sacha inchi leaves. Firstly, the preliminary phytochemical screening was done. The leaves give positive test for alkaloid, flavonoid, glycoside, terpene, steroid, reducing sugar, saponin, tannin and phenolic compound but cyanogenic glycoside was not found. The mineral content was determined by EDXRF spectroscopic technique. The main minerals present in sacha inchi leaves are calcium and potassium. The antioxidant activity of ethanol extract was determined by DPPH assay. The IC<sub>50</sub> value of ethanol extract was found to be 179.60 µg mL<sup>-1</sup>. Moreover, the antimicrobial activity of ethanol extract was investigated by agar well diffusion method on seven selected microorganisms. Among selected microorganisms, the ethanol extract showed the highest activity on *Bacillus pumilus* and high activities on *Agrobacterium tumefaciens*, *Bacillus subtilis*, *Candida albicans*, *Escherichia coli*, *Pseudomonas fluorescens* and *Staphylococcus aureus*. In addition, oral acute toxicity test of ethanol extract was studied by Organization of Economic Cooperation and Development (OECD) guideline (425). According to oral acute toxicity test, the tested sacha inchi leaves can be considered relatively safe to the dose level of 5000 mg/kg body weight. No toxicity effects after oral acute exposure of ethanol extract to mice were observed.

**Keywords:** phytochemicals, antioxidant activity, antimicrobial activity, acute toxicity

### Introduction

Plants have been a valuable source of natural products for a long period of time to maintain human health. Natural products have been used in the treatment of several diseases for centuries, among them, wound healing. To heal, the wound or burn needs to free of infection. Human beings have relied on natural products as a resource of drug for thousands of years. Herbal drugs constitute only those traditional medicines, which primarily use medicinal plant preparation for therapy (Nascimento *et al.*, 2013). According to world health organization, traditional medicine is the synthesis of therapeutic experience of the generation of indigenous systems of medicine. In literature, sacha inchi leaves make a wonderful, aromatic tea that not only tastes delicious but is gluten free and contains antioxidants, leading to health benefits which include helping to reduce blood sugar levels, cholesterol and blood. Among different medicinal plants, *Plukenetia volubilis* L., a perennial oilseed vine belonging to the Euphorbiaceae family native to the rainforests of South America was selected for chemical analysis.

### Botanical Aspect of *P. volubilis* L.

Scientific name	-	<i>Plukenetia volubilis</i> L.
Family	-	Euphorbiaceae
Genus	-	<i>Plukenetia</i>
Species	-	<i>volubilis</i>
English name	-	Sacha inchi, mountain peanut
Myanmar name	-	Kyalpe
Part used	-	Leaves



**Figure 1** Sacha inchi leaves

<sup>1</sup> Dr, Lecturer, Department of Chemistry, Yenanchaung University

<sup>2</sup> Lecturer, Department of Chemistry, Magway University

<sup>3</sup> Dr, Lecturer, Department of Chemistry, Yenanchaung University

## **Medicinal Uses of Sacha inchi Leaves**

Sacha inchi botanical extract is supposed to support the healthy functioning of the brain, heart and nervous system and to help maintain healthy levels of cholesterol and blood pressure. Encourages weight loss. It regenerates the nervous system's cells, enhancing the mood and communication abilities. It relieves the pain caused by arthritis. It cures certain skin condition. It prevent the onset of inflammation, distribute essential nutrients throughout the body, balance the mood (Health benefits times, 2020).

## **Materials and Methods**

### **Sample Collection and Preparation**

The sample sachu inchi leaves to be analyzed was collected from Kyaukpadaung Township, Mandalay Region. The sachu inchi leaves were cut into small pieces and air dried. And then, the sample was powdered by mortar and pestle. It was stored in well stoppered bottle and used throughout the experiment.

### **Preliminary Phytochemical Test of Sacha inchi Leaves**

Phytochemical investigation of sachu inchi leaves powder was done according to standard procedure (Harbone, 1984).

### **Qualitative Elemental Analysis of Sacha inchi Leaves by EDXRF Spectrometry**

The determination of minerals containing in sachu inchi leaves was studied by Energy Dispersive X-ray Fluorescence (EDXRF) spectrometer. The measurement was carried out at University of Research Centre (URC), Yangon.

### **Screening of Antioxidant Activity of Ethanol Extract of Sacha inchi Leaves by DPPH Assay**

The antioxidant activity of ethanol extract of sachu inchi leaves was studied by DPPH (2, 2-diphenyl-1-picryl-hydrazyl) radical scavenging assay method. This assay has been widely used to evaluate the free radical scavenging effectiveness of various flavonoids and polyphenols in food system (Marinova *et al.*, 2011).

### **Determination of Antimicrobial Activity of Ethanol Extract of Sacha inchi Leaves**

The antimicrobial activity of ethanol extract of leaves was tested by employing Agar well diffusion method in Meiktilar University. The tested microorganisms are *Agrobacterium tumefaciens*, *Bacillus pumilus*, *Bacillus subtilis*, *Candida albicans*, *Escherichia coli*, *Pseudomonas fluorescens* and *Staphylococcus aureus*.

### **Determination of Acute Toxicity of Ethanol Extract of Sacha inchi Leaves**

The acute toxicity test on 95 % ethanol extract of the sachu inchi leaves could be carried out according to OECD (Organization of Economic Co-operation and Development) guidelines 425. The test substance 95 % ethanol extract of the sachu inchi leaves were administered orally in a single dose by using cannula. One group was served as the control and only vehicle distilled water was given orally. Three mice were used for each doses level. In this study, the starting dose 175 mg/kg body weight test substance was given to 3 mice. Mice were observed after dosing at least once during the first 30 min periodically during the first 24 h with special attention given during the first 4 h and daily up to 14 days.



**Figure 2** Weighing fasted body weight of each female albino mice



**Figure 3** Administration of leaves solution to the test mouse

## Results and Discussion

### Phytochemical of Sacha inchi Leaves

Preliminary phytochemical screening was carried out in order to know the different types of chemical constituents present in the leaves of *plukenetia volubilis* L. According to phytochemical tests, it gives positive tests for alkaloid, flavonoid, steroid, terpene, glycoside, reducing sugar, phenolic, saponin, tannin and cyanogenic glycoside is negative. These results are shown in Table 1. These phytochemical compounds are key micronutrients needed for the body immune system. These have a broad range of protective benefits from reducing inflammation and speeding healing to preventing infection and fighting cancer.

**Table 1 Results of Phytochemical Tests of Sacha inchi Leaves**

No.	Tests	Solvent Extract	Test Reagents	Observation	Results
1.	Alkaloid	1% HCl	Dragendorff's reagent Wagner's reagent	Orange ppt Brown ppt	+ +
2.	Flavonoid	95 % EtOH	Mg ribbon, Conc: HCl	pink colour	+
3.	Steroid	95 % EtOH	Acetic anhydride, Conc: H <sub>2</sub> SO <sub>4</sub>	Green colour	+
4.	Terpene	95 % EtOH	Acetic anhydride, CHCl <sub>3</sub> , Conc: H <sub>2</sub> SO <sub>4</sub>	Reddish brown colour	+
5.	Glycoside	Distilled Water	10 % lead acetate	White ppt	+
6.	Reducing Sugar	Distilled Water	Benedict's solution	Brick red ppt	+
7.	Phenolic	Distilled Water	10 % FeCl <sub>3</sub>	Greenish blue colour	+
8.	Saponin	Distilled Water	Shaking	Permanent frothing	+
9.	Tannin	Distilled Water	Dil :H <sub>2</sub> SO <sub>4</sub> , 10 % FeCl <sub>3</sub>	Brown ppt	+
10.	Cyanogenic glycoside	Distilled Water	Sodium picrate solution	No brick red colour	-

(+) = presence (-) = absence ppt = precipitate

### Qualitative Elemental Analysis of Sacha inchi Leaves

The elemental content of sacha inchi leaves were determined by EDXRF technique. The observed elements are shown in Figure 4 and Table 2. In accordance with Table 2, sacha inchi leaves contain significant amounts of calcium and potassium was the second most element. These minerals are considered to be essential in human nutrition to keep the blood pressure regulated.

Calcium is required for the development of bones and teeth, muscle contraction and nerve transmission. The primary functions of potassium in the body include regulating fluid balance and controlling the electrical activity of the heart and other muscles. These elements are essential because they play key roles in several body functions.

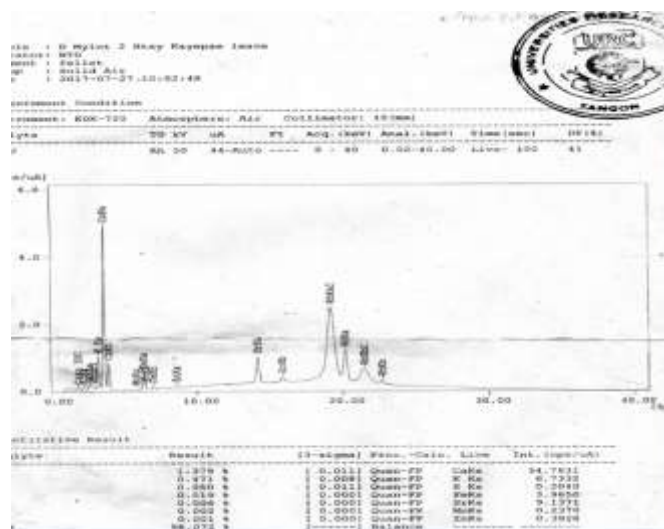


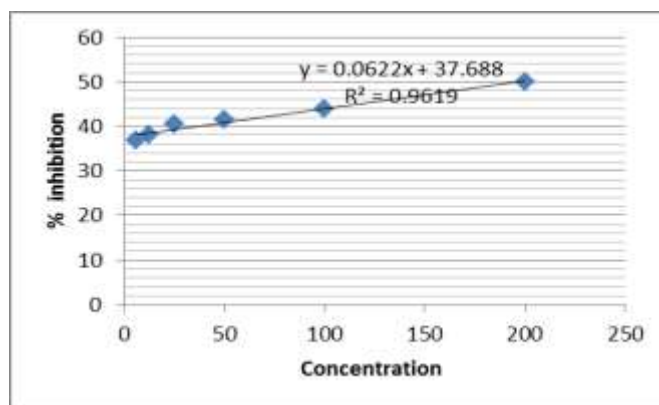
Figure 4 EDXRF spectrum of sacha inchi leaves

Table 2 Relative Abundance of Elements in Sacha inchi Leaves

No.	Symbols	Relative abundance
1	Ca	1.379
2	K	0.471
3	S	0.050
4	Fe	0.019
5	Sr	0.006
6	Mn	0.002
7	Zn	0.001
8	C <sub>2</sub> H	98.072

### Screening on Antioxidant Activity of Ethanol Extract of Sacha inchi Leaves

Antioxidant activity of ethanol extract of sacha inchi leaves were studied by DPPH assay. The percent oxidative inhibition values of leaves extract measured at different concentration and the results are tabulated in Table 3. As the concentration increased, the absorbance value decreased i.e., increase in radical scavenging activity of each extract usually expressed in terms of % inhibition. The 50% inhibition concentration (IC<sub>50</sub>) for leaves extract was calculated by linear regressive excel program.



**Figure 5** Percent inhibition activity of ethanol extract of Sacha inchi leaves

**Table 3** Antioxidant Activity of Sacha inchi Leaves

Concentration of sample (µg/mL)	Mean absorbance	Mean % inhibition	IC <sub>50</sub> (µg/mL)
200	0.205	49.85632	179.60
100	0.218	43.95887	
50	0.228	41.38817	
25	0.231	40.61697	
12.5	0.241	38.04627	
6.25	0.246	36.76093	

**Antimicrobial Activity of Ethanol Extract of Sacha inchi Leaves**

Antimicrobial activity of leaves have been investigated by Agar well diffusion method on seven selected microorganisms. Agar well diffusion method is based on the zone diameter in millimeter (mm) of Agar well. The larger the zone diameter is the more activity on the tested microorganisms. According to Table 4, the result informs that responds highest activity on *B. pumilus* and high activity on *C. albicans*, *S. aureus*, *A.tumefaciens*, *B. subtilis*, *E. coli* and *P. fluorescens*.

**Table 4** Inhibition Zone Diameters of Ethanol Extract of Sacha inchi Leaves

No.	Microorganisms	Inhibition zone diameters
1	<i>A. tumefaciens</i>	<b>13 mm</b> (++)
2	<i>B. pumilus</i>	<b>19 mm</b> (+++)
3	<i>B. subtilis</i>	<b>15 mm</b> (++)
4	<i>C. albicans</i>	<b>14 mm</b> (++)
5	<i>E.coli</i>	<b>16 mm</b> (++)
6	<i>P.fluorescens</i>	<b>15 mm</b> (++)
7	<i>S.aureus</i>	<b>15 mm</b> (++)

Agar well- 8 mm, 8 mm -12 mm (+), 13 mm-17 mm (++) , 18mm - above (+++)

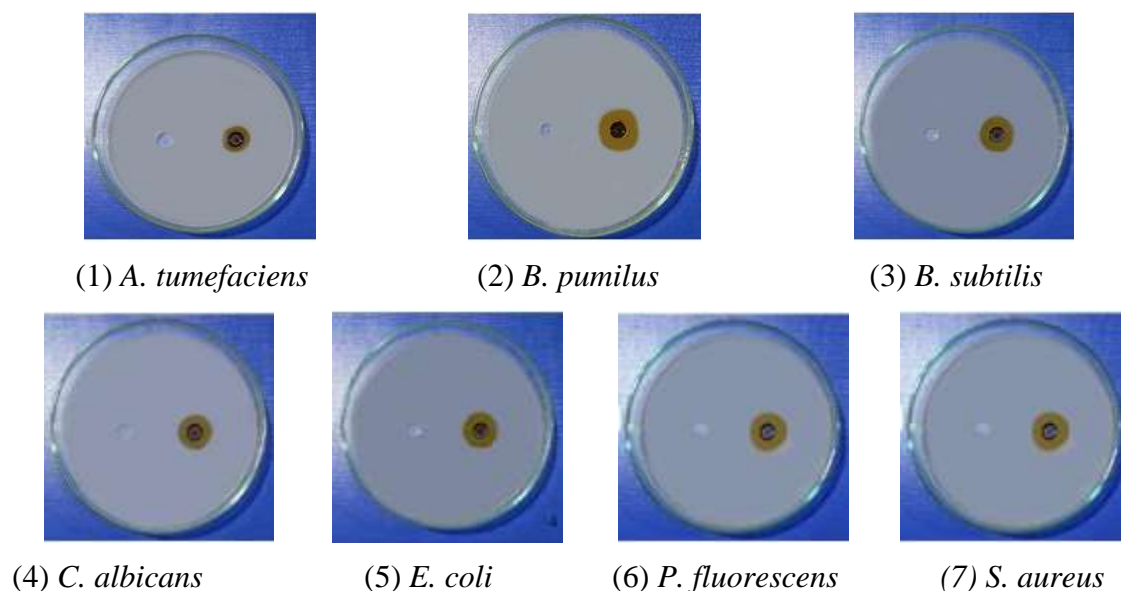


**Figure 6** Inhibition zones of ethanol extract of sacha inchi leaves

### Acute Toxicity of Ethanol Extract of Sacha inchi Leaves

For safety profile, the ethanol extracts of sacha inchi leaves were tested for acute toxicity study on albino mice. This tested was done according to OECD guidelines (425). In this experiment different groups of mice were used by calculating of AOT-425. The different groups of mice were administered with 4 different doses (175 mg/kg, 550 mg/kg, 1750 mg/kg, 5000 mg/kg) of ethanol extract of leaves of sacha inchi and vehicle (distilled water) 10 mL/kg body weight (control) were kept under observation for two weeks. The resultant data based on body weights record and cage side observation are presented in Table 5 and Table 6.

**Table 5 Acute Toxicity Study of Sacha inchi Leaves Based on Daily Body Weight Record and Mortality Record**

Test dose	Dosage of extract (mg/kg)	Sex	Body weight of mice (g)		Mortality up to 14 days
			Day 0	Day 14	
1	175	Female	35	37	Nil
2	550	Female	37	43	Nil
3	1750	Female	27	29	Nil
4	5000	Female	26	26	Nil
5	5000	Female	30	31	Nil
6	5000	Female	27	33	Nil

**Table 6 Acute Toxicity Study of Ethanol Extract of Sacha inchi Leaves Based on Cage Side Observations**

No.	Parameters	Observations
1	Condition of the fur	Normal
2	Skin	Normal
3	Subcutaneous swellings	Nil
4	Abdominal distension	Nil
5	Eyes-dullness	Nil
6	Eyes-opacities	Nil
7	Pupil-diameter	Normal
8	Ptosis	Nil
9	Colour and consistency of the faeces	Normal
10	Wetness of soiling of the perineum	Nil
11	Condition of teeth	Normal
12	Breathing abnormalities	Nil
13	Gait	Nil

### Conclusion

In this research work, sachu inchi leaves were selected for preliminary phytochemical examination. It was found that alkaloid, flavonoid, glycoside, steroid, terpene, phenolic, reducing sugar, saponin and tannin but cyanogenic glycoside was not found. The minerals, Ca, K, S, Fe, Sr, Mn and Zn were observed in sachu inchi leaves. Among these elements calcium concentration is distinctly higher than other elements. According to the antioxidant activity study of ethanol extract of leaves using DPPH assay, the  $IC_{50}$  value was found to be  $179.60 \mu\text{g mL}^{-1}$ . Furthermore, the antimicrobial activity of ethanol extract of sachu inchi leaves were also investigated by employing Agar well diffusion method against seven selected microorganisms. It was observed that the ethanol extract of the leaves exhibited the highest activity on *B. pumilus* and high activity on remaining microorganisms. Moreover, from the determination of oral acute toxicity, all the tested mice from treated groups increased body weight for all the 14 days as compared with 0 day body weight. From the daily body weight record the tested mice at all dose levels showed no death. The  $LD_{50}$  value of the test substance was found to be more than 5000 mg/kg based on body weight. From the cage-side observations record, the tested animals at all dose levels showed no significant changes in behaviors before and after administration. Thus the ethanol extract of sachu inchi leaves can be considered free from toxic effects up to the dose level of 5000 mg/kg for oral administration. Therefore, the sachu inchi leaves can be used in medicinal and pharmaceutical industries.

### Acknowledgements

We would like to gratefully acknowledge to Dr Soe Myint Thein, Pro-rector, Yenanchaung University for his permission and we are deeply indebted to Dr Lin Lin Tun Professor and Head, Department of Chemistry, Yenanchaung University, for her valuable advice and kind encouragement for research paper. We would like to express our profound gratitude to the Myanmar Academy of Arts and Science, for giving permission to submit this paper.

## References

- Buzarbarua. A. (2000). A Text Book of Practical Plant Chemistry. Dept. of Botany, Cotton College, Guwahati, New Delhi, 7361.
- Harbone. J.B. (1984). Phytochemical Methods-A guide to modern techniques of plant analysis. London: 2<sup>nd</sup> Ed., Chapman and Hall, 701-710.
- Lenka S., Petra H.C., Iva V. And Danter C.H. (2015). "Effect of Thermal Processing on Phenolic Content, Tocopherols and Antioxidant Activity of Sacha Inchi Kernels". *Journal of Food Processing and Preservation*, Issn 1745-4549.
- Marinova, G. and Batchvarov, V. (2011). "Evaluation of the Methods for Determination of the Free Radical Scavenging Activity by DPPH". *Bulgarian Journal of Agricultural Science*, 17, 11-24.
- Monoroe. S., Polk. R. (2000) "Antimicrobial use and bacterial resistance". *Curr Opin Microbial*, 3(5): 496-501.
- Nascimento. A.K.L., Melo-Silveira. R.F., Dantas-Santo. N., Fernandes, J.M. and Zucolotto. S.M. (2013). "Antioxidant and Antiproliferative Activities of Leaf Extracts from *Plukenetia volubilis* L. (Euphorbiaceae)". *Evidence-Based Complementary and Alternative Medicine*, 1, 1-10.
- OECD. (2008). Test No. 425: Acute Oral Toxicity Up-and-Down Procedure, OECD Guideline for the Testing of Chemicals, Section 4. French.

## Online Materials

- Health benefits times. (2020). "Health benefits of Sacha Inchi". [https://www.healthbenefitstimes.com/sacha inchi facts and health benefits-Health Benefits Times](https://www.healthbenefitstimes.com/sacha-inchi-facts-and-health-benefits).

## REPARATION AND CHARACTERIZATION OF LIQUID GLUCOSE FROM THE SWEET POTATO STARCH OF *POMOEA BATATAS* L. (SHWE-KAN-ZUN-U)

Kyawt Kay Khaing<sup>1</sup>, Mar Mar Soe<sup>2</sup>, Win Naing<sup>3</sup>

### Abstract

The present work deals with isolation and identification of liquid glucose from sweet potato tuber *Ipomoea batatas* L. (Shwe-ka-zun-u). From the preliminary phytochemical investigation, alkaloids, carbohydrates,  $\alpha$ -amino acids, flavonoids, glycosides, saponins, steroids, tannins, terpenoids, phenolic compounds, starch, organic acids, reducing sugars were found to be present and the cyanogenic glycosides was absent in the tuber of sweet potato. In addition, sweet potato tuber contains the content of water (42.15 %), total solid (57.85 %), nitrogen (0.192 %), ash (1.91 %), fat (0.72 %), starch (48.34 %) and crude fibre (1.97 %). According to ED XRF data analysis, K (65.705 %), Ca (21.918 %), Fe (6.025 %), Rb (3.487 %) and Mn (2.865 %) were observed. The contents of soluble matters using water, ethanol and petroleum were 6.01, 4.14 and 2.23 %, respectively. The yield percent and dextrose equivalent of liquid glucose prepared by enzymatic method and acid hydrolysis method were respectively found to be 11.95 and 11.04 %, 40.37 and 37.30., determined by Fehling's solution method. Similarly, the yield percent of liquid glucose prepared by enzymatic method and acid hydrolysis method were observed as 22.43 and 21.78 %, 75.78 and 73.58, respectively, determined by phenol-sulphuric acid assay. The prepared liquid glucose was characterized by paper chromatographic method. The characteristics of prepared liquid glucose obtained by enzyme hydrolysis and acid hydrolysis were indicated as specific gravity (1.08 and 1.02), refractive index (1.42 and 1.30), viscosity (1.5282 cP and 0.7864 cP), pH (4.4 and 4.8), water content (25.67 % and 31.95 %), total solid (74.33 % and 68.05 %) and sulphated ash (0.048 % and 0.069 %), respectively.

**Keywords:** *Ipomoea batatas* L., sweet potato tuber, liquid glucose, termamyl enzyme, paper chromatography

### Introduction

The sweet potato (*Ipomoea batatas* L.) is a dicotyledonous plant that belongs to the bindweed or morning glory family, *Convolvulaceae*. Its large, starchy, sweet-tasting, tuberous roots are a root vegetable (Purseglove, 1968). The young leaves and shoots are sometimes eaten as greens. The plant is herbaceous perennial vine, bearing alternate heart-shaped or palmately lobed leaves and medium-sized sympetalous flowers. Sweet potato cultivars with white or pale yellow flesh are less sweet and moist than those with red, pink or orange flesh. The sweet potato (*Ipomoea batatas*) is one of the most important food crops in the world and provides not only staple food but also important as an industrial raw materials. Originating in South America, it is now grown all over the world spreading throughout the tropical and sub-tropical countries. The sweet potato tubers are rich in starch, sugars, minerals and vitamins. In Asian countries, some edible tubers are also used as traditional medicine.

The production of glucose syrup from sweet potato actually is produce the glucose from sweet potato starch, because the sweet potato with more protein and fiber. Liquid glucose is also a main ingredient of candies and sweets. In the pharmaceutical industry, it is used as a cost-effective replacement to sugar syrup preparations and is also used in tablets for coating and as a granulating agent.

Liquid glucose is widely used in the confectionery, biscuit and food canning industries, as a thickener, sweetener and to modify the mouth feel of food preparations. Glucose liquids are

---

<sup>1</sup> Dr, Assistant-Lecturer, Department of Chemistry, Dagon University

<sup>2</sup> Dr, Assistant-Lecturer, Department of Chemistry, Dagon University

<sup>3</sup> Dr, Professor and Head, Department of Chemistry, Taungoo University

obtained by the hydrolysis of starch in which the long-chain carbohydrate molecules are broken down into series of low molecular weight carbohydrates. Liquid glucose is an aqueous solution of nutritive saccharide obtained by starch hydrolysis, by using corn and rice as raw material, which is purified and concentrated to required solids. It is usually odorless and clear yellow colored viscous liquid sweet syrup which is processed and stored under hygienic conditions.

The present study was focused on the preliminary phytochemical tests, chemical analysis, preparation and characterization of liquid glucose from sweet potato tuber by using Termamyl enzyme and HCl hydrolysis methods.

## **Materials and Methods**

### **Collection and Preparation of Plant material**

The tuber of *I. batatas* (Shwe-ka-zun-u) was collected from Taikkyi Township, Yangon Region. The tuber sample was transformed into powder and stored in air-tight container.

### **Preliminary Phytochemical Test**

A few grams of dried tuber powder sample of *I. batatas* was subject to the tests of alkaloids, carbohydrates,  $\alpha$ -amino acids, flavonoids, glycosides, saponins, steroids, tannins, terpenoids, phenolic compounds, starch, cyanogenic glycosides, organic acids and reducing sugars according to the standard procedures (Finar, 1968; M-Tin Wa, 1972; Marini-Bettolo *et al.*, 1981; Robison, 1983; Shriner *et al.*, 1980; Trease and Evans, 1996).

### **Chemical Analysis of Sweet Potato Tuber**

The water content of dried powder tuber sample was determined by the Dean and Stark method (AOAC, 1995), total solid content by the oven drying method (Pearson, 1976), nitrogen content by the Micro-Kjeldahl distillation method (AOAC, 1995), the ash content by the gravimetric method, fat content by the soxhlet extraction method (Joslyn, 1956), water-soluble matter, ethanol-soluble matter and petroleum ether-soluble matter contents by the British Pharmacopoeia method. The starch content was calculated by multiplying the sugar content with factor 0.93. The crude fibre content was determined by the acid and alkali digestion method, shown in Table 2. The relative abundance of elements was determined by Energy Dispersive X-ray Fluorescence, shown in Table 3.

### **Preparation of Liquid Glucose from Sweet Potato Tuber**

#### **Determination of optimum saccharification time**

Starch 100 g was mixed with 500 mL of distilled water and cooked with pressure cooker for about 30 min until the starch solution become sticky and waxy in nature. Liquefaction of the starch slurries was carried out using a thermostable  $\alpha$ -amylase (125 mL of termamyl enzyme). The pH of the slurry was adjusting to 6.0 and reaction was carried out in a stirred reactor with enzyme at 65 °C for 2 h. The resulting solution (prepared liquid glucose) was cooled to 30 °C. Saccharification was carried out for 5 days at 30 °C.

Dextrose equivalent (D.E) of the saccharified solution was determined daily by phenol-sulphuric acid assay method. The results are recorded in and the standard calibration curve was plotted by dextrose equivalent against the saccharification time. From this curve, the optimum saccharification time was obtained.

### **Preparation of liquid glucose from sweet potato tuber by using enzyme and acid**

For enzyme, the dried powder tuber of sweet potato 100 g was mixed with 500 mL of distilled water and cooked with pressure cooker for about 30 min until the starch solution become sticky and waxy in nature. Liquefaction of the starch slurries was carried out using a thermostable  $\alpha$ -amylase (125 mL of termamyl enzyme). The pH of the slurry was adjusting to 6.0 and reaction was carried out in a stirred reactor with enzyme at 65 °C for 2 h. The resulting solution (liquid glucose) was cooled to 30 °C. Saccharification was carried out for 72 h which was the optimum saccharification time obtained from determination of optimum saccharification time at 30 °C and was stopped by heating to 90 °C for 10 min. The hydrolysate was double filtered using a nylon cloth and filter paper so as to get the clear hydrolysate. The hydrolysate was clarified with 10 g of animal charcoal and filtered, and then measured the value of reducing sugar (glucose).

In acid hydrolysis method, the dried powder tuber of sweet potato 100 g was mixed with 500 mL of distilled water and cooked with pressure cooker for about 30 min until the starch solution become sticky and waxy in nature. The starch solution was removed from the pot and cooled to 30 °C. Aqueous solution at pH 5.5 was treated with 5 % fuming hydrochloric acid at 40 °C with stirring for 20 min. The mixture was cooled to 30 °C and after 72 h, 0.1 M  $\text{Na}_2\text{CO}_3$  was added into this slurry to neutralize. The hydrolysate was double filtered using a nylon cloth and filter paper so as to get the clear hydrolysate. The hydrolysate was clarified with 10 g of animal charcoal and filtered, and then measured the value of reducing sugar (glucose).

### **Quantitative Determination of Glucose in the Prepared Liquid Glucose from Sweet Potato Tuber**

#### **Fehling's solution method (Volumetric method)**

First, Fehling's solution was standardized with glucose solution. The standardization of Fehling's solution was carried out with the standard glucose solution. The results showed that the volume of the sugar solution required to reduce 10 mL of Fehling's solution must be in the range of 17 mL to 34 mL (equivalent to 0.15 % to 0.3 % reducing sugar solution) so that the error for titration would be minimum. Standard glucose (ca. 2 g) was weighed, dissolved in distilled water and made up to mark in a volumetric flask (1000 mL). Standard glucose solution was freshly prepared to standardize Fehling's solution. Fehling's solution 10 mL was pipetted into a conical flask and glucose solution 15 mL was added from a burette. The mixture was heated on a hot plate till it boiled. When the solution in the flask had boiled for about 15 s, the blue colour of the solution turned red and the major portion of copper was precipitated as cuprous oxide. Methylene blue indicator 1 mL was then added and the liquid was boiled for another 2 min. Small quantity of standard liquid glucose solution 1 mL was added in portion, keeping the liquid boiling, till the colour of the indicator disappeared. The titration was carried out so that it was completed within 5 min. And then standard liquid glucose solution 1 mL was added and boiled for 15 s. Methylene blue indicator 3 drops was added and these mixture solution was boiled for another 2 min and titrated with glucose solution till the colour of the indicator disappeared. The volume of glucose solution required for the reduction of 10 mL of Fehling's solution was noted. From the titre the amounts of glucose required to reduce 10 mL Fehling's solution was calculated (AOAC, 1995).

#### **Phenol-sulphuric acid assay method (UV spectrophotometric method)**

For preparation of standard glucose solution, 0.2 g of glucose was exactly weighed and dissolved in 100 mL of distilled water. 1, 2, 3, 4, 5, 6, 7, 8, 9 and 10 mL of these solutions were down out and placed in each 100 mL of volumetric flask and diluted to the mark with distilled water. These solutions contained 20, 40, 60, 80, 100, 120, 140, 160, 180 and 200  $\mu\text{g}$  of glucose per mL, respectively.

One mL each of the prepared glucose liquid solution and the above ten standard glucose solutions (20, 40, 60, 80, 100, 120, 140, 160, 180 and 200  $\mu\text{g}$  of glucose per mL) were introduced into each test tube. One mL of 5 % phenol solution was added to each test tube and mixed. A blank was prepared with 1 mL of distilled water instead of sugar solution, 5 mL of concentrated sulphuric acid was added again to each test tube. Each test tube was agitated during the addition of acid. After about 10 min, the tubes were shaken again and placed in water-bath at 30 °C for 20 min. The yellow orange colour was stable for several hours. Absorbance was measured at 490 nm using CIBA Corning Spectrophotometer 259 (Pearson, 1976).

A standard curve was plotted by the absorbance of the standard glucose solutions against the concentration in  $\mu\text{g}$  per mL. Using this standard curve, the concentration of glucose in the sample and dextrose equivalent was then calculated (Conn and Stumpf, 1972).

### **Characterization of the Prepared Liquid Glucose by Paper Chromatography**

The prepared liquid glucose by enzymatic method and acid hydrolysis method was screened by means of ascending paper chromatography using appropriate standards and solvent system. The solvent in this technique moved upward against the gravitational pull (Whistler and Wolfrom, 1964). The paper was cut into small paper (7.5  $\times$  15 cm in size). About 5  $\mu\text{L}$  of samples (two isolated liquid glucoses, standard glucose, standard galactose) were spotted on the paper using a capillary tube. The paper was placed in a chromatographic chamber with *n*-butanol: pyridine: water (10: 3: 3) solvent system. When the solvent reached the height of about 15 cm from the place of origin, it was taken out. The paper chromatogram was dried in an oven (at a temperature 60 °C). The spots on paper chromatogram were detected by viewing directly under UV 254 nm and 365 nm light and by spraying the dried paper with aniline phthalate reagent. Then, the paper was heated at 80-110 °C in an oven for exactly 3 min. The separated sugars were revealed as brown spots for hexoses and the paper chromatogram. The  $R_f$  values of liquid glucose were measured (Whistler and Wolfrom, 1964).

### **Determination of Physiochemical Properties of the Prepared Liquid Glucose**

The prepared liquid glucose was determined the specific gravity by Baume's hydrometer, the refractive index by an Abbe 60, refractometer (Jacobs, 1958), the viscosity by the U-tube viscometer (ASTM, 1966), the colour by the Lovibond Tintometer, water content by oven drying method (Pearson, 1976), sulphated ash by the gravimetric method and pH is measured by pH meter.

## **Results and Discussion**

Preliminary phytochemical analysis was performed in order to know the different types of compounds present in sweet potato tuber. The results on phytochemical testes are summarized in Table 1.

The Dean and Stark method is more accurate than oven drying method because the water content from oven drying method contains bound water, adsorbed water and bulk or free water. Nitrogen content was determined by using the Micro-Kjeldahl distillation method. Ash is the inorganic residue remained after the organic matter has been burnt away, shown in Table 2. Fats were determined by the soxhlet extraction method using petroleum ether (b.pt 40-60 °C). The petroleum ether cannot extract non-fat constituents such as starches and proteins. Determination of water soluble matters, alcohol soluble matters and petroleum ether-soluble matters were carried out to know the amount of total solids soluble in water, in alcohol and in petroleum ether (b.pt 40-60 °C). Starch content in the sweet potato tuber was also determined by using distilled water and dilute sulphuric acid. Starch is a water-soluble complex, carbohydrate found naturally in many

vegetable products. The crude fibre is the insoluble and combustible organic residue with remains after the sample has been treated under prescribed conditions. The results are shown in Table 2.

X-ray spectrometer permits simultaneous analysis of light element to heavy element. Shimadzu EDX-700 spectrometer can analyze the element from Si to U under vacuum condition. In the present work, relative abundance of element present in sweet potato tuber sample was determined by ED-XRF spectrometer. It can be seen that essential minerals for human such as potassium and calcium in tuber was predominant. Potassium (K) is important in regulating the body fluid volume and also widely distributed in foods. Potassium is essential in maintaining water or intracellular fluid balance. The daily intake may range from 1900-5600 mg. Calcium (Ca) with which decreases the toxicity of other ions, is a major mineral constituents of the body (Monier, 1950). Ca is important for the health of bone and teeth, but it also affects muscles, hormones and nerve function. Iron (Fe) is essential nutrients for men (Bowman, 1980). Rubidium (Rb) in its chemical properties, it is closely resembles potassium. Among them, potassium (65.705 %) was higher than other elements in the sample, shown in Table 3.

Liquid glucose from sweet potato was prepared by using termamyl enzyme for 5 days at 30 °C. The dextrose equivalent (D.E) of the saccharide solution was measured daily by phenol-sulphuric acid assay method and these values are shown in Table 4 and Figure 1. According to the Figure 1, the optimum saccharification time was 48 h and the dextrose equivalent was 75.78. Dextrose equivalent is very important for sugar chemistry. The dextrose equivalent value (D.E) of commercial liquid glucose is the reducing sugar content, as dextrose, calculated on the basis of the solid matter.

The amounts of glucose in the prepared liquid glucose from sweet potato by enzymatic and acid hydrolysis methods were determined by the Lane and Eynon's Method (Lane and Eynon, 1923) and phenol-sulphuric acid assay method (Dubois *et al.*, 1956). Standard glucose curve was used for quantitative determination and standard calibration curve was shown in Figure 2 and Table 5. The amount of glucose in the prepared liquid glucose and dextrose equivalent are shown in Table 6.

Most of the physical characteristics of liquid glucose can be judged visually. The liquid glucose is light brown, viscous liquid having a bunt sugar smell. The colour was determined by using the Lovibond Tintometer. It was observed that yellow colour value of liquid glucose obtained from acid hydrolysis was very high compared to the corresponding red and blue values. The red colour value of liquid glucose obtained by enzymatic method was very high compared to the corresponding yellow and blue values. Specific gravity is the ratio of the mass of a unit volume of the sample to the mass of a unit volume of water at 30 °C. The specific gravity of liquid glucose from enzyme and acid hydrolysis were determined by hydrometer. The amount of total solid present would be related to the specific gravity. Hydrometers constructed for the determination of specific gravity of sugar solution are called saccharometers under which name, they are known in breweries. The refractive index, as normally measured, is the ratio of the velocity of the light in air to the velocity of the light in the substance being determined. Refractive index of liquid glucose from enzyme and acid hydrolysis were determined by the Abbe-refractometer, at 30 °C. Refractive indices of liquid glucoses have been found to provide a reliable indication of the dry weight of solid in the solution. The viscosity of a substance is the shearing resistance of a liquid film which separates two horizontal plates, one of which is being moved across the other. The viscosity of liquid glucose from enzyme and acid hydrolysis were determined by U-tube viscometer. Water contents of liquid glucose from enzyme and acid hydrolysis were determined by oven drying method. The pH of liquid glucose was obtained by using enzymatic method and acid hydrolysis method. The two prepared liquid glucose (by using enzymatic method and acid hydrolysis method)

were heated with concentrated sulphuric acid and the ash was expressed as “sulphated ash”. The results are shown in Table 8.

**Table 1 Result of Phytochemical Investigation on Tuber of *I. batatas***

Sr. No.	Tests	Extract	Test reagents	Observation	Remark
1.	Alkaloids	10 % acetic acid in EtOH	Mayer's reagent Dragendroff's reagent sodium picrate solution	white ppt blue-black ppt yellow ppt	+
2.	Carbohydrates	H <sub>2</sub> O	10 % $\alpha$ -naphthol, H <sub>2</sub> SO <sub>4</sub> (conc.)	pink colour	+
3.	$\alpha$ -amino acids	H <sub>2</sub> O	Ninhydrin reagent	violet spot on paper	+
4.	Flavonoids	EtOH	Mg ribbon, HCl (conc.)	pink colour	+
5.	Glycosides	H <sub>2</sub> O	10 % lead acetate	white ppt	+
6.	Saponins	H <sub>2</sub> O	distilled water	frothing	+
7.	Steroids	Benzene	acetic anhydride & H <sub>2</sub> SO <sub>4</sub> (conc.)	green colour	+
8.	Tannins	EtOH	1 % FeCl <sub>3</sub> and gelatin solution	greenish-yellow colour	+
9.	Terpenoids	CHCl <sub>3</sub>	acetic anhydride & H <sub>2</sub> SO <sub>4</sub> (conc.)	blue colour	+
10.	Phenolic compounds	H <sub>2</sub> O	1 % potassium ferricyanide & 1 % ferric chloride	deep green colour	+
11.	Starch	H <sub>2</sub> O	I <sub>2</sub> solution	bluish-black colour	+
12.	Cyanogenic glycosides	H <sub>2</sub> O	conc: H <sub>2</sub> SO <sub>4</sub>	no brick red	-
13.	Organic acids	H <sub>2</sub> O	bromocresol blue	blue colour	+
14.	Reducing sugars	H <sub>2</sub> SO <sub>4</sub>	Benedict's solution	brick-red ppt	+

Presence = (+), Absence = (-), Precipitate = (ppt)

**Table 2 Chemical Analysis of Tuber of *I. batatas***

No.	Principal Components	Observation Value (%)	Literature Value (%)*
1.	Water Content (Wet-matter)	42.15	68.5-72.3
2.	Total solid Content	57.85	31.5-27.7
3.	Nitrogen Content (Crude Protein)	0.192	0.182-0.553
4.	Ash Content	1.91	0.7-1.0
5.	Fat Content	0.72	0.2-0.4
6.	Water-soluble Matter Content	6.01	-
7.	Ethanol-soluble Matter Content	4.14	-
8.	Petroleum Ether-soluble Matter Content	2.23	-
9.	Starch (Wet-matter)	48.34	25.6-31.0
10.	Crude Fiber Content	1.97	0.7-1.0

\*(AOAC, 1995)

**Table 3 Relative Abundance of some Elements in Tuber of *I. batatas* by ED XRF Method**

No.	Element	Relative Abundance (%)
1.	Potassium (K)	65.705
2.	Calcium (Ca)	21.918
3.	Iron (Fe)	6.025
4.	Rubidium (Rb)	3.487
5.	Manganese (Mn)	2.865

**Table 4 Change in Sugar Content of Saccharified Solution with Termamyl Enzyme in Different Saccharification Times**

Sr. No.	Saccharification time (h)	Sugar content (%)
1.	0	0
2.	12	18.01
3.	24	30.11
4.	48	41.52
5.	72	38.43
6.	96	36.78
7.	120	34.54

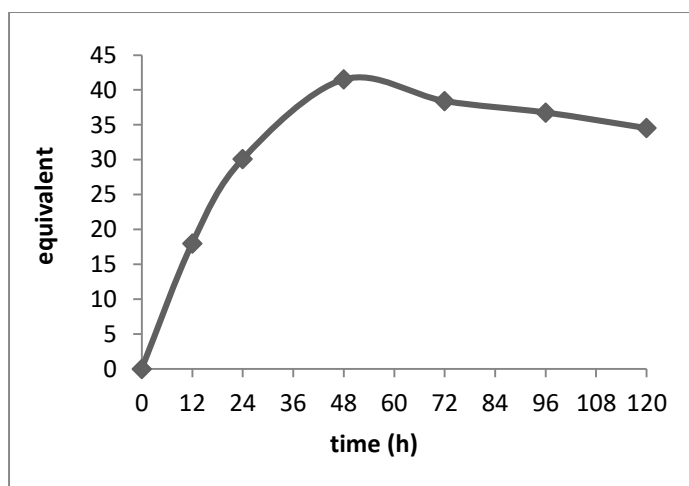


**Figure 1** Plot of variation of glucose content percent for glucose syrup with incubation period

**Table 5 Absorbance of the Orange Yellow Colour of Standard Glucose Solution of Various Concentrations in the Phenol-sulphuric Acid Assay**

Amount of Glucose (µg/mL)	Absorbance at 490 nm
100	0.031
200	0.062
300	0.102
400	0.129
500	0.161
600	0.193
700	0.238
800	0.262
900	0.289
1000	0.319

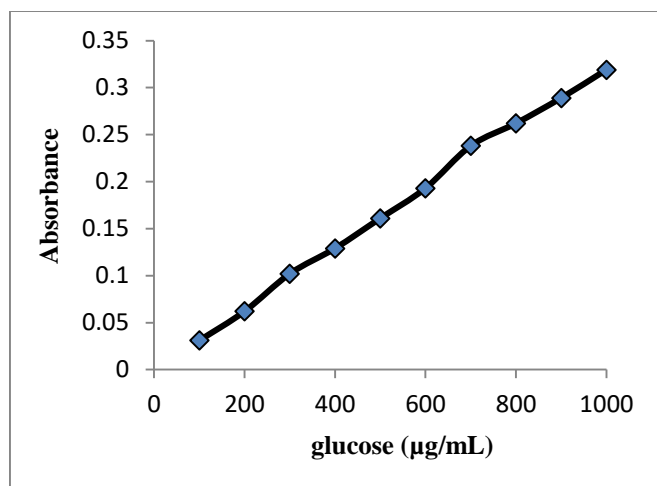


**Figure 2** Plot of absorbance as a function of weight of glucose

**Table 6** Glucose Content of the Prepared Liquid Glucose from *I. batatas*

Name of method	Glucose content from enzyme hydrolysis		Glucose content from acid hydrolysis	
	Glucose content (%)	D.E	Glucose content (%)	D.E
Volumetric method	11.95	40.37	11.04	37.30
Spectrophotometric method (Phenol-sulphuric acid assay method)	22.43	75.78	21.78	73.58

D.E = Dextrose Equivalent

**Table 7** Paper Chromatography of the Prepared Liquid Glucose

No.	Sugars	R <sub>f</sub> values	Observation
1.	Liquid glucose (enzymatic method)	0.71	Brown colour
2.	Liquid glucose (acid hydrolysis method)	0.72	Brown colour
3.	Standard galactose	0.68	Brown colour
4.	Standard glucose	0.71	Brown colour



Solvent System= *n*-butanol : pyridine : water (10: 3: 3)

Spray reagent = aniline phthalate reagent

S<sub>1</sub> = Liquid glucose (acid hydrolysis method)

S<sub>2</sub> = Liquid glucose (enzymatic method)

S<sub>3</sub> = Standard galactose

S<sub>4</sub> = Standard glucose

**Figure 3** Paper chromatogram of the prepared liquid glucose from *I. batatas*

**Table 8 Physicochemical Properties of the Prepared Liquid Glucose *I. batatas***

No.	Physicochemical properties	Liquid glucose from enzyme	Liquid glucose from acid
1.	Specific gravity	1.08	1.02
2.	Refractive Index at 30 °C	1.42	1.30
3.	Viscosity (cP) at 28 °C	1.5282	0.7864
4.	Water content (%)	25.67	31.95
5.	Total solid (%)	74.33	68.05
6.	Sulphated ash (%)	0.048	0.069
7.	Colour		
	(Red)	46.1	0.1
	(Yellow)	0.4	62.2
	(Blue)	0.3	0.3
8.	pH	4.4	4.8

### Conclusion

From the overall assessment for the present work concerning with the phytochemical constituents and liquid glucose from enzyme and acid hydrolysis of *I. Batatas* (Shwe-ka-zun-u) tuber, the following inferences could be deduced. In the present work on the Sweet Potato tuber sample, preliminary phytochemical tests revealed the presence of alkaloids, carbohydrates,  $\alpha$ -amino acids, flavonoids, glycosides, saponins, steroids, tannins, terpenoids, phenolic compounds, starch, organic acids and reducing sugars and the absence of cyanogenic glycosides in it.

Chemical analysis of the tuber sample revealed water, total solid, nitrogen, ash, fat, starch and crude fiber contents. Qualitative elemental analysis of the tuber sample by Ed XRF method showed that K, Ca, Fe, Rb and Mn. The results indicated relatively high contents of potassium and calcium. According to the elemental result, this sample was found to be effective for good; potassium and calcium are especially important for mineral elements which are necessary for the body in trace amount. The soluble matter for water, ethanol and petroleum ether were respectively determined.

The optimum saccharification time for liquid glucose (by using enzyme) was 48 h. The optimum saccharification time for liquid glucose (by using enzyme) was 48 h. The yield percent of liquid glucose prepared by enzymatic method and acid hydrolysis method were observed to be 11.95 % and 11.04 % determined by Fehling's solution volumetric method, and 22.43 % and 21.78 % determined by phenol-sulphuric acid assay, respectively. The dextrose equivalent of these two prepared liquid glucose were determined by volumetric and spectrophotometric methods, and found to be (40.37, 75.78) in enzymatic method and (37.30, 73.58) in acid hydrolysis method.

The prepared liquid glucoses from enzyme and acid hydrolysis were characterized by Paper Chromatographic method.

Physicochemical properties of liquid glucose prepared by hydrolysis with enzyme and acid such as specific gravity, refractive index, viscosity, water content, total solid, sulphated ash, colour and pH were determined respectively.

The prepared liquid glucoses were observed as colourless liquid and their identification test values are in close agreement with literature values.

## Acknowledgements

The authors would like to acknowledge to Dr Cho Cho Win, Professor and Head, Dr Khin Than Win, Professor, Department of Chemistry, Dagon University and Dr Win Naing, Professor and Head (Retd.), Taungoo University for generously and kindly providing to do this research work. And the authors would like to express our gratitude to the Department of Higher Education, Ministry of Education, Myanmar, for their permission to do this research and also the Myanmar Academy of Arts and Science for allowing presenting this paper.

## References

- AOAC (1995). "Official Methods of Analysis. Association of Official Analytical Chemists". *The Association: Arlington*, 15<sup>th</sup> Ed., vol. 2, p. 985
- A.S.T.M. (1996). "American Standard of Testing and Method". "Designation". D. 2515-66, p 430-432
- Bowman, W. C. and Rand, M. J. (1980). *Textbook of Pharmacology*. Oxford: Blackwell Scientific Pub., p 423
- Conn, E. E. and Stumpf, P. K. (1972). "Outlines of Biochemistry". New York: 3<sup>th</sup> Ed., Wiley and Sons, p 72
- Duboiset, M. Gilles, K. A., Hamilton J. K., Rebers, P. A. and Smith, F. (1956). "Colorimetric Method for Determination of Sugar, and Related Substances". *Anal. Chem.*, vol. 28, p 350-356
- Finar, I. L. (1968). *Organic Experiment*. New York: 4<sup>th</sup> Ed., D-C Health and Company, p 132
- Jacobs, M. B. (1958). *Chemical Analysis of Foods and Food Products*. London: D. Van Notstrand Company, Inc., 3<sup>rd</sup> Ed., p 46-47
- Joslyn, M.A. (1956). *Methods in Food Analysis, Physical, Chemical and Instrumental Method of Analysis*. 2<sup>nd</sup> Ed., p 483
- Lane, J. H. and Eynon, L. (1923). "Chemical Analysis of Foods and Food Products". *Journal of Society Chemical Industry*. vol. 42, p 32-37
- M-Tin Wa. (1972). "Phytochemical Screening Methods and Procedures". *Phytochemical Bulletin of Botanical Society of America Inc.*, vol. 5(3), p 4-10
- Marini, G. B., Bettolo-Nicoletti, M., Patomia, M., Galeffi, C. and Messona, I. (1981). "Plant Screening by Chemical and Chromatographic Procedures Under Field Conditions". *J. Chormate.*, vol. 46(2), pp. 359-363
- Monier-Williams, G. W. (1950). *Trace Elements in Foods*. New York: 2<sup>nd</sup> Ed., John Wiley and Sons, Inc., p. 64
- Pearson, D. (1976). "The Chemical Analysis of Foods". New York: Churchill Livingstone, 7<sup>th</sup> Ed., p. 493
- Puresglove, J. W. (1968). "Tropical Crops: Dicotyledons, Longman Scientific and Technical". New York: John Wiley and Sons, Inc., vol. 2, p. 654
- Robinson, T. (1983). "The Organic Constituents of Higher Plants". North Amherst, MA: Cordus Press, 5<sup>th</sup> Ed., p. 353
- Shriner, R. L., Fuson, R. C., Curtin, D. Y. and Morrill, T. C. (1980). *The Systematic Identification of Organic Compounds" A Laboratory Manual*, New York: 6<sup>th</sup> Ed., John Wiley and Sons, p 34-38
- Trease, G. E and Evans, W. C. (1996). *Trease and Evans pharmacognosy*. London: 14<sup>th</sup> Ed., WB Saunders Company Limited, p. 191, 293
- Whistler, R. L and Wolfrom, M. L. (1964). *Methods in Carbohydrate Chemistry*. New York: Academic Press, vol. 4, p. 335

## A STUDY ON SOME WATER QUALITY ASSESSMENT OF GAMOEYIEK CREEK WATER SAMPLE NEAR NORTH DAGON TOWNSHIP AND TREATED WITH *MORINGA OLEIFERA* L. (DANT-DA-LUN) SEEDS

Thin Thin Hlaing<sup>1</sup>, Ohnmar Aung<sup>2</sup>, Zaw Naing<sup>3</sup>

### Abstract

In the present work, the Ngamoeyeik creek water sample was collected from North Dagon Township, Yangon Region. Some physicochemical properties (pH, turbidity, conductivity, chemical oxygen demand, biochemical oxygen demand, total alkalinity, total hardness, total suspended solids and total dissolved solids) of the creek water sample were determined by standard method. Elemental analysis of some trace elements (Cr, Mn, Fe, Cu, Zn, Pb, Cd, Mg, Ca, K, Na and As) of the creek water sample were measured by atomic absorption spectrophotometer (AAS). Bacteriological properties of creek water sample were investigated by AOAC method. The conventional treatment design for creek water was modified by coagulation and flocculation approach. In the lab study, the experiments with two parameters such as doses of *M. oleifera* seeds powder (1, 2, 3, and 4 g/L) and contact times (1, 2, 3 and 4 h) were conducted to study their effects on the flocculation process. This process showed in significant reducing of turbidity. The optimum conditions for water treatment by using *M. oleifera* (Dant-da-lun) seeds powder are 2 g/L dose and 1 h of contact time. After treatment the observed values of (pH, total suspended solids, total dissolved solids, Mn, K, Cd, Mg, total coliform and *E.coli*) are significantly reduced.

**Keywords:** TDS, pH, Turbidity, *M. oleifera* seeds

### Introduction

Water is one of the most important compounds to the ecosystem. Better quality of water described by its physical, chemical and biological characteristics. But some correlation was possible among these parameters and the significant one would be useful to indicate quality of water, due to increased human population, industrialization, use of fertilizers in agriculture and man-made activity. It is therefore necessary that the quality of drinking water should be checked at regular time interval because due to use of contaminated drinking water, human population suffers from a variety of water borne diseases (Mohamed, 2018). The most important use of water in agriculture is for irrigation, which is a key component to produce enough food. Irrigation takes up to 90 % of water withdraw in some developing countries. Other uses are as a scientific standard for dinking, washing, transportation, chemical uses, heat exchange, fire extinction, recreation, water industry, industrial application and food processing (Choy, 2015). In future, even more water will be needed to produce food because the earth's population is forecast to rise to 9 billion by 2050. The availability and quality of water always have played on important part in determining not only where people can live, but also their quality of life .In rural and undeveloped countries people living in extreme poverty are presently drinking highly turbid and microbiologically contaminated water as they lack of knowledge of proper drinking water treatment and also not afford to use high cost of chemical coagulants. Chemical coagulants like Aluminium sulphate (alum), FeCl<sub>2</sub> is used in Municipal drinking water treatment plant for purification process (Hendrawati *et al.*, 2016). This excess use of amount of chemical coagulants can affect human health e.g., aluminum has also been indicated to be a causative agent in neurological diseases such as pre- senile dementia. To overcome chemical coagulant problems it is necessary to increase the use of natural coagulants for drinking water treatment. Naturally occurring coagulants are usually presumed safe for human health. Some studies on natural coagulants have been carried out and various natural coagulants were produced or extracted form microorganisms, animals or plants.

---

<sup>1</sup> Dr, Lecturer, Department of Chemistry, Dagon University

<sup>2</sup> Dr, Lecturer, Department of Chemistry, Dagon University

<sup>3</sup> Dr, Associate Professor, Department of Chemistry, Dagon University

One of these alternatives is *Moringa oleifera* L. seeds. It is a native tree of the sub-Himalayan parts of North-west India, Pakistan and Afghanistan. *M. oleifera* is a perfect example of a so-called "multipurpose tree". Earlier studies have found *M. oleifera* to be non-toxic, and recommended it to use as a coagulant in developing countries. The use of *M. oleifera* has an added advantage over the chemical treatment of water because it is biological and has been reported as edible. *M. oleifera* seeds act as a natural absorbent and antimicrobial agent as their seeds contain 1 % active ployelectrolyte's that neutralize the negatively charged colloid in the dirty water (Sasikala *et al.*, 2016). This protein can be therefore nontoxic natural ploypeptide for sedimentation of mineral particles and organics in the purification of drinking water. These seeds are also act as antimicrobial agent against variety range of bacteria and fungi. The seed contain number of benzyl isothiocynate and benzyl glucosinolate which act as antibiotic. It is believed that the seed is an organic natural polymer (Amaglo *et al.*, 2010).

*M. oleifera* L. is a highly valued plant, distributed in many countries of the tropics and subtropics Figure 1. Myanmar name of *M. oleifera* L. is Dant-da-lun. English name and botanical name are drumstick and *Moringa oleifera* Lam. Moringaceae is the family of *M. oleifera* L. and part of *M. oleifera* L. is used as seeds.

The aims of the present work, are to investigate the different parameters of water quality of Ngamoeyeik creek water sample treated with *M. oleifera* seeds powder and treated water sample can be suitably used or not for customers near the creek in crowded area.



**Figure 1** (a) pods and (b) seeds of *Moringa oleifera* L. (Dant-da-lun)

## Materials and Methods

### Sample Collection and Storage

In this research, the water sample was collected from Ngamoeyeik creek near North Dagon Township. The sample was collected in polyethylene bottles which had been washed with a detergent and rinsed with water, diluted nitric acid solution and distilled water. Sampling site was recorded with GPS detector. The sampling site is represented in Figure 2.

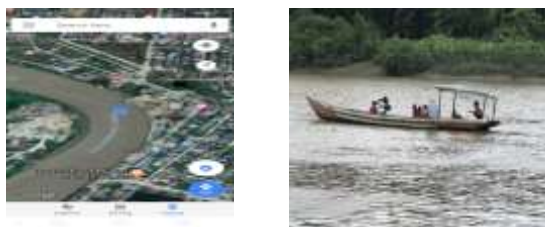


**Figure 2** Satellite image and sampling site

### Determination of Some Physicochemical Properties and Some Bacteriological Activities of Ngamoeyeik Creek Water Sample

In this research, all chemicals were used of analytical reagent grade. In all investigations, the recommended standard methods and techniques involving both standard and modern methods were provided. Some physicochemical properties (pH, turbidity and conductivity) of creek water sample treated with *M. oleifera* seeds powder were measured by digital meter (HANNA

instrument). Total suspended solids and total dissolved solids were determined by filtration and evaporation methods. Total alkalinity and total hardness were determined by titration methods. Some trace elements of water sample were detected by AAS method. Bacteriological properties of creek water sample were investigated by AOAC method (AOAC, 1990).

### Coagulation and Flocculation Process

Coagulating material was added to the supernatants formed from sedimentation process, for determining the effect of the type, dose and time on the coagulation and flocculation of contaminants (turbidity).

### Collection and Preparation of *M. oleifera* L. (Dant-da-lun) Seeds

Coagulating material used in this study is *M. oleifera* seeds were collected from Thanlyin Township, Yangon Region. Good quality of *M. oleifera* seeds were harvested when they were fully matured which was determined by observing if there were any cracked pods on the plants. The pods were plucked and cracked to obtain the seeds which were air dried for 2 week. The seeds are taken and removed its wings and coat from their seeds. Fine powder was prepared by using mortar and pestle and this powder was directly used as coagulant for water treatment (Ndabigengesere *et al.*, 1995).

### Effect of Different Doses on the Removal of Turbidity in Water Sample by Using *M. oleifera* Seeds Powder

1, 2, 3 and 4 g of *M. oleifera* seeds powder were added separately into the beakers containing 1000 mL of water sample. The mixtures in the beaker were stirred thoroughly for 1 h using glass rod. The suspension was left to stand without disturbance at 1 h and the supernatants formed were decanted and subjected to determine the turbidity. They are represented in (Figure 3).

### Effect of Different Contact Times on the Removal of Turbidity in Water Sample by Using *M. oleifera* Seeds Powder

The dose 2 g of *M. oleifera* seeds powder were added separately into a beakers containing 1000 mL of water sample. The mixtures in the beakers were stirred thoroughly for 1 h using glass rod. The suspension was left to stand without disturbance at various time 1, 2, 3 and 4 h. The obtained supernatants were decanted and subjected to determine the turbidity (Figure 4).



**Figure 3** Water samples before and after treatment



**Figure 4** Water samples before and after treatment



**Figure 5** Turbidity apparatus and pH meter

## Results and Discussion

### Collection of Water Sample from Ngamoeyik Creek

In the present study, creek water sample was collected near North Dagon Township, Yangon Region on February 2019. The collected water sample was investigated by conventional methods as well as modern instrumental techniques.

### Effect of Different Doses on the Removal of Turbidity in Water Sample by *M. oleifera* Seeds Powder

The percent removal of turbidity of water sample is 99.503 %, 99.590 %, 99.408 % and 99.560 %, respectively. The maximum reduction of turbidity was found to be 99.590 % in sample. According to the results, the effective dose of *M. oleifera* seeds powder in the removal of turbidity was found to be 2 g/L. These data are shown in Table 1.

Turbidity in creek water is caused by the presence of suspended matter such as clay, silt, finely divided organic and inorganic matter, plankton and other microscopic organisms.

**Table 1** Effect of Different Doses on the Removal of Turbidity in Water Sample by *M. oleifera* Seeds Powder

Doses (g L <sup>-1</sup> )	Removal of Turbidity (%)
1	99.503
2	99.590
3	99.408
4	99.560

### Effect of different contact times on the removal of turbidity in water sample by *M. oleifera* seeds powder

In this study, the optimum dose 2 g L<sup>-1</sup> of *M. oleifera* seeds powder was used for the removal of turbidity. The contact times were varied at 1, 2, 3 and 4 h. The percent removal of turbidity of water sample are 99.570 %, 99.361 %, 99.470 % and 99.343 %, respectively. The maximum reduction of turbidity was found to be 99.570 % in sample. According to the results, optimum contact time was 1 h. These data are shown in Table 2.

**Table 2 Effect of Different Contact Times on the Removal of Turbidity in Water Sample by *M. oleifera* Seeds Powder**

Time (h)	Removal of Turbidity (%)
1	99.570
2	99.361
3	99.470
4	99.343

**Some Physicochemical Properties of Creek Water Sample Before and After Treatment by Using *M. oleifera* Seeds Powder**

In the present study, creek water sample was collected from Ngamoeyeik creek, North Dagon Township. The collected water sample was investigated before and after treatment with *M. oleifera* seeds powder (2 g/L dose) by standard methods as well as modern instrumental techniques. In this research, pH values of water sample were determined as 7.24 and 6.5, respectively. The observed values of pH were within the WHO standards. These pH values are suitable for aquatic life. The turbidity values of water sample were recorded as (>1050) NTU and 4.3 NTU, respectively. According to the visualization and measurement results, the turbidity of water sample was reduced after treatment of *M. oleifera* seeds powder (Figures 3 and 4). So *M. oleifera* seeds powder removed 90 % to 99 % of turbid in the treated water. The observed values of conductivity of water sample were recorded as 3.30  $\mu\text{S}/\text{cm}$  and 2.9  $\mu\text{S}/\text{cm}$ , respectively. The observed values were lower than WHO standards. The values of biochemical oxygen demand of water sample were observed 1.0 and 2.0 ppm and chemical oxygen demand were detected 0.65 and 2.32 ppm, respectively. These results were slightly lower than the WHO standard. The values of total alkalinity and total hardness of water samples before and after treatment were measured 20, 10 and 204, 250 respectively. The observed values of total alkalinity were within WHO standard and total hardness were slightly greater than WHO standard. Total suspended solids were observed 18325 and 0.92 ppm and total dissolved solids were recorded as 14.5 and 2.624 ppm, respectively. High concentration of suspended solid can lower creek water quality by absorbing light. Suspended solids clog fish gills, reduce growth rates, decrease resistance to disease. All of these data are shown in Table 3.

**Table 3 Some Physicochemical Properties of Ngamoeyeik Creek Water Sample Treatment with *Moringa oleifera* L. (Dant-da-lun) Seeds**

Parameters	Observed values		WHO Standard (2017)
	Before treatment	After treatment	
pH	7.24	6.5	6.5-8.5
Turbidity (NTU)	> 1050	4.3	5-25
Conductivity ( $\mu\text{S}/\text{cm}$ )	3.30	2.98	600
COD	0.65	2.32	10
BOD	1.0	2.0	5.0
Total alkalinity (ppm of $\text{CaCO}_3$ )	20	10	90-100
Total hardness (ppm of $\text{CaCO}_3$ )	204	250	20-200
TSS (ppm)	18325	0.92	150
TDS (ppm)	14.5	2.624	500

### Some Elemental Analysis of Creek Water Sample before and after Treatment by Using *M. oleifera* Seeds Powder

Elemental analysis is a process where a sample of some material is analyzed for its elemental. In this study, some elements (Cr, Mn, Fe, Cu, Zn, Pb, Cd, Mg, Ca, K, Na and As) were investigated by AAS method. Before and after treatment of water samples, the observed values of Cr, Fe, Cu, Pb were not measured in the present investigation. The values of Mn, Zn, Cd and As were determined as 0.046, 0.023, 0.043 and 0.01 respectively. After treatment, Mn, Zn, Cd and As were not detected. The values of Mg and Ca, before and after treatment of water samples were determined as 5.108, 4.804 and 18.11, 33.13 respectively. Before and after treatment of water samples, the observed values of K were as 217.9 and 21.52. The values of Na were recorded as 35.27 and 106.5. After treatment, some metals were not detected. These results are shown in Table 4.

**Table 4** Some Elemental Analysis of Ngamoeyeik Creek Water Sample before and after Treatment with *M. oleifera* (Dant-da-lun) Seeds

Parameters	Observed values (ppm)		WHO Standard (2017)
	Before treatment	After treatment	
Cr	ND	ND	0.1
Mn	0.046	ND	0.4
Fe	ND	ND	0.3
Cu	ND	ND	1.0
Zn	0.023	ND	3
Pb	ND	ND	0.01
Cd	0.043	ND	0.003-0.005
Mg	5.108	4.804	50
Ca	11.18	33.13	65
K	217.9	21.52	8
Na	35.27	106.5	30-60
As	0.01	ND	-

ND = not detected

### Some Bacteriological Properties of Ngamoeyeik Creek Water Sample before and after Treatment by Using *M. oleifera* (Dant-da-lun) Seeds

In this present study, before treatment of total coliform was found as 56 cfu/mL in sample. After treatment with *M. oleifera* seeds powder, the number of total coliform was recorded as 10 cfu/mL in sample. The results are presented in Table 5.

In this present study, before treatment of *E. coli* was found as 7 cfu/mL in sample. After treatment with *M. oleifera* seeds powder, the number of *E. coli* was recorded as 1 cfu/mL in sample. The results are presented in Table 5.

**Table 5** Some Bacteriological Properties of Ngamoeyeik Creek Water Sample before and after Treatment by Using *M. oleifera* (Dant-da-lun) Seeds

Parameters	Observed values (cfu/mL)		WHO Standard (2017)
	Before treatment	After treatment	
Total coliform	56	10	0
<i>E. coli</i>	7	1	0

## Conclusion

The water sample from Ngamoeyeik Creek at North Dagon Township, Yangon Region were collected and their physicochemical properties by conventional methods and modern instrumental techniques, elemental analysis by AAS method, bacteriological properties of before and after treatment by AOAC method using *M. oleifera* seeds powder. According to the overall results, it was concluded that *M. oleifera* seeds are the effective natural bioflocculants for water treatment process with low environmental risks. Therefore, *M. oleifera* seeds can be applied as environmental friendly biosorbent material for multi-purposes. This research program can contribute economically and environmentally entire society of Myanmar especially in the rural areas where no facilities are available for the treatment of drinking water.

## Acknowledgements

I would like to express our profound thanks to Dr. Nu Nu Yee and Dr. Nay Thew Kyi, Pro-Rectors, Dagon University for their kind permission and encouragement to carry out this work. I am indebted to Dr. Cho Cho Win, Professor and Head of the Department of Chemistry, Dagon University for her enthusiastic reading and comments for this work.

## References

- Amaglo, N. K., Bennett, R. N. and Lo Curto, R. B. (2010). "Profiling Selected Phytochemicals and Nutrients in Different Tissues of the Multipurpose Tree *Moringa oleifera* L., Grown in Ghana". *Food Chem.*, vol. 122, pp. 1047-1054
- AOAC. (1990). "Official Methods of Analysis of the Association of Official Analytical Chemists". Ed. Helrich, K. Virginia; 15<sup>th</sup> Ed. 1, AOAC Inc.
- Choy, S. P. (2015). "A review on common vegetables and legumes as promising plant-based natural coagulants in water clarification". *International Journal of Environmental Science and Technology*, vol. 12 (1), pp. 367-390
- Hendrawati, Y., Nurhasni, I. R., Rohaeti, E., Effendi, H. and Darusman, L. K. (2016). "The use of *Moringa oleifera* Seed Powder as Coagulant to Improve the Quality of Wastewater and ground Water". *IOP Conference Series, Earth and Environment Science*, vol. 31, p. 12033
- Mohamed, S. A. R. (2018). "Application of Green Synthesis Ag-NPs from *Lawsonia inermis* (Henna) Plant as Antifungal & Non Toxic Nonmaterial in Drinking Water Purification". *Chemistry Research Journal*, vol. 3 (1), pp. 64-73
- Ndabigengesere, A., Narasia S. K., and Talbot, B. J. (1995). "Active Agents and Mechanism of Coagulation of Turbid Waters using *Moringa oleifera*". *Water Research*, vol. 29 (2), pp. 703-710
- Sasikala, S. and Muthuraman, G. (2016). "A Laboratory Study for the Treatment of Turbidity and Total Hardness Bearing Synthesis Wastewater/ Ground Water Using *Moringa Oleifera*". India: Chem, vol. 2, p. 112
- World Health Organization. (2017). "Guideline for Drinking Water Quality". Geneva, Switzerland: World Health Organization

## STUDY ON WATER QUALITY AND TREATMENT OF TUBE WELL WATER SAMPLES FROM SHWEBO TOWNSHIP, SAGAING REGION

Su Lay Yee<sup>1</sup>, Tin Tin Latt<sup>2</sup> and Nwe Thuzar Htwe<sup>3</sup>

### Abstract

In this study, the water samples were collected from three different locations of Shwebo Township, Sagaing Region. Collected water samples were treated by filtration method by using chipping stones (2"), rice husk char (2") and sand (2"). Physicochemical parameters such as pH, turbidity, total suspended solid (TSS), total dissolved solid (TDS), total hardness, total alkalinity, chloride, salinity, dissolved oxygen (DO), chemical oxygen demand (COD), biochemical oxygen demand (BOD) of water samples before and after treatment were also investigated by standard method. The mineral elements such as sodium (Na), magnesium (Mg), calcium (Ca) and lead (Pb) contents were also analyzed by atomic absorption spectrometer and arsenic content was determined by arsenator. The obtained results were compared with the WHO standard. The result of mineral determination revealed sodium (Na), Calcium (Ca) and magnesium (Mg) composition in water samples of before and after treatment were found to be within the WHO standard. Furthermore, toxic element lead and arsenic were not detected all samples of before and after treatment. However, water samples showed high total suspended solid (TSS), total dissolved solid (TDS), total alkalinity, chloride, salinity, biochemical oxygen demand (BOD) values indicating poor water quality.

**Keywords:** water quality, physicochemical parameters, ground water, filtration

### Introduction

The quality of water is vital concern for mankind because it directly linked with human health. Now a day, the menace of water borne diseases and epidemics still looms large on the horizons of developed and developing countries. The polluted water is the culprit in all such cases. We need water every day for various domestic, irrigation and drinking purposes (Degremont, 1991). Groundwater is generally considered to be much cleaner than surface water. However, several factors such as discharge of industrial, agricultural and domestic wastes, land use practices, geological formation, rainfall patterns and infiltration rate affect the groundwater quality. Water gets polluted due to contamination by foreign matter such as microorganism, chemicals, industrial or other wastes. The major problem with the ground water is that once contaminated, it is difficult to restore its quality. Hence there a great need for the protection and management quality. Therefore, the physical and chemical parameters of the particular area will be changed. The quality of water varies with depth of water. Seasonal changes are governed by the extent and composition of dissolved salts depending upon subsurface environment (Saravanakumar, *et al.*, 2011). The main objectives of the physicochemical parameters are to know the suitability of the ground water for domestic and drinking purposes.

### Physicochemical Parameters

It is very essential and important to test the water before it is used for drinking, domestic, agricultural or industrial purpose. Water must be tested with different physicochemical parameters. Selection of parameters for testing of water is solely depends upon for what purpose we going to use that water and what extent we need its quality and purity. Pollution of groundwater is an impairment of quality by chemicals, heat or bacteria to a degree, that does not necessarily create and actual public health hazards, but does adversely affect such water for domestic, farm, municipal or industrial use. Water does content different types of floating, dissolved, suspended

---

<sup>1</sup> Dr, Associate Professor, Department of Chemistry, Shwebo University

<sup>2</sup> Dr, Lecturer, Department of Chemistry, Shwebo University

<sup>3</sup> Lecturer, Department of Chemistry, Shwebo University

and microbiological as well as bacteriological impurities. Some physical test should be performed for testing of its physical appearance such as temperature, color, odour, pH, turbidity, TDS etc., while chemical tests should be performed for its BOD, COD, dissolved oxygen, alkalinity, hardness and other characters (Ellis, 1989).

### Trace Elements in Water

Trace elements are generally present in small concentration in natural water system. Many trace elements are essential nutrients however certain trace elements such as As, Cd, and Hg are known to be persistent environment contamination and toxic to most form of life. Trace elements are generally present in small concentration in natural water system (Adeyeye, 1994). Sodium and potassium are chemical commonly found in soils and rocks. Sodium and potassium are often associated with chloride and bromide. In these forms they readily dissolve in water. In soil containing appreciable amounts of clay, these metals are not mobile. Consequently, concentration increases as residence time in ground water increases.

Lead is a naturally occurring toxic metal found in the Earth's crust. Drinking water delivered through lead pipes or pipes joined with lead solder may contain lead. Much of the lead in global commerce is now obtained from recycling (Adefemi and Awokunmi, 2010). Its widespread use has resulted in extensive environmental contamination, human exposure and significant public health problems in many parts of the world.

Arsenic (As) is a naturally occurring element, due to the presence of arsenical minerals, volcanic emissions and inputs from geothermal sources as well as a consequence of anthropogenic activities, such as mining activities, combustion of fossil fuels and the use of arsenical pesticides. Arsenic exists in both organic and inorganic forms in nature; inorganic arsenic is mostly found in natural water systems (Malana and Khosa, 2011). Long-term exposure to arsenic from drinking water and food can cause cancer and skin lesions. It has also been associated with cardiovascular disease and diabetes. The world health organization (WHO) guideline value of arsenic in drinking water is 10 ppb.

## Material and Methods

### Collection of Samples

In this study, water samples were collected from Shwebo Township, Sagaing Region (Figure 1). Water supplies were throughout this area mostly from tube wells as well as Mahar Nandar pond. Three water samples were collected from different sites (Table 1). The sampling was carried out in January, 2019. The sample bottles were labelled with date and sampling source and immediately brought to the laboratory. The samples were analysed for their physicochemical parameters for water quality.

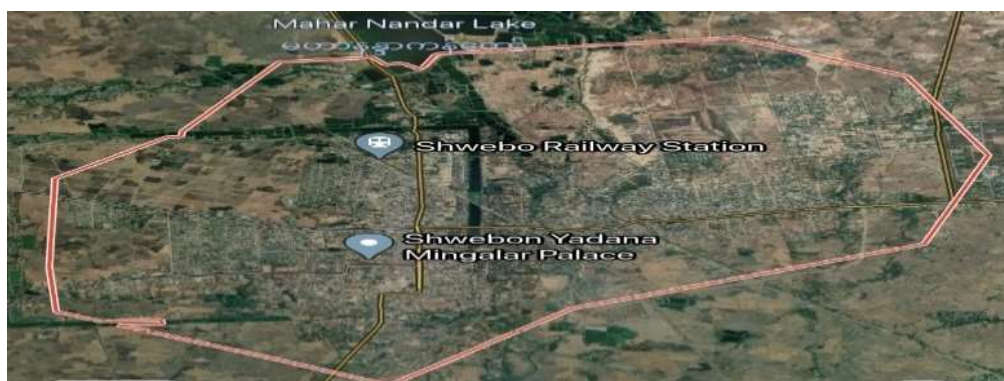


**Figure 1** Map of sample collected area

**Table 1 Location of Sampling Sites**

Sample	Latitude (N)	Longitude (E)	Depth of tube well
1	22° 33.580'	095° 41.567'	365 ft
2	22° 33.601'	095° 41.598'	1100 ft
3	22° 33.594'	095° 41.586'	650 ft

**Preparation of Water Treatment System**

Filtration is a process which improved the water quality by the removal of suspended solids, colloidal matter and the reduction of number of bacteria, colour, odour etc. Sand filters are used as a step in the water treatment process of water purification. Rice husk char is used for adsorption of pollutant from water and waste water. Therefore, a filter was designed, using locally available adsorbents, such as rice husk char, sand and chipping stone which removes the physical and chemical impurities from water. Collected water samples were filtered by use of chipping stones (2"), rice husk char (2") and sand (2").



**Figure 2** Chipping stones, rice husk char and sand for water treatment



**Figure 3** Filtration of water sample

**Determination of Physicochemical Properties**

The experiments and measurements were carried out at the Department of Chemistry, Shwebo University. The samples were analyzed for their physicochemical parameters such as pH, turbidity, total suspended solid, total dissolved solid, total hardness, total alkalinity, dissolved oxygen, chemical oxygen demand, biochemical oxygen demand, trace element (Na, Ca and Mg) and toxic elements (Pb and As) contents by using standard method (APHA,1985). AR grade reagents were used for the analysis and distilled water was used for preparation of solutions. The methods used for estimation of various physicochemical parameters are tabulated in Table 2. The result data was compared with WHO drinking water standard (WHO, 2012).

**Table 2 Methods Used for Determination of Physicochemical Parameters**

No.	Parameter	Method
1	pH	pH meter
2	Turbidity	Turbidimeter
3	TDS and TSS	Filtration method
4	Total hardness	EDTA- titration method
5	Alkalinity	Acid base titration method
6	Chloride and salinity	Silver Nitrate method
7	DO	Iodometric method
8	COD	Palintest photometer 7500
9	BOD	Lovibond-BD 600 photometer
10	Na, Mg, Ca, Pb	Atomic absorption spectrometer
11	As	Arsenator

## Results and Discussion

### Physical Parameters of Water Samples

Some physical parameters of water samples are summarized in Table 3. The pH value of water sample before treatment was found to be 8.02 to 8.37 and pH values were found to be 7.72 to 7.78 after treatment. The acceptable pH for WHO standard is between 6.5 and 8.5 usually indicating good quality. If the pH is less than 6.5, it discontinues the making of vitamins and minerals in the human body. More than 8.5 pH values cause the taste of water saltier. The pH value of water sample before and after treatment exist within the standard range. The turbidity value of water sample before treatment was found to be 2.13 to 2.99 NTU. The turbidity value of the water sample after treatment were found to be 0.25 to 0.87 NTU. Turbidity should ideally be below 5 NTU, since the appearance of water with a turbidity of less than this value is usually acceptable to consumers.

Solids refer to the suspended and dissolved matter in water. the total suspended solid value of water sample before treatment were found to be 200 to 800 ppm. The acceptable total suspended solid value for WHO standard is 150 ppm. The total suspended solid values of water before treatment exist higher than the standard range and the total suspended solid of all water samples decrease to 200 ppm after treatment. In this research, the total dissolved solid of water samples before treatment were found to be 1000 ppm and after treatment were 757 to 986 ppm. The acceptable total dissolved solid value for WHO standard is 500 ppm. The total dissolved solid value of water sample before and after treatment were over the standard range. These water samples also found high alkalinity, chloride and salinity. Hence, these samples were not acceptable to use as drinking water.

**Table 3 Physical Parameters of Water Samples before Treatment and after treatment**

Sample	pH		Turbidity (NTU)		TSS (ppm)		TDS (ppm)	
	*BT	*AT	*BT	*AT	*BT	*AT	*BT	*AT
1	8.37	7.75	2.99	0.25	200	200	1000	953
2	8.02	7.78	2.13	0.87	300	200	1000	757
3	8.30	7.72	2.59	0.60	800	200	1000	986
WHO standard (2017)	6.5 – 8.5		5		150		500	

\*BT = Before Treatment

\*AT = After Treatment

\*TDS = Total Dissolved Solids

\*TSS = Total Suspended Solids

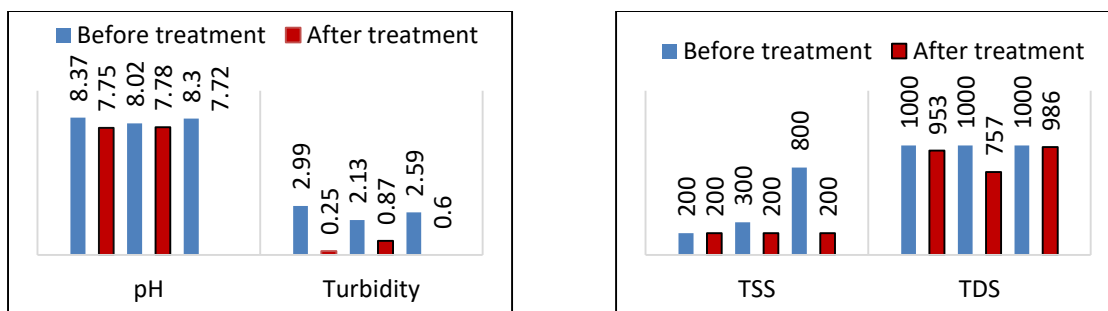


**Figure 4** Comparison of pH, turbidity, TSS and TDS of water samples for before treatment and after treatment

### Chemical Parameters of Water Samples

The values of some chemical parameter found in water samples were shown in Table 4 and Figure 5. Regarding total hardness of all studied samples considered safe for drinking purposes, the hardness value of water sample before treatment were found to be 112 to 180 ppm of CaCO<sub>3</sub>. The hardness values of the water sample after treatment were found to be 56 to 80 ppm of CaCO<sub>3</sub>. The acceptable hardness value for WHO standard is 500 ppm of CaCO<sub>3</sub>. These results showed that hardness of water was good agreement with WHO standards.

Alkalinity of water is measure of its capacity to neutralize acids. This is due to the primarily salts of weak acids or strong bases. Bicarbonates represent the measure form of alkalinity. The alkalinity values of water samples before treatment were found to be 300 to 700 ppm of CaCO<sub>3</sub>. The alkalinity values of the water samples after treatment were found to be 280 to 520 ppm of CaCO<sub>3</sub>. The acceptable alkalinity value of drinking water for WHO standard is 150 ppm of CaCO<sub>3</sub>. The alkalinity values of both water samples of before and after treatment were found to be higher than the standard range. High alkalinity may be due to presence of salts of metal ions.

High chloride ion concentration indicates organic pollution in the water. Chloride is a natural substance present in all portable water as well as sewage effluents as metallic salt. In the study area, the chloride ranged from 480 to 600 ppm for before treatment and after treatment, it was found to be 400 to 450 ppm. The chloride values were greater than the drinking water quality standards. The reported the range of chloride was 250 ppm. The water salinity found range from 896 to 1113 ppm for before treatment and 752 to 826 ppm after treatment which is higher than the maximum permissible limits 500 ppm.

**Table 4** Chemical Parameters of Water Samples before Treatment and after treatment

Sample	Total hardness (ppm of CaCO <sub>3</sub> )		Total alkalinity (ppm of CaCO <sub>3</sub> )		Chloride (ppm)		Salinity (ppm)	
	*BT	*AT	*BT	*AT	*BT	*AT	*BT	*AT
1	112	80	700	520	600	400	1113	752
2	172	56	300	280	480	400	896	752
3	180	72	400	320	600	450	1113	826
WHO standard (2017)	500		150		250		500	

\*BT = Before Treatment, \*AT = After Treatment,

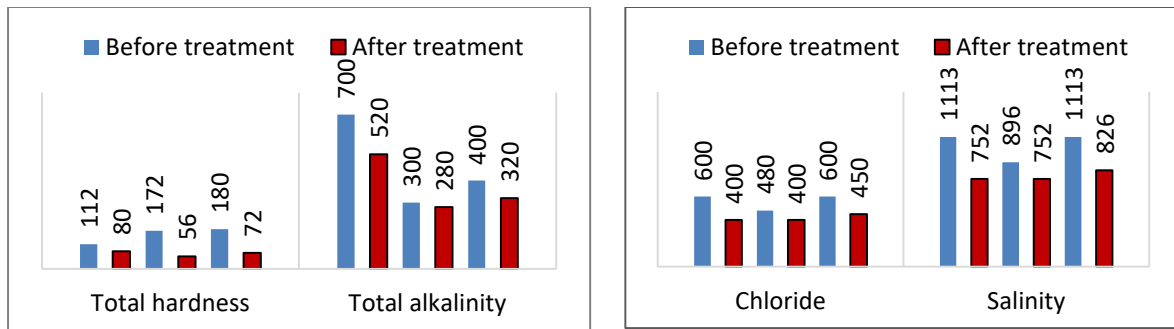


**Figure 5** Comparison of total hardness, total alkalinity, chloride and salinity of water samples before treatment and after treatment

### Biochemical Parameters of Water Samples

Some biochemical characteristics of water samples were shown in Table 5 and Figure 6. Dissolved oxygen (DO) reflects the physical and biological processes prevailing in the water. The DO values indicate the degree of pollution in water bodies. In this research, the dissolved oxygen of water samples before treatment were found to be 1.46 to 3.25 ppm. The dissolved oxygen of the water sample after treatment were found to be 1.35 to 2.75 ppm. The dissolved oxygen values of water samples were within the acceptable WHO standard (<5 ppm).

BOD and COD are two common measures of water quality that reflect the degree of organic matter pollution of a water body. So, poor quality of water such as high COD, BOD can cause waterborne diseases like diarrhea, cholera etc. COD of water samples before treatment were found to be in the range of 0.02 to 0.28 ppm. COD values of the water sample after treatment were found to decrease to 0.01 ppm. The chemical oxygen demand values of water samples were within the standard range.

BOD is used for determination of requirement of oxygen for stabilizing household and industrial wastes. The effluents disposed by domestic and industries into the surface and ground water contaminate the quality of the water which can be assessed by BOD determination (Sawyer, *et al.*, 1994). According to WHO drinking water standard, BOD should not exceed 6 ppm. The biochemical oxygen demand (BOD) of water samples before treatment was found to be 4 to 9 ppm. The biochemical oxygen demand of the water samples after treatment were found to be 3 to 7 ppm. The biochemical oxygen demand of water samples 2 and 3 were found higher than the standard range.

### Trace Elements of Water Samples

The results of the mineral elements concentration in water samples are shown in Table 6 and Figure 7. According to the AAS results, Na contents of water samples were found in the range of 172.3 to 175.3 ppm before treatment and it was found in the range of 145.0 to 166.2 ppm after treatment. The sodium content of samples was found to be high as well as salinity. Mg contents were 7.052 to 9.314 and 5.238 to 6.844 ppm before treatment and after treatment respectively. Ca contents were 8.951 to 10.665 and 6.197 to 6.821 ppm before treatment and after treatment, respectively. According to the results of sodium, calcium and magnesium composition of all water samples before and after treatment were also found to be within WHO acceptable level of drinking water. Toxic elements Pb and As were not detected in all samples.

**Table 5 Biochemical Parameters of Water Samples before Treatment and after Treatment**

Sample	DO (ppm)		COD (ppm)		BOD (ppm)	
	*BT	*AT	*BT	*AT	*BT	*AT
1	3.25	2.75	0.02	0.01	4	3
2	2.89	2.56	0.28	0.01	8	7
3	1.46	1.35	0.25	0.01	9	7
WHO standard (2017)	5		10		6	

\*BT = Before Treatment \*AT = After Treatment \*DO = Dissolved Oxygen

\*COD = Chemical Oxygen Demand \*BOD = Biochemical Oxygen Demand

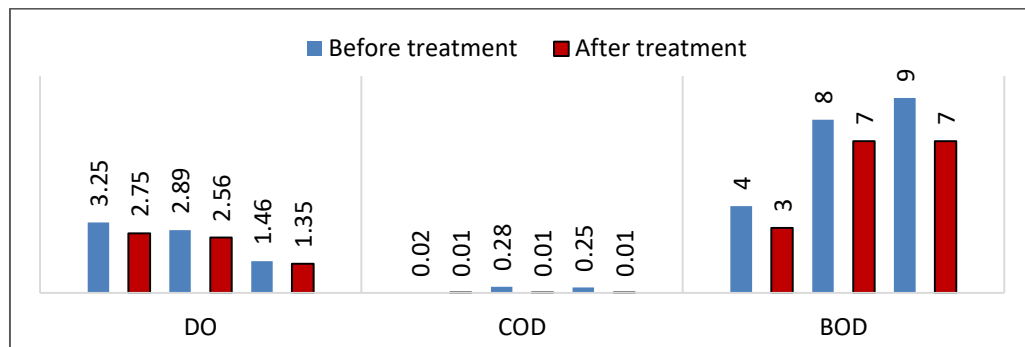


**Figure 6** Comparison of DO, COD and BOD of water samples before treatment and after treatment

**Table 6** Element Contents of Water Samples before Treatment and after treatment

Mineral element	Relative abundance of elemental contents (ppm)						WHO standard (2017)
	Before Treatment			Before Treatment			
	Sample 1	Sample 2	Sample 3	Sample 1	Sample 2	Sample 3	
Na	173.9	175.3	172.3	145.0	166.2	165.4	200
Mg	8.040	7.052	9.314	5.556	5.238	6.844	150
Ca	8.981	8.951	10.665	6.775	6.821	6.197	75
Pb	0.00	0.00	0.00	0.00	0.00	0.00	0.01
As	0.00	0.00	0.00	0.00	0.00	0.00	0.001

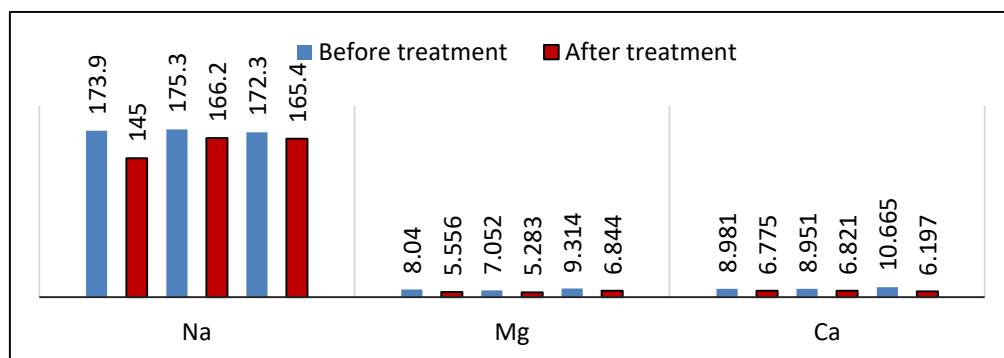


**Figure 7** Comparison of Na, Mg and Ca contents of water samples before treatment and after treatment

## Conclusion

The water samples were collected from different locations of Shwebo Township, Sagaing Region. The water samples were treated by filtration of chipping stones (2"), rice husk char (2") and sand (2"). The water samples of before and after treatment were analysed for physicochemical properties, trace elements and heavy metals pollution. According to the experimental results, total suspended solid (TSS), total dissolved solid (TDS), total alkalinity, chloride, salinity and biochemical oxygen demand (BOD) of water samples were found higher than WHO standard. But these physicochemical parameters could be reduced after filtration. Na, Mg and Ca contents of all water samples before and after treatment were also found to be within WHO acceptable level of drinking water. Furthermore, toxic elements such as lead and arsenic were not detected in all of the samples, before and after treatment. The water samples from the study area cannot be regarded as being of good quality for drinking. Based on the results of this research, chipping stone, rice husk char and sand can be considered as low cost and locally available natural filter for removing of some impurities from tube well water. Thus, it was attributed to lack of adequate protection for most ground water sources especially the public ones.

## Acknowledgements

The authors would like to express their profound gratitude to the Department of Higher Education, Ministry of Education, Myanmar, for provision of opportunity to do this research and Myanmar Academy of Arts and Science for allowing to present this paper. Special thanks are extended to Professor and Head, Dr Nyunt Nyunt Sein, Department of Chemistry, Shwebo University for her guidance and invaluable suggestions.

## References

- Adefemi, S. O. and Awokunmi, E. E. (2010). "Determination of Physicochemical Parameters and Heavy Metals in Water Samples from Itaogbolu Area of Ondo-State, Nigeria", *African Journal of Environmental Science and Technology*, vol 4(3), pp. 145-148
- Adeyeye, E. I. (1994). "Determination of Heavy Metals in Illisha Africana, Associated Water, Soil Sediments from Some Fish Ponds", *International Journal of Environmental Study*, vol.45, pp. 231-240
- APHA. (1985). *Standard Methods for Examination of Water and Wastewater*. Washington D. C.: 20<sup>th</sup> Edition, American Public Health Association, pp.116-268
- Degremont, G. (1991). *Water Treatment Handbook*. Netherland: 6<sup>th</sup> Edition, Lavoisier Publishing
- Ellis, K. V. (1989). *Surface Water Pollution and Its Control*, London: Macmillan Press Ltd., Basingstoke, pp. 97-101
- Malana M. A. and Khosa, M. A. (2011). "Ground Water Pollution with Special Focus on Arsenic, Dera Ghazi Khan-Pakistan." *Journal of Saudi Chemical Society*, vol. 15 (1), pp. 39-47
- Saravanakumar, K. and Ranjith, R.K. (2011). "Analysis of Water Quality Parameters of Ground Water near Ambattur Industrial Area, Tamil Nadu, India". *Indian Journal of Science and Technology*, vol. 4 (5), pp. 1732-1736
- Srivastava, S., Kumar, M., Singh, J., Srivastava, K. K and Singh, G. (1999). "Determination of Physicochemical Parameters of Deoli Bhorus Dam water". *Indian J. Environmental Protection*, vol. 19 (9), pp. 271-279
- WHO. (2017). "Guidelines for Drinking-Water Quality", Geneva: 4<sup>th</sup> ed.; World Health Organization, pp-126-380

# REMOVAL OF CALCIUM ION FROM WATER BY LUFFA SPONGE *L. AEGYPTIACA*

Thin Thin Swe<sup>1</sup>, Su Myat Noe<sup>2</sup>

## Abstract

Hardness is one of the common water quality problems throughout the world. Luffa sponge can be used as a sorbent material to reduce dissolved calcium and magnesium in hard water. This paper deals with removal of calcium ions from water by using luffa sponge as a sorbent. The luffa sponge sample was collected from Taunggyi Township, Shan State. In order to find out the types of organic constituents present in luffa sponge sample, preliminary phytochemical investigation was carried out by test tube method. Some physicochemical parameters such as ash, moisture and fibre contents of luffa sponge were determined by AOAC methods. The alkali modified luffa sponge sample was prepared by treating with NaOH solution. The feasibility of alkali modified luffa sponge as metal ions adsorbent for Ca<sup>2+</sup> ions from aqueous solution was studied in batch experiments at room temperature. Sorption efficiency of alkali modified luffa sponge for calcium ions was investigated by varying pH, initial metal concentration, contact time and sorbent dose. The residual metal ions in aqueous solution will be determined by complexometric titration. Alkali modified luffa sponge and metal loaded alkali modified luffa sponge were characterized by EDXRF and FT IR analyses. It was inferred that alkali modified luffa sponge can be considered as an effective sorbent in the treatment of hard water.

**Keywords:** AOAC methods, hard water, calcium removal, luffa sponge, phytochemical investigation

## Introduction

Luffa (*Luffa cylindrica*(L.) Rome syn *L. aegyptiaca* Mill.) commonly called sponge gourd, luffa, vegetable sponge, bath sponge or dish cloth gourd, is a member of cucurbitaceous family. Luffa sponge contains an abundance of oxygen-containing functional groups such as phenolic, alcoholic, ketonic structures which can serve as adsorption sites for binding metals and will form sorbent-metal macromolecular complexes with high stability through ionic and coordinate covalent bonding. This feature is the basis for the application of luffa sponge in the removal of metal contaminants from water (Adie *et al.*, 2013). Calcium is unique among nutrients, in that the body's reserve is also functional increasing bone mass is linearly related to reduction in fracture risk. Calcium that reaches the lower small intestine actually protects against kidney stones by binding oxalic acid in food and reducing its absorption. Calcium ingested from water together with food would have the same effect. Epidemiological evidence is strong that dietary calcium reduces the incidence of kidney stones (Cotruvo *et al.*, 2009). In recent years, faced with the need for new material more efficient, economical, biodegradable, use of plant material for the disposal of toxic products in aqueous effluents has received a significant credibility. Adsorption process is considered as the most effective technique for remediation of contained water owing to its technical feasibility and cost-effectiveness. Luffa sponge may provide an alternative option and be used to partly replace the activated carbon (AD *et al.*, 2015). The main aim of this work is to modify luffa sponge by using alkali and to apply it in the treatment of hard water.

## Materials and Methods

### Sample Collection and Preparation

Luffa sponge sample (*L. aegyptiaca*) was chosen to use as a sorbent in this work. Luffa sponge was collected from Taunggyi Township, Southern Shan State in December, 2018. The sample was cut into small strips and washed with distilled water and dried in oven at 105 °C for

---

<sup>1</sup> Dr, Associate Professor, Department of Chemistry, Taunggyi University

<sup>2</sup> Candidate, MSc, Department of Chemistry, Taunggyi University

24 h. It was then ground to fine power and stored in air-tight container. Tap water sample was collected from Taunggyi University Campus.

### **Phytochemical Investigation on Luffa Sponge Sample**

In order to find out the types of organic constituents in luffa sponge sample, preliminary phytochemical investigation was carried out by test tube methods.

### **Determination of Moisture, Ash and Fiber Contents**

The physicochemical parameters such as moisture, ash and fiber contents of luffa sponge were determined by AOAC methods (AOAC, 1996).

### **Investigation on the Removal of Calcium (II) Ions from Aqueous Solution**

#### **(a) Modification of luffa sponge**

Dried luffa sponge (1 g) was soaked for 24 h and then washed with distilled water. Then, it was dried in oven at 105 °C for 24 h to obtain dried material. And then, this dried material was grinded with electric grinder. After powder was achieved, this powder was treated with 2 M NaOH for 24 h and then stirred at 30 min and placed at room temperature for overnight. Treated carbon was achieved. It was washed with distilled water after dried in furnace. Finally alkali modified sample was obtained (Abay, 2015).

#### **(b) Preparation of stock solution**

Aqueous stock solution (1000 mg L<sup>-1</sup>) of calcium (II) ions was prepared by dissolving calcium chloride in deionized water. Solutions of desired metal concentrations were then prepared by dilution of the stock solution with deionized water. Fresh dilutions were used for each study. The pH of the solutions was adjusted by using 0.1 M hydrochloric acid and 0.1 M sodium hydroxide.

#### **(c) Effect of pH on metal sorption**

The sorption studies were carried out by batch technique. The initial concentration of calcium solution was 200 mg L<sup>-1</sup>. In order to determine the effect of different pH on sorption, metal solution was divided into six samples and their pH was adjusted to 2, 3, 4, 5, 6, and 7. For each test run, 5 g of modified luffa sponge sample was added into a 100 mL of the metal solution. The suspension was then shaken in a shaker for 1 hour at room temperature. At the end of equilibrium time, the sample was separated by decantation. The residual metal ion in aqueous layer was determined by complexometric titration using EBT indicator (Vogel, 1962).

#### **(d) Effect of initial metal concentration on sorption**

The concentrations of metal ion solutions prepared from their respective stock solutions were: 5, 10, 50, 100, 200, 500, and 1000 mg L<sup>-1</sup>. The pH for experiment was taken as optimal pH 6. For each test run, a 100 mL of the metal solution was added into 5 g of modified luffa sponge sample. The suspension was then shaken in a shaker for 1 h at room temperature. At the end of equilibrium time, the sample was separated by decantation. The residual metal ion in aqueous layer was determined by complexometric titration using EBT indicator (Vogel, 1962).

#### **(e) Effect of contact time on metal sorption**

A five-gram of modified luffa sponge sample was mixed with 100 mL of metal ion solution. The initial concentration of metal solution was 200 mg L<sup>-1</sup>. The pH for experiment was taken as optimal pH 6. The sample solution was shaken with shaker for a predetermined time interval. The time intervals for test runs were: 10, 20, 30, 40, 50, 60 and 90 min. At the end of prescribed contact

time, the residual solution was analyzed for  $\text{Ca}^{2+}$  ion by complexometric method. The equilibrium time is defined as the contact time required for the metal concentration in the solutions to reach constant value.

**(f) Effect of sorbent doses on metal sorption**

Dependence of metal sorption on the sorbent dose was studied by varying the amount of modified luffa sponge sample from 1 to 9 g L<sup>-1</sup>, while keeping other parameters (pH, metal concentration and contact time) constant. The pH was adjusted to the optimal pH 6. The initial concentration of metal solution was 200 mg L<sup>-1</sup>. The contact time was 1 h. The residual metal content was determined by complexometric titration.

**Characterization of Luffa Sponge Sample**

**(a) Determination of relative abundance of elements (EDXRF)**

The elements present in the modified and calcium loaded luffa sponge were measured by means of an EDXRF spectrometer at the Department of Physics, Taunggyi University.

**(b) Determination of FT IR spectrum**

Functional groups present in the modified and calcium loaded luffa sponge were analyzed by using FT IR spectrometer at Department of Chemistry, Taunggyi University.

**Determination of Hardness of Tap Water before and after Treatment by Luffa Sponge**

**(a) Determination of total hardness**

The 10 mL each of the water samples before and after treatment was pipetted out into a clean conical flask. The 1 mL ammonia buffer and 1 drop of EBT indicator were added and titrated against EDTA from the burette. The end point was the change of colour from wine red to clear blue.

**(b) Determination of permanent hardness**

The 100 mL of the given sample of water was pipetted out into a clean beaker and boiled for 60 min. It is then filtered to remove the precipitate formed due to the decomposition of temporary hardness producing salts. The filtrate was made up to 100 mL in standard measuring cylinder using distilled water. The 10 mL of the solution is pipetted out into a conical flask. The 1 mL ammonia buffer and 1 drop of EBT indicator were added and titrated against EDTA from the burette. The end point is the change of colour from wine red to clear blue.

**(c) Determination of temporary hardness**

The temporary hardness was calculated from the total and permanent hardness.

Temporary hardness = Total hardness – Permanent hardness

**Results and Discussion**

**Phytochemical Investigation of Luffa Sponge**

According to the phytochemical investigation of luffa sponge, glycoside, protein, polyphenol and carbohydrate were present in the sample while alkaloids,  $\alpha$ -amino acids, flavonoids, reducing sugars, saponins, starch, steroids, terpenoids and tannins were not present in luffa sponge. These phytochemicals do not adversely affect water when luffa sponge is used as a sorbent in water.

### Moisture, Ash and Fiber Contents of Luffa Sponge

The physicochemical parameters such as moisture, ash and fiber contents of luffa sponge were determined. It was found that fiber was present as major constituent in luffa sponge and the result are shown in Table 1.

**Table 1 Physicochemical Parameters of Luffa Sponge**

No.	Parameters	Content (%)
1	moisture	10.40
2	fiber	69.23
3	ash	0.40

### Modification of Luffa Sponge

Alkali modified luffa sponge was used for the adsorption of water hardness. The purpose of treating luffa sponge using NaOH is to increase the number of adsorption sites on the surface of sorbent. The treatment with alkali chemically modifies the surface of luffa sponge fiber. The main action of NaOH on the fiber is to remove the lignin binder of the cellulosic material (Abay, 2015).

### Sorption of Calcium onto the Modified Luffa Sponge

The feasibility of modified luffa sponge as metal ion adsorbent for removing calcium ions from aqueous solution was investigated. The effects of various experimental parameters (pH, metal concentration, contact time and sorbent dose) were studied in batch sorption experiments at room temperature. Luffa sponge was found to absorb  $\text{Ca}^{2+}$  ions employed in the study.

The effect of pH on % removal of calcium ions is shown in Table 2 and Figure1. The minimum percent removal of  $\text{Ca}^{2+}$  ions was at pH 2. As the pH of the solution increased from 2 to 7, calcium ions showed an increase in binding to the sorbent with optimum binding occurring at pH 6. The percent removal of  $\text{Ca}^{2+}$  ion from aqueous solution of  $200 \text{ mg L}^{-1}$  initial metal concentration onto modified luffa sponge at  $5 \text{ g L}^{-1}$  dose after 60 min contact time was 75.49 % at pH 6. It was observed that the percent removal of  $\text{Ca}^{2+}$  ions decreased with further increased in pH beyond the optimum pH. This finding has been attributed to the formation of anionic hydroxide complexes that decreased the concentration of free metal ions, thereby the sorption capacity of metal ions accordingly decreased (Stephen and Sulochana, 2004).

**Table 2 Effect of pH on % Removal of Calcium Ion by Luffa Sponge.**

pH	2	3	4	5	6	7
Percent removal of $\text{Ca}^{2+}$ ion (%)	8.82	29.41	46.08	65.68	75.49	64.70

(initial calcium concentration =  $200 \text{ mg L}^{-1}$ ; sorbent dose =  $5 \text{ g L}^{-1}$ ; contact time = 60 min)

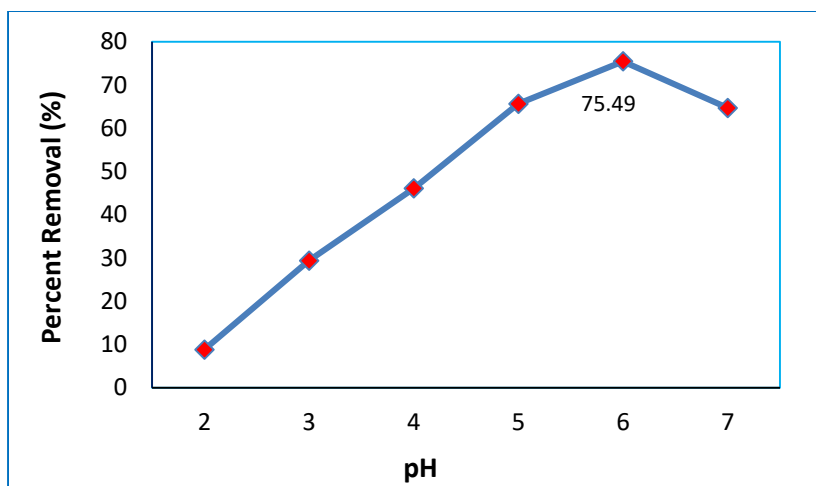


**Figure 1** Effect of pH on calcium removal by luffa sponge (initial calcium concentration = 200 mg L<sup>-1</sup>; sorbent dose = 5 g L<sup>-1</sup>; contact time = 60 min).

Effect of initial metal concentration on Ca<sup>2+</sup> ions removal by modified luffa sponge is shown in Table 3 and Figure 2. Initial concentrations of Ca<sup>2+</sup> ions were varied from 5 to 1000 mg L<sup>-1</sup> while keeping other parameters fixed at their optimal values. It was observed that percent removal of metal decreased with increase in initial metal concentration. At their respective optimal pH, high percent removal of Ca<sup>2+</sup>, 84.90 % was observed at initial metal concentration, 5 mg L<sup>-1</sup>. When initial concentration was varied from 5 to 1000 mg L<sup>-1</sup>, the percentage of metal removal markedly decreased. The absolute amount of metal removal per unit mass of luffa sponge significantly decreased with increasing initial metal concentration. This can be attributed to the increase of contact between metal ion and adsorbent. Thus, initial metal concentrations have a considerable effect on binding of metal ions to the sorbent and concentration always correlated with the quantity of metal fixed on the material. At lower concentration, the ratio of initial number of mole of metal ions to the available surface area is larger (Yu *et al.*, 2003).

**Table 3** Effect of Concentration on % Removal of Calcium Ion by Luffa Sponge

Initial metal concentration (mgL <sup>-1</sup> )	5	10	50	100	200	500	1000
Percent removal of Ca <sup>2+</sup> ion (%)	84.90	80.05	78.49	76.36	75.49	73.70	34.40

(sorbent dose = 5 g L<sup>-1</sup>; pH = 6; contact time = 60 min)

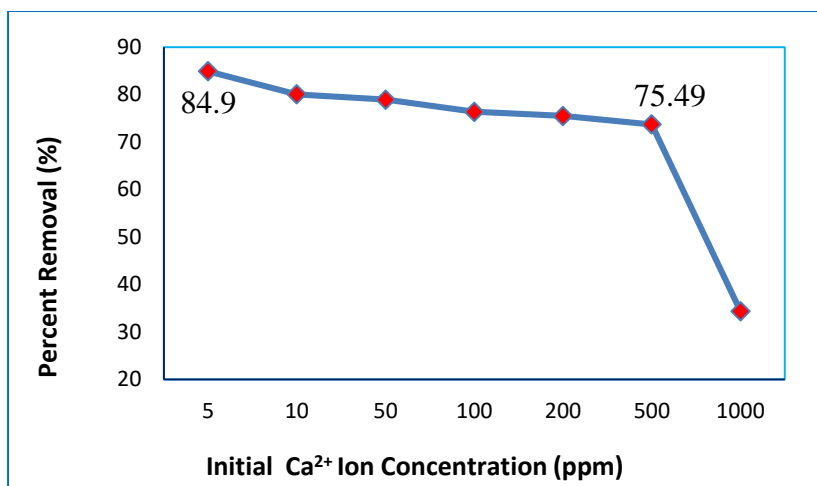


**Figure 2** Effect of initial metal concentration on calcium removal by luffa sponge  
(sorbent dose = 5 g L<sup>-1</sup>; pH = 6; contact time = 60 min)

Time-dependency studies offered data about the change in metal removal related to time. In this study, the minimum time necessary for modified luffa sponge to be in contact with the metal ion solutions was elucidated. The percent removal Ca<sup>2+</sup> ions with respect to contact time for initial metal concentration of 200 mg/L onto modified luffa sponge at 5 g L<sup>-1</sup> dose at pH 6 was studied by varying the contact time from 10 to 90 min. After that the rate of Ca<sup>2+</sup> ions removal increased gradually and reached the equilibrium value at about 60 min. The results are presented in Table 4 and Figure 3.

**Table 4** Effect of Contact Time on % Removal of Calcium Ion by Luffa Sponge

Contact Time (min)	10	20	30	40	50	60	90
Percent removal of Ca <sup>2+</sup> ion (%)	53.92	53.92	54.90	64.70	65.68	75.49	75.49

(sorbent dose = 5 g L<sup>-1</sup>; pH = 6; initial calcium concentration = 200 mg L<sup>-1</sup>)

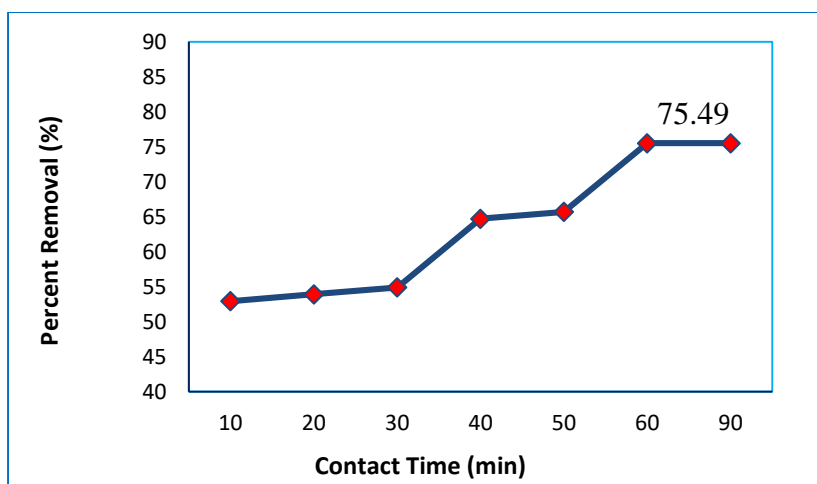


**Figure 3** Effect of contact time on calcium removal by luffa sponge  
(Sorbent dose = 5 g L<sup>-1</sup>; pH = 6; initial calcium concentration = 200 mg L<sup>-1</sup>)

The dependence of  $\text{Ca}^{2+}$  ions removal on sorbent dose were studied by varying the amount of sorbent, modified luffa sponge, from 1 to 10  $\text{g L}^{-1}$ , while keeping other parameters at constant. The results are presented in Table 5 and Figure 4. As the absorbent dosage increased from 1 to 9  $\text{g L}^{-1}$ , the percentage of  $\text{Ca}^{2+}$  ions removal increased from 65.68 % to 87.25 %. With more than 8  $\text{g L}^{-1}$  of sorbent dose, the equilibrium of calcium removal was reached and the percent of removal remained stable. Increasing the dose further did not affect the percentage removal. To sum up, increase in  $\text{Ca}^{2+}$  ions removal with increase in modified luffa dose is due to the greater availability of exchangeable sites or surface area at higher concentration of the sorbent. However, after a certain dose of sorbent, the maximum sorption is attained and hence the amount of ions bound to the sorbent and amount of free ions remains constant even with further addition of sorbent (Adbel-Ghani *et al.*, 2007).

**Table 5 Effect of Sorbent Dose on % Removal of Calcium Ion by Luffa Sponge**

Sorbent dose ( $\text{g L}^{-1}$ )	1	2	3	4	5	6	7	8	9
Percent removal of $\text{Ca}^{2+}$ ion (%)	65.68	66.67	67.64	68.63	75.49	77.45	85.29	87.25	87.25

(initial calcium concentration = 200  $\text{mg L}^{-1}$ ; contact time = 60 min; pH = 6)

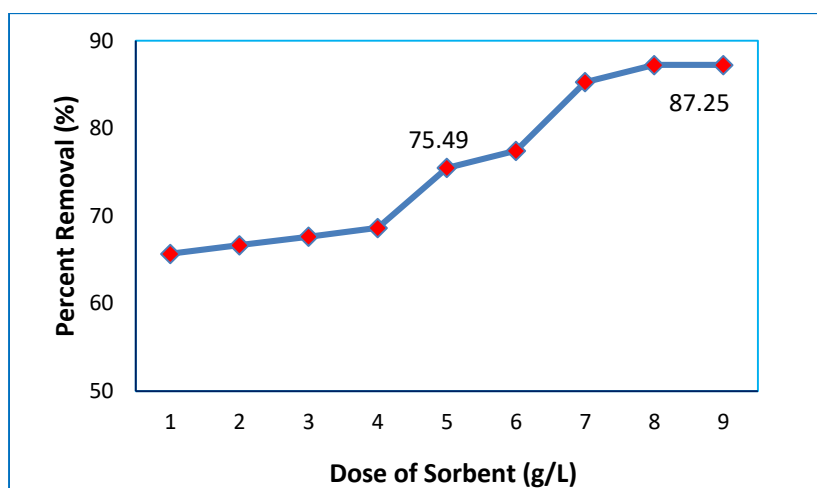
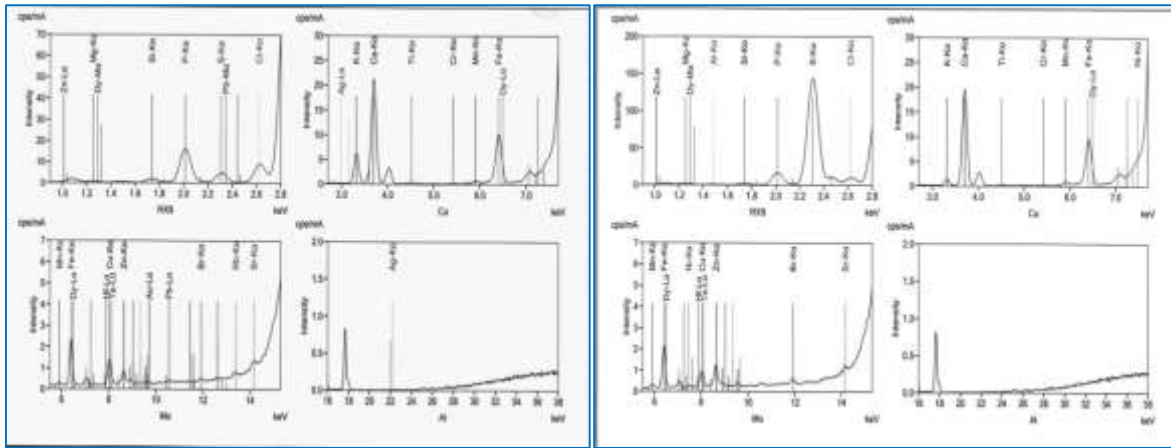


**Figure 4** Effect of sorbent dose on calcium removal by luffa sponge  
(initial calcium concentration = 200  $\text{mg L}^{-1}$ ; contact time = 60 min; pH = 6)

**Characterization of Modified and Calcium Loaded Luffa Sponges**

**(a) EDXRF Analysis**

EDXRF spectra of the samples shown in Figures 5 represent the relative abundance of elements present in modified and calcium loaded luffa sponges samples. According to qualitative EDXRF analysis Cl, S, K, P, Fe, Br, Cu and Zn were found to be present in modified luffa sponge. Figure 5(b) shows the presence of  $\text{Ca}^{2+}$  ion sorbed on luffa sponge.

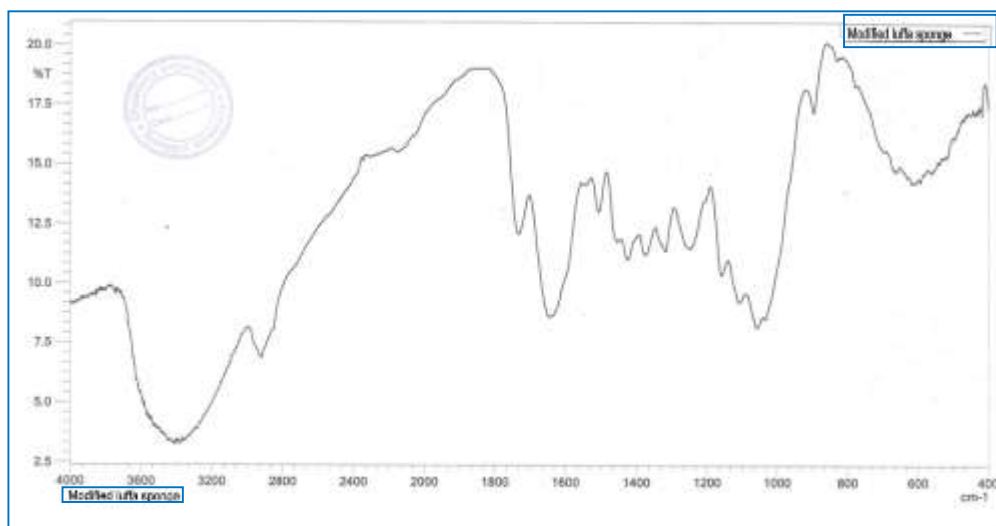


(a) modified luffa sponge

(b) calcium loaded luffa sponge

**Figure 5** EDXRF spectra of (a) modified and (b) calcium loaded luffa sponges**(b) FT IR Analysis**

FT IR spectra of modified and calcium loaded luffa sponge are showed in Figures 7 and 8. FT IR spectrum of modified luffa sponge exhibited stretching frequency of  $\text{-OH}$  groups at  $3600\text{-}3200\text{ cm}^{-1}$ . Aliphatic  $\text{C-H}$  stretching vibration was observed at  $2900\text{ cm}^{-1}$ . The band at  $1560\text{ cm}^{-1}$  was attributed to  $\text{C=C}$  stretching vibration of aromatic and aliphatic rings. The bands between  $1470$  and  $1120\text{ cm}^{-1}$  were provided from  $\text{-CH}_2$  bending. From the analysis of IR spectrum, it may be inferred that ionisable (carboxylic and phenolic groups) and polar functional groups (hydroxyl, methoxy) abundantly consist of luffa sponge. Characteristic vibration of metal- oxygen bonding was observed at  $840\text{-}860\text{ cm}^{-1}$  and  $850\text{ cm}^{-1}$  for calcium loaded modified luffa sponge.

**Figure 7** FT IR spectrum of modified luffa sponge

**Table 6 Infrared Spectral Data of Modified Luffa Sponge**

Observed band (cm <sup>-1</sup> )	Mode of vibration
3600-3200	$\nu_{\text{O-H}}$ (O-H Stretching of O–H stretching of aromatic or aliphatic alcohol; carboxylic acid)
2900	$\nu_{\text{C-H}}$ (aliphatic C-H Stretching)
1680	$\nu_{\text{C=O}}$ (C=O Stretching of carbonyl group)
1560	$\nu_{\text{C=C}}$ (aromatic or alkenic stretching vibrations)
1470	$\delta_{\text{C-H}}$ (out of plane C-H deformation)
1120	$\delta_{\text{C-H}}$ (in plane deformation of C-H)

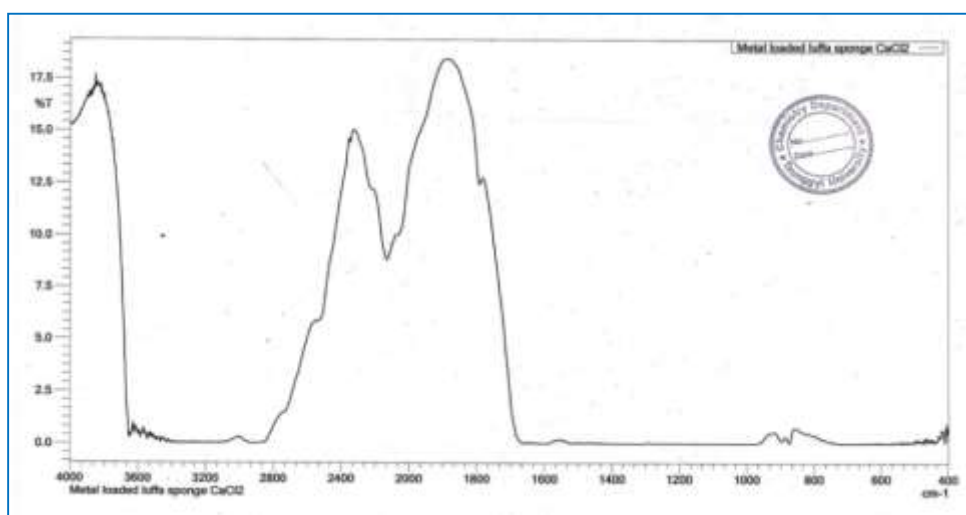


**Figure 8** FT IR spectrum of calcium loaded luffa sponge

**Hardness of Tap Water Sample before and after Treatment**

Hardness in tap water is due to the presence of dissolved salts of calcium and magnesium. It is unfit for drinking, bathing, washing and it also forms scales in boilers. Hence it is necessary to estimate the amount of hardness producing substances present in water sample. The hardness of tap water collected from Taunggyi University Campus was reduced by alkali modified luffa sponge.

**Table 8 Hardness of Tap Water Sample before and after Treatment with Luffa Sponge**

Hardness	Before treatment (ppm as CaCO <sub>3</sub> )	After treatment (ppm as CaCO <sub>3</sub> )	% Reduction
Total hardness	280	130	53.57
Permanent hardness	170	40	76.47
Temporary hardness	110	90	18.18

## Conclusion

According to phytochemical results, glycoside, protein, polyphenol and carbohydrate were present in the sample. According to physicochemical parameters study, fiber was present as major constituent in luffa sponge. Sorption efficiency of modified luffa sponge for calcium (II) ion ( $\text{Ca}^{2+}$ ) was investigated by varying pH, initial metal concentration, sorbent dose and contact time. The highest removal efficiency was observed for calcium at pH 6. The optimum percent removal of calcium from  $200 \text{ g L}^{-1}$  solution by modified luffa sponge ( $5 \text{ g L}^{-1}$  dose) was 75.49 % of calcium, after 60 min contact time. The characterization of alkali modified and metal loaded alkali modified luffa sponge was carried out by EDXRF and FT IR analyses. From the analysis of FT IR spectrum, it may be inferred that ionisable (carboxylic and phenolic groups) and polar functional groups (hydroxyl, methoxy) abundantly consist of luffa sponge. The characteristic vibration of metal-oxygen bonding was observed the spectra of metal loaded modified luffa sponge samples. It was observed that the hardness of tap water collected from Taunggyi University Campus can be reduced by modified luffa sponge. It was found that the total hardness, permanent hardness and temporary hardness of tap water were reduced. It was inferred that alkali modified luffa sponge can be considered as an effective sorbent in the treatment of hard water. Removal of other metals such as Cd, Cu, Pb, Ni, Zn from water should also be studied by using luffa sponge as a sorbent.

## Acknowledgements

The authors would like to thank the Myanmar Academy of Arts and Science for allowing to present this paper. The authors also thank to Professor and Head Dr Ah Mar Yi, Department of Chemistry, Taunggyi University for her invaluable guidance and permission to use the research facilities for the research work.

## References

- Abay, A. K. (2015). "Removal of Water Hardness Causing Constituents Using Alkali Modified Sugarcane Bagasse and Coffee Husk". *International Journal of Environmental Monitoring and Analysis*, vol. 3(1), pp. 7-16
- AD, C., Benalia, M., Laidani, Y., Elmsellem, H., Ben Saffedine, F., Nouacer, I., Djedid, M., El Mahi, B. and Hammouti, B. (2015). "Adsorptive Removal of Cadmium from Aqueous Solution by *Luffa cylindrica*: Equilibrium, Dynamic and Thermodynamic". *Journal for Medicinal Chemistry, Pharmaceutical Chemistry, Pharmaceutical Sciences and Computational Chemistry*, vol. 7(12), pp. 388-397
- Adbel-Ghani, N.T., Hefny, M. and El-Chaghaby, G.A.F. (2007). "Removal of Lead from Aqueous Solution Using Low Cost Abundantly Available Adsorbents". *Inter. J. Envi. Sci. and Technol.*, vol. 4(1), pp. 67-73
- Adie, D.B., Igboro, S.B., Daouda, N. and Eledere, E. (2013). "Determination of the Filter Potential of Luffa Sponge (*luffa aegyptiaca*) in Water Quality Analysis". *American International Journal of Contemporary Research*, vol. 3(3), pp.1-4
- AOAC. (2000). *Official Method of Analysis*. Washington DC: 17<sup>th</sup> Ed., Association of Analytical Chemists, pp. 526-530
- Cotruvo, J. and Bartram, J. (2009). *Calcium and Magnesium in Drinking Water: Public Health Significance*. Geneva, WHO Press, pp. 1-36
- Stephen, B. And Sulochana, N. (2004). "Carbonised Jackfruit Peel as an Adsorbent for the Removal of Cd (II) from Aqueous Solution". *Bioresource and Technology*, vol. 94, pp. 49-52
- Vogel, A.I. (1961). *A Text Book Quantitative Inorganic Analysis*. London: 3<sup>rd</sup> Ed., Longmans, Green & Co. Ltd., pp. 415-444
- Yu, L.J., Dorris, K.L. Shukl, A. and Margrave, J.L. (2003). "Adsorption of Chromium from Aqueous Solutions by Maplet Dust". *J. Haz. Mater.*, vol.100, pp. 53-63

## PREPARATION OF SOAP IN THE PRESENCE OF LOCALLY AVAILABLE NATRON

Khin Moh Moh Hlaing<sup>1</sup>, Than Zaw<sup>2</sup>, Mya Hinn Aye Khaing<sup>3</sup>, Aung Kyaw Moe<sup>4</sup>,  
Ni Ni Aung<sup>5</sup>, Swe Zin Tun<sup>6</sup>

### Abstract

This research work concerns with the preparation of soap from palm oil with locally available natron by hot process method. Locally available natron sample was collected from Aigther village, Wundwin Township, Mandalay Division in winter season. The purified natron was characterized by available modern techniques ED XRF and FT IR analyses. The physicochemical properties of prepared soaps such as texture, color, foam stability (%), foam height (cm), pH, degree of absorption activity (%) and antimicrobial activity etc. were determined. According to the physicochemical properties, all of the prepared soaps were found in the pH range of (10.2-10.8). This pH range was skin friendly pH and was accepted by National Agency for Food and Drug Administration and Control (pH 8-11). Antimicrobial activity of prepared soaps was investigated by agar well diffusion method at Meiktila University. The prepared soaps were found to be active against with *Bacillus subtilis*, *Staphylococcus aureus*, *Pseudomonas fluorescens*, *Bacillus pumilus*, *Candida albicans* and *Escherichia coli* (*E.coli*). From the preparation's stand point, the prepared soaps were utilized not only as laundry soap but also as medicated soap.

**Keywords:** natron, hot process method, antimicrobial, laundry soap, medicated soap

### Introduction

As protection of the body from the outside, the skin has various problems such as dry skin, premature aging, chronic diseases like cancer. This can be caused by air pollution resulting in many free radicals, exposure ultraviolet, and also less care for cleanliness. The main treatment for maintaining skin health is to use soap regularly. The use of chemical will side effect on sensitive skin, while soaps with natural ingredient will provide the maximum nutrition on the skin (Putri and Anindia, 2017).

For generations, hand washing with soap and water been considered a measure of personal hygiene, bacteria are very diverse and present everywhere such as in soil, water, sewage, standing water and even in human body. Bacteria's that attacks on human body is of great importance with reference to health. In 1961 the U.S. public Health Service recommendations directed that personal wash their hands with soap and water for 1 to 2 minutes before and after client contact (Rama *et al.*, 2011).

Soap is sodium or potassium salt of fatty acid produced by saponification reaction using sodium or potassium hydroxide. Based on its chemical properties as an anionic surface active agent (surfactant), soap is used to clean and wash skin and clothing. The fatty acids, such as stearic, palmitic, myristic, lauric and oleic acids, contribute to lathering and washing properties of the soaps. The chemical characteristics of soap depend on several factors: the strength and purity of alkali, the kind of oil used, completeness of saponification and age of the soap. Such chemical characteristics include moisture content, total fatty acids (TFM), pH, free alkali, and percent chloride (Mak-Mensah and Firempong, 2011).

---

<sup>1</sup> Dr, Lecturer, Department of Chemistry, Meiktila University

<sup>2</sup> Lecturer, Department of Chemistry, Meiktila University

<sup>3</sup> Dr, Lecturer, Department of Chemistry, Meiktila University

<sup>4</sup> Lecturer, Department of Chemistry, Meiktila University

<sup>5</sup> Dr, Professor, Department of Chemistry, Meiktila University

<sup>6</sup> MSc Candidate

Natron, with its chemical composition of sodium carbonate 10-hydrate, had various applications in ancient technologies, ranging from the mummification of bodies to soap production and glassmaking (Jackson *et al.*, 2018). This white powdery material is an evaporate deposit of alkaline lakes and is found in nature as fragile, whitish stone chunks and it remains a crucial industrial component of soap/detergent and glass industries today (Reade *et al.*, 2005). In modern mineralogy the term natron has come to mean only the sodium carbonate decahydrate (hydrated soda ash) that makes up most of the historical salt. Historical natron was harvested directly as a salt mixture from dry lake beds in ancient Egypt, and has been used for thousands of years as a cleaning product for both the home and body. Blended with oil, it was an early form of soap. It softens water while removing oil and grease. Undiluted, natron was a cleanser for the teeth and an early mouthwash. The mineral was mixed into early antiseptics for wounds and minor cuts. Natron can be used to dry and preserve fish and meat. It was also an ancient household insecticide, and was used for making leather as well as a bleach for clothing. Today, natron is not used as readily in modern-day society due to being replaced with commercial detergent items along with soda ash, which made up for its use as a soap, glass-maker and household items (Noble, 1969).

### Materials and Methods

Soap is common cleansing agent well known to everyone. Soaps are produced for varieties of purpose ranging from washing, bathing, medication etc. The use of locally available raw materials in soap production was carried out. The soap was prepared using palm oil, coconut oil and natron by hot process method.

#### Sample Collection and Purification of Natron Sample

The natron (sample) were collected from Aigther village, Wundwin Township, Mandalay Region in September, 2018. The sample collected area of natron was shown in Figure 1.



**Figure 1** Sample collected area of natron

The collected natron sample (300 g) was purified by dissolution with 5 L distilled water and stand for three days. After standing for three days the solution was filtered to get the clear filtrate. Then the filtrate was gently heated to use throughout the research.



(a)



(b)

**Figure 2** Natron (a) unrefined (b) purified

### Characterization of the Purified Natron Sample

The purified natron was characterized by using modern techniques such as EDXRF and FT IR.

### Preparation of Soap using Natron and Lye (Sodium hydroxide) and without Natron

About 5 g of sodium hydroxide was added to 20 mL distilled water in a beaker and stirred to get sodium hydroxide solution. At the same time 20 mL of coconut oil was added to the beaker containing 20 mL of ethyl alcohol and heated together a few minutes. After cooling the sodium hydroxide solution, the two solutions were heated together and gently stirred to turn pasty. When all the paste had formed, 5 g of natron was added and the beaker was cooled at room temperature. Then 5 g of sodium chloride was added and filtered. Finally, the soap paste was washed with distilled water and filtered using a linen cloth, and then a small amount of water was added to soften it whilst heating. The soap was placed in cast and allowed to dry. The same procedure was carried out with palm oil. The prepared soap samples were denoted by SN.I for palm oil and SN.II for coconut oil.

The same procedure was carried out by using 10 g of lye (sodium hydroxide) and without addition of natron. The prepared soap samples were denoted by SL.I for palm oil and SL.II for coconut oil.

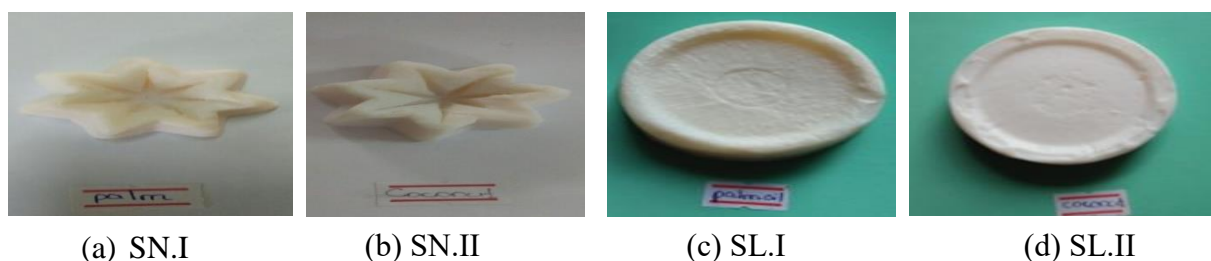


**Figure 3** (a) Prepared soap using natron and lye with palm oil  
 (b) Prepared soap using natron and lye with coconut oil  
 (c) Prepared soap using lye with palm oil  
 (d) Prepared soap using lye with coconut oil

### Determination of Physicochemical Properties of the Prepared Soaps

All the prepared soaps (SN.I, SN.II, SL.I and SL.II) were determined by texture, color, foam stability, foam height and pH. Then, the prepared soaps (SN.I and SN.II) and commercial soaps (Shwe war) were determined water absorption activity and antimicrobial activity (Zauro *et al.*, 2016).

## Results and Discussion

### Characterization of the Purified Natron

The chemical composition of the purified natron was shown by EDXRF spectrum and represented in Figure 4. From the EDXRF spectrum, the trace amount of elements such as P, Al, K, Zn, Br, Fe and Cu were present. The spectrum indicated that S (89.07 %), Si (4.597 %) and P (4.313 %) are the major constituents in the purified natron. It is a semi quantitative value measured on a matrix basis.

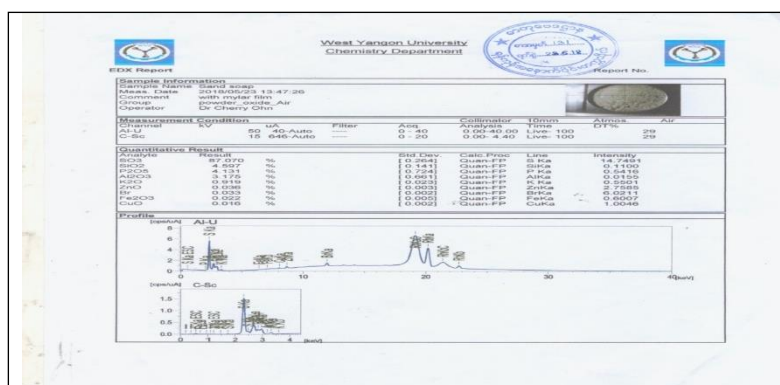


Figure 4 EDXRF spectrum of natron (purified)

The functional groups present in the purified natron were also studied by FT IR analysis. The FT IR spectrum of purified natron is shown in Figure 5 and the spectral assignment of purified natron was tabulated in Table 1. It can be observed that the frequency range was 4000-600  $\text{cm}^{-1}$ . The strong stretching band at 2200-2000  $\text{cm}^{-1}$  in spectrum is attributed to the aromatic thiocyanate. The sharp peak at 876.66  $\text{cm}^{-1}$  in the spectrum are silica group in natron of Si-H stretching and Si-O stretching respectively. The strong stretching band at 778.29  $\text{cm}^{-1}$  represent P-O-P and aromatic alkene.

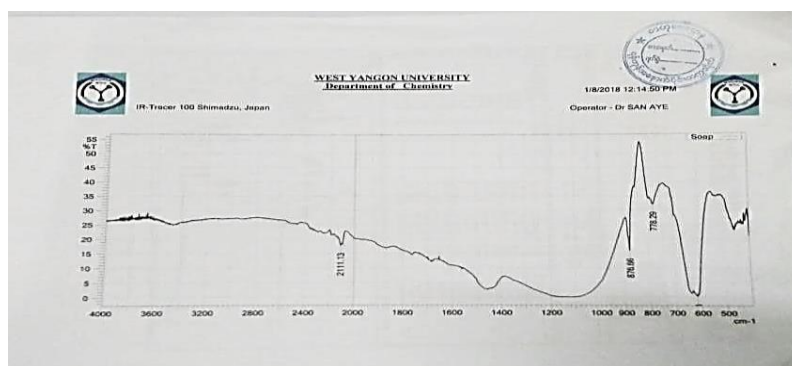


Figure 5 FT IR spectrum of natron (purified)

Table 1 FTIR Spectral Assignment of Natron (purified)

Observed wave number ( $\text{cm}^{-1}$ )	Literature Frequency ( $\text{cm}^{-1}$ )	Possible Assignment
2111.13	2000-2200	C=C, SCN (aromatic) stretching,
876.66	800-950	Si-H stretching, Si-O stretching
778.29	700-800	P-O-P stretching, aromatic amine

## Physicochemical Properties of the Prepared Soap

### pH

pH values of the prepared soaps are presented in Table 2. pH is a chemical parameter for knowing characteristic of the soap kind of alkaline or acidic. pH of the prepare soap was strongly basic in nature. According to the literature, the pH values of all soaps were in the range of National Agency for Food and Drug Administration and Control (pH value of 8-11).

## Foam Stability

The foam stability was determined by measuring the time it takes for the lather formed by the soap with pure water to collapse. The foam height (6.7 cm) of soap prepared with palm oil containing natron was higher than that of coconut oil (2.5 cm). Palm oil is very popular for its ability to add hardness to soap and produce creamy leather (Azeman *et al.*, 2015). A good foam stability criterion is when subjected to a foam stability range of about 60-70 % in the first five minutes (Wara *et al.*, 2014). In each soap formula containing stearic acid so that the resulting foam stability is good enough to be proved in the foam stability data within the first minutes.

**Table 2 Physicochemical Properties of the Prepared Soaps Using Natron with Lye and without Natron**

Parameters	SN.I	SN.II	SL.I	SL.II
Texture	soft	hard	soft	hard
Colour	white	white	white	white
Foam stability (%)	89.55	20	89.71	17.77
Foam height (cm)	6.7	2.5	7	4.5
pH	10.4	10.3	10.2	10.5

According to the physicochemical properties, the prepared soaps (SN.I, SN.II, SL.I and SL.II) were nearly the same properties. Therefore, the amount of lye (sodium hydroxide) can be reduced by using natron in the preparing of soap with suitable oils.

## Water Absorption Activity of the Prepared Soap

The dissolution of soap in water is very important, if the soap is very soluble water it is not suitable for commercially used and not effective for customers. The degree of absorption (%) of prepared soap (SN.I and SN.II) and commercial soap sample (Shwe war) are shown in Figure 6 as a function of absorption time in water. According to this result, the prepared soap SN.I and SN.II showed the decreasing in absorption (%) than the commercial soap sample. In addition, the prepared soap SN.I was the least absorption (%) than that of SN.II and commercial soap (Shwe war). Therefore, it can be concluded that the prepared soap may be used in laundry soap.

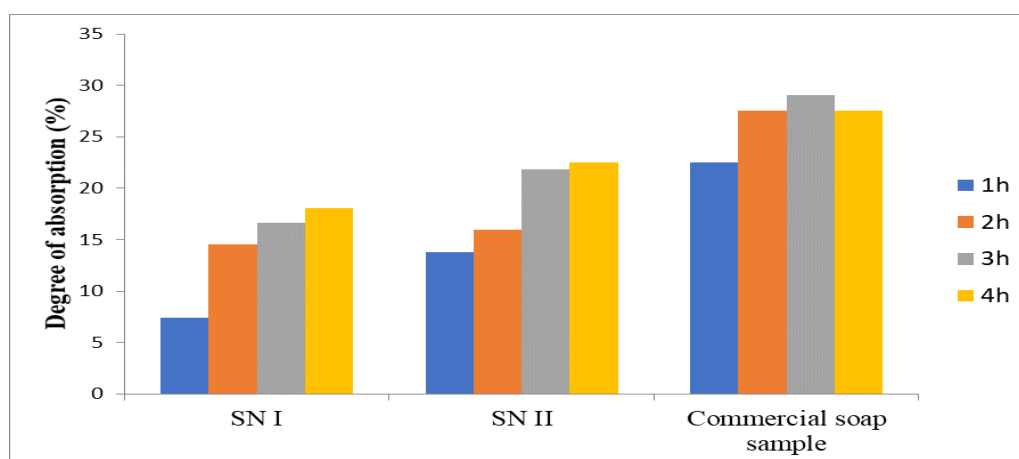


**Figure 6** Degree of absorption (%) of the prepared soap with time

### Antimicrobial Activity of the Prepared Soap

Antimicrobial activity of prepared soap SN.I, SN.II, purified natron and commercial soap sample (Shwe war) were shown in Table 2. The tested organisms were *Agrobacterium tumefaciens* (plant disease), *Bacillus pumilus* (fever), *Bacillus subtilis* (fever), *Candida albicans* (candidosis), *Escherichia coli* (*E.coli*) (cholera, diarrhea and vomiting urinary tract infection), *Pseudomonas fluorescens* (Plant disease) and *Staphylococcus aureus* (skin disease, food poison and wound infection) species, as seen in Figure 7 and Figure 8. The prepared soaps SN.I, SN.II, purified natron and commercial soap sample (Shwe war) were used for the agar medium cultivation. It was evident from the antimicrobial activity studies, the prepared soaps SN.I, SN.II and purified natron showed antimicrobial activity against all the given strains. This is due to the fact that the purified natron contained sulphur, as a major constituent in this sample from EDXRF analysis. Moreover, from FT IR analysis, it can be seen strong stretching band at 2200-2000  $\text{cm}^{-1}$  in spectrum is attributed to the aromatic thiocyanate. Consequently, these results were agreed with EDXRF and FT IR observations. From these studies, prepared soap SN.I, SN.II and natron (purified) were better than the commercial soap sample (Shwe War). Therefore, it can be concluded that according to the antimicrobial activity, purified natron and prepared soap SN.I and SN.II may be commonly used antimicrobial in medicated soap.

**Table 4 Antimicrobial Activities of Prepared Soap (SN and SL), Natron (purified), and Commercial Soap (Shwe war)**

Sample	<i>B. subtilis</i>	<i>S. aureus</i>	<i>P. fluorescens</i>	<i>B. pumilus</i>	<i>C. albicans</i>	<i>E. coli</i>	<i>A. tumefaci-ens</i>
SN.I	+++	+++	+++	++	+++	+++	+++
SN.II	++	++	+++	++	++	+++	+++
Commercial (Shwe war)	++	++	++	++	+++	++	++
Natron	23.30 mm	22.41 mm	21.64 mm	17.79 mm	21.69 mm	18.61 mm	21.62 mm
	+++	+++	+++	++	+++	++	+++
Control	-	-	-	-	-	-	-

Auger Well -10mm

10mm~14mm (+) low activity

15mm~19mm (++) medium activity

20mm~above (+++) high activity

*B. subtilis*

*S. aureus*

*P. fluorescens*

*B. Pumilus*

*C. albicans*

*E. coli*

*A. tumefaciens*

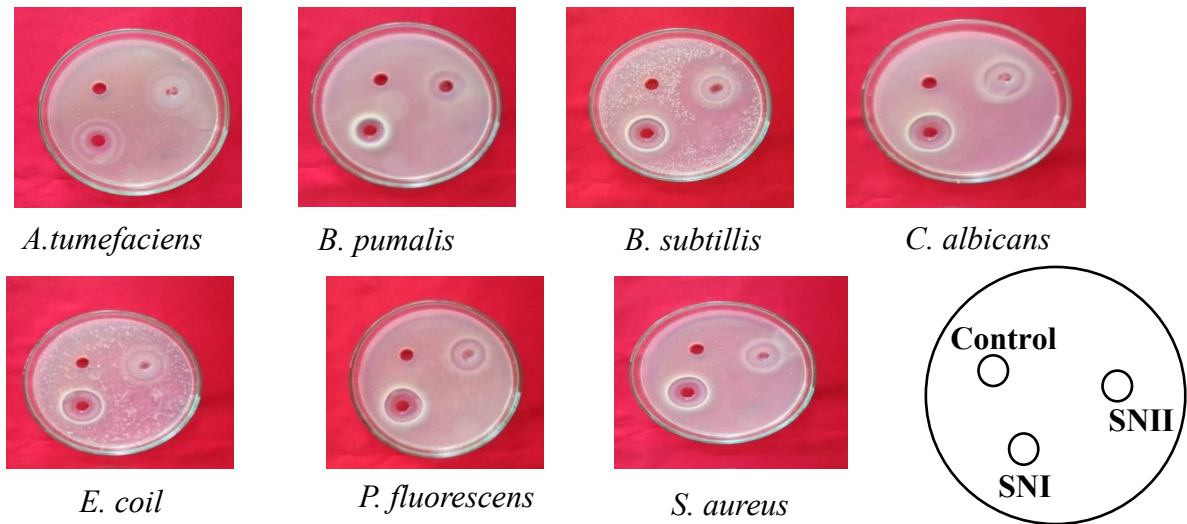


**Figure 7** Antimicrobial activity of SN.I and SN.II

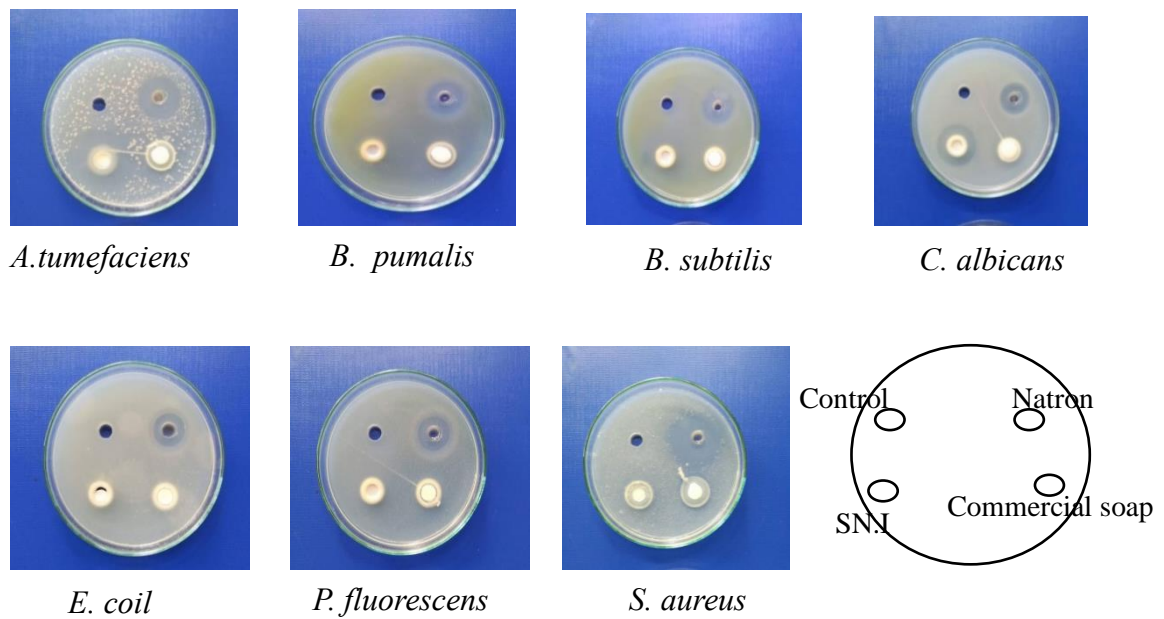


**Figure 8** Antimicrobial activity of natron (purified), SN.I and commercial soap (Shwe war)

### Conclusion

The preparation of soap from locally available natron with palm oils was successfully achieved using a hot- process method. The purified natron was characterized by EDXRF and FT IR analyses. The chemical composition of EDXRF spectrum showed sulphur (87.07 %) was the major constituent in natron sample and the other elements (Si, P, Al) contained trace elements. The pH of the prepared soaps from natron was in the range of 10.2-10.8 and it was strongly basic in nature. The pH values of all soaps were in the range of National Agency for Food and Drug Administration and Control (pH value of 8-11). Therefore, the amount of natron added was not affected the pH of the soap. The prepared soap SN.I and SN.II showed the decreasing absorption (%) than the commercial soap sample. Therefore, the prepared soaps are suitable for customers commercially used. From the antimicrobial activity studies, the prepared soaps SN.I, SN.II and purified natron showed antimicrobial activity against all the given strains. Especially, it was suitable for production of toilet and bathing soap due to antimicrobial activity on *Escherichia coli* (*E.coli*) and *S. aureus*. This fact was due to the presence of purified natron contained sulphur.

According to the antimicrobial activity, prepared soaps from natron may be commonly used antimicrobial medicated soap and laundry soap making. Therefore, it can be concluded that the using of natron instead of lye will save the environment from the potential harmful effect on pollution that commonly associate with these synthetic chemicals.

### Acknowledgements

We would like to thank to the Department of Higher Education, Ministry of Education in Myanmar, for giving as the opportunity to do this research. Our deepest gratitude is expressed to Dr Ba Han, Rector, Meiktila University, his encouragement and kind help to do this research. Thanks, all of teachers are also extended to Department of Chemistry, Meiktila University), for their helpful advice.

### References

- Azeman, N.H., Yusof, N.A. and Othman A.I. (2015). "Detection of Free Fatty Acid in Crude Palm Oil". *Asian Journal of Chemistry*, Vol 27(5), pp.1569-1573
- Jackson, C. M., Paynter, S., Nenna, M. D. and Degryse, P. (2018). "Glassmaking using Natron from El-Barnugi (Egypt); Pliny and the Roman Glass Industry", *Archaeol Anthropol Science*, Vol 10, pp. 1179-1191
- Mak-Mensah, E. E. and Firempong, C. K. (2011). "Chemical Characteristics of Toilet Soap Prepared from Neem (*Azadirachta indica* A. Juss), Seed Oil", *Asian Journal of Plant Science and Research*, Vol 1(4), pp 1-7  
ISN: 2249-7412
- Noble, J.V. (1969). "The Technique of Egyptian Faïence". *American Journal of Archaeology*, Vol 73(4), pp. 435-439
- Putri, S. and Anindia, F. (2017). "Manufacture of Solid Soap Based on Crude Papain Enzyme and Antioxidant from Papaya". *IOP Conference: Earth and Environmental Science*, Vol 105(1), pp.1-7
- Rama, B. P., Prajna, P. S., Menezes, P.M. and Shetty, P. (2011). "Antimicrobial Activities of Soap and Detergents". *Advances in Bioresearch*, Vol 2(2), pp. 52-62
- Reade, W., Freestone, I.C. and Simpson, S.J. (2005). "Innovation or Continuity? Early First Millennium BCE Glass in the Near East: The Cobalt Blue Glasses from Assyrian Nimrud", *Annales du 16e Congres de l' Association Internationale pour l'Histoire du Verre*, Vol 16, pp. 23-27
- Wara, A. A., Babayemi, A. W. and Buga, M. L. (2014). "Properties of Soaps Produced from Selected Seed Oils". *International Conference on Agriculture, Environmental and Biological Science*, Vol 14, pp. 44-47
- Zauro, S. A., Abdullahi, M. T., Aliyu, A., Muhammad, A., Abubakar, I. and Sani, Y. M. (2016). "Production and Analysis of Soap using Locally Available Raw-Materials". *Elixir Appl. Chem*, Vol 96, pp.41479-41483

## COMPARATIVE EVALUATION OF THE PELLETIZED BIOMASS FUEL FROM DIFFERENT SOLID WASTES

Thet Naing Soe<sup>1</sup>, Khin Chaw Win<sup>2</sup>, Phyu Phyu Myint<sup>3</sup>, Ni Ni Than<sup>4</sup>

### Abstract

This research is aimed to convert the vegetable waste into valuable products as an alternative and sustainable fuel source. This study investigated the potential use of fuel pellets that are produced from the wastes such as radish leaf, rice husk and rice husk char. Some physicochemical properties such as moisture content, ash content, bulk density, and chemical composition (N and S %) of different solid waste samples were carried out using appropriate analytical methods. Furthermore, pellets were produced from radish leaf, rice husk and rice husk char using cassava stem and local algae (*Spirogyra sp.*) as a binder. The properties of fuel pellets (compact and relax densities, heating value, energy densities, pellet moisture content) were determined as a function of types and sample composition (60 to 80 % w/w) by applied pressure (1.7 MPa). Also comparative studies of the different samples such as radish leaf (R) with rice husk (H) and rice husk char (C) and their toasted samples (TR, TH and TC) were conducted. The results showed that energy densities ranged from 6.183 to 7.613 kJcm<sup>-3</sup>, 0.366 to 4.387 kJcm<sup>-3</sup> and 0.909 to 1.648 kJcm<sup>-3</sup> for the samples R, H and C whereas energy-densities ranged from 9.003 to 11.072 kJcm<sup>-3</sup>, 0.369 to 4.760 kJcm<sup>-3</sup> and 1.116 to 1.876 kJcm<sup>-3</sup> for the samples TR, TH and TC, respectively. The heating value was also found in the range of 13.188 - 14.336 kJg<sup>-1</sup>, 13.375 kJg<sup>-1</sup> and 2.425 - 5.214 kJg<sup>-1</sup> for samples R, H and C, and 13.737 - 14.010 kJg<sup>-1</sup>, 12.656 - 13.333 kJg<sup>-1</sup> and 2.891 - 5.567 kJg<sup>-1</sup> for samples TR, TH and TC, respectively. From the findings, the radish leaf waste was found to have good pelletizing and combustion characteristics under the conditions considered because of their high density, high heating value and low pellet moisture content. Properties of the densified products (pellets) appeared to be comparable to US PFI requirements.

**Keywords:** radish leaf, rice husk and rice husk char, physicochemical properties, densification, fuel pellets

### Introduction

Agricultural and forest-based industries in developing and emerging economies generate a substantial amount of vegetable solid wastes residue and waste that could, in principle, be used for energy production (Bauen, and Slade, 2013). Vegetable wastes resources are found almost everywhere and can become a reliable and renewable local energy source. Energy produced from vegetable wastes can reduce reliance on an overloaded electricity grid and can replace expensive fuels used in local industries (Armesto *et al.*, 2002). Among these vegetable wastes, radish (*Raphanus sativus*) is one of the major vegetable crops grown throughout the country. It is widely grown in different parts of the country mainly by small and marginal farmers.

Rice husk is a by-product of rice milling. The prevalence and year-round production of rice crops on both an industrial and small scale means that rice husks are an attractive biomass fuel because they are not only readily available in large quantities but are also easy to collect. Furthermore, combusting the husk solves the problem of waste husk disposal. A large quantity of rice husks is produced annually in some countries and these residues are left to rot away or they are burned like other agricultural wastes. These residues could however be used to generate heat energy for domestic and industrial cottage applications (Fapetu, 2000).

The conversion of biomass to energy can be achieved through various technologies such as direct/stove, biomass briquette and boiler combustion; thermochemical conversion (which includes

---

<sup>1</sup> Lecturer, Department of Chemistry, Pakokku University

<sup>2</sup> Dr, Lecturer, Department of Chemistry, University of Yangon

<sup>3</sup> Dr, Professor, Department of Chemistry, Loikaw University

<sup>4</sup> Dr, Professor (Head), Department of Chemistry, University of Yangon

gasification, pyrolysis and liquefaction); and biochemical conversion (anaerobic fermentation biogas, bioethanol and biodiesel) (Oladeji, 2011 and Qiao *et al.*, 2011).

The major limitations of direct combustion are the low heating efficiency and difficulty in handling, storage and transportation resulting from the low bulk density and high moisture content of the biomass materials (Li *et al.*, 2017 and Tumuluru *et al.*, 2011). Srivastava *et al.*, 2014 converted vegetable market waste to briquettes without pre-treatment and without using any external binders. Therefore, relying on biomass for the production of pellets or briquettes is a potential solution to solid waste problems in developing countries as well as the high dependence on fuel wood.

The PFI is a North American trade association based in Arlington, Virginia, that represents a range of contributors to the pellet industry, including companies that manufacture wood pellets and pellet manufacturing equipment, or provide other products and services to the densified biomass industry at large.

The aim of the present research work is to convert the vegetable waste into valuable products as an alternative and sustainable fuel source. In this work, densification of radish leaf waste was carried out using cassava stem and algae as binding agents and also comparative with rice husk and rice husk char wastes. Effect on properties of the pellets (compact and relax densities, heating value, energy densities, pellet moisture content) were evaluated as a function of types and algae to leaf mixture ratio (60 to 80 % w/w).

## Materials and Methods

### Collection and Preparation of Solid Waste Samples

Radish leaf wastes were collected from Pyin Oo Lwin Township, Mandalay Region during June and August, 2018. Also rice husk and rice husk char samples were collected from Hle-dan Market, Kamayut Township, Yangon Region during May, 2019.

The radish leaf wastes were cleaned in water, dried naturally in sunlight for at least 5 days. Clean and dried leaf waste were reduced in size using burner and sieved into 40 mesh size. Whereas rice husk sample was naturally dried naturally in sunlight for 1 day, and pulverized with burner to reduce in size. Also rice husk char was dried naturally in sunlight for 1 day, and pulverized with burner to reduce in size and then sieved into 40 mesh sizes.

Moreover, cassava stem was collected from Lashio Township, Northern Shan state and algae (*Spirogyra* sp.) were also collected from Thahton hostel, Yangon University campus. Cassava stem and algae were also dried naturally under the sun by spreading on a steel plate for at least 3 days. After which, they were sieved into 40 mesh size. In this preparation, densifications of different solid wastes were carried out using cassava stem and algae as binding agents.

### Determination of the Physicochemical Properties of Raw Materials

The different solid wastes were cleaned in water, dried naturally under sunlight for at least 5 days, and reduced in size. The moisture content (dry basis) of raw materials was determined using the Infrared moisture analyzer method (FD 660). To determine the ash content, the samples were placed in reweighed crucible and ignited in a muffle furnace at 600 °C for 2 h until the substance turned into ash (LabTech). After ashing, the crucible was cooled in a desiccator and weighed (AOAC, 2000). For bulk density determination, the graduated cylinder was filled with the dry sample. The cylinder was placed in a tapping box and gently tapped until there was no more reduction in volume and the bulk density was calculated (Tapping method). The sulphur contents

of the samples were determined as barium sulphate by precipitation method (AOAC method). Total nitrogen contents of the samples were measured by Dumas Nitrogen Analyzer (NDA 701).

### Preparation of Raw Materials for the Fuel Pellets

Pelletizing at moderate conditions may be effective with inexpensive binding agents from natural sources. Prior to densification, blending was performed by weight ratios into 100 % waste samples. Using radish leaf raw materials, three composite samples: (i) 10 % algae, 10 % cassava stem and 80 % radish leaf (R1), (ii) 10 % algae, 20 % cassava stem and 70 % radish leaf (R2), (iii) 10 % algae, 30 % cassava stem and 60 % radish leaf (R3) were prepared. The same ratio as the previous one but pre-toasted at 100 °C before combination were conducted for samples TR1, TR2 and TR3. Also using rice husk sample, three composite samples: (i) 10 % algae, 10 % cassava stem and 80 % rice husk (H1), (ii) 10 % algae, 20 % cassava stem and 70 % rice husk (H2), (iii) 10 % algae, 30 % cassava stem and 60 % rice husk (H3) were prepared. The same ratio as the previous one but pre-toasted at 100 °C before combination were conducted for samples TH1, TH2 and TH3. Also using rice husk char sample, three composite samples: (i) 10 % algae, 10 % cassava stem and 80 % rice husk char (C1), (ii) 10 % algae, 20 % cassava stem and 70 % rice husk char (C2), (iii) 10 % algae, 30 % cassava stem and 60 % rice husk char (C3) were prepared. The same ratio as the previous one but pre-toasted at 100 °C before combination were conducted for samples TC1, TC2 and TC3.

### Densification Procedure

Each pellet mass loading was approximately 17.0 to 20.0  $\pm$  1.0 g. A compacting (densifying) apparatus used is shown in Figure 1, comprising a piston, a closed-end cylinder and a base. Internal diameter was 27 mm, indicating the resultant pellet size. The compacting apparatus was mounted with 1.7 MPa to the material. Eighteen composite samples with different weight ratios were taken into 250 mL beaker. For each test condition, about 20 mL distilled water was added slowly with constant stirring. A holding time of 1 h was used for each pellet.

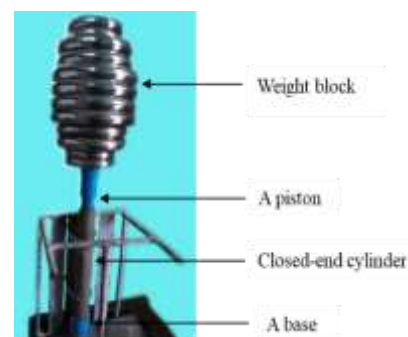


**Figure 1** Manual densification unit

### Determination of the Physicochemical Properties of Fuel Pellet

The resultant pellets were subsequently evaluated for various physicochemical properties, including compact and relax densities, energy density, heating value, pellet moisture content and SEM. The pellet density was determined based on the pellet mass per volume. In this work, the compact and relax densities were used and defined as that of the pellet determined immediately after compaction and that determined after storage for one week, respectively. The energy density ( $\text{kJ cm}^{-3}$ ) used in this work was defined as the product between heating value ( $\text{kJ g}^{-1}$ ) and relax density ( $\text{g cm}^{-3}$ ) of the pellet. The heating value of the pellet was determined using bomb calorimeter (DRI). The pellet moisture content (dry basis) was determined using the infrared moisture analyzer method (FD 660). A scanning electron microscope (SEM) was determined by University Research Center (Jeol JXA- 840 A).

## Preparation of Fuel Pellet from Biomass

According to the physicochemical parameters of Lab-Scale Fuel Pellet, mixture ratio of R2 sample was chosen as the most potent sample for further optimization process to fuel pellets production. So, radish leaf (1284.62 g) and algae (153.85 g) were thoroughly mixed and mixed again cassava stem (230.77 g) with 1000 mL of distilled water. They were thoroughly mixed and heated to obtain syrup, which were sundried for 1 to 2 days. The mixtures were loaded into the pellet mill (Figure 2) for about 15 min. The resultant (densified) pellets were obtained



**Figure 2** Pellet Mill

## Results and Discussion

### Biomass Characteristics

The different solid waste samples in urban areas are seasonally available biomass residues that may potentially be utilized to produce biomass pellets. The biomass pellets comprised many small pieces of leaf packed together and shaped into solid cylinder, holding together by manual densification of solid bridges. Binding agents impart cohesive qualities to powdered material during the production of pellet. In this research work, the different solid waste samples and binding agents are shown in Table 1. Moisture contents, ash contents and bulk density based on the dry solid samples (radish leaf, rice husk and rice husk char) were found 0.16 to 11.85 %, 18.22 to 91.00 % and 0.32 to 0.41 g mL<sup>-1</sup> whereas sulphur and nitrogen contents were found 0.36 to 0.63 % and 0.42 to 4.64 %, respectively. For the binding agents (cassava stem and algae) the moisture contents, ash contents and bulk density were found to be 0.11- 0.19 %, 18.00 - 76.00 % and 0.10 - 0.39 g mL<sup>-1</sup> whereas sulphur and nitrogen contents were 0.44 - 0.73 % and 7.46 - 10.63 %, respectively.

**Table 1** Some Physicochemical Properties of Different Solid Samples

No.	Sample	Moisture (%)	Ash (%)	Bulk density (g mL <sup>-1</sup> )	Total S (%)	Total N (%)
1	Radish leaf	11.85	18.22	0.37	0.36	3.03
2	Rice husk	0.31	21.00	0.41	0.46	4.64
3	Rice husk char	0.16	91.00	0.32	0.63	0.42
4	Cassava stem	0.09	18.00	0.10	0.44	7.46
5	Algae	0.11	76.00	0.39	0.73	10.63

### Physical Appearance of the Fuel Pellets

Figure 3 shows pictorial views of the pellets after one week storage. It was evident that radish leaf pellets (R2) processed at room temperature by applied pressure (1.7 MPa) could retain the pellet form. They would need to be pelletized at higher pressures to form very tight pellets. For processing at room temperature and pre-toasted at 100 °C, all cases were found to be successful in forming pellets. But all cases could not retain the pellet form under low pressure even with binder. From the pictures, the densification of different solid wastes was carried out using cassava stem and local algae as a binder by various mixture ratios and conditions.

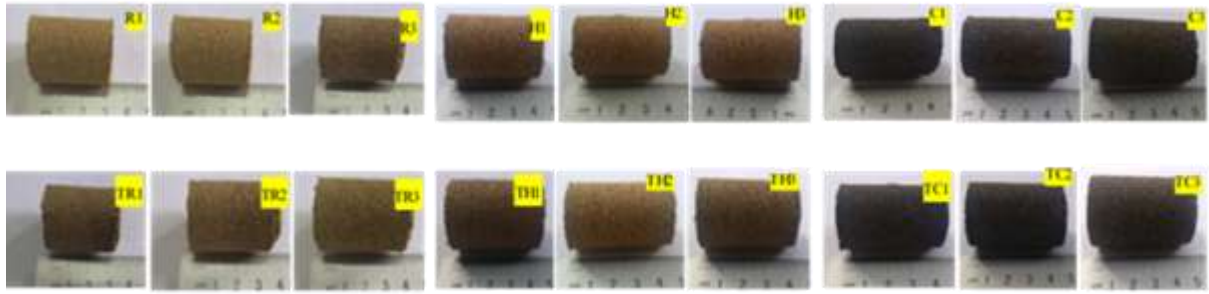


**Figure 3** Appearance of fuel pellets densified using different ratio and types of samples

**Compact and Relax Densities of Fuel Pellets**

Measurement of length and diameter of the pellets was under taken immediately and after storage for one week. This was used to calculate their corresponding volume and density from a fixed mass input. Compacted density was always higher than relaxed density because the expansion of pellet dimension affected change in pellet volume. The results of the experiments carried out on the properties of the radish leaf, rice husk and rice husk char pellets are presented on Table 2. It was observed that change in density of the pellets after storage was rather small for those compressed using radish leaf. Also change in density of the pellets after storage was rather large for those compressed using rice husks and rice husk char. From the finding, it was clear that the ratio of radish leaf had positive impact on the pellet density.

**Table 2** Variation in Pellet Densities with Different Conditions

No.	Raw materials	Pellet sample	Compact densities (g cm <sup>-3</sup> )	Relax densities (g cm <sup>-3</sup> )
1.	Radish leaf	R1	0.596	0.572
		R2	0.547	0.531
		R3	0.467	0.453
		TR1	0.832	0.806
		TR2	0.746	0.718
		TR3	0.702	0.651
2.	Rich Husk	H1	0.772	0.366
		H2	0.895	0.385
		H3	0.800	0.328
		TH1	0.737	0.369
		TH2	0.721	0.351
		TH3	0.789	0.357
3.	Rich Husk Char	C1	0.829	0.375
		C2	0.920	0.348
		C3	0.846	0.316
		TC1	0.838	0.386
		TC2	0.767	0.367
		TC3	0.702	0.337

**Heating Value, Energy Density and Pellet Moisture of Fuel Pellets**

The heating value and energy density of fuel pellets results of this study are as shown in Table 3. A little difference in the energy content of mixture ratios were observed on table 3 using

radish leaf with different conditions but more difference in the energy content of mixture ratios were observed using rice husk and rice husk char with different conditions. The energy density ( $\text{kJ/cm}^3$ ) used in this work was defined as the product between heating value ( $\text{kJ/g}$ ) and relax density ( $\text{g cm}^{-3}$ ) of the pellet.

Significant differences in heating values were found between pellet samples. The maximum heating value 14.336  $\text{kJ/g}$  of sample R2 and the maximum heating value 14.010  $\text{kJ/g}$  of sample TR2 are shown in Table 3. The minimum heating values of R1 (13.188  $\text{kJ/g}$ ) and TR1 (13.737  $\text{kJ/g}$ ) are shown in Table 3, and the maximum heating values of H3 (13.375  $\text{kJ/g}$ ) and TH3 (13.33  $\text{kJ/g}$ ) are also shown in Table 3. The heating values of H1 and H2 and TH1 were not detected. The maximum heating value (5.214  $\text{kJ/g}$ ) of the sample C3, ranged from 2.425 to 5.214  $\text{kJ/g}$ , and that of the sample TC3 (5.567  $\text{kJ/g}$ ), ranged from 2.891 to 5.567  $\text{kJ/g}$  are also shown in Table 3. From the finding, the pellet sample R2 possessed more heating value than other pellet samples that can meet domestic needs such as cooking and water boiling (Tippayawong *et al.*, 2018).

The results in Table 3 show that as the moisture content increases the heating value reduces. The minimum moisture contents for pellet samples R2, H1 and TC2 were observed as 2.896 %, 0.510 % and 0.386 % respectively. Higher moisture content implies a lower heating value as each unit mass of fuel contains less oven dry biomass - which is the part of the fuel that actually undergoes combustion to release heat (Tokan *et al.*, 2016).

**Table 3 Variation in Heating Values, Energy Densities and Pellet Moisture with Different Conditions**

No.	Raw materials	Pellet sample	Heating values ( $\text{kJ g}^{-1}$ )	Energy densities ( $\text{kJ cm}^{-3}$ )	Pellet moisture (%)
1.	Radish leaf	R1	13.188	7.544	4.002
		R2	14.336	7.613	2.896
		R3	13.649	6.183	2.834
		TR1	13.737	11.072	2.958
		TR2	14.010	10.059	3.764
		TR3	13.830	9.003	7.302
2.	Rich Husk	H1	ND	0.366	0.510
		H2	ND	0.385	0.512
		H3	13.375	4.387	0.574
		TH1	ND	0.369	1.092
		TH2	12.656	4.442	0.519
		TH3	13.333	4.760	0.949
3.	Rich Husk Char	C1	2.425	0.909	0.415
		C2	4.040	1.406	0.861
		C3	5.214	1.648	0.579
		TC1	2.891	1.116	0.676
		TC2	4.029	1.479	0.386
		TC3	5.567	1.876	0.623

### SEM Analysis

The appearance of fuel pellets by grinding mill using raw samples of (a) radish leaf (b) rice husk and (c) rice husk char was indicated by SEM micrograph (Figures 4). In these SEM micrograph, appearance of fuel pellets and rice husk char were observed as similar pattern of pores and attributed on the surface of the all samples. Also rice husk can be seen that stick structure and

attributed on the surface of the all samples. The more pronounced morphological character was shown by appearance of fuel pellet samples.

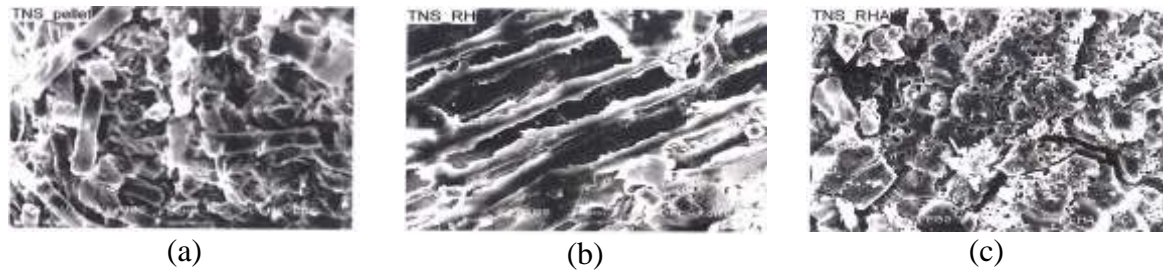


**Figure 4** Scanning electron micrographs of (a) Appearance of fuel pellets by grinding mill, (b) Rice husk and (c) Rice husk char

**Comparison of Fuel Pellets with an International Standard**

Biomass pellets are currently graded by the US PFI. Pellet quality is a largely dependent on type of feedstock and process parameters. In this work, comparison of our densified products against the US PFI requirement was made for some indicators. Results were shown in Table 4 and Table 5. It can be seen that Radish leaf pellets obtained from this work were in some compliance with the US PFI and German standard requirements.

**Table 4 Comparison of Fuel Pellet Properties against PFI Fuel Grade Requirements**

No.	Properties	Observed values		PFI premium	PFI utility	PFI standard
		R1 to C3	TR1 to TC3			
1.	Diameter (mm)	27	27	6.35 - 7.25	6.35 - 7.25	6.35 - 7.25
2.	Length (% > 38 mm)	1.2 - 1.5	1.2 - 1.6	≤ 1.0	≤ 1.0	≤ 1.0
3.	Energy density (kJ/cm <sup>3</sup> )	0.366 - 7.613	0.369 - 11.072	-	-	-
4.	Heating value (kJ/g)	2.425 - 14.336	2.891 - 14.010	*15.501 - 19.501	-	* >17.999
5.	Moisture (%)	0.415 - 4.002	0.386 - 7.302	≤ 8.0	≤ 10.0	≤ 8.0

\*Garcia-Maraer and Carpio (2015)

**Fuel Pellets Prepared by Commercial Scale**

Based on the compact and relax densities, heating value, energy density and pellet moisture content, the densification of radish leaf wastes was chosen for further use as commercial fuel pellets. So, the radish leaf waste, mixture ratio R2 could be suggested for the production of fuel pellet between the different solid wastes (Figure 5). Also commercial pellets obtained from this work were in approximately compliance with the US PFI and German standard requirements.



**Figure 5** Appearance of fuel pellets densified by commercial scale

**Table 5 Comparison of Commercial Pellet Properties against PFI Fuel Grade Requirements**

No.	Properties	Observed values	PFI premium	PFI utility	PFI standard
1	Energy density (kJ/cm <sup>3</sup> )	14.329	-	-	-
2	Heating value (kJ/g)	14.803	*15.501 - 19.501	-	* >17.999
3	Moisture (%)	0.312	≤ 8.0	≤ 10.0	≤ 8.0

\* Garcia-Maraer and Carpio (2015)

### Conclusion

The present work deals with conversion of the vegetable waste into valuable products as an alternative and sustainable fuel source. In converting the radish leaf waste into pellets, the physical and combustion characteristics of the pellets were investigated, and comparative study were also conducted with rice husk and rice husk char pellets in order to establish suitability for use as fuel. The work draws the following conclusion: high efficient and durable solid fuel for domestic use was produced, from radish leaf, with heating value ranging from 12.482 - 14.336 kJ/g on the sample R2 whereas heating value ranging from 12.807 - 14.010 kJ/g on the sample TR2. Also use of radish leaf (60 - 80% w/w) offer any marked improvement of the physical characteristics of the pellets. They were also compared to requirements for fuel pellets in the US PFI in order to assess their potential for future use in pellet firing systems. From the findings between different solid wastes, R2 sample could be suggested for the production of fuel pellet because of their high density, heating value, low pellet moisture content.

### Acknowledgements

The authors would like to express their profound gratitude to the Myanmar Academy of Arts and Science for giving permission to submit this paper.

### References

- A.O.A.C. (2000). "Methods in Food Analysis. Pearson's Chemical Analysis of Foods", *Association of Official Analytical Chemists*. America: 17<sup>th</sup> Ed<sup>n</sup>., Food Science and Technology
- Armesto, L., Bahillo, A., Veijonen, K., Cabanillas, A. and Otero, J. (2002), "Combustion behaviour of rice husk in a bubbling fluidised bed", *Biomass and Bioenergy*. vol. 23(3), pp. 171-79
- Bauen, A. and Slade, R. (2013). "Biomass Use on a Global Scale", *Encyclopedia of Sustainability Science and Technology*. pp. 1607-18
- Fapetu, O. P. (2000). "Production of Charcoal from Tropical Biomass for Industrial and Metallurgical Process", *Nigerian Journal of Engineering Management*. vol. 1(2), pp. 34-37
- Garcia-Maraver, A. and Carpio, M. (2015). "Factors Affecting Pellet Quality", *WIT Transactions on State of the Art in Science and Engineering*, vol. 85, pp. 26-27
- Li, Y., Zhou, L. and Wang, R. (2017). "Urban biomass and methods of estimating municipal biomass resources". *Renewable and Sustainable Energy Reviews*, vol. 80, pp. 1017-1030
- Oladeji, J. T. (2011). "Agricultural and forestry wastes and opportunities for their use as an energy sources in Nigeria: An Overview", *World Rural Obs*. vol. 3, pp. 107-112
- Qiao, W., Yan, X., Ye, J., Sun, Y., Wang, W. and Zhang, Z. (2011). "Evaluation of biogas production from different biomass wastes with/without hydrothermal pretreatment", *Renew. Energy*. vol. 36, pp. 3313-3318
- Srivastava, N. S. L., Narnaware, S. L., Makwana, J. P., Singh, S. N. and Vahora, S. (2014). "Investigating the energy use of vegetable market waste by briquetting", *Renew. Energy*. vol. 68, pp. 270-275
- Tippayawong, N., Jaipa, C. and Kwanseng, K. (2018). "Biomass Pellets from Densification of Tree Leaf Waste with Algae", *Agricultural Engineering International: CIGR Journal*, vol. 20(4), pp. 119-125
- Tokan, A., Muhammad, M. H., Japhet, J. A. and Kyauta, E. E. (2016). "Comparative analysis of the effectiveness of rice husk pellets and charcoal as fuel for domestic purpose", *Journal of MechMechanical and Civil Engineering (IOSR-JMCE)*. Nigeria: vol. 13, Issue 5 ver. VI, pp. 21- 27
- Tumuluru, J. S., Wright, C. T., Hess, J. R. and Kenney, K. L. (2011). "A review of biomass densification systems to develop uniform feedstock commodities for bioenergy application", *Biofuel Bioprod. Biorefin.* vol. 5, pp. 683-707

## ASSESSING THE APPLICATION OF IRON OXIDE PARTICLES FOR REMEDIATION OF INSECTICIDE CONTAMINATED SOIL

Swe Sint<sup>1</sup>, Phyu Phyu Myint<sup>2</sup>, Saw Hla Myint<sup>3</sup>

### Abstract

In this study, iron oxide particles were synthesized and used to remediate insecticide contaminated soil. The influence of experimental variables such as reaction time, and particle dosage of iron oxide particles on the soil remediation were studied. The green synthesis of iron oxide particles was prepared by reducing iron (III) chloride solution with tea leaves extract for remediation of the soil. The optimized quantity of iron oxide particles was found to be 0.01 mL/kg of soil contaminated with 0.002  $\mu\text{g g}^{-1}$  of cypermethrin insecticide. The physicochemical properties of the soil sample were determined. Iron oxide particles were prepared by green method and characterized by modern techniques such as XRD, FT IR, TG-DTA and FESEM analyses. The degradation of insecticides residue in contaminated soil was studied. The residual insecticide in soil samples extracted from the experimental plot was examined by using UV-Vis spectrophotometer. Insecticide residue did not increase but firstly increased than decreased. The soil urease activity in the treated and contaminated soil was also determined. The stabilization of urease activity in the soils studied was due to iron oxide particles and these had light influence on soil organic matter. These results suggest that only proper amount of iron oxide particles plays a dominating role to control the urease activity of the soils.

**Keywords:** cypermethrin, remediation, iron oxide particles, contaminated soil, urease activity

### Introduction

In recent years, the phasing out of organophosphate products such as diazinon and chlorpyrifos has prompted an increased use of pyrethroid insecticides for agricultural pest control (Bootharaju *et al.*, 2012). Because of this concerns regarding the fate, toxicity, diffusion, and transformation of pyrethroids have significantly increased. Once the insecticide enters the soil it is partitioned between soil particles and soil solution. In soil particles, cypermethrin particularly binds with the soil organic matter. If organic matter is associated with soil particles, then it is favourable for binding insecticide.

Cypermethrin is classed as a type II pyrethroid and is commonly found in rivers, sediments, soils, and even foodstuffs (XIE *et al.*, 2008). It possesses carcinogenic and cocarcinogenic potential and can produce compounds with endocrine activities, such as 3-phenoxybenzoic acid (PBA). Degradation of PBA is thus a vital step for remediation of cypermethrin pollution. One of the most important processes influencing the environmental behavior of an insecticide is its degradation in soil. Hydrolysis of the ester linkage producing PBA and cyclopropane carboxylic derivatives is the main degradation pathway of cypermethrin in soil. However, PBA is more mobile and persistent than cypermethrin in soils and it presents an environmental risk greater than its parent molecule. Degradation of PBA is a vital step for remediation of cypermethrin pollution.

---

<sup>1</sup> Assistant Lecturer, Department of Chemistry, University of Yangon

<sup>2</sup> Dr, Professor, Department of Chemistry, Loikaw University

<sup>3</sup> Dr, Part-Time Professor, Department of Chemistry, University of Yangon

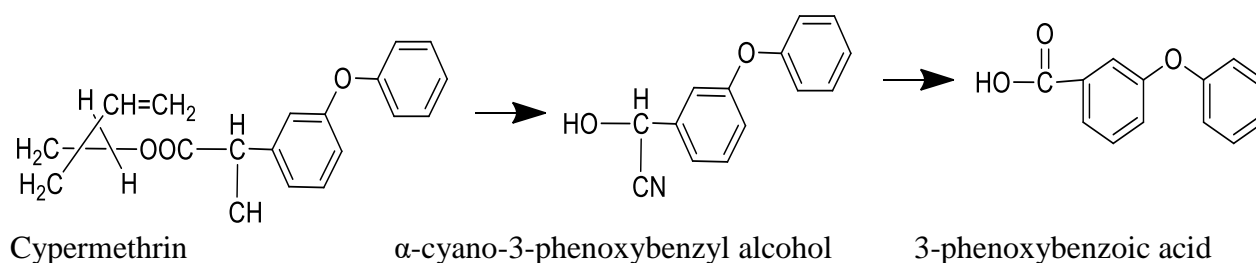


**Figure 1** Degradation pathway of cypermethrin in soil

Iron oxides form naturally through the weathering of Fe-containing rocks both on land and in the oceans. They have attracted much attention due to their fine magnetic properties and applications in modern science (Fernández-García *et al.*, 2007). Moreover, urea added to soils as fertilizer is rapidly hydrolyzed to ammonium carbonate in most soils through soil urease activity. Urease is a nickel containing enzyme which catalyzes the hydrolysis of urea to ammonia and carbon dioxide, it is produced by bacteria, algae, fungi and plants (Hameed *et al.*, 2018). The main role of urease is to allow the microorganisms to use urea as a source of nitrogen. Furthermore, urease plays an important role in nitrogen cycle in plants, urease produced by bacteria, also, acts as a virulence factor in many human infections. Ureases is the enzyme that degrades urea and is widely considered to be a good proxy of nitrogen (N) mineralisation. The aim of the present research work is to assess the application of iron oxide particles for remediation of insecticide contaminated soil by using green synthesized iron oxide particles and to determine the activities of urease enzyme of insecticide-contaminated soil.

## Materials and Methods

### Preparation of iron oxide particles

Iron oxide particles were synthesized by green method. Briefly, by adding 0.01 M  $\text{FeCl}_3 \cdot 6\text{H}_2\text{O}$  solution to the tea extract in a 1:1 volume ratio.  $\text{Fe}_3\text{O}_4$  particles were immediately obtained with the reduction process (Kanagasubbulahshmi *et al.*, 2017). The mixture was stirred for 60 min and then allowed to stand at room temperature for another 30 min to obtain colloidal suspension. Mixture was centrifuged and washed several times with ethanol and then dried at  $60^\circ\text{C}$  under vacuum. Finally, the black iron oxide particles were obtained. Tea leaves have the best reduction capability against ferric chloride when compared to other parts of the plants that is observed by the external color change (Bharadwaz *et al.*, 2015).

### Characterization of iron oxide particles

The prepared black iron oxide particles were characterized by XRD, FT IR and TG-DTA techniques at the Universities Research Center, University of Yangon and by FESEM technique at the Science and Industrial Research, Osaka University. The prepared iron oxide particles were characterized by means of XRD method and estimated the crystallite size of these particles according to Debye-Scherrer's formula. The prepared iron oxide particles were characterized by means of FT IR method and estimated the functional group of the iron oxide particles. The TG-DTA was used to investigate the decomposition and phase formation that occurs during heat treatment of the prepared iron oxide particles. The FESEM signals that derived from electron sample interactions reveal information about the sample including external morphology (texture), chemical composition, and crystalline structure and orientation of materials making up the sample.

## Soil Sample Collection

Soil samples were collected from the surface layer (0-20 cm depth) of an agricultural field located in Phya Thee Village (at 21° 48' latitude north and 94° 57' longitude east), Myaing Township, Pakokku District, Magway Region, cropped with a chilli and tomato rotation without treatment of any pyrethroids for several years.



**Figure 2** Sampling site of soil in Phya Thee village

## Physicochemical Properties of Soil Sample

The moisture content of the soil samples was determined according to the reported method. The pH content of the soil sample was determined according to the standard method by using pH meter. Electrical conductivity of the soil sample was determined by using electrical conductivity meter. Organic matter content of the soil sample was determined by using walkley and black method based upon the oxidizable organic matter content. Total N content was determined by using Kjeldahl's method. Cation exchange capacity content of the soil samples were determined according to the method of Kappen (Jaremko *et al.*, 2014). Total P of the soil samples was determined by using Olsen method for neutral and alkaline soil (measured by spectrophotometer). Potassium content of the soil samples was determined by using ammonium acetate extraction method (measured by Flame photometer).

## Experimental Design for Determining Insecticide Degradation in Soil

Dried soil samples (10 g), H<sub>2</sub>O (1mL) and 0.0001% cypermethrin (1mL) were placed in 150 mL aliquots. Fe<sub>3</sub>O<sub>4</sub> particles were dissolved in water at doses of 0 % Fe<sub>3</sub>O<sub>4</sub> (P 0), 1% Fe<sub>3</sub>O<sub>4</sub> (P 1), 2% Fe<sub>3</sub>O<sub>4</sub> (P 2), 3% Fe<sub>3</sub>O<sub>4</sub> (P 3), respectively. A control soil sample, without adding iron oxide particles, was prepared in a similar manner. Each treatment in triplicate was amended with cypermethrin dissolved in water to obtain insecticide concentration of 0.002 µg/g, which is the common residual field concentration after application in contaminated soils. All the containers were covered with perforated aluminum foil to ensure gas exchange and then incubated at 25 °C. The samples were aged for several weeks. After 1, 2, 3, 4 and 5 weeks, soil samples were collected to determine the amount of secondary metabolite of cypermethrin (3-phenoxy benzoic acid, 3- PBA) formed.

## Extraction of 3-phenoxy benzoic acid in soil and characterization

Three samples from each treatment were used to determine the residue of PBA in the soil. In brief, PBA was extracted from 10 g soil samples using methanol and dichloromethane (3:1, v/v) and placed in shaker at 150 rpm for 30 min. The supernatant liquid was centrifuged at 5000 rpm for 15 min in three times. The residual insecticide (as its metabolite 3-phenoxybenzoic acid, 3-PBA) in contaminated soil samples extracted from the experimental plot was examined by using UV-Vis spectrophotometer.

### Determination of the urease enzyme activity in soil and characterization

The activity of the urease enzyme ( $\text{mg NH}_4^+ \text{-N g}^{-1} \text{ soil h}^{-1}$ ) was measured by the determination of ammonia released after soil sample incubation with a urea solution by using colorimetric methods (Jingjing *et al.*, 2015). A 10 g of fresh soil was placed in a 100 mL volumetric flask and treated with 1 mL of toluene, 10 mL buffer (pH-7) and 5 mL of 10 % urea solution (freshly prepared). After a throughout mixing the flask was incubated for 3 h at 37 °C in dark. After incubation the volume of the flask was made to 100 mL distilled water and shaken thoroughly and transferred the filtrate through Whatman No.5 filter paper. The ammonia released as a result of urease activity was measured by indophenol blue method. 0.5 mL of the filtrate was taken into a 25 mL volumetric flask and 5 mL of distilled water was added. Then 2 mL of phenolate solution (mixture of 20 mL of stock A (62.5 g phenol crystals dissolved in a minimum volume of methanol and make up the volume up to 100 mL with ethyl alcohol after adding 18.5 mL acetone and 20 mL of stock B (27 g NaOH dissolved in 100 mL distilled water and kept in freezer)) was added. Therefore, 1.5 mL of sodium hypochlorite solution was added. The final volume of the flask was increased up to 25 mL with distilled water and the blue colour was read out with the spectrophotometer at 630 nm. Urease activity was determined by a calibration curve.

## Results and Discussion

### Characteristics of Prepared Iron Oxide Particles

The green synthesis of iron oxide particles using extract of green tea which is a cheap and local resource. Synthesized iron oxide particles utilizing green tea (*Camellia sinensis*) extract containing a range of polyphenols. Polyphenols in plants act as both a reducing agent and a capping agent to provide a robust coating on metal particles in a single step and leads to colour change yellowish brown to brownish black. This colour change gave the confirmation of the synthesis of iron oxide particles. This denotes the tea leaves have premier competence to synthesize of iron oxide particles than other parts of the plants such as seeds, fruit.

The XRD analysis results of iron oxide powders prepared at 60 °C are shown in Figure 3. The results indicate that, at 200 °C or 1 h, no other obvious diffraction peaks are found, except the peaks belonging to  $\alpha\text{-Fe}_2\text{O}_3$  phase. The XRD pattern points out that the product reduced at 300 °C is a mixture of  $\text{Fe}_3\text{O}_4$  and  $\alpha\text{-Fe}_2\text{O}_3$  phases with  $\text{Fe}_3\text{O}_4$  as the main phase. The crystalline natures of the prepared iron oxides were identified by XRD analysis. Four miller indices [(111), (311), (422), and (531)] of magnetite sample matched with the standard data. This revealed that the resultant iron oxide are cubic structure. After that, the particle sizes of iron oxide samples was calculated by using Debye-Scherrer's equation and the particle size of iron oxide particles was found to be 33.518 nm.

The FT IR spectrum of iron oxide particles is shown in Figure 4 (Nakamoto, 1997). The absorption peaks at 893.07, 792.77, 572.88, and 451.36  $\text{cm}^{-1}$  correspond to the vibration of Fe-O group. FT IR analysis gave the stretching vibrations at 3448, 1622, 572 and 451  $\text{cm}^{-1}$ . These peaks represent the reducing agent role in the formation of  $\text{Fe}_3\text{O}_4$  particles. The peak at 3448  $\text{cm}^{-1}$  corresponds to the -OH bond stretching denotes the aqueous phase as well as the reduction of ferric chloride. Remaining unclear peaks represents small amount of organic acids which is responsible for the low pH of the sample which helps to the synthesis of the  $\text{Fe}_3\text{O}_4$  particles. The peaks at 572 and 451  $\text{cm}^{-1}$  correspond to the inorganic stretching indicates the  $\text{Fe}_3\text{O}_4$  particles.

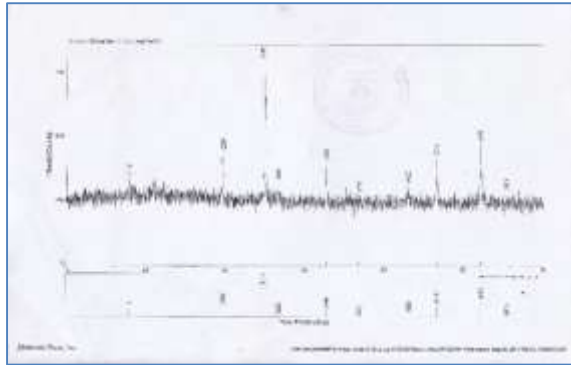


**Figure 3** XRD diffractogram of prepared iron oxide particles

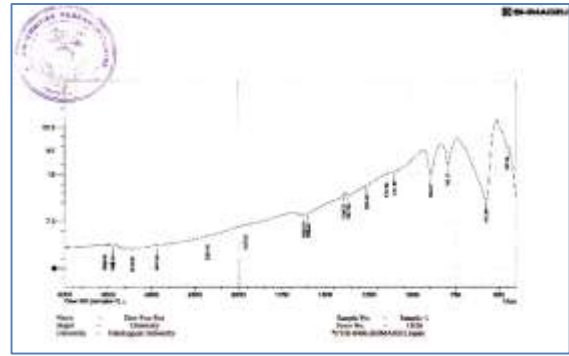


**Figure 4** FT IR spectrum of prepared iron oxide particles

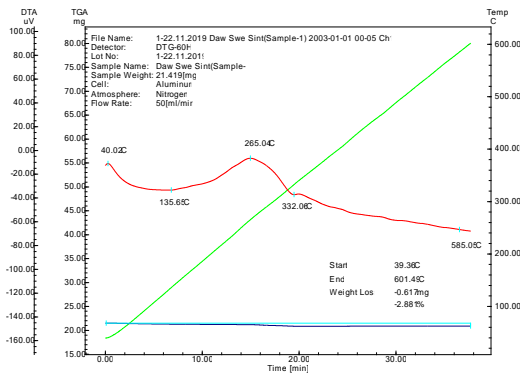


**Figure 5** TG-DTA thermograph of prepared iron oxide particles

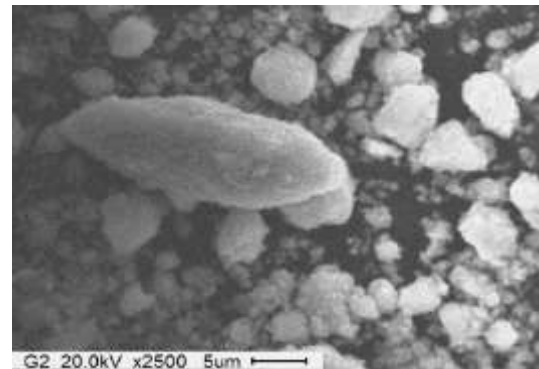


**Figure 6** FESEM microphotograph of prepared iron oxide particles

TG and DTA curve of iron oxide particles is shown in Figure 5. The temperature range is 40 °C to 600 °C. TG-DTA analysis, it was found that total weight loss is 2.881 %. One exothermic peak and one endothermic peak were corresponding to phase transition and oxidation reaction takes place in the sample. The endothermic peak was observed at about 332.06 °C due to the removal of organic volatile materials and the exothermic peak was observed at about 265.04 °C. From DTA data, above 200 °C, exothermic peak and endothermic peak were observed due to the phase transformation. In this research, surface morphology of the prepared iron oxide samples were studied by using FESEM as shown in Figure 6. From the FESEM result of iron oxide particles by green method indicated that the particles are spherical in shape with a narrow size distribution and it can be seen that the particles agglomeration, indicating a good connectivity between the grains together and the pore size of which is 0.7 cm. The FESEM micrographs indicated the porous nature of the surface.

**Physicochemical Properties of Soil Sample**

The soil has the sandy loam texture. This research used a soil with low nitrogen, very low organic carbon and electrical conductivity (EC), medium cation exchange capacity (CEC), high K<sub>2</sub>O and very high phosphorous (P) content in order to scientifically investigate on the degradation of cypermethrin. The pH value of the contaminated soil was found to be 8.079. The electrical conductivity value of the contaminated soil was found to be 0.09 μS/cm. The organic carbon content of the contaminated soil was found to be 0.36 %. Humus content of the contaminated soil was found to be 0.62 %. The nitrogen value of the contaminated soil was found to be the lowest value 0.13 %. CEC is important for maintaining adequate quantities of plant available calcium Ca<sup>++</sup>

(19.10) meq/100 g,  $Mg^{++}$  (0.68) meq/100 g,  $K^+$  (0.43) meq/100 g, and  $Na^+$  (0.85) meq/100 g, respectively. The highest phosphorous content of the contaminated soil was found to be 45.03 ppm.

**Table 1 Characteristics of the Soil Sample**

Test Parameter	Content
Texture	Sandy loam
Sand (%)	67.56
Silt (%)	15.00
Clay (%)	17.44
Organic carbon (%)	0.36
Humus (%)	0.62
Total Nitrogen (%)	0.13
CEC (meq/100 g)	21.06
Phosphorus (ppm)	45.03
$K_2O$ (mg/100 g)	20.27
Exchangeable $Ca^{++}$ (meq/100 g)	19.10
Exchangeable $Mg^{++}$ (meq/100 g)	0.68
Exchangeable $K^+$ (meq/100 g)	0.43
Exchangeable $Na^+$ (meq/100 g)	0.85

### The iron oxide particles efficiency on soil remediation

After 4 weeks' incubation, the amounts of PBA degradation were found to be slightly higher in the 2<sup>nd</sup> week in all treatments with respect to Control (P0). These findings indicated that adequate addition of iron oxide particles could increase the degradation of cypermethrin. However, the degradation levels were similar after a long enough incubation period. Apparently, there is no movement of cypermethrin from soil to air and its degradation in soil is mostly attributed to microorganisms.

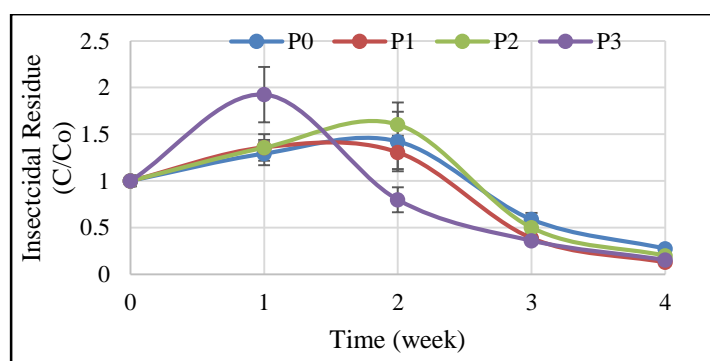


**Figure 7** Insecticide residue in soil by different dosage of iron oxide particles treatments

### Enhancement of Urease Enzyme Activity

The effect of iron oxide particles on urease activity was found to be increased during the incubation periods. The results of determination of urease enzyme activity in contaminated in soil are shown in Figure 8.

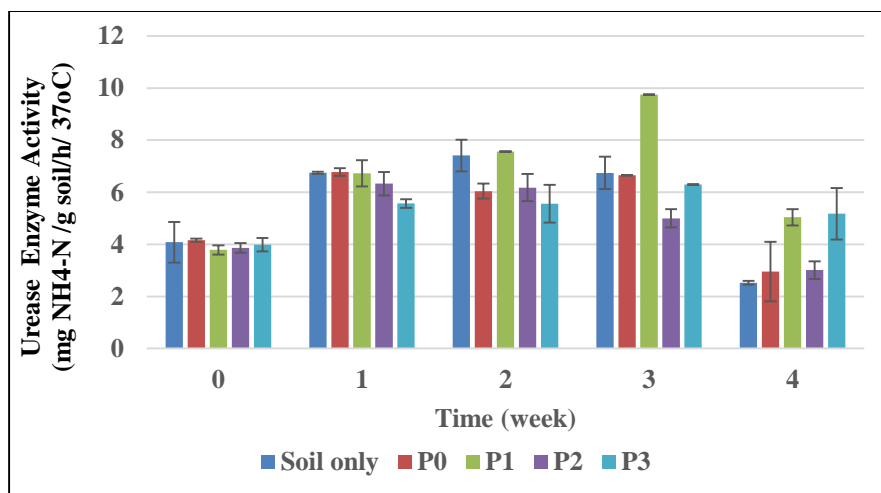


**Figure 8** Urease Enzyme Activity of insecticide contaminated soil

The change of urease activity depended on iron oxide particles dosage. In blank stage, urease activity had a slight increase. Under the addition of different iron oxide particles, all treatments showed a little positive impact on urease activity. The present study showed that urease enzyme quality was improved by addition of proper iron oxide particles. In 1 week, urease activity content of five treatments had little difference. But in the 3<sup>rd</sup> week period, it had the highest value of urease activity due to the high 1 % iron oxide particles. At the 4 weeks, urease activity in soil was found to decrease. Moreover, the first two had very little change in all treatments, this means that proper dose of iron oxide particle is conducive to the preservation of urease activity. However, urease activity picked up quickly in jointing stage and reached the top of growth. These results clearly indicate that urease activity in iron oxide particles treatment increased compared to dose and time. P1 treatment of urease activity was higher than other treatments, moreover, 3 week in four stages had the highest urease activity. Thus, the different dose of iron oxide particles and soil urease activity related to the time.

### Conclusion

In this research, synthesis of iron oxide particles by green method were carried out. The results of this study suggest that addition of iron oxide particles could enhance degradation of cypermethrin and its most persistent metabolite, PBA. Thus, in agricultural practice, adequate application of iron oxide particles was an efficient method to reduce the accumulation of cypermethrin and PBA in soil and significantly decreased environmental risks. The present study showed that high soil urease activity due to iron oxide particles. The variance analysis results indicated iron oxide particles can influence the soil urease activity. It is concluded that proper iron oxide particles is important for the beneficial to the remediation of insecticide contaminated soil.

### Acknowledgements

The authors would like to express their profound gratitude to the Myanmar Academy of Arts and Science for giving permission to submit this paper and to Professor and Head, Dr Daw Ni Ni Than, Department of Chemistry, University of Yangon, for her kind encouragement.

## References

- Bharadwaz, A. and Battacharjee, C. (2012). "Extraction of Polyphenol from Dried Tea Leaves". *International Journal of Scientific and Engineering Research*, vol. 3(5), pp. 1-5
- Bootharaju, M.S, and Pradeep, T. (2012). "Understanding the Degradation Pathway of the Pesticide, Chlorpyrifos by Noble Metal Nanoparticles". *Langmuir*, vol. 28, pp. 2671-2679
- Fernández-García, M., and José A. R. (2007). *Metal Oxide Nanoparticles*. Upton, USA: Brookhaven National Laboratory, pp. 1-60
- Hameed, H.D. and Entesar, H. E. (2018). "Evaluation of purified urease activity from *Proteus mirabilis* using iron oxide nanoparticles and measurement of urea concentration in blood". *Engineering and Technology Journal*, vol. 36, pp. 152-155
- Jaremko, D. and Kalembasa, D. (2014). "A comparison of methods for the determination of cation exchange capacity of soils". *Ecological Chemistry and Engineering S. Journal*, vol. 21(3), pp. 487-498
- Jingjing, S., Mijia, Z., Xiaoqia, Y., Chi, Z. and Jun, Y. (2015). "Microbial, Urease Activities and Organic Matter Responses to Nitrogen Rate in Cultivated Soil". *The Open Biotechnology Journal*, vol. 9, pp. 14-20
- Kanagasubbulahshmi, K. and Kadirvelu, K. (2017). "Green Synthesis of Iron Oxide Nanoparticles using *Lagenaria siceraria* and Evaluation of its Antimicrobial Activity". *Journal of Life Science*, vol. 2, pp.422-427
- Nakamoto, K. (1997). *Infrared and Raman Spectra of Inorganic and Coordination Compounds*, New York: Parts A and B, John Wiley & Sons, pp. 52-68
- XIE, W.-J., Jian-Min, Z., Huo-Yan W. and Xiao-Qin, C. (2008). "Effect of Nitrogen on the Degradation of Cypermethrin and Its Metabolite 3-Phenoxybenzoic Acid in Soil", *Pedosphere*, vol. 18(5), pp. 638-644

## EFFECTIVENESS OF SAPONIN ON PHYTOREMEDIATION OF PETROLEUM-CONTAMINATED SOIL

Myat Hnin Ei<sup>1</sup>, Phyu Phyu Myint<sup>2</sup>, Ni Ni Than<sup>3</sup>

### Abstract

This study aims to evaluate efficiency of saponin, a natural surfactant, in remediation the soils which are smeared by crude oil and it was conducted based on the soil properties of oil ring no. (52), Nyaungdon Twonship, Ayeyarwaddy Region in 2019. For this purpose, soil properties were initially studied in this zone including soil texture, pH, moisture, nitrogen content, phosphorus content and potassium content. Crude saponin was extracted from the vegetable waste materials such as Onion (*Allium cepa* L.) skin, Ka Nyut (*Asparagus officinalis* L.) hard stem and Hin Nu Nwe (*Amaranthus paniculatus* L.) hard stem by the yield percent of 14.55 %, 2.53 % and 2.12 %, respectively. The studied phases included variables of saponin concentration within ranges of 250, 500 and 1000 ppm, contact time (10 week) and concentration of oil within ranges of 0.1-10 % in soil. The findings from assessment showed that the conditions under concentration of saponin (1000 ppm) on 0.1 % oil contaminated soil. The removal efficiency percentage of crude oil on 10 weeks contact time was observed 24.89 %. A laboratory study was extended to assess the potentials of local grass (Bermuda grass) under normal environmental conditions with or without surfactants in remediating soil contaminated with crude oil. The results of the phytoremediation of contaminated soil showed that significant reduction 76.3 % of crude oil was observed by natural saponin. It was also observed that the crude oil in the polluted soil was reduced by 72.4 % as a result of plant only, similar to commercial surfactant (SLES) treatment 72.1 %. This research indicates the soil remediation by Onion skin saponin, making better use of Bermuda grass and contributing to environmental protection.

**Keywords:** vegetable waste, saponin, Onion skin, petroleum contaminated soil, oil extraction, phytoremediation, Bermuda Grass

### Introduction

As raw material for production of petroleum and other chemicals, crude oil has become one of the most important energy sources in the world. However, the soil, water and air has contaminated by crude oil as a result of exploration, production, maintenance, transportation, storage and accidental release, add hazardous chemicals to the ecosystem. So, pollution has become a major global problem. Management of pollution is still a challenge to the humans. Among them, soil can be contaminated by many different human activities. Soil can be subjected to remediation techniques for the purposes of site decontamination.

Fortunately, surfactants can promote the removal of organic compounds and heavy metals from contaminated soils. Saponins are steroid or triterpene glycoside compounds found in variety of plants and derive their name from the soapwort plant. Saponins are traditionally used as natural detergents. Saponins show the unique properties of foaming and emulsifying agents (Bajad and Pardeshi, 2015). It is also called natural surfactant.

Surfactants are substances whose molecules consist of a water soluble (hydrophilic) and an oil soluble (hydrophobic) part. They have the tendency of accumulating at oil-soil and oil-water interfaces. The addition of surfactant to the washing solution (crude oil contaminated soil) to reduce the surface and interfacial tension at the air-water and oil-water interface, thereby reducing the capillary force that holds the oil and soil, which may lead to the mobilizing and (or) the solubility of the oil. The mechanisms behind surfactant removal of petroleum oil from soil studied (Deshpande *et al.*, 1999).

---

<sup>1</sup> PhD Candidate, Department of Chemistry, University of Yangon

<sup>2</sup> Dr, Professor, Department of Chemistry, Loikaw University

<sup>3</sup> Dr, Professor (Head), Department of Chemistry, University of Yangon

Currently, chemical surfactants have been used in enhanced solubilization for organic compounds and removal of heavy metals, usually synthesized by chemical materials (Wei *et al.*, 2015). Compared with chemical surfactants, biosurfactants were isolated from plants produced by microorganisms. It shows the excellent performance for remediation process owing to their lower toxicity, better surface activity, readily biodegradable and huge environmental compatibility (Mnif *et al.*, 2015).

Bioremediation is the use of biological processes to degrade, transform, or essentially remove contaminants from soil. This process relies on microorganisms (bacteria and/or fungi) and plants. For this reason, bioremediation is widely used to remediate organic contaminants and can be an effective means of mitigating.

Phytoremediation is applied to provide long-term rehabilitation of the residual oil-contamination. Phytoremediation is a bioremediation process that uses various types of plants to remove, transfer, stabilize, and (or) destroy contaminants in soil. Use of green plants and their microorganisms to reduce environmental problems without the need to excavate the contaminant material and dispose of it elsewhere.

Bermuda grass was selected for phytoremediation. Myanmar name is Myin-sa-myet, Mye-sa-myet. It was distributed in Myanmar, India, Philippines and South Africa. The stem of Bermuda grass has 12-24 cm high, slender, round, shoots and roots arise from nodes, most of the stems and growing points are covered with leaf sheath. The leaf of Bermuda grass has linear, 2-3 mm wide, blue green. Bermuda grass has a deep root system; in drought situations with penetrable soil, the root system can grow to over 2 m deep. Bermuda grass has been used as a phytoextraction (Adomako *et al.* 2010). It has also been used for arsenic and mercury (Weaver *et al.*, 1984). Certain mechanisms such as phytoextraction, phytostabilisation, phytodegradation, rhizoremediation and rhizofiltration occur, allowing plants to remediate both organic and inorganic substances (Zoller and Reznik, 2009).

The aim of the present research work is to study the phytoremediation of petroleum contaminated soil by using natural surfactant (saponin) from vegetable wastes on soil washing process and by using the Bermuda grasses.

## Materials and Methods

### Collection and Preparation of Vegetable Waste Samples

Vegetable waste samples were collected in June, 2018 from Kamayut Township, Yangon Region of Myanmar. They were identified by the Department of Botany, University of Yangon.

The two collected vegetable waste samples, Hin Nu Nwe and Ka Nyut were washed with tap water and dried for a while to remove water. These two fresh samples were sliced very small. The dried sample of Onion skin was also sliced very small. All samples are used directly without further modification (Laufenberg *et al.*, 2003).

### Extraction and purification of saponin

The selected waste samples (5 g) were placed in beakers 250 mL, extracted with 100 mL of aqueous ethanol in a water bath for 2 h with continuous stirring until discolored. The mixture was filtered and combined this solution and was concentrated to about 40mL. The residue was transferred to separation funnel, and defatted with petroleum ether. The aqueous layer was recovered while the petroleum ether layer was discarded. The purification process was repeated. 60 mL of *n*-butanol was added. The *n*-butanol extracts were washed with 10 mL of 50 % aqueous sodium chloride. The remaining solution was heated in a water bath. After evaporation, the samples

were dried in the oven to constant weight and the saponins content was calculated (De Geyter *et al.*, 2007).

### Identification of saponin

Saponin was identified by spectroscopy method and chemical method. Firstly, the crude saponin was identified by FT IR. And then, the crude saponin was determined by foaming test and emulsifying test.

In foaming test, the selected waste samples were extracted with water, and filtered, the filtrate in test tubes with various volume ratios. Then, the permanent foaming was observed and measured the foaming height. In emulsifying test, the selected waste samples were extracted with water, and filtered, the filtrate in test tubes, and it was warmed in water bath, the stable persistent froth, was mixed with liquid paraffin and shaken vigorously, then observed for the formation of emulsion, indicate the presence of saponins. Emulsifying capacity was measured at some important variables such as contact time and saponin concentration were selected in 1:1 volume ratio of saponin to paraffin. The operation variables used were saponin concentration (25-200  $\mu\text{g/mL}$ ) and contact time (15-60 min).

### Collection of Soil Sample

The soil sample was collected from the upper layer (0-20 cm) of oil ring no. (52), Nyaungdon Township, Ayeyarwaddy Region. The soil was air-dried, crushed and passed 40mm sieve to remove the larger clods and trash.

### Characterization of Soil Sample

Soil texture and pH were characterized by pipetting method based upon the Strobe's law and standard method by using pH meter. The moisture content in the soil was determined by oven dry method (Schneekloth *et al.*, 2002). The organic matter was investigated by Walkley and black method based upon the oxidizable organic matter content. And then, total nitrogen and phosphorous content in the soil were determined by Kjeldahl's method, Olsen method for neutral and alkaline soil (measured by spectrophotometer). Finally, the total potassium and humus content were characterized by Ammonium Acetate extraction method (measured by Flame photometer) and ignition method.

### Preparation of contaminated soil sample

The collected soil sample was dried at room temperature. The dried sample was sieved (40 mm) mesh. The soil was spread on plastic tray and air dried. A 40 mm mesh screen separated the larger clods and trash. The soil was mixed by hand with lubricant oil in various concentrations (0.1, 1, and 10 %).

### Bench Study

The collected soil sample was treated with lubricant (0.1 %, 1 % and 10 %) and three different concentrations of saponin. This mixture was added n-hexane and acetone (5:1) ratio, shaken 10 min at the shaker, filtered and centrifuged this mixture. It was evaporated and calculated the constant weight of dried extract.

### Phytoremediation

Phytoremediation is a bioremediation process that uses various types of plants to remove, transfer, stabilize, and (or) destroy contaminants in soil. Use of green plants and their

microorganisms to reduce environmental problems without the need to excavate the contaminant material and dispose of it elsewhere.

The tropical grass sample (Bermuda grass) was used for this phytoremediation process. The collected petroleum contaminated soil sample was treated with 1% lubricant oil and saponin concentration (250 ppm). The composite soil mixture was filled into plastic pots (1kg soil per pot) and treated with four different designs (plant only, plants with natural surfactant, plants with commercial surfactant (SLES) and without plant).

The oil remaining in soil was determined by using (5:1) ratio of n-hexane and acetone. Twenty millilitres of this solvent mixture was added to the soil, shaken for 10 min and filtered. And then, the liquid decanted was added in the centrifuge tube and was centrifuged at 2500 rpm for 15 min. Weekly, crude oil residue was extracted from spiked soil samples from each vessel and studied on removal efficiency according to this procedure (Phyu Phyu Myint *et al.*, 2013).

## Results and Discussion

### Extraction and Identification of Saponin

Crude saponin was extracted from the selected vegetable waste samples by lead-acetate method. The yield percent of crude saponin were calculated. The yield % of saponin were found 14.55 % in Onion skin, 2.53 % in Ka Nyut hard stem, and 2.12 % in Hin Nu Nwe hard stem. Onion skin has the highest saponin content. The results obtained are present in Table 1.

**Table 1 Yield % of Saponin Content in Collected Samples**

No.	Sample Name	Sample Condition	Yield (saponin content)
1	Onion skin ( <i>A. cepa</i> )	dried	14.55
2	Ka Nyut hard stem ( <i>A. officinalis</i> )	fresh	2.53
3	Hin Nu Nwe hard stem ( <i>A. paniculatus</i> )	fresh	2.12

According to FT IR spectral data, saturated and unsaturated H/C group and cyclic alcohol group were observed in the extracted crude saponin. FT IR was identified by PerkinElmer Spectrum Two at University of Yangon. This spectral data is present in Figure 1.

FT IR analysis of the vegetable waste samples has absorption bands and wave numbers ( $\text{cm}^{-1}$ ) of the prominent peaks obtained are described in Table 2. The peaks of frequency of above  $3000 \text{ cm}^{-1}$ ,  $1500 \text{ cm}^{-1}$ ,  $1300 \text{ cm}^{-1}$ ,  $1000 \text{ cm}^{-1}$  and  $700 \text{ cm}^{-1}$  were strong while the others vary from medium to weak. The peak at  $3500\text{-}3200 \text{ cm}^{-1}$  was assigned to the OH stretching. The peak intensity at nearly  $1600 \text{ cm}^{-1}$  was assigned to C=C skeletal stretching of alkene. The absorption band at  $1390\text{-}1380 \text{ cm}^{-1}$  was assigned to CH bending. The peak at  $700 \pm 20 \text{ cm}^{-1}$ , CH bending will present and at  $1390\text{-}1310 \text{ cm}^{-1}$  was assigned to the OH bending.

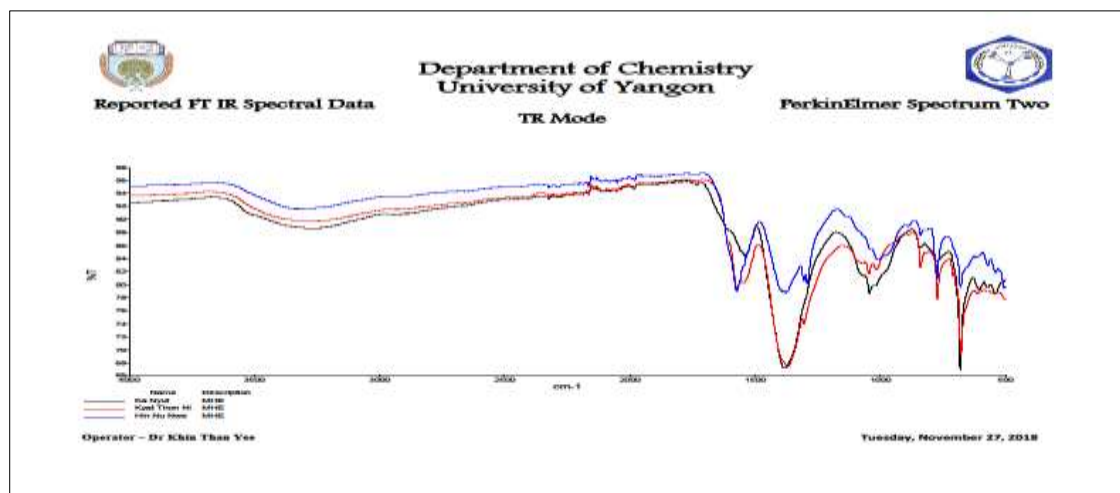


Figure 1 FT IR spectra of saponin from the selected samples

Table 2 FT IR Spectral Data of Saponin from the Selected Samples

Wave number (cm <sup>-1</sup> )			Band Assignment
Onion skin	Ka Nyut hard stem	Hnin Nu Nwe hard stem	
3242.51	3271.37	3326.32	$\nu_{OH}$ of hydroxyl group
1571.62	1541.27	1571.10	$\nu_{C=C}$ of alkene
1370.76	1380.36	1376.06	$\delta_{CH}$ of gem dimethyl group
1045.35	1043.20	1007.00	$\nu_{CH-OH}$ in cyclic alcohol
771.80	773.53	772.55	$\delta_{CH}$ out of plane wagging

### Characterization of Saponin

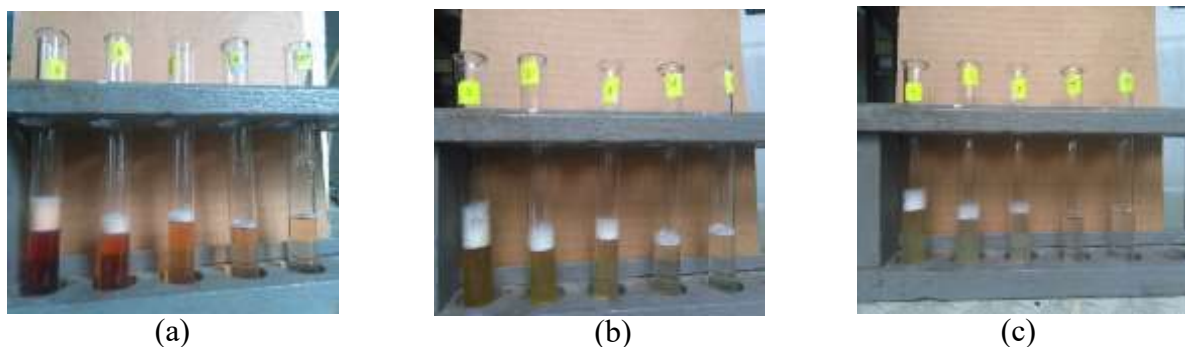
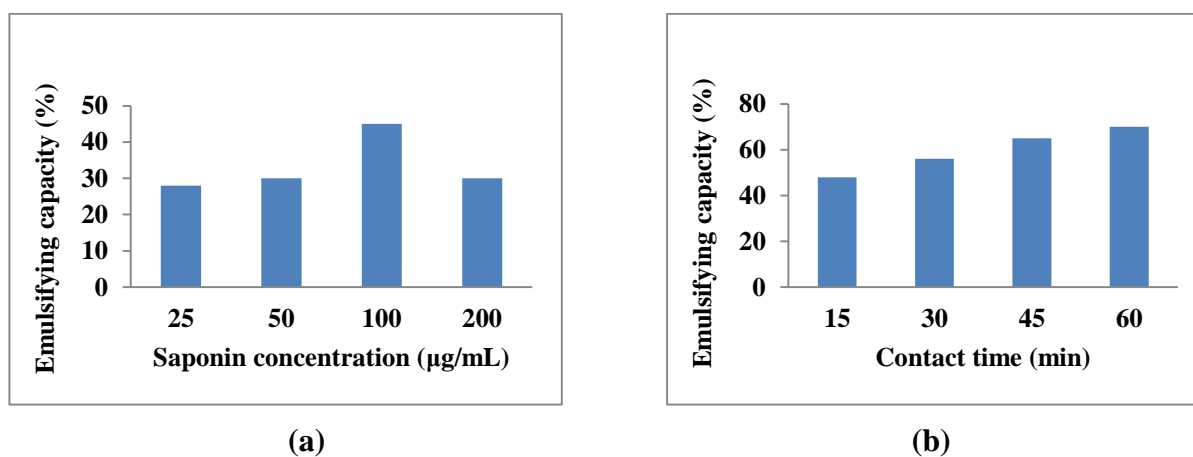
Permanent foaming capacity of crude saponin extract was determined by Froth test using various volume ratio. By Froth test, higher concentration of saponin increases the permanent foaming high as shown in Figure 2. These results obtained are present in Table 3. The foam value was calculated by using the method developed by taking the foam height after 2 min dissipation and subtracting the foam interface (Dini *et al.*, 2009).

### Changes of emulsifying capacity as a function of saponin concentration

Although three samples showed higher forming capacity of their saponin extracts, Onion skin was chosen for further studies since it possesses the highest amount of saponin in compare with other two samples. Thus, emulsifying capacity of Onion skin saponin was determined by the variation of time and saponin concentration. According to these data, emulsifying capacity changes with contact time and saponin concentration (100  $\mu\text{g/mL}$ ) indicated the highest emulsifying capacity. Emulsifying capacity was changed with saponin concentration are present in Figure 3 (a) and varied with contact time are shown in Figure 3 (b).

**Table 3 Permanent Foaming Capacity of Saponin Extracted from Different Vegetable Wastes**

Saponin extract (v/v % in H <sub>2</sub> O)	Permanent foaming capacity (%)		
	Onion skin	Ka Nyut hard stem	Hnin Nu Nwe hard stem
100	40	40	40
80	25	25	33.3
60	14.28	23.08	25
40	7.69	14.29	3.32
20	4	7.69	3.32

**Figure 2** Foaming capacity of saponin extracted from (a) Onion Skin (b) Ka Nyut hard stem and (c) Hnin Nu Nwe hard stem**Figure 3** Changes of emulsifying capacity as a function of (a) saponin concentration and (b) contact time

### Physicochemical Properties of Soil Sample

The physicochemical properties including soil texture, pH, moisture, nitrogen content, phosphorus content and potassium content of soil sample were characterized and the result obtained were present in Table 4. The soil texture was determined by laboratory analysis. The soil samples were averagely sandy loam and (33.12 % sand, 52.00 % silt and 14.88 % clay) with very low contents of nitrogen, phosphorous and potassium (<1 %) were shown in Table 4. Oceanic waters contain only about 0.04 percent of potassium in contrast with about 2.45 percent in the earth's crust. A soil with 0.29 % of total potassium would be rated very low in this element. Potassium as nitrogen and phosphorous must be in an available form, or in other words soluble in the soil moisture, before plants can utilize it. Without sufficient available of potassium in the soil

crop plants suffer in reduced vigor, greater susceptibility to disease, impairment of growth process. Potassium might be considered to stand between nitrogen and phosphorous in its effects on plant growth. A lack of available potassium in the soil is very likely to result in poor quality of the crop (Zhang and Kang, 2013).

**Table 4 Characteristics and Physico-chemical Properties of Crude Oil Contaminated Soil**

<b>Test Parameter</b>	<b>Result</b>
Texture	Sandy loam
Sand (%)	33.12
Silt (%)	52.00
Clay(%)	14.88
pH	9.16
Moisture content (%)	0.13
Humus	1.20
Organic matter content (%)	1.27
Total Nitrogen content (%)	0.11
Total Phosphorus content (ppm)	1.00
Potassium content (mg/100 g)	0.29

#### **Efficiency of Saponin on Remediation of Petroleum Contaminated Soil (Bench Study)**

A laboratory bench study was conducted to assess the removal efficiency of saponin on 1 % crude oil contaminated soil. Various concentration (250, 500 and 1000 ppm) of saponin treatments along with control (no saponin) were applied. All treatments showed the results of residual crude oil 96.97 %, 90.99 %, 75.11 % in soil treatment by 250, 500 and 1000 mg saponin/kg of soil whereas 95.94 % residue was found in control soil. The results were shown in Table 5. According to these data, the concentration of saponin (1000 ppm) decreases the highest residual percent of crude oil in soil during 10 weeks treatment.

#### **Efficiency of Saponin on Remediation of Petroleum Contaminated Soil (Phytoremediation)**

A laboratory study was extended to assess the potentials of local grass (Bermuda grass) under normal environmental conditions with or without surfactants in remediating soil contaminated with crude oil. Each 1 kg of the contaminated soil sample (1% oil in soil) was distributed into nine plastic pots. The Bermuda grasses were transplanted into six pots for two treatments (three pots for plant with commercial surfactant (sodium lauryl ether sulfate-SLES) and three pots for plants with natural surfactant). The other three pots served as Control with plant only. The results of the phytoremediation of contaminated soil showed that significant reduction (76.3 %) of crude oil was observed by natural saponin. It was also observed that the crude oil in the polluted soil were reduced by 72.4 % as a result of plant only, similar to surfactant (SLES) treatment (72.1 %). These data were present in Table 8. According to phytoremediation data, the contaminated soil with plant decreases the residual percent of crude oil in soil.

**Table 5 Changes of Residual Percent of Crude Oil in Soil during 10 Weeks Treatment**

Time (week)	Residual crude oil (%) in treated soil by			
	Saponin (0 ppm)	Saponin (250 ppm)	Saponin (500 ppm)	Saponin (1000 ppm)
0	100.00	100.00	100.00	100.00
2	104.80	103.95	102.21	91.27
4	97.42	97.69	96.98	89.01
6	96.48	97.66	96.40	85.63
8	97.77	98.45	92.32	79.40
10	95.84	96.97	90.99	75.11

**Table 6 Residual Percent of Crude Oil in Saponin Enhanced Phytoremediation**

Time (week)	Residual crude oil (%) in treated soil by		
	Soil+Oil+Plant	Soil+Oil+Plant+Saponin	Soil + Oil+Plant+SLES
0	100.0	100.0	100.0
4	23.7	27.0	27.3
6	24.3	25.8	27.3
8	26.0	24.7	27.2
10	27.6	23.7	27.9

SLES = Sodium Lauryl Ether Sulfate

### Conclusion

The yield % of saponin was found to be highest of 14.55 % in Onion skin, in compare with that of Ka Nyut hard stem (2.53 %) and Hin Nu Nwe hard stem (2.12 %). By Froth test, higher concentration of saponin increases with the permanent foaming high. According to FT IR spectral data, saturated and unsaturated H/C group and cyclic alcohol group were observed in the extracted crude saponin. Emulsifying capacity of Onion skin saponin was changed with saponin concentrations and then saponin (100 µg/mL) possesses the highest emulsifying capacity. Emulsifying capacity was also changed with contact time between saponin solution and paraffin. Crude saponin extracted from Onion skin is potentially applied on the petroleum biodegradation in soil sample. A laboratory study was conducted to assess the potentials of natural saponin and local grasses under normal environmental conditions in remediating soil contaminated with engine oil. Results obtained showed a considerable reduction in the crude oil level of the soil samples compared to the unplanted control soil samples, moreover, the grasses and the saponin showed great promising potential as phytoremediating agents in order to clean-up of crude oil contaminated soil.

### Acknowledgements

The authors would like to express their profound gratitude to the Department of Higher Education (Lower Myanmar), Ministry of Education, Yangon, Myanmar, for provision of opportunity to do this research and Myanmar Academy of Arts and Science for allowing to present this paper.

## References

- Adomako, E. E., Deacon, C. and Meharg, A. A. (2010). "Variations in Concentrations of Arsenic and Other Potentially Toxic Elements in Mine and Paddy Soils and Irrigation Waters from Southern Ghana". *Water Qual Expo Health*, vol. 2, pp.115-124.
- Aye Sandar Linn, Phyu Phyu Myint, and Daw Hla Ngwe. (2013). "Assessment of Tropical Grasses (*Eleusine indica* L., *Axonopus compressus* (Sw.) P.Beauv., *Coelachyrum piercei* Benth.) for Phytoremediation of Hydrocarbon Contaminated Soil". *Myanmar Academy of Arts and Sci.*, vol. 11 (1), pp. 105-118.
- Bajad, P. N., and Pardeshi, A.B. (2015). "Qualitative and Quantitative Analysis of Saponin as Bioactive Agent of *Sapindus emarginatus*". *Int. J. of Sci. and Res. (IJSR)*, vol. 5 (10), pp. 351-354.
- De Geyter, E., Lambert, E., and Geelen, D. (2007). "Novel Advances with Plant Saponins as Natural Insecticides to Control Pesticides". *Pest Tech.* vol. 1, pp.96-105.
- Deshpande. S., Shiau, B.J., Wade, D., Sabatini, D.A., and Harwell, J.H. (1999). "Surfactant section for enhancing ex situ soil washing". *Water Res.*, vol. 33 (2): pp. 351-360.
- Dini, I., Tenore, G. C., and Dini, A. (2009). "Saponins in Ipomoea Botatastubers: Isolation, Characterization, Quantification and Antioxidant Properties". *Food Chem.*, vol. 11 (3), pp. 411-419.
- Laufenberg, G., Kunz, B. and Nystroem, M. (2003), "Transformation of Vegetable Waste into Value Added Products: (A) The Upgrading Concept; (B) Practical Implementations". *Bioresour. Technol.*, vol. 8 (7), pp. 167-198.
- Mnif, I., Mnif, S., Sahnoun, R., Maktouf, S., Ayedi, Y., Ellouzechaabouni, S. and Ghribi, D. (2015). "Biodegradation of diesel oil by a novel microbial consortium: comparison between co-inoculation with biosurfactant-producing strain and exogenously added biosurfactants". *Environ. Sci. Pollut. Res.*, vol. 22, pp.14852-14861.
- Weaver, R. W., Melton, J. R., Wang, D., Duple, R. L. (1984). "Uptake of Arsenic and Mercury from Soil by Bermuda grass *Cynodon Dactylon*". *Environmental Pollution*, vol. 33, pp.133-142.
- Wei, Y., Liang, X., Tong, C., Guo, Z., Dang, Z. (2015). "Enhanced solubilization and desorption of pyrene from soils by saline anionic-nonionic surfactant systems". *Colloids Surfaces A Physicochem. Engin. Aspects*, vol. 468, pp. 211-218.
- Zhang, T., and Y., Kang, (2013). "Shallow sand- filled niches beneath drip emitters made reclamation of an impermeable saline-sodic soil possible while cropping with *Lycium barbarum* L.", *Agric. Water Manage.* 119, 54-64
- Zoller,U., and Reznik, A. (2009). In-situ Surfactant/Surfactant-nutrient Mix-enhanced Bioremediation of NAPL (fuel) Contaminated Sandy Soil aquifer, *Environmental Sci. and Pollutant Res.*, vol. 2 (13), pp. 392-397.

## PREPARATION AND CHARACTERIZATION OF CHICKEN FEET COLLAGEN FOR BIOMEDICAL APPLICATION

Lae Lae Mon Win<sup>1</sup>, Thinzar Nu<sup>2</sup>, Cho Cho<sup>3</sup>

### Abstract

In this study, collagen was extracted from chicken feet and its biomedical application was investigated. The chicken feet were collected from poultry Myanmar market. The collagen was extracted from chicken feet by using acid solubilized method. The yield percent of crude was found to be 10.08 %. And then the crude collagen was purified by dialysis method, purified collagen was found to be 8.32 %. Both crude and purified collagens were characterized by using SEM, UV-visible and FT IR analysis. The SEM images of collagen to be regular and uniform with networking of porous on the surface. The absorption bands of crude and purified collagen were found to be near 230 nm in UV spectra. In the FT IR spectra, absorption bands of collagen sample indicated the presence of N-H, O-H, C=O, -CH<sub>2</sub>, -CH<sub>3</sub> groups in the sample. The antimicrobial activity of both collagen samples were determined by agar well diffusion method. In this experiment, both samples were found to be high activities against six microorganisms such as *Bacillus subtilis*, *Staphylococcus aureus*, *Pseudomonas aeruginosa*, *Bacillus pumilus*, *Candida albicans* and *Escherichia coli*, which showed that collagen possessed the high antimicrobial activity against all tested microorganisms. The wound healing effect of both collagens was investigated. It was found that the purified collagen was well-developed in healing of burn wound with well-developed sebaceous glands, sweat glands and hair follicles in epidermis layer of skin. This research therefore contributes to academics as well as biomedical application.

**Keyword:** Chicken feet, collagen, acid-solubilized method, antimicrobial activity, biomedical

### Introduction

Collagen was first found and defined as gelatin by extractive cooking of bones at the beginning of 1800's. This family of proteins was studied by scientists in different areas. Collagens are the most abundant high molecular weight proteins in both invertebrate and vertebrate organisms, including mammals and possess mainly a structural role, exciting different types according with their specific organization in distinct tissues (Almeida and Lannes, 2013). It is mainly presented in all connective tissues, including animal skins, bones, cartilages, tendon and blood vessels. It is involved in the formation of fibrillar and microfibrillar networks of the extracellular matrix and basement membranes. Collagen is the major components of the extracellular matrix nearly 28 types of collagen have been identified. All of them have triple helix characteristic but the length of the helix, the size and nature of non - helical portion various from one to another type (Kirti and Khora, 2015). The collagen types were classified by their size, function and distribution which differ considerably in their amino acid composition. Among all the current variants of collagens, type I, II, III and V are the most prevalent and they are all fibrillar-forming collagens. Every collagen type has its special amino acid composition, and each performs a distinctive role in the tissue (Hashim, 2015).

The collagen family consists of 28 different proteins, which account for 25% -35% of the total protein mass in mammals and play a pivotal role in the structure of several tissues, such as skin and bones, providing rigidity and integrity (Silvipriya, *et al.* 2015). The stability of collagen helix is closely correlated with the total amino acid content in a collagen molecule. Collagen contains rather larger amount of polar amino acid residues (arginine, lysine, aspartate, and glutamate) besides high contents of glycine and amino acids (Kiew and Don, 2013). The chemical

---

<sup>1</sup> Lecturer, Department of Chemistry, Yangon University of Education

<sup>2</sup> Dr, Associate Professor, Department of Chemistry, University of Yangon

<sup>3</sup> Dr, Professor, Department of Chemistry, University of Yangon

cross – linkers used may be either relatively small bifunctional molecules or polyfunctional macromolecules. Poultry feet are abundant in collagen and also have been extracted as medical material such as collagen film, and collagen powder for wound exudate control (Lee and Singla, 2001).

Recently, consumers had rejected some foods and cosmetics that were prepared from beef collagen due to the fear of bovine spongiform encephalopathy. Thus, it is desirable to seek an alternative source of collagen from the other animal species rather than from cattle. Chicken feet may be a good collagen source and could be used to replace beef collagen. Collagen was extracted from different raw materials has been used for clarifying beverages, in cosmetics, in casings for meat products and in a host of biomedical application. Medical applications of collagen include use in drug delivery systems, sponges for burns and wounds and in tissue engineering (Liu, 2001).

### **Materials and Methods**

The chicken feet sample was collected from Hledan Market, Kamayut Township, Yangon. The chicken feet were cut proper size and washed with water to removed impurities. The collagen was extracted according to the method of Liu, 2001 and Lin, 2013 with slight modification. Repeated defatting processes were performed to extract lipids and triglycerides by stirring the chicken feet in 1:8 (w/v) of 90 % ethanol for 48 h at 4 °C. The residues were soaked with 0.05 M disodium salt of EDTA with a solid/ solvent ratio of 1:8 (w/v). The mixture was stirred for 24 h and then the solution was decanted and the residue was washed with distilled water, until the water was clear. The liquid suspension was decanted and the residues were subsequently soaked into 0.1 M NaOH at a sample / alkali solution ratio of 1: 8 (w/v) and stirred for 72 h at 4 °C then the liquid suspension was decanted and the residue was washed with distilled water, until the water was clear. Inorganic compounds were removed by soaking the defatted sample in 0.1 M HCl solution with solid/ solvent ratio of 1:8 (w/v). The mixture was stirred for 24 h. Then the solution was decanted and the residues were washed with distilled water until the neutral pH. After being wash with water, the residues were soaked in 0.5 M acetic acid with a sample per solvent ratio of 1:10 (w/v) at 4 °C for 5 days with a stirring. The chicken feet suspended solution was filtered by using cheese cloth to remove the residues. Then the solution was centrifuged at 15000 rpm for 30 min at 4 °C, the crude collagen solution was obtained. Crude collagen purification was achieved by convenient salting out process performed at 4 °C for 24 h with gentle agitation: NaCl was carefully added to the supernatants until a final concentration of 0.9 M was achieved. The collagen solutions were dialyzed against 0.1 M acetic acid and distilled water at 4 °C for 4 days and then dried at 30 °C for 3 days. And then the crude and purified collagens were characterized by SEM, UV, and FT IR. The antimicrobial activity of both collagen samples was determined by agar well diffusion method. The preliminary characterization and bioactivity test was made for biomedical application of collagens. The biomedical application of crude and purified collagens was further studied by animal test.

### **Results and Discussion**

Chicken feet may be a good collagen source and could be used to replace beef collagen (Liu, 2001). There are three major methods of collagen extraction producer such as neutral-salt solubilized collagen, acid-solubilized collagen and pepsin-solubilized collagen. Organic acids are capable of solubilizing non-crosslink collagens and also of breaking some of the inter-strand cross-links in collagen, which leads to a higher solubility of collagen during the extraction process. Therefore, acidic solutions, especially acetic acid, are commonly used to extract collagen. In this study, collagen was extracted from chicken feet by acid solubilized method with acetic acid. The yield percent of crude and purified collagens were found to be 10.08 and 8.23 %, respectively.

### Scanning Electron Microscopy (SEM)

Figure 1 (a) and 1 (b) show the surface morphology of crude and purified collagens. There were observed fibril like structures. The SEM images of collagen to be regular and uniform with networking of porous on the surface. Generally uniform network structure of collagen as drug carrier is propitious, for well-proportioned distribution of drugs. Based on the SEM results, chicken feet collagen is suitable for the preparation of collagen based products.

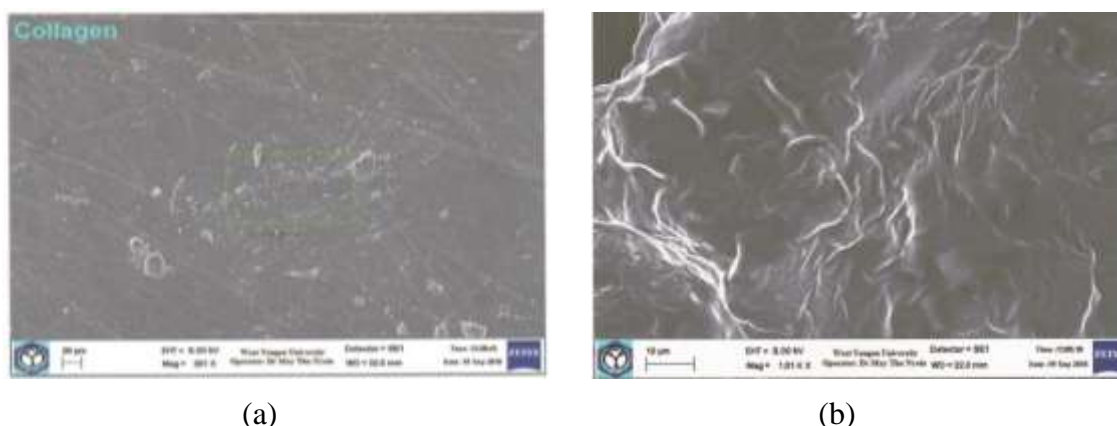


**Figure 1** SEM images of (a) crude collagen and (b) purified collagen

### UV-visible Spectra of Extracted Collagen

Figure 2 (a) and 2 (b) show the UV-visible spectra of crude and purified collagen. The ultraviolet spectra of extracted crude and purified collagen showed the maximum absorbance near 232 nm. Moreover, a shoulder or smaller peak in the 250-290 nm region is absent because of the negligible amount of tyrosine residues and the absence of tryptophan in the extracted collagen.

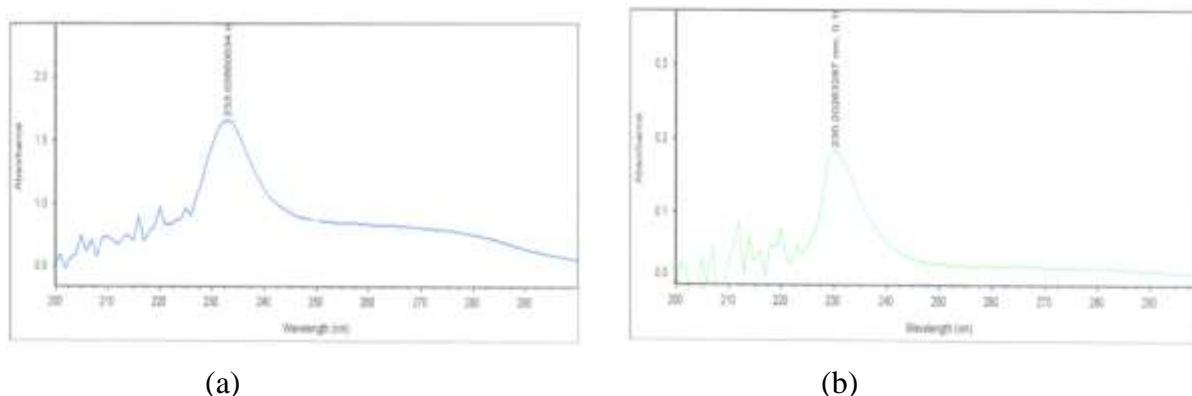


**Figure 2** UV-visible spectrum of (a) crude collagen and (b) purified collagen

### Fourier Transform- Infrared (FT IR) Analysis

The FT IR spectroscopy provides information regarding interaction via analysis of FT IR spectra corresponding to stretching or bending vibrations of particular bonds. Figure (3, a) shows the FT IR spectra of extracted crude collagen. The amide B band at  $2924\text{ cm}^{-1}$  was assigned to the asymmetrical  $\text{CH}_2$  stretching. The amide II band,  $1456\text{ cm}^{-1}$  was assigned to the NH bending coupled with CN stretching vibration. The peak of amide III band was found at  $1165\text{ cm}^{-1}$ .

Figure (3, b) shows FT IR spectra of purified collagen. According to Doyle (1975), a free N-H stretching vibration occurs in the range of  $3400\text{-}3440\text{ cm}^{-1}$  and when the N-H group of a peptide is involved in a hydrogen bond, the position is shifted to lower frequencies. The amide A

band of purified collagen was found at the  $3283\text{ cm}^{-1}$  was assigned to the hydrogen bonding in the NH group of the peptide, which is the main functional group of the collagen. The amide B peak at  $2930\text{ cm}^{-1}$ , was represented the asymmetrical stretching of  $\text{CH}_2$ . The amide I band was found at  $1632\text{ cm}^{-1}$ , which associated with the stretching vibration of carbonyl groups ( $\text{C}=\text{O}$ ) along the poly peptide backbone. The amide II at  $1537\text{ cm}^{-1}$  was assigned to the NH bending coupled with CN stretching vibration. The amide II band indicates the secondary structure of collagen. The amide III band,  $1237\text{ cm}^{-1}$  was related to triple helical structure of collagen.

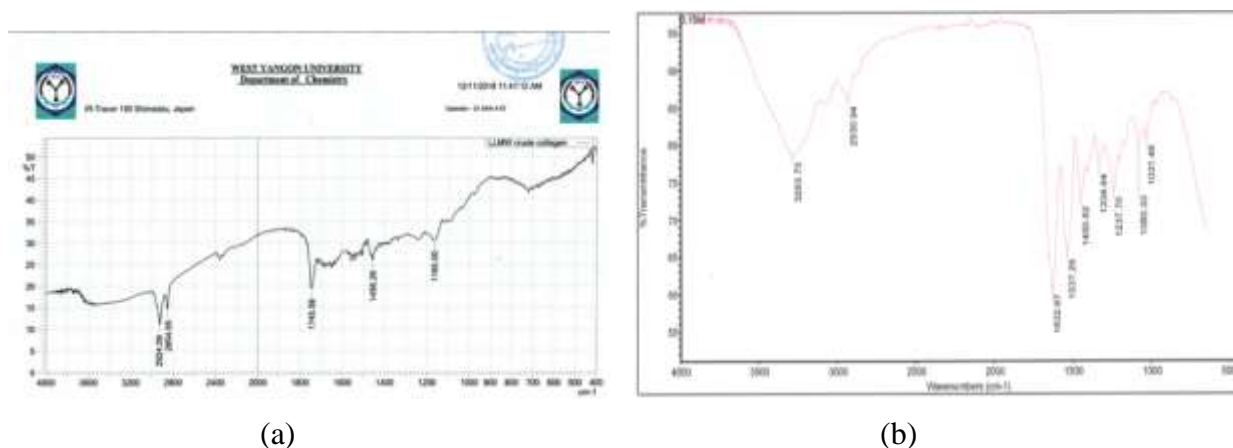
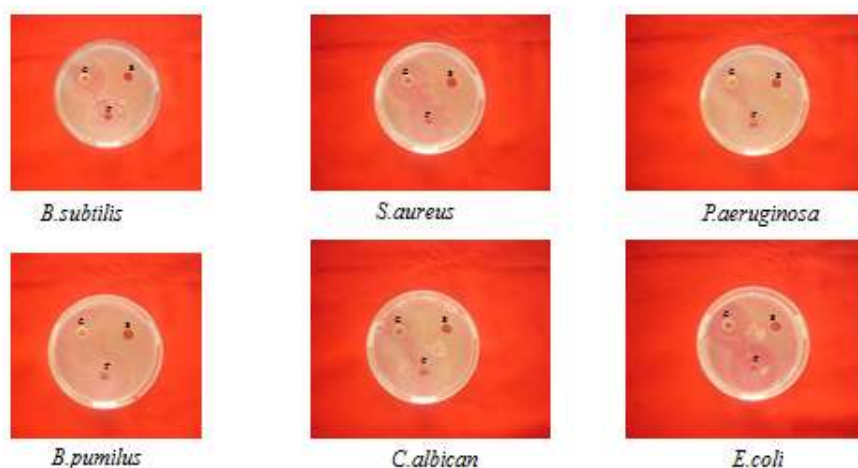


**Figure 3** FT IR spectrum of (a) crude collagen and (b) purified collagen

### Antimicrobial Activity of Collagen

Antimicrobial activity of crude collagen and purified collagen was investigated against six species of microorganisms by employing agar well diffusion method. The samples were tested on six species of microorganisms including *Bacillus subtilis*, *Staphylococcus aureus*, *Pseudomonas aeruginosa*, *Bacillus pumilus*, *Candida albicans* and *Escherichia coli*. The results are shown in Figure 4 and Table 1. It was found that crude and purified collagen showed highest antimicrobial activity against all tested microorganisms with inhibition zone diameter higher than 20 mm. So, it may be inferred that the collagens extracted from the chicken feet can be effective in the formulation of medicine for the treatment of diseases such as soft tissue infection, bone and joint infection, ear infection, burn infection and as a surgical homeostatic agent.



C= Crude collagen, P = Purified collagen, S = Solvent (Acetic acid)

**Figure 4** Antimicrobial activities of crude collagen and purified collagen against six microorganisms

**Table 1 Antimicrobial Activity of Crude and Purified Collagen**

Samples	Inhibition zone diameter (mm)					
	<i>B.subtilis</i>	<i>S.aureus</i>	<i>P.aeuginosa</i>	<i>B.pumilus</i>	<i>C.albican</i>	<i>E.coli</i>
Crude collagen	36 (+++)	35 (+++)	40 (+++)	35 (+++)	38 (+++)	35 (+++)
Purified collagen	38 (+++)	37 (+++)	40 (+++)	36 (+++)	40 (+++)	36 (+++)
Control (10 % acetic acid)	-	-	-	-	-	-

Agar well -10 mm

10 mm ~ 14 mm (+) → normal

15 mm ~ 19 mm (++) → high

20 mm above (+++) → highest

### Biomedical Application of Chicken Feet

This test was carried out at Department of Medical Research (DMR). The incision skins of rats were treated with sofretulle, crude collagen, purified collagen and commercial collagen. The progress of the treatment was recorded at a specified time interval. The results were shown in Figure 6. The healing rate of burned and scabs drop time were recorded on days 0, 2, 9 and 17. On days 2, the wound area increased initially and the progress of all burned skins were not significantly observed. On days 9, crude collagen, purified collagen and commercial collagen treated wounds relieved conspicuous redness on the wound border which is a sign of vascularization and re-epithelization. On days 17, shaving was performed on all rats, since hair had grown extensively. The burn wounds were almost completely healed that were treated with crude, purified and commercial collagen. From the observation crude and purified collagens have been shown to significantly accelerate the burn wound healing. After 17 days, histopathological finding of the skin lesions was carried out by haematoxylin and eosin (H & E) method and recorded by using light microscope with specific images. The results showed that the treatment with purified collagen and commercial collagen were better than the crude collagen and sofretulle. This histopathological section of rat skin showed incomplete epithelialization in epidermis, dermis and subcutaneous tissue in no treatment group. Standard group of rat skin showed re-epithelialization of healing process but focal epidermal lesion is still present. The wound healing is still in progress and partially developed re-epithelialization of healing process and focal epidermal lesion is still present in epidermal layer by treatment with crude collagen and commercial collagen. Good wound healing in skin lesion of rat model was observed because presence of well-developed granulation tissues accompanied with well-developed sebaceous glands and sweat gland and hair follicles in epidermis and dermis layers of skin by the treatment with purified collagen. Better degree of wound healing was observed in this group by treatment with purified collagen than that of other. These results were showed in Figure 7.



**Figure 5** Preparation of burn wound on rat model

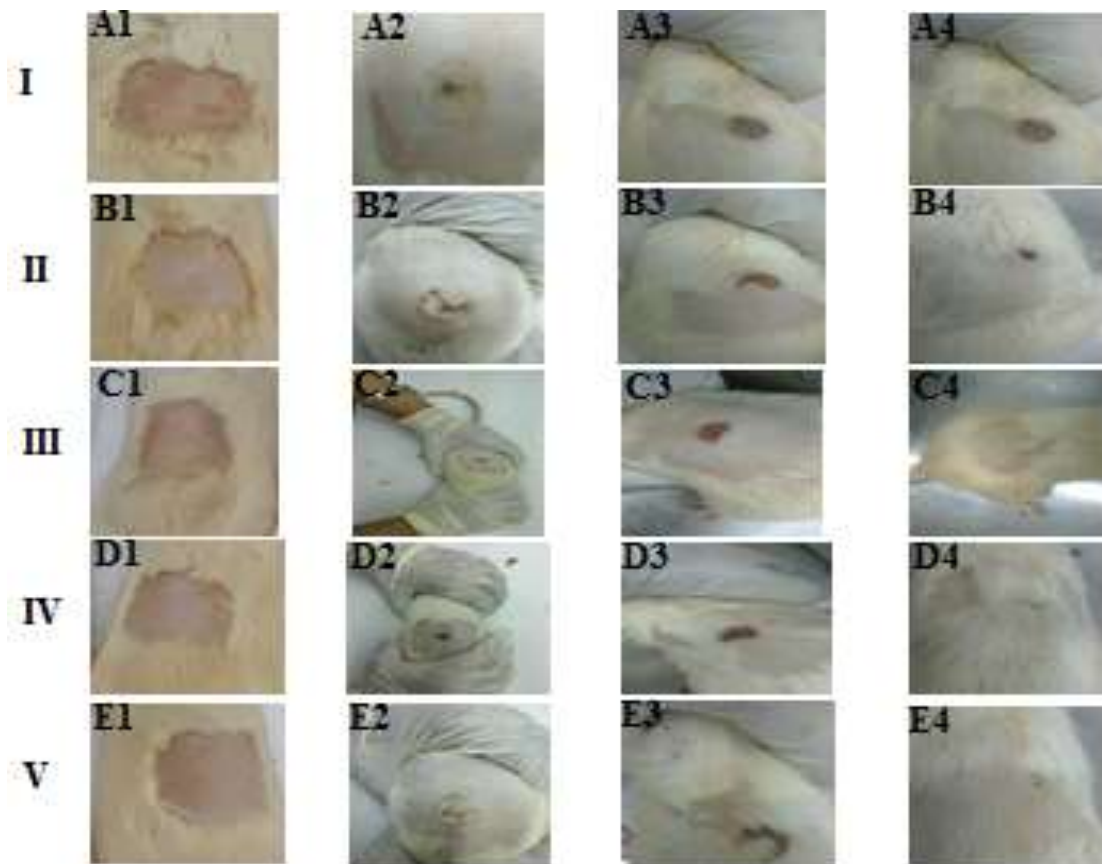


**Figure 6** Burn wound activity of treatment on 17 days (I control, II sofretulle, III crude collagen, IV purified collagen and V commercial collagen)

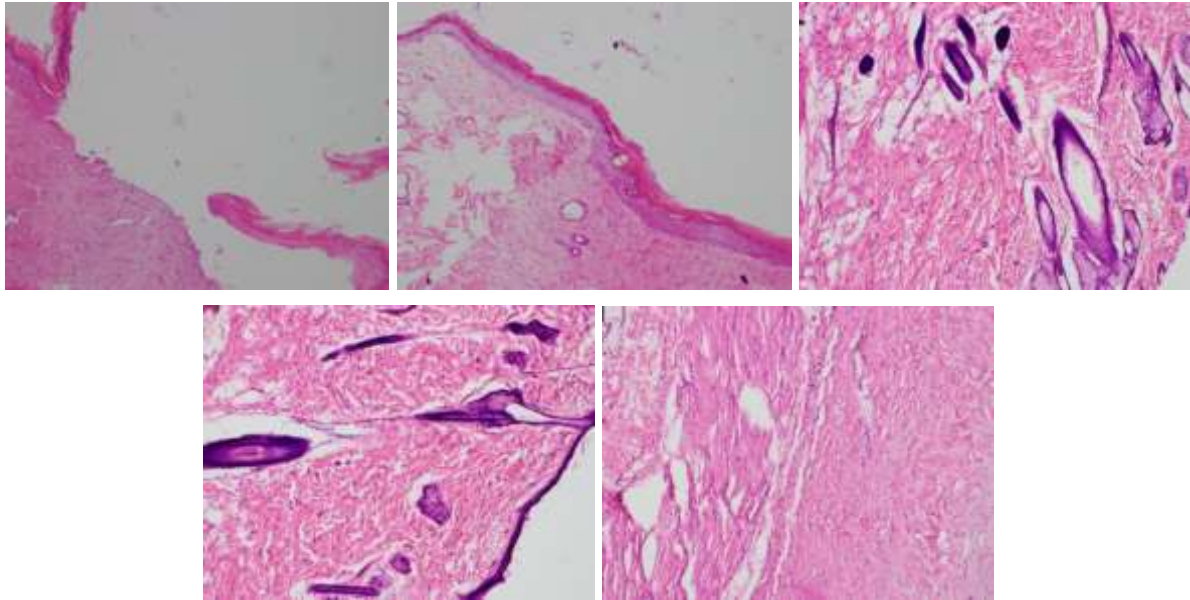


**Figure 7** Hematoxyline and eosin-stained section of biopsies for the morphological evaluation of skin lesions of burn skin treated with crude collagen, purified collagen and commercial collagen on days 17

### Conclusion

In this research, chicken feet were used as a source of collagen for biomedical application. Collagen was extracted from chicken feet by method of Liu, 2001 with slight modification and then crude collagen was purified by the method of Lin, 2013. The yield percent of crude and purified collagens were found to be 10.08 and 8.23 %, respectively. The micro architecture of collagen was studied by using Scanning Electron Microscopy, SEM. From the SEM result, both crude and purified collagens were identified as fibrillar structure. According to UV spectrum analysis, collagens were found to be the highest intensity of absorbance peak is 232 nm and no more other peaks were observed. The FT IR spectra data of collagen indicated the presence of N-H, C=O, C-H, O-H, CH<sub>2</sub>. From the screening of antimicrobial activity of collagens, it can be concluded that the collagens showed the pronounced antimicrobial activity against all tested microorganisms. So, it may be inferred that chicken feet collagen can be used in the biomedical and pharmaceutical fields as a potential material for construction of tissue engineering scaffold and wound dressing system. The chicken feet collagens were studied in biomedical field especially burn wound healing compared standard sofretulle drug. The significant improved in burn contraction by visually was observed when using the chicken feet collagen on days 17 after burning. Histopathological finding under microscope also reported that the skin treated with collagen exhibited good wound healing and well developing granulation tissue composed of sebaceous glands, sweat glands and follicles in epidermis and dermis layers. From these results chicken feet collagen was better than the standard sofretulle drug for burn wound healing. Therefore, this research contributes to academic as well as biomedical application.

### Acknowledgements

The authors would like to express their profound gratitude to the Department of Higher Education (Lower Myanmar), Ministry of Education, Yangon, Myanmar, for provision of opportunity to do this research and Myanmar Academy of Arts and Science for following to present this paper.

## References

- Almeida, P.F. and S.C. Lannes. (2013). "Extraction and Physicochemical Characterization of Gelatin from Chicken by-product". *Journal of Food Process Engineering*, vol. 36 (6), pp. 824-833
- Doyle, B. B., E. R. Blout and E. G. Bendit. (1975). "Infrared Spectroscopy of Collagen and Collagen-Like Polypeptides". *Biopolymer*, vol. 14 (5) pp. 937-957
- Hashim, P., M. Ridzwan, J. Bakar and H.D. Mat. (2015). "Collagen in Food and Beverage Industries". *International Food Research Journal*, vol. 22 (1), pp.1-8
- Kiew, P. L. and M.M. Don. (2013). "The Influence of Acetic Acid Concentration on the Extractability of Collagen from the Skin of *Hybrid Claris sp.* And its Physicochemical Properties: A Preliminary study". *Focusing on Modern Food Industry*, vol.2 (3), pp.123-128
- Kirti,S. and S. Khora. (2015). "Isolation and Characterization of Collagens Extracted from the Skin of Pufferfish, *Lagocephalus wheeneri*". *Research Journal of Pharamaceutical, Biological and Chemical Sciences*, vol. 6 (6) pp. 863-870.
- Lee, C. H. and A. Singla. (2001). "Biomedical Applications of Collagen". *International Journal of Pharmaceutics*, vol. 221 (2), pp.1-22
- Lin, C. W., M. Loughram and T.Y.Tsai. (2013). "Evaluation of Convenient Extraction of Chicken Skin Collagen using Organic Acid and Pepsin Combination". *J. Chin. Soc. Anim. Sic*, vol. 42 (1), pp. 27-28
- Liu, D. C., Y. K. Lin and M.T. Chen. (2001). "*Optimum condition of Extracting Collagen from Chicken Feet and its characteristic*". Department of Animal Science, National Chung-Hsing University, Taiwan, vol. 3 (6), pp. 24-33
- Silvipriya, K.S., K.K., Kumar and A. R. Bhat. (2015). "Collagen: Animal Sources and Biomedical Application". *Journal of Applied Pharmaceutical Science*, vol.5 (3), pp.123-127

## PREPARATION OF SECRETED PROTEINS FROM *STREPTOMYCES* SP. SIREXAA-ETO HYDROLYZE CMC AND CELLULOSE

Nang Naunge Ying<sup>1</sup>, Taichi Takasuka<sup>2</sup>, Ye Myint Aung<sup>3</sup>

### Abstract

One of the insect associated bacterium, *Streptomyces* sp. SirexAA-E (SirexAA-E), was described to be highly cellulolytic. SirexAA-E grew well on cellulose and other plant cell wall materials such as xylan, and secretes a suite of specialized enzymes depending on the available carbon sources in the growth medium. Non-crystalline cellulose (CMC) and chemically pretreated miscanthus were used as sole carbon sources, and secreted enzymes were compared between two culture conditions. In the presence of CMC, several prominent cellulases were determined by SDS-PAGE. While in the presence of miscanthus, dozens of enzymes including above cellulases were determined, thus I decided to use miscanthus as a sole carbon sources to prepare the culture supernatant of Sirex AA-E. The optimum condition of cultivation of SirexAA-E on miscanthus was determined with regard to protein yield (mg/L) and quality. It was confirmed that 5 days with 1 mL inoculum into 50 mL culture gave the highest protein yields with intact form of secreted proteins.

**Keywords:** SirexAA-E, CMC, SDS-PAGE, miscanthus, inoculum, secreted proteins.

### Introduction

Plant biomass is the most abundant of carbon source on earth, and its deconstruction and subsequent catabolism are key components of global carbon cycling. (Schlesinger, 2000 & Klemm 2005). The main energy in plant biomass is stored in plant cell walls, primarily in the recalcitrant polysaccharides cellulose and hemicellulose (Kirk, 1987, Awungacha, 2015 & Lynd, 2002). Efficient breakdown of these insoluble polymers is difficult, and only a limited number of bacterial and fungi have this capability (Lynd, 2002). *Streptomyces* the largest genus of Actinobacteria and over 1000 *Streptomyces* sp. from both free livings and eukaryotic symbionts are reported (Book, 2016, Lewin, 2016 & Poulsen, 2011). Because of the great potential for their capability (Lynd, 2002). *Streptomyces* the largest genus of Actinobacteria and over 1000 *Streptomyces* sp. from both free livings and eukaryotic symbionts are reported (Book, 2016, Lewin, 2016 & Poulsen, 2011). Because of the great potential for their secondary metabolites for human health and other applications, *Streptomyces* have been capability (Lynd, 2002). *Streptomyces* the largest genus of Actinobacteria and over 1000 *Streptomyces* sp. from both free livings and eukaryotic symbionts are reported (Book, 2016, Lewin, 2016 & Poulsen, 2011). Because of the great potential for their secondary metabolites for human health and other applications, *Streptomyces* have been the most extensively studied microorganisms in the past decades (Alvarez, 2017, Clardy, 2006, Demain, 2009 & Adams, 2011). Recently, multiple insect symbionts of *Streptomyces* were described, and a potential application for biofuels production has been identified because of their high plant cell wall degradation potential (Book, 2016).

*Streptomyces* is the largest genus of Actinobacteria and an ecologically important group in the soil environment. They play as essential roles in the decomposition of biomass polymers especially hemicellulose (Cantarel, 2009, Crawford, 1978, Good fellow, 1983 & McCarthy, 1992). *Streptomyces* use a wide range of carbon sources and produce antimicrobial secondary metabolites (Goodfellow, 1983 & Schlatter, 2009). Although, the cellulose-degrading ability of *Streptomyces*

---

<sup>1</sup> Graduate school of Agriculture, Hokkaido University, Japan

Lecturer, Department of Chemistry, Patheingyi University, Myanmar

<sup>2</sup> Dr Associate Professor, Research Faculty of Agriculture, Hokkaido University, Japan

<sup>3</sup> Dr Professor and Head, Department of Chemistry, Patheingyi University, Myanmar

was not well described in the past, novel isolate, *Streptomyces* sp. SirexAA-E, originally isolated from the wood devastating wood wasp, was shown to possess very high cellulose-degrading potential (Fig. 1), (Bianchetti, 2013).

In this study, we examined the growth, in the presence of biomass, SirexAA-E secreted enzymes that hydrolyzed CMC and cellulose.

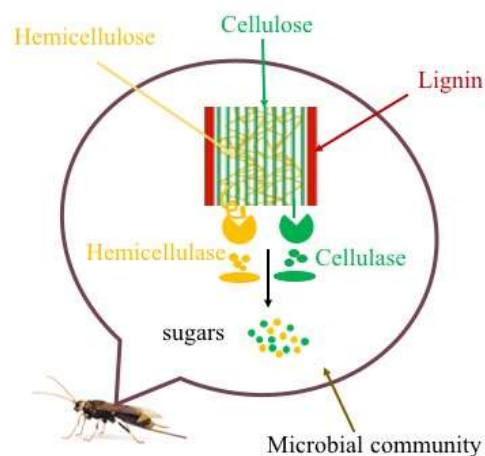


**Figure 1** Schematic diagram of wood wasp symbiont microbial community that decomposes plant cell wall structures by using various cellulases and hemicellulases to produce sugars.

## Materials and Methods

### 1 General reagents

Media for the growth and cultivation of bacterial cells were used Carboxymethyl cellulose (CMC) (Sigma-Aldrich, MO, USA), and biomass (miscanthus prepared in this study). Cellulose (Avicell) used in the cellulase activity measurements was purchased from Sigma-Aldrich.

### 2 Growth of organisms

Sirex AA-E was grown in YME medium Table 1. Cultures were incubated for 2 days at 30°C. Different days and different amount of inoculum (mL of inoculum into 50 mL M63 minimum medium: are shown in (Table 2). The sole carbon source (0.5%, wt/vol) in the medium was carboxymethyl cellulose (CMC) or biomass (miscanthus). Cultures were incubated with shaking condition at 250 rpm at 30 °C for the number of days as shown in (Table 3).

### 3 Preparation of secretomes

Supernatants were prepared from growing cultures by centrifuging the culture medium for 10 min at 4200×g at 4°C to remove insoluble polysaccharides and cells. The supernatant fraction was then passed through a 0.45 μm glass fiber filter (AS ONE co., Osaka) to remove remaining cells. The concentration of secreted proteins in the supernatants was determined by Bio-Rad protein assay kit (Bio-Rad). For enzyme assays, the supernatants were concentrated to 1 mg/mL by using centrifugal ultrafiltration (VIVASPIN 20, Germany).

**Table 1 Preparation of YME medium**

Reagents	Volume
Yeast Extract	4.0 g
Malt Extract	10.0 g
Dextrose or D-glucose	0.4 g
Distilled H <sub>2</sub> O to bring	1L

**Table 2 Preparation of M63 minimal medium**

Reagents	Volume
K <sub>2</sub> HPO <sub>4</sub>	53.6 g
KH <sub>2</sub> PO <sub>4</sub>	26.2 g
(NH <sub>4</sub> ) <sub>2</sub> SO <sub>4</sub>	10.0 g
1 M MgSO <sub>4</sub>	1 mL
thiamine	1 mL (1 mg/mL)
Distilled H <sub>2</sub> O to bring	1L

**Table 3 Incubation of cultures time**

Inoculum (mL) in 50 mL culture	Incubation time (days)
1.0 mL	3 days
5.0 mL	3 days
10.0 mL	3 days
1.0 mL	5 days
5.0 mL	5 days
10.0 mL	5 days
1.0 mL	6 days
3.0 mL	6 days
5.0 mL	6 days
1.0 mL	9 days
3.0 mL	9 days
5.0 mL	9 days

#### 4. Enzyme activity measurements

Reduced sugar assays were carried out by mixing biomass secretome preparations with polysaccharide-containing substrates including carboxymethyl cellulose CMC and cellulose. Enzyme hydrolysis reactions were carried out using 0.1 mg/mL of miscanthus secreted protein from the culture supernatant were incubated with 10 mg/mL of either CMC or cellulose in 10 mM sodium phosphate, pH 6, at 40 °C for 20 h. The reaction will be stopped by heating for 5 min at 95 °C. Reducing sugar content was determined by the dinitrosalicylic acid (DNS) assay. D-glucose was used to obtain a standard to quantify the amount of reducing end products. The enzyme activity in each solution ( $\mu\text{mol}$  reducing sugar/mg per hour) was calculated.

## Results and Discussions

### Growth of SirexAA-E with two different carbon sources

SirexAA-E grew well in 50 mL of M63 minimal medium containing two different carbon sources including 0.5% carboxymethyl cellulose (CMC) and 0.5% pretreated miscanthus. The

protein contents were analyzed for the culture supernatant from two different carbon sources by SDS-PAGE and also different amount of inoculum were tested, 0.5, 1.0 and 2.0 mL in 50 mL of M63 minimal medium for 7 days at 30 °C, to test proteins amount and quality of proteins (Fig. 2). In the SDS-PAGE analysis of proteins from the CMC and biomass culture supernatants, around 47 kDa and 61 kDa proteins can be seen, respectively, which are indicative of the presence of untruncated reducing and non-reducing end cellobiohydrolases. In the following protein gel analyses, thus I utilize these two protein bands as indicators of quality of secreted proteins. From this result, among two different carbon sources in the culture medium, different amount of proteins were observed and also different inoculum showed improvement of protein amount in the culture supernatants. I concluded that the use of miscanthus as a sole carbon source in the growth medium of SirexAA-E was more relevant to prepare secreted proteins than that of CMC. Thus, I decided to optimize the secreted protein production by using the medium containing miscanthus as sole carbon source.

To optimize culture conditions, SirexAA-E was grown on 0.5% (w/v) miscanthus for 3 and 5 days at 30°C with different amount of inoculum (1.0, 5.0 and 10.0 mL) in the 50 mL of M63 minimum medium, and analyzed by the SDS-PAGE (Fig. 3) and the concentration of proteins in the supernatant was measured (Table 4). Also the culture supernatants from 6 and 9 days at 30°C with different amount of inoculum (1.0, 3.0 and 5.0 mL) in 50 mL of M63 minimum medium were analyzed by SDS-PAGE (Fig. 4) and the concentration of proteins in the supernatant was measured (Table 5). In the 3 days culture supernatants, the following concentrations of secreted proteins were obtained from the 1.0 mL of inoculum (0.045 µg/µL), 5.0 mL of inoculum (0.083 µg/µL), and 10.0 mL of inoculum (0.080 µg/µL), respectively. In Fig. 2.2., the SDS-PAGE analysis showed that two indicators (47 kDa and 61 kDa bands) seem to be intact. In the 5 days culture supernatants, the following concentrations of secreted proteins were obtained from the 1.0 mL of inoculum (0.358 µg/µL), 5.0 mL of inoculum (0.478 µg/µL), and 10.0 mL of inoculum (0.428 µg/µL) respectively. In Fig. 2.2., the SDS-PAGE analysis showed that two indicators (47 kDa and 61 kDa) seem to be intact. In the 6 days culture supernatants, the following concentrations of secreted proteins were obtained from the 1.0 mL of inoculum (0.154 µg/µL), 3.0 mL of inoculum (0.107 µg/µL), and 5.0 mL of inoculum (0.153 µg/µL), respectively. In Fig. 2.3., the SDS-PAGE analysis showed that two indicators (47 kDa and 61 kDa) were intact. In 9 days culture supernatants, the following concentrations of secreted proteins were obtained from the 1.0 mL of inoculum (0.144 µg/µL), followed by 3.0 mL of inoculum (0.153 µg/µL), and 5.0 mL of inoculum (0.141 µg/µL), respectively. In contrast to other samples, one of the two indicators (47 kDa and 61 kDa), 61 kDa protein seem to be proteolytically truncated. Thus, from these results, I concluded that the culture supernatant from the 5 days culture gave the highest protein production with no apparent truncation by secreted proteases.

**Table 4 SDS-PAGE analysis for 3 & 5 days of biomass secretomes**

Inoculum (mL/ days)	Concentration of proteins (µg/µL)
1.0 mL-3 days	0.045
5.0 mL- 3 days	0.083
10.0 mL- 3 days	0.080
1.0 mL- 5 days	0.358
5.0 mL- 5 days	0.478
10.0 mL- 5 days	0.428

**Table 5 SDS-PAGE analysis for 6 & 9 days of biomass secretomes**

Inoculum (mL/ days)	Concentration of proteins (µg/µL)
1.0 mL-6 days	0.154
3.0 mL- 6 days	0.107
5.0 mL- 6 days	0.153
1.0 mL- 9 days	0.144
3.0 mL- 9 days	0.153
5.0 mL- 9 days	0.141

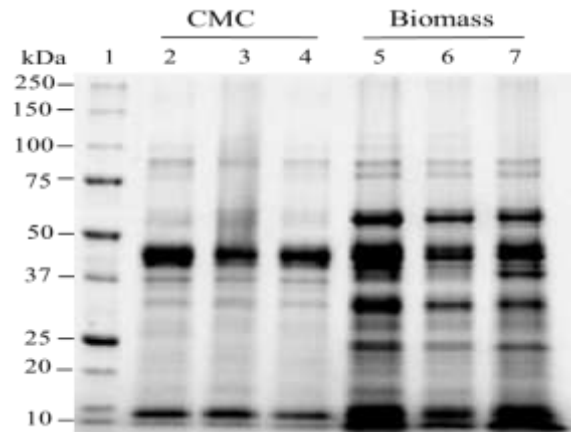


**Figure 2** SDS-PAGE analysis of two difference carbon sources in 7 days inoculum.

Secretome analysis by 10% SDS-PAGE gel. SireAA-E was grown on either 0.5% CMC or biomass (miscanthus) for 7 days at 30°C with different amount of inoculum (0.5, 1.0 and 2.0 mL) in 50 mL culture. Lane 1 is Mw marker. Lanes 2 to 4 are 0.5, 1.0 and 2.0 mL inoculum in 50 mL 0.5% CMC M63 minimum medium, respectively. Lanes 5 to 7 are 0.5, 1.0 and 2.0 mL inoculum in 50 mL 0.5% miscanthus M63 minimum medium, respectively. 10.0 µg equivalent of total secretome was used.

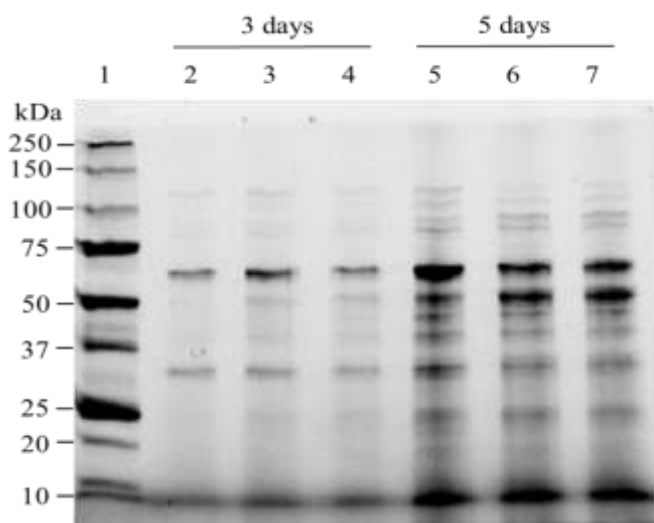


**Figure 3** The SDS-PAGE analysis of biomass secretomes in 3 & 5 days inoculum Secretome analysis was done by 10% SDS-PAGE gel.

SireAA-E was grown on 0.5% miscanthus for 3 and 5 days at 30°C with different amount of inoculum (1.0, 5.0 and 10.0 mL) in 50 mL of M63 minimum medium. Lane 1 is Mw marker. Lanes 2 to 4 are 1.0, 5.0 and 10.0 mL inoculum in 50 mL 0.5% miscanthus M63 minimum medium after 3 days respectively. Lane 5 to 7 are 1.0, 5.0 and 10.0 mL inoculum in 50 mL 0.5% miscanthus M63 minimum medium after 5 days respectively. 2.0 µg equivalent of total secretome was used.

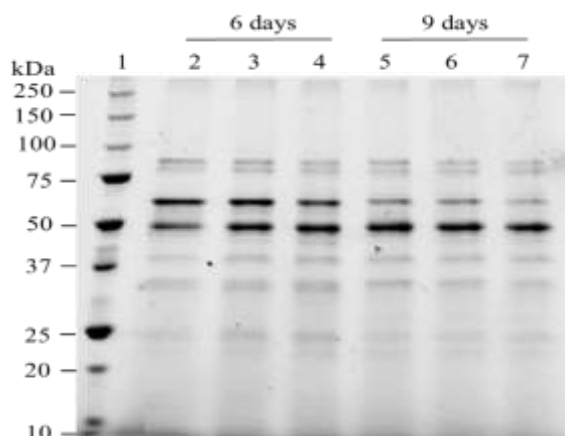


**Figure 4** The SDS-PAGE analysis of biomass secretomes in 6 & 9 days inoculum.

Secretome analysis by 10% SDS-PAGE gel. SireAA-E was grown on 0.5% miscanthus for 6 and 9 days at 30°C with different amount of inoculum (1.0, 3.0 and 5.0 mL) in 50 mL culture. Lane 1 is Mw marker. Lanes 2 to 4 are 1.0, 3.0 and 5.0 mL inoculum in 50 mL 0.5% miscanthus M63 minimum medium after 6 days incubation, respectively. Lanes 5 to 7 are 1.0, 3.0 and 5.0 mL inoculum in 50 mL 0.5% miscanthus M63 minimum medium after 9 days incubation, respectively. 2.0 µg equivalent of total secretome was used.

### Reaction of the biomass secretome

The culture supernatant containing SirexAA-E miscanthus secreted proteins from 1.0, 5.0 and 10.0 mL inoculum for 5 days at 30°C were tested for their ability to degrade CMC and cellulose to test polysaccharide-degrading enzyme activities from three different inoculum conditions (n = 3) (Fig. 3). Secretome activity was measured after incubating with CMC or cellulose for 20h at 40°C. The biomass secretome showed the highest polysaccharide-degrading activities for CMC substrate in all inoculum compared to the cellulose substrate. In contrast to the CMC hydrolysis reaction, the miscanthus secretome showed limited hydrolysis on the cellulose substrate due to the high crystalline nature (Fig. 5).

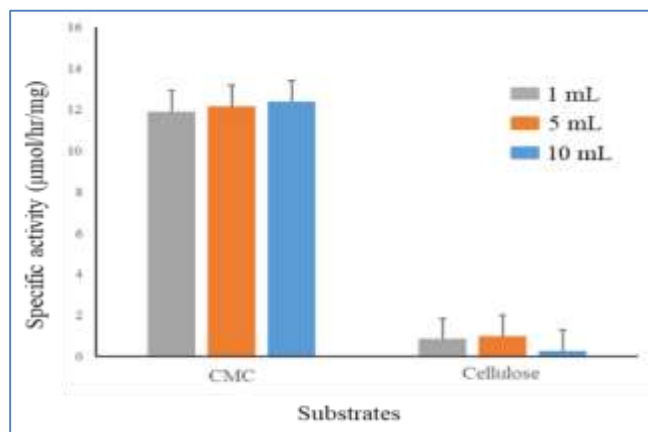


**Figure 5** Determination of the specific activity (µg/hr/mg) of the culture supernatants from CMC and crystalline cellulose for polysaccharide degradation.

Different amount (1.0, 5.0 and 10.0 mL) of inoculum was tested for 5 days at 30°C. Biomass activity from SirexAA-E culture supernatant was measured after growth on CMC and cellulose. Secretome activity was measured after incubating prepared secretomes with the substrate for 20 hrs at 40°C. Error bars indicate the standard deviation from three independent experiments from secretome. (P<0.05)

## Conclusion

In this study, it attempted to discover that 5 days with 1 mL inoculum into 50 mL culture gave the highest protein yields with intact form of secreted proteins. We examined the growth, in the presence of biomass, SrexAA-E secreted enzymes that hydrolyzed CMC and cellulose. The biomass secretome showed the highest polysaccharide-degrading activities for CMC substrate in 1 mL inoculum.

## Acknowledgements

Special thanks go to the government of Japan through Monbukagakusho (MEXT) for awarding me a rear privilege of a fully funded scholarship to pursue my master's degree at Hokkaido University, one of the most prestigious Universities in Japan. I also give thanks to the government of the Republic of the Union of Myanmar for allowing me to pursue further studies and ensuring that my study leave was processed. I would also like to express my deepest gratitude to my supervisor Associate Professor Taichi Takasuka for his guidance, advice, and help throughout my study in Japan. Furthermore, I would like to thank Dr Ye Myint Aung, Head of Professor, Department of Chemistry, Patheingyi University, Myanmar for his reviewing of this research paper, support and encouragement.

## References

- Adams, A. S., Jordan, M. S., Adams, S. M., Suen, G., Goodwin, L. A., Davenport, K. W., Currie, C. R. & Raffa, K. F. (2011). "Cellulose-degrading bacteria associated with the invasive woodwasp *Sirex noctilio*". *ISME J.* vol. 5, pp 1323-1331.  
doi:10.1038/ismej.2011.14.
- Alvarez, A., Saez, J. M., Davila Costa, J. S., Colin, V. L., Fuentes, M. S., Cuozzo, S. A., Benimeli, C. S., Polti, M. A. & Amoroso, M.J. (2017). "Actinobacteria: Current research and perspectives for bioremediation of pesticides and heavy metals". *Chemosphere*, vol. 166, pp 41-62.  
doi:10.1016/j.chemosphere.2016.09.070.
- Awungacha L. C, Busse N, Herrenbauer M, Czermak P (2015). "Photocatalytic based degradation processes of lignin derivatives". *International Journal of Photoenergy*, vol. 12, pp, 1-18  
doi: [https://doi.org/ 10.1155.137634](https://doi.org/10.1155.137634).
- Bianchetti, C.M., Harmann, C.H., Takasuka, T.E., Hura, G.L., Dyer, K., & Fox, B.G. (2013). "Fusion of Dioxxygenase and Lignin-binding Domains in a Novel Secreted Enzyme from Cellulolytic *Streptomyces* sp. SirexAA-E". *The journal of biological chemistry*, vol. 288, no. 25, pp 18574–18587.
- Book, A. J., Lewin, G. R., McDonald, B. R., Takasuka, T. E., Wendt-Pienkowski, E., Doering, D. T., Suh, S., Raffa, K. F., Fox, B. G. & Currie, C.R. (2016). "Evolution of High Cellulolytic Activity in Symbiotic *Streptomyces* through Selection of Expanded Gene Content and Coordinated Gene Expression". *PLoS Biol.* Vol. 14, pp 1-21.
- Cantarel, B. L. *et al* (2009). "The carbohydrate-Active enzymes database (CAZy): an expert resource for glycogenomics". *Nucleic Acids Res*, vol. 37, pp 233-238.
- Clardy, J., Fischbach, M. A. & Walsh, C. T. (2006). "New antibiotics from bacterial natural products", *Nat. Biotechnol*, vol. 24, pp 1541-1550.
- Crawford, D. L (1978). "Lignocellulose decomposition by selected *Streptomyces* strains".  
*Appl Environ Microb*, vol. 35, pp 1041-1045.
- Demain, A. L. & Sanchez, S. (2009). "Microbial drug discovery: 80 Years of progress", *J. Antibiot. (Tokyo)*, vol. 62, pp 5-16. doi:10.1038/ja.2008.16.
- Goodfellow, M. & Williams, S. T (1983). "Ecology of actinomycetes". *Annu Rev. Microbiol*, vol. 37, pp 198-216.

- Kirk TK, Farrell RL. (1987). "Enzymatic 'combustion': The microbial degradation of lignin". *Annual review of Microbiology*, **vol. 41**, pp. 465-505.
- Klemm, D., Heublein, B., Fink, H. P. & Bohn, A. (2005). "Cellulose: fascinating biopolymer and sustainable raw material". *Angew. Chem. Int. Ed. Engl*, **vol. 44**, pp 3358-3393.
- Lewin, G. R., Carlos, C., Chevrette, M. G., Horn, H. A., McDonald, B. R., Stankey, R. J., Fox, B. G. & Currie, C. R (2016). "Evolution and Ecology of Actinobacteria and Their Bioenergy Applications", *Annu. Rev. Microbiol*, **vol. 70**, pp 235-254.
- Lynd, L. R., Weimer, P. J., van Zyl, W. H. & Pretorius, I. S. (2002). "Microbial cellulose utilization: fundamentals and biotechnology". *Microbiol. Mol. Biol. Rev.* **vol. 66**, pp 506-577.
- McCarthy, A.J.& Williams, S.T (1992). "Actinomycetes as agents of biodegradation in the environment a review". *Gene*, **vol. 115**, pp 189-192.
- Poulsen, M., Oh, D. C., Clardy, J. & Currie, C. R. (2011). "Chemical analyses of wasp- associated Streptomyces bacteria reveal a prolific potential for natural products discovery", *PLoSOne*. **Vol 6**. doi:10.1371/journal.pone.0016763.
- Schlatter, D. et al (2009). "Resource amendments influence density and competitive phenotypes of Streptomyces in soil". *MicrobEcol*, **vol. 57**, pp 413-420.
- Schlesinger, W. H. & Andrews, J. A. (2000). "Soil respiration and the global carbon cycle". *Biogeochemistry*, **vol. 48**, pp. 7-20.

## APPLICATIONS OF MODIFIED CHITOSAN COMPOSITE MEMBRANES

Nan Yu Nwe<sup>1</sup>, Zaw Naing<sup>2</sup>, Khin Than Yee<sup>3</sup>, Cho Cho<sup>4</sup>

### Abstract

The modified chitosan composite membranes (CASG-1 to CASG-4) were prepared with various ratios of chitosan, alginate, starch and glycerol by using casting and autoclaving methods. These membranes have smooth surfaces, highly transparent and pale yellow colour. The mechanical properties such as tensile strength, elongation at break and tear strength of these prepared membranes were determined. Based on the mechanical properties of the prepared composite membranes CASG-2 was chosen for biomedical applications. The antimicrobial activities of prepared membranes were tested by agar well diffusion method. The skin irritation test was conducted by Draize's method. The selected composite membranes (CASG-2) indicated that there is no irritation potential in albino rabbit skin. The selected composite membrane (CASG-2) was used to test in burn wound healing compared with standard sufre tulle drug. It was found that CASG-2 composite membrane was better than standard drug, sufre tulle for burn wound healing.

**Keywords:** composite membranes, mechanical properties, antimicrobial activities, skin irritation test, wound healing

### Introduction

Higher molecular weight chitosan has been reported to have good membrane forming properties as a result of intra and intermolecular hydrogen bonding. The chitosan membrane characteristics, however, varied from one report to another due to their excellent properties and numerous applications like biocompatible coatings and membrane. Differences in the source of chitin used to produce chitosan, its properties, solvent used, method of membrane preparation, type of amount of copolymer, plasticizer used, affect the quality of chitosan membrane. These membranes have been studied in morphological aspects as well as in properties such as crystalline, porosity, and capacity of ion exchanger, etc. (Kurihara, 1994). Recently the formation of hybrid membranes of chitosan with inorganic networks has been also studied. The ability of chitosan membranes may permit its extensive use in the formation of membrane dosage forms or as drug delivery system. Chitosan could be dissolved in dilute organic acid such as lactic acid and acetic acid, prior to being cast into membranes. In order to assure for safety of biomedical application, skin irritation test should be carried out. This must be done to determine the risk of irritation due to the contact between the chemicals or formulations and human skin (More *et al.*, 2013). Irritation is manifested by a tissue system in response to stimuli of either exogenous or endogenous origins (Carson *et al.*, 1964). It has also been advocated as wound healing agent in the forms of a bandage. Its effect on wound healing in urogenital tissue has also been investigated (Nakatsuka *et al.*, 1992). In this work, composite membranes were tested on rabbit skin instead of human skin. Scoring system of rabbit skin irritation and response categories of irritation were shown in Table 1 (OECD TG 404, 2002) and Table 2 (Draize *et al.*, 1944). Chitosan's unique properties make it useful for a broad variety of industrial and biomedical applications. In the present study, modified chitosan composite membranes were prepared and it may be used for medical purposes.

---

<sup>1</sup> 3-PhD, Candidate, Department of Chemistry, University of Yangon

<sup>2</sup> Dr, Associate Professor, Department of Chemistry, Dagon University

<sup>3</sup> Dr, Lecturer, Department of Chemistry, West Yangon University

<sup>4</sup> Dr, Professor, Department of Chemistry, University of Yangon

**Table 1 Scoring System of Rabbit Skin Irritation**

Reaction	Score
<b>Erythema</b>	
No erythema	0
Very slight erythema	1
Well defined erythema	2
Moderate to severe erythema	3
Severe erythema (beet redness) to eschar formation	4
<b>Oedema</b>	
No oedema	0
Very slight oedema	1
Well defined oedema	2
Moderate oedema (raising approximately 1mm)	3
Severe oedema (raising more than 1 mm and extended beyond the area of exposure)	4
<b>Total possible score for primary irritation</b>	<b>8</b>

OECD TG 404, 2002

**Table 2 Response Categories of Irritation**

Evaluations	Score
No Irritant	0.0
Negligible Irritant	0.1- 0.4
Slight Irritant	0.41-1.9
Moderate Irritant	2.0-4.9
Severe Irritant	5.0-8.0

Draize, Woodward &amp; Calvery, 1944

## Materials and Methods

### Sample Collection

Chitosan sample was purchased from Shwe Poe Co. Ltd., Hlaing Tharyar Township, Yangon Region.

Starch was prepared from maize grain, *Zea mays* L. and this sample was procured from Insein Market, Yangon Region.

### Preparation of Chitosan-Alginate-Starch-Glycerol (CASG) Composite Membranes

Modified chitosan composite membranes (CASG) were prepared by using 1.5 % (w/v) chitosan, 3 % (w/v) sodium alginate, 0.3 % (w/v) starch solution and various ratio of glycerol 0.05 %, 0.10 %, 0.15 % and 0.20 % and the prepared membranes were denoted as CASG-1, CASG-2, CASG-3 and CASG-4, respectively. The glycerol was also used as plasticizer for flexibility of membranes. The resulting modified composite solutions were autoclaved at a pressure of 0.1 MPa and  $121 \pm 1$  °C for 1 h.

## **Mechanical Properties of Prepared Composite Membranes**

### **Determination of thickness**

Thickness of the prepared CASG-1 to CASG-4 composite membranes was measured by using NSK micrometer. The thickness of the membranes was measured at 5 points (center and 4 corners) using digital micrometer.

### **Determination of tensile strength and elongation at break**

The prepared CASG-1 to CASG-4 composite membranes were cut off according to JIS K 7127 (1987) and the shape and dimension of test pieces were obtained. The both ends of test pieces were firmly clamped in the jaw of testing machine. One jaw was fixed and the other was moveable. The rate of moveable jaw was hold 100 mm/min. The resulting data was shown at the recorder. This procedure for tensile strength was repeated for three times.

### **Determination of tear strength**

The specimen was cut off by using die-cutting. Specimen was cut with a single nick (0.05 mm) at the entire of the inner concave edge by a special cutting device using a razor blade. The clamping of the specimen in the jaw of test machine was aligned with travel direction of the grip in 100 mm/min. The order of the machine showed the highest force to tear from a specimen nicked. The procedure was repeated three times for each result.

### **Screening of Antimicrobial Activities of the Prepared Composite Membranes by Agar Well Diffusion Method**

The prepared composite membranes: CASG-1 to CASG-4 were tested with *Bacillus subtilis*, *Staphylococcus aureus*, *Pseudomonas aeruginosa*, *Bacillus pumilus*, *Candida albicans* and *E. coli* species to investigate the nature of antimicrobial activity. After preparing the bacteriological media, the dried membranes were placed on the agar with flamed forceps and gently pressed down to ensure proper contact. The plates were incubated immediately or within 30 min after incubation or after overnight incubation at 37 °C.

### **Skin Irritation Test**

Firstly, the albino rabbits were divided into two groups. Each group was included one rabbit. The 3 cm<sup>2</sup> area of hair from back quarter of each albino rabbit was shaved by using the shaver and cleaned by the clean water. The group-A used as control (with any treatment), and the group-B was treated with CASG-2 composite membrane respectively. The skin area of treated with CASG-2 albino rabbit was checked after 2 h later. If the area was shown redness, the animal was suffering the skin irritation. It observed redness with control to compare treated with CASG-2.

### **Animal experiment (burn wound healing)**

Each Wistar albino rat was anaesthetized by injection Ketamine HCl and Xylazine (Anaesthesia) allowed for 30-45 min. Then the Ringer's Lactate solution was induced by intraperitoneally to resist the heat effect. The hair from dorsal side of Wistar albino rat was shaved. A 150 g cylindrical metal rod (1 cm diameter) heated to 100 °C in boiling water with an insulated rubber handle was used for the infliction of burns. Temperature was monitored using a thermometer. Burn infliction was limited to the loin area of all anaesthetized rats. The skin was pulled upwards, away from the underlying viscera, creating a flat surface. The rod was located on its own weight for 20 s on each rat. The average wound size was 1 cm in diameter.

### Histopathological finding

The skin lesions samples were obtained by necropsy was fixed with formalin for routine histopathological processing. Hematoxylin and eosin (H & E) stained and evaluated blinded manner by two observers using a light microscope with specific image analysis software from Olympus. For the morphological evaluation of skin lesions, a collagen fiber, inflammatory cell, blood vessel and granulation tissue of skin tissues were examined under a microscope by the pathologist.

## Results and Discussion

### Aspect of Membrane Preparation

In this preparation, modified chitosan-alginate-starch-glycerol composite membranes (CASG-1 to CASG-4) were prepared by using solvent casting and autoclaving method. These modified chitosan composite membranes (CASG-1 to CASG-4) showed smooth surface texture, transparent and pale yellow colour. These membranes to be employed as wound dressing, it should be durable, stress resistant, flexible, pliable and elastic.

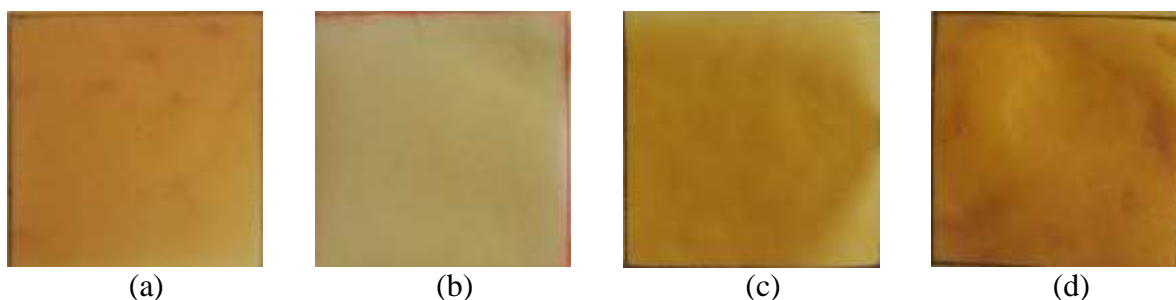


**Figure 1** Modified composite membranes: (a) CASG-1 (b) CASG-2 (c) CASG-3 and (d) CASG-4

### Mechanical Properties

The mechanical properties such as tensile strength, tear strength and elongation at break are important parameters for showing the nature of membranes. The mechanical properties of CASG-1 to CASG-4 composite membranes are shown in Tables 3 and Figure 2. The more the tensile strength of membrane, the higher is the elasticity of the membrane. This means to point out that CASG-2 composite membrane are more flexible and more elastic.

**Table 3 Mechanical Properties of the Modified Chitosan Composite Membranes**

Membrane	Tensile strength ( MPa)	Elongation at break (%)	Tear strength ( kNm <sup>-1</sup> )
CASG- 1	16.00	13.00	15.70
CASG- 2	20.50	18.00	42.50
CASG- 3	13.20	15.00	20.00
CASG- 4	9.20	32.00	14.40

CASG- 1 = Chitosan (1.5 %) +Alginate (3.0 %) +Starch (0.3 %) +Glycerol (0.05 %) w/v

CASG- 2 = Chitosan (1.5 %) +Alginate (3.0 %) +Starch (0.3 %) +Glycerol (0.10 %) w/v

CASG- 3 = Chitosan (1.5 %) +Alginate (3.0 %) +Starch (0.3 %) +Glycerol (0.15 %) w/v

CASG- 4 = Chitosan (1.5 %) +Alginate (3.0 %) +Starch (0.3 %) +Glycerol (0.20 %) w/v

Thickness = ~ 0.10 mm

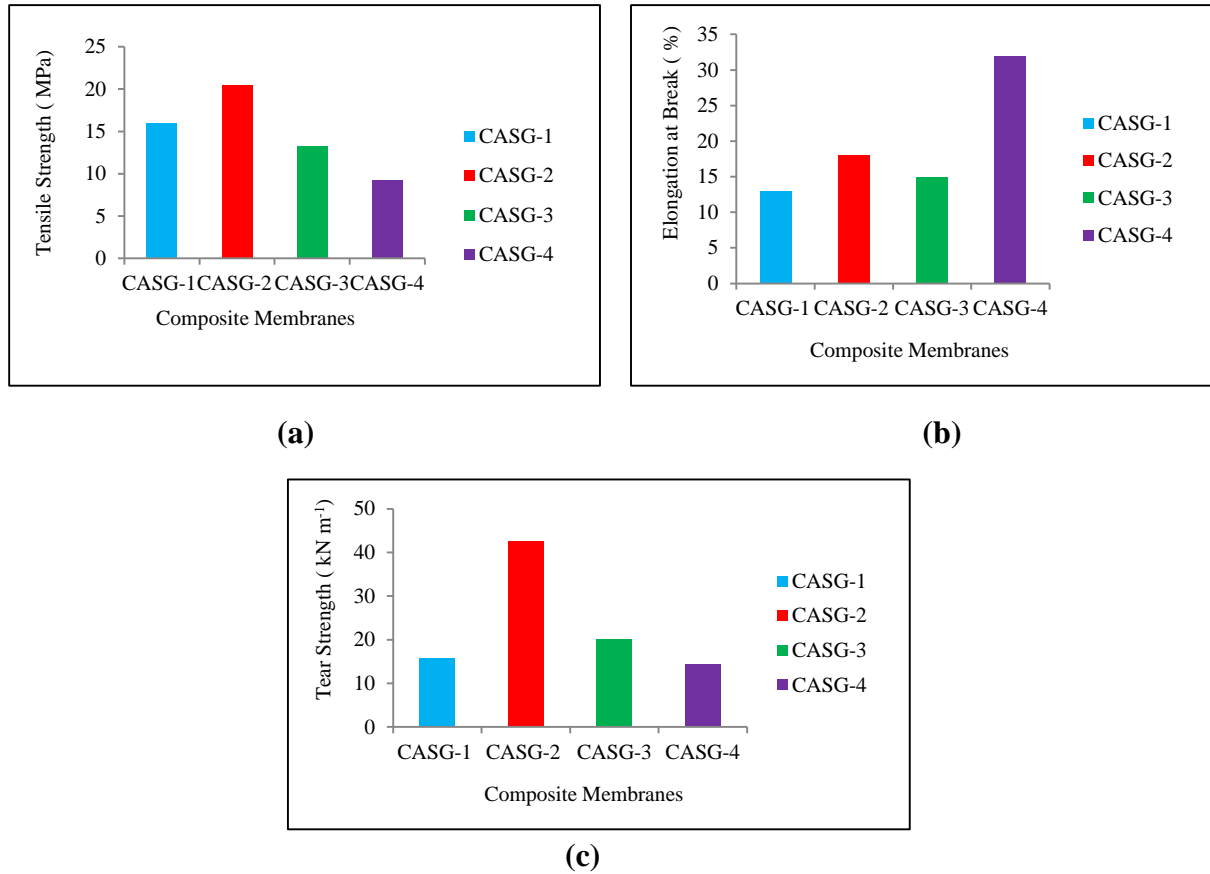


**Figure 2** Mechanical properties: (a) tensile strength (b) elongation at break and (c) tear strength of the chitosan composite membranes

### Antimicrobial Activities of the Prepared Composite Membranes

Antimicrobial activities of the prepared CASG-1 to CASG-4 composite membranes were studied. These membranes were tested on six different strains of human pathogenic bacteria, *Bacillus subtilis*, *Staphylococcus aureus*, *Pseudomonas aeruginosa*, *Bacillus pumilus*, *Candida albicans*, and *E. coli*. To strengthen the finding, the antimicrobial activity of the all prepared membranes was determined by agar well diffusion method. Antimicrobial activities of the all prepared membranes were evaluated based on the diameters of clear inhibition zone surrounding the agar well. The prepared CASG-1 to CASG-4 composite membranes showed medium antimicrobial activities in the range of inhibition zone diameters (12 ~19 mm). Among them, the modified CASG-2 composite membrane showed that highest activity against six microorganisms (16 ~19 mm). The resulting data are shown in Table 4 and Figure 3.

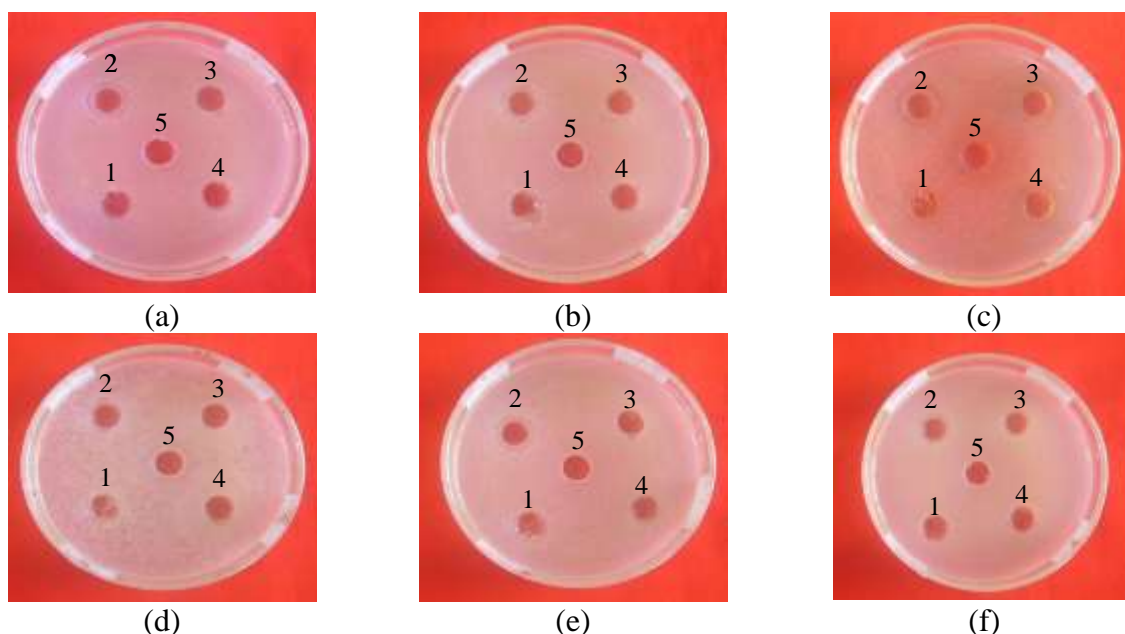


**Figure 3** Antimicrobial activities of prepared chitosan composite membranes (1) CASG-1 (2) CASG-2 (3) CASG-3 (4) CASG-4 and (5) control

- (a) *Bacillus subtilis* (d) *Bacillus pumilus*  
 (b) *Staphylococcus aureus* (e) *Candida albicans*  
 (c) *Pseudomonas aeruginosa* (f) *E. coli*

**Table 4** Antimicrobial Activities of the Prepared Composite Membranes: CASG-1 to CASG-4

Membranes	Inhibition zone diameters (mm) of the samples against different organisms					
	(a)	(b)	(c)	(d)	(e)	(f)
Control	-	-	-	-	-	-
CASG-1	13(+)	15(++)	16(++)	14(+)	13(+)	16(++)
CASG-2	16(++)	17(++)	17(++)	16(++)	18(++)	19(++)
CASG-3	12(+)	15(++)	12(+)	13(+)	13(+)	16(++)
CASG-4	14(+)	16(++)	13(+)	14(+)	17(++)	18(++)
Ager well – 10 mm	*Organisms*					
10 mm ~ 14 mm (+)	(a) <i>Bacillus subtilis</i>		(N.C.T.C-8236)			
15 mm ~ 19 mm (++)	(b) <i>Staphylococcus aureus</i>		(N.C.P.C-6371)			
20 mm above (+++)	(c) <i>Pseudomonas aeruginosa</i>		(6749)			
	(d) <i>Bacillus pumilus</i>		(N.C.I.B-8982)			
	(e) <i>Candida albicans</i>					
	(f) <i>E. coli</i>		(N.C.I.B-8134)			

### Skin Irritation Test

The irritant response was observed according to post-test observation periods. The animals were observed at 24, 48 and 72 h examination on these skin areas. Group-A rabbit (without treatment) showed no erythema and no oedema signs. Group-B rabbit (treated with CASG-2) composite membrane showed no erythema and oedema at 24, 48 and 72 h observation. Thus, it can be concluded that CASG-2 composite membrane has no irritation potential. These results were shown in Table 5 and Figure 4.

**Score of Primary Irritation (SPI)**

$$SPI = \frac{\sum \text{Erythema and oedema grade at 24, 48 and 72 h}}{\text{Number of observation}}$$

**Primary Irritation Index (PII)**

$$PII = \frac{\sum SPI (Test) - \sum SPI (Control)}{\text{Number of animals}}$$

**Table 5 Score of Primary Irritation (SPI) and Primary Irritation Index (PII) for Rabbits (Control and Treated with Composite Membrane CASG-2)**

Observation periods	Rabbit numbers (Group)					
	A (control)			B (CASG-2)		
	A <sub>1</sub>	A <sub>2</sub>	A <sub>3</sub>	B <sub>1</sub>	B <sub>2</sub>	B <sub>3</sub>
24 h (Erythema & Oedema score)	0	0	0	0	0	0
48 h (Erythema & Oedema score)	0	0	0	0	0	0
72 h (Erythema & Oedema score)	0	0	0	0	0	0
SPI	0			0		
PII	0			0		
Category	No irritant			No irritant		

\* Draize *et al.*, 1944 & OECD TG 404, 2002

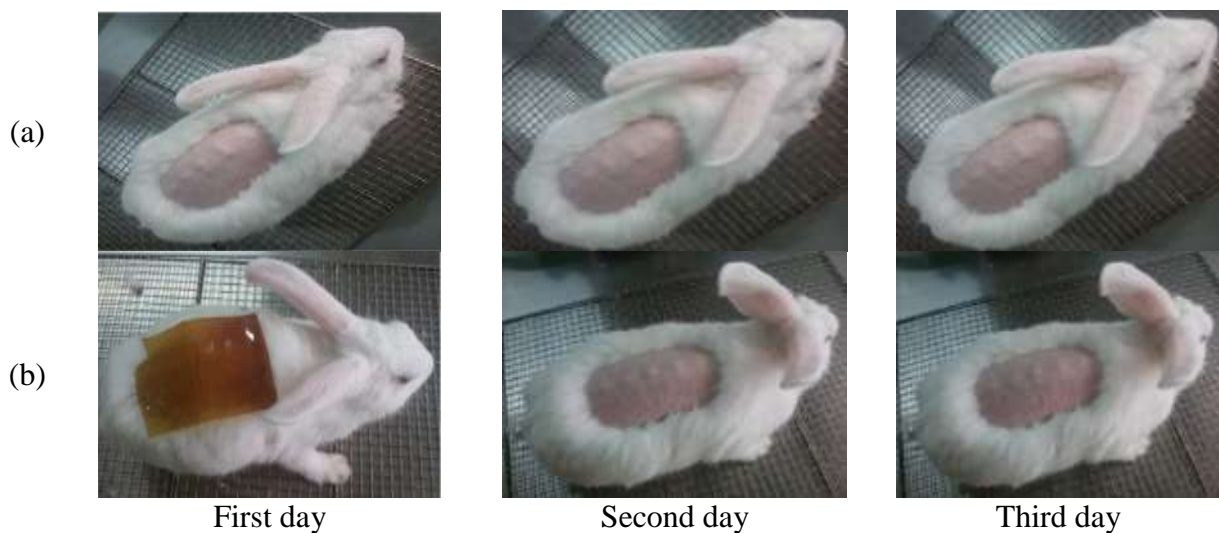


**Figure 4** Physical appearances of albino rabbits skin test for (a) control and (b) treated with CASG-2 composite membrane

**Appearance changes of burned skin**

On days 5 and days 10, the wound area increased initially and the progress of all burned skins improvements were not significantly observed. On days 15, the crust was sloughed off completely in CASG-2 treated skin. On days 21, shaving was performed on all rats, since hair had grown extensively. The burn wound was almost completely healed that was treated with CASG-2.

From the observations, CASG-2 has been shown to significantly accelerate the burn wound healing. These results were shown in Figure 5.

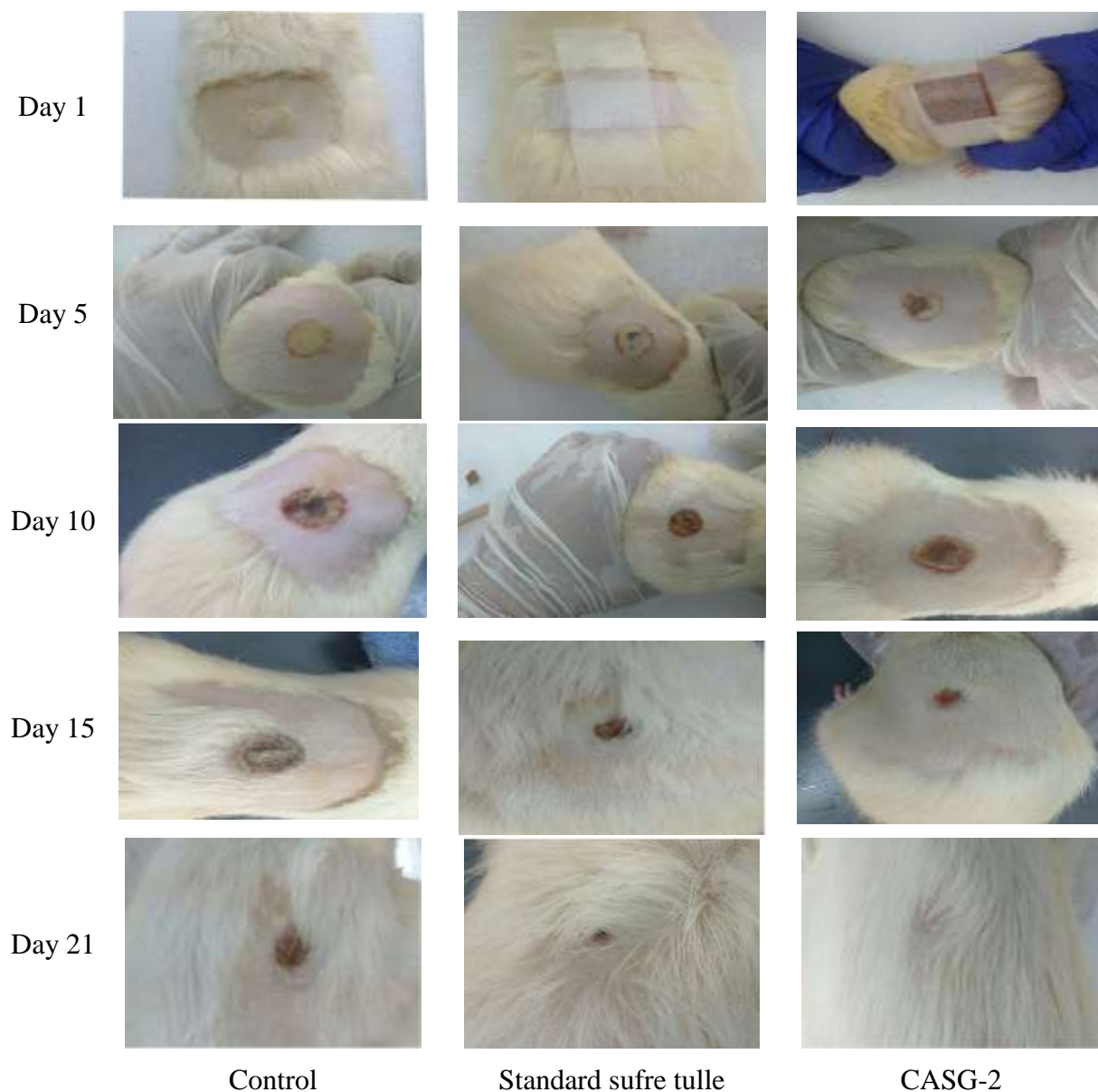


**Figure 5** Treatment of burn skin by using control, standard sufre tulle and CASG-2 composite membranes

### Histopathological examination

The crust layer of thin epidermis is detached from wound area. A few area of interrupted lining epithelium is still present in epidermis of control (no treatment) rat skin. The treated with sufre tulle (standard drug), there had a few sebaceous glands and sweat glands in epidermis layer without hair follicles. In the case of using CASG-2 as therapeutic agent of burned wound, well-developed sebaceous glands, sweat glands and hair follicles in epidermis and dermis layers of skin. Good wound healing in skin lesion of rat model.

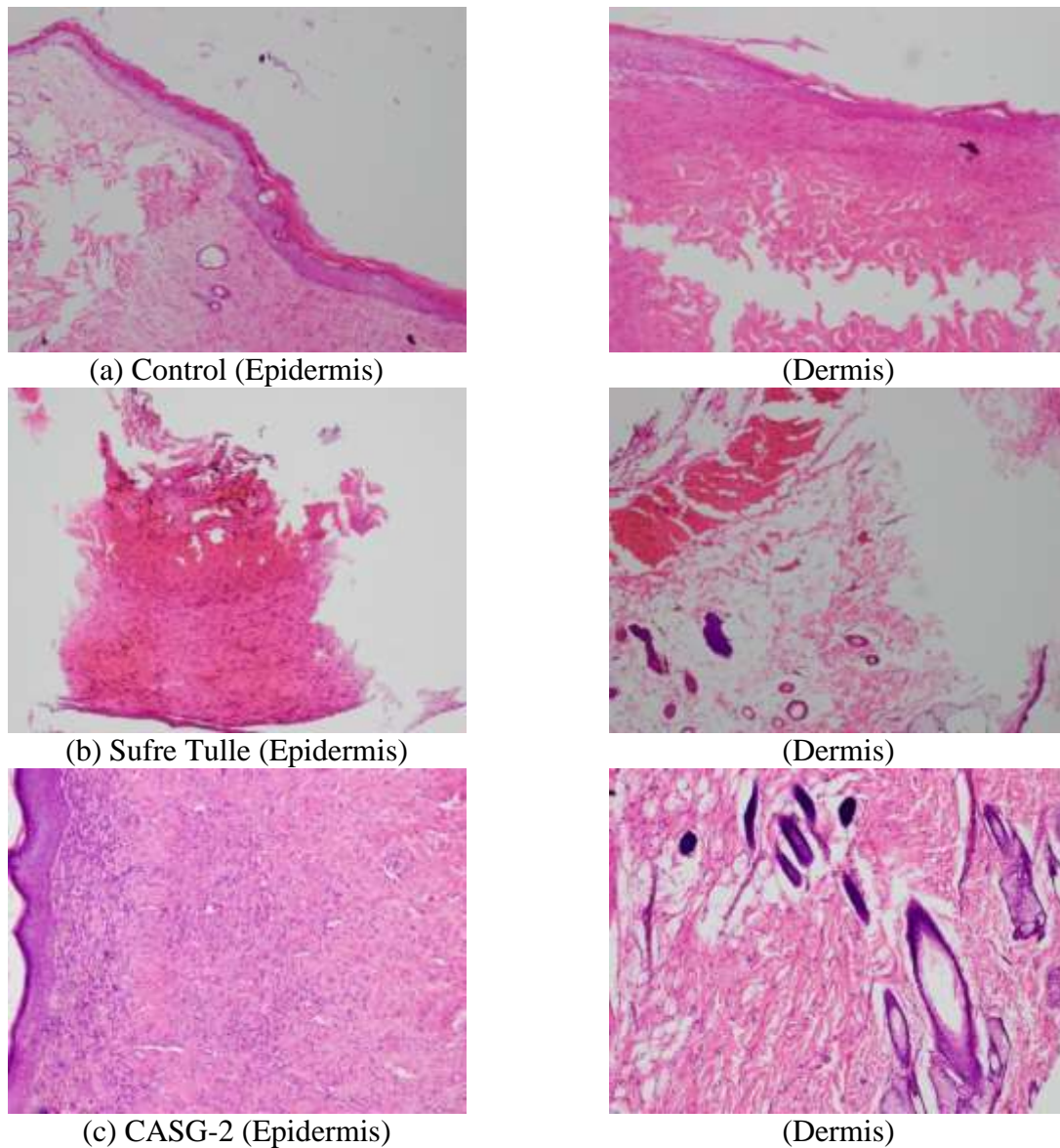


**Figure 6** Histopathological examination (H& E) stained for morphological evaluation of burn skin (a) control, (b) treated with standard sufre tulle and (c) CASG-2 (after day 21) epidermis and dermis

### Conclusion

In this study, polymer blended membranes consisting of chitosan, sodium alginate, starch and glycerol solution were prepared. The various ratios of modified chitosan-alginate-starch-glycerol (CASG-1 to CASG-4) composite membranes were prepared by solvent casting technique under autoclaving conditions at 121 °C and 0.1 MPa for 1 h. These modified composite membranes showed clear, smooth surface, flexible, highly transparent and light yellow colour. Based on the mechanical properties such as tensile strength, elongation at break and tear strength, the optimum condition was achieved by using 1.5 % (w/v) of chitosan, 3.0 % (w/v) of sodium alginate, 0.3 % (w/v) of starch solution, 0.1 % (w/v) of glycerol. According to mechanical properties, CASG-2 composite membrane was chosen as membrane to apply selected for biomedical applications. The antimicrobial activities of prepared CASG-1 to CASG-4 composite membranes were tested by agar well diffusion method. The prepared composite membranes gave antimicrobial activities, especially CASG-2 composite membrane indicated the highest activity on six microorganisms.

Skin irritation test showed that selected composite membrane: (CASG-2) was no irritation potential in albino rabbit skin. Based on the overall results, the selected composite membranes (CASG-2) are suitable to be used as wound healing and wound dressing for biomedical application.

### Acknowledgements

The authors would like to express their profound gratitude to the Department of Higher Education, Ministry of Education, Yangon, Myanmar, for provision of opportunity to do this research and Myanmar Academy of Arts and Science for allowing to present this paper.

### References

- Carson, S., M. S. Weinberg and R. Goldhamer. (1964). "An Improved Method for Testing the Safety of Hair Dye Preparation". *Journal of the Society of Cosmetic Chemists*, vol. 16, pp. 747-761
- Draize, J. H., G. Woodward and H. O. Calvery. (1944). "Methods for the Study of Irritation and Toxicity of Substance Applied Topically to the Skin and Mucous Membrane". *Journal of Pharmacology and Experimental Therapeutics*, vol. 3, pp. 377-390
- Kurihara, M. (1994). "Thermal Effect on the Microhardness of Chitosan Films". *Pure Appl. Chem.*, vol. 31(11), pp. 1791-1799
- More, B. H., S. N. Sakharwade, S. V. Tembhurne and D. M. Sarkarkar. (2013). "Evaluation for Skin Irritancy Testing of Developed Formulations Containing Extract of *Butea monosperma* for Its Topical Application". *International Journal of Toxicology and Applied Pharmacology*, vol. 3, pp. 10-13
- Nakatsuka, S. and L. A. Andrady. (1992). "Permeability of Vitamin B<sub>12</sub> in Chitosan Membranes, Effect of Crosslinking and Blending with poly (vinyl alcohol) on Permeability". *J. Appl. Polym. Sci.*, vol. 44, pp. 7- 28
- OECD TG 404. (2002). *OECD Guideline for Testing of Chemicals*. Organization of Economic, Commercial and Development

## **PREPARATION AND CHARACTERIZATION OF POLYMERIC MATERIAL OF CELLULOSE ACETATE-POLYVINYL ALCOHOL FILM**

Hnin Yu Wai<sup>1</sup>, Thi Dar Khaing<sup>2</sup>, Khin Kay Thi Han<sup>3</sup>

### **Abstract**

This work is mainly concerned with the preparation of polymeric material from cellulose acetate with polyvinyl alcohol (PVA) and glutaraldehyde as used as cross linker and the study of their characteristics. The films were prepared by mixing various proportions of cellulose acetate with various proportions of polyvinyl alcohol and fixed proportion of glutaraldehyde by blending, casting technique. The prepared films were investigated according to physicochemical parameters such as thickness, tensile strength, elongation at break, tear strength and physicochemical parameters such as water uptake and swelling properties. The optimum ratios for preparing films were chosen according to their physicochemical properties. The most favorable conditions for preparing film namely CPF 3 was found to be 20 mL of 2 % w/v cellulose acetate, 80 mL of 4 % w/v PVA and 25 mL of 0.025 M glutaraldehyde. It was found that the film CPF 3 possessed 27.30 MPa of tensile strength, 24.60 % of elongation at break and 58.90 kNm<sup>-1</sup> of tear strength. All prepared films showed plain, clear, smooth surface, flexible, highly transparent and light white colour. The prepared films can be used in packaging materials.

**Keywords:** Cellulose acetate, polyvinyl alcohol, films, tensile strength

### **Introduction**

The importance of polymeric materials has increased in recent years due to their unique properties and the potential to be beneficial for resource conservation. Novel polymeric materials are a key research field at Fraunhofer IFAM for adhesive bonding, paint/lacquer technology and fiber reinforced plastics. These materials are opening up a host of new technical opportunities (Cascone, 1997).

Cellulose acetate which is an abundant natural fiber resource with an excellent tensile strength is widely used in oral pharmaceutical products and is regarded as a nontoxic, nonirritant and biodegradable material (Liu *et al.*, 2012). Among its wide array of applications, cigarette filters, high absorbent diapers, semipermeable membranes for separation processes, fibers, films for biomedical domain and mats for transdermal drug delivery can be included. In addition, a long term antimicrobial effect for wound healing application (Ragauskas, 2016).

Cellulose acetate is an environmental friendly substance for making membranes since it is a non-toxic material and low can be available at cost. Membranes made from cellulose acetate have been used for brackish water or seawater desalination and for filtering methanol, ethanol and urea in a reverse osmosis process. Cellulose acetate was used for its excellent film forming properties (Darunee and Tripo, 2008).

Synthetic polymers have been widely used in biosensors poly (vinyl alcohol) solid supports. The hydrogels most commonly known are PVA and their copolymers and their structures can be controlled by physical and chemical crosslinking of chains. PVA is a synthetic water-soluble hydrophilic polymer. The basic properties of PVA are dependent on the degree of polymerization or on the degree of hydrolysis. It has been widely used in adhesives, emulsificants, in the textile and paper industry applications and in the attainment of amphiphilic membranes for enzyme immobilization. Most recently, PVA has been used in pharmaceutical and biomedical

---

<sup>1</sup> Dr, Lecturer, Department of Chemistry, University of Yangon

<sup>2</sup> Lecturer, Department of Chemistry, Hpa-an University

<sup>3</sup> Lecturer, Department of Chemistry, Hpa-an University

applications for controlled drug release tests due to its degradable and non-toxic properties. Chemical crosslinking is a highly versatile method to create and modify polymers, where properties can be improved, such as mechanical, thermal and chemical stability. Also, a novel class of materials called organic-inorganic hybrids would combine properties of organic polymers with ceramics. Hybrids would combine properties of organic polymers with ceramics. These different components can be mixed at length scales ranging from nanometer to micrometer, in virtually any ratio leading to the so-called hybrid organic-inorganic (Zhang *et al.*, 2009).

The aim of this research is to prepare and characterize the polymeric material of cellulose acetate-polyvinyl alcohol film. The prepared polymeric material films have been assessed according to their physicochemical properties.

## Materials and Methods

All specific chemicals used were cited in details in each experimental section. The apparatus consists of conventional laboratory glass ware and modern equipment. Some of the instruments used in the experiments are Balance (Precision Balance, AWS, PN-2100A, China), Magnetic Stirrer Oven (Universal Oven, Memmert, UFB-400, Germany), Furnace (Thermo scientific, USA), melamine plate, FTIR (Fourier Transform Infrared Spectrophotometer, Shimadzu, IR Prestige-21, Japan), SEM (Scanning Electron Microscope, Evo-18, Brandi cars ZEISS, Germany) and TG-DTA (DTA-60H, Hi-TGA 2950) thermal analyzer.

### Collection of Samples

In the experiments, commercial cellulose acetate, polyvinyl alcohol (Molecular weight 20,000, degree of hydrolysis 98 %) and glutaraldehyde were purchased from the British Drug House (BDH) Chemical Ltd, England. All other chemicals used were of analytical reagent grade.

### Determination of Physicochemical Properties of Cellulose Acetate and Polyvinyl Alcohol

The physicochemical properties (moisture content, ash content, solid content, bulk density and pH) of the samples were determined by conventional methods and the results are presented in Table 1.

### Characterization of Cellulose Acetate and Polyvinyl Alcohol

#### FT IR analysis

FT IR analysis was performed in order to characterize the functional groups of samples. A Perkin-Elmer Spectrum GX, USA was used for FT IR analysis. The FT IR spectra of cellulose acetate and polyvinyl alcohol are shown in Figures 1 and 2 and the description data are presented in Tables 2 and 3.

#### SEM analysis

The morphology of prepared cellulose acetate and polyvinyl alcohol was studied by using Scanning Electron Microscope (JSM-5160, JEOL Ltd., Japan) for analysing micro and macro pores present on the surface of the samples. The scanning electron micrographs of cellulose acetate and polyvinyl alcohol are shown in Figures 3 and 4.

### Preparation of Cellulose Acetate and Polyvinyl Alcohol Films

In this research, all of the cellulose acetate - polyvinyl alcohol films were prepared by blending casting method.

### **On the Aspect of the Preparation of Cellulose Acetate - Polyvinyl Alcohol Films**

Clear solution of PVA 4 % w/v was prepared by dissolving 4 g of PVA in 100 mL of water by stirring with magnetic stir for 20 min at room temperature, to get a clear solution. Clear solution of cellulose acetate 2 % w/v in acetone by stirring with magnetic stir for 30 min at 100 °C. Next, (40, 30, 20, 10, 0) mL of the prepared CA solution and (60, 70, 80, 90, 100) mL of prepared PVA solution and were thoroughly mixed by stirring each pair in the given order for 20 min. The polymer solution was cooled to room temperature and (0.025 M, 25 mL) glutaraldehyde was slowly added and allowed to undergo gelation for 10 min. The solution was casted onto cleaned and dried melamine plate at room temperature for three days.

### **Determination of the Physicochemical and Physicomechanical Properties of Cellulose Acetate - Polyvinyl Alcohol Films**

The physicochemical and physicomechanical properties (thickness, tensile strength, elongation at break, and tear strength) of the prepared CPF films were determined by the conventional method and modern techniques. The resulting data are presented in Table 4 and Figures 5, 6 and 7.

### **Determination of the Water Uptake Properties of Cellulose Acetate - Polyvinyl Alcohol Films**

The water uptake of the prepared CPF 3 films are shown in Figure 8 and the resulting data are presented Table 5.

### **Determination of the Degree of Swelling Properties of Cellulose Acetate - Polyvinyl Alcohol Films**

The degree of swelling of the prepared CPF 3 films are shown in Figure 9 and the resulting data are presented in Table 6.

### **Characterization of the CPF 3 Film**

#### **FT IR analysis**

The FT IR spectrum of CPF 3 film is shown in Figure 10 and the description data is presented in Table 7.

#### **SEM analysis**

The scanning electron micrograph of CPF 3 film is presented in Figure 11.

#### **TG-DTA analysis**

Thermal analysis of the sample was determined by a DTA-60H (Hi-TGA 2950) thermal analyzer. The sample (*ca.* 5 mg) was required and measured in the temperature range 0~600 °C at 20.00 °C/min and nitrogen gas at 50.00 mL/min. The TG-DTA thermogram of CPF 3 film is shown in Figure 12 and the description data is presented in Table 8.

### **Determination of Biodegradation**

#### **Soil Burial Test**

Biodegradation of prepared CPF 3 films were determined by soil burial test examining the morphology changes. Sample geometry on degradation was also recorded by photo. The physical appearances of CPF 3 films are shown in Figure 13.

## Results and Discussion

Table 1 shows that the physicochemical properties (moisture content, ash content, bulk density, and pH) of the cellulose acetate and polyvinyl alcohol determined by the conventional methods. The pH values of samples were determined by pH meter. The moisture content of cellulose acetate and polyvinyl alcohol were determined by oven drying method at 115-120 °C to obtain constant weight. It can be observed that moisture content of the cellulose acetate is 15.24 %, ash content is 5.00 %, solid content is 84.76 %, bulk density is 52.50 g mL<sup>-1</sup> and pH is 6.20. It can be observed that moisture content of the polyvinyl alcohol is 33.00 %, ash content is 6.50 %, solid content is 67.00 %, bulk density is 0.30 g mL<sup>-1</sup> and pH is 6.70.

**Table 1 Physicochemical Properties of Cellulose Acetate and Polyvinyl Alcohol**

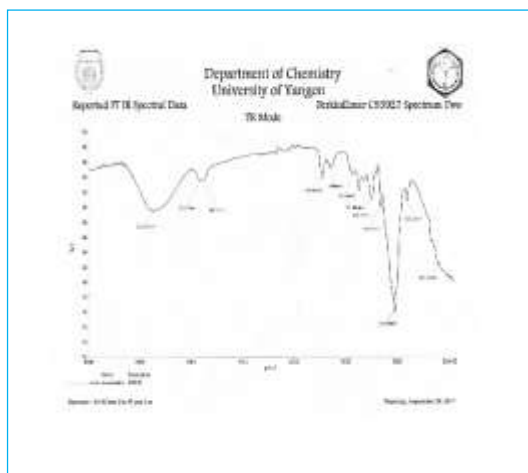
No.	Physicochemical Properties	Cellulose Acetate	Polyvinyl Alcohol
1.	Moisture content ( % )	15.24	33.00
2.	Ash content ( % )	5.00	6.50
3.	Solid content ( % )	84.76	67.00
4.	Bulk density ( g mL <sup>-1</sup> )	52.50	0.30
5.	pH	6.20	6.70

### Characterization of Cellulose Acetate and Polyvinyl Alcohol

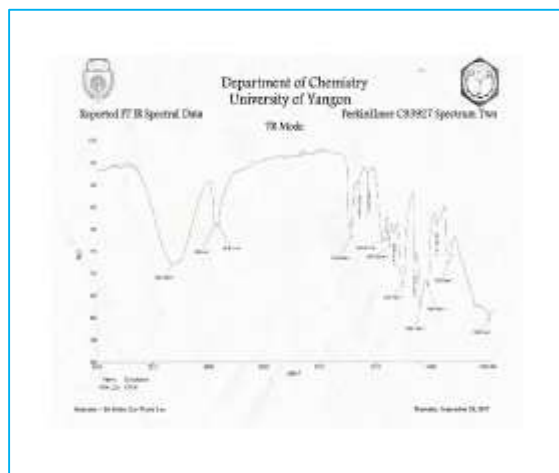
#### FT IR analysis

Figure 1 shows the FT IR spectrum of cellulose acetate. The spectrum of CA shows a weak and broad band at 3369 cm<sup>-1</sup>, 2919 cm<sup>-1</sup>, 1728 cm<sup>-1</sup>, 1437 cm<sup>-1</sup>, 1019 cm<sup>-1</sup>. These peaks are assigned to the O-H stretching of hydroxyl group, C-H asymmetric stretching, C=O symmetric stretching acetyl group, C-H stretching of CH<sub>3</sub>, C-O-C asymmetric stretching for ether bridge and pyranose ring, respectively. The presence of PEG in the spectrum is manifested only as an outstanding increase of the signal for OH groups and CH stretching at 3289 cm<sup>-1</sup>.

Figure 2 shows the FT IR spectrum of polyvinyl alcohol. The main peak of PVA observed at at 3305 cm<sup>-1</sup>, 2916 cm<sup>-1</sup>, 1714 cm<sup>-1</sup>, 1423 cm<sup>-1</sup>, 1248 cm<sup>-1</sup>, 943 cm<sup>-1</sup>. These peaks are assigned to the O-H stretching of hydroxyl group, C-H as symmetric stretching, C=O carbonyl stretching, C-H bending of CH<sub>2</sub>, C-O stretching acetyl group, C-C stretching, respectively.



**Figure 1** FT IR spectrum of cellulose acetate



**Figure 2** FT IR spectrum of polyvinyl alcohol

**Table 2 FT IR Band Assignments of Cellulose Acetate**

Observed wave number (cm <sup>-1</sup> )	Literature wave number (cm <sup>-1</sup> )	Band assignment
3369	3200-3600	O-H (stretching)
3289	3330-3500	O-H and C-H (stretching)
2919	2850-2940	C-H (stretching)
1728	1695-1735	C=O (symmetric stertching)
1437	1400-1480	C-H (bending ester methyl group)
1019	1320-1380	C-O-C (asymmetric stretching of ether )

\*(Silverstein *et al.*, 2003)

**Table 3 FT IR Band Assignments of Polyvinyl Alcohol**

Observed wave number (cm <sup>-1</sup> )	Literature wave number (cm <sup>-1</sup> )	Band assignment
3305	3200-3600	O-H (stretching)
2916	2850-2940	C-H (stretching)
1714	1705-1750	C=O (stretching)
1423	1260-1440	C-H (bending of CH <sub>2</sub> )
1248	1050-1330	C-O (stretching of acetyl group)
943	750-1300	C-C (stretching)

\*(Silverstein *et al.*, 2003)

**SEM analysis**

Surface morphology of cellulose acetate and polyvinyl alcohol are presented in Figures 3 and 4. It is obviously seen that large non-uniform cavities and pores are on the surface of the cellulose acetate whereas the fibrils with uncrosslinks nature of PVA is observed.



**Figure 3** SEM photomicrograph of cellulose acetate

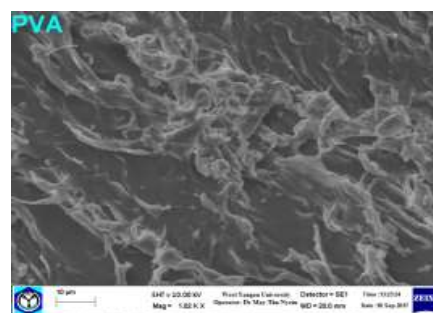


**Figure 4** SEM photomicrograph of polyvinyl alcohol

**On the Aspect of the Preparation of Cellulose Acetate - Polyvinyl Alcohol Films Determination of the Physicomechanical Properties of Cellulose Acetate - Polyvinyl Alcohol Films**

For all of the prepared films, physicochemical and physicomechanical parameters were determined. Among these parameters, tensile strength is more specific than other for determining films quality. CPF 1, CPF 2, CPF 3, CPF 4 and CPF 5 films were prepared. The results of the physicochemical and physicomechanical properties of CPF 1 to CPF 5 films are presented in Table 4 and Figures 5, 6 and 7. The most favorable conditions for preparing film namely (CPF 3) was

found to be with 20 mL of 2 % w/v cellulose acetate, 80 mL of 4 % w/v PVA and 25 mL of 0.025 M glutaraldehyde. It was found that CPF 3 has the highest tensile strength among them. Moreover, the water uptake tests of the films are also found to be satisfactory. The film CPF 3 has the equilibrium water uptake percentage among them in Table 5. Therefore, film CPF 3 was chosen to make the most suitable film.

**Table 4 Physicomechanical Properties of Films with Various Proportions of Cellulose Acetate - Polyvinyl Alcohol Films**

Properties	Cellulose Acetate - PVA Films				
	CPF 1	CPF 2	CPF 3	CPF 4	CPF 5
Thickness (mm)	0.10	0.11	0.19	0.23	0.18
Tensile strength (MPa)	15.20	19.40	27.30	18.20	17.20
Elongation at break (%)	17.90	22.00	24.60	20.40	18.28
Tear strength (kN/m)	38.40	48.80	58.90	52.60	52.00

CPF 1 = (2 % w/v, 40 mL) C + (4 % w/v, 60 mL) P + Glutaraldehyde (0.025 M, 25 mL)

CPF 2 = (2 % w/v, 30 mL) C + (4 % w/v, 70 mL) P + Glutaraldehyde (0.025 M, 25 mL)

CPF 3 = (2 % w/v, 20 mL) C + (4 % w/v, 80 mL) P + Glutaraldehyde (0.025 M, 25 mL)

CPF 4 = (2 % w/v, 20 mL) C + (4 % w/v, 90 mL) P + Glutaraldehyde (0.025 M, 25 mL)

CPF 5 = (2 % w/v, 0 mL) C + (4 % w/v, 100 mL) P + Glutaraldehyde (0.025 M, 25 mL)

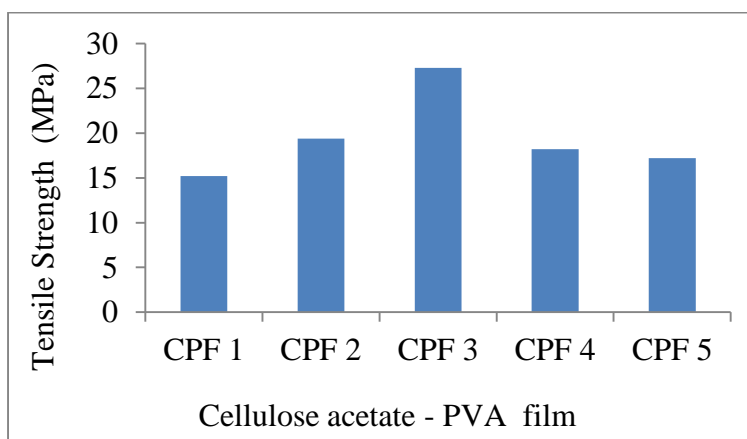


**Figure 5** Tensile strength of cellulose acetate- polyvinyl alcohol films

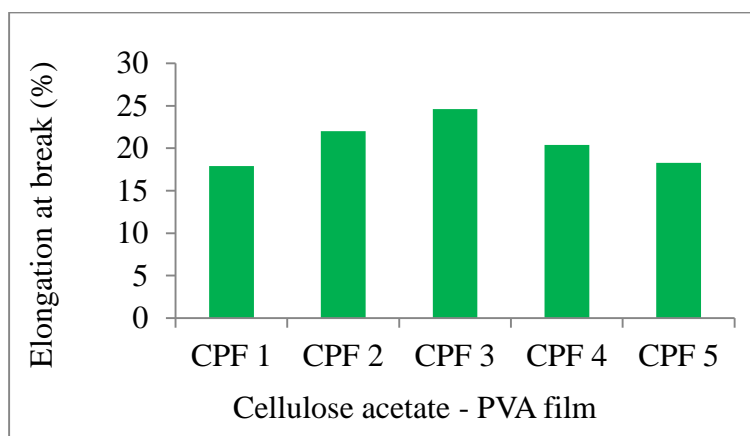


**Figure 6** Elongation at break of cellulose acetate- polyvinyl alcohol films

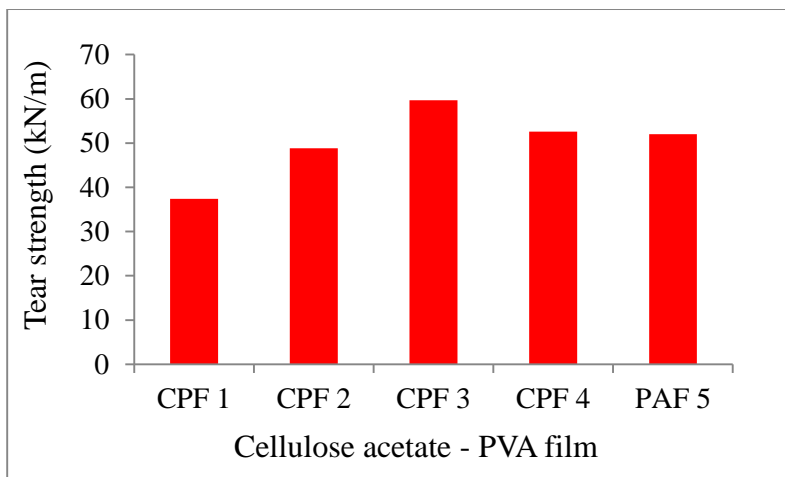


**Figure 7** Tear strength of cellulose acetate- polyvinyl alcohol films

**Determination of Water Uptake Properties of Cellulose Acetate - Polyvinyl Alcohol Films**

The degree of water uptake was investigated with increasing immersion time. The water uptake was one of the most significant parameter when a film to be used as packaging materials. The water uptake was the amount of water entrapped in the matrix including bound water. The water absorption properties of CPF 3 films were studied for varying time intervals such as 10 min, 20 min, 30 min, 40 min, 50 min and 60 min. The water uptakes as a function of time for CPF 3 films are shown in Table 5 and Figure 8.

**Table 5** Water Uptake of Cellulose Acetate -Polyvinyl Alcohol Films

Films	Water Uptake (%)					
	10 min	20 min	30 min	40 min	50 min	60 min
CPF 1	10.2	12.8	15.7	17.6	20.4	26.9
CPF 2	15.5	18.6	20.5	22.4	26.0	28.6
CPF 3	19.3	22.4	25.6	27.3	24.2	32.4
CPF 4	22.1	24.7	27.3	29.5	32.4	34.6
CPF 5	25.4	28.0	31.5	33.6	37.8	40.2

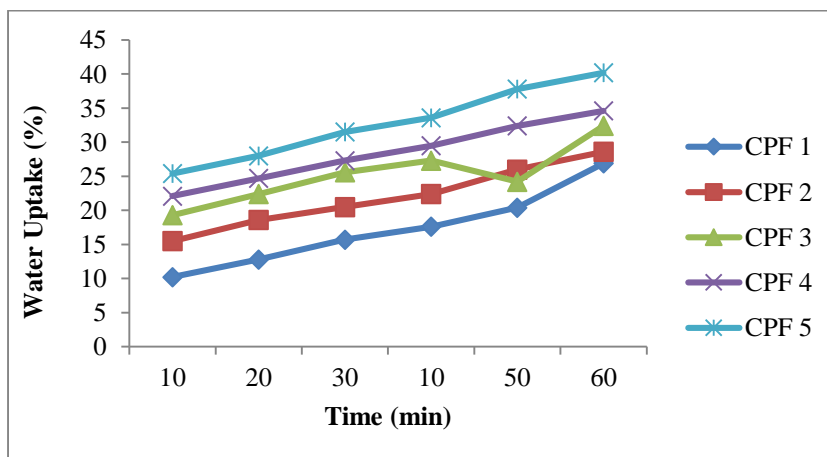


**Figure 8** Water uptake of cellulose acetate - polyvinyl alcohol films as a function of contact time

## Determination of Degree of Swelling Properties of Cellulose Acetate - Polyvinyl Alcohol Films

The degree of swelling of CPF 3 films with different compositions are shown in Table 6 and Figure 9 as a function of immersion time in distilled water at room temperature. For a given blend composition time, mostly the degree of swelling increased with increasing immersion time. The degree of swelling of CPF 3 films from 10 min to 60 min was slightly difference for all prepared films.

**Table 6 Degree of Swelling of Cellulose Acetate - Polyvinyl Alcohol Films**

Films	Degree of Swelling (%)					
	10 min	20min	30min	40mn	50 min	60min
CPF 1	8.3	11.2	13.7	16.2	19.36	21.1
CPF 2	12.4	13.6	15.9	18.3	22.6	25.3
CPF 3	15.5	17.2	17.2	20.4	21.4	23.6
CPF 4	19.2	21.4	21.4	23.0	25.9	27.2
CPF 5	21.4	24.6	24.6	26.4	29.8	30.8

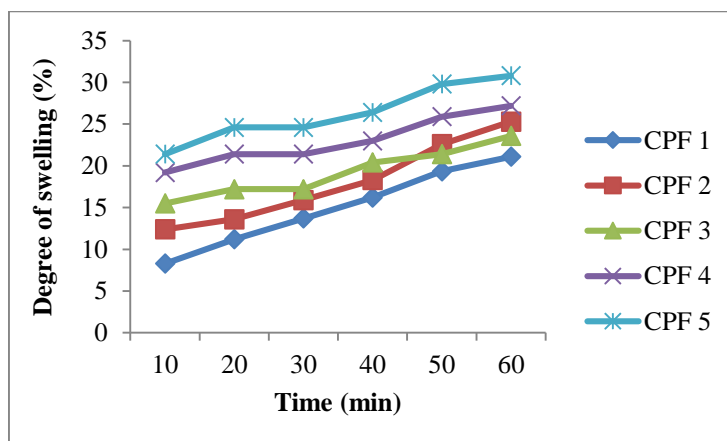


**Figure 9** Degree of swelling of cellulose acetate - polyvinyl alcohol films as a function of contact time

### Characterization of CPF 3 Film

#### FT IR analysis

Figure 10 shows the FT IR spectrum of CPF 3 film. The bands at  $3271\text{ cm}^{-1}$ ,  $2922\text{ cm}^{-1}$ ,  $1648\text{ cm}^{-1}$ ,  $1416\text{ cm}^{-1}$ ,  $1328\text{ cm}^{-1}$ ,  $1087\text{ cm}^{-1}$ ,  $832\text{ cm}^{-1}$  may be due to O-H stretching, C-H stretching, C=O (stretching), C-H (bending of  $\text{CH}_3$ ), C-H (bending of  $\text{CH}_3$ ), C-O (stretching of CH-OH) and C-C (stretching) respectively.

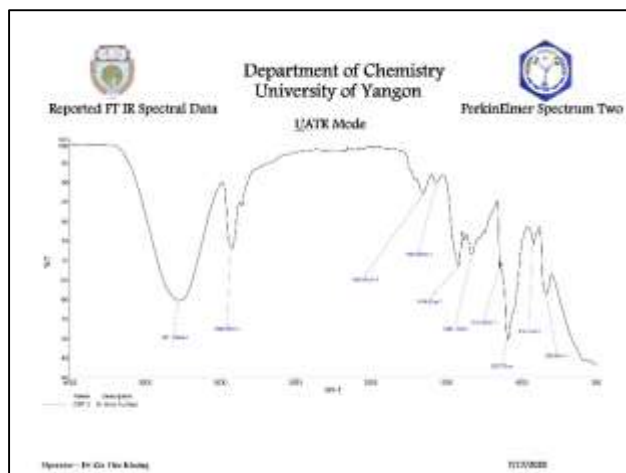


Figure 10 FT IR spectrum of CPF 3 film

Table 7 FT IR Band Assignments of CPF 3 Film

Observed wave number (cm <sup>-1</sup> )	Literature wave number (cm <sup>-1</sup> )	Band assignment
3271	3200-3600	O-H (stretching)
2922	2850-2940	C-H (stretching)
1648	1705-1750	C=O (stretching)
1416	1260-1440	C-H (bending of CH)
1328	1300-1350	C-H (bending of CH <sub>3</sub> )
1087	1000-1125	C-O (stretching of CH-OH)
832	750-1300	C-C (stretching )

\*(Silverstein *et al.*, 2003)

### SEM analysis

Surface morphology of CPF 3 is presented in Figure 11. Generally, the images show that the cellulose was homogeneously dispersed in the PVA matrix. The white dots, having different sizes on the film can be considered as cellulose. The amount of these smaller white dots was found to increase with increasing cellulose content indicating that these smaller white dots were mostly indicating of cellulose dispersed in PVA matrix.

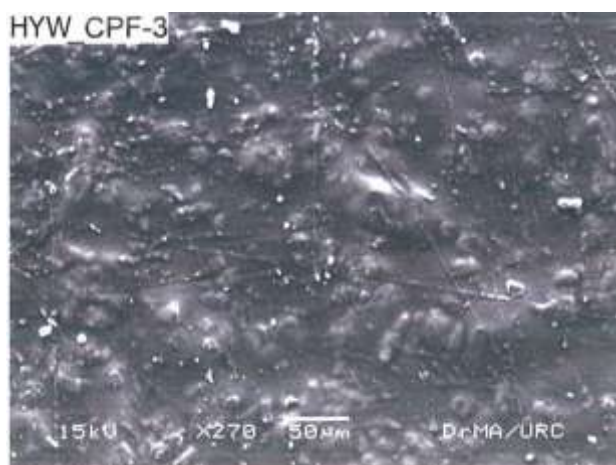
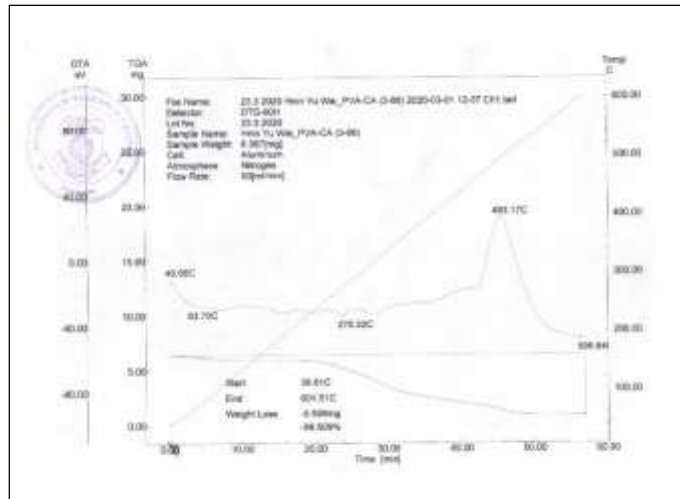


Figure 11 SEM photomicrograph of CPF 3 film

**TG DTA analysis**

Thermal stability of film CPF 3 is shown in Figure 12. It was investigated by TG-DTA analysis. On the basis of the thermogram of CPF 3 film, in first stage, the weight loss % about 8.16 % that was found within the temperature range of 38 °C to 80 °C. This is due to the dehydration of surface giving an endothermic peak at 63.70 °C. In the second stage, the weight loss % about 22.76 % was found within the temperature range of 80 °C to 300 °C. This is due to the decomposition of polymer backbone giving an endothermic peak at 275.32 °C. In the third stage, the weight loss % about 55.57 % that was found within the temperature range of 300 °C to 600 °C. This is due to the degradation of polymer backbones and burning into char giving an exothermic peak at 493.17 °C in Table 7.



**Figure 12 TG TDA thermogram of CPF 3 film**

**Table 8 Thermal Analysis Data of CPF 3 Film**

Sample	TG		DTA		Remarks
	Break in Temperature (°C)	Weight loss (%)	Peak Temperature (°C)	Nature of peak	
CPF 3	38-80	8.16	63.70	endothermic	Dehydration due to surface water
	80-300	22.76	275.32	exothermic	Decomposition of polymer backbone
	300-600	55.57	493.17	exothermic	Degradation of polymerbackbones and completely burn

**On the Aspect of Biodegradation**

The environment friendly degradable plastic has been developed by gelling the cellulose acetate with the synthetic polyvinyl alcohol (PVA) polymer. One of the objectives of development of CPF 3 film is to make easy throw away materials from degradable plastic to alleviate waste disposal problems by means of environmental degradation. In this work, biodegradation of CPF 3 film was tested by soil burial method actual condition of waste disposal. Uniformly sized samples were buried in the soil from waste disposal. The physical appearance of CPF 3 films buried in the soil is shown in Figure 13. The Figure 13 shows biodegradation nature of CPF 3 film for 3 months

interval. These figures clearly showed significant deformation of films observed at films at each investigation period.

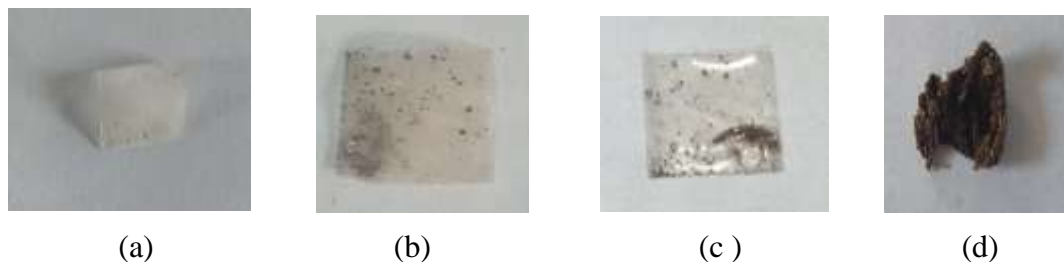


**Figure 13** The physical appearances of CPF 3 film (a) Before burial test (b) After one month (c) After four month (d) After seven month

### Some Possible Application of Prepared Films

The prepared cellulose acetate - polyvinyl alcohol films will be widely used in packaging materials. The photographs of CPF films are presented in Figure 14 and the photograph of the prepared food packaging box is in shown Figure 15.



**Figure 14** Photographs of CPF film



**Figure 15** Photograph of the prepared food packaging box

### Conclusion

Polymeric materials consisting of cellulose acetate and polyvinyl alcohol films were prepared. The various types of cellulose acetate - polyvinyl alcohol films were prepared by blending, casting technique. According to the physicomechanical properties such as tensile strength, elongation at break (%) and tear strength, the optimum conditions was achieved by using 80 mL of polyvinyl alcohol and 20 mL of cellulose acetate. All prepared cellulose acetate - polyvinyl alcohol films showed plain, clear, smooth surface, flexible, transparent to light white

colour. According to physicochemical properties, film (CPF 3) sample was chosen as optimum conditions for the preparation of cellulose acetate - polyvinyl alcohol films. The prepared cellulose acetate - polyvinyl alcohol film will be widely used in packaging materials.

### Acknowledgements

The author would like to express her deepest gratitude to the Department of Higher, Ministry of Education, Yangon, Myanmar, for the provision of opportunity to do this research and Myanmar Academy of Arts and Science for allowing to present this paper. Thanks are also due to the Rubber Research and Development Centre for the necessary research testing and Universities' Research Center (URC) for TG TDA, SEM and thank are extended to Department of Chemistry, University of Yangon for FT IR.

### References

- Bhongsuwan, D. and Bhongsuwan, T. (2008). "Preparation of Cellulose Acetate Membranes for Ultra-Nano-Filtrations". *Journal of Membrane Science*, vol. 43, pp. 311-317
- Cascone, M. G. (1997). "Dynamic Mechanical Properties of Bioartificial Polymeric Materials". *International Journal of Polymer*, vol. 43, pp. 55-69
- Liu, X., Lin, T. and Geo, Y. (2012). "Electrospun Cellulose a\Acetate Nanofibers: the Present Status and Gamut of Biotechnological Applications". *Journal of Biotechnology Advances*, vol. 31, pp. 421-437
- Rauauskas, J. (2016). "Preparation and Characterization of Bioartificial Polymeric Material:Biolayer of Cellulose Acetate-PVA", *International Journal of Polymer Science*, vol. 33, pp.68-75
- Silverstein, R. M., Webster, F. X. and Kiemle, D. J. (2003). *Spectrometric Identification of Organic Compounds*. New York: 7th Edition, John Wiley and Sons, Inc.
- Zhang, Q. G., Liu, Q. L., Zhu, A. M., Xiong, Y. and Ren, L. (2009). "Evaporation Performance of Quaternized Poly (vinylalcohol) and its Crosslinked Membranes for the Dehydration of Ethanol". *Journal of Membrane Science*, vol. 3, pp. 20-30

# FABRICATION OF ARECA NUT FIBRE-RUBBER COMPOSITES USING TAGUCHI OPTIMIZATION

Thwe Thwe Soe<sup>1,2</sup>, Htin Zaw Myint<sup>3</sup>, Saw Hla Myint<sup>4</sup>

## Abstract

In the present work, Taguchi method; a Design of Experiment (DOE) technique was used to optimize the process parameters to prepare the areca nut fibre - natural rubber composite possessing desired qualities, using minimum of time and resources. The tools and techniques such as, orthogonal array, signal-to-noise ratio (S/N), and the optimum condition were employed in Taguchi method to study the process parameters of the areca nut fibre - natural rubber composite. Three factors, namely fibre treatment type, fibre length and fibre loading (that is, loading of fiber) were considered as the process parameters. Three levels for each parameter were used. Accordingly, a suitable orthogonal array L<sub>9</sub> (3<sup>3</sup>) was selected and experiments were conducted. After conducting the experiments the mechanical properties (hardness, and tear strength) of the prepared areca nut fibre - natural rubber composites were measured and (S/N) ratios were calculated. With the help of graphs, optimum parameter values were obtained and the confirmation experiments were carried out, and satisfactory agreement was obtained.

**Keywords;** Taguchi method, orthogonal array, signal-to-noise ratio, optimum condition

## Introduction

A composite material system is composed of two or more physically distinct phases whose combination produces aggregate properties that are different from those of its constituents. Composites can be very important because of its strong and stiff, yet very light in weight, so ratios of strength to weight and stiffness to weight are several times stronger than steel or aluminum and also possible to achieve combinations of properties not attainable with metals, ceramics, or polymers alone.

Natural rubber (NR) is one of the main elastomers and widely used to prepare many rubber compounding products. NR is frequently reinforced by assimilation of the filler to improve its mechanical properties like; tensile strength, modulus, tear strength, elongation at break, hardness, rebound resilience and abrasion resistance (Khalil *et al.*, 2014). For this purpose, fillers are commonly used for rubber. Effectiveness of the reinforcing filler depends on numerous factors such as particle size, surface area and shape of filler. Nowadays, there has been growing interest in the use of industrial and agriculture waste such as areca nut fibre as fillers for rubber and their blends. The benefits of these fillers include low cost, easy availability and protection to our environment.

In the recent years, Taguchi method is a statistical method developed by Genichi Taguchi. Initially it was developed for improving the quality of goods manufactured (manufacturing process development), later its application was expanded to many other fields in Engineering, such as Biotechnology etc. Professional statisticians have acknowledged Taguchi's efforts especially in the development of designs for studying variation. Success in achieving the desired results involves a careful selection of process parameters and bifurcating them into control and noise factors. Selection of control factors must be made such that it nullifies the effect of noise factors. Taguchi method involves identification of proper control factors to obtain the optimum results of the process (Srinivas and Venkatesh, 2012). Orthogonal Arrays (OA) are used to conduct a set of

---

<sup>1</sup> Assistant Lecturer, Department of Chemistry, Yangon University of Education

<sup>2</sup> PhD Student, Department of Chemistry, University of Yangon

<sup>3</sup> Dr, Associate Professor, Department of Chemistry, Iashio University

<sup>4</sup> Dr, Part-Time Professor, Department of Chemistry, University of Yangon

experiments. Results of these experiments are used to analyze the data and predict the quality of components produced (Rahul *et al.*, 2014).

### Process Optimization

Process optimization can be defined as the method of finding the conditions that will give the maximum or minimum value desired of a response.

Taguchi method minimizes the effect of uncontrollable or noise factors. It determines the optimum combination of controllable factors that will give the best value of the desired response. It is a multi-response optimization where a balance is to be achieved between a number of desired responses. Taguchi experimental design is one of the most commonly used techniques of process optimization. Taguchi method is a robust design method, because it reduces the variation of the quality of product by making the process less sensitive to the noise. The fundamental principle of robust design is to improve the quality of a product by minimizing the effect of the causes of variation without eliminating the causes.

### Approach to Product/Process Development

Many methods have been developed and implemented over the years to optimize the manufacturing processes. Some of the widely used approaches are as given below:

1. Best-guess" experiments
2. One-factor-at-a-time (OFAT) experiments
3. Statistically designed experiments (Taguchi Method belongs to this method.)

In the present work, Taguchi method was used where the design parameters change simultaneously. It uses orthogonal array (OA) to reduce the number of experiments to run. Calculation of the signal-to- noise ratio (S/N) is done to predict the optimum values of input parameters to achieve the target quality of the product.

### Orthogonal Array

There are different orthogonal arrays, *i.e.*, the OA shown on the right is called  $L_9(3^3)$  OA. The advantage of using OA is that it reduces the total number of experiments to be carried out: *e.g.*, for the 3 factors & 3 levels case (*i.e.*, each factor can have three values), all possible combinations of factor levels requires  $3^3 = 27$  experiments; but using  $L_9(3^3)$  OA requires only 9 experiments. Columns of the array are mutually *orthogonal*. It means that for any pair of columns, all combinations of factor levels occur and they occur equal number of times. This is called the balancing property and it implies orthogonality. The number of *columns* of an array represents the maximum *number of factors* that can be studied using that array. Each number under a column is a level of the factor represented by the column. The number of *rows* of an orthogonal array represents the *number of experiments*.

**Table 1. L<sub>9</sub> (3<sup>3</sup>) Orthogonal Array**

Experiment Number	Column		
	1	2	3
1	1	1	1
2	1	2	2
3	1	3	3
4	2	1	2
5	2	2	3
6	2	3	1
7	3	1	3
8	3	2	1
9	3	3	2

### Steps Involved in Taguchi Method

The use of Taguchi's parameter design involves the following steps;

1. Deciding the important process *parameters* and their *levels*, response parameter and its characteristics.
2. Selecting the appropriate OA and assigning the parameters to its various columns.
3. Conducting experiments for the levels given in each row, random order, and noting down the value of the response parameters. Each experiment is run three times.
4. Studying factors effects and finding out the optimum combination of the parameters. Calculating to predict the best value of the response characteristic.
5. Calculating the range within which the experimental value should lie and conducting confirmation experiment
6. Performing analysis of variance (ANOVA) to find out the significance of the various factors and their relative contribution.

### Materials and Methods

The Taguchi method is well known by simplification of experimental plan and feasibility of study of interaction between various parameters. In this method a less number of experiments are carried out, hence time and cost are reduced considerably. Main effect analysis is performed based on the average output of the quality characteristic at each parameter. Using the main effect and S/N ratio a prediction of the best combination of optimum parameters can be calculated (YathiAjay *et al.*, 2015).

### Design of Experiment (Taguchi Methodology)

The important process *parameters (factors)* and their *levels*, response parameter (hardness and tear strength in our case) (see below) and its characteristics was decided. Then an appropriate orthogonal array (OA) was chosen and the selected parameters and their levels were assigned to it. And then, each experiment was done according to the set of parameter levels in each row of the OA, in random order of rows. Each experiment was repeated three times and the values of the response parameters were recorded. The effect of factors on each level was calculated and the optimum combination of the parameters was chosen graphically. To do this, the chosen type of signal-to-noise ratio was calculated (the larger the better on our case) (see below). The best value of the predicted response characteristic was calculated and validated by running the experiment with the calculated optimum combination of input parameters.

Response Names ; Hardness (IRHD) and Tear Strength (kN/m)

Response Types ; Larger-the-better ,  $SN_L = -10 \log \left[ \frac{1}{n} \sum_{i=1}^n \frac{1}{y_i^2} \right]$

### Selecting of processing parameters

Three processing parameters (or) factors, each with three levels were chosen. (The non-linear behavior of the response characteristic can only be studied if more than two levels of a parameter were used.)

Factor one is the type of fibre (its three levels are: untreated, alkali treatment and potassium permanganate treatment). Choosing these processing types was based on the more reactive groups on the areca fiber surface, and effective areca fiber surface area for good adhesion with the natural rubber matrix. Furthermore, chemically treated areca fiber surface became more hydrophobic and there is improvement in surface characteristics such as wetting, adhesion and porosity of areca fibers, which improve interfacial adhesion between the treated areca fiber surface and the natural rubber matrix.

Factor two is the fibre length. It was also one of the parameters chosen due to its influence on the strength of the composite (20 mm is reported to be the upper limit (Rameez *et al.*, 2016)). The three levels are: 5, 10 and 15 mm fibre lengths.

Finally, factor three is the fibre loading. It also has effects on the strength of a composite (Rameez *et al.*, 2016). The three levels are: 5, 10 and 15 % by loading. Thus three levels are selected for each parameter (Table 2). Nine experiments have been done with different combinations of levels of parameters according to  $L_9$  orthogonal array was carried out (Table 3).

**Table 2 The Parameters for Three Levels of Selected Factors**

Factors	Level -1	Level-2	Level-3
Fibre treatment type	Untreated	Alkali treated	KMnO <sub>4</sub> treated
Fibre length (mm)	5	10	15
Fibre loading (%)	5	10	15

**Table 3 The Combination of Different Levels of Parameters According to  $L_9$  Orthogonal Array**

Experiment No.	Column		
	Fibre treatment type	Fibre length (mm)	Fibre loading (%)
1	Untreated	5	5
2	Untreated	10	10
3	Untreated	15	15
4	NaOH	5	10
5	NaOH	10	15
6	NaOH	15	5
7	KMnO <sub>4</sub>	5	15
8	KMnO <sub>4</sub>	10	5
9	KMnO <sub>4</sub>	15	10

### Synthesis of Natural Rubber Composites Reinforced by Areca Nut Fibre

Natural rubber smoked sheets for the experiments were procured from Myanmar Gone Yee Rubber Plantation, Bago Region. The areca nut fibre-rubber composites were prepared and their mechanical characteristics were recorded at Rubber Research and Development Centre in Yangon.



**Figure 1** Natural rubber

**Materials**

Natural rubber smoked sheet grade 1, zinc oxide, stearic acid, mercapto benzothiazole, oil, antioxidant, sulphur, untreated, alkali treated and potassium permanganate treated areca nut fibre.

**Procedure**

Natural rubber smoked sheet Figure 1 was first rolled at 60°C for 5 minutes on a Two Roll Mill to break out the fibrous bond of rubber polymer chain. This step is called mastication. Then mercapto benzothiazole (MBT) was mixed on rolling. After ½ minute zinc oxide and stearic acid were added simultaneously and rolled for 2 minutes. And then petroleum oil was added and rolled for one minute. Sulphur was added and rolled about 3-4 minutes until thick sheet was obtained. Vulcanized rubber was obtained. Finally, the vulcanized rubber was mixed separately with untreated and treated fibres (various ratios according to Table 4) on rolling. The fibre loadings based on 100 g of rubber were in weight. Total mixing duration was 10 to 15 minutes. During mixing whenever the roller becomes too hot, water was sprayed on the roller (The temperature must be maintained at 60°C). The matrix material thus obtained for composite preparation was being allowed to age for 24 hours. Procedure for preparation of natural rubber–areca nut matrix and the composite was shown in Figure 2.

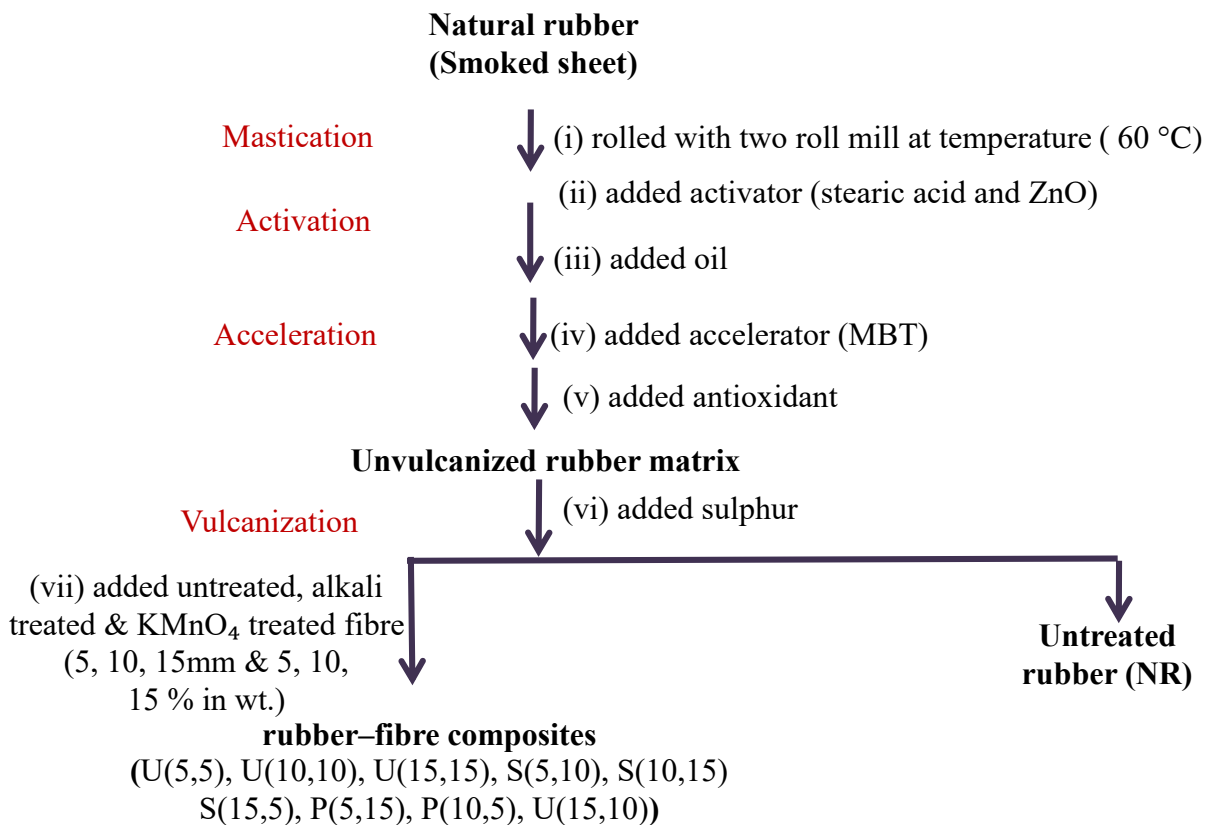


**Figure 2** Flow diagram for the preparation of rubber-areca nut fibre composite

## Making composites

The molded plates of aging matrix were compressed for shaping by Hand Press Machine). Firstly, the plates were hot pressed at 153-160 °C ( Hardness for 8 minutes and Tear Strength for 6 minutes) under 1000 lb in<sup>-2</sup> loading. By mixing reinforcing agents nine samples were prepared and compositions of these samples were illustrated in Table 4.

**Table 4 Composition of Prepared Natural Rubber Composites Reinforced by Areca Nut Fibre**

Sr. no.	Ingredient (g)	natural rubber (NR)	Composite								
1	Natural rubber	100	100	100	100	100	100	100	100	100	100
2	Zinc oxide	5	5	5	5	5	5	5	5	5	5
3	Stearic acid	2.5	2.5	2.5	2.5	2.5	2.5	2.5	2.5	2.5	2.5
4	Petroleum oil	3	3	3	3	3	3	3	3	3	3
5	MBT	1.8	1.8	1.8	1.8	1.8	1.8	1.8	1.8	1.8	1.8
6	Antioxidant	1	1	1	1	1	1	1	1	1	1
7	Sulphur	2	2	2	2	2	2	2	2	2	2
8	Areca nut fibre	-	U (5, 5)	U (10,10)	U (15,15)	S (5,10)	S (10,15)	S (15,5)	P (5,15)	P (10,5)	P (15,10)

NR = Natural rubber

U (5, 5) = Composites with untreated areca nut fibre (5 mm in length and 5 % in loading of fibre to rubber)

U (10, 10) = Composites with untreated areca nut fibre (10 mm in length and 10 % in loading of fibre to rubber)

U (15, 15) = Composites with untreated areca nut fibre (15 mm in length and 15 % in loading of fibre to rubber)

S (5, 10) = Composites with alkali treated areca nut fibre (5 mm in length and 10 % in loading of fibre to rubber)

S (10, 15) = Composites with alkali treated areca nut fibre (10 mm in length and 15 % in loading of fibre to rubber)

S (15, 5) = Composites with alkali treated areca nut fibre (15 mm in length and 5 % in loading of fibre to rubber)

P (5, 15) = Composites with permanganate treated areca nut fibre (5 mm in length and 15 % in loading of fibre to rubber)

P (10, 5) = Composites with permanganate treated areca nut fibre (10 mm in length and 5 % in loading of fibre to rubber)

P (15, 10) = Composites with permanganate treated areca nut fibre (15 mm in length and 10 % in loading of fibre to rubber)

## Determination of the Mechanical Properties of the Areca Nut Fibre-Natural Rubber Composites

### Reinforced by areca nut fibre

Comparative determination of mechanical properties of natural rubber composites reinforced by areca nut fibre such as hardness and tear strength were carried at the Rubber Research and Development Centre in Yangon.

### Determination of hardness

The hardness of a composite also depends on the distribution of the fibre into the matrix. Better dispersion of the fibre into the matrix with minimization of voids between the matrix and the fibre enhanced this hardness. Hardness is a measurement in degree and based on the penetration into the rubber of a definite indenter under a set load. Three scales are commonly used. IRHD (International Rubber Hardness Degree), Shore A, and Shore D. For hard materials over 90, Shore A scale is used. IRHD is preferred for most specifications, but Shore A is also in widespread use.

## Materials

Natural rubber sheet, Rubber composite

## Apparatus

Wallace Rubber Hardness Tester Figure 4

## Procedure

Hardness is a measure of an elastomer's response to a small surface stress. The test was based on the measurement of the indentation of a rigid ball into the rubber Figure 3 under specified conditions. The specified test piece was placed in a Wallace rubber hardness tester Figure 4 and the vibrator was switched on. Hardness is a measurement in degree based on the penetration into the rubber of a definite indenter used. After 30 seconds, the hardness was read directly in IRHD on the micrometer gauge.



**Figure 3** Prepared samples to determine hardness



**Figure 4** Wallace rubber hardness tester

## Determination of tear strength

### Materials

Natural rubber sheet, Rubber-Fibre composite

### Apparatus

H-5000E Tensile Testing Machine Figure 5

### Procedure

The determinations were carried out at standard laboratory temperature in the H-5000E Tensile Testing Machine Figure 5. The test pieces were cut 100 mm length and the machine was started and the change in the test piece monitored continuously. Tear strength is a resistance to the growth of a cut or nick in a vulcanized fiber-rubber specimen when tension was applied. Tear strength is an important consideration, both as the finished article was being removed from the mold and as it performs in actual service.



**Figure 5** Determination of tear strength

### Results and Discussion

Since hardness and tear strength are the criteria that were chosen to study the optimum parameters, then in determination of S/N ratio, the larger- the- better quality characteristic has been selected.

After performing experimental design and tabulating performance data, appropriate signal-to-noise (S/N) ratio was calculated.

$$\text{S/N ratio for "larger is better"} : \text{SN}_L = -10 \log \left[ \frac{1}{n} \sum_{i=1}^n \frac{1}{y_i^2} \right]$$

Where,  $n$  is number of repetitions of each experiment and

$y_i$  is the measured result for  $i^{\text{th}}$  repetition of each experiment

**Table 5 Results for Determination of Signal-to-Noise Ratios for Hardness and Tear Strength of the Composites Prepared According to L<sub>9</sub> Orthogonal Array Design**

Expt No.	Hardness (IRHD)			S/N Ratio (dB)	Tear Strength (kN/m)			S/N Ratio (dB)
	R1	R2	R3		R1	R2	R3	
1	38	36	36	31.277	22.3	27.5	27.5	28.092
2	45	40	42	32.503	23.0	21.9	22.2	26.986
3	51	45	47	33.529	18.2	14.7	17.3	24.362
4	40	47	45	32.808	16.0	22.6	20.4	25.598
5	43	48	48	33.282	20.7	24.0	23.6	27.088
6	40	42	40	32.178	20.9	25.5	24.1	27.329
7	44	41	43	32.590	19.4	18.9	19.0	25.619
8	37	38	38	31.517	23.0	28.1	27.1	28.222
9	42	40	40	32.178	19.3	28.6	26.9	27.537
Total	380	377	379	291.864	182.8	211.8	208.1	240.833
Overall mean of hardness = 42.074				Mean, m=32.429	Overall mean of tear strength = 22.322			Mean, m= 26.759

Then the mean S/N ratios at each level for various factors have to be calculated. The factor levels corresponding to the highest average S/N ratio will give the optimized condition of maximum efficiency. The S/N ratio for the individual control factors are calculated as given below;

Effects of factor A at Level 1,  $m_{A1} = (n_1 + n_2 + n_3) / 3$

where  $n_1$  is the signal-to-noise ratio of the first row

where  $n_2$  is the signal-to-noise ratio of the second row, etc.

Effect of factor A at level 2,  $m_{A2} = (n_4 + n_5 + n_6) / 3$

Effect of factor A at level 3,  $m_{A3} = (n_7 + n_8 + n_9) / 3$

Effect of factor B at level 1,  $m_{B1} = (n_1 + n_4 + n_7) / 3$

Effect of factor B at level 2,  $m_{B2} = (n_2 + n_5 + n_8) / 3$

Effect of factor B at level 3,  $m_{B3} = (n_3 + n_6 + n_9) / 3$

Effect of factor C at level 1,  $m_{C1} = (n_1 + n_6 + n_8) / 3$

Effect of factor C at level 2,  $m_{C2} = (n_2 + n_4 + n_9) / 3$

Effect of factor C at level 3,  $m_{C3} = (n_3 + n_5 + n_7) / 3$  (YathiAjay *et al.*, 2015)

**Table 6 The Effects of Factor on Individual Levels for Hardness**

Factor Levels	Fibre treatment type		Fibre length (mm)		Fibre loading (%)	
	Raw data	S/N ratio	Raw data	S/N ratio	Raw data	S/N ratio
L1	42	32.437	41	32.225	38	31.657
L2	44	<b>32.756</b>	42	32.434	42	32.496
L3	40	32.095	43	<b>32.628</b>	46	<b>33.134</b>

**Table 7 The Effects of Factors on Individual Levels for Tear Strength**

Factor levels	Fibre treatment type		Fibre length (mm)		Fibre loading (%)	
	Raw data	S/N ratio	Raw data	S/N ratio	Raw data	S/N ratio
L1	21.6	26.480	21.5	26.436	25.1	<b>27.881</b>
L2	22.0	26.672	23.7	<b>27.432</b>	22.3	26.707
L3	23.4	<b>27.126</b>	21.7	26.410	19.5	25.690

The optimum factor levels can be easily identified from the graphs showing the variation of S/N ratio (Y-axis) with the Levels (X-axis) for different factors. The graphs for hardness and tear strength are shown below.

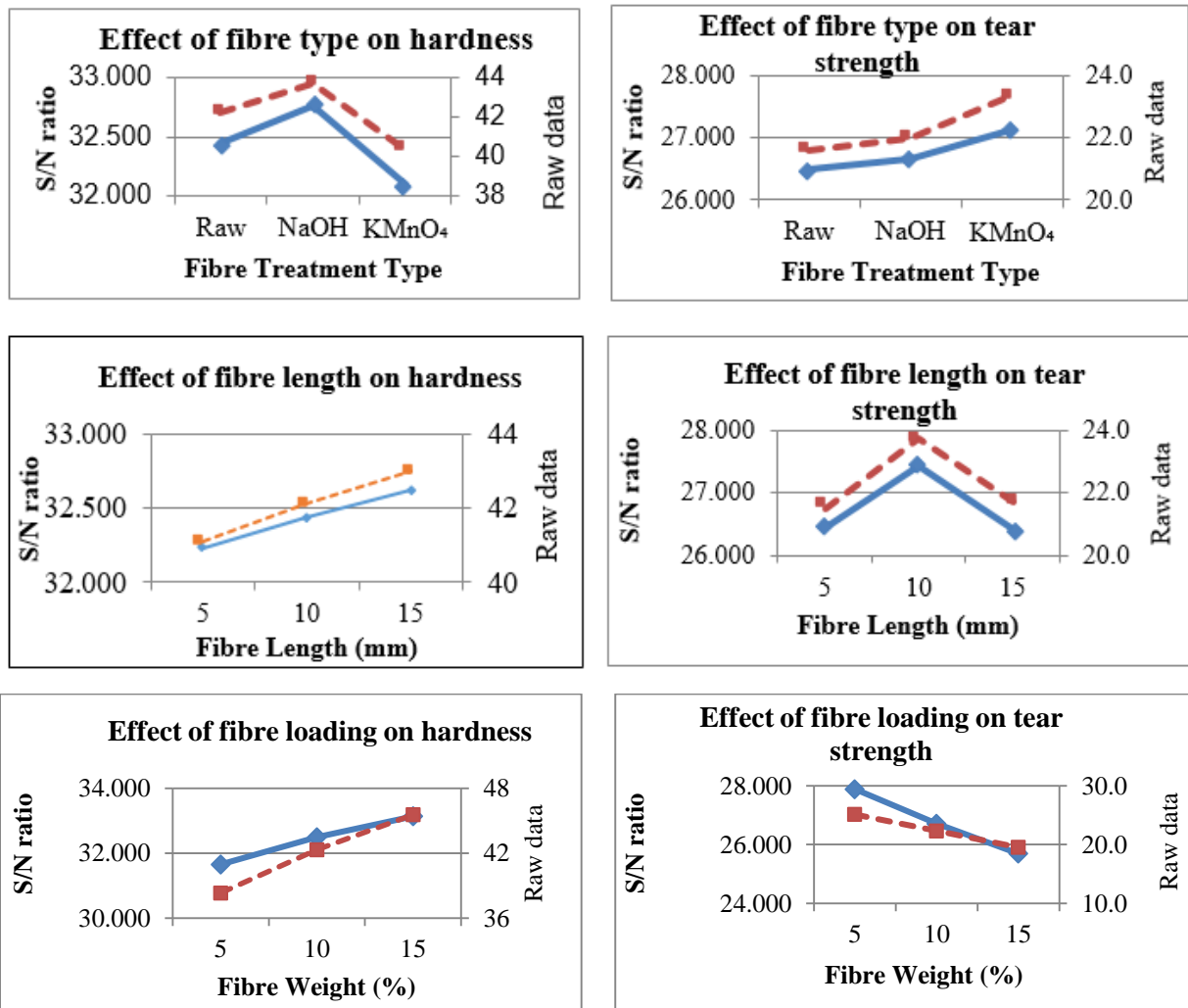


**Figure 5** Effect of the largest fibre type, fibre length and fibre loading on hardness and tear strength

### Hardness and Tear Strength Test Result

From the graphs, the optimum combination input parameters for hardness can be observed as: the fibre treatment type NaOH treatment, fibre length 15 mm and fibre loading 15 % weight. Similarly, for tear strength the optimum combination input parameters are: fibre treatment type KMnO<sub>4</sub> treatment, fibre length 10 mm and fibre loading 5 % weight.

**Table 8 Optimum Combinations of Values of Factor Levels for each Property Measured**

Property measured	Factor levels		
	Fibre treatment type	Fibre length (mm)	Fibre loading (%)
Hardness	NaOH	15	15
Tear strength	KMnO <sub>4</sub>	10	5

### Calculation of Optimum S/N ratio and the Prediction of the Corresponding Optimum Value of the Property

The optimum condition of the three process parameters for hardness is A<sub>2</sub>B<sub>3</sub>C<sub>3</sub>, (A= fibre type, B= fibre length, C= fibre loading) then the theoretical value of  $\eta$  under the optimum conditions, denoted by  $\eta_{opt}$  is given by:

$$\eta_{opt} = m + (m_{Ai} - m) + (m_{Bj} - m) + (m_{Ck} - m)$$

Where i, j, k are the best levels, respectively, for factors A, B and C.

The corresponding optimum value of larger-the-better type of response characteristic is given by

$$y_{opt}^2 = 1 / 10^{-\eta_{opt}/10}$$

**Table 9 Example Calculated for Hardness of Optimum S/N Ratio**

Factor levels	Fibre treatment type		Fibre length (mm)		Fibre loading (%)	
	Raw data	S/N ratio	Raw data	S/N ratio	Raw data	S/N ratio
L1	42	32.437	41	32.225	38	31.657
L2	44	<b>32.756</b>	42	32.434	42	32.496
L3	40	32.095	43	<b>32.628</b>	46	<b>33.134</b>

Optimum Value -  $m_{Ai}$ ,  $m_{Bj}$ ,  $m_{Ck}$

	$m_{A2}$	$m_{B3}$	$m_{C3}$	$m$	$\eta_{opt}$	$y_{opt}$
Hardness	32.756	32.628	33.134	32.429	33.660	48.20

### Comparison of Optimum Condition and Experimental results for Mechanical Properties

It can be clearly shown from this table for theoretical optimum conditions and experimental results data of hardness and tear strength are nearly the same. So, NaOH, 15 mm, 15 % is more significant than other fibre treatment and filler content for hardness. The highest tear strength is KMnO<sub>4</sub>, 10 mm, 5 % more significant. Therefore, Taguchi’s Method of parameter design can be performed with lesser number of experiments as compared to that of other analyses. Taguchi’s method can be applied for analyzing any other kind of problems as described in this paper. It is

found that the parameter design of the Taguchi method provides a simple, systematic, and efficient methodology for optimizing the process parameters.

**Table 10 Optimum Values**

	$m_{Ai}$	$m_{Bj}$	$m_{Ck}$	$m$	$n_{opt}$	$y_{opt}$
Hardness	32.756	32.628	33.134	32.429	33.660	48.20
Tear Strength	27.126	27.432	27.881	26.759	28.920	27.93

**Table 11 Experimental Results for Mechanical Properties**

	Hardness (IRHD)	Tear Strength (kN/m)
NaOH 15, 15	58.6	19.8
KMnO <sub>4</sub> 10, 5	50.6	26.1
Rubber only	30.0	24.1

### Conclusion

Instead of the conventional one-factor-at-a-time (OFAT) method, the present work manipulates multiple variables simultaneously using statistical technique (design of experiments (DOE)) known as Taguchi method. This method has successfully provided the optimum values of the selected process parameters to be used to prepare two samples of areca nut fibre-natural rubber composites with preferential qualities, hardness for the one and tear strength for the other. Experiments were done according to a L<sub>9</sub> orthogonal array and the results were analysed using the conceptual signal-to-noise (S/N) ratio approach to get the optimum parameter values to effect the desired quality of each composite sample:

- For the highest hardness - NaOH treated fibre, with fibre length (15 mm), and fibre loading (15 %) should be used.
- For the highest tear strength - KMnO<sub>4</sub> treated fibre, with fibre length (10 mm), and fibre loading (5 %) should be used.

The difficulty to tear is due to the high interfacial locking between the fibre and matrix. Both samples also were found to possess higher values of the respective selected qualities than the rubber without fibre.

These results clearly evidenced that chemical treatments are very effective in surface modification of the areca fibers and improving the mechanical properties of areca fiber reinforced natural rubber composite. So, these chemically treated areca fiber reinforced natural rubber composites are suitable for applications where hardness or tear strength are required, while at the same time reducing environmental issues caused by the unused betel nut shells. All these results have been realized with economy of time and resources by using Taguchi design of experiment.

### Acknowledgements

The authors would like to express their gratitude to the Department of Higher Education (Lower Myanmar), Ministry of Education, Myanmar, for the permission to do this research and also to the Myanmar Academy of Arts and Science for giving the opportunity to read this paper.

## References

- Khalil, A., Nizami, S. S. and Riza, N. Z. (2014) "Reinforcement of Natural Rubber Hybrid Composites Based on Marble Sludge/ Silica and Marble Sludge/ Rice Husk Derived Silica". *Journal of Advanced Research*, vol. 5, pp. 165-173
- Rameez, M., Alexander, R., Joy, R. T., Mathew, R. and Kumar, H. (2016). "Fabrication and Testing of Reinforced Composites using Natural Rubber and Natural Fibre". *International Journal for Innovative Research in Science & Technology Research*, vol. 2(11), pp. 626-635
- Rahul, K., Kumar, K. and Bhowmik, S. (2014). "Optimization of Mechanical Properties of Epoxy Based Wood Dust Reinforced Green Composite using Taguchi Method". *Procedia Materials Science*, 5, 688-696
- Srinivas, A., and Venkatesh, Y. D. (2012). "Application of Taguchi Method for Optimization of Process Parameters in Improving the Surface Roughness of Lathe Facing Operation". *International Refereed Journal of Engineering and Science*, vol 1(3), pp. 13-19.
- YathiAjay, A. V., Ramkumar, B. Vishnu, U. and John, P. (2015). "Optimization of Process Parameters to Maximize the Efficiency of a Vacuum Pump Using Taguchi Method and ANOVA". *International Journal of Science, Engineering and Technology Research*, vol. 4 (4), pp. 747-751.

## PREPARATION OF SILVER COLLOIDAL SOLUTION COATED CERAMIC FILTER AND ITS ANTIMICROBIAL ACTIVITY

Thazin Oo<sup>1</sup>, Zaw Naing<sup>2</sup>, May Zin Oo<sup>3</sup>, Cho Cho<sup>4</sup>

### Abstract

In this research work, the silver colloidal solution was synthesized by using silver nitrate and watery extract of bamboo leaves as reducing agents. The optimum ratio of red clay, brown clay and rice husk (6:3:1 w/w) were used for preparing porous ceramic filters. Silver colloidal solution was coated on prepared ceramic filter and silver coated filter, was obtained. EDXRF and SEM were used to examine the silver percent content of coated and uncoated ceramic filters. EDXRF analysis showed that silver (0.166 %) was present in coated filter and absent in uncoated filter. The antimicrobial activities of uncoated filter and coated filter by agar well diffusion method were tested on *Bacillus pumilus*, *Bacillus subtilis*, *Candida albicans*, *Escherichia coli*, *Pseudomonas fluorescens* and *Staphylococcus aureus* strains. The coated filter showed high antimicrobial activities on six microorganisms but not on the uncoated filter. Based on the results, prepared silver coated ceramic filters may be used as ecofriendly, environmental friendly and most effective filter material for water treatment due to its antimicrobial activities.

**Keywords:** silver colloidal solution, ceramic filter, antimicrobial activity, bamboo leaves, watery extract

### Introduction

The World Health Organization (WHO) assessed in 2000 that 1.1 billion peoples do not have access to 'improved drinking water sources'. Consumption of unsafe water continues to be one of the major causes of the 2.2 million diarrhoeal disease deaths occurring annually, mostly children in developing countries. According to the WHO a short-term solution to meet the basic need of safe drinking water can be found in household water treatment and safe storage (HWTS). An appropriate technology complies with WHO guidelines on the quality and quantity of water. It ensures the guarantee that water for personal or domestic use is safe and therefore free from microorganisms, chemical substances and hazards that constitute a threat to a person's health (Halem, 2006). People have to collect their own water outside their own water outside their homes and then store the water in the household due to the lack of water supply, and contaminations could occur during the water collection, transport, and storage, which cause a high chance of water-borne disease infection (Mohamed, 2018).

Silver nanoparticles (AgNPs) can be easily incorporated into drinking water purifiers so as to deliver safe and clean water at low cost. Nevertheless, the large demands in nanoparticles availability and high microbial loading during disinfection of drinking water still limits AgNPs either for household (point-of-use) water treatment or when specialized treatment is required (Simeonids *et al.*, 2016). Deposition of AgNPs in the bacterial cell surface can affect cell membrane permeability. Nanoparticles can destroy both bacterial cell wall and cell membrane well (Likus, 2013). There have been several reports on the use of AgNPs in the field of medicine. The AgNPs have been used as therapeutic agents, as glyconano sensors for disease diagnosis and as nano carriers for drug delivery (Srikar *et al.*, 2016).

Ceramic-water filtration by using ceramics is an inexpensive and effective type of filtration method that relies on the small pore size of ceramic material to filter dirt, debris, and bacteria out of water. Typically bacteria, protozoa, and microbial cysts are removed but the filters are not

---

<sup>1</sup> PhD Candidate, Department of Chemistry, University of Yangon

<sup>2</sup> Dr, Associate Professor, Department of Chemistry, Dagon University

<sup>3</sup> Dr, Lecturer, Department of Chemistry, Dagon University

<sup>4</sup> Dr, Professor, Department of Chemistry, University of Yangon

effective against viruses since they are small enough to pass through to the other "clean" side of the filter. Ceramic when combined with silver impregnated carbon is called sterasyl that is ideal for filtering microbiologically unsafe water; however sterasyl does not remove fluoride. The only disadvantage of ceramic materials is the brittle nature which may develop hairline cracks during handling (Padmaja *et al.*, 2007). In the present investigation an attempt is made to prepare a silver colloidal solution coated ceramic filter and it can be used as a filter for microbiologically unsafe water.

## Materials and Methods

### Preparation of Silver Colloidal Solution

2:1 (v/v) ratio of 3 mM silver nitrate solution and bamboo leaves extract were mixed and stirred for 1 h with a magnetic stirrer. The reduction reaction was completed after 2 days with the appearance of a reddish brown colour which confirms the formation of a silver colloidal solution.



Figure 1 Silver colloidal solution

### Preparation of Porous Ceramic Filters

The 60 % of red clay, 30 % of brown clay and 10 % rice husk were mixed with weight by weight ratio. 30 mL of distilled water was added to the clay mixture and thoroughly mixed to obtain until paste. And then, the resulting clay paste was put into plastic mold and pressed to obtain ceramic filters. The filters were dried for 2 days in air and heated at 800 °C for 2 h.

### Coating of Porous Ceramic Filter with Silver Colloidal Solution

The filter was immersed in 25 mL of silver colloidal solution for 1 h. After that, the filter was removed from the silver colloidal solution and dried at room temperature. Figure 2 (b) shows the prepared silver coated porous ceramic filter.



(a)



(b)

Figure 2 Porous ceramic filters (a) uncoated filter and (b) coated filter

## Characterization of Ceramic Filters by Modern Techniques

### EDXRF analysis

The energy dispersive X-ray fluorescence spectrums (EDXRF) of composite beads were recorded on Perkin Elmer 700, EDXRF spectrometer.

### SEM analysis

A scanning electron microscope (JSM-5610 Model SEM, JEOL-Ltd., Japan) was used to record the micrograph images of uncoated filter and coated filter.

### Antimicrobial activity using agar well diffusion method

The agar plates containing tested organisms were punched to make the wells (8 mm in diameter) using sterile cork borer and filled with the stock solution (0.2 mL) and then these plates were incubated at room temperature for 24 h. After incubation, the diameters of the growth inhibition zones surrounding the wells were measured in mm. These zones indicated the presence of antimicrobial activities which inhibit the growth of tested organisms selectively (Collins, 1965).

## Results and Discussion

### Visual Observation of Silver Colloidal Solution

The silver colloidal solution prepared by using 3mM of silver nitrate solution and bamboo leaves extract was confirmed by changing in colour from pale yellow to reddish brown due to the formation of silver colloidal solution. Figure 1 shows the silver colloidal solution.

### Characterization of Uncoated Filter and Coated Filter

#### EDXRF analysis

The chemical compositions of minerals that present in the uncoated and coated filter were determined by EDXRF and their compositions are shown in Table 1. Their respective spectra are described in Figures 3 and 4. According to EDXRF analysis, silver is absent in uncoated filters and present in coated filters.

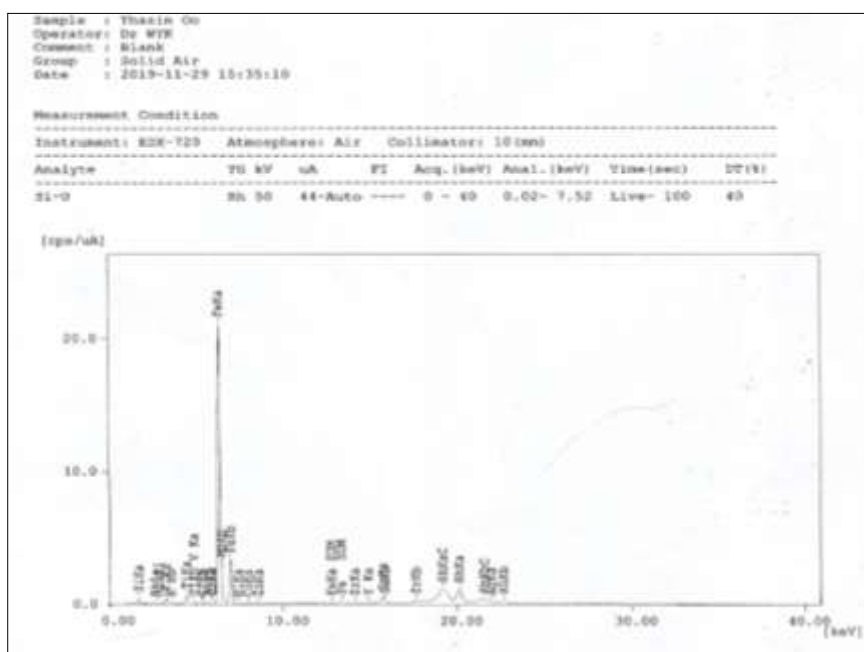


Figure 3 EDXRF spectrum of uncoated filter

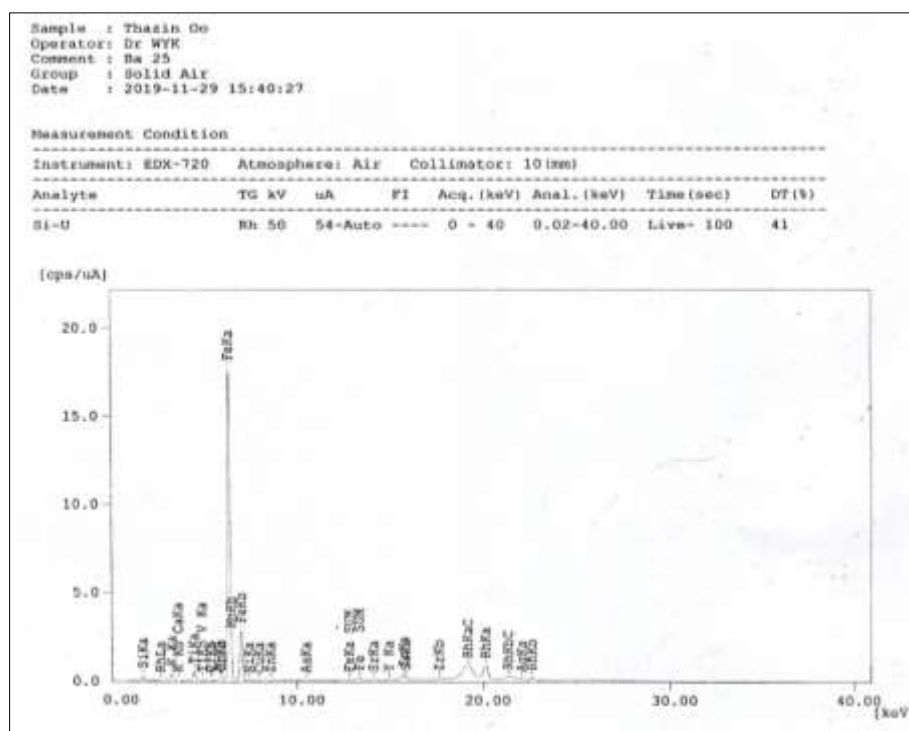


Figure 4 EDXRF spectrum of coated filter

Table 1 Elemental Analysis of Uncoated and Coated Filter

Elements	Relative abundance (%)	
	Uncoated filter	Coated filter
Si	62.123	58.572
Fe	28.816	31.151
K	6.004	6.613
Ti	2.084	2.198
Mn	0.247	0.249
Zr	0.231	0.205
Ag	<b>ND</b>	<b>0.166</b>
Cr	0.131	0.129
Ni	0.062	0.072
Zn	0.053	0.062

ND – not detected

### SEM Analysis

SEM micrographs of silver coated and uncoated filters were described in Figures 5 (a) and (b). It can be seen that uncoated and coated filters have different morphologies. The pores are indicated by black areas in the micrograph of the uncoated filter. In the SEM micrograph of the coated filter, there was a lack of the black areas due to the presence of silver. In Figure 5 (a) the black areas showed the pores of the uncoated filter.

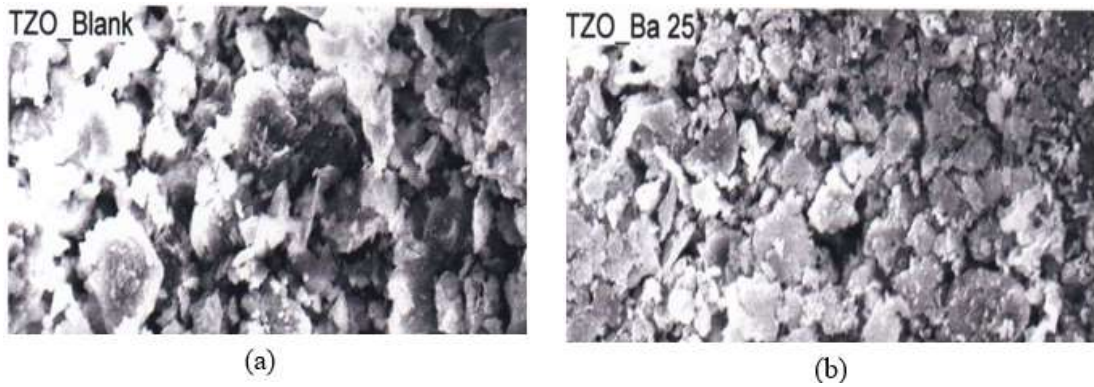


**Figure 5** SEM micrographs of (a) uncoated filter (b) coated filter

**Antimicrobial Activities of Uncoated and Coated Filters**

The uncoated and coated filter exhibited an antimicrobial activity against *Bacillus pumilus*, *Bacillus subtilis*, *Candida albicans*, *Escherichia coli*, *Pseudomonas fluorescens* and *Staphylococcus aureus*. Figure 6 and Table 2 showed the antimicrobial activities of uncoated filters on six microorganisms. Figure 7 and Table 2 showed the antimicrobial activities of coated filters against six microorganisms. According to the test the uncoated filter showed no antimicrobial activities on six microorganisms and the coated filter showed high activity against six microorganisms due to the presence of silver.

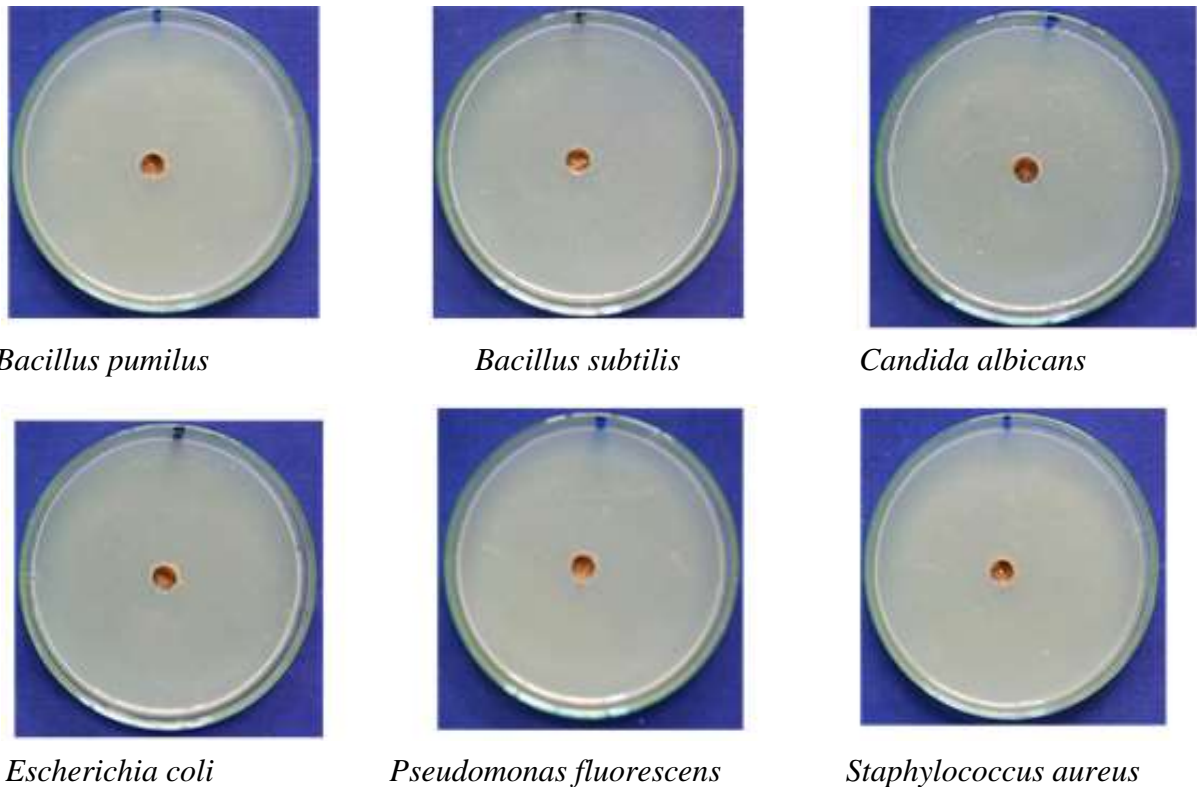


**Figure 6** Antimicrobial activities of uncoated filter

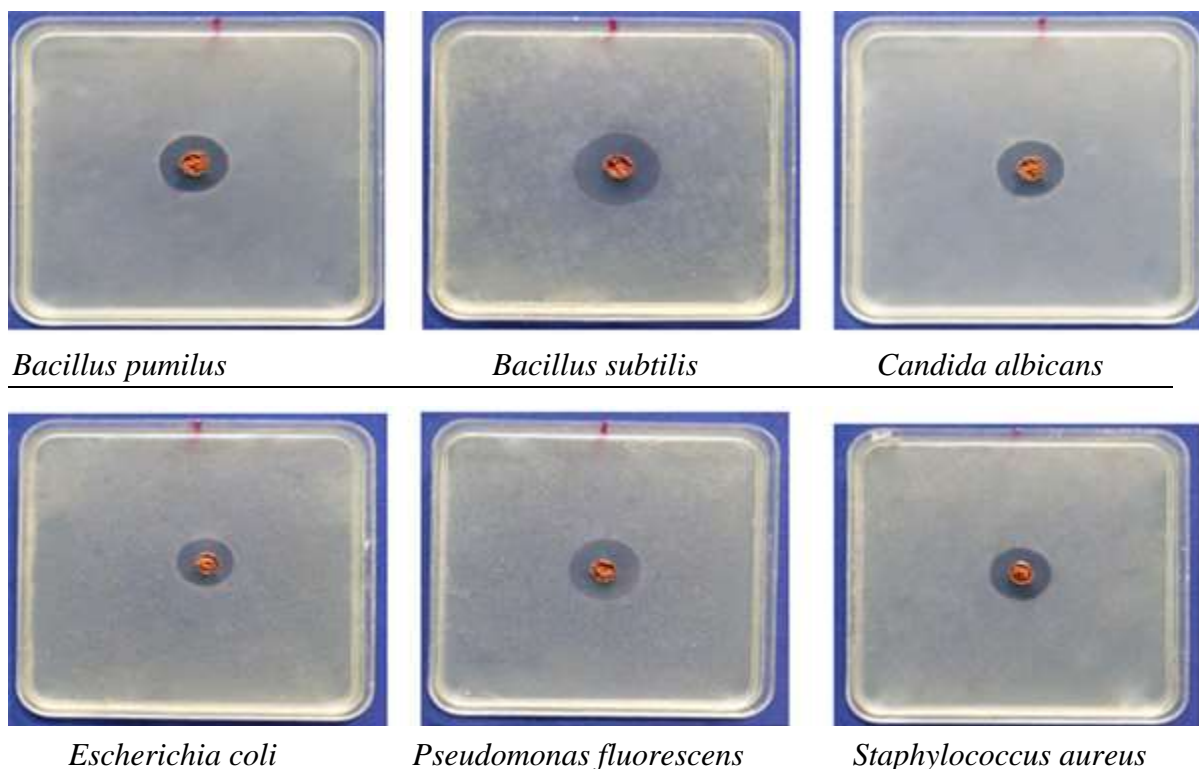


**Figure 7** Antimicrobial activities of coated filter

**Table 2** Antimicrobial Activities of Coated and Uncoated Filters

Organisms	Inhibition zone diameter (mm)	
	Uncoated filter	Coated filter
<i>Bacillus pumilus</i>	–	22 (+++)
<i>Bacillus subtilis</i>	–	26 (+++)
<i>Candida albicans</i>	–	22 (+++)
<i>Escherichia coli</i>	–	20 (+++)
<i>Pseudomonas fluorescens</i>	–	24 (+++)
<i>Staphylococcus aureus</i>	–	26 (+++)

Diameter of Agar Well – 8 mm

No activity (-)

10 mm ~ 14 mm - mild activity (+)

15 mm ~ 19 mm - medium activity (++)

20 mm ~ above - high activity (+++)

### Conclusion

Silver colloidal solution was successfully prepared from silver nitrate solution by bamboo leaves extract as reducing agent. Porous ceramic filters were prepared by using optimum ratios of red clay, brown clay and rice husk with 6:3:1 w/w at 800°C. Silver colloidal solution coated and uncoated ceramic filters were examined by EDXRF and SEM analyses. EDXRF analysis revealed that silver was found to be 0.166 % in a coated filter. According to SEM analysis, SEM micrographs of uncoated and coated filters have different microstructures. The morphology of coated filters showed a distribution of silver particles on pores of ceramic surfaces. And also an antimicrobial activity test was performed by using an uncoated filter and coated filter. Concerning the antimicrobial activities, uncoated filter did not show activity but coated filter showed high activity against six microorganisms. Therefore, the prepared silver colloidal solution coated filters

are nontoxic, simple and cost-effective ceramic filters and it can be used for filtering microbiologically unsafe water.

### Acknowledgements

The authors would like to express their profound gratitude to the Department of Higher Education, Ministry of Education, Yangon, Myanmar, for provision of opportunity to do this research and Myanmar Academy of Arts and Science for following to present this paper.

### References

- Collin, C.H. (1965). "*Microbiological Method*". Butterworth and Co., Publishers Ltd., London
- Halem, D.V. (2006). *Ceramic silver impregnated pot filters for household drinking water treatment in developing countries*. M.Sc Thesis Water Management Department, Delft University of Technology
- Likus, W., Bajor, G. and Siemianwicz, K. (2013). "Nanosilver-does it have only one face?". *ACTABP Biochemical Polonica* vol. 60 (4), pp. 495-501
- Mohamed, S.A.R. (2018). "Application of Green Synthesis Ag-NPs from *Lawsonia inermis* (Henna) Plant as Antifungal & Non Toxic Nonmaterial in Drinking Water Purification". *Chemistry Research Journal*, vol. 3 (1), pp. 64-73
- Padmaja, K., Cherukuri, J. and Reddy, M.A. (2007). "Conventional to Cutting Edge Technologies in Drinking Water Purification - A Review". *International Journal of Innovative Research in Science, Engineering and Technology*, vol. 3(2), pp. 9375-9385
- Simeonidis, K., Mourdikoudis, S. and Kaprara, E. (2016). "Inorganic engineered nanoparticles in drinking water treatment: a critical review". *Environmental Science Water Research Technology*, vol. 2, pp. 43-70
- Srikar, S.K., Giri, D.D., Pal, D.B., Mishra, P.K. and Upadhyay, S.N. (2016). "Green Synthesis of Silver Nanoparticles: A Review". *Green and Sustainable Chemistry*, vol. 6, pp. 34-56

## CHARACTERIZATION OF SILICA FROM CLAY MINERALS IN KYAUKPADAUNG TOWNSHIP AND ITS APPLICATION ON LEAD CONTAMINANT WASTE WATER

Theingi Win<sup>1</sup>, Myint Myint Htay<sup>2</sup>, Htun Min Latt<sup>3</sup>

### Abstract

In this research, the clay sample was collected from Khin Phone Chone Village, Kyaukpadaung Township, Mandalay Region. Elemental Analysis of the clay sample was determined by EDXRF technique. The extraction of silica from sample was performed by using various concentration of NaOH and HCl, 2 M, 4 M, 6 M, 8 M and 10 M. Then, silica was prepared from the sample using various stirring time and different temperature. For the sample, stirring time 60 min, 90 min and 120 min were used. By using different temperature such as 60 °C, 80 °C, 100 °C, the optimum temperature for silica extraction was chosen at 80 °C for the sample. The extracted silica was characterized by using EDXRF, FT-IR, XRD and SEM analysis. From EDXRF data, the highest amount of silica were found to be 81.892%. From FT IR spectra, the peak at 1052 cm<sup>-1</sup> for extracted silica was indicated the presence of Si-O stretching. SEM image showed that silica from clay has amorphous nature. The adsorption behavior of extracted silica has been studied. Waste water from lead acid battery industry were treated with extracted silica by using standing method. Before and after treatment, the quantities of waste water were determined. After treatment, the percent removal was found to be 64.76% from sample (1) and 34.84% for sample (2).

**Keywords:** Clay, Silica, EDXRF, FT IR, XRD, SEM analysis, standing method

### Introduction

Clay minerals are the characteristic minerals of the earth's near surface environments. They form in soils and sediments, and by diagenetic and hydrothermal alteration of rocks. Water is essential for clay mineral formation and most clay minerals are described as hydrous aluminosilicate. Structurally, the clay minerals are composed planes of cations, arranged in sheets, which may be tetrahedrally or octahedrally coordinated (with oxygen), which in turn are arranged into layers often described as 2:1 if they involve units composed of two tetrahedral and one octahedral sheet, or 1:1 if they involve units of alternating tetrahedral and octahedral sheets. Additionally some 2:1 clay minerals have inter layer sites between successive 2:1 units which may be occupied by interlayer cations, which are often hydrated. The planer structure of clay minerals give rise to characteristic platy habit of many and to perfect cleavages (Amonette, *et al.*, 1994).

Clay minerals are included in several health care formulations. In particular, they are presented in many semisolid preparations with functions, including stabilization of suspensions and emulsions viscosizing and other special rheological tasks, adsorption of greases, control of heat release, etc (Barnhisel, *et al.*, 1989).

Silica is another name for the chemical compound silicon dioxide. Each unit of silica includes one atom of silicon and two atoms of oxygen. Silica makes up the mineral called quartz and it is the most abundant mineral in the earth's crust. It is the main component of most sand and the primary ingredient in glass. Today, there are many industrials, fillers, electronics and water filtration. In this research work, clay mineral was used as precursor in silica extraction (Ghosh, *et al.*, 2013).

Nowadays lead contamination in a environment is a very important problem of worldwide concerning due to its highly toxic and nonbiodegradable in nature. There are many ways that lead

---

<sup>1</sup> Lecturer, Department of Chemistry, University of Magway.

<sup>2</sup> Dr, Lecturer, Department of Chemistry, Yenanchaung Degree College.

<sup>3</sup> Dr, Lecturer, Department of Chemistry, University of Magway

is released into aquatic system such as natural phenomenon, urban, agricultural and industrial activity.

Adsorption process is considered very effective in industrial wastewater treatment. It proves superior to the other processes by being sludge free and can completely remove even very minute amounts of heavy metal in wastewater. Adsorption process using silica is very effective for removal of heavy metal from wastewater but its high cost has provided the search for alternatives and low-cost adsorption (Sone, *et al.*, 2009).

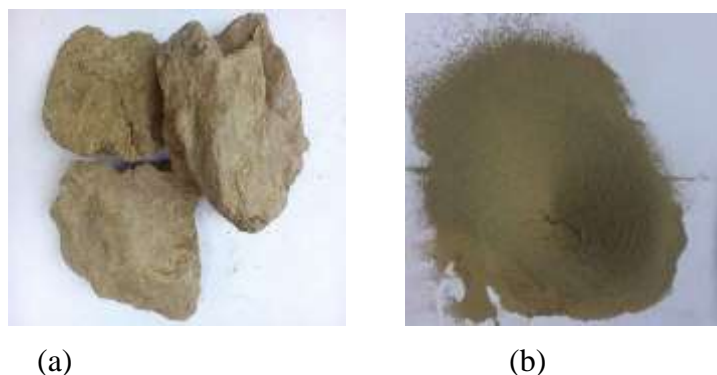
## Materials and Methods

### Sample Collection

Clay sample was collected from Khin Phone Chone Village, Kyaukpadaung Township, Mandalay Region. Afterwards, pieces of macroorganic matters were discarded the clay aggregates were broken up by grinding lightly in motor and pestle. Then, it was meshed through 40 mesh size sieve and the fine powder sample was stored for further uses.



**Figure 1** Sample collection site of Kyaukpadaung Township



(a)

(b)

**Figure 2** (a) and (b) Clay sample in Khin Phone Chone Village, Kyaukpadaung ownship

### Determination of Mineral Content in Clay Mineral

The selected clay sample was measured at the Department of Physics, University of Mandalay by EDXRF technique.

### **Preparation of Silica from Clay Sample with Various Concentrations**

(10 g) of sample was weighed accurately and placed in beaker. And then the sample was washed with 100 mL of distilled water and filtered by filter paper. After that, the residues were used for silica extraction 100 mL of 2 M NaOH was added to the residue in beaker. The beaker was covered for 60 min heated at 80 °C and constant stirring. The solution was filtered by filter paper and carbon residues were washed with 100 mL of boiling water. The filtrate and washing were allowed to cool at room temperature and were precipitated 2 M HCl with constant stirring to pH4. Silica gel started to precipitate when pH decreased to <10. The silica gel was aged for 18 h. This gel filtered by filter paper and dried at 80 °C for 12 h. Similarly, 4 M, 6 M, 8 M and 10 M NaOH and HCl were used for above same procedures to prepare silica.

### **Preparation of Silica by Various Temperature**

According to former procedure, silica powder was prepared by using various temperatures (60 °C, 80° C and 100 °C).

### **Preparation of Silica by Various Reaction Time**

According to former procedure, silica powder was prepared by using various reaction times (60 min, 90 min and 120 min).

### **Characterization of Extracted Silica from Clay Mineral**

#### **Determination of Elemental Contents by EDXRF Technique**

The oxide powder was determined by EDXRF analyzer (EDX-700 spectrometer) to examine the presence of elements in the powder. It was measured at Monywa University. The EDXRF spectrum result of oxide powder is shown on Table 5.

#### **FT IR Analysis**

Prepared pure silica sample was analyzed by FT IR spectrophotometer. The procedure was used in accordance with recommended standard procedure as reported in FT IR spectrophotometer catalogue. The characteristic feature of FT IR spectrum of prepared pure silica is show in Figure 7. The spectral assignment for prepared pure silica sample is also presented in Table 6.

#### **XRD Analysis**

The oxide powder was characterized by X-Ray Diffractometer (XRD 6000, Shimadzu, Japna) for phase analysis at the West Yangon University. The XRD pattern of silica is indicated in Figure 8.

#### **SEM Analysis**

The oxide powder was characterized by SEM (JEOL-JSM-5610 Series, Japan) analyzer to know the particle size and surface morphology of the powder. It was measured at the West Yangon University. The SEM microgram of oxide powder is indicated in Figure 9.

### **Determination of Removal Efficiency of Silica by Standing Method**

#### **(Column method)**

#### **Materials**

Lead (II) nitrate

Sodium hydroxide solution (0.1 - 1.0 M)

Hydrochloric acid (0.1- 1.0 M)

## Apparatus

Column, Measuring Cylinder, Beaker, Funnel, Filter Paper

## Procedure

(5 g) of silica was weighed and placed in the column. 120 mL of mg/mL of lead aqueous solution was poured into the column containing silica. The lead solution was passed through the silica and the filtrate was collected at room temperature the flow rate was 15 drops per minute. After that,  $Pb^{2+}$  ion in the filtrate was determined by atomic adsorption spectrophotometer.

## Sample Collection (Waste water)

The waste water sample was collected from Shwe Nan Taw Battery Factory, Industrial Zone (2), Mandalay Region. Two different site of waste water were collected. Sample (I) was collected from the wastewater tank of the industry and sample (II) was collected from pond behind the Shwe Nan Taw Battery Factory. The wastewater from the tank drains directly into this pond.

## Treatment of Wastewater by Extracted Silica (Standing Method)

### Materials

Industrial Wastewater

### Apparatus

Column, Measuring Cylinder, Beaker, Filter Paper

### Procedure

(5 g) of silica was weighed and placed in the column. 120 mL of waste water of was poured into the column containing silica. The industrial wastewater was passed through the silica and filtrate was collected at room temperature. The flow rate was 15 drops per minute. Before and after treatment,  $Pb^{2+}$  ion concentration was determined by atomic absorption spectrophotometer. Lead content in waste water (before and after treatment) is indicated in Table 7 and 8.

## Results and Discussion

### Mineral Contents of Clay Sample by EDXRF Analysis

The observed spectrum indicates that 11.850% Si, 4.826% Fe, 3.740% Al, 0.487% K and 0.434% Ca for clay sample. Silica is the rich mineral in clay sample. In this research work, clay sample was used as precursor in silica extraction. For qualitative determination of elements in clay sample, EDXRF spectrophotometer was used. The relative abundance of elements in clay sample is presented in Table 1.

**Table 1 Relative Abundance of Mineral Contents in Clay Sample by EDXRF Analysis**

No.	Elements	Relative Abundance (%)
1	Si	11.850
2	Fe	4.826
3	Al	3.740
4	K	0.487
5	Ca	0.434

### Silica Content with Various Concentrations of NaOH and HCl

In silica extraction, various concentrations of NaOH and HCl (2M, 4M, 6M, 8M and 10 M) were used. The yield percent are shown in Table 2 and Figure 3.

Silica content is directly proportion to the concentration of NaOH and HCl. Optimum concentration was found to be 8 M for both NaOH and HCl. Beyond these concentrations the silica content does not change.

**Table 2 Yield (%) of Silica with Various Concentrations**

No.	Concentration (M)		Weight of silica (g)	Yield of silica (%)
	NaOH	HCl		
1	2	2	1.5	15
2	4	4	1.6	16
3	6	6	2.5	25
4	8	8	3.8	38
5	10	10	3.8	38

Sample - 10 g, Reaction time - 60 min

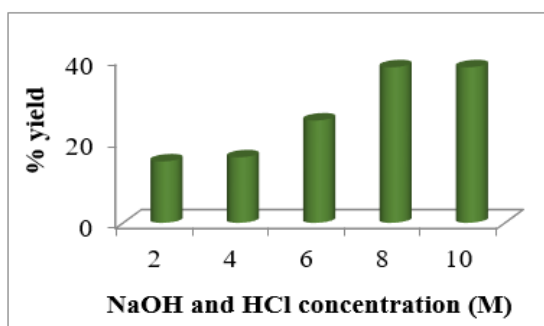


**Figure 3 Yield (%) of silica with various concentration of NaOH and HCl**

**Silica Content with Various Reaction Time of Clay Sample**

In silica extraction, various reaction time (60 min, 90 min and 120 min) were used in 8 M NaOH and HCl. The yield percent are shown in Table 3 and Figure 4.

Silica content is directly proportion to the reaction time used. Optimum times was found to be 90 min. Beyond these times, the silica content is decreased.

**Table 3 Yield (%) of Silica with Various Reaction Time**

No.	Concentration of NaOH (M)	Concentration of HCl (M)	Time (min)	Weight of silica (g)	Yield of silica (%)
1	8	8	60	3.8	38
2	8	8	90	5.0	50
3	8	8	120	3.9	39

Sample - 10 g

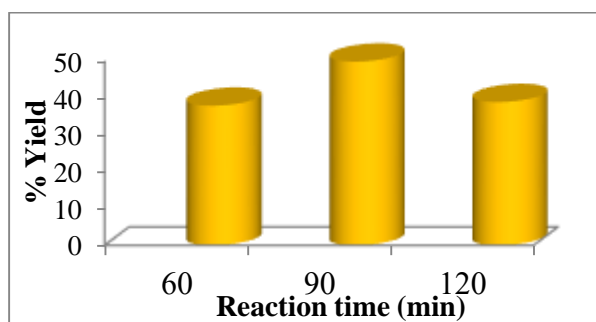


**Figure 4 Yield (%) of silica with various reaction time**

### Silica Content with Various Temperature

In silica extraction, various temperature (60°, 80° and 100° C) were used in 8 M NaOH and HCl. The yield percents are shown in Table 4 and Figure 5.

Silica content is directly proportion to the various temperature. Optimum temperature was found to be 80 °C. Beyond these temperature, the silica content is decreased.

**Table 4 Yield (%) of Silica with Various Temperature**

No.	Concentration of NaOH (M)	Concentration of HCl (M)	Temperature (°C)	Weight of silica (g)	Yield of silica (%)
1	8	8	60	38	38
2	8	8	80	4.5	45
3	8	8	100	4.0	40

Reaction time - 90 min, Sample - 10 g

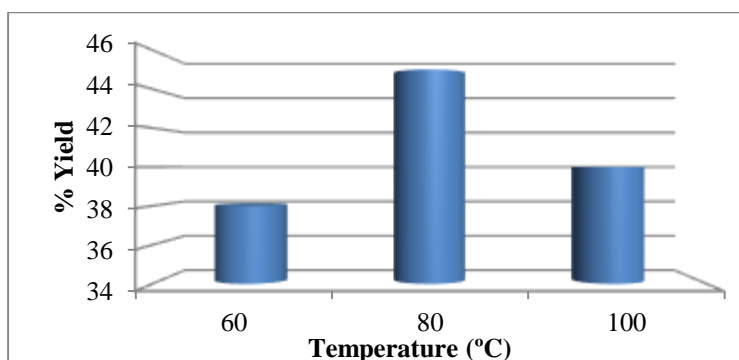


**Figure 5** Yield (%) of silica with various temperature

### Characterization of Extracted Silica

#### EDXRF Analysis of Extracted Silica

For qualitative determination of elements in pure silica powder samples, EDXRF technique was used. EDXRF spectrum of the prepared pure silica samples are shown in Figure 6. The relative abundance of metals oxide in these samples are presented in Table 5.

According to EDXRF analysis, it can be observed that silica (SiO<sub>2</sub>) contents were found to be the highest (78.162%) in these samples. When the results of EDXRF for pure silica were compared with XRD diffractogram, it was found that these results were agreed with each other.

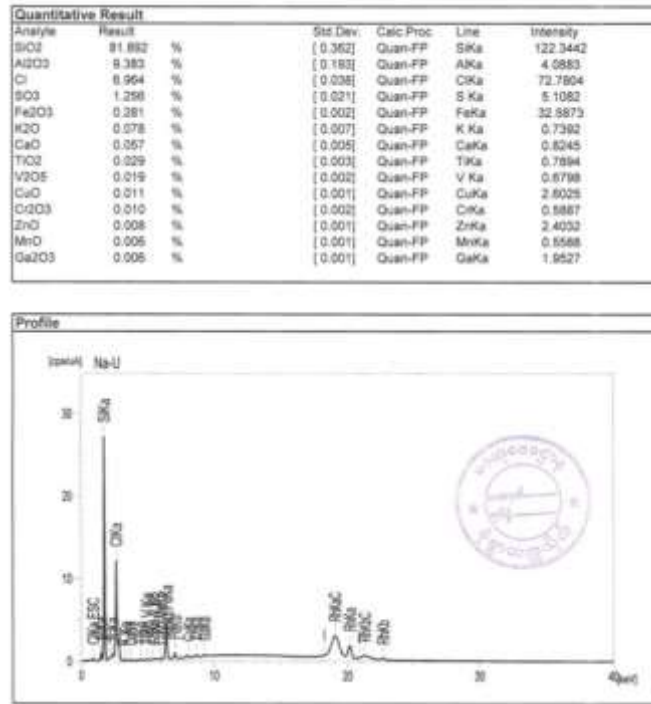


Figure 6 EDXRF spectrum of extracted Silica

Table 5 Relative Abundance of Some Oxides in the Extracted Silica

No	Analyte	Relative Abundance (%)
1	SiO <sub>2</sub>	78.162%
2	Al <sub>2</sub> O <sub>3</sub>	11.519%
3	Cl	8.282%
4	SO <sub>3</sub>	1.124%
5	Fe <sub>2</sub> O <sub>3</sub>	0.635

**FT IR Spectra of Pure Silica**

The FT IR spectrum of extracted silica sample is shown in Figure 7. The bond assignment of extracted silica sample is tabulated in Table 6. According to FT IR data, the bands at 1052cm<sup>-1</sup> (Si-O stretching vibration), 789 cm<sup>-1</sup> (Si-O-Si stretching vibration), 442 cm<sup>-1</sup> (Si-O in-plane bending vibration) were observed in this sample.

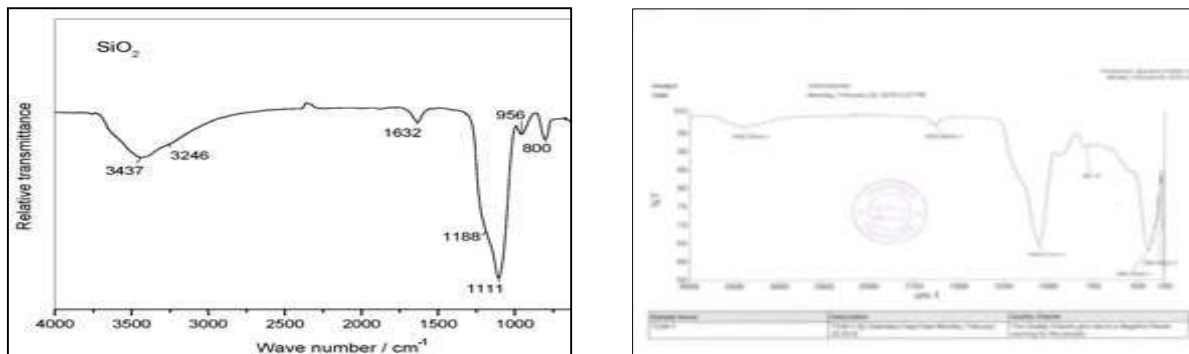


Figure 7 FT IR spectra of reference silica and extracted silica

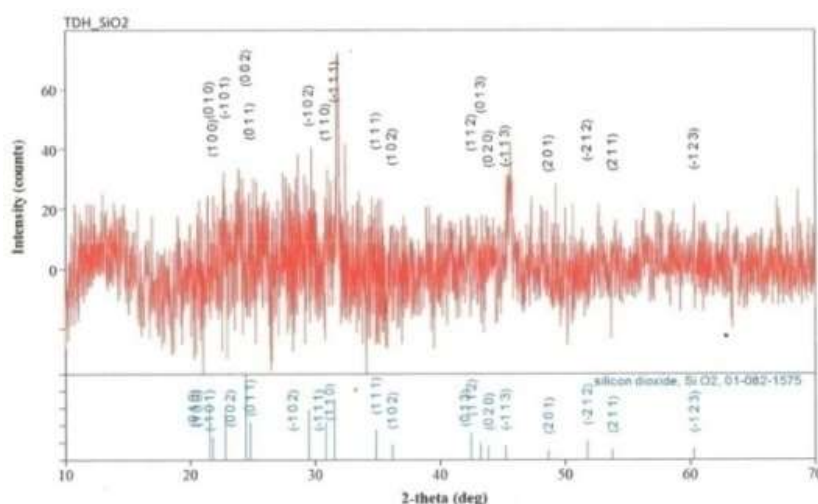
**Table 6 Vibrational Mode for SiO<sub>2</sub> Groups per unit Cell of Extracted Silica**

Assignment	Spectral region assigned for polymorphs of SiO <sub>2</sub> (cm <sup>-1</sup> )	Spectral region assigned for polymorphs of SiO <sub>2</sub> (cm <sup>-1</sup> ) Literature value*
Si-O stretching vibration (motion primarily associated with the oxygen atom)	1052	1200 – 1000
Si-O stretching vibration (motion primarily associated with the silicon atom)	789	825 – 600
Si-O bending vibration	442 392	600 – 390
Distortion modes	383	380 – 100

\* Ellis, 1958

### XRD Diffractogram of Extracted Silica

The X-ray diffraction pattern of extracted silica is shown in Figure 8. These XRD pattern shows ten characteristic peaks (123), (211), (212), (201), (113), (020), (102), (111), (110), (011) for extracted silica. These peaks support the amorphous nature for extracted silica.

**Figure 8** X-ray diffractogram of extracted silica

### SEM Analysis of Extracted Silica with 8 M HCl from Clay Powder

SEM measurement for surface analysis was carried on silica from clay mineral. The SEM micrographs of extracted silica are shown in Figures 9 (a) and (b). It can be clearly seen that the crystalline and amorphous nature of silica was observed in SEM images. From surface morphology of silica sample, many small pores and particles with diameter <10 μm were seen on the surfaces of silica sample.



Figure 9 SEM micrographs of extracted silica from clay powder

**Removal Efficiency of Silica**

The removal efficiency of silica was determined by using aqueous lead solution (100 ppm) with two methods such as shaking and column methods. Shaking method is more effective than standing method. But shaking method is not benefited for waste water treatment. Thus, only standing method is used for waste water treatment along this research. The percent removal of metal ion (Lead) was described in Table (7).

$$\% \text{ removal of metal ion} = \frac{C_o - C_e}{C_o} \times 100$$

C<sub>o</sub> = initial concentration (ppm)

C<sub>e</sub> = final concentration (ppm)

**Table 7 Percent Removal of Metal Ion (Lead)**

Method	Initial concentration (ppm)	Final concentration (ppm)	% removal
Standing	36.51	12.86	64.77

**Lead Content in Waste Water**

Lead content in waste water determined by using AAS method. This results are described in the following Table 8.

According to AAS results, silica can remove 64.76% of Lead from sample (1) and 34.84% of lead from sample (2). Comparing the removal % of lead it can be clearly seen that the adsorption efficiency is depended on the concentration of adsorbate. These results indicate that the standing method is depended on the flow rate.

**Table 8 Determination of Lead Content in Waste Water (Before and After treatment)**

No	Lead (ppm)	Before treatment	After treatment	% removal
1	Sample (1)	2.049	0.722	64.76
2	Sample (2)	0.597	0.389	34.84

## Characterization of Extracted Silica and Lead Adsorbed Silica

### EDXRF spectra of extracted silica

The EDXRF spectrum of extracted silica is shown in Figure 10. These spectra shown 62.891% of silicon and small amount of some minerals are presented in extracted silica.

### EDXRF spectrum of lead adsorbed silica (sample-1)

The EDXRF spectrum of lead adsorbed silica for sample (1) is shown in Figure 11. Silica can adsorb 27.194% of lead from waste water.

### EDXRF spectrum of lead adsorbed silica (sample -2)

The EDXRF spectrum of lead adsorbed silica for sample (2) is shown in Figure 12. Silica can adsorbed 0.265% of lead from waste water.

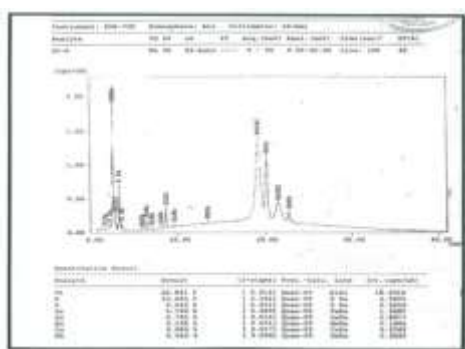


**Figure 10** EDXRF spectrum of extracted silica

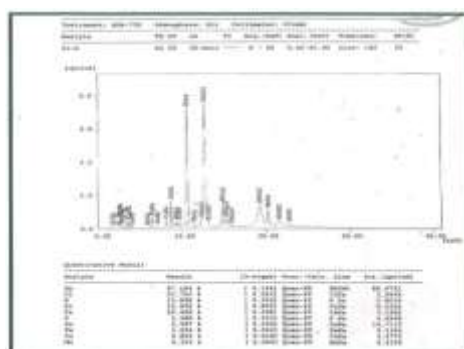


**Figure 11** EDXRF spectrum of lead adsorbed silica (sample -1)

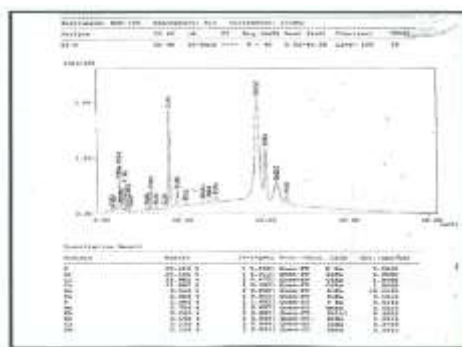


**Figure 12** EDXRF spectrum of lead adsorbed silica (sample - 2)

## Conclusion

In this research work, silica was extracted from Montmorillonite, clay mineral. The clay mineral was collected from Khin Phone Chone Village, Kyaukpadaung Township. The silicon contents found in clay minerals were determined by EDXRF. The observed spectra indicated that the amount of silicon was the highest, 11.850% in clay sample.

In silica extraction, the optimum condition such as NaOH concentration in the range of (2 to 10 M) was determined. 8M NaOH was found to be highest yield 38.00% of silica. Increasing the alkali solution, increase the % yield of SiO<sub>2</sub> till 8.0 M, beyond these concentrations silica content does not significantly change.

The alkaline extraction was investigated at various reaction time of 60, 90 and 120 min. Silica content is directly proportion to the reaction time used. Optimum time was found to be 90 min. Beyond these time, the silica content is decreased. The preparation of silica was investigated at various temperature of 60 °C, 80 °C and 100 °C. Optimum temperature was found to be 80 °C.

The extracted silica was characterized by using EDXRF, FT IR, XRD and SEM analysis. From EDXRF data, the highest amount of silica were found to be 81.892% for clay sample.

From FTIR spectra, the peak at 1052  $\text{cm}^{-1}$  for extracted silica was indicated the presence of Si-O stretching modes involving motion primarily associated with the oxygen atom. It is obvious that the extracted silica is identical to reference silica.

Crystal structure identification was achieved by X-ray diffraction (XRD), from the XRD diffractogram ten characteristic peaks for  $\text{SiO}_2$  (silica) observed in extracted pure silica. SEM image showed that silica from clay has amorphous nature.

The adsorption character of silica was determined by using lead solution (100 ppm) with two methods, shaking and standing method. It can be absorb (96.65%) for shaking and (64.77%) for standing method, respectively. In this research work, only standing method was used to treatment of wastewater.

In addition, the silica was used in treatment of lead contaminant wastewater from lead-acid battery factory. Silica can reduce pollutant level of wastewater. Toxic heavy metal pollutants cause several environmental problems to environment. The most common heavy metal pollutant is lead. Silica can also reduce lead content in wastewater. The lead content in wastewater sample (1) and (2) were found to be 2.049 ppm and 0.597 ppm respectively.

After treatment, the lead content left was to 0.722 ppm and 0.389 ppm. The % removal was found to be 64.76% for sample (1) and 34.84% for sample (2).

EDXRF spectra data, lead adsorbed silica for sample (1) and sample (2) were found to be 27.194% and 0.265% respectively.

In this research work, one of the abundant clay minerals, montmorillonite can be converted into valuable product (silica) used for several applications in industry. The silica obtained is very amorphous. The pure silica was synthesized from clay sample, successfully.

### Acknowledgements

I am extremely grateful to Dr Khin Maung Oo, Rector, Dr Thidar Aung, Professor and Head, Department of Chemistry, Magway University, for their permitting, understanding, kindly helps and good guidance on my study.

### References

- Amonette, J.E., Zelazny, L. W., Eds. (1994). *Quantitative Methods in Soil Mineralogy*; Soil Science Society of America Miscellaneous Publication: Madison, WI.
- Barnhisel, R.; P., Bertsch. (1989). Chlorites and Hydroxy-Inter-layered Vermiculite and Smectite. In *Minerals in Soil Environments*; Dixon, J., Weed, S., Eds.; Soil science Society of America: Madison, WI, 729-788.
- Brady, N. (1990). Soil Colloids: Their Nature and Practical Significance. *The Nature and Properties of Soils*, 10th Ed.; Macmillan Publishing Co.: New York, 177-212.
- Brindley, G.W. (1955). "Clays and clay Technology". California Division of Mines, Sanfranciso, Bulletin 169, P.33.
- Ghosh, R., and Bhattacharjee, S. (2013). "A Review Study on Precipitated Silica and Activated Carbon from Rice Husk", *Chemical Engineering & Process Technology*, Department of Chemical Engineering, Calcutta Institute of Technology, India, 4 (4) 1-7.
- Sone, H., Fugetsu, B., Tanaka, S. (2009). "Selective elimination of Lead (II) Irons by alginate/polyurethane composite foams," *Journal of Hazardous Materials*, Vol. 162, pp.423-428.

## ISOLATION, IDENTIFICATION AND CHROMIUM ADSORPTION BEHAVIOUR OF A CHROMIUM-RESISTANT *PAECILOMYCES* sp.

Ohnmar Aye<sup>1</sup>, Khin Myo Myint<sup>2</sup>

### Abstract

The present study was carried out to investigate metal resistant and adsorption strain. A chromium-resistant fungus M-1 was isolated from soil sample by conventional plating method. The isolated fungus was studied on the basis of morphological, microscopical characteristics and identified with the help of literature keys of Ando (2016). According to morphology and distinct characters, the fungal strain was identified as *Paecilomyces* sp. The fungal growth in metal resistant against Cr<sup>6+</sup> ion at different concentration of 10 mM, 20 mM, 30 mM, 40 mM and 50 mM was studied. It was observed that *Paecilomyces* sp. was found to be resistant against 50 mM of Cr<sup>6+</sup> ion. The biomass of chromium-resistant fungus was used for biosorption experiment by varying contact time and biomass dose. The biosorption of Cr<sup>6+</sup> ion from industrial wastewater by chromium-resistant biomass showed 45.48 % removal and 1.9058 mg g<sup>-1</sup> of Cr<sup>6+</sup> ion at optimum contact time 8 h and biomass dose 0.4 g respectively. From the results, that *Paecilomyces* sp. showed chromium-resistant behaviour and biosorption potential for removal of Cr<sup>6+</sup> ion from industrial wastewater.

**Keywords:** chromium-resistant, biosorption, contact time, biomass

### Introduction

Microbes often have other genetically determined defences against harmful metals when they cannot detoxify them. Fungi can be screened as potential bioremediation agents due to their greater growth capacity and reach by virtue of mycelial branching, a greater potential to produce a number of enzymes, and they are good accumulators of various metals. Exploration of various habitats may lead to fungal strains with diverse potentials.

Industrial and metallurgical processes release a wide range of toxic metal pollutants as their waste products. Chromium is one of the metals of most immediate concern according to the World Health Organization (1984). Chromium may be present in effluent in various chemical forms. Hexavalent chromium compounds tend to be more mobile and toxic than trivalent chromium compounds (Calder, 1988) while Cr(VI) may be detrimental to human beings and animals and have pronounced adverse effects on plants and aquatic life. Most of the current methods of chromium removal are expensive and inconsistent, and may generate toxic sludge that requires careful disposal (Wild, 1987). Bioremediation using various microorganisms can be a more promising alternative than chemical treatment of such toxicants. Microbes (both prokaryotes and eukaryotes) have the ability to bind metal ions in the external environment at the cell surface, or to transport them into the cell. Some may form metabolic products such as acids or ligands that dissolve base metals dissolved in mineral or anions such as sulfide or carbonate that precipitate dissolved metal ion (Ehrlich, 1997).

The aim of the study was to examine the potential of metal tolerant fungal strain associated with metal tolerant and accumulate hexavalent chromium, one of the most hazardous heavy metals, its effect on fungal biomass production and thus, to examine their application as biosorption process for wastewater treatment.

---

<sup>1</sup> Dr, Associate Professor, Department of Chemistry, Dawei University

<sup>2</sup> Dr, Professor, Department of Botany, Loikaw University

## Materials and Methods

### Media Used for Isolation

(1) Beef-extract Peptone Medium (Ando, 2004)		(2) Potato Dextrose Agar (PDA) Medium (Ando, 2004)	
Beef-extract	3.0 g	Potato	200 g
Peptone	10.0 g	Dextrose	20 g
NaCl	10.0 g	Agar	18 g
DW	1.0 L	DW	1.0 L
pH	6.5	pH	6.5

(After autoclaving chloramphenicol 0.03 g was added to both media.)

### Isolation of Chromium-Resistant Fungi

Chromium-resistant fungus was isolated by using conventional plate method. The stock solution of  $\text{Cr}^{6+}$  ion containing concentration of  $1000 \text{ mgL}^{-1}$  was prepared by dissolving 2.829 g of potassium dichromate,  $\text{K}_2\text{Cr}_2\text{O}_7$  in 1000 mL of deionized water and this solution was further diluted with water to desired concentration of test solution. Soil suspension was added to beef-extract peptone liquid medium containing 2mM of  $\text{Cr}^{6+}$  ion solution. The cultures were incubated on a rotatory shaker at room temperature, 180 rpm for 3-5 days. The spore suspension was spotted on metal containing agar plates (PDA). The plates were incubated at  $25^\circ\text{C}$  for 7 days and the growth of the chromium-resistant fungus M-1 was observed.

### Identification of Isolated Fungi

Fungal isolate was studied for its morphological features under light microscope. The culture was identified on the basis of morphological (colonial morphology, colour, shape, diameter and colony appearance) and microscopical characteristics (septation in mycelium, shape and structure of conidia).

### Metal-Tolerant Test for Fungi

The metal tolerance of fungi was determined by liquid (PDB) and solid (PDA) media. In liquid medium, 1 mL inoculum (spore suspension) was inoculated in 500 mL of Potato Dextrose Broth medium containing different concentrations of  $\text{Cr}^{6+}$  i.e., 25, 50 and 100 mM, as potassium dichromate. Each set was prepared in triplicate. One set of medium without  $\text{Cr}^{6+}$  was also inoculated, which was kept as control. The inoculated flasks were incubated at room temperature for 15 days and effect of chromium on biomass (and in that way tolerance to  $\text{Cr}^{6+}$ ) was recorded in terms of dry weight of the inoculated fungi.

A series of solid PDA media which contained different concentrations of 10, 20, 30, 40 and 50 mM of  $\text{Cr}^{6+}$  ion. The spore suspension was spotted on metal containing agar plates. The strain was orderly inoculated and cultivated from low concentration to high concentration level. The inoculated plates were incubated at  $25^\circ\text{C}$  at least for 15 days to observe the growth of fungus with chromium-resistant. Three replicates for each concentration were recorded. The PDA medium without metal was also inoculated as a control plate. The concentration which fungal isolates fail to grow was estimated as minimum inhibitory concentration. MIC is defined as the lowest concentrations of metal that inhibit visible growth of the isolate (Hassen and Saidi, 1998).

## Study on Biosorption of Toxic Heavy Metal Cr<sup>6+</sup> Ion from Industrial Wastewater

The biosorption process was generally applied for the removal of toxic heavy metal Cr<sup>6+</sup> ion from industrial wastewater.

Industrial wastewater sample was collected from Shwe Lin Ban Industrial Zone, Shwe Phyi Thar Township, Yangon in November, 2018. The wastewater sample was taken at a distance of about 1 m from the point source of drainage and at a depth of 0.2 m below the surface of water with sterilized prewashed polyethylene container. The initial concentration of Cr<sup>6+</sup> ion in the wastewater was analyzed by Atomic Absorption Spectrophotometer (AAS) from Ministry of Education, Department of Research and Innovation (DRI), Yangon.

In this study, the fungal isolate *Paecilomyces* sp. was used as biosorbent for removal of Cr<sup>6+</sup> metal ion from industrial wastewater. The heavy metal removal was determined by the effect of biomass dose (0.1 g, 0.2 g, 0.3 g, 0.4 g and 0.5 g) and contact time (2 h, 3 h, 4 h, 6 h, 8 h, and 10 h).

## Results and Discussion

### Identification of Isolated Fungi

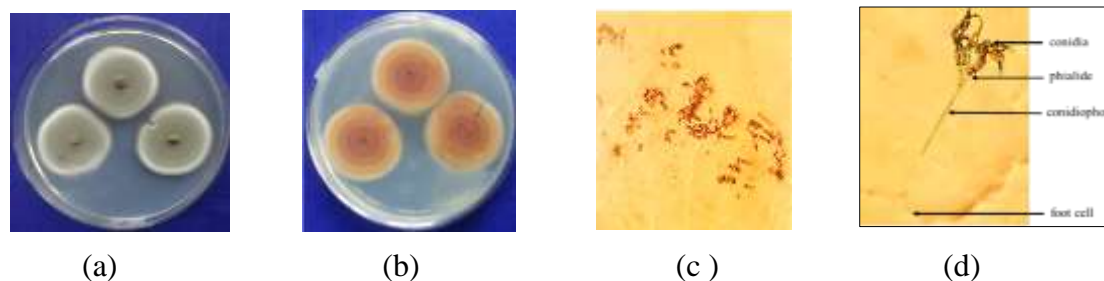


**Figure 1** Morphological characters of isolated fungi (a) Front view (b) Reverse view (c) Conidia (d) Microscopical description

### Morphological and Microscopical Description of M-1

The colonies of isolated fungus M-1 grow rapidly and mature within 3 days. The colonies are flat and powdery or velvety in texture. The colour is initially white and becomes pale green or olive brown colour. The reverse colour is yellowish brown (Figure 1 a, b).

The microscopic character showed mycelia had septate hyaline hyphae and branches. Slender conidiophores are grown out from mycelia. The conidia are long, dry chains of single-celled, smooth or rough hyaline to darkly coloured, ovoid conidia are produced in the basipetal succession from the phialides (Figures 1 c, d). The phialides of this fungus taper towards their apices and are organized slightly apart from each other. The phialides of *Penicillium* have thicker apices and are organized in tight clusters. Colonies of *Penicillium* are commonly blue-green in colour while those of *Paecilomyces* are not (Samson, 1974).

### Identification key of isolated fungi

The isolated fungus was identified as *Paecilomyces* sp. according to keys of Ando, (2016) as follow.

1. Conidial Ontogeny -
  - (i) Conidial production is chain
  - (ii) Type of conidial production is Phialo type
  - (iii) Type of conidial ontogeny is Enteroblastic chain

2. Conidiophores - Typical conidiophores with branches
3. Conidiophores - Elongate along with conidial production
4. Arrangement of Conidiogenous cells  
- Independent (Parallel)
5. Development of Conidiogenous cells  
- Stable
6. Conidial production loci of Conidiogenous cells - Mono
7. Conidia (i) Shape - Simple  
(ii) Spore - Amerospore
8. Hyphae - with septa regularly
9. Identified this fungus as *Paecilomyces* sp.

### Scientific Classification

Kingdom : Fungi  
 Phylum : Ascomycota  
 Class : Eurotiomycetes  
 Order : Eurotiales  
 Family : Trichocomaceae  
 Genus : *Paecilomyces* sp.

**Table 1 Morphological and Physical Characteristic of the Isolated Fungi**

Characteristics	<i>Paecilomyces</i> sp.
Colony diameter	42.3 mm
Conidial colour	Brown
Conidial shape	Elliptic or ovoid
Conidiophore colour	Hyaline
Mycellial colour	Pale green
Colonial reverse	Brownish yellow
No. of sterigmata	Present in one series

### Screening of Metal-Tolerant Fungi



**Figure 2** Growth of *Paecilomyces* sp. after exposure to concentration of  $\text{Cr}^{6+}$  ion in PDB medium

In this study, chromium-tolerant fungus was screened by PDB and PDA medium. Fungus *Paecilomyces* sp. showed luxuriant growth in PDB medium containing  $\text{Cr}^{6+}$  ion. Effect of  $\text{Cr}^{6+}$  ion on growth of fungi was estimated in terms of dried weight of biomass (Figure 3). The biomass was dried at  $60^\circ\text{C}$  to obtain constant weight. The results suggested that biomass production was higher in control and lower in  $\text{Cr}^{6+}$  metal ion treated media.

**Table 2 Dry Cell Weight of Fungal Biomass *Paecilomyces* sp.**

No.	Cr <sup>6+</sup> Concentration (mM)	Dry weight (g/100 mL)
1	Control	1.234
2	25	0.523
3	50	0.427
4	100	0.211

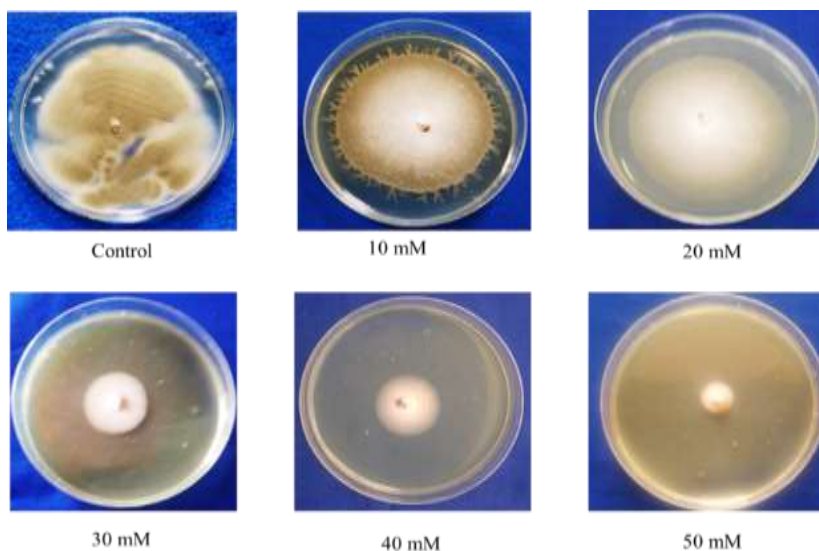


**Figure 3** Growth of *Paecilomyces* sp. after exposure to different concentration of Cr<sup>6+</sup> ion in PDA medium

In solid PDA medium, *Paecilomyces* sp. appeared white density mycelia and maximum growth of isolates at 10 mM. When the metal ion concentration gradually increased, the fungal cultural growth was inhibited. Then the metal concentration reached 50 mM, the fungi can failed to grow after culturing for 15 days, and 50 mM was thought as the MIC of Cr<sup>6+</sup> ion. It was found that the low concentration of the metal, less toxicity to fungal cell whereas higher concentration of metal, high toxicity to the cell and more inhibited the cell growth.

**Study on Biosorption of Toxic Heavy Metal Cr<sup>6+</sup> Ion from Industrial Wastewater**

**Table 3 Effect of Biomass Dosage on Removal of Cr<sup>6+</sup> Ion by *Paecilomyces* sp.**

Contact time = 8 h  
 pH = 6.0  
 Temperature = 30°C

Dosage (g)	Initial Concentration (mg/L)	Final Concentration (mg/L)	Percent removal
0.1	0.62	0.394	36.45
0.2	0.62	0.380	38.71
0.3	0.62	0.356	42.58
0.4	0.62	0.338	45.48
0.5	0.62	0.344	44.51

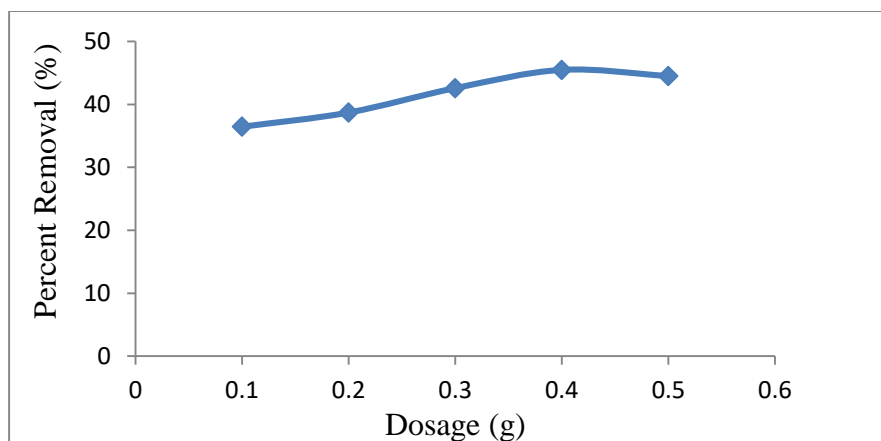


**Figure 4** Effect of biomass dosage on removal of  $\text{Cr}^{6+}$  ion by *Paecilomyces* sp.

**Table 4** Effect of Contact Time on Removal of  $\text{Cr}^{6+}$  Ion by *Paecilomyces* sp.

Biomass dose = 0.4 g  
 pH = 6.0  
 Temperature = 30°C

Contact Time (h)	Initial concentration (mg/L)	Final concentration (mg/L)	Percent removal
2	0.62	0.380	38.70
4	0.62	0.368	40.64
6	0.62	0.357	42.41
8	0.62	0.338	45.48
10	0.62	0.359	42.09

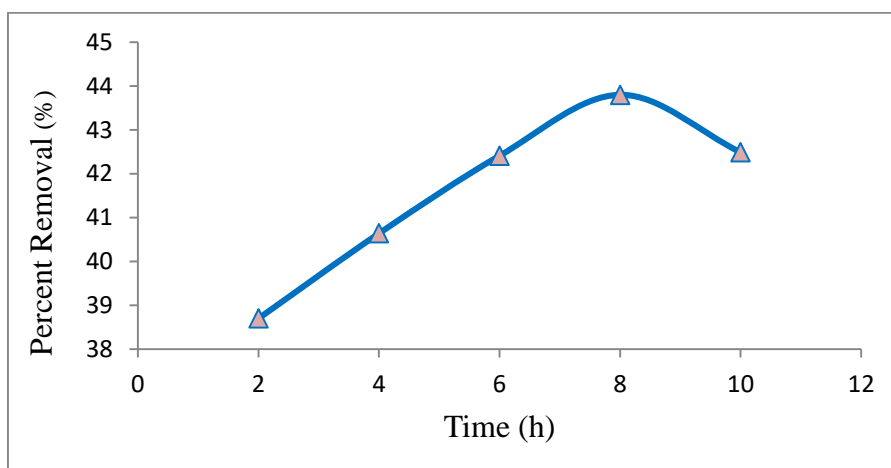


**Figure 5** Effect of contact time on removal of  $\text{Cr}^{6+}$  ions by *Paecilomyces* sp.

Table 3 and Figure 4 showed the effect of biomass dose on percent removal of metal ions. It was observed that removal percent increased with increased in dosage and significantly decreased at dosage 0.5 g. This may be due to the increase in surface area and number of available active site for adsorption of metal ions with saturation of cell surface.

The removal percent on effect of contact time are shown in Table 4 and Figure 5. It was found that percent removal increased gradually to the maximum adsorption and then to attain

equilibrium with increased in contact time. It may be explained by initial rapid uptake due to surface adsorption and subsequent slow uptake due to the specific sites is saturated with metal ions.

### Adsorption Isotherm Assessment

Langmuir equation which is valid for monolayer sorption on to a surface with a finite number of identical sites and the linearized form of this model equation is given as

$$\frac{C_e}{q_e} = \frac{C_e}{q_{\max}} + \frac{1}{(q_{\max} b)}$$

Where  $C_e$  is the equilibrium concentration,  $q_{\max}$  is the maximum amount of the metal ion per unit weight of the adsorbent to form a complete monolayer and  $b$  is a constant related to the affinity of the binding sites.  $q_{\max}$  and  $b$  can be determined from the linear plot of  $C_e/q_e$  versus  $C_e$ .

The empirical Freundlich model also considers mono molecular layer coverage of solute by the adsorbent.

$$\log q = \log K + \frac{1}{n} \log C$$

Where,  $K$  and  $n$  are the Freundlich constants characteristics of the system. The  $q_{\max}$  value of these isotherm models reflects the metal affinity to the sites of biomass. That is the number of metal ions which form a complete monolayer on the surface of the biomass. Adsorption isotherm shows the distribution of solute between the liquid and solid phases and can be described by the standard Langmuir isotherm (Figure 6 and Table 5) and Freundlich isotherm model (Figure 7 and Table 6). The linearized Langmuir and Freundlich adsorption isotherm parameters showed the value of linear regression coefficients. The coefficients of determination ( $R^2$ ) are 0.9730 for Langmuir model and 0.9998 for Freundlich isotherm model and the values for linear regression ( $R^2$ ) indicated that the adsorption nature is well fitted with both models.

**Table 5 Langmuir Isotherm Data for the Biosorption of  $Cr^{6+}$  ion by *Paecilomyces* sp.**

$C_e$ (mmol L <sup>-1</sup> )	$q_e$ (mmol g <sup>-1</sup> )	$C_e/q_e$ (g L <sup>-1</sup> )
6.02	19.86	0.30
6.04	9.87	0.61
6.05	6.57	0.92
6.06	4.92	1.23
6.07	3.92	1.54

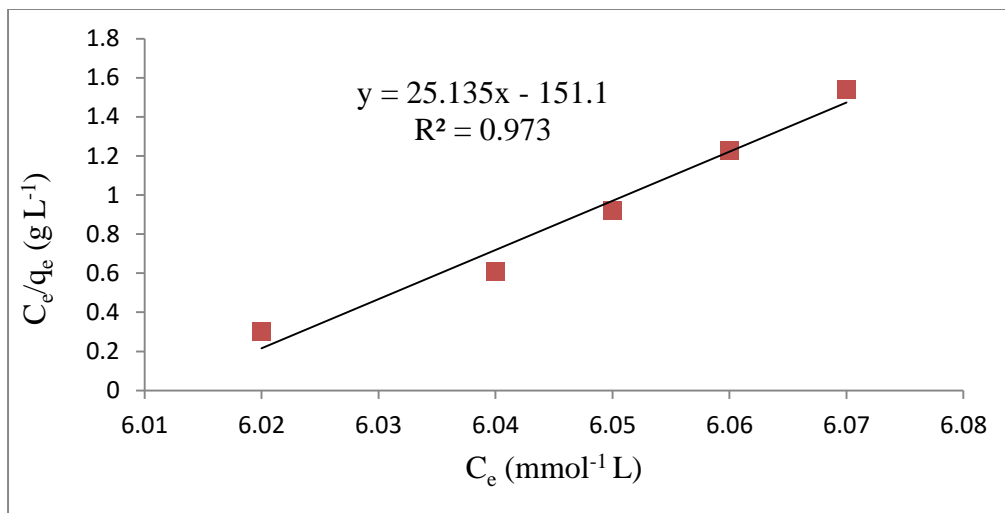


Figure 6 Langmuir adsorption isotherm of Cr<sup>6+</sup> ion by *Paecilomyces* sp.

Table 6 Freundlich Isotherm Data for the Biosorption of Cr<sup>6+</sup> ion by *Paecilomyces* sp.

$C_e$ (mmol L <sup>-1</sup> )	$q_e$ (mmol g <sup>-1</sup> )	$\log C_e$ (mmol L <sup>-1</sup> )	$\log q_e$ (mmol g <sup>-1</sup> )
6.0274	19.8629	0.7801	- 0.10783
6.0480	9.8798	0.7816	- 0.10701
6.0563	6.5728	0.7822	- 0.10668
6.0635	4.9205	0.7827	- 0.10639
6.0738	3.9261	0.7835	- 0.10598

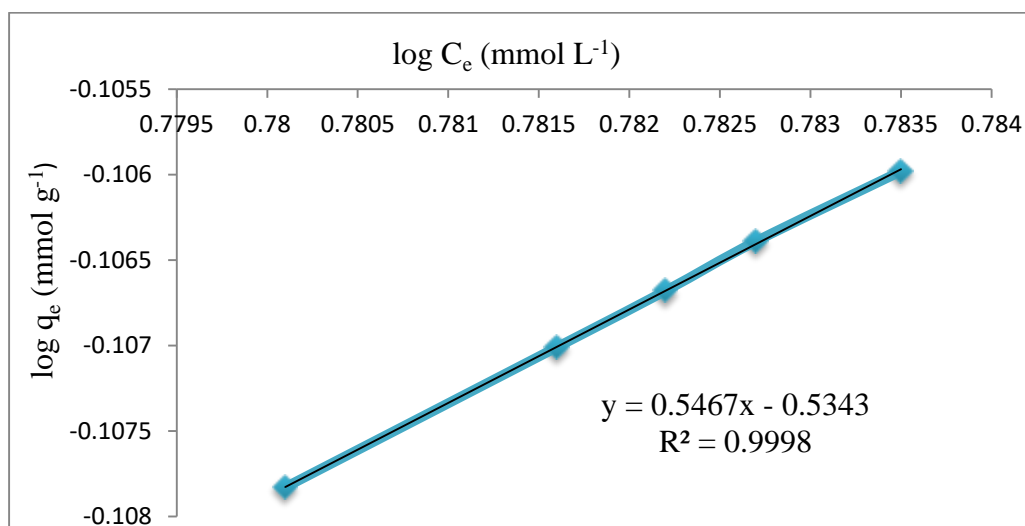


Figure 7 Freundlich adsorption isotherm of Cr<sup>6+</sup> ion by *Paecilomyces* sp.

**Table 7 Isotherm Parameters for the Biosorption of Metal Ions**

Metal Ions	Biomass	Langmuir Model		Freundlich Model			
		$q_{\max}$ (mg g <sup>-1</sup> )	R <sup>2</sup>	b (L mg <sup>-1</sup> )	K <sub>f</sub>	R <sup>2</sup>	n
Cr <sup>6+</sup>	<i>Paecilomyces</i> sp.	1.9058	0.9730	0.0036	0.3137	0.9998	1.9632

### Conclusion

Soil fungi was isolated from agriculture soil samples by using conventional plate method. Morphological and microscopic characters of the isolated fungi were identified by using keys of Ando (2016). According to morphology and distinct characters, chromium-resistant fungus M-1 was identified as *Paecilomyces* sp. Fungal isolate was tested for their tolerance against different concentrations of Cr<sup>6+</sup> metal ion. In PDB liquid medium, isolate exhibited fair tolerance towards high chromium concentration. The results suggested that biomass production was higher in control and lower in Cr<sup>6+</sup> metal ion treated media. In solid PDA medium, the metal concentration reached 50 mM, the fungus failed to grow after culturing for 15 days and 50 mM was thought as the MIC of chromium ion. Thus, it can be concluded both media have similar potential to tolerate various concentration of Cr<sup>6+</sup> ion. In the biosorption study of wastewater treatment, the industrial wastewater was collected and initial metal ion concentrations of chromium in collected sample was analyzed. According to results, ability of *Paecilomyces* sp. was found to adsorb the chromium ion with maximum removal of 45.48 % at optimum dose 0.4 g and contact time 8 h.

The results of this study revealed that the fungal cell of *Paecilomyces* sp. has greater potential application for the removal of chromium ion from industrial wastewater sample.

### Acknowledgements

Special thanks are extended to Ministry of Education, Department of Higher Education for the permission of the research project. We feel a deep sense of gratitude to Dr Theingi Shwe, Rector, Dawei University for her invaluable encouragement. We would be grateful to Dr Khin May Aung and Dr Cho Cho Myint, Pro-rectors, Dawei University for their continuous suggestions. Thanks are also extended to Dr Khin Aye May, Professor, Department of Chemistry, for her guidance, encouragement and invaluable suggestions.

### References

- Ando, K. (2004). *Isolation and Identification of Fungi*. Workshop, Biotechnology Development Centre, Patheingyi University.
- Ando, K. (2016). *Identification of Mitosporic Fungi*. Biological Resource Center, National Institute of Technology and Evaluation (NITE), Japan. pp. 64-85
- Calder, L. (1988). "Interaction of Fungi with Toxic Metals". *New Phytol*, vol. 20. pp. 215-219.
- Ehrlich, H. L. (1997). "Microbes and Metals". *Applied Microbiology Biotechnology*, vol. 48. pp. 687-692
- Hassen, A. and Saidi.N. (1998). "Resistance of Environmental Bacteria to Heavy Metal". *Bioresour, Technol.* vol. 64. pp. 7-15
- Samson, R. A. (1974). "*Paecilomyces* and Some Allied Hyphomycetes". *Stud. Mycol*, vol. 6. pp. 1-119.
- Wild, J. (1987). "*Liquid Waste from the Metal Finishing Industry in Surveys in Industrial Wastewater Treatment*". New York: John Wiley and Sons. pp. 21-62

## SOME CHEMICAL CONSTITUENTS AND SOME BIOLOGICAL ACTIVITIES OF *PICRASMA JAVANICA* FRUIT

Yi Yi Win<sup>1</sup>, Yin Yin Htwe<sup>2</sup>, Zin Thu Khaing<sup>3</sup>, Saw Hla Myint<sup>4</sup>

### Abstract

In the present study, two compounds were isolated from the fruit of *Picrasma javanica* and identified as 1-ethyl-4-methoxy- $\beta$ -carboline and 1-ethyl- $\beta$ -carboline on the basis of their spectroscopic data; UV, IR, <sup>1</sup>H and <sup>13</sup>C NMR in conjunction with 2D experiments (COSY, HSQC, HMBC) and comparison with published literature. For the cytotoxic effect of *P. javanica* fruit ethanol and water extracts; by brine shrimp assay method, the LC<sub>50</sub> values were found to be 135  $\mu$ g/mL for the ethanol extract and 318  $\mu$ g/mL for the water extract. Moreover, the antioxidant potential of ethanol and water extracts was evaluated by DPPH radical scavenging activity, using ascorbic acid as standard and both extracts showed a good antioxidant activity with IC<sub>50</sub> values of 7.71  $\mu$ g/mL and 12.19  $\mu$ g/mL, respectively. Total phenol content by Folin-Ciocalteu reagent method gave 43.06  $\pm$  0.5 mg GAE/g for the ethanol extract and 21.96  $\pm$  1.3 mg GAE/g for the water extract. Furthermore, the anti-inflammatory activity of the ethanol and water extracts by protein denaturation method was 44.44 % and 42.15 %, respectively, at a concentration of 1000  $\mu$ g/mL.

**Keywords:** *Picrasma javanica* fruit, cytotoxicity, antioxidant, anti-inflammatory,  $\beta$ -carboline

### Introduction

The genus *Picrasma* (Simaroubaceae) comprises about six to nine species native to temperate to tropical regions of Asia and tropical regions of America. The species are shrubs and trees growing up to 20 m high. *Picrasma* species are commonly used in traditional medicine to cure various diseases. They have long been used in herbal medicine as anemopyretic cold, sore throat, dysentery, eczema, nausea, loss of appetite, diabetes mellitus and *falciparum* malaria: the most dangerous type of malaria (Scragg and Allan, 1993). Several alkaloids and quassinoids have been reported from the genus *Picrasma*. *Picrasma javanica* Blume (Synonyms: *Picrasma nepalensis* A.W. Bennet and *Picrasma philippinensis* Elmer.) grows in Java Island at 150-1400 m altitude. The plant occurs from the North-Eastern India throughout South East Asia to the Solomon's islands (Heyne, 1987). The flowers are numerous and whitish. The fruit is a drupe, green, red or blue when it ripens (Figure 1). Traditionally, the plant (also known as Yar-baw-jaw as well as Nann-paw-kyawt in Ka-yin State, Myanmar) is used as a febrifuge where it is known to be a substitute for quinine. Leaves have been applied to festering sore and fruit for inflammation. To date, however, nothing was reported in literature, so far, concerning the chemical composition and biological activities of the fruit of this plant. Therefore, it is deemed worthy of research interest in the fruit of this plant. This paper reports the isolation and identification of two alkaloids from the fruit of *Picrasma javanica*, namely 1-ethyl-4-methoxy- $\beta$ -carboline (**1**) and 1-ethyl- $\beta$ -carboline (**2**) and evaluates the cytotoxic effect, and antioxidant and anti-inflammatory activities of the ethanol and water extracts of the fruit.

---

<sup>1</sup> Dr, Associate Professor, Department of Chemistry, Dawei University

<sup>2</sup> Dr, Lecturer, Department of Chemistry, Mawlamyine University

<sup>3</sup> Dr, Lecturer, Department of Chemistry, University of Yangon

<sup>4</sup> Dr, Part-time Professor, Department of Chemistry, University of Yangon



**Figure 1** Photographs showing *Picrasma javanica* (a) Plant and (b) Fruit

## Materials and Methods

### General Experimental Procedure

The FTIR spectra were recorded on a Perkin Elmer GX system FTIR spectrophotometer. UV spectra were recorded on a Shimadzu UV-1800 spectrophotometer. The  $^1\text{H}$  and  $^{13}\text{C}$  NMR spectra were recorded in  $\text{CDCl}_3$ ,  $\text{CD}_3\text{OD}$  on JEOL and Varian Inova 400 or 600 MHz spectrometers. The MS spectra were recorded on a Varian MAT 95 Finigan (70eV) ESI-Mass spectrometer. Silica gel 60 (70-230 mesh) Merck was used for column chromatography. TLC analyses were carried out on 0.25 mm silica gel 60 F<sub>254</sub> precoated on glass plate, Whatman.

### Sample Collection

*P. javanica* fruit used in this study was collected from Naung-ka-mying Township, Ka-yin State (Figure 1). The collected sample was washed with water, and air dried to a constant weight at room temperature for one month. The dried sample was subsequently milled into coarse powder using a grinding mill and then stored in an airtight plastic container for the experimental works.

### Preparation of Crude Extracts

The dried fruit powder (300 g) was percolated with ethanol (1000 mL) for 21 days and filtered. This procedure was repeated three times. The combined filtrate was evaporated under reduced pressure by means of a rotatory evaporator to give the ethanol extract. Water extract was prepared by boiling 300 g of dried fruit powder sample in 1000 mL of distilled water for 6 h and filtered and the filtrates were combined followed by heating on water bath and sand bath to give the extract. These extracts were screened for cytotoxic effect, and antioxidant and anti-inflammatory activities.

### Isolation of Compounds

The fruit powder of *P. javanica* (1.5 kg) was extracted with EtOH till exhaustion to produce a dark solid extract (60 g), which was then suspended in water (500 mL) and successively partitioned with petroleum ether and ethyl acetate to obtain petroleum ether (1.5g) and ethyl acetate (7.1 g) extracts after removing solvent in vacuum. The ethyl acetate extract was chromatographed on a silica gel column by gradient elution with *n*-hexane–ethyl acetate (100:0–25:75) to obtain six fractions. Then, fraction B was further subjected to silica gel column chromatography by gradient elution with *n*-hexane: ethyl acetate (80:20–75:25) to give three sub-fractions of B-1 (70 mg), B-2 (80 mg) and B-3 (350 mg). Sub-fraction B-2 was subjected to preparative thin layer chromatography using toluene: chloroform: ethyl acetate (15: 5: 2 v/v) as developing solvent system to yield compound [1] (20 mg) and compound [2] (5 mg). The structures of the isolated compounds were elucidated and identified by modern spectroscopic techniques, namely UV, FT IR,  $^1\text{H}$  NMR,  $^{13}\text{C}$  NMR, DEPT, and 2D NMR:  $^1\text{H}$ - $^1\text{H}$  COSY,  $^1\text{H}$ - $^{13}\text{C}$  HSQC and  $^1\text{H}$ - $^{13}\text{C}$  HMBC.

Compound [1]: Pale yellow crystals; UV  $\lambda_{\max}$  (EtOH) nm: 259, 303, 346;  $\lambda_{\max}$  (MeOH/HCl) nm: 248, 303, 367; IR  $\nu_{\max}$  (KBr)  $\text{cm}^{-1}$ : 3471 (–NH), 3085 (aromatic C–H), 1635 (>C=N–), 1593 and 1220 (aromatic benzene and ar–C–O–Me), 1118 (=C–N<) and 2918 and 2854 (–CH<sub>3</sub> and –CH<sub>2</sub>–); <sup>1</sup>H NMR (CDCl<sub>3</sub>, 500 MHz) and <sup>13</sup>C NMR (CDCl<sub>3</sub>, 125 MHz) see Table 1.

Compound [2]: Pale yellow amorphous; UV  $\lambda_{\max}$  (MeOH) nm: 242, 285, 348;  $\lambda_{\max}$  (MeOH/HCl) nm: 247, 308, 371; IR  $\nu_{\max}$  (KBr)  $\text{cm}^{-1}$ : 3471 (–NH), 3085 (aromatic C–H), 1635 (>C=N–), 1593 (aromatic benzene and ar–C–O–Me), 1118 (=C–N<) and 2918 and 2854 (–CH<sub>3</sub> and –CH<sub>2</sub>–); <sup>1</sup>H NMR (CDCl<sub>3</sub>, 500 MHz) and <sup>13</sup>C NMR (CDCl<sub>3</sub>, 125 MHz) see Table 2.

### Determination of Cytotoxicity by Brine Shrimp Lethality Bioassay

Brine shrimp lethality bioassay method indicates cytotoxicity as well as a wide range of pharmacological activities e.g., anticancer, anti-viral and pesticidal properties. The experiment was carried out using the method described by McLaughlin with slight modifications (McLaughlin *et al.*, 1982). Brine shrimp eggs were obtained from a pet shop. Briefly, *Artemia salina* cysts (brine shrimp eggs, 0.1 g) were allowed to hatch in artificial seawater, containing 3.8 g/L sodium chloride. The larvae (nauplii) were placed in the prepared water for 48 h at 25 °C under constant aeration and illumination to ensure survival and maturity before use. Stock solutions (10 mg/mL) of fruit extracts were prepared in clean test tubes of 10 mL volume to obtain five final concentrations (800, 400, 200, 100, 25  $\mu\text{g/mL}$ ). Ten nauplii were collected with the aid of a pipette and added to the serially diluted test solutions. Test was carried out in triplicate. The negative control consisted of ten nauplii per tube in sea water without plant extract while potassium dichromate was used as the positive control. After the 24 h incubation at 25 °C, a magnifying lens was used to count the number of dead larvae. Larvae were considered dead only if they did not move for few seconds after pricking with sharp object during observation and the percentage mortality was calculated as follows.

$$\% \text{ Mortality} = \frac{A}{A + B} \times 100$$

Where, A = number of dead nauplii and B = number of live nauplii

The 50 % mortal concentration (LC<sub>50</sub> value) was calculated using a linear regressive excel programme.

### Investigation of Antioxidant Capacity

#### (i) Determination of total phenolic content

The total phenolic content of the ethanol and water extracts of *P. javanica* fruit were determined with Folin-Ciocalteu reagent by using the method developed by Harbertson and Spayd (Harbertson and Spayd, 2006). A 0.5 mL of extract sample (0.1 %), 2.5 mL of 1/10 dilution of Folin-Ciocalteu reagent and 2.0 mL of sodium carbonate (7.5 %, w/v) in water were mixed and incubated for 15 min at 45 °C. The reaction was kept in the dark for 30 min and after centrifuging the absorbance of blue color from different samples was measured at 765 nm with a visible spectrophotometer. The phenolic content was calculated as gallic acid milligram equivalents GAE/g of dry plant material on the basis of a standard curve of gallic acid. All determinations were carried out in triplicate.

#### (ii) Determination of *in vitro* antioxidant action by DPPH free radical scavenging assay

The radical scavenging and antioxidant activity of ethanol and water extracts of *P. javanica* fruit was estimated alongside the free radical DPPH (Brand-Williams *et al.*, 1995). Various

concentrations (2.5, 5, 10, 20 and 40 µg/mL) of the extracts, and commercial antioxidant (ascorbic acid) (1.5 mL) were incubated with a 0.002 % DPPH solution (1.5 mL) for about 30 min at room temperature in the dark. A vortex machine was employed to ensure a thorough mixing and the absorbance was read at 517 nm by UV-Vis spectrophotometer. The control solution was also prepared by mixing 1.5 mL of 0.002 % DPPH and 1.5 mL of EtOH solutions. The capacity of the crude extracts to scavenge DPPH free radicals was calculated using the following equation:

$$\% \text{ Inhibition} = \frac{A_{\text{DPPH}} - (A_{\text{sample}} - A_{\text{blank}})}{A_{\text{DPPH}}} \times 100$$

Where,  $A_{\text{DPPH}}$  = absorbance of DPPH in EtOH solution

$A_{\text{sample}}$  = absorbance of test sample and DPPH solution

$A_{\text{blank}}$  = absorbance of test sample in EtOH solution

The dose-response curve was plotted, and the  $IC_{50}$  value of the commercial antioxidant and crude extracts were calculated by using a linear regressive excel programme.

### Determination of *In Vitro* Anti-inflammatory Activity by Protein Denaturation Method

Anti-inflammatory activity of ethanol and water extracts of *P. javanica* fruit was evaluated by protein denaturation method (Elias and Rao, 1988). The reaction mixture consisted of 0.2 mL of egg albumin (from fresh hen's egg), 2.8 mL of phosphate buffered saline (pH 6.4) and 2 mL of varying concentrations (25, 100, 200, 400, 800 µg/mL) of the test extracts and diclofenac sodium which was used as reference. Similar volume of double-distilled water served as control. Then the mixtures were incubated at  $37 \text{ }^{\circ}\text{C} \pm 2 \text{ }^{\circ}\text{C}$  in an incubator for 15 min and then heated at  $70 \text{ }^{\circ}\text{C}$  for 5 min. After cooling, the turbidity was measured at 660 nm with spectrophotometer. The percentage inhibition of protein denaturation was calculated by using the following formula;

$$\% \text{ Inhibition} = \frac{A_{\text{control}} - A_{\text{sample}}}{A_{\text{control}}} \times 100$$

Where,  $A_{\text{control}}$  = absorbance of control

$A_{\text{sample}}$  = absorbance of test sample

The 50% inhibition of protein denaturation ( $IC_{50}$  value) was calculated using a linear regressive excel programme.

## Results and Discussion

### Structure Elucidation of Isolated Compounds

The ethyl acetate soluble fraction from ethanol extract of *Picrasma javanica* fruit was subjected to a succession of chromatographic procedures, including silica gel chromatography to afford two pure isolates. The structures of the isolated compounds in Figures 2 and 3 were established from spectroscopic analysis, especially, NMR spectra in conjunction with 2D experiments (COSY, HMQC, and HMBC) and direct comparison with published data. The  $^1\text{H}$  and  $^{13}\text{C}$  NMR data of isolated compound **1** (Figures 7-10) resemble strikingly with those reported for 1-ethyl-4-methoxy- $\beta$ -carboline (Ohmoto *et al.*, 1987). The IR spectral data also revealed the presence of singlet -NH group ( $3471 \text{ cm}^{-1}$ ), aromatic =CH- group ( $3085 \text{ cm}^{-1}$ ) group, >C=N- group ( $1635 \text{ cm}^{-1}$ ), aromatic benzene and ar-C-O-Me group ( $1593 \text{ cm}^{-1}$  and  $1220 \text{ cm}^{-1}$ ) and =C-N< group ( $1118 \text{ cm}^{-1}$ ). In UV spectral data, the absorption maximum for the lowest energy  $\pi \rightarrow \pi^*$  electronic transition observed at 346 nm in EtOH shifted 21 nm to a longer wavelength maximum at 367 nm by addition of HCl to the EtOH solution. This indicates a  $\beta$ -carboline structure (Tarzi *et al.*, 2005). The isolated compound **1** must therefore be 1-ethyl-4-methoxy- $\beta$ -

carboline: DEPT,  $^1\text{H}$ - $^1\text{H}$  COSY,  $^1\text{H}$ - $^{13}\text{C}$  HSQC and  $^1\text{H}$ - $^{13}\text{C}$  HMBC data of compound **1** also agreed with the structure of 1-ethyl-4-methoxy- $\beta$ -carboline (Figure 2 and the comparative spectral data in Table 1).

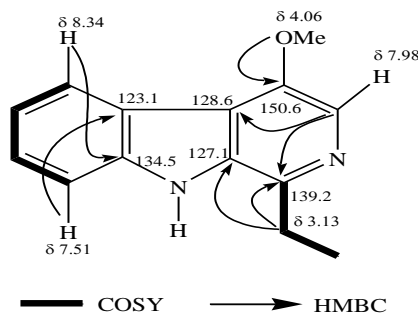


**Figure 2** Structure of compound **1** (1-ethyl-4-methoxy- $\beta$ -carboline)

**Table 1**  $^1\text{D}$  and  $^2\text{D}$  NMR Spectral Data ( $\text{CDCl}_3$ , 500 and 125 MHz) of Compound **1** and Reported Data ( $\text{CDCl}_3$ , 500 and 125 MHz) of 1-ethyl-4-methoxy- $\beta$ -carboline ( $J_{\text{Hz}}$  Value in Parenthesis)

Position	C-type (DEPT)	compound <b>1</b>		1-ethyl-4-methoxy- $\beta$ -carboline*		$^1\text{H}$ - $^1\text{H}$ COSY	$^1\text{H}$ - $^{13}\text{C}$ HMBC
		$^1\text{H}$ NMR ( $\delta_{\text{H}}/\text{ppm}$ )	$^{13}\text{C}$ NMR ( $\delta_{\text{C}}/\text{ppm}$ )	$^1\text{H}$ NMR ( $\delta_{\text{H}}/\text{ppm}$ )	$^{13}\text{C}$ NMR ( $\delta_{\text{C}}/\text{ppm}$ )		
1	C	-	139.2	-	139.2		
2	-	-	-	-	-		
3	=CH-	7.98, s	120.6	8.00, s	120.6		H-3 $\rightarrow$ C-1, C-4b
4	C	-	150.6	-	150.6		
4a	C	-	123.1	-	123.1		
4b	C	-	128.6	-	128.6		
5	=CH-	8.34, d (8.0)	124.5	8.35, d (8.0)	124.5	H-5 $\rightarrow$ H-6	H-5 $\rightarrow$ C-8a
6	=CH-	7.29, m	120.2	7.27, m	120.2	H-6 $\rightarrow$ H-5	
7	=CH-	7.50, t (7.6)	127.6	7.49, m	127.6	H-7 $\rightarrow$ H-8	
8	=CH-	7.51, m	111.2	7.49, m	111.2	H-8 $\rightarrow$ H-7	H-8 $\rightarrow$ C-4a
8a	C	-	134.5	-	134.5		
8b	C	-	127.1	-	127.1		
9	-	-	-	-	-		
1'	$\text{CH}_2$	3.13, q (7.6)	26.5	3.13, q (8)	26.5	H-1' $\rightarrow$ H-2'	H-1' $\rightarrow$ C-1, C-8b
2'	$\text{CH}_3$	1.36, t (7.6)	14.4	1.37, t (8)	14.4	H-2' $\rightarrow$ H-1'	H-2' $\rightarrow$ C-1
4-OMe	$\text{CH}_3$	4.06, s	56.1	4.07, s			4OMe $\rightarrow$ C-4

\* Ohmoto *et al.*, 1987

## Compound 2

There is a slight difference from compound **1** in  $^1\text{H}$  and  $^{13}\text{C}$  NMR data of the compound **2** (Figures 11 and 12), the methoxyl group signal at C-4 disappeared and the new aromatic methine signal appeared at  $\delta_{\text{H}}$  7.82 ppm and  $\delta_{\text{C}}$  112.8 ppm. The aromatic methine proton signal ( $\delta_{\text{H}}$  7.82 ppm) was correlated to the neighbouring proton ( $\delta_{\text{H}}$  8.42 ppm) in  $^1\text{H}$ - $^1\text{H}$  COSY spectrum (Figure 13) and  $\delta_{\text{C}}$  112.8 ppm in the HMQC spectrum of compound **2** (Figure 14) compared to

compound **1** (Table 1). This fact confirms that –OMe group was replaced by an aromatic hydrogen at C-4. The aromatic =CH at C-4 was confirmed by HMBC correlation of H-4 with C-8b (Figure 15). The comparison of  $^1\text{H}$  and  $^{13}\text{C}$  NMR chemical shifts as well as the observed coupling constants with the reported values (Prinsep, 1990) were presented in Table 2. Thus compound **2** was proposed as 1-ethyl- $\beta$ -carboline (Figure 3).

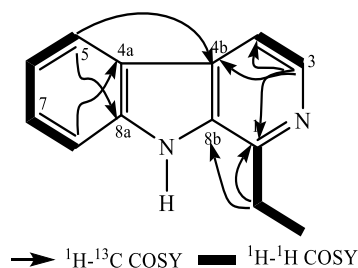


**Figure 3** Structure of compound **2** (1-ethyl- $\beta$ -carboline)

**Table 2**  $^1\text{D}$  and  $^2\text{D}$  NMR Spectral Data ( $\text{CDCl}_3$ , 500 and 125 MHz) of Compound **1** and Reported Data ( $\text{CDCl}_3$ , 500 and 125 MHz) of 1-ethyl- $\beta$ -carboline ( $J_{\text{Hz}}$  Value in Parenthesis)

Position	C- type (DEPT)	Compound <b>2</b>		1-ethyl- $\beta$ -carboline*		$^1\text{H}$ - $^1\text{H}$ COSY	$^1\text{H}$ - $^{13}\text{C}$ HMBC
		$^1\text{H}$ NMR ( $\delta_{\text{H}}/\text{ppm}$ )	$^{13}\text{C}$ NMR ( $\delta_{\text{C}}/\text{ppm}$ )	$^1\text{H}$ NMR ( $\delta_{\text{H}}/\text{ppm}$ )	$^{13}\text{C}$ NMR ( $\delta_{\text{C}}/\text{ppm}$ )		
1	C	-	146.6	-	146.8	-	-
2	-	-	-	-	-	-	-
3	=CH-	8.42, d (5.1)	138.8	8.43, d (5.3)	138.7	H-3→H-4	H-3→C-1, C-4, C-4b
4	=CH-	7.82, d (5.1)	112.8	7.83, d (5.3)	112.9	H-4→H-3	H-4→C-8b
4a	C	-	122.1	-	122.0	-	-
4b	C	-	128.6	-	128.6	-	-
5	=CH-	8.11, d (8.0)	121.7	8.11, d (8.0)	121.7	H-5→H-6, H-7	H-5→C-4b, C-8a
6	=CH-	7.28, t (7.6)	120.1	7.27, m	119.9	H-6→H-5	-
7	=CH-	7.52, t (7.6)	128.2	7.49, m	128.1	H-7→H-5, H-8	-
8	=CH-	7.52, m	111.4	7.49, m	111.5	H-8→H-7	H-8→C-4a
8a	C	-	140.1	-	140.3	-	-
8b	C	-	133.8	-	-	-	-
9	-	-	-	-	-	-	-
1'	$\text{CH}_2$	3.16, q (7.6)	27.2	3.16, q (7.6)	27.2	H-2'	H-1'→C-1, C-8b
2'	$\text{CH}_3$	1.42, t (7.6)	12.6	1.41, t (7.6)	12.6	H-1'	H-2'→C-1

\* Prinsep, 1990

### Determination of Cytotoxic Effect

The cytotoxicity of ethanol and water extracts of *P. javanica* fruit was determined by using brine shrimp lethality bioassay. The percent mortality of brine shrimp in different concentrations and  $\text{LC}_{50}$  value of extracts and that of positive control; potassium dichromate was shown (Table 3 and Figure 4). From the results,  $\text{LC}_{50}$  value of EtOH extract showed 135  $\mu\text{g}/\text{mL}$  and that of  $\text{H}_2\text{O}$  extract was 380  $\mu\text{g}/\text{mL}$ . It could be deduced that EtOH and  $\text{H}_2\text{O}$  extracts of *P. javanica* fruit had

medium toxicity due to LC<sub>50</sub> values between 100 and 500 µg/mL. Therefore, the cytotoxic effect of the extracts might be due to the presence of cytotoxic compounds in the fruit extracts.

**Table 3 Percent Mortality and LC<sub>50</sub> Value of Crude Extracts of *P. javanica* Fruit**

Extracts	% Mortality of Brine Shrimp ±SD in Different Concentrations of Sample (µg/mL)					LC <sub>50</sub> (µg/mL)	Toxicity Profile
	25	100	200	400	800		
EtOH	31±0.65	47±0.78	55±0.48	62±1.09	68±1.05	135	Toxic
Water	19±0.75	35±0.77	42±0.49	52±0.33	56±0.62	380	Toxic
*K <sub>2</sub> Cr <sub>2</sub> O <sub>7</sub>	42±0.56	61±0.73	72±1.15	80±0.60	88±0.61	48	Highly Toxic

\*- positive control and N = 10 (no. of shrimps).

Score for LC<sub>50</sub>: highly toxic; 0-100 µg/mL, toxic; 100-500 µg/mL, non-toxic; > 1000 µg/mL (Mentor *et al.*, 2014)

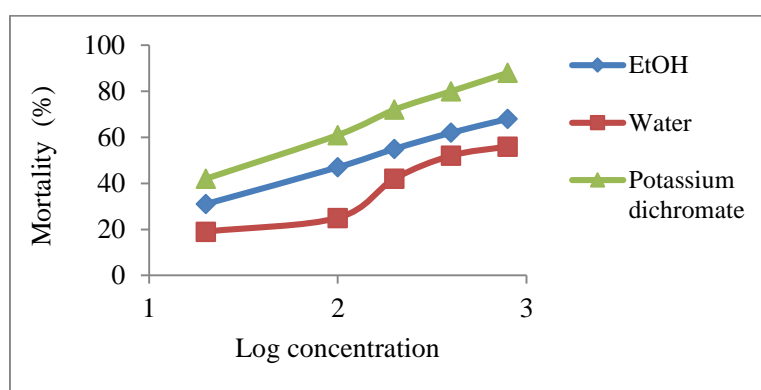


**Figure 4** Brine shrimp mortality of crude extracts of *P. javanica* fruit for 24 h

### Determination of Total Phenolic Content

The total phenol content of ethanol extract of *P. javanica* fruit ( $43.06 \pm 0.5$  mg GAE/g) was found to be higher than water extract ( $21.96 \pm 1.3$  mg GAE/g) (Table 4). Several studies have described the antioxidant properties of medicinal plants which are rich in phenolic compounds. These correlations indicated that high total phenol contents in ethanol extract contributed to high antioxidant and anti-inflammatory activities of this extract.

### Determination of *In Vitro* Antioxidant Effect

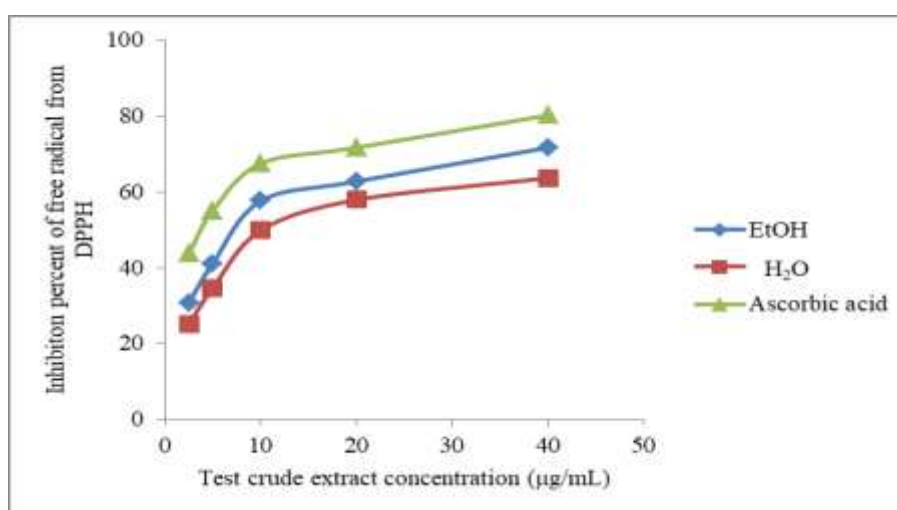
In the DPPH free radical scavenging assay, the ethanol extract of *P. javanica* fruit revealed maximum free radical scavenging activity (IC<sub>50</sub> = 7.71 µg/mL) when compared to ascorbic acid (IC<sub>50</sub> = 3.87 µg/mL) (Table 4 and Figure 5). This prominent free radical scavenging activity may be due to synergistic activity of various chemical entities present in the extractive.

**Table 4** Percent Inhibition of DPPH Free Radicals, IC<sub>50</sub> Value and Total Phenolic Content of Crude Extracts of *P. javanica* Fruit

Extracts	Inhibition of DPPH Free Radicals (% Mean± SD) at Different Concentrations (µg/mL)					IC <sub>50</sub> (µg/mL)	Total phenol content (mg GAE/g)
	2.5	5	10	20	40		
EtOH	30.80 ±1.06	41.14 ±0.44	57.63 ±1.56	62.78 ±1.44	71.68 ±0.42	7.71	43.06 ± 0.5
Water	25.17 ±0.16	34.66 ±0.44	44.85 ±1.47	57.91 ±0.79	63.68 ±1.53	12.19	21.96 ± 1.3
Ascorbic acid*	43.81 ±0.88	55.09 ±0.11	67.5 ±0.36	71.71 ±1.06	80.21 ±0.44	3.87	-

Data are expressed as means ± SD from triplicate experiments.

\*- positive control

**Figure 5** Percent inhibition of DPPH free radicals of crude extracts of *P. javanica* fruit tested

#### Determination of *In Vitro* Anti-inflammatory Effect

Protein denaturation is the process by which proteins lose their tertiary structure and secondary structure. Protein denaturation is a well-documented cause of inflammation. From the results of this study, the ethanol and water extracts of *P. javanica* fruit are effectively inhibiting the protein denaturation (albumin) caused by heat. The protein denaturation percent inhibition was 42.51 % and 44.44 %, respectively, for the ethanol and water extracts at a concentration of 1000 µg/mL, whereas diclofenac sodium had produced 89.19 % inhibition (Table 5 and Figure 6).

**Table 5** Inhibition Effect of Test Crude Extracts of *P. javanica* Fruit on Protein Denaturation

Extracts	Inhibition (% Mean± SD) at Different Concentrations (µg/mL)			
	100	200	500	1000
EtOH	29.44±0.11	32.79±1.36	37.30±0.32	44.44± 0.79
Water	27.33± 1.30	29.26±0.88	33.83±0.44	42.51±1.32
Diclofenac sodium*	74.41± 2.11	76.72±2.61	81.48± 1.53	89.19±1.02

Data are expressed as means ± SD from triplicate experiments. \*- positive control

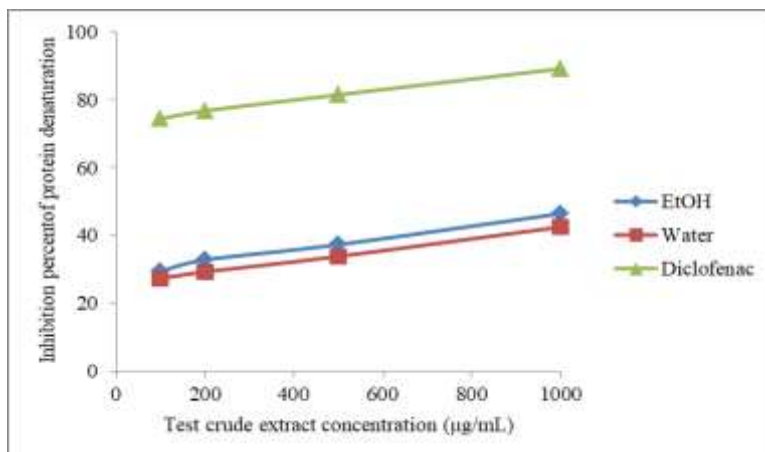


**Figure 6** A plot of inhibition percent of protein denaturation against various concentrations of crude extracts of *P. javanica* fruit tested

**Analysis Supplementary data for Compound 1**

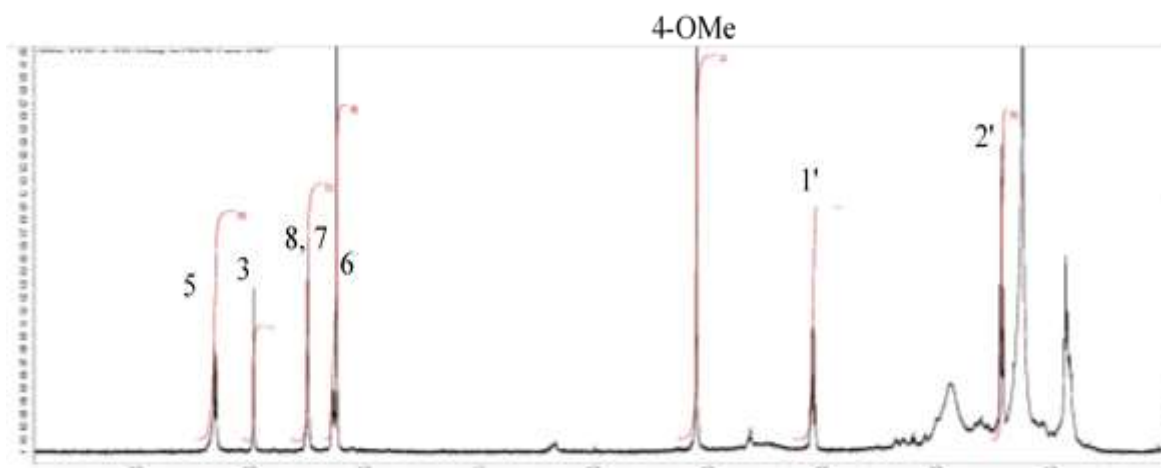


**Figure 7** <sup>1</sup>H NMR spectrum of compound 1 (CDCl<sub>3</sub>, 500 MHz)

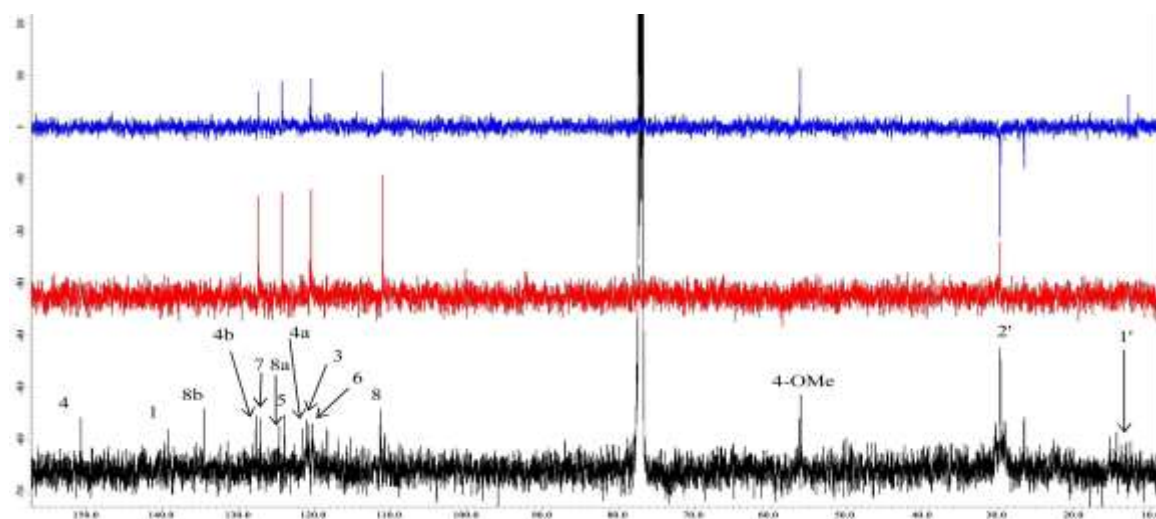


**Figure 8** <sup>13</sup>C NMR and DEPT spectra of compound 1 (CDCl<sub>3</sub>, 125 MHz)

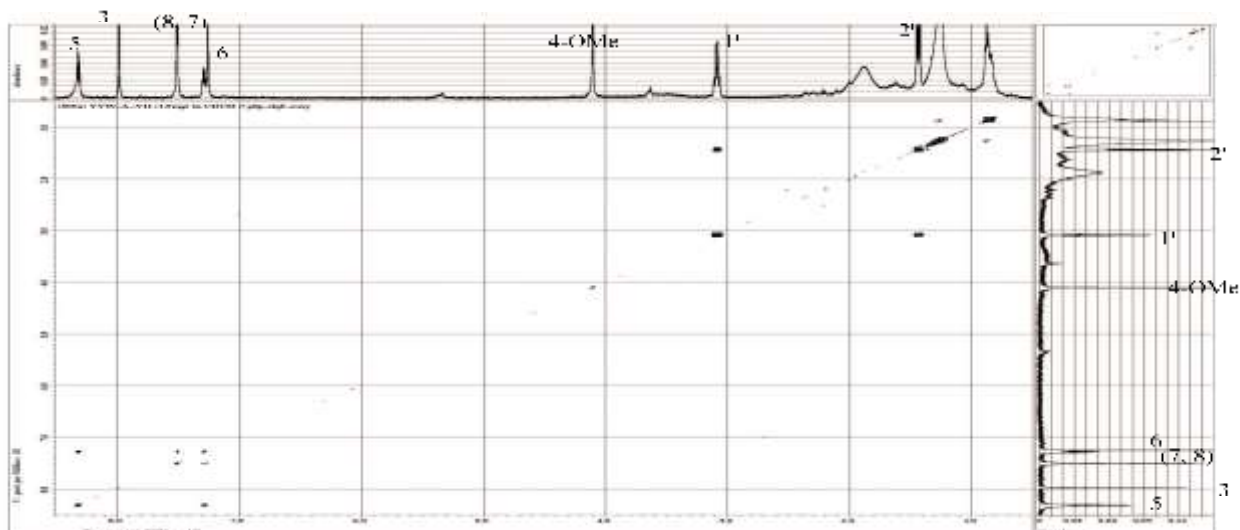


**Figure 9**  $^1\text{H}$ - $^1\text{H}$  COSY spectrum of compound **1** ( $\text{CDCl}_3$ , 500 MHz)

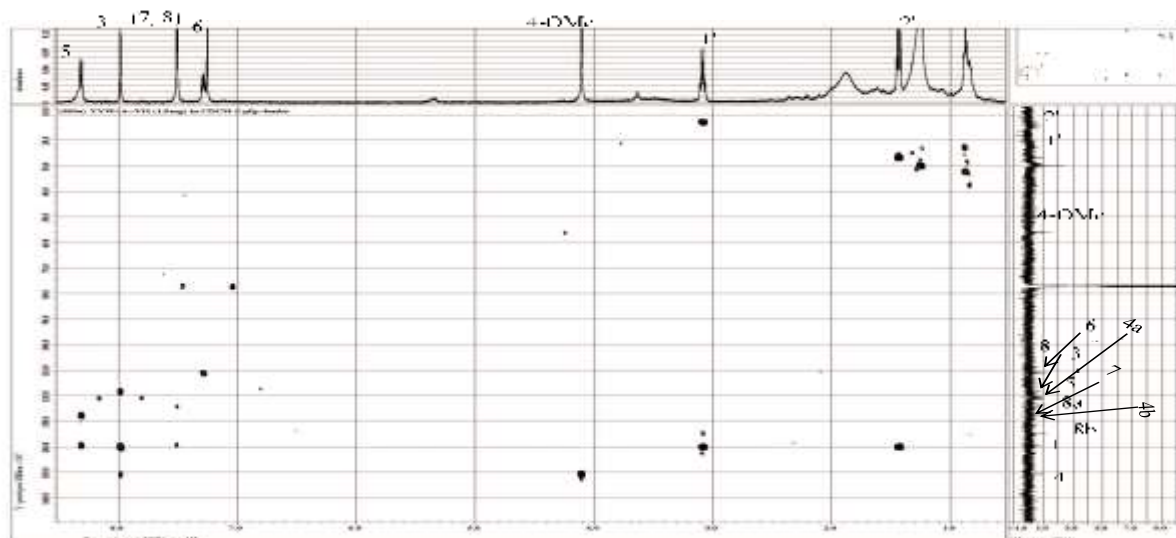


**Figure 10**  $^1\text{H}$ - $^{13}\text{C}$  HMBC spectrum of compound **1** ( $\text{CDCl}_3$ , 500 MHz)

### Compound **2**

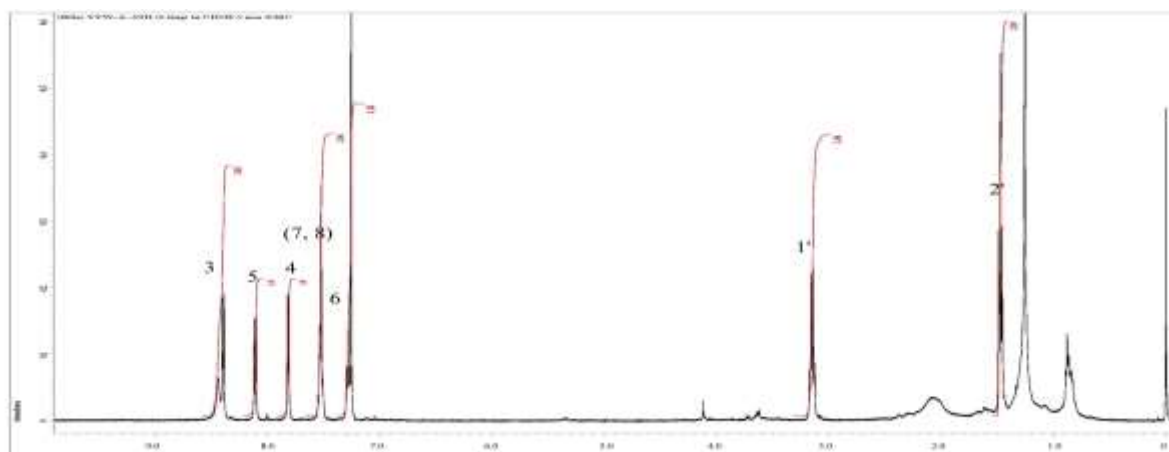


**Figure 11**  $^1\text{H}$  NMR spectrum of compound **2** ( $\text{CDCl}_3$ , 500 MHz)

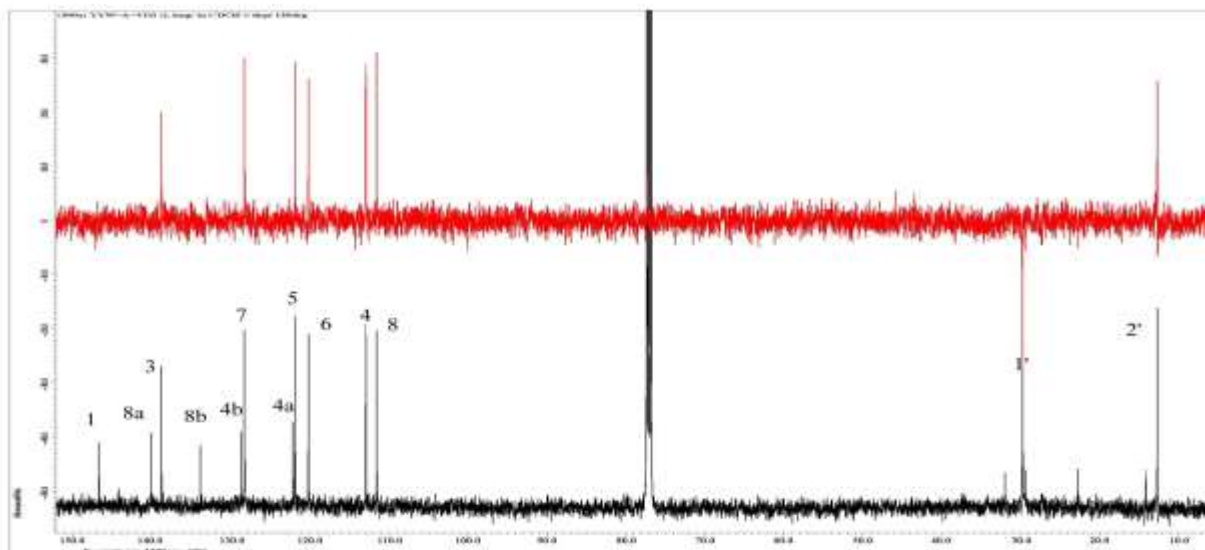


**Figure 12**  $^{13}\text{C}$  NMR and DEPT spectra of compound **2** ( $\text{CDCl}_3$ , 125 MHz)

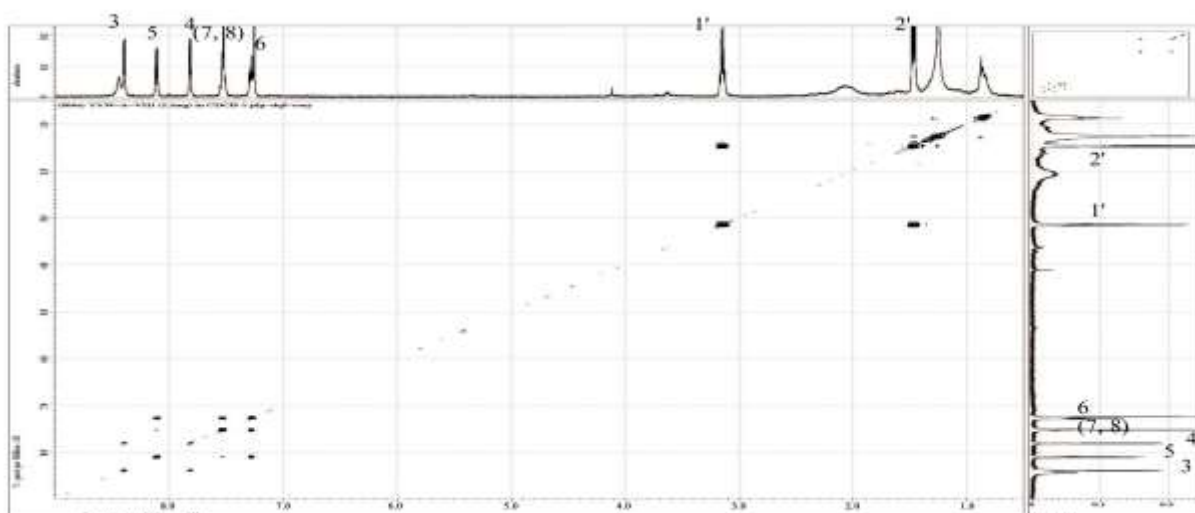


**Figure 13**  $^1\text{H}$ - $^1\text{H}$  COSY spectrum of isolated compound **2** ( $\text{CDCl}_3$ , 500 MHz)

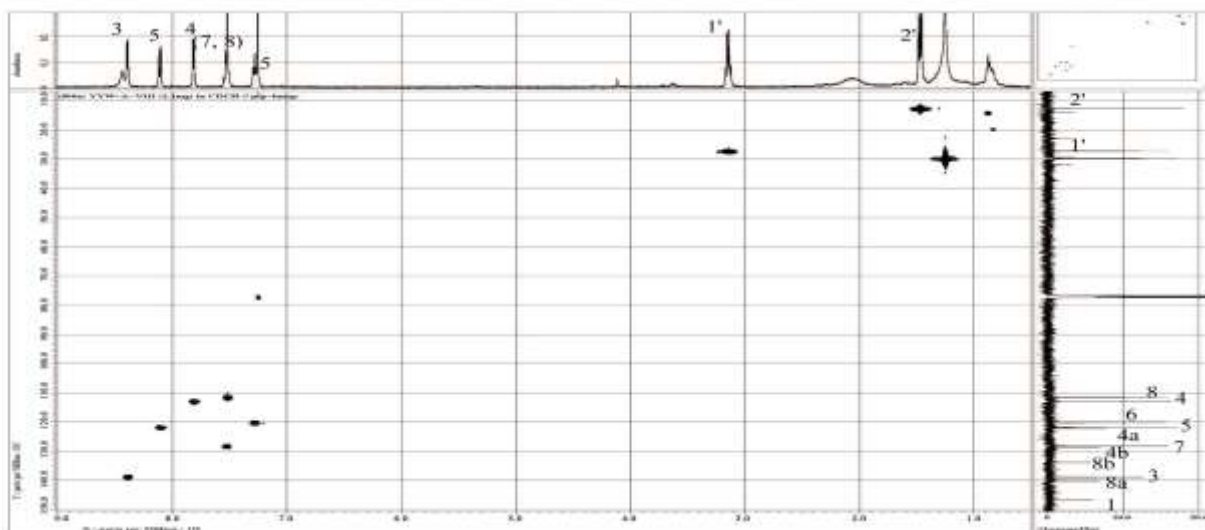


**Figure 14**  $^1\text{H}$ - $^{13}\text{C}$  HMQC spectrum of compound **2** ( $\text{CDCl}_3$ , 500 MHz)

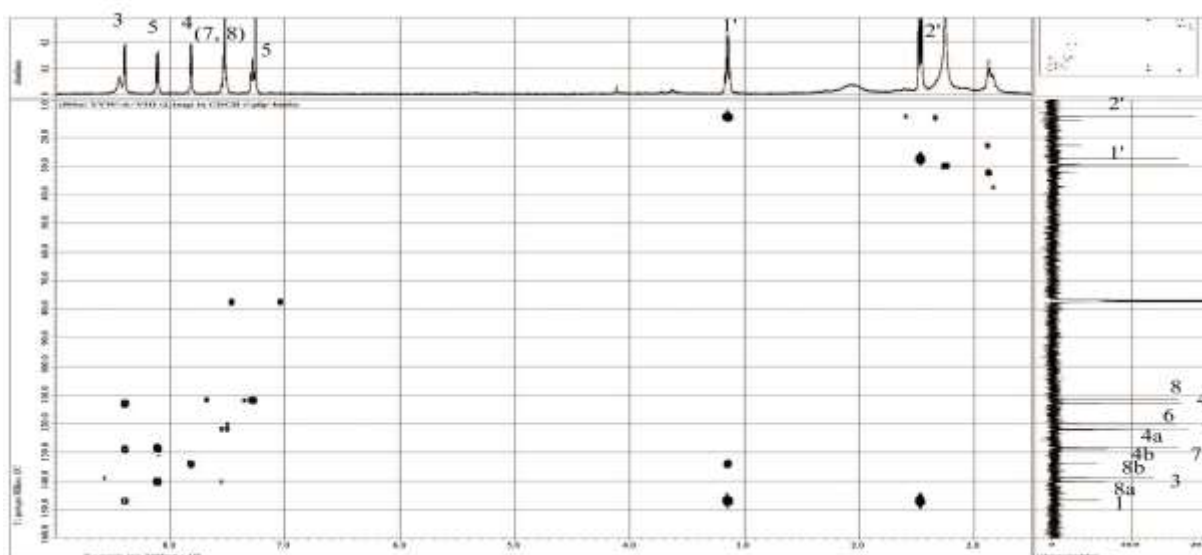


**Figure 15**  $^1\text{H}$ - $^{13}\text{C}$  HMBC spectrum of compound **2** ( $\text{CDCl}_3$ , 500 MHz)

### Conclusion

This research revealed some chemical constituents such as alkaloids; 1-ethyl-4-methoxy- $\beta$ -carboline (**1**) and 1-ethyl- $\beta$ -carboline (**2**), cytotoxicity, antioxidant and anti-inflammatory activities of the *P. javanica* fruit. In fact, the present research showed that the ethanol and water extracts of *P. javanica* fruit possess not only antioxidant but also anti-inflammatory effects as well as cytotoxicity. Therefore, the research findings will contribute to some extent to the search for the *in vivo* antioxidant and anti-inflammatory agents of plant origin and also to the development of the role of Myanmar traditional medicinal formulation, especially in the treatment of the related diseases.

### Acknowledgements

The authors acknowledge to the Myanmar Academy of Arts and Science and the Department of Higher Education (Yangon Office), Ministry of Education, Myanmar for giving the opportunity to submit this paper.

### References

- Brand-Williams, W., Cuvelier, M.E. and Berset, C. (1995). "Use of Free Radical Method to Evaluate Antioxidant Activity". *Lebensm. Wiss. Technol.*, vol. 28, pp. 25-30.
- Elias, J.G. and Rao, M. N. (1988). "Inhibition of Albumin Denaturation and Anti-inflammatory Activity of Dehydrozingerone and its Analogs". *Indian. J. Exp Biol.*, vol. 26, pp. 540-542.
- Harbertson, J. and Spayd, S. (2006). "Measuring Phenolic in the Winery". *Am.J. Enol. Vitic.*, vol. 57, pp. 280-288.
- Heyne, K. (1987). "Tumbuhan Berguna Indonesia II". *Badan Litbang Kehutanan, Jakarta*, vol. 4, pp. 493-494.
- Mentor, R., Hamidi, B. and Panovska, T. K. (2014). "Toxicological Evaluation of the Plant Products Using Brine Shrimp (*Artemia salina* L.) Model". *M Pharm. Bull.*, vol. 60(1), pp. 9-18.
- McLaughlin, J. L., Meyer, B.N., Ferringni, N.R., Puam, J.E., Lacobsen, B.L. and Nichols, E.D. (1982). "Brine Shrimp: A Convenient General Bioassay for Active Constituents". *Planta Med.*, vol. 45, pp. 31-32.
- Ohmoto, T., Koike, K. and Kagei, K. (1987). "Alkaloids from *Picrasma javanica* Growing in Indonesia". *Sho. Zas.*, vol.41(4), pp. 338-340.
- Prinsep, R.M. (1990). *Studies on Marine Natural Products*. PhD Thesis, Department of Chemistry, University of Canterbury, Christchurch, New Zealand.
- Scragg, A.H. and Allan, E.J. (1993). "Picrasma Quassinoides Bennet (Japanese Quassia Tree): *In Vitro* Culture and Production of Quassin". *Biotechnology in Agriculture and Forestry*, vol. 21, pp. 249-268.
- Tarzi, O.I., Ponce, M.A., Cabrerizo, F.M., Bonesi, S.M. and Erra-Balsells, R. (2005). "Electronic Spectroscopy of the  $\beta$ -Carboline Derivatives Nitronorharmanes, Nitroharmanes, Nitroharmines and Chloroharmines in Homogeneous Media and in Solid Matrix". *Arkivoc*, vol. 12, pp. 295-310.

## STUDIES ON BIOACTIVITY AND STRUCTURE ELUCIDATION OF ISOLATED BIBENZYL DERIVATIVES FROM *DENDROBIUM PULCHELLUM* ROOT EXTRACTS

Pann Yone<sup>1</sup>, Hnin Yu Win<sup>2\*</sup>, Thida Win<sup>3</sup>

### Abstract

The objective of the present study is to investigate bioactive metabolites from *Dendrobium pulchellum* roots. Bibenzyl derivatives extracted by acetate ethyl namely, 4-(4-hydroxy-3-methoxyphenethyl)-2, 6-dimethoxyphenol (1) and 4-(3,4-dimethoxy-phenethyl)-2,6-dimethoxy phenol (2) were isolated by using separation techniques such as thin layer and column chromatography. The structure elucidation the isolated compounds was performed based on NMR and mass. Moreover, the antioxidant activity of crude extract was evaluated by using DPPH (2,2-diphenyl-1-picrylhydrazyl) radical scavenging assay. Furthermore, the acute toxicity and antimicrobial activities of crude extracts were also examined.

**Keywords:** *Dendrobium pulchellum*, bibenzyl, NMR, mass, DPPH

### Introduction

Plants are used for variety of purpose and are also really important for the earth and for all living things. They provide us with food, fiber, shelter, medicine and fuel. Plant is an important source of medicine and plays a key role in world health. Medicinal herbs or plants have been known to an important potential source of therapeutic or curative aids. Man used medicinal plant or medicinal herbs since ancient times as they believed that medicinal plants can supply us with medical treatment and other effects. Since that time early man valued these medicinal plants. Nowadays, two-third of the people living in rural areas depends on medicinal herbs as primary health care. The term of medicinal plants involve a various types of plants used in herbalism and these contain a rich resource of active ingredients. Moreover, these plants play an important role in the development of human cultures around the whole world (Hassam, 2012). Medicinal plant consists of a wide range of secondary metabolites or compounds such as tannins, terpenoids, alkaloids, flavonoids that shows the curative effect of the plants most especially the antimicrobial activities (Oladej, 2016).

In Myanmar, there are many traditional plants which have been reputed for their various kinds of activities and usefulness in pharmacology. Therefore, the study of traditional plant and their usage in therapy play a very important role. In the present work, medicinal orchid *Dendrobium pulchellum* was selected for isolation of pure bioactive compounds. *Dendrobium pulchellum* is belonged to the family Orchidaceae and it is locally known as Kyaung-myet-lone (or) Sin-ma-myet-kwin (Figure1). *Dendrobium* genus are used for therapeutic activities such as anticancer, hypoglycemic, antimicrobial, antidiabetic, anti-inflammatory, antiherpetic, antimalarial, antioxidant, immunomodulatory, hepatoprotective and neuroprotective activities (Singh *et al.*, 2012). *Dendrobium pulchellum* was found to inhibit the lung cancer cell motility and invasion through suppression of endogenous reactive oxygen species (Kowitdamrong *et al.*, 2013).

---

<sup>1</sup> Lecturer, Department of Chemistry, Mandalay University

<sup>2</sup> Dr, Associate Professor, Department of Chemistry, University of Mandalay

<sup>3</sup> Dr, Rector (Rtd.), University of Mandalay

\*Corresponding author: Hnin Yu Win, Department of Chemistry, University of Mandalay, email: snowhninyuwin@gmail.com



**Figure 1** Roots, plants and flowers of *Dendrobium pulchellum* Roxb.ex Lindl.

## Materials and Methods

### General Experimental Procedure

$^1\text{H}$  NMR spectra: Varian Unity 300 (300.542 MHz), Bruker AMX 300 (300.542 MHz), Varian Inova 500 (499.8 MHz).  $^{13}\text{C}$  NMR spectra: Varian Unity 300 (75.5 MHz), Varian Inova 500 (125.7 MHz). Chemical shifts were measured relatively to tetramethylsilane as internal standard. 2D NMR spectra: H, H COSY spectra ( $^1\text{H}$ ,  $^1\text{H}$ -Correlated Spectroscopy), HMBC spectra (Heteronuclear Multiple Bond Connectivity) and HMQC spectra (Heteronuclear Multiple Quantum Coherence). Thin layer chromatography (TLC): DC-Folien Polygram SIL G/UV<sub>254</sub> (Macherey-Nagel & Co.). Column chromatography (CC): MN silica gel 60: 0.05-0.2 mm, 70-270 mesh (Macherey-Nagel & Co). Sephadex LH-20 (Pharmacia) was used for size exclusion chromatography. Commercial grade reagents and solvents were purchased from Super Shell Co. Ltd, Yangon. Common laboratory apparatus were used. PerkinElmer C93927 was used for FT IR spectra measurement. The antimicrobial activities of plant extracts were measured in Pharmaceutical and Food Research Department (PFRD), Insein, Yangon.

### Plant Material

The roots of *Dendrobium pulchellum* were collected from Mawlu Township, Sagaing Region, Myanmar. The root materials were cut into small pieces and dried at room temperature for about one month.

### Preliminary Phytochemical Analysis

The various solvent extracts of root sample were prepared to analyze the presence of certain phytochemicals such as alkaloids, flavonoids, phenolic compounds, polyphenols, saponins, steroids, tannins, terpenes, glycoside, lipophilic and reducing sugar by the standard method of Harborne (Harborne, 1998).

### Biological Activities of Various Crude Extracts

Antimicrobial tests were performed at Pharmaceutical and Food Research Department (PFRD), Insein Township, Yangon Region. Antimicrobial activities of crude extracts were tested by agar-well diffusion method on six test microorganisms such as *Bacillus subtilis*, *Staphylococcus aureus*, *Pseudomonas aeruginosa*, *Bacillus pumilus*, *Candida albicans* and *Escherichia coli*.

### Measurement of DPPH Radical Scavenging Activity by Spectrophotometric Method

Antioxidant activity of ethyl acetate extract was determined by DPPH radical scavenging assay. The control solution was prepared by mixing 1.5 mL of 0.002% DPPH solution and 1.5 mL of ethanol. Moreover, the blank solution could be prepared by mixing 1.5 mL of test sample solution and 1.5 mL of ethanol. Furthermore, the test sample solutions were also prepared by gently

mixing 1.5 mL of 0.002 % DPPH solutions and 1.5 mL of test sample solution in various concentrations (0.78125, 1.5625, 3.125, 6.250, 12.5, 25, 50, 100, 200 and 400 mg/mL). Then, the resulting mixture was homogenized by applying vortex mixer. After that, the solutions were allowed to stand for 30 min at room temperature. Then, the absorbance value of each solution was measured at 517 nm by using UV-Vis spectrophotometer. The measured absorbance values were applied to calculate inhibition percentage by the equation:

$$\% \text{ inhibition} = \frac{\text{Abs}_{\text{DPPH}} - [\text{Abs}_{\text{sample}} - \text{Abs}_{\text{Blank}}]}{\text{Abs}_{\text{DPPH}}} \times 100$$

Where, % inhibition = % inhibition of test sample,  $\text{Abs}_{\text{DPPH}}$  = absorbance of control solution,  $\text{Abs}_{\text{sample}}$  = absorbance of test sample solution,  $\text{Abs}_{\text{blank}}$  = absorbance of blank solution. The antioxidant power ( $\text{IC}_{50}$ ) is expressed as the test substances concentration ( $\mu\text{g/mL}$ ) that result in a 50% reduction of initial absorbance of DPPH solution and that allows to determine the concentration.  $\text{IC}_{50}$  (50% inhibition concentration) values were calculated by linear regressive excel program (Kiattsin *et al.*, 2016). Ascorbic acid was used as a reference compound in the same concentration range as the test compound.

### Acute Toxicity Test

Study on acute toxicity of ethyl acetate extract of the roots of *Dendrobium pulchellum* was performed at Department of Biotechnology, Mandalay Technological University, Patheingyi Township, Mandalay Region, Myanmar. The study was carried out to assess the acute toxicity on oral administration (Gallagher, 2003).

### Sample preparation for acute toxicity

About (100 g) of air dried roots of *Dendrobium pulchellum* were percolated with ethyl acetate (3 L) for two months. The extract was filtered and the filtrate was evaporated to dryness under reduced pressure to attain ethyl acetate extract (2.25 g).

### Method

Both sexes of healthy albino ICR (Institute of Cancer Research) strain mice (30 to 35 g) were randomly selected and kept in their cages for at least 5 days prior to the experiment for acclimatization of laboratory conditions. Before the experiment, the animals were kept fasting overnight for 18 h but were allowed with free access to water. Following period of fasting, mice were weighed and dose was calculated according to the body weight. Then, the test substance was dissolved in distilled water for required concentration and administered orally in a single dose by using disposable syringe. One group was served as the control and only distilled water was given orally. Five groups of mice (five mice in each group) were used for each dose level. Each dose of (500 mg/kg, 1000 mg/kg, 1500 mg/kg, 2000 mg/kg and 2500 mg/kg) were administered orally to five groups of mice (Figure 2). Mice were observed after dosing at least one during the first 30 min, periodically during the first 24 h, with special attention given during the first 4 h and daily up to 10 days. Signs of toxicity and mortality of the mice were recorded. Changes in fur, eyes, mucous membranes, respiratory rate, autonomic central nervous systems and behavioral pattern were observed. At the end of the test (i.e 10 days) the mice were weighed (Litchfield and Wilcoxon, 1949).



**Figure 2** Administration of ethyl acetate extract to the experimental mice

### Extraction and Isolation of Pure Compounds

The air dried roots sample of *Dendrobium pulchellum* (700 g) were percolated with methanol (10L) for one month. The methanol crude extracts were filtered and evaporated the solvent under reduced pressure. The residue was extracted with ethyl acetate to attain 11.3 g of ethyl acetate crude extracts. The obtained crude extracts were subjected to silica gel by using various solvent systems of n-hexane and ethyl acetate. After purification on Sephadex LH-20 with methanol only, mixture of bibenzyl derivatives 1 and 2 were isolated from selected fraction II (Figure 3) as oily form.

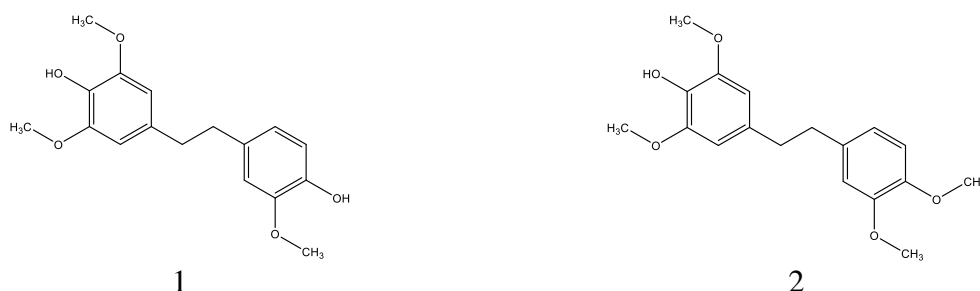


**Figure 3** Compounds isolated from the roots of *Dendrobium pulchellum*

## Results and Discussion

### Phytochemical Constituents

Preliminary phytochemical analysis was performed in order to know different types of organic compounds present in root of *Dendrobium pulchellum*. Analysis of the extract of root sample revealed the presence of phytochemicals such as alkaloids, flavonoids, phenolic compounds, polyphenols, saponins, steroids, tannins, terpenes, glycoside, carbohydrates, lipophilics and reducing sugars. These phytochemicals are known to exhibit medicinal as well as physiological activities.

### Antimicrobial Activities

The antimicrobial activities of various solvent extracts of the roots of *Dendrobium pulchellum* were examined by using agar-well diffusion method as shown in Table 1.

**Table 1** Antimicrobial Activities of Various Solvent Extracts on Different Microbial Strains

Sample	Solvent extracts	Inhibition zone (mm)					
		I	II	III	IV	V	VI
<i>Dendrobium pulchellum</i> roots	n-hexane	-	13	13	-	11	11
	EtOAc	15	-	13	14	14	14
	MeOH	14	11	12	12	12	13

Agar-well – 10 mm

10 mm ~ 14 mm (+)

15 mm ~ 19 mm (++)

20 mm above (+++)

I = *Bacillus subtilis*

II = *Staphylococcus aureus*

III = *Pseudomonas aeruginosa*

IV = *Bacillus pumilus*

V = *Candida albicans*

VI = *Escherichia coli*

According to antimicrobial assay, n-hexane extract responded low activities on *Staphylococcus aureus*, *Pseudomonas aeruginosa*, *Candida albicans* and *Escherichia coli*, except *Bacillus subtilis* and *Bacillus pumilus*. The methanol extract showed low activities on all selected microorganisms. Ethyl acetate extract exhibited medium activities on *Bacillus subtilis* and low activities on *Pseudomonas aeruginosa*, *Bacillus subtilis*, *Candida albicans* and *Escherichia coli* except *Staphylococcus aureus*.

### Determination of Acute Toxicity

The mice (five per group) administered with 500 mg/kg, 1000 mg/kg, 1500 mg/kg, 2000 mg/kg and 2500 mg/kg doses of ethyl acetate extract of *Dendrobium pulchellum* roots were observed for 10 days (Table 2). At the end of observation period, all the mice were alive, did not show any toxic symptoms such as diarrhea, inactivity, restlessness, aggressiveness, eye-dullness, breathing, abnormalities, etc. and did not exhibit loss and obvious changes of body weight. Hence, the test substance can be considered relatively safe.

**Table 2 Acute Toxicity Study of Ethyl Acetate Extract of *Dendrobium pulchellum* Roots Based on Mortality Record**

Dose Sample (mg/kg)	No. of mice	Observation	Day											
			0	1	2	3	4	5	6	7	8	9	10	
2500	5	Alive	5	5	5	5	5	5	5	5	5	5	5	5
		Dead	0	0	0	0	0	0	0	0	0	0	0	0
2000	5	Alive	5	5	5	5	5	5	5	5	5	5	5	5
		Dead	0	0	0	0	0	0	0	0	0	0	0	0
1500	5	Alive	5	5	5	5	5	5	5	5	5	5	5	5
		Dead	0	0	0	0	0	0	0	0	0	0	0	0
1000	5	Alive	5	5	5	5	5	5	5	5	5	5	5	5
		Dead	0	0	0	0	0	0	0	0	0	0	0	0
500	5	Alive	5	5	5	5	5	5	5	5	5	5	5	5
		Dead	0	0	0	0	0	0	0	0	0	0	0	0
Control (25 % EtOH)	5	Alive	5	5	5	5	5	5	5	5	5	5	5	5
		Dead	0	0	0	0	0	0	0	0	0	0	0	0

### Determination of Antioxidant Activity

Antioxidant activities of crude extract were expressed as percentage of DPPH radical inhibition or IC<sub>50</sub> values (µg/mL). The absorbance of standard ascorbic acid and ethyl acetate extract in different concentrations are described in Table 3.

**Table 3 Absorbance of Standard Ascorbic Acid and Ethyl Acetate Extract**

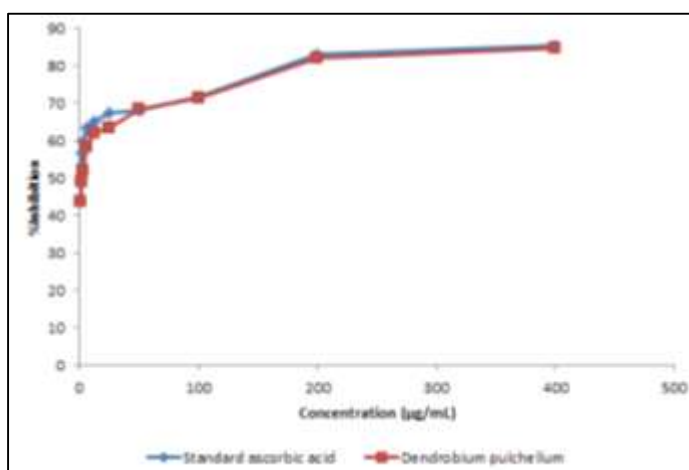
No.	Concentration (µg/mL)	Ascorbic acid		<i>Dendrobium pulchellum</i>	
		Abs <sub>sample</sub>	Abs <sub>blank</sub>	Abs <sub>sample</sub>	Abs <sub>blank</sub>
1	0.78125	0.200	0.001	0.219	0.001
2	1.5625	0.169	0.001	0.198	0.002
3	3.125	0.158	0.002	0.189	0.003
4	6.250	0.145	0.003	0.165	0.004
5	12.5	0.138	0.003	0.152	0.005
6	25	0.130	0.004	0.148	0.006
7	50	0.125	0.001	0.130	0.007
8	100	0.111	0.001	0.119	0.008
9	200	0.068	0.002	0.078	0.009
10	400	0.059	0.002	0.069	0.010

The inhibition percentage of standard ascorbic acid and ethyl acetate extract in different concentration are described in Table 4 and Figure 4.

**Table 4 Percent Inhibition of Standard Ascorbic Acid and Ethyl Acetate Extract**

No.	Concentration (µg/mL)	% Inhibition	
		Standard ascorbic acid	<i>Dendrobium pulchellum</i>
1	0.78125	48.71	43.81
2	1.562	56.70	49.23
3	3.125	59.79	52.06
4	6.25	63.40	58.51
5	12.5	65.20	62.11
6	25.0	67.53	63.40
7	50.0	68.04	68.30
8	100	71.65	71.39
9	200	82.98	82.22
10	400	85.31	84.79

\* Absorbance of DPPH (Control) = 0.388

**Figure 4** Percent Inhibition in Different Concentration of Standard Ascorbic Acid and Ethyl Acetate Extract of *Dendrobium pulchellum*

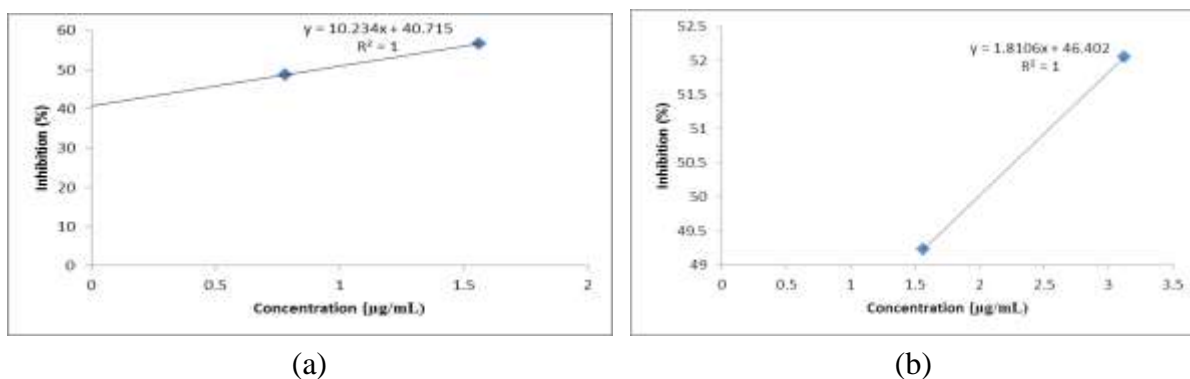


**Figure 5** (a) Linear regression analysis for IC<sub>50</sub> value of standard ascorbic acid and (b) ethyl acetate extract of *Dendrobium pulchellum*

**Table 5** The Linear Regression Equations and IC<sub>50</sub> Values

No.	Test Solution	Regression Equations	IC <sub>50</sub> (µg/mL)
1	Ascorbic acid	$y = 10.234x + 40.715$	0.9072
2	<i>D. pulchellum</i>	$y = 1.8106x + 46.402$	1.987

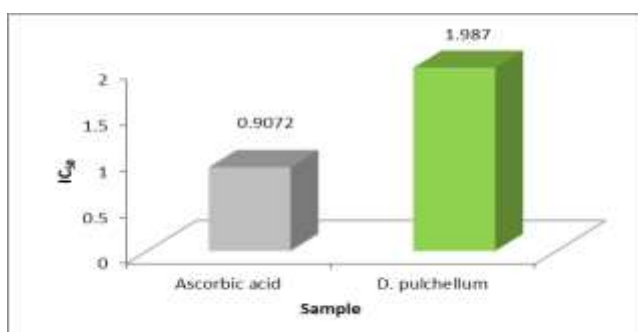


**Figure 6** Histogram of IC<sub>50</sub> values of standard ascorbic acid and *Dendrobium pulchellum* extract

The IC<sub>50</sub> value is a parameter used to measure antioxidant activity and it is defined as the sample extract concentration required for 50 % scavenging of DPPH radicals under experiment condition employed. The smaller IC<sub>50</sub> value corresponds to a higher antioxidant activity. The IC<sub>50</sub> values was calculated by linear regressive excel program (Table 5, Figure 5). According to the results, the significant antioxidant property with IC<sub>50</sub> value of 1.987 µg/mL which is comparable to ascorbic acid solution, standard antioxidant. The comparison of IC<sub>50</sub> values of standard ascorbic acid with crude extracts are shown in Figure 6.

### Structure Elucidation

In the aromatic region of <sup>1</sup>H NMR spectrum, Figure 8(a), one doublet methine proton at  $\delta$  6.83 ppm ( $\delta_c = 114.1$  ppm,  $J = 7.83$  Hz) showed ortho coupling with another doublet methine proton at  $\delta$  6.67 ( $\delta_c = 121.0$  ppm,  $J = 7.82$  Hz). In the DQF-COSY spectrum, Figure 8(d), these two methine protons showed correlation as expected. In the HMBC spectrum, Figure 8(f), doublet methine proton at  $\delta$  6.83 showed  $\beta$ -correlation with two  $sp^2$  quaternary carbons at  $\delta$  133.5, 146.2 ppm and  $\alpha$ -coupling with one  $sp^2$  quaternary carbon at  $\delta$  143.7 ppm. Moreover, another methine proton at  $\delta$  6.67 ppm showed  $\beta$ -coupling with one  $sp^2$  methine carbon at  $\delta$  111.2 ppm and one  $sp^2$  quaternary carbon at  $\delta$  143.7 ppm. Furthermore in HMBC spectrum, Figure 8(f), one

methine proton at  $\delta$  6.60 which is attached to carbon at  $\delta$  111.2 ppm showed  $\beta$  correlation with one  $sp^2$  quaternary carbon at  $\delta$  143.7 ppm and one  $sp^2$  methine carbon at  $\delta$  121.0 ppm and  $\alpha$ -coupling with one  $sp^2$  quaternary carbon at  $\delta$  146.2 ppm. Therefore, fragment (a) could be assigned as shown in Figure 7.

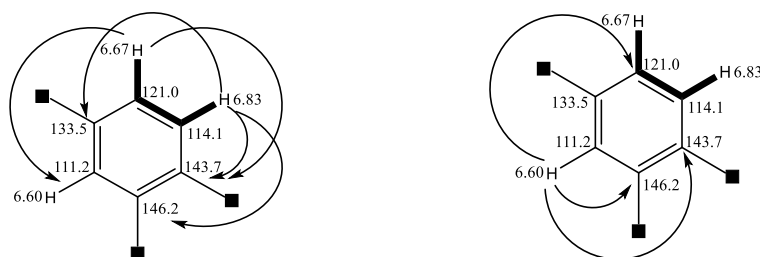
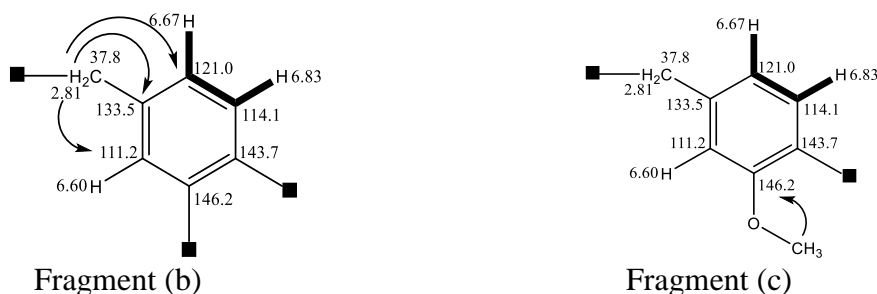


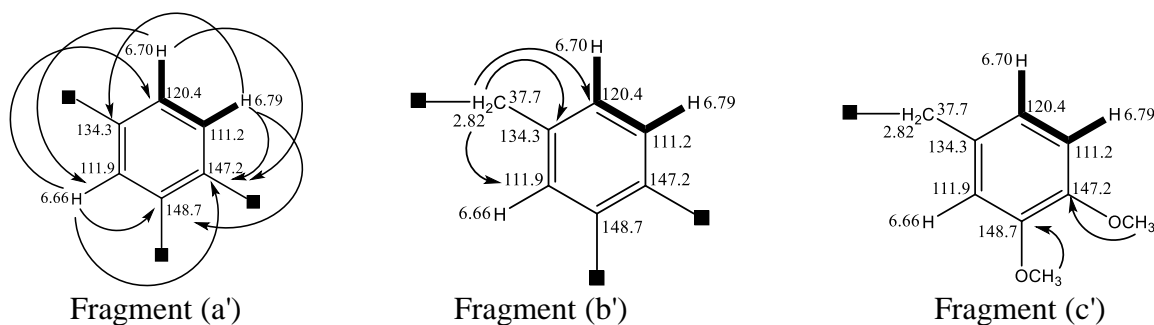
**Figure 7** (—) COSY and (→) HMBC correlations in fragment (a)

Moreover, in the HMBC spectrum, Figure 8(f), methylene protons at  $\delta$  2.81 which is attached to carbon at  $\delta$  37.8 ppm showed  $\beta$ -correlation with two  $sp^2$  methine carbons at  $\delta$  111.2 and 121.0 and  $\alpha$ -coupling with  $\delta$  133.5 ppm. Similarly, two methine protons at  $\delta$  6.67 ppm ( $\delta_c$  121.0 ppm) and  $\delta$  6.60 ppm ( $\delta_c$  111.2 ppm) showed  $\beta$ -coupling with methylene carbon at  $\delta$  37.8 ppm. Thus, the extended fragment (b) could be assigned.



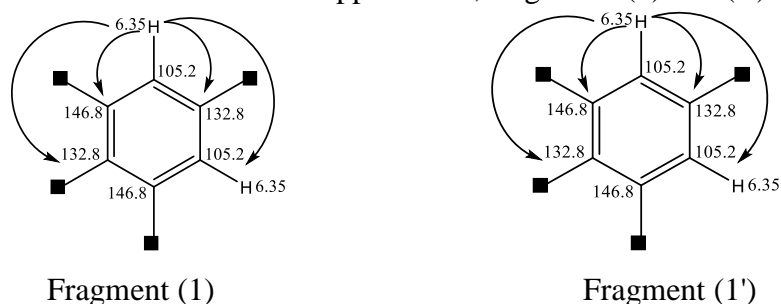
Moreover, singlet methoxy proton at  $\delta$  3.82 ppm showed HMBC correlation to  $sp^2$  quaternary carbon at  $\delta$  146.2 ppm and fragment (c) was elucidated.

Similarly, in the aromatic region of the  $^1\text{H}$  NMR spectrum, Figure 8(a), one doublet methine proton  $\delta$  6.79 ppm ( $\delta_c$  111.2 ppm,  $J = 8.10$  Hz) showed ortho coupling with another methine proton at  $\delta$  6.70 ppm ( $\delta_c = 120.4$  ppm,  $J = 8.08$  Hz). In DQF-COSY spectrum, Figure 8(d), these two methine protons showed correlation as expected. In the HMBC spectrum, Figure 8(f), the methine proton at  $\delta$  6.79 showed  $\alpha$ -correlation with one  $sp^2$  quaternary carbon at  $\delta$  147.2 and one methine carbon at  $\delta$  120.4 ppm and  $\beta$ -correlation with two  $sp^2$  quaternary carbons at  $\delta$  134.3 and 148.7 ppm. Moreover, one methine proton at  $\delta$  6.70 ppm ( $\delta_c$  120.4 ppm) showed  $\beta$ -coupling with one  $sp^2$  quaternary carbon at  $\delta$  147.2 ppm and one  $sp^2$  methine carbon at  $\delta$  111.9 ppm. Furthermore, in the HMBC spectrum, Figure 8(f), one methine proton at  $\delta$  6.66 ppm ( $\delta_c$  111.9 ppm) showed  $\beta$ -correlation with one  $sp^2$  quaternary carbon at  $\delta$  147.2 ppm and one methine carbon at  $\delta$  120.4 ppm. Therefore, fragment (a') could be assigned. In addition, the methylene protons  $\delta$  2.82 ppm showed  $\beta$ -correlation with two  $sp^2$  methine carbons at  $\delta$  111.9 and 120.4 ppm and  $\alpha$ -coupling with one  $sp^2$  quaternary carbon at  $\delta$  134.3 ppm which gave fragment (b'). On the other hand, the appearance of  $\beta$ -long range signals between two methoxy singlets  $\delta$  3.82 and 3.83 ppm with two  $sp^2$  quaternary carbons at  $\delta$  147.2 and 148.7 ppm led to fragment (c').

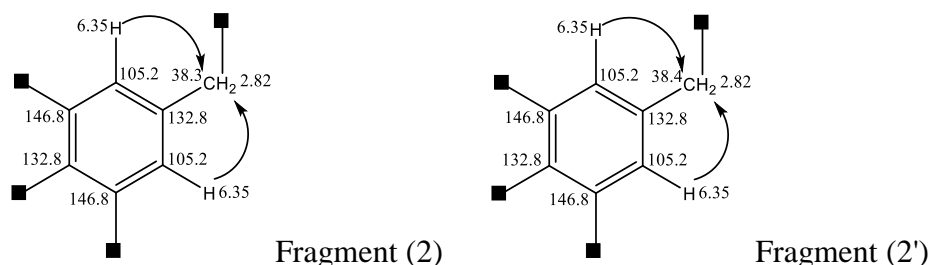


In the aromatic region of  $^1\text{H}$  NMR spectrum, Figure 8(a), the signal at  $\delta$  6.35 ppm with the integration of four protons was detected. By the analysis of HMQC together with  $^{13}\text{C}$  NMR spectra, the proton signal at  $\delta$  6.35 ppm was connected to methine carbon at  $\delta$  105.2 ppm. Therefore, the signal at  $\delta$  105.2 ppm must be four methine carbons. According to integration of the signals in  $^{13}\text{C}$  NMR spectrum, Figure 8(b), the signals at  $\delta$  132.8 and 146.8 ppm were belonged to four carbons in each signal.

The four methine protons at  $\delta$  6.35 ppm in  $^1\text{H}$  NMR spectrum, Figure 8(a), were ascribed to two 1, 2, 3, 5-tetrasubstituted benzene ring. In the HMBC spectrum, Figure 8(f), two equivalent protons at  $\delta$  6.35 ppm showed correlation with one  $sp^2$  methine carbon at  $\delta$  105.2 and two  $sp^2$  quaternary carbons at  $\delta$  132.8 and 146.8 ppm. Thus, fragments (1) and (1') could be assigned.



Furthermore, the two equivalent methine protons at  $\delta$  6.35 ppm from fragment (1) and (1') showed HMBC cross signals to two methylene carbons at  $\delta$  38.3 and 38.4 ppm respectively. Therefore, the fragment (2) and (2') could be assigned.

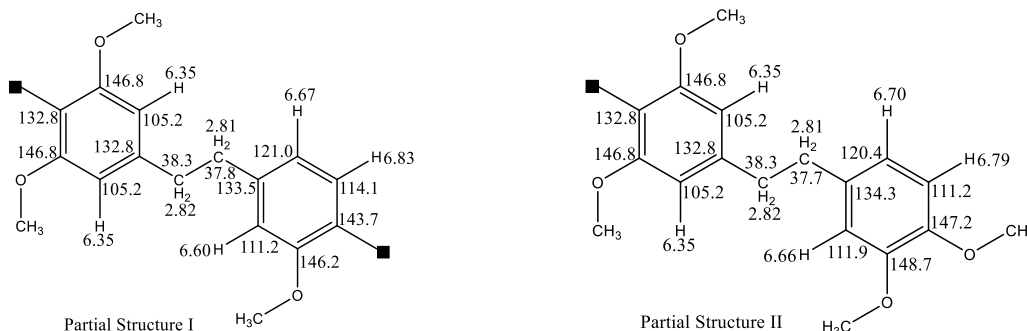


In the HMBC spectrum, Figure 8(f), the two methylene protons at  $\delta$  2.82 ppm ( $\delta_c$  38.3, 38.4 ppm) showed  $\beta$ -correlation with two equivalent  $sp^2$  methine carbons at  $\delta$  105.2 ppm. Thus, the fragment (2) and (2') could be confirmed. Furthermore, in the HMBC spectrum, Figure 8(f), the methylene protons at  $\delta$  2.82 ppm ( $\delta_c$  38.3 ppm) from fragment (2) showed  $\beta$ -correlation with one  $sp^2$  quaternary carbons at 133.5 ppm from fragment (c). The methylene protons at  $\delta$  2.82 ppm ( $\delta_c$  37.8 ppm) from fragment (c) showed  $\beta$ -correlation with one  $sp^2$  quaternary carbon at  $\delta$  132.8 ppm from fragment (2). Therefore, the fragment (c) and (2) could be connected and partial structure I could be assigned.

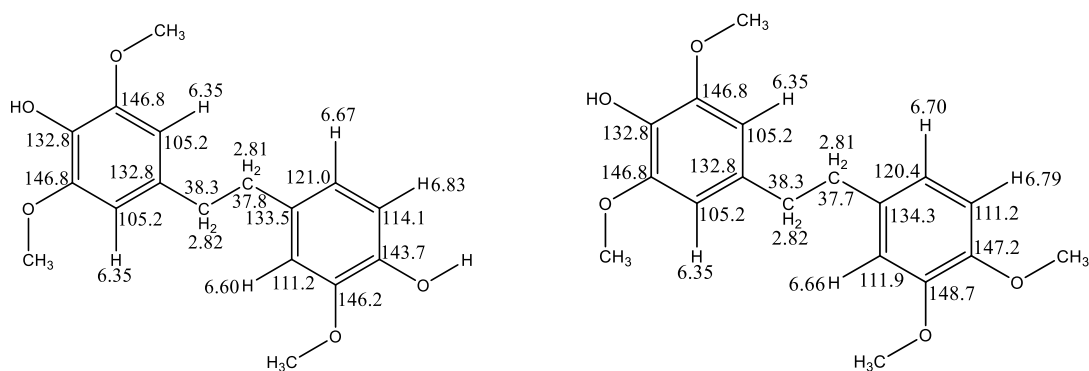
Similarly, the methylene proton at  $\delta$  2.82 ppm ( $\delta_c$  38.4 ppm) from fragment (2') showed  $\beta$ -correlation with one  $sp^2$  quaternary carbon at  $\delta$  134.3 ppm from fragment(c'). The methylene

protons at  $\delta$  2.82 ppm ( $\delta_C$  37.7 ppm) from fragment (c') showed  $\beta$ -correlation with one  $sp^2$  quaternary carbon at  $\delta$  132.8 ppm from (2'). Therefore, the fragment (c') and (2') could be connected and partial structure II could be drawn.

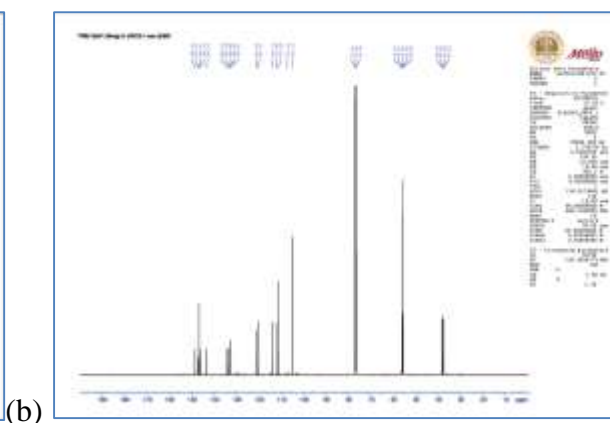
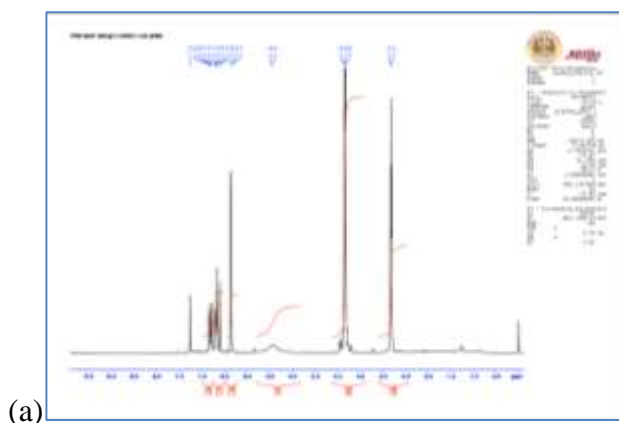
The singlet methoxy signals at  $\delta$  3.84 ppm ( $\delta_C$  55.7, 55.8, 55.9, 56.2 ppm) showed correlation with four  $sp^2$  quaternary carbons at  $\delta$  146.8 ppm from partial structure I and II.

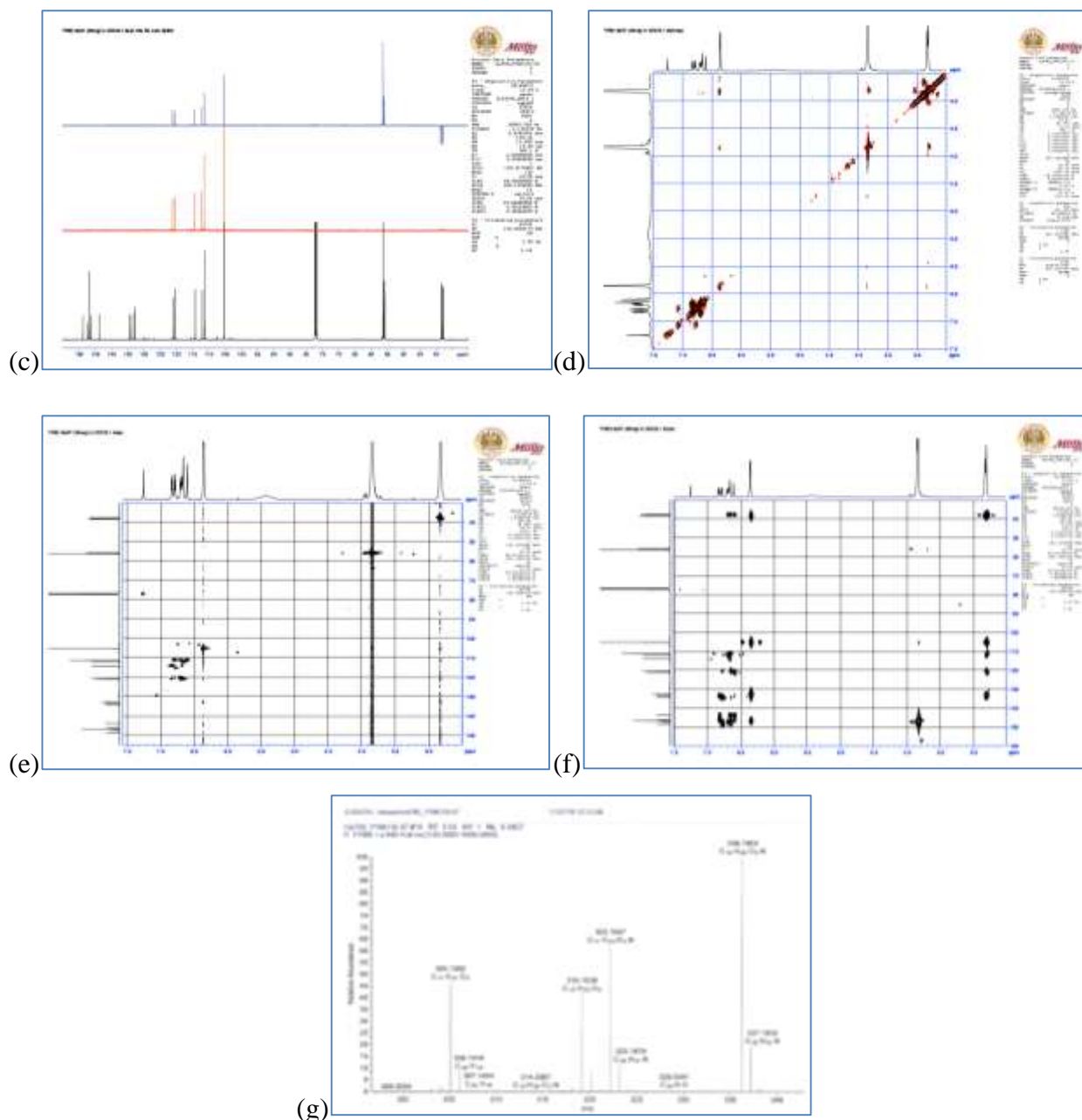


In addition, (+)-DART mass spectrum, (Figure 8g) revealed two pseudomolecular ion peaks  $[M+H]^+$  at  $m/z$  305.1362 and 319.1538 respectively. The two molecular mass were deduced as 304 and 318. Their molecular formula was  $C_{17}H_{20}O_5$  and  $C_{18}H_{22}O_5$ . Therefore, the remaining two hydroxyl groups were attached to two  $sp^2$  quaternary carbons at  $\delta$  143.7 and 132.8 ppm in partial structure I and one hydroxyl group was attached to one  $sp^2$  quaternary carbons at  $\delta$  132.8 ppm in partial structure II, and complete structures of two bibenzyl derivatives 1 and 2 were obtained.



Structures of compound 1 and 2





extracts showed high antioxidant activity with  $IC_{50}$  of 1.987  $\mu\text{g/mL}$  which is comparable to  $IC_{50}$  0.9072  $\mu\text{g/mL}$  of ascorbic acid. Finally, two bibenzyl derivatives from ethyl acetate extract were isolated and characterized by NMR and mass studies.

### Acknowledgements

The authors thank Dr Yoshiaki Takaya, Associate Professor, Faculty of Pharmacy, Meijo University for NMR and mass measurements. The authors thank Dr Yi Yi Myint, Professor and Head, Department of Chemistry, University of Mandalay and Dr Mi Mi Hlaing, Professor and Head, Department of Chemistry, Mandalay University for their permission to submit the paper.

### References

- Gallagher, M.E. (2003). "Toxicity Testing Requirements, Methods and Proposed Alternatives". vol. 26. pp. 257-258.
- Hassam, B.A.R. (2012). "Medicinal Plants (Important and Uses)." *Pharmaceut Anal Acta.*, vol. 3, pp. 1-5.
- Kiattsin, K., Nantarat, T., and Leelapornpisid, P. (2016). "Evaluation of Antioxidant and Anti-tyrosinase Activities as well as Stability of Green and Roasted Coffee Bean Extracts from *Coffea arabica* and *Coffea canephora* Grown in Thailand". *Journal of Pharmacognosy and Phytotherapy.* vol. 8, pp. 182–192.
- Kowitdamrong, A., Chanvorachote, P., Sritularak, B. and Pongrakhananon, V. (2013) "Moscatilin Inhibits Lung Cancer Cell Motility and Invasion via Suppression of Endogenous Reactive Oxygen Species." *Bio Med Research International journal*, vol. 1, pp. 1-11.
- Litchfield, J.T., and Wilcoxon, F. (1949). "A Simplified Method of Evaluating Dose-effect Experiments". *The Journal of Pharmacology and Experimental Therapeutics*, vol. 96, pp. 99-113.
- Oladeji, O. (2016). "The Characteristics and Roles of Medicinal Plants: Some Important Medicinal Plants in Nigeria. *Natural Products: An India Journal*, vol. 12, pp. 1-8.
- Singh, S., Singh, A. K., Kumar, S., Kumar, M., Pandey, P. K., and Singh, M.C.K. (2012). "Medicinal Properties and Uses of Orchids: A Concise Review". *Elixir International Journal*, vol. 52, pp. 11627-11634.

## IDENTIFICATION AND ANTIMICROBIAL ACTIVITY OF SELECTED SOIL FUNGUS, HMF-33

Hlaing Myint Thu<sup>1</sup>, Su Su Latt<sup>2</sup>, San Yu Maw<sup>3</sup>, Zar Zar Yin<sup>4</sup>

### Abstract

The present research work was focused on the identification and extraction of antimicrobial active soil fungus HMF-33. This fungus was isolated by serial dilution method from the soil of Naung Taw village, Homalin Township. The macroscopic and microscopic characters of HMF-33 were observed on the Blakeslee's Malt Extract Agar (BMEA Medium), Czapek-Dox Agar (CZA Medium), Malt Extract Agar (MEA Medium), Glucose Ammonium Nitrate Agar (GAN Medium), Potato Glucose Agar (PGA Medium) and incubated for 7 days at room temperature. According to the results, selected fungus HMF-33 was identified as the genus *Penicillium* sp. In the investigation of fermentation medium (FM), eight kinds of fermentation media was studied by using various carbon and nitrogen sources. Among them, FM 6 showed the higher antimicrobial activity than other fermentation media on seven test organisms. In the results of paper chromatography, n-butanol was the most suitable solvent for extraction of antimicrobial secondary metabolites from fermented broth of HMF-33 and bioautographic assay showed R<sub>f</sub> values had 0.92 on *Bacillus subtilis* and 0.90 on *Candida albicans*. Furthermore, crude extract 33.0g yielded from 17.5L of fermented broth of *Penicillium* sp., HMF-33 and showed highly antimicrobial activities (20.53-32.94mm) against (gram positive, gram negative bacteria and fungi) ten test organisms. Crude extract of *Penicillium* sp. (HMF 33) possessed broad spectrum bioactivity. Therefore, crude extract of *Penicillium* sp. may be used by the pharmaceutical industries for the production of antimicrobial compounds from local sources.

**Keywords:** bioautographic assay, secondary metabolites, antimicrobial activities, *Penicillium* sp., broad spectrum

### Introduction

*Penicillium* derives its name from the latin word "Penicillius" meaning "little brush" (Pitt, 1979). The subgenus (verticillate nature) can be determined by the number of branch points (rami) between the phialide which bears the conidia on the tip and the stipe (hyphal stalk). Isolates with one such branch point are monoverticillate, two branches-biverticillate, three branches – terverticillate and four branches – quarterverticillate (pitt, 1991). Identification of *Penicillium* species should focus on the implementation of both morphological and molecular identification methods.

Solvent extraction provides the ease of liquid handing, the potential for high throughput operation, and the potential for adaptation to continuous operation (Schugerl, 1993). There are three main methods that are used to extract secondary metabolites namely; liquid-liquid extraction, reverse phase micelles and solid phase extraction. The most commonly used and favoured methods is the liquid- liquid extraction. <sup>1</sup>

Antibiotics play a very important role in controlling infectious diseases (Sarkaret *al.*, 2014). Antibiotics are produced by bacteria, fungi, sponges etc. Antimicrobial compounds are used to kill or retard the growth of the living organisms. Therefore, the aim of the research work was to identify genus level of HMF 33 and to produce antimicrobial metabolite from HMF 33, *Penicillium* sp.

---

<sup>1</sup> Lecturer, Department of Chemistry, Sagaing University

<sup>2</sup> Lecturer, Department of Botany, Sagaing University

<sup>3</sup> Dr, Lecturer, Department of Chemistry, Taungoo University

<sup>4</sup> Dr, Associate Professor, Department of Botany, Patheingyi University

## Materials and Methods

### Method for Collection of Soil Sample

The soil sample was collected from Naung Taw village, Homalin Township, during July 2017. The soil sample was collected from Naung Taw village (up to 15 cm depth) into sterilized polythene bags after removing the surface soil for the isolation of fungi and brought to the laboratory of Biological Resources and Biotechnology Development Center at Patheingyi University.

### Isolation of Fungi from the Soil Sample

Strain HMF-33 was isolated by the serial dilution method (Dubey and Maheshwari, 2002) from the soil of Naung Taw village (N 24° 49' 39.211"E 95° 07' 07.066"), Homalin Township.

### Culture and identification of HMF-33

HMF-33 was identified in the level of genus on different media such as Blakeslee's Malt Extract Agar (BMEA Medium), Czapek- Dox Agar (CZA Medium), Malt Extract Agar (MEA Medium), Dichloram Rose Bengal- Chloramphenicol Agar (DRBC Medium), Glucose Ammonium Nitrate Agar (GAN Medium), Potato Glucose Agar (PGA Medium). Morphological features of HMF-33 cultures were studied, the major and remarkable macroscopic features in species identification were the colony diameter and color (surface and reverse). Riddle's classic slide culture method (Riddle, 1950) was used for microscopic study of HMF-33. Microscopic characteristics for the identification were conidia length, conidia width, conidia shape, conidia ornamentation, stipe length, stipe width, stipe ornamentation, phialide shape and branching pattern. The identification of fungus HMF-33 was undertaken by the method of Ando, 2016, literature reviews and references key (Ando, 2004).

### Agar Well Diffusion Method

Isolated strains were performed by agar well method (Collins, 1965) for the antimicrobial activities. Cork borer was used to make the wells (8 mm in diameter) in the autoclaved basal antimicrobial test-medium. Wells impregnated with 3-7 days old culture fermented broth (20µL/well) were incubated at room temperature for 24-28 h. After 24-28 h of incubation, the clear zones were measured. Therefore, the diameter of clear zones had been observed as potent activity as shown by respective strain. Clear zones surrounding the wells indicated the presence of antimicrobial activities which inhibit the growth of the test organisms selectively.

### Test Organisms

The test organisms used for this experiment were *Agrobacterium tumefaciens* NITE 09678, *Bacillus pumilus*, *Bacillus subtilis* IFO 90571, *Candida albicans* NITE 09542, *Escherichia coli* AHU5436, *Pseudomonas fluorescens* IFO94307, *Malassezia furfur*, *Micrococcus luteus*, *Staphylococcus aureus* AHU8465, *Saccromyces cereviciae*, *Salmonella typhi*. The organisms were obtained from National Institute of Technology and Evaluation (NITE, Japan), and Pharmaceutical Research Department, Yangon, Myanmar.

### Paper Chromatography

Paper chromatography was performed to know how to extract the bioactive compounds from fermentation broth by using which solvent system (Tomitta, 1988). The filter paper and four solvent systems; n-butanol-acetic acid –water (3:1:1), n-butanol saturated with water, ethyl acetate saturated with water and 20% NH<sub>4</sub>Cl were used for preliminary characterization of antibiotics. The fermented broth (10µl) were spotted by capillary tube on the paper and allowed to dry. The papers

were chromatographed in each solvent. Then, bioautography was done to check the antimicrobial activity of each. Each paper was placed on assay agar plates, in the same method as paper disc assay, except that after one hour the paper was taken out, then the plates were incubated for 24-36 hours. The inhibitory zone place was measured yielding a  $R_f$  values were measured for the corresponding bioactive compounds.

### **Extraction of Bioactive Metabolite from Culture Filtrate of HMF-33**

The fungal culture in fermentation medium was incubated with shaking for four days at room temperature. When the incubation period was complete, mycelia was filtered off, soaked on solvents (such as ethyl acetate and n- butanol) for 24 hrs and filtered, resulting in an organic layer. The antimicrobial metabolite was extracted by liquid-liquid extraction with solvents. Equal volume (1:1 v/v) of culture filtrate and solvents were taken in a separating funnel and agitated for about 30 minutes. Then the mixture was allowed to stand till complete separation to upper and lower layer (phase) was formed. The upper (solvent) layers were evaporated to get concentrated crude extract (Petit *et al.*, 2009). The extracts were tested for antimicrobial activity by using agar well diffusion assay.

## **Results and Discussion**

### **Colony Characters and Growth of HMF-33**

In the study of morphological of HMF-33, six differential culture media were used for identification of HMF-33. A culture time of seven days was generally required for identification of HMF-33 strain. Using differential media like BMEA, CZA, MEA, GAN, DRBC, PGA media with colony and microscopic characters of HMF-33 growth on these culture media enable to discriminate HMF-33. Fungus HMF-33 has different growth, different surface and reverse color on different media. Isolates of single species may appear different if grown on various media (Raper and Thom, 1949). The surface color of HMF-33 were greenish yellow, gray, yellowish green, white on six different media and reverse color of HMF-33 were yellow, pink, white cream and yellow on BMEA, CZA, MEA, GAN, DRBC, PGA media. Mushimiyimana *et al.*, 2016 mentioned that colonies on CYA, MEA and YES with *Penicillium sp* and *Penicillium crustosum* are white to cream, yellow and dark green colour on observe whereas in reverse pale, yellow, orange, light brown, and dark brown. The reverse colony was usually pale to yellowish or brownish. Ando, 2004 stated that as the results of the observation of spore production, fungi are identified under genus level. For the identification of fungi under species level, media described and used in the descriptions or the monographs of each genus will be used. In generally, PDA, MEA, LCA, CZA and OA media are used for the identification media. Therefore, the media for identification varied with each fungus group. Ando, 2004 mentioned that many fungi grow robustly on BMEA medium. In the studying of colony growth of HMF-33, Colony growth of HMF-33 have excellent growth 39.00-45.89mm on BMEA medium, followed by 39.00-39.20mm on MEA medium, 37.13-37.48mm on PGA medium, 33.90-39.54mm on CZA, 24.55-24.65mm on DRBC, 19.88-21.00mm on GAN medium respectively (Table 1 and Figure 1) and colony texture of HMF-33 on six different media was almost valutinuous.

**Table 1 Colony Morphology of HMF-33 on Different Media at Seven Days**

Culture Media	Surface colour	Reverse colour	Size of Colonial Growth (mm)
BMEA	Greenish yellow	Yellow	39.00-45.89
CZA	Greenish yellow	Yellow	33.90-39.54
MEA	Gray in the center Yellow in the periphery	Yellow	39.00-39.20
GAN	Yellowish green	Pink	19.88-20.00
DRBC	White	White cream	24.55-24.65
PGA	Yellowish green	Yellow	37.13-37.48

10-20mm = Poor growth      20-30mm = Moderate growth  
 30-40mm = Good growth      40 to above = Excellent growth

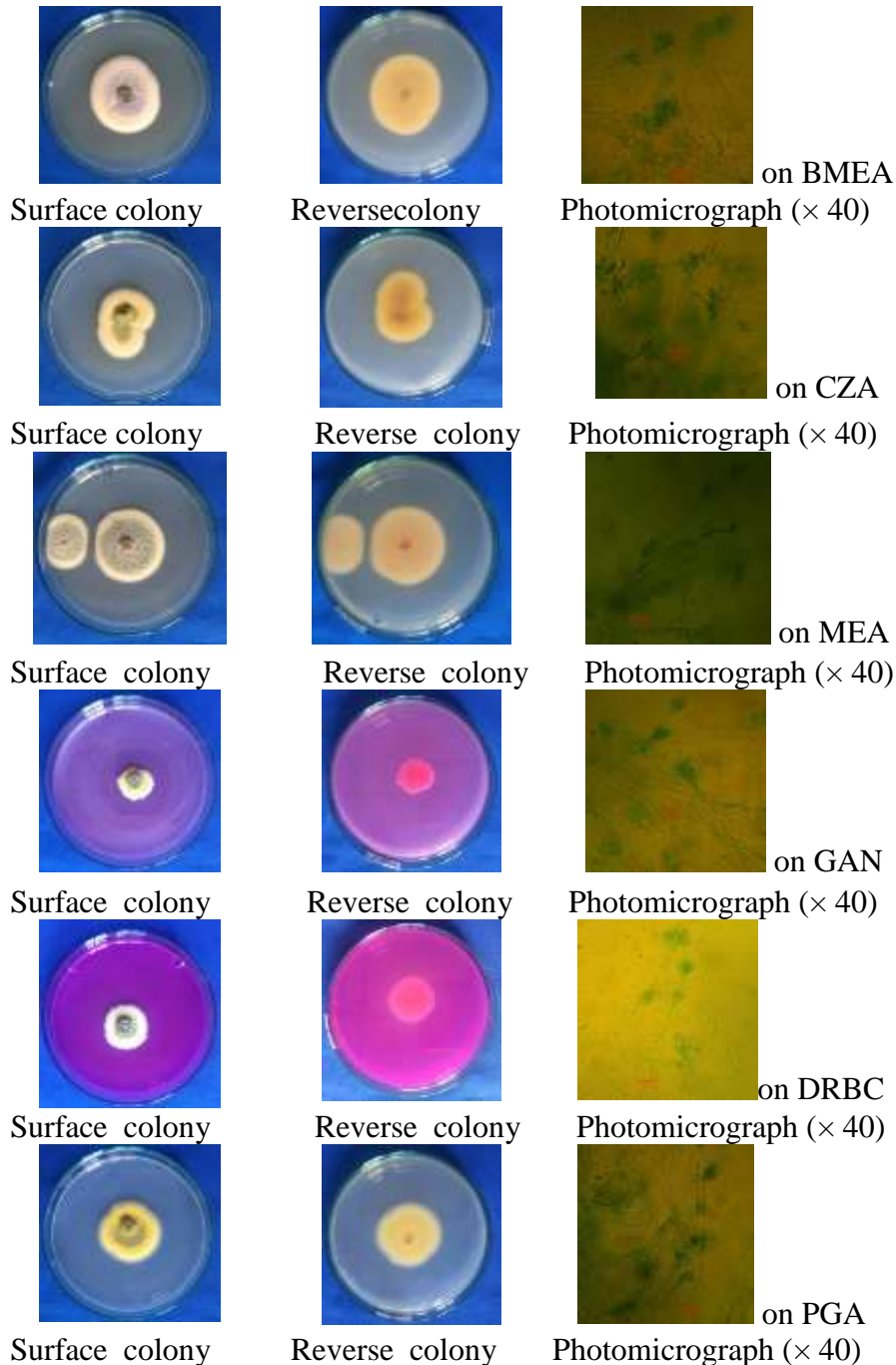


**Figure 1** Colony and microscopic characters of isolated fungus HMF-33 in six (BMEA, CZA, MEA, GAN, DRBC, PGA) differential media at seven days

### Microscopic Character of Fungus HMF-33

In the microscopic characters of HMF-33, conidiophores were biverticillate, appressed elements, born from surface hyphae, stipes were smooth walled,  $100-120\mu\text{m} \times 2.5-3\mu\text{m}$  and have a cluster of four metulae; cylindrical,  $7.5-8\mu\text{m} \times 2-2.5\mu\text{m}$ . Phialids were cylindrical tapering to a distinct column,  $7.5-8\mu\text{m} \times 2-2.5\mu\text{m}$ . Conidia were small in size ( $2-2.5\mu\text{m}$ ), globose in simple shape with smooth and chain in production (Figure 2). These microscopic characters were similar to the investigation of the *Penicillium* species of Ando (2004). Tiwari, 2011 also reported that *Penicillium rubrum* showed aerial mycelium; strips long smooth wall bearing biverticillate *penicillin* narrow and the conidia was smooth strongly. *Penicillium* variable showed smooth, much shorter hyphae, conidiophores typically biverticillate and *P. multicolor* showed septate hyphae and conidia were spheroidal. The regular production of biverticillate *Penicillin* with 4 to 6 terminal metulae, and phialides, which were flask shaped and distinctly shorter than metulae by *Penicillium* isolate are indicatives that it belongs to the subgenus *Furcatum* section (pitt, 2000). Barnett, 1969 also reported that conidiophores arising from the mycelium singly or less often in synnemata, branched near the apex to form a brush-like, conidia-bearing apparatus; ending in phialides which pinch off conidia in dry chain; conidia hyaline or brightly colored in mass, one celled, mostly globose or ovoid, produced basipetally. According to above evidence, HMF-33 may be identified as the genus *Penicillium* sp.

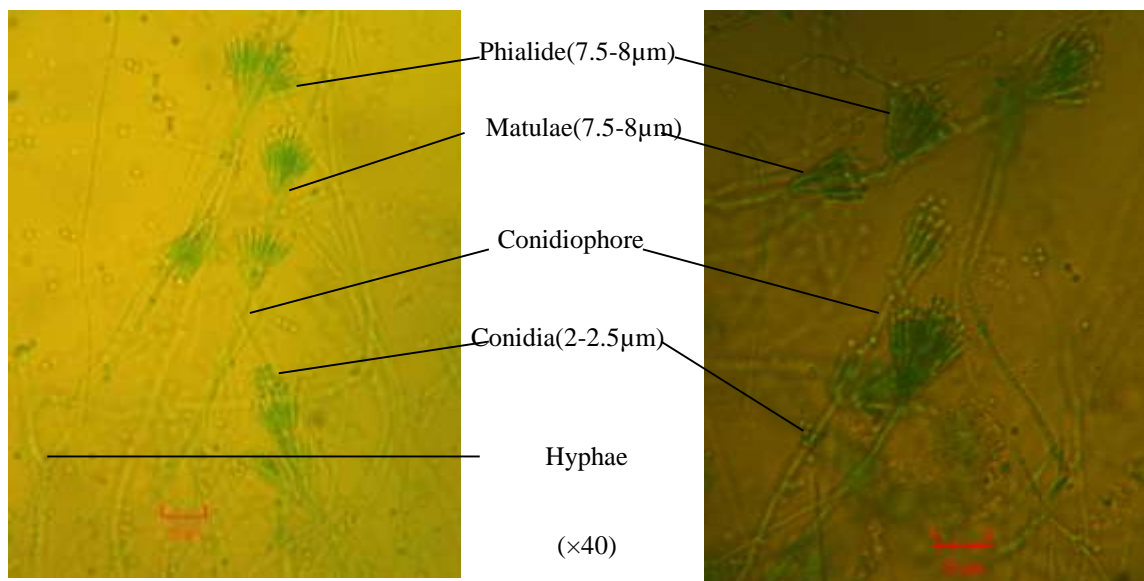


**Figure 2** Microscopic Examination of Selected Fungus HMF-33

### Effect of Different Concentration of Carbon and Nitrogen on Fermentation Media by HMF-33, *Penicillium* sp

Carbon and nitrogen sources from fermentation medium of Ando,2004 was substituted by dextrose 3.2g, fructose 2.4g, casein 0.24g and yeast extract 2.4g in 100ml of fermentation medium. The eight fermentation media were performed for antimicrobial activities with test organisms such as *Bacillus subtilis* and *Candida albicans*. Among of all fermentation media, fermentation medium FM-6 showed maximum antimicrobial activity 30.88mm against *Bacillus subtilis* and 31.61mm against *Candida albicans*, followed by FM-3 (30.07mm and 31.08mm), FM-5 (28.71mm-29.11mm), FM-4 (28.28mm-29.47mm), FM-1 (27.50mm-29.68mm), FM-8 (25.68mm and 27.23mm), FM-2 (24.33mm and 24.66mm), FM-7 (22.68mm and 23.92mm) against *Bacillus subtilis* and *Candida albicans* (Table 2 and Figure 2). HMF-33, *Penicillium* sp produced red pigment in fermentation media including dextrose. Mendez *et al.*, 2011 mentioned that *P.*

*purpurogenum* can produce colorants in both solid and liquid media. *P. purpurogenum* DPUA 1275 was studied to produce yellow, orange, and red extracellular colorants during culture on an orbital shaker (Santos-Ebinuma *et al.*, 2013).

**Table 2 Antimicrobial Activity of HMF 33, *Penicillium sp* on the Fermentation Medium with the Various Carbon and Nitrogen Concentrations**

Fermentation media	Two test organisms and Inhibition Zone (mm)	
	<i>Bacillus subtilis</i>	<i>Candida albicans</i>
FM 1	27.50	29.68
FM 2	24.33	24.66
FM 3	30.07	31.08
FM 4	28.28	29.47
FM 5	28.71	29.11
<b>FM 6</b>	<b>30.88</b>	<b>31.61</b>
FM 7	22.68	23.92
FM 8	25.68	27.23



**Figure 2 (a)** Production of red pigment by HMF-33 in Fermentation including dextrose

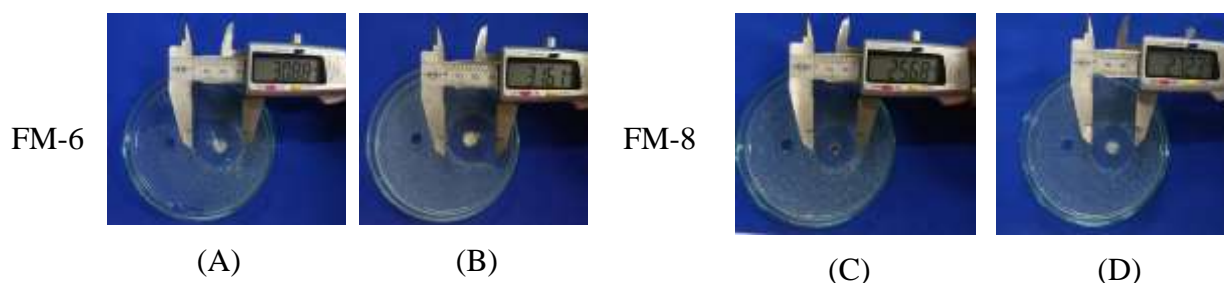


**Figure 2 (b)** Antimicrobial Activity of HMF 33 on the Fermentation Medium with the Various Carbon and Nitrogen Concentrations against *Bacillus subtilis* (A, C) and *Candida albicans*(B, D), (FM-6, FM-8)

### Antimicrobial Activity of HMF-33, *Penicillium sp* on the Suitable Synthetic Fermentation Medium

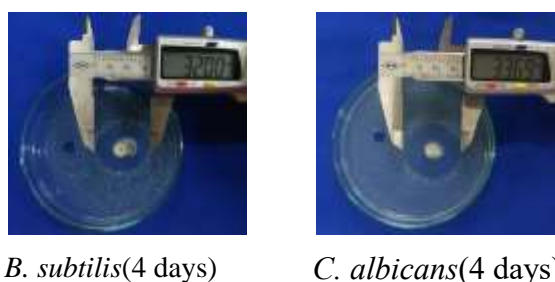
When synthetic fermentation medium was performed together with the optimal fermentation parameters such as 48h of seed culture, 5% inoculum size, temperature 25 °C, pH 6.5, dextrose concentration 3.2 % (w/v), yeast extract concentration 0.24 % (w/v), 250mL of fermentation vessel size with shaking culture, antimicrobial activity of HMF 33, *Penicillium spp.* exhibited inhibition zone 24.56mm against *Agrobacterium tumefaciens* at 4 days, 26.72mm against *Bacillus pumilus* at 4 days, 32.00mm against *Bacillus subtilis* at 4 days, 33.61mm against *Candida albicans* at 4 days, 26.42mm against *Escherichia coli* at 4 days, 25.08mm against *Pseudomonas fluorescens* at 5 days, 25.56mm against *Staphylococcus aureus* at 5 days (Table 3 and Figure 3).

**Table 3 Antimicrobial Activity of HMF-33, *Penicillium* sp on the Suitable Synthetic Fermentation Medium (6) against Seven Test Organisms**

Fermentation Periods(Days)	Seven test organisms and Inhibition Zone (mm )						
	1	2	3	4	5	6	7
2	20.60	20.02	20.90	22.17	21.21	16.61	22.47
3	21.43	21.67	23.30	24.62	24.50	21.79	24.41
4	24.56	26.72	32.00	33.69	26.42	24.16	24.16
5	23.20	25.83	24.64	25.75	25.07	25.08	25.56
6	22.89	25.30	22.40	25.07	24.86	23.19	23.61
7	20.40	18.40	19.73	19.77	19.64	14.09	21.31

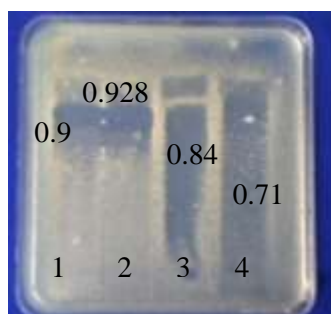
1. <i>Agrobacteriumtumefaciens</i>	4. <i>Candida albicans</i>	7. <i>Staphylococcus aureus</i>
2. <i>Bacillus pumilus</i>	5. <i>Escherichia coli</i>	
3. <i>Bacillus subtilis</i>	6. <i>Pseudomonasfluorescens</i>	



**Figure 3** Antimicrobial Activity of HMF-33, *Penicillium* sp on the Suitable Synthetic Fermentation Medium (6) against Seven Test Organisms

Paper Chromatography of Fermented Broth of HMF-33, *Penicillium* sp

In this study, four solvents (20% NH<sub>4</sub>CL, n-Butanol saturated with water, n-Butanol-Acetic acid-Water (3:1:1) and ethyl acetate saturated with water) were used. According to the R<sub>f</sub> values, 0.92 and 0.90, n-Butanol was more extractable the antimicrobial metabolites than other solvents, followed by n-Butanol-Acetic acid-Water (3:1:1) 0.9 and 0.84 and the lower R<sub>f</sub> value by ethyl acetate saturated with water (0.84 and 0.71), but 20% NH<sub>4</sub>CL was not clearly showed inhibitory zones and R<sub>f</sub> value ( Fig 4 -a and b).



**Solvent system**

1. n-Butanol-Acetic acid-Water (3:1:1)
2. n-Butanol saturated with water
3. Ethyl acetate saturated with water
4. 20% NH<sub>4</sub>CL

**Figure 4** (a) Paper Chromatography bioautographic assay (against *Bacillus subtilis*)



### Solvent system

1. n-Butanol-Acetic acid-Water (3:1:1)
2. n-Butanol saturated with water
3. Ethyl acetate saturated with water
4. 20% NH<sub>4</sub>CL

(b) Paper Chromatography bioautographic assay (against *Candida albicans*)

### Comparison of antimicrobial activity of metabolite in HMF-33, *Penicillium* sp extracted with different solvents of EtOAc and n-BuOH

When using EtOAc solvent, equal volume (1:1 v/v) of culture filtrate and ethyl acetate resulted in inhibition zone shown 19.15mm and 17.94mm against *Bacillus subtilis* and *Candida albicans* at upper layer. Antimicrobial activities showed 22.30mm and 19.13mm against *Bacillus subtilis* and *Candida albicans* at lower layer. Fermented broth of HMF-33 showed 20.55mm, 17.10mm against *Bacillus subtilis* and *Candida albicans*. When using n-BuOH solvent, equal volume (1:1 v/v) of culture filtrate with n-butanol showed inhibition zone was 23.33mm against *Bacillus subtilis* and 21.79mm against *Candida albicans* at upper layer. Antimicrobial activities showed 15.60mm and 12.64mm against *Bacillus subtilis* and *Candida albicans* at lower layer. Fermented broth of HMF-33, *Penicillium* sp showed 20.60mm, 17.27mm against *Bacillus subtilis* and *Candida albicans*. These results were shown in (Table 5 and Figure 5).

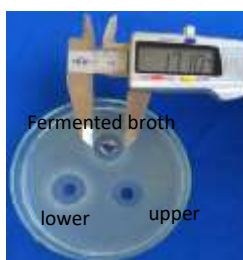
**Table 5** Comparison of antimicrobial activity of metabolite in HMF-33, *Penicillium* sp extracted with different solvents

Extracted with different solvents (1:1 v/v)	Two test organisms and Inhibition Zone (mm)					
	<i>Bacillus subtilis</i>			<i>Candida albicans</i>		
	1	2	3	1	2	3
EtoAc Extract	20.55	19.15	22.30	17.10	17.94	19.13
BuOH Extract	20.60	23.33	15.60	17.27	21.79	12.64

1. Fermented broth 2. Upper layer 3. Lower layer



against *Bacillus subtilis*



against *Candida albicans*

**Figure 5** (a) Antimicrobial activity of metabolite in HMF-33, *Penicillium* sp extracted with EtOAc solvent

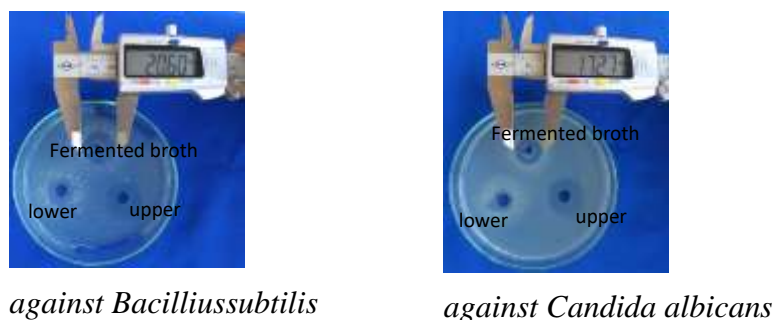


**Figure 5 (b)** Antimicrobial activity of metabolite in HMF-33, *Penicillium* sp extracted with BuOH solvent

**Extraction Antimicrobial Metabolites from HMF-33, *Penicillium* sp**

According to the results of paper chromatography (PPC), comparison with different solvents of EtOAc and n-BuOH, extracted with equal ratio (1:1 v/v) of culture filtrate and n-butanol to yield 33.0g of brown solid crude extract. Preparation of n-butanol extract from fermented broth of HMF-33, *Penicillium* sp was shown in Figure 6.

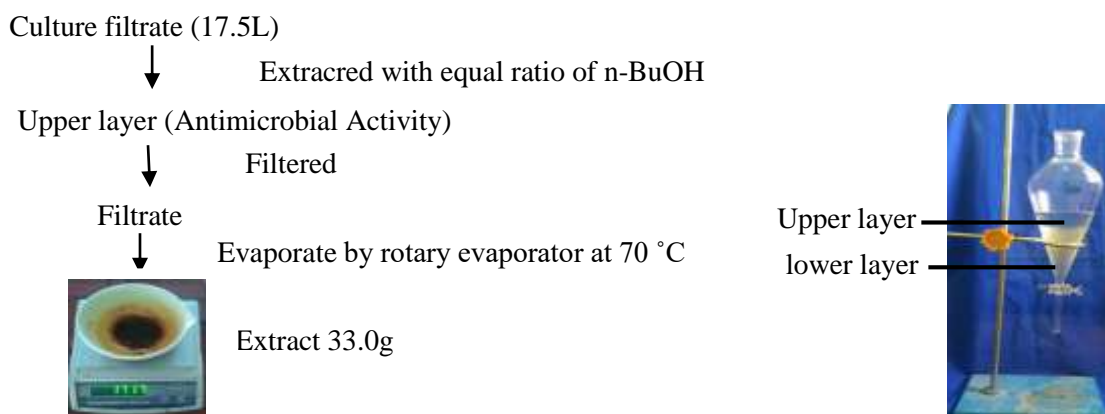


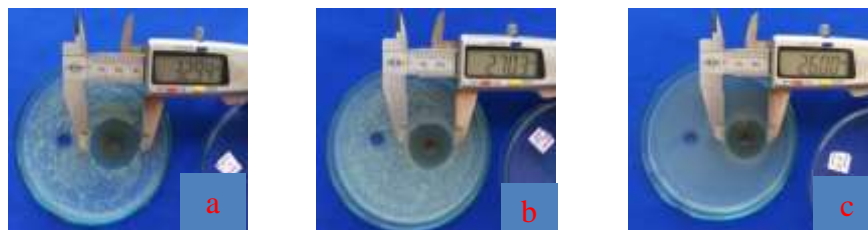
**Figure 6** Flow diagram for preparation of n-BuOH extract from fermented broth of HMF-33, *Penicillium* sp

**Antimicrobial Activity of Crude Extract of HMF-33**

Antimicrobial Activity of Crude Extract of HMF-33 was found to be most effective against all test organisms. Crude Extract of HMF-33 showed antimicrobial activities 22.42mm against *Agrobacterium tumefaciens*, 26.86mm against *Bacillus subtilis*, 32.94mm against *Candidaalbicans*, 22.41 against *Escherichia coli*, 20.53mm against *Malasseza furfur*, 27.03mm against *Micrococcus luteus*, 27.56mm against *Pseudomonas fluorescens*, 26.00mm against *Staphylococcus aureus*, 22.58mm against *Saccromyces cereviciae*, 25.23mm against *Salmonella typhimurium* respectively ( Table 7 and Figure 7).According to these results, crude extract of HMF-33, *Penicillium* sp shown broad spectrum in its mode of action as inhibited the growth of all test pathogens.

**Table 7** Antimicrobial Activity of Crude Extract of HMF-33, *Penicillium* sp

Sample	Ten Test Organisms and Inhibition Zone (mm)									
	1	2	3	4	5	6	7	8	9	10
Crude extract (n-BuOH)	22.42	26.86	32.94	22.41	20.53	27.03	27.56	26.00	22.58	25.23
1. <i>Agrobacteriumtumefaciens</i>	5. <i>Malasseza furfur</i>			9. <i>Sacromycescereviciae</i>						
2. <i>Bacillus subtilis</i>	6. <i>Micrococcus luteus</i>			10. <i>Salmonella typhimurium</i>						
3. <i>Candida albicans</i>	7. <i>Pseudomonas fluorescens</i>									
4. <i>Escherichia coli</i>	8. <i>Staphylococcus aureus</i>									

**Figure 7** Antimicrobial Activity of Crude Extract of HMF-33, *Penicillium* sp on (a) *Candida albicans* (b) *Micrococcus luteus* (c) *Staphylococcus aureus*

### Conclusion

This study revealed that selected fungus HMF-33 was identified as the genus level, *Penicillium* sp by observation of macroscopic and microscopic characters. According to the result of bioautographic assay, fermented broth of *Penicillium* sp extracted with equal ratio (1:1 v/v) of n-butanol yielded 33.0g of brown solid crude extract. Though it is not much about the chemical nature as identified the crude extract of *Penicillium* sp, HMF-33 showed broad spectrum in its mode of action as inhibited the growth of all test organisms (plant and animal pathogen). It may be suggested that *Penicillium* sp from soil of local sources may facilitate the new products (bioactive compounds) discovery process.

### Acknowledgements

We would like to thank to the Department of Higher Education, Ministry of Education in Myanmar, for giving us the opportunity to do this research. Our deepest gratitude is expressed to Dr zaw win, Rector, Sagaing University, for his encouragement, kind guidance, and kind help to do this research. We wish to thank the Myanmar Academy of Arts and Science for allowing to present this paper.

### References

- Ando, K., Suto, M and Inada, S. (2004). *Sampling and Isolation Methods of Fungi*. Department of Biotechnology, National Institute of technology and Evaluation (NITE)
- Ando, K. (2004). Workshop on Taxonomy and Identification of Fungi. Biological Resource Center, Patheingyi University, Myanmar.
- Ando, K. (2016). "Identification Key of Mitosporic Fungi". Basic Laboratory Workshop, Biological Resource Center, National Institute of Technology and Evaluation (NITE). Japan
- Barnett, H. L. (1969). *Illustrated Genera of Imperfect Fungi*. Busness Publishing Company; U.S.A., PP. 62-63
- Collins, C.H. (1965). *Microbiological Methods*. Landon: 5<sup>th</sup> Edition, Butterworth and Co., Publishers Ltd.
- Dubey, R.C. and Maheshwari, D. K.. (2002). *Practical Microbiology*. New Dehli: Chand and Company Ltd., Ram Nagar

- Mendez, A., Perez, C., Montanez, J. C., Martinez, G. and Aguilar, C. N. (2011). Red Pigment Production by *Penicillium purpurogenum* GH2 is Influenced by pH and Temperature. *J. Zhejiang Univ. sci.*
- Mushimiyimana, I., Anastase, K and Phenias, N. (2016). Colonial and Morphological Characteristics of various fungi Species Isolated from Soil in Bangalore city. India; Bulletin of Environment, Pharmacology and Life Sciences. Petit, P., Lucas, E. M. F., Abreu, L.M., Pfenning, L.H, and Takahashi, J. A. (2009).
- Noval Antimicrobial Secondary Metabolites from a *Penicillium sp.* Isolated from Brazilian Cerrado Soil. Brazil; *Electronic Journal of Biotechnology* ISSN: 0717-3458. vol. 12, pp.1-9.
- Pitt, J. I. (1979). “**The Genus *Penicillium* and its Teleomorphic States *Eupenicillium* and *Talaromyces***”. London; Academic Press, vol. 4, pp.16-23.
- Pitt, J. I. (1991). “**A Laboratory Guide to Common *Penicilium* species**”. Australia; Commonwealth Scientific and Industrial Research Organization, Food Research Laboratory, N. S. W.
- Pitt, J. I. (2000). “**A Laboratory Guide to Common *Penicillium* species**”. Australia; 3<sup>rd</sup> edition, Food science, Australia Publishers, pp. 197.
- Raper, K. B. and Thom, C. (1949). A Manual of the *Penicillia*. Baltimore. The Williams and Wilkins Company.
- Riddle, R. W. (1950). “Permanent Stained Mycological Preparation Obtained by Slide Culture”. *Mycologia*, Vol.42, pp.256-270.
- Santos-Ebinuma., V. Carvalho, M. F. S. Teixeira, P. J. Adalberto. 2013. Submerged Culture Conditions for Production of Alternative Natural Colorants by a New Isolated *Penicillium purpurogenum* DPUA 1275. Brazil; *J. Microbiol. Biotechnol.*, vol.23 (6), pp.802-810.
- Sarkar P, Bhagavatula S, Suneetha, V. (2014). *J Appl Pharm Sci.* 4(1), 61-65.
- Schugerl, K. (1993). “Liquid-liquid extraction (small molecules), in biotechnology”. Vol, 3, p.558-589.
- Tiwari, K. L., Jadhav, S. k, and Kumar, A. (2011). “Morphological and Molecular Study of Different *Penicillium* Species”. India; *Middle-East journal of scientific Research*, vol.7(2): pp.203-210.
- Tomita, F. (1988). Laboratory Method. Japan, Hokkaido University.

## HEAVY METAL TOLERANCE AND BIOSORPTION POTENTIAL OF *ASPERGILLUS NIGER* ISOLATED FROM SOLID MINING WASTE

Mar Mar Aye<sup>1</sup>, Ye Myint Aung<sup>2</sup>, Ei Ei Mon<sup>3</sup>, Kyae Hmone Win<sup>4</sup>

### Abstract

The fungi are the most common and efficient group of the heavy metal resistant microbial family which have potential for metal biosorption study. In this research work, ten fungi were isolated from solid mining waste and soil sample. The isolated fungi were screened for their heavy metals tolerance to different concentrations (0-20 mM) of Cr<sup>6+</sup>, Cu<sup>2+</sup>, Cd<sup>2+</sup>, and Ni<sup>2+</sup> solutions. Minimum inhibitory concentrations (MICs) for (Cr<sup>6+</sup>, Cu<sup>2+</sup>, Cd<sup>2+</sup>, and Ni<sup>2+</sup>) were also determined by the agar diffusion method. Most of the isolates were tolerant of the metals. Among all fungal strains, isolated from solid mining waste, *Aspergillus niger* was the highest resistant to Cu<sup>2+</sup> ion up to 20 mM. Thus *A. niger* exhibiting great tolerance to metal ion was used for biosorption study. The optimum parameters for biosorption (pH, contact time, initial metal concentration and adsorbent dose) were studied. The maximum removal efficiency of copper was observed around 60.27 % at pH 4.5 with 0.1g adsorbent dose for 5h. Metal sorbed adsorbents were characterized by FT IR and SEM analysis. In FT IR spectra, changes in spectral data of biomass were observed after absorption of Cu (II) by *A.niger*. Scanning electron microscopy indicated that the morphology of the biomass considerably changed after metal sorption. It could be concluded that *A.niger* possessed significant heavy metal tolerance and biosorption potential against Cu<sup>2+</sup> ions.

**Keywords:** *Aspergillus niger*, metal tolerance, heavy metals, MIC, biosorption

### Introduction

Heavy metal pollution is one of the most important environmental problems today because of their toxicity, bio-accumulation tendency, the threat to human life and the environment. Heavy metals are presented in nature and industrial wastewater, so the presence of heavy metals in surface and groundwater pose a contamination problem. A large number of industries can produce and discharge wastes containing different heavy metals into the environment. The main sources of heavy metal pollution are metal plating, mining, battery manufacturing, tanneries, petroleum refining, pigment manufacture, pesticides, etc. (Igwe and Abia, 2003). The release of large quantities of hazardous materials into the natural environment has resulted in several environmental problems and due to their non-biodegradability and persistence, can accumulate in the environmental elements such as food chain, and thus may pose a significant danger to human health (Hlihor *et al.*, 2013).

In recent years, microbial biomass has emerged as an option for developing an economic and eco-friendly wastewater treatment process, therefore, applying biotechnology in controlling and removing metal pollution has been paid much attention, and gradually becomes a hot topic in the field of metal pollution control because of its potential application. An alternative process is a biosorption, which utilizes various certain natural materials of biological origin, including bacteria, fungi, yeast, algae, etc. Fungal organisms like *Aspergillus niger*, *Sreptomycetes noursei*, *Pseudomonas aeruginosa*, and *Rhizopus arrhizus* have been reported for removal of heavy metals, such as Pb, Cd, and, in particular, Ni (II) (Sar *et al.*, 2000). Heterotrophic fungi such as *Mucor* sp., *Aspergillus* sp., *Penicillium* sp., and *Yarrowta* sp. can remove both soluble and insoluble metal species from solutions and can leach metal cations from solid waste (Heinfling *et al.*, 1997). Metal

---

<sup>1</sup> Lecturer, Department of Chemistry, Patheingyi University

<sup>2</sup> Professor and Head Department of Chemistry, Patheingyi University

<sup>3</sup> Lecturer, Department of Chemistry, Meiktila University

<sup>4</sup> Lecturer, Department of Chemistry, Patheingyi University

\* Contributed equally

resistance is defined as the ability of an organism to survive metal toxicity using a mechanism produced in direct response to metal species concerned. This ability of the microorganisms to grow in the presence of heavy metals has potential use in bioremediation of polluted waters (Desai *et al.*, 2015).

The application of fungal organisms in the field of biosorption technology has become a part of active research by environmental scientists. Heavy metal tolerance fungi might be present in metal contaminated places. The objective of this study is to isolate and screen heavy metal tolerant (Pb, Cd, Cr, Cu) fungi from contaminated waste and soil and to evaluate their biosorptive potential against heavy metals under laboratory conditions.

## Materials and Methods

### Sample Collection and Heavy Metals Analysis

The solid mining wastes were collected from near Lepantaung copper mine, Salingyi Township, Sagaing Region. The solid waste samples were air-dried and sieved to achieve the homogeneity and stored in the plastic container for subsequent experiments. Samples were stored in the refrigerator (4°C) for the isolation of fungi. Soil samples were utilized for the isolation of microorganisms especially fungi. These soil samples were collected from Kanyin-pin-hla village, Laymyethna Township, Ayeyarwady Region. Soil texture and pH were analyzed at the Department of Agriculture (Land Use), Giorgione, Insein Township, Yangon. Soil samples and mining waste were analyzed by Atomic Absorption Spectrometry (AAS) for the concentration of copper, cadmium, nickel, and chromium at the Innovation Center, Department of Higher Education.

### Isolation of Fungi from Mining Waste and Soil

The fungal strains were isolated from soil and solid mining waste by serial dilution method (Hayakawa and Kobayashi, 2005). The dilution technique was made by placing one gram of the sample in the test tube containing 10 mL of sterile distilled water and tenfold serial dilution was made by transferring 1 mL of the suspension to another test tube containing 9 mL of distilled water. This step was repeated ten times to obtain a dilution of  $10^{-10}$ . Each volume 0.1 mL from the test tubes ( $10^{-3}$ ), ( $10^{-6}$ ), ( $10^{-9}$ ) was taken and placed on the plate containing Lignocellulose Agar (LCA) culture medium. Chloramphenicol was added to the medium after autoclaving for 15 min at 121 °C to arrest bacterial growth. After 5 to 7 days incubation, larger identical colonies from each plate were isolated. Isolated fungi from master plates were transferred to the medium plate Potato Dextrose Agar (PGA) to obtain pure cultures. The pure cultures were stored in (PGA) slant culture before further analysis.

### Screening for Metal Resistance Fungi

The metal resistance properties of ten isolated fungi were determined by the spot plate's method (Zafar *et al.*, 2007) using  $K_2CrO_4$ ,  $CuSO_4$ ,  $CdSO_4$  and  $NiSO_4$  metal solutions Potato dextrose agar medium was used for heavy metal resistance experiments. The metal solution was added to the sterile medium and made up the concentrations of (5, 10, 15 and 20 mM). Then the test fungi were spotted on metal-containing plate and control plates. The duplicated cultures were carried out in this work. The plates were incubated for 10 days to observe the growth of the spotted area. Metal tolerance was observed as the minimum inhibitory concentration (MIC) of the heavy metal that inhibited the visible growth of test fungi.

### Morphological Characterization of Highest Metal Resistant Fungal Isolates

The highest Cu resistance fungus (MR-02) was characterized. The fungus was cultured on Potato Dextrose Agar (PDA), Czapek-Dox Agar (CZA), and Meat Extract Agar (MEA) medium.

After seven days, fungal isolates were studied for its morphological features under the light microscope (at 40x). The isolates were mounted on slide with the help of lactophenol cotton blue. The fungal isolates were identified by comparing these morphological characteristics by using fungal identification manuals.

### Preparation of Fungal Biomass

A liquid medium of potato dextrose broth (PDB) with a pH value adjusted to 5 was prepared. 5 days old culture of fungi from LCA plate culture was inoculated into the 500 mL flask containing 100 mL sterile medium incubated at 25°C for 7 days. The fungal cell mass was determined by filtering the culture medium through weighed Whatman filter paper No. (1). Mycelium was thoroughly washed with generous amounts of deionized water, re-suspended and washed again. The biomass thus obtained was suspended in 0.5N sodium hydroxide solutions for 15 min. The pretreated biomass was washed with deionized water until the pH of the solution was in a near neutral range (pH 6.8-7.2). The pretreated fungal biomass was autoclaved for 15min at 121°C. Then the fungal biomass was dried in an oven at 60°C for constant weight. When the biomass was dry, it was powdered and stored in the desiccator.

### Studies on Biosorption

Testing for biosorption efficiency different concentrations of *Aspergillus niger* biomass was combined with 100 mL of CuSO<sub>4</sub> solution in 250 mL Erlenmeyer flasks. The flasks were placed on a shaker with a constant speed of 150 rpm and left to equilibrate. Samples were collected at predefined time intervals. The adsorbate was decanted and separated from the adsorbent using Whatman No.1 filter paper. The supernatant was analyzed by AAS. The effect of pH on the copper biosorption using *A.niger* was investigated on a wide pH ranged from 3 to 6. The effect of initial metal ion concentration was also altered. The dosage of biosorbent was also investigated with varying concentration of dead fungal biomass (0.02- 0.14 g). The contact time of the biosorbent with the metal ion solution (1- 6 h) was also optimized further. The removal percentage of copper was calculated by using the following formula:

$$E (\%) = \left( \frac{C_i - C_f}{C_i} \right) \times 100$$

where, C<sub>i</sub> = the initial copper concentration

C<sub>f</sub> = the final copper concentration

E = metal removal efficiency (%)

### Characterization of Fungal Biomass

#### FT IR analysis

The functional groups present on the dried fungal biomass *Aspergillus niger* before and after biosorption were analyzed by FT IR Spectrophotometer, Perkin Elmer. The spectra were recorded over the range 4,000 – 400 cm<sup>-1</sup> using the recommended standard procedures as described in FT IR Spectrophotometer.

#### SEM analysis

The surface morphology and fundamental physical properties of *Aspergillus niger* biomass before and after biosorption were characterized by using scanning electron microscope (SEM) for a visual inspection of external porosity and micro texture.

## Results and Discussion

### Characteristics of Soil Samples and Heavy Metals Concentrations

The properties of soil that was used for isolation of fungi were analyzed. The pH range of soil conditions was 6.24. The soil type was silt loam. The soil texture was determined depending upon the percentage of sand, silt, and clay (Table 1). It was observed that  $\text{Cu}^{2+}$  had the highest concentration in the solid mining waste  $106.26 \text{ mg kg}^{-1}$  and the  $\text{Ni}^{2+}$ ,  $\text{Cr}^{6+}$ , and  $\text{Cd}^{2+}$ , were 76.73, 40.33 and  $76.82 \text{ mg kg}^{-1}$ . The  $\text{Cr}^{6+}$ ,  $\text{Cu}^{2+}$ ,  $\text{Cd}^{2+}$ , and  $\text{Ni}^{2+}$  contents in soil sample were very lower and some were not detected (Table 2).

**Table 1 Analytical Data of Soil Sample**

Samples	Texture (%)				pH	Soil type
	Sand	Silt	Clay	Total		
Soil	4.30	76.00	18.20	98.50	6.24 (slightly acid)	silt loam

**Table 2 Concentrations of Metal in Soil and Solid Mining Waste Samples**

Samples	Metal concentration(mg/kg)				pH
	$\text{Cu}^{2+}$	$\text{Ni}^{2+}$	$\text{Cr}^{6+}$	$\text{Cd}^{2+}$	
Soil	0.004	0.014	0.007	ND	6.24
Solid Waste	106.26	76.73	40.33	76.82	8.2

\* ND - Not Detected

### Isolation of Fungi from Soil and Solid Mining Waste

Ten fungal strains were isolated from soil and mining waste by the serial dilution method. They were designated as MR-01, MR-02, MR-03, MR-04, and MR-05 which were isolated from metal contaminated waste and MR-06, MR-07, MR-08, MR-09, and MR-10, which were isolated from soil. It can be seen that fungi are able to grow in the heavy metals contaminated places.

### Screening for Metal Resistance Fungi

The isolated fungi tolerance to metal ions such as  $\text{Cr}^{6+}$ ,  $\text{Cu}^{2+}$ ,  $\text{Cd}^{2+}$ , and  $\text{Ni}^{2+}$  were determined by varying concentration. The MICs of fungal isolates against on the four metals ion are shown in Table 3. Most of isolated fungi resisted the individual metal in different concentration except MR-03 and MR-07. MR-01 showed resistance up to 5 mM concentration of  $\text{Cu}^{2+}$ ,  $\text{Cd}^{2+}$ , and  $\text{Cr}^{6+}$ . The highest metal resistance fungus (MR-02) is shown in Figure 2. Some fungal isolate can resist at higher concentration of heavy metals due to the various biological factors. Malik (2004) have been reported that the concentration of heavy metal was affected on the growth of fungi. Heavy metal resistant microorganisms play an important role in the bioremediation of heavy metal contaminated places. (Ray and Ray, 2009). Among all fungal isolates, MR-02 showed the highest resistance up to 20 mM concentration (Figure 2). Thus MR-02 was selected for biosorption study of  $\text{Cu}^{2+}$  ions.

**Table 3 Minimum Inhibitory Concentration of Heavy Metals Tolerated by Resistant Fungi**

Strain No.	MIC of Heavy Metal Ions (mM)			
	Cd <sup>2+</sup>	Cr <sup>6+</sup>	Ni <sup>2+</sup>	Cu <sup>2+</sup>
MR-01	5	5	-	5
MR-02	-	-	5	20
MR-03	-	-	-	-
MR-04	-	-	-	15
MR-05	-	-	-	5
MR-06	-	10	-	10
MR-07	-	-	-	-
MR-08	-	5	5	-
MR-09	-	5	5	5
MR-10	-	5	-	5

(-) = No growth

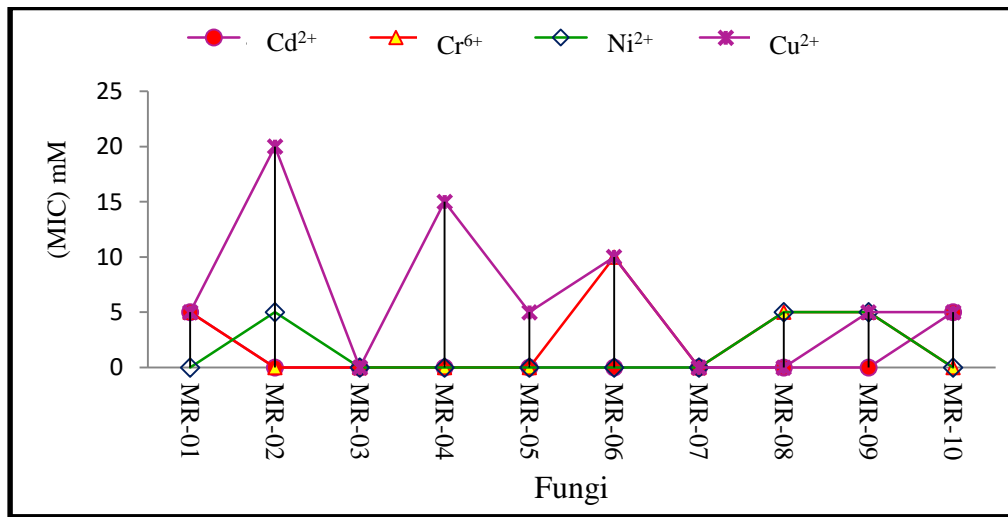


**Figure 1** MIC of all fungal isolates against metals

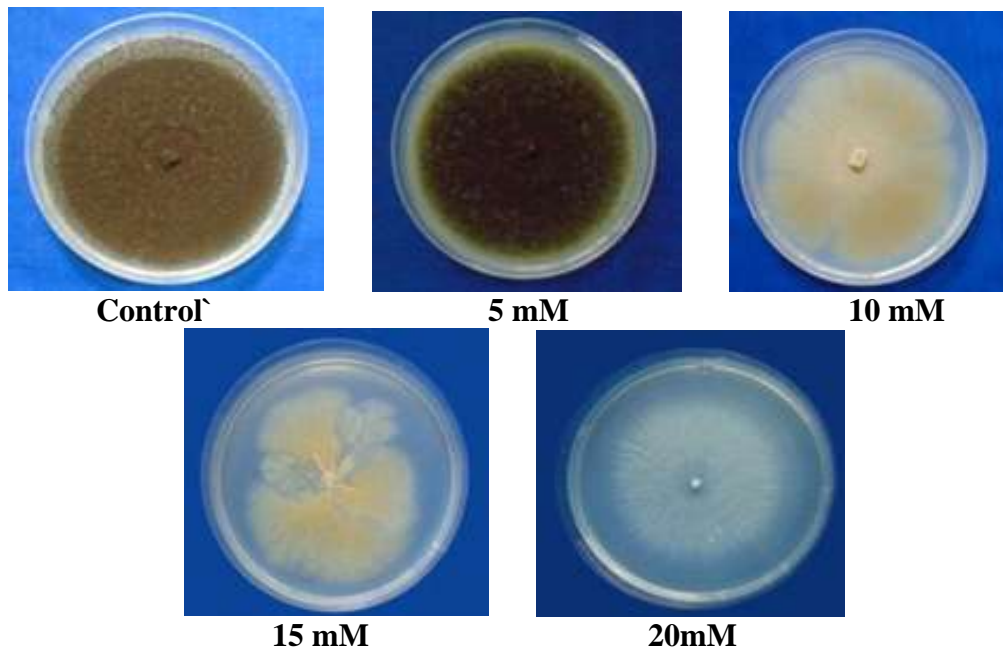


**Figure 2** The growth of *Aspergillus niger* with different concentration of (Cu<sup>2+</sup>) ions for 10 days

## Morphological Characteristics

Microscopical Characters of isolates MR-02 was observed under compound microscope. Isolates MR-02, colony showed typically black powdery. Conidiophores arising from long, broad, thick-walled, mostly brownish. Conidia in large, radiating heads, mostly globose, irregularly roughened 4.0 - 5.0  $\mu\text{m}$  diameters. Based on the works of literature, references (Domsch, 1993; Ando, 2016) and morphological and microscopically characters, the characters of fungus MR-02 was identified as *Aspergillus niger*.

## Evaluation of Biosorption Efficiency

*Aspergillus niger* biomass showed biosorption efficiency on Cu (II) ions. Maximum biosorption was 60.27% and minimum absorption was 11.11%. The effect of the Cu (II) ions removed by *A. niger* biomass are shown in Figures 3 and 4. Results are in agreement with (Gadd, 1993) who reported that fungi are able to grow in the presence of heavy metals due to physiological adaptation and such adaptation may be associated with increased metal sorption capacity.

## Effect of biosorbent dosage and initial metal concentration on Cu(II) ions on biosorption

In the effect of biomass dosage on biosorption, biomass dosages were varied between 0.02 -0.14 g while the initial copper ion concentration and pH were 0.2-1.4mg/mL and 3-6. It was found that optimum adsorption was 60.12 % at 0.1g of *A. niger* biomass for  $\text{Cu}^{2+}$  (Figure 3-a). Further increase in the biosorbent dosage, the biosorption efficiency had not increased.

The initial heavy metal ions concentration is an important parameter in adsorption since a certain amount of adsorbent can adsorb a certain amount of heavy metal ions. The biosorbent optimum dose was found to be 0.1g. The results represented in Figure 3-b, showed that maximum percent removal of *A. niger* for  $\text{Cu}^{2+}$  ion was 60.23 % with initial concentration at 1.0 mg/mL. After that the adsorption capacity was decreased with the increasing metal ion concentration. It may be due to the surface of the biomass has less adsorption sites. The results are in agreement with the literature studies reporting high metal ion biosorption at high metal ion concentrations (Gulnaz *et al.*, 2005). Percent copper ion removal decreased from 40.31 to 21.11% when the initial  $\text{Cu}^{2+}$  concentration was raised from 1.2 to 1.4 mg/mL.

## Effect of pH

The pH was an important parameter for adsorption of metal ions from aqueous solution because it affected the solubility of the metal ions, concentration of the counter ions on the functional groups of the adsorbent and the degree of ionization of the adsorbate during reaction. Biomass had active sites capable of binding metal ions. Such bond formation could be accompanied by displacement of protons and was dependent in part on the extent of protonation which was determined by the pH (Volesky, and Holan, 1995). To examine the effect of pH on the  $\text{Cu}^{2+}$  removal efficiency, the pH was varied from 3 to 6. Pretreated fungal biomasses of *Aspergillus niger* was contacted  $\text{Cu}^{2+}$  ions in separate solutions at concentration of 1.0 mg/mL for 5 h respectively. Figure 4(b) showed that the uptake of metal ions depended on pH. It was observed that *Aspergillus niger* exhibited maximum sorption capacity for the  $\text{Cu}^{2+}$  in the pH of 4.5 with maximum efficiency 60.27 %. Above this pH substantial declined in metals uptake was evidenced which represented the pH factor being highly sensitizing element. In similar findings by earlier investigators it has been attributed to protonation or poor ionization of acidic functional group of cell wall at low pH, inducing a weak complex affinity between the cell wall and the metal ions (Chergui *et al.*, 2007). The reduction in metal ions uptake by fungus at high pH can be explained on the basis that at higher pH values the metal ions may accumulate in the cells or the intra-fibular capillarity of the cell walls by a combined sorption of micro precipitation mechanism (Beveridge,

1986). With an increase in pH, the negative density on cell surface increased due to deprotonation of the binding sites thus improved biosorption of heavy metal ions.

### Effect of contact time

In the effect of contact time, metal solution concentration of 1.0 mg/mL was adjusted to the maintain optimum pH 4.5 and biosorbent 0.1 g. The filtrate was collected by using Whatmann filter at different time intervals of 1, 2, 3, 4, 5 and 6 h. As can be seen in Figure 4(b) the percentage removal of ions increased with increasing the shaking time. A sharp increase was observed at optimum time of 5 h for biosorption of  $\text{Cu}^{2+}$  by *A.niger*. At the equilibrium maximum adsorption for  $\text{Cu}^{2+}$  was observed as 60.26 %. This result was important, as equilibrium time was one of the important parameters for an economical wastewater treatment system.

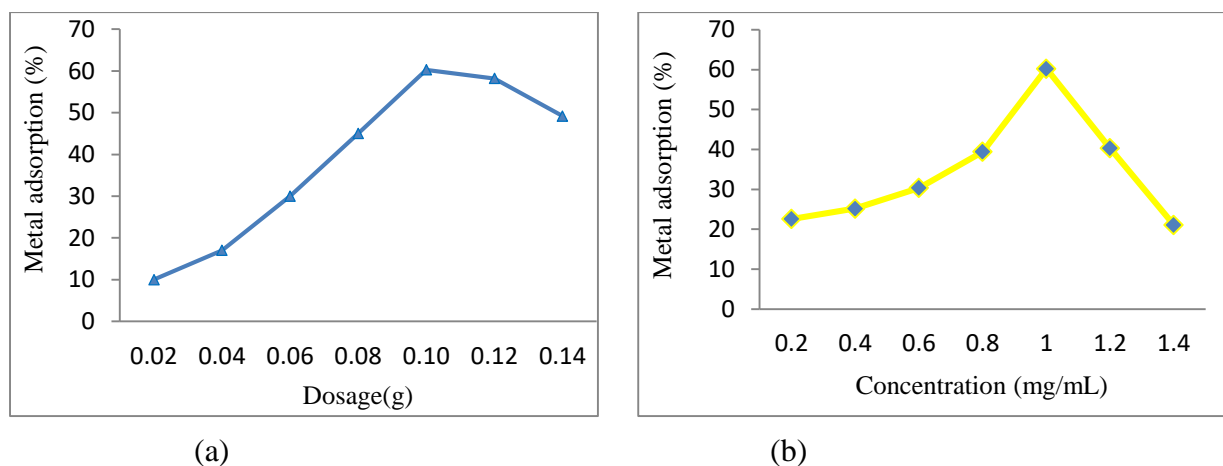


**Figure 3** (a) Effect of biosorbent dosage on Cu(II) ions biosorption by *Aspergillus niger*  
(b) Effect of initial metal concentration on Cu(II) ions biosorption by *Aspergillus niger*

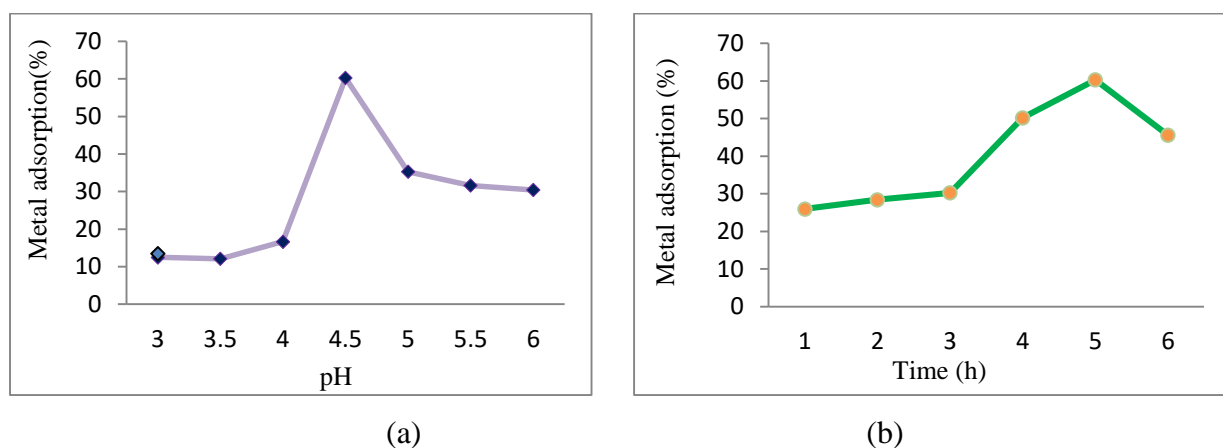


**Figure 4** (a) Effect of pH on Cu (II) ions biosorption by *Aspergillus niger* (b) Effect of contact time on Cu (II) ions biosorption by *Aspergillus niger*

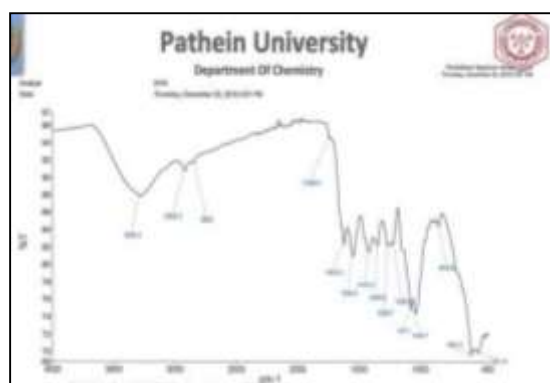
### FT IR Analysis of Fungal Biomass Before and After Cu II Biosorption

The negatively charged functional groups present in the biomass were identified by FT IR spectrum. Table 4 shows the FT IR spectral data of *Aspergillus niger* biomass. In Figure 5-a, *A. niger* fungal biomass shows stretching vibrations at  $3285$ ,  $1740$  and  $1040 \text{ cm}^{-1}$ , which indicates the presence of the (-OH); (-C=O); (-C-O) respectively. It was found that the FT IR spectra of before and after biosorption of heavy metal Cu II were not significantly different but after biosorption some of the peaks were shifted and gave the more sharp (Figure 5-b). Changes in wave number at

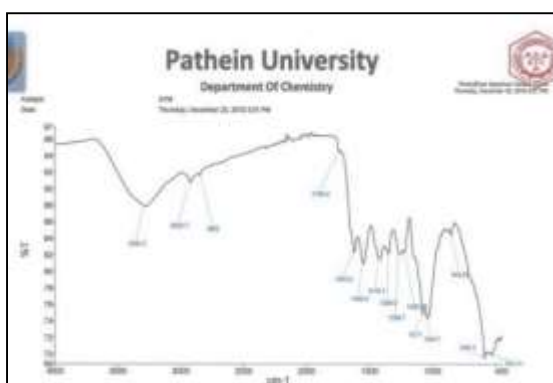
3285, 2852, 1740, and 1040  $\text{cm}^{-1}$  in metal-bounded biomass could be assigned to participation of -OH, C-H, C=O and -C-O groups in biosorption process of copper II ions .

**Table 4 FT IR Spectral Data for Pretreated *Aspergillus niger* Biomass Before and After  $\text{Cu}^{2+}$  Biosorption**

Fungal biomass	Functional groups	Wave number ( $\text{cm}^{-1}$ )	
		Before $\text{Cu}^{2+}$ biosorption	After $\text{Cu}^{2+}$ biosorption
	$\nu_{\text{O-H}}$ of alcohol	3285	3276
	$\nu_{\text{C-H}}$ of $\text{CH}_2$ and $\text{CH}_3$	2924, 2852	2924, 2855
	$\nu_{\text{C=O}}$	1740	1746
<i>Aspergillus niger</i>	$\nu_{\text{C=C}}$ of aromatic ring	1622, 1549	1622, 1543
	$\delta_{\text{C-H}}$ of $\text{CH}_3$	1416, 1346	1410, 1370
	$\nu_{\text{C-O}}$ of alcohol	1040	1028



(a)

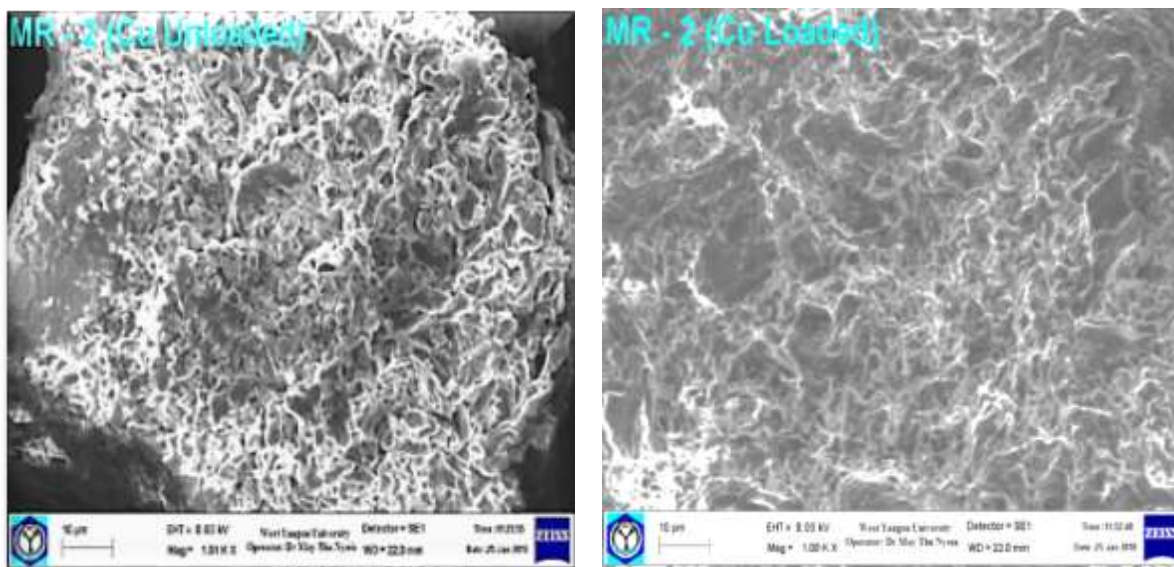


(b)

**Figure 5** FT IR analysis of alkali pretreated *Aspergillus niger* (a) before and (b) after biosorption

### SEM Analysis of Fungal Biomass Before and After $\text{Cu}^{2+}$ Biosorption

Scanning electron microscopy (SEM) had been a primary tool for characterizing the surface morphology and fundamental physical properties of the adsorbent surface. It was useful for determining the particle shape, porosity and appropriate size distribution of the adsorbent (Arami *et al.*, 2008). SEM micrographs of *Aspergillus niger* biomass before (Figure 6-a) and after (Figure 6-b) adsorption of  $\text{Cu}^{2+}$  were compared. The SEM micrographs of *Aspergillus niger* without metal stress (control) possessed a rough, heterogeneous and a large surface area. As seen in Figure, the adsorbents had some heterogeneity which is supposed to be the active site for metal  $\text{Cu}^{2+}$  binding. After  $\text{Cu}^{2+}$  adsorption, the surface of fungal biomass was flattened (Figure 6-b). The SEM micrographs of fungal biomass *Aspergillus niger* showed the changes in the structure after sorption indicating the effective adsorption of copper II ions in the interstices and cavities on the external surface of this biosorbent. Results are in agreement with the Mondal, *et al.* (2017) who indicated that the surface changes occurred after binding of  $\text{Cu}^{2+}$  ions onto the surface of *A. niger* biomass.



(a)

(b)

**Figure 6** SEM micrographs of *Aspergillus niger* fungal biomass (a)  $\text{Cu}^{2+}$  ions unloaded (b)  $\text{Cu}^{2+}$  ions loaded

### Conclusion

In this study, ten fungal strains were isolated from solid mining waste and soil sample. The isolated fungal strains were screened for their tolerance to four metal ions ( $\text{Cu}^{2+}$ ,  $\text{Cd}^{2+}$ ,  $\text{Ni}^{2+}$  and  $\text{Cr}^{6+}$ ). Among them, fungus *Aspergillus niger* isolated from metals contaminated waste showed the highest  $\text{Cu}^{2+}$  tolerance up to (20 mM). This study reveals that heavy metal contaminated places might be considered as a precious natural source of the resistant fungal strains. Thus the fungal biomass of *A. niger* was evaluated for biosorption study of Cu (II) ions from aqueous solution. The maximum sorption efficiency of biomass *A. niger* for the  $\text{Cu}^{2+}$  ions was 60.27 % at pH 4.5. Biomass of *A. niger* exhibited sorption potential to bind with  $\text{Cu}^{2+}$  ions and uptake Cu (II) ions from the aqueous solution. Though the mechanism of sorption potential with  $\text{Cu}^{2+}$  ions should be further studied. The results of the present study suggest that *Aspergillus niger* isolated from solid mining waste in metal contaminated places can be useful for the biosorption of heavy metals from wastewater.

### Acknowledgements

The authors would like to thank the Department of Higher Education, Ministry of Education, Myanmar, for the permission of doing this research and also to the Myanmar Academy of Arts and Science for allowing to present this paper.

### References

- Ando, K., (2016) "Identification of Mitosporic Fungi, Basic Laboratory Workshop, Biological Resource Center, National Institute of Technology and Evaluation, (NITE), Japan."
- Arami, M., Limaee, N. Y., and Mahmoodi, N. M. (2008) "Evaluation of the Adsorption Kinetics and Equilibrium for the Potential Removal of Acid Dyes Using a Biosorbent" *Chemical Engineering Journal*, vol. 139(1), pp. 2-10.
- Bektas., N and Kara, S. (2004) "Removal of Lead from Aqueous Solutions by Natural Clinoptilolite: Equilibrium and Kinetic Studies" *Separation Purification Technol.*, vol. 39, pp.189-200
- Beveridge, T. J. (1986) "The Immobilization of Soluble Metals by Bacterial Walls." *In Biotechnology and Bioengineering Symposium* vol. 16, pp.127-139.

- Chergui.A., Bakhit. M.Z., Chahboub. A., Haddoum. S., Selatnia. A., and Junter.G.A. (2007) "Simultaneous Biosorption of  $\text{Cu}^{2+}$ ,  $\text{Zn}^{2+}$ , and  $\text{Cr}^{6+}$ , from Aqueous Solutions by *Streptomyces rimosus* Biomass" *Desalination*, vol. 206(1-3), pp.179-184
- Desai, H., Patel. D., and Joshi. B. (2015) "Screening and Characterization of Heavy Metal Resistant Fungi for its Prospects in Bioremediation of Contaminant Soil. *Int. Journal Curr. Microbiol. App.*" vol. 5(2), pp.78-94.
- Domsch, K. H., Gams. W., and Anderson. T. H. (1993) "Compendium of Soil Fungi". vol.1, London : Academic Press, UK.
- Gadd, G.M. and Whlte, C. (1993). "Bioremediation: Microbial Treatment of Metal Pollution - A Working Biotechnology?" *Trends in Biotechnology*, TIBTECH vol. 11 ( 8 ) pp. 115, 353-359.
- Gulnaz. O., Saygideger , S. and Kusvuran. E. (2005) " Study of Cu (II) Biosorption by Dried Activated Sludge: Effects of Physico-Chemical Environment and Kinetic Study" *Journal,Hazar. Mater.* vol. 120 pp.193-200
- Hayakawa, A., and Kobayashi., M. (2005) "Screening for Rare *Actinomycetes* from Soil." *Journal of Microbiol.*, vol. 76, pp.240-242.
- Heinfling, A., Bergbauer, M. and Szewzyk. U., (1997)"Biodegradation of Azo and Phthalo Cyanine Dyes by *Trametes versicolor* and *Bjerkandera adusta*. *Applied Microbial Biotechnology*, vol. 48, pp. 261-266.
- Hlihor, R. M., Diaconu. M., Fertu. D. Chelaru. C., Sandu. I. , Tavares . T. and Gavrilesu., M. (2013). "Bioremediation of Cr(VI) Polluted Wastewaters by Sorption on Heat Inactivated *Saccharomyces cerevisiae* Biomass" *Int. Journal Environ. Res.* vol. 7(3), pp. 581-594.
- Igwe, J. C., and Abia. A. A. (2003): "Maize Cob and Husk Mill Wastes Water Pollution. as Adsorbents for Removal of Cd, Pb and Zn ions from Waste Water" *The Physical Scientist.*vol. 2, pp. 83-92.
- Malik A. (2004) "Metal Bioremediation through Growing Cell" *Int. Journal Environ .* vol. 30, pp. 271–278
- Mehra, R. K., and Winge. D. R. (1991) "Metal Ion Resistance in Fungi: Molecular Mechanisms and Their Regulated Expression" *Journal of Cellular Biochemistry*, vol. 45(1), pp.30-40
- Mondal, N. K., Samanta. A., Dutta. S., and Chatteraj, S. (2017)"Optimization of Cr (VI) Biosorption onto *Aspergillus niger* using 3-level Box-Behnken Design: Equilibrium, Kinetic, Thermodynamic and Regeneration Studies" *Journal of Genetic Engineering and Biotechnology*, vol.15(1), pp.151-160
- Ray, S. A., and Ray. M. K. (2009) "Bioremediation of Heavy Metal Toxicity with Special Reference to Chromium " *Journal of Am Med Sci*, vol. 2(2), pp. 57-63.
- Sar, P., Kazy, S. K., Asthana, S. and Singh. P. (1999) "Metal Adsorption and Desorption by Lyophilized *Pseudomonas aeruginosa*" *International Biodeterioration and Biodegradation*, vol. 44 (2-3), pp. 101-110
- Volesky, B., and Holan, Z.R. (1995) " Biosorption of Heavy Metals" . *Biotech Prog.*, vol. 11, pp. 235-250
- Yin, P., Yu. Q., Jin. B.and Ling. Z. (1999) " Biosorption Removal of Cadmium from Aqueous Solution by Using Pretreated Fungal Biomass Cultured from Starch Wastewater" *Water Research*, vol.33(8), pp. 1960-1963
- Zafar, S., F.Aqil., I. Ahmad., (2007) " Metal Tolerance and Biosorption Potential of Filamentous Fungi Isolated from Metal Contaminated Agricultural Soil" *Bioresource Technology*, vol. 98(13), pp. 2557-2561.

## NUTRITIONAL VALUES, TOTAL PHENOLIC, TOTAL FLAVONOIDS AND ANTIOXIDANT ACTIVITY OF RED AND WHITE FLOWER PETALS OF *SESBANIA GRANDIFLORA* (L.) PERS.

Khin Myo Myint Tun<sup>1</sup>, Ma San Aye<sup>2</sup>, Swe Mar Win<sup>3</sup>

### Abstract

The objectives of this research work were to evaluate the nutritional values, phytochemicals, total phenolic, total flavonoid and antioxidant activity of red and white flower petals of *Sesbania grandiflora* (L.) Pers. Red and white flower petals possess nutritional values of moisture (6.13 and 5.28 %), ash (4.37 and 5.10 %), fiber (1.40 and 3.60 %), protein (5.99 and 8.32 %), fat (0.83 and 1.53 %), carbohydrates (81.28 and 76.17 %) and energy value (357 and 352 kcal/100 g), respectively. Both varieties of flower samples contain plenty of phytochemicals such as alkaloids, phenolic compounds, flavonoids, steroids, terpenoids, glycosides,  $\alpha$ -amino acids, starch, reducing sugars, carbohydrates, saponin and tannins. The total phenolic content was determined by Folin-Ciocalteu assay and expressed as gallic acid equivalent. Total phenolic content of red flower petals was found to contain 185.15  $\mu\text{g}$  GAE/mg of ethanol extract and 82.08  $\mu\text{g}$  GAE/mg of aqueous extract. Total phenolic content of white flower petal was found to contain 134.38  $\mu\text{g}$  GAE/mg of ethanol extract and 55.92  $\mu\text{g}$  GAE/mg of aqueous extract. Total flavonoid content was determined by aluminium chloride colourimetric method and expressed as quercetin equivalent. It was observed that red flowers contain total flavonoid content of 356.85  $\mu\text{g}$  QE/mg of ethanol extract and 285.33  $\mu\text{g}$  QE/mg of aqueous extract, and white flowers contain 45.33  $\mu\text{g}$  QE/mg of ethanol extract and 22.30  $\mu\text{g}$  QE/mg of aqueous extract. Antioxidant activity of each extract was evaluated by DPPH assay. In DPPH assay,  $\text{IC}_{50}$  values were used to determine the antioxidant potential of the sample. Among the extracts ethanolic extracts of both red and white flower varieties exhibited higher DPPH radical scavenging activity with  $\text{IC}_{50}$  value of 213.67  $\mu\text{g}/\text{mL}$  and 322.31  $\mu\text{g}/\text{mL}$ , respectively. *S. grandiflora* can be regarded as promising candidates for natural plant sources of antioxidant with high values.

**Keywords:** *Sesbania grandiflora*, nutritional values, phytochemicals, phenolic, flavonoid, antioxidant activity

### Introduction

*Sesbania grandiflora* (L.) Pers. is a popular Myanmar medicinal plant which belongs to family Leguminosae. It is small, erect, fast-growing and sparsely branched tree that reaches 15 m in height. All *Sesbania* species have pinnately compound leaves where each leaf is divided into multiple leaflets. The leaves can be up to 30 cm long with 5-15 paired leaflets that are oblong to elliptic in shape and about 3 cm in length. The flowers of *S. grandiflora* are large and 7-9 cm long. Two varieties of *S. grandiflora* are recognized as red flower variety and white flower variety (Bahera *et al.*, 2012). In Myanmar, red flower variety is called *Pauk-pan-ni* and white flower variety is called *Pauk-pan-byu*. The photographs of *S. grandiflora* plants and flowers are shown in Figures 1 and 2.

The bioactive chemical constituents of *S. grandiflora* are leucocyanidin and cyanidin present in seeds. Oleanolic acid and its methyl ester and kaempferol-3-rutinoside are present in flowers. The bark contains tannins and gum. Saponin and sesbanimide are observed in seeds (Outtara, 2011; Vijay *et al.*, 2009).

All parts of *S. grandiflora* are used for medicine as well as vegetables in Southern Asia and India. In Folk Medicine it is reported to be aperient, diuretic, emetic, emmenagogue, febrifuge, laxative, and tonic. It is also used for the treatment of bruises, catarrh, dysentery, fevers, headaches,

---

<sup>1</sup> Dr, Associate Professor, Department of Chemistry, West Yangon University

<sup>2</sup> Dr, Lecturer, Department of Chemistry, West Yangon University

<sup>3</sup> Lecturer, Department of Chemistry, West Yangon University

smallpox, sores, sore throat and stomatitis. It also possesses anxiolytic, anticonvulsive and hepatoprotective properties (Alli and Salwau, 2011; Mbatchou, 2011; Vijay *et al.*, 2009). The present study evaluates the nutritional values, phytochemicals, total phenolic, total flavonoids and antioxidant activity of red and white flowers petals of *S. grandiflora* (*Pauk-pan-ni* and *Pauk-pan-byu*).



**Figure 1** Photographs of *Sesbania grandiflora* plants and flowers (red variety)



**Figure 2** Photographs of *Sesbania grandiflora* plant and flowers (white variety)

## Materials and Methods

### Collection and Preparation of Plant Materials

The red and white flowers of *S. grandiflora* (*Pauk-pan-ni* and *Pauk-pan-byu*) were collected near Professor Housing, West Yangon University, Yangon, Myanmar in the month of February 2019. The flowers and plant sample were authenticated by the botanists of Botany Department, West Yangon University.

The red and white flowers of *S. grandiflora* were harvested and carefully separated the flower petals from the other parts of flowers. The flower petals were dried under shade for one week and then dried in an air oven at 50 °C. The dried flower petals were ground by using a mechanical grinder. The dried powdered samples were stored in an air tight bottle and placed in cool and dry place.

### Determination of Nutritional Values

The nutritional values such as moisture, ash, crude protein, crude fiber, crude fat, carbohydrate contents and energy value of *S. grandiflora* flower petals were determined at Research Laboratory of Chemistry, West Yangon University. The analyses were carried out according to A.O.A.C method (A.O.A.C, 2000).

### Phytochemical Screening in *S. grandiflora* Flower Petals

Preliminary qualitative phytochemical screening were carried out for alkaloids, phenolic compounds, flavonoids, steroids, terpenoids, glycosides,  $\alpha$ -amino acids, cyanogenic glycosides, starch, reducing sugars, carbohydrates, saponins and tannins following the standard procedures (Harborne, 1998; Kokate *et al.*, 2009).

### Preparation of Plant Extracts

**Ethanolic extract:** Each of the dried powder samples (50 g) was immersed in ethanol (500 mL) for 7 days at room temperature with frequent agitation. The ethanolic extract was filtered and filtrate was concentrated to dryness using rotatory evaporator under reduced pressure. The ethanolic extracts of each sample were kept in the desiccator for 3 days and then stored in airtight bottle at 4 °C.

**Aqueous extract:** Each of the dried powder samples (50 g) was boiled with distilled water (500 mL) on water bath for 30 min. The extract was filtered and the filtrate was evaporated on water bath. The resultant aqueous extracts were kept in the desiccator and then dry paste extracts were stored in airtight bottle at 4 °C until further use.

### Determination of Phenolic Contents

The total phenolic content was determined for ethanolic and aqueous extracts of flower petals of *S. grandiflora* using the Folin-Ciocalteu method (Ainsworth and Gillespie, 2007). 0.5 mL of sample extract solution (250  $\mu$ g/mL in methanol) was mixed with 0.5 mL methanol and 5 mL Folin-Ciocalteu reagent (1:10 v/v). The mixture was incubated at 37 °C for 30 min. After 30 min, 4 mL of 1 M sodium carbonate was added to the above mixture and kept at room temperature for 15 min. The absorbance was measured utilizing a UV spectrophotometer (Shimadzu, UV-1800) at 760 nm against a blank without sample extract. The same procedure was repeated for the standard solution of gallic acid and the standard calibration line was constructed as shown in Figure 3. Then the content of phenolics in each extract was expressed in terms of gallic acid equivalent ( $\mu$ g GAE/mg of extract).

### Determination of Flavonoid Contents

The content of flavonoids in the examined plant extracts (ethanolic and aqueous) was determined by using aluminium chloride colourimetric method (Afify *et al.*, 2012). An aliquot of 0.5 mL of each extract solution (250  $\mu$ g/mL in methanol) was mixed with 1.5 mL methanol, 0.1 mL of 10 % aluminium chloride, 0.1 mL of 1 M potassium acetate and 2.8 mL distilled water. The mixture was incubated for 40 min at room temperature followed with the measurement of absorbance at 415 nm using Shimadzu, UV-1800 UV-Visible spectrophotometer. The calibration curve was plotted using standard quercetin as shown in Figure 5. The total flavonoid contents of each sample extract were expressed as quercetin equivalent in terms of ( $\mu$ g QE/mg of extract).

### DPPH Radical Scavenging Activity Assay

The radical scavenging activity (RSA) of the crude extracts was adopted the measure antioxidant activity using the DPPH method (Yan-Hwa *et al.*, 2000; Aryal *et al.*, 2019). Briefly, 1.5 mL of extract solution (25-800 µg/mL in ethanol) was added to 1.5 mL of DPPH (0.002 %) solution. The mixture was kept aside in a dark area for 30 min and absorbance was measured at  $\lambda_{\max}$  517 nm against equal amount of DPPH and ethanol as a control. The absorbance of sample in ethanol without DPPH was determined as sample blank. Ascorbic acid was used as standard antioxidant compound in the experiment. The percentage of DPPH radical scavenging (% RSA) was estimated using the equation:

$$\% \text{ RSA} = \frac{A_{\text{control}} - [A_{\text{sample}} - A_{\text{blank}}]}{A_{\text{control}}} \times 100$$

Where;           % RSA= radical scavenging activity  
                    $A_{\text{control}}$  = absorbance of DPPH in ethanol  
                    $A_{\text{sample}}$  = absorbance of DPPH with sample solution  
                    $A_{\text{blank}}$  = absorbance of sample in ethanol without DPPH

## Results and Discussion

### Nutritional Values

Proteins, carbohydrates, fats, vitamins, minerals and water are the nutrients that are essential for life and contribution to the caloric value of the body. In the present study, proximate analyses were carried out for the red and white flower petals of *S. grandiflora* to know the nutritional significance of the frequently consumed species in the traditional medicines. Proximate compositions *viz.* moisture, ash, crude protein, crude fat, crude fiber, carbohydrates and energy values were carried out using standard methods for food analysis (A.O.A.C, 2000). The analyses of nutritional values were performed at Department of Chemistry, West Yangon University. These analyses revealed some interesting findings and the results obtained from proximate analysis are presented in Table 1. These flower samples are low in protein and fat, however rich in carbohydrates. Moreover, the flowers of *S. grandiflora* are energy's high source, as 100 g of plant materials can give approximately 357 kcal and 352 kcal energy for red and white flowers, respectively.

**Table 1 Nutritional Values of Red and White Flower Petals of *S. grandiflora***

Parameter	Nutritional Value (%)*	
	Red Flower	White Flower
Moisture	6.13	5.28
Ash	4.37	5.10
Fiber	1.40	3.60
Protein	5.99	8.32
Fat	0.83	1.53
Carbohydrate	81.28	76.17
Energy Value (kcal/100 g)	357	352

\* based on the weight of dried sample

## Phytochemical Constituents

The qualitative tests for phytochemicals in red and white flower petals of *S.grandiflora* were carried out and a number of phytochemicals showed positive results in their specific tests. In the present study, the phytochemical screening of flowers of *S. grandiflora* revealed the presence of alkaloids, phenolic compounds, flavonoids, steroids, terpenoids, glycosides,  $\alpha$ -amino acids, starch, reducing sugars, carbohydrates, saponins and tannins. The results are indicated in Table 2.

**Table 2 Phytochemicals of Red and White Flower Petals of *S. grandiflora***

No	Phytochemical Constituents	Red Flower	White Flower
1	Alkaloids	+	+
2	Phenolic compounds	+	+
3	Flavonoids	+	+
4	Steroids	+	+
5	Terpenoids	+	+
6	Glycosides	+	+
7	$\alpha$ -Amino acids	+	+
8	Cyanogenic glycosides	-	-
9	Starch	+	+
10	Reducing sugars	+	+
11	Carbohydrates	+	+
12	Saponin	+	+
13	Tannins	+	+

**Note:** (+) = presence (-) = absence

## Total Phenolic Content

The total phenolic content of ethanolic and aqueous extracts of red and white flowers of *S.grandiflora* was estimated by Folin-Ciocalteu's method using gallic acid as standard. The reagent is formed from a mixture of phosphotungstic acid and phosphomolybdic acid which after oxidation of phenols is reduced to a mixture of blue oxides of tungsten and molybdenum. The blue coloration produced has a maximum absorption in the region of 760 nm and proportional to the total quantity of phenolic compounds originally present. The gallic acid solution of concentration (3.125 -100  $\mu\text{g/mL}$ ) was used for the construction of calibration curve ( $y=0.0052x + 0.1073$ ) with a regression coefficient ( $R^2=0.9907$ ) as shown in Figure 3.

The total phenolic content of red and white flowers extracts were expressed as  $\mu\text{g GAE/mg}$  of plant extract and shown in Table 3 and histogram is shown in Figure 4. Among the extracts, the higher phenolic contents (185.15 and 134.38  $\mu\text{g GAE/mg}$ ) were found in ethanolic extracts of red and white flower petals, respectively. Significant amount of phenolic content was observed in aqueous extracts of red flower (82.08  $\mu\text{g GAE/mg}$ ) and white flower (55.92  $\mu\text{g GAE/mg}$ ).

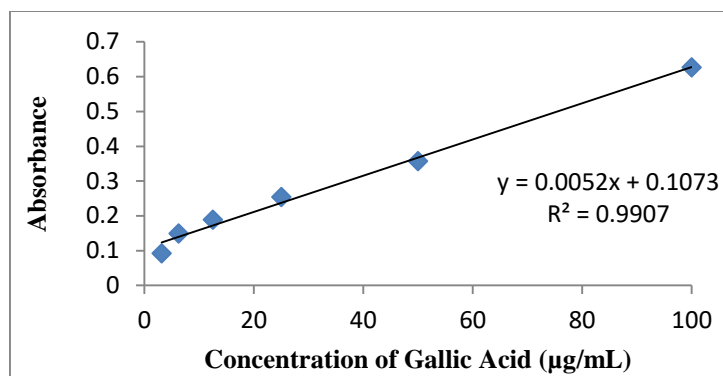


Figure 3 Standard curve of gallic acid

Table 3 Total Phenolic Contents in Red and White Flower Petals of *S. grandiflora*

Extract (250 µg/mL)	Total Phenolic Content (µg GAE/mg of extract)	
	Red Flower	White Flower
Ethanol	185.15	134.38
Aqueous	82.08	55.92

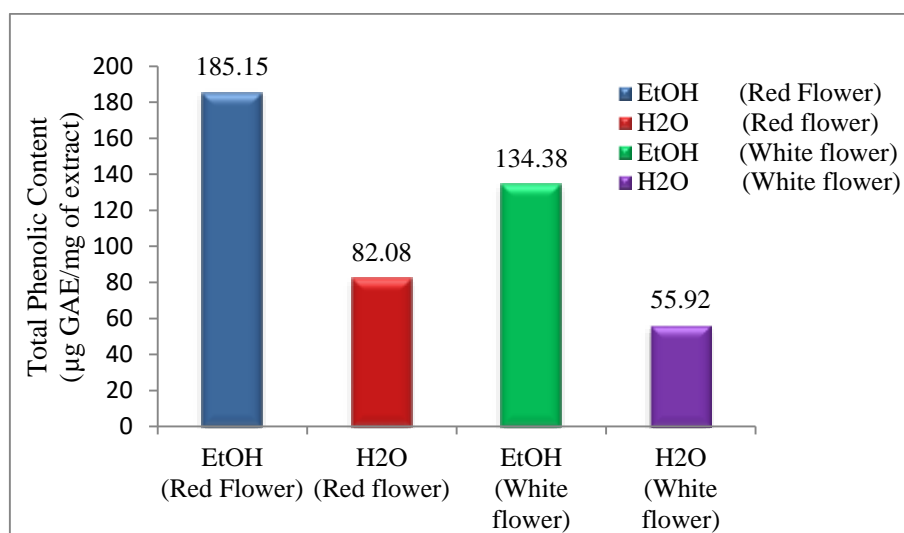


Figure 4 Histogram of total phenolic content of flower petals of *S. grandiflora*

### Total Flavonoid Content

The total flavonoid content in ethanolic and aqueous extracts of the red and white flower petals of *S. grandiflora* were determined using spectrophotometric method with aluminium chloride. Quercetin was used as standard and total flavonoid content was expressed in µg quercetin equivalence (µg QE/mg of extract). The total content of flavonoids in extracts was determined from the regression of the calibration curve ( $y=0.0033x-0.0064$ ,  $R^2 = 0.9934$ ) expressed in Figure 5. The total flavonoid contents in ethanolic and aqueous extracts of red and white flowers are indicated in Table 4 and histogram shown in Figure 6. It was observed that red flower variety possessed the highest amount of flavonoids than those of white flower variety. Both ethanolic and aqueous extracts of red flower contained 356.85 µg QE/mg and 285.33 µg QE/mg of extract, respectively, however, 45.33 µg QE/mg and 22.30 µg QE/mg of total flavonoids were observed in

white flowers. Since the various colour of plant parts are caused by the flavonoid compounds, red flowers of *S. grandiflora* contain more content of flavonoids.

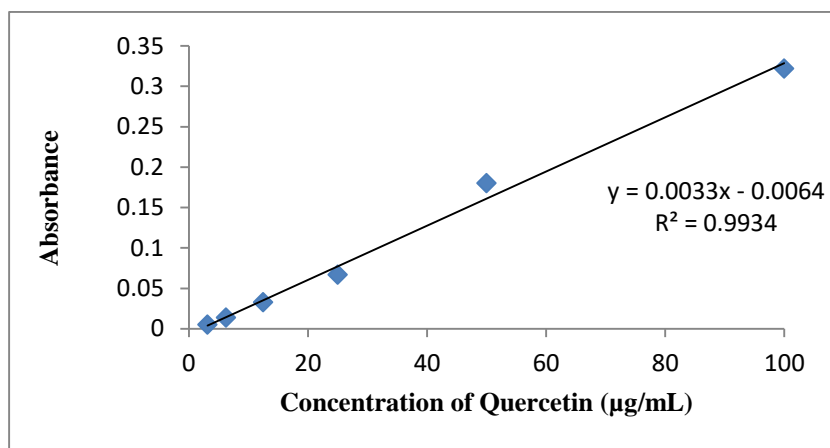


Figure 5 Standard curve of quercetin

Table 4 Total Flavonoid Contents in Red and White Flower Petals of *S. grandiflora*

Extract (250 µg/mL)	Total Flavonoid Content (µg QE/mg of extract)	
	Red Flower	White Flower
Ethanol	356.85	45.33
Aqueous	285.33	22.30

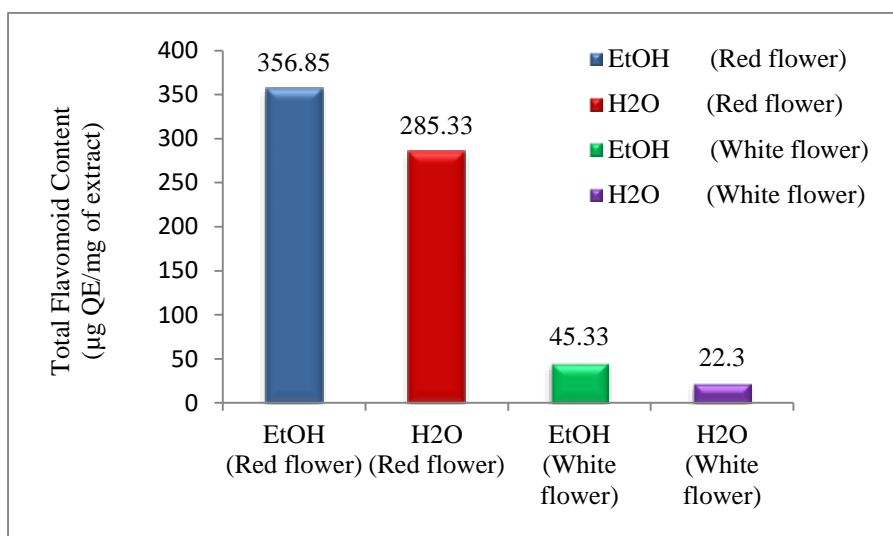


Figure 6 Histogram of total flavonoid content of flower petals of *S. grandiflora*

### Evaluation of Antioxidant Activity

The antioxidant activity of ethanolic and aqueous extracts from flower petals of *S. grandiflora* was determined using DPPH reagent. DPPH is very stable free radical. A freshly prepared DPPH solution exhibits a deep purple colour with an absorption maximum at 517 nm. This purple colour generally fades when antioxidant molecules quench DPPH free radicals and converted them into a colourless or yellow product, resulting in a decrease in absorbance at 517 nm (Amarowicz *et al.*, 2003).

The antioxidant activity of different extracts from flowers of *S.grandiflora* is expressed in terms of percentage of radical scavenging activity (% RSA) and  $IC_{50}$  values. The radical scavenging activities of flower extracts of *S. grandiflora* are shown in Table 5 and Figure 7. The obtained values of % RSA varied from 5.20 % to 82.13 % in various dosages of sample extracts. The  $IC_{50}$  value was calculated to determine the concentration of the sample required to inhibit 50 % of DPPH radical. The lower the  $IC_{50}$  value, the higher the antioxidant activity of the samples (Li *et al.*, 2009). The observed  $IC_{50}$  values of each extract and standard ascorbic acid are expressed in Table 6. The highest capacity to scavenge DPPH radicals was found in ethanolic extracts of both red and white flowers varieties with  $IC_{50}$  values of 213.67  $\mu\text{g/mL}$  and 322.21  $\mu\text{g/mL}$ , respectively. A moderate activity was observed in aqueous extracts of both red and white species of *S.grandiflora*.

**Table 5 Radical Scavenging Activity of Red and White Flower Petals of *S.grandiflora***

Concentration ( $\mu\text{g/mL}$ )	% RSA			
	Red Flower		White Flower	
	EtOH extract	H <sub>2</sub> O extract	EtOH extract	H <sub>2</sub> O extract
25	14.61	5.33	10.50	5.20
50	18.54	8.00	14.67	7.82
100	33.03	12.00	20.43	10.34
200	48.31	23.33	36.85	20.57
400	73.03	49.33	58.37	40.24
800	82.13	64.00	70.32	50.09

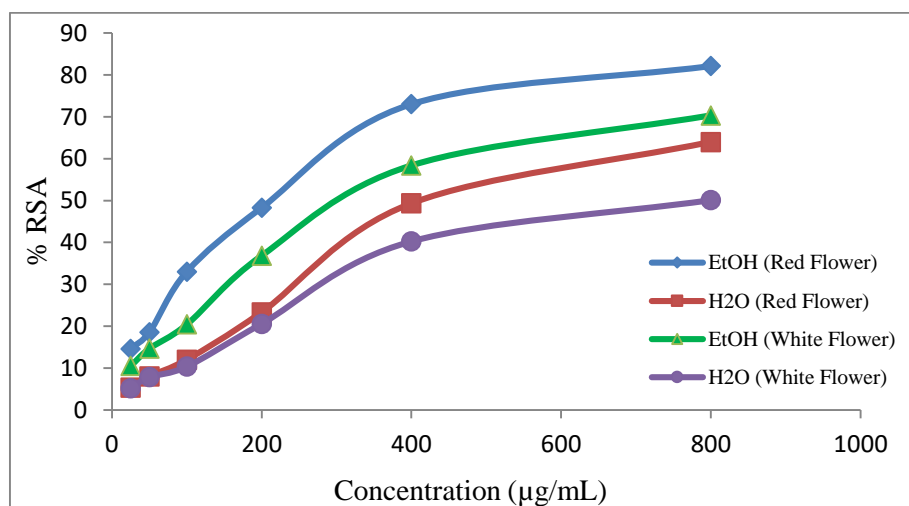


**Figure 7** Radical scavenging activity of red and white flower petals of *S.grandiflora*

**Table 6  $IC_{50}$  Values of Ascorbic Acid and Extracts of *S. grandiflora***

Sample	$IC_{50}$ Value ( $\mu\text{g/mL}$ )
Red Flower	
EtOH extract	213.67
H <sub>2</sub> O extract	417.98
White Flower	
EtOH extract	322.21
H <sub>2</sub> O extract	797.15
Ascorbic Acid	6.25

## Conclusion

The present study reported the nutritional values, phytochemicals, the total phenolic, total flavonoid contents and antioxidant activity of red and white flower varieties of *S. grandiflora*. Ethanolic extracts of both varieties were found to possess the higher phenolic and flavonoid contents and showed the higher antioxidant activity compared to aqueous extract. The results of this work suggested the importance of *S. grandiflora* as a source of active constituents known for their antioxidant properties.

## Acknowledgements

The authors are thankful to Myanmar Academy of Arts and Science for the submission of this research paper. Special thanks are expressed to Professor and Head Dr Sanda Khar and Professor Dr Myint Ngwe, Department of Chemistry, West Yangon University for their encouragements, providing necessary research facilities to carry out the research work.

## References

- A.O.A.C. (2000). *Official Methods of Analysis of the Association of Official Analytical Chemists*. 17<sup>th</sup> Edition, Washington D.C.
- Afify, E.A., El-Beltagi, H.S., El-Salam, S.M. and Omran, A.A. (2012). "Biochemical Changes in Phenols, Flavonoids, Tannins, Vitamin E,  $\beta$ -Carotene and Antioxidant Activity during Soaking of Three White Sorghum Varieties". *Asian Pacific Journal of Tropical Biomedicine*, vol. 2(3), pp.203-209
- Ainsworth, E. A. and Gillespie, K. (2007). "Estimation of Total Phenolic Content and other Oxidation Substrates in Plant Tissues using Folin-Ciocalteu Reagent". *Nature Protocols*, vol. 2 (4), pp. 875-877
- Alli, L. A. and Salwau, A. (2011). "Antiplasmodial Activity of Aqueous Root Extract of *Acacia nilotica*". *AJBR*, vol. 5, pp. 214-219
- Amarowicz, R., Pegg, B.R., Rahimi-Moghaddam, P., Bar, B. and Well, J.A. (2003). "Free Radical Scavenging Capacity and Antioxidant Activity of Selected Plant Species from the Canadian Prairies". *Food Chem.*, vol. 84, pp.551-562
- Aryal, S., Baniya, M.K., Danekhu, K., Kunwar, P., Gurung, R. and Koirala, N. (2019). "Total Phenolic Content, Flavonoid Content and Antioxidant Potential of Wild Vegetables from Western Nepal". *Plants*, vol. (8)96, pp.1-12
- Bahera, M., Karki, R. and Shekar, C. (2012). "Preliminary Phytochemical Analysis of Leaf and Bark Methanolic Extract of *Sesbania grandiflora*". *The Journal of Phytopharmacology*, vol.1 (2), pp.10-20
- Harborne, J.B. (1998). *Phytochemical Methods, A Guide to Modern Techniques of Plant Analysis*. 3<sup>rd</sup> Edition, Chapman and Hall, New York, pp.60-210
- Kokate, C.K., Purohit, A.P. and Gokhale, S.B. (2009). *Pharmacognosy.*, Nirali Prakashan: 17<sup>th</sup> Edition, Pune, pp. 99-445
- Li, X., Wu, X. and Huang, L. (2009). "Correlation between Antioxidant Activities and Phenolic Contents of Radix *Angelicae Sinensis* (Danggui)". *Molecules*, vol. 14(12), pp. 5349-5361
- Mbatchou, V. C. (2011). "Antibacterial Activities of Seed Pod Extracts of *Acacia nilotica* Wild to *Artemia salina* Larvae". *Journal of Applied Biosciences*, vol.40, pp. 2738-2745
- Outtara, M. B. (2011). "Antibacterial Potential and Antioxidant Activity of Polyphenols of *Sesbania grandiflora*". *Current Research Journal of Biological Sciences*, vol. 3(4), pp.351-356
- Vijay, D.W., Kalpana, V. W., Yogyata, N.T. and Shubhangi, A. S. (2009). "Phytochemical, Pharmacological and Phytopharmaceutics Aspects of *Sesbania grandiflora* (Hadga): A Review". *Journal of Pharmacy Research*, vol.2 (5), pp. 889-892
- Yan-Hwa, C., Chao-Lin, C. and Hsia-Fen, H. (2000). "Flavonoid Content of Several Vegetables and their Antioxidant Activity". *J. Sci. Food Agric.*, vol. 80, pp. 561-566

## INVESTIGATION OF PHYTOCONSTITUENTS AND SOME BIOACTIVITIES OF LEAVES AND BARKS OF *HOLOPTELEA INTEGRIFOLIA* R. (PHYAUK-SEIK)

Tha Zin Nwe Oo<sup>1</sup>, Mya Thandar Aung<sup>2</sup>, Saw Hla Myint<sup>3</sup>

### Abstract

Due to the increasing resistance of pathogens to the antibiotics, the plant kingdom is more focused than ever because the most parts of the plants have the ability to synthesize a wide variety of chemical compounds that possess important biological functions. The selected Myanmar medicinal plant, *Holoptelea integrifolia* R. (Phyauk-seik), belonging to family Ulmaceae, is known to have many bioactivities. This research deals with phytochemical and medico-chemical investigations of leaves and barks of *H. integrifolia*. The preliminary phytochemical investigation revealed the presence of many valuable phytochemicals in both samples. Based on DPPH assay method, the 70% EtOH extracts of leaves and barks of *H. integrifolia* showed the mild antioxidant activity by comparing with the standard ascorbic acid. The antimicrobial activity of PE, EtOAc and 70 % EtOH extracts of leaves and barks were screened on six microorganisms, namely *B. subtilis*, *S. aureus*, *P. fluorescens*, *A. flavus*, *C. albicans* and *E. coli* by paper disc diffusion assay. All of the tested extracts, except PE extract of barks exhibited the antimicrobial activity with inhibition zone diameters ranged between 8 mm ~ 18 mm for leaves and 10 mm ~ 22 mm for barks, while the PE extract of barks did not show the activity. The antiproliferative activity of PE, EtOAc and 70 % EtOH extracts of leaves and barks of *H. integrifolia* were determined by MTT assay on two human cancer cell lines: A 549 (lung) and HeLa (cervix). All of the tested extracts of leaves exhibited mild activities on two tested cancer cell lines with IC<sub>50</sub> values > 100 µg/mL. And, PE and 70 % EtOH extracts of barks exhibited significant activities on two tested cell lines with IC<sub>50</sub> values < 20 µg/mL, except the EtOAc extract, while the EtOAc extract of barks showed mild activity on cervix cancer cell line with IC<sub>50</sub> value > 100 µg/mL.

**Keywords:** *Holoptelea integrifolia*, Phyauk-seik, antioxidant activity, antimicrobial activity, antiproliferative activity, MTT assay

### Introduction

Myanmar is a fortunate country with a large number of medicinal plants. Most of the plants have been used as the traditional medicines from ancient times. They are widely used in Myanmar by the majority of the population either as an alternate or as a supplement to modern medicines. In this research, one of the Myanmar medicinal plant *Holoptelea integrifolia* R., Phyauk-seik, commonly called as India Elm tree have been selected for chemical analysis.



**Plant**

**Leaves**

**Barks**

**Figure 1** Photographs of plant, leaves and barks of *H. integrifolia* (phyauk-seik)

<sup>1</sup> Candidate, Second Year PhD Student, Department of Chemistry, University of Yangon

<sup>2</sup> Lecturer, Department of Chemistry, University of Yangon

<sup>3</sup> Professor, Department of Chemistry, University of Yangon

It is widely distributed all over tropical and temperate regions of Northern Hemisphere and the family Ulmaceae consists of 15 genera and 200 species (Sandhar *et al.*, 2011). *H. integrifolia* is a roadside tree possessing wide range of biological activities. Traditionally it used for the treatment of inflammation, wound healing, leprosy, diabetes, hemorrhoids, rheumatism and intestinal cancers in many countries (Danthala *et al.*, 2017).

It is a large, spreading, glabrous and deciduous tree as illustrated in Figure 1. Barks are 6-8 mm thick, grey, pustular and exfoliating in somewhat corky scales. Leaves are elliptic-ovate, acuminate, base rounded or sub-cordate. Flowers are greenish-yellow, polygamous in short racemes or fascicles on the leafless branches. Fruit is sub-orbicular samara with two membranous wings. Seed is one and flat. And, unpleasant odour appears on cutting the barks and crushing the leaves. The wood is light yellow, lustrous, interlocked-grained, medium and even-textured, moderately heavy and strong. Flowering occurs in February-March and fruiting March onwards (Shastri, 2007).

This plant has been reported to possess various chemical constituents. Different parts of the plant like stem bark, heartwood, leaves, seed, pollen and root are the major sources of various medicinally important phytochemicals. Two triterpenoids fatty acid esters holoptelin-A and B, 2-amino naphthaquinone, friedelin, epifriedelinol,  $\beta$ -sitosterol and its  $\beta$ -D-glucose,  $\beta$ -amyrin, betulin and betulinic acid are derived from stem bark. And, hexacosanol, octacosanol, 1, 4-naphthalenidone,  $\beta$ -sitosterol and  $\beta$ -amyrin are derived from leaves (Sharma, 2009; Mondal *et al.*, 2016). The aim of the present study is to screen the preliminary phytoconstituents and some bioactivities such as antioxidant, antimicrobial and antiproliferative activities of leaves and barks of *H. integrifolia*.

## Materials and Methods

### Collection and Preparation of Plants Materials

*Holoptelea integrifolia* (phyauk-seik) leaves and barks were collected from Nyaung Bin Seik Quarter, Mawlamyine Township in Mon State and identified at the Department of Botany, Mawlamyine University.

After collection, the leaves and barks of *H. integrifolia* were cleaned thoroughly with distilled water to remove any type of contamination. Then, the collected plant materials were shade dried to retain its vital phytoconstituents and subjected to size reduction. The powder of the samples were separately stored in air tight bottles and kept in a cool, dark and dry place until analyses were commenced.

### Preliminary Phytochemical Tests

The preliminary phytochemical detection of leaves and barks of *H. integrifolia* were carried out with standard phytochemical methods (Evans *et al.*, 2003; Harborne, 1984; Marini-Bettolo *et al.*, 1981; M-Tin Wa, 1972; Robinson, 1983; Shriner *et al.*, 1980; Trease *et al.*, 1978).

### Preparation of Plant Extracts for Biological Activity

The crude extracts of leaves and barks of *H. integrifolia* were prepared by extracting the sample with different solvents like pet ether (PE), ethyl acetate (EtOAc) and 70 % ethanol (EtOH) by successive maceration method at ambient temperature. All of these extracts were kept for the determination of antioxidant, antimicrobial and antiproliferative activities.

### Determination of Antioxidant Activity

The antioxidant activity of 70 % EtOH extracts of leaves and barks of *H. integrifolia* and standard ascorbic acid were investigated by DPPH (2,2-diphenyl-1-picryl-hydrazyl) free radical scavenging assay (Ashokkumar and Ramaswamy, 2013). DPPH radical scavenging activity was determined by spectrophotometric method.

### Preparation of sample and DPPH solutions

Each extract 2 mg and 10 mL of EtOH were thoroughly mixed by shaker. The mixture solution was filtered and the stock solution was obtained. The sample solutions (100, 50, 25, 12.5 and 6.25 µg/mL concentrations) were prepared from the stock solution by dilution with appropriate amounts of EtOH.

DPPH 2.364 mg was thoroughly dissolved in 100 mL of EtOH. This solution was freshly prepared in the brown coloured reagent bottle and stored in the fridge for no longer than 24 h.

### Procedure for antioxidant activity

The control solution was prepared by mixing 1.5 mL of 60 µM DPPH solution and 1.5 mL of 95 % EtOH using shaker. And, the blank solution was prepared by mixing 1.5 mL of test sample solution and 1.5 mL of 95 % EtOH. The sample solution was also prepared by mixing thoroughly 1.5 mL of 60 µM DPPH solutions and 1.5 mL of test sample solution. The sample solution was allowed to stand at room temperature for 30 min. Then, the absorbance of these solutions was measured at 517 nm by using UV-Visible spectrophotometer. Absorbance measurements were done in triplicate for each concentration and then the mean values obtained were used to calculate % inhibition of oxidation by the following equation,

$$\% \text{ Oxidative Inhibition} = \frac{A_c - (A - A_b)}{A_c} \times 100 \%$$

Where, % oxidative inhibition = % oxidative inhibition of test sample

$A_c$  = absorbance of the control (DPPH alone)

$A_b$  = absorbance of the blank (EtOH + Test sample solution)

$A$  = absorbance of test sample solution

Then  $IC_{50}$  (50 % inhibitory concentration) values were also calculated by linear regressive excel program (Brand-Williams *et al.*, 1995). The antioxidant activity is expressed as % radical scavenging activity (% RSA) and 50 % inhibition concentration ( $IC_{50}$ ). When the concentrations of the samples were increased, the absorbance values decreased i.e. % inhibition or radical scavenging activities also increased.

### Screening of Antimicrobial Activity

An antimicrobial is a substance that destroys microorganisms or inhibits their growth. The antimicrobial activity of different crude extracts such as PE, EtOAc and 70 % EtOH extracts of leaves and barks of *H. integrifolia* were tested with six microorganisms such as *Bacillus subtilis*, *Staphylococcus aureus*, *Pseudomonas fluorescens*, *Aspergillus flavus*, *Candida albicans* and *Escherichia coli* species by using paper disc diffusion assay. These tests were performed at Department of Botany, University of Yangon.

### Preparation of broth medium

Isolated bacterial strains grown on nutrient agar were inoculated into 50 mL conical flasks containing 10 mL of sterile growth medium. Then, they were incubated at 30 °C for 72 h on a reciprocal shaker at 200 rpm.

### Procedure for paper disc diffusion assay

Test organisms 0.3 mL was added to assay medium, then poured into plates. After solidification, paper discs impregnated with broth samples of PE, EtOAc and 70 % EtOH extracts of leaves and barks of *H. integrifolia* were applied on the test plates and these plates were incubated for 24-36 h at 30 °C. After incubation, clear zones (inhibitory zones) surrounding the test discs indicate the presence of bioactive compounds which inhibit the growth of test organisms.

### Determination of Antiproliferative Activity

*In vitro* antiproliferative activities of PE, EtOAc and 70 % EtOH extracts of leaves and barks of *H. integrifolia* were determined with two human cancer cell lines A 549 (lung cancer) and HeLa (cervix cancer). The antiproliferative activity was measured by MTT (3-(4, 5-dimethylthiazol-2-yl) - 2, 5-diphenyltetrazolium bromide) assay (Win *et al.*, 2015). These tests were done at Department of Natural Products Chemistry, Institute of Natural Medicine, and University of Toyama, Japan. This assay detects the reduction of MTT by mitochondrial dehydrogenase to blue formazan product, which reflects the normal function of mitochondria and cell viability.

### Preparation of sample and control solutions by serial dilution method

Each 1 mg of the PE, EtOAc and 70 % EtOH extracts of leaves and barks of *H. integrifolia* was dissolved in 100 µL of dimethyl sulfoxide (DMSO) solution to get 10000 µg/mL sample solution. It is necessary to mix with a vibrator. And the two eppendorf tubes for each sample were used for serial dilution.

The fresh medium 686 µL was added in the first eppendorf tube and then another fresh medium 540 µL was put into the second tube. The stock sample solution 14 µL was added to the 686 µL fresh medium with first eppendorf tube and vibrated well for solubility. And then 60 µL from the first eppendorf tube was added to the 540 µL fresh medium with second eppendorf tube and slowly pipetted up and down 2 to 3 times. Finally, 200 and 20 µg/mL of serial solutions were obtained and kept in the refrigerator.

The control solutions were serially prepared as described above procedure. Instead of sample extract, 5-fluorouracil (5 FU) was used for the positive control. Only DMSO was used for negative control.

### Preparation of cell growth

The cell was taken from the stock and transferred into a 15 mL centrifuge tube followed by addition of 5 mL of respective medium. The suspension cell was centrifuged in the refrigerated centrifuge machine 1000 rpm for 3 min. After the centrifugation, the supernatant was carefully removed without disturbing the cell pellet. And then fresh medium 2 mL was gently added to the side of the tube and slowly pipetted up and down 2 to 3 times to re-suspend the cell pellet. The suspension cell was centrifuged for 3 min. The supernatant was carefully removed without disturbing the cell pellet. The cell suspension was diluted with 6 mL of medium. Finally, the cells were transferred to the desired sterile container and the cells were incubated until 70 -100 % cell confluences for 7 days at an incubator.

### Procedure for antiproliferative activity

After the cell growth, the 70-100 % cell in the medium was aspirated with aspirator. The cell was washed with 5 mL of phosphate buffer saline (PBS) 2 times. The cells are trypsinised with 4 mL of trypsin and incubated for 2–3 min. And then the medium 1 mL was added to stop trypsinization. The cell suspension was transferred to 15 mL centrifuge tube. The tube (cell suspension) was centrifuged in the refrigerated centrifuge machine 3000 rpm with the same centrifuge tube for 3 min. After the centrifugation, the supernatant was carefully removed without disturbing the cell pellet and the cell was found at the bottom of the centrifuge tube. The cell in the centrifuge tube was added with 3 mL of fresh medium gently to the side of the tube and slowly pipetted up and down 2 to 3 time to re-suspend the cell pellet. The number of cell was counted with Haemocytometer.

The cell solution 10  $\mu$ L was mixed in the 40  $\mu$ L of Tryphan blue. The chamber and the covered slip were cleaned with alcohol (70 % EtOH). The chamber was dried and the over slip was fixed in position. The cell was harvested and the 10  $\mu$ L of the cell was added to the Haemocytometer (do not overfill). And then the chamber was placed in the inverted microscope under a 10  $\times$  objective and phase contrast was used to distinguish the cell. The cell was counted in the large, central gridded square (1 mm<sup>2</sup>). The gridded square was circled and multiplied by 10<sup>4</sup> to estimate the number of cells per millimeter. The number of cells was counted by the following equation,

$$\text{No. of cells in stock} = \text{counted cell}/4 \times 10^4 \times \text{dilution factor} \times \text{volume of stock cell solution}$$

After the cell counting, the cell was added with 50 mL (500  $\mu$ L) of medium for 12 plates. 10 mL (100  $\mu$ L) medium of cell was filled in 96 well plates. The cell in 96 well plates was incubated in an incubator for 24 h. After the incubation, the medium was removed by absorption machine (very carefully) and washed with 100  $\mu$ L PBS solution. And then 100  $\mu$ L each of the different concentrations of sample and control solution was added in the 96 well plates. The sample solutions in 96 well plates with cells were incubated in an incubator for 72 h.

The sample solution with cell and medium was added with 100  $\mu$ L MTT reagent. And then the 96 well plates were incubated in an incubator for 3 h. After the incubation, cells in the medium were aspirated with aspirator. The cell was washed with 5 mL of PBS for 2 times. Then, DMSO was added about 100  $\mu$ L per well and the 96 well plates were placed in the dark for 15 min. And then, the absorbance of each solution was measured at 570 nm by using UV-visible spectrophotometer. The percent cell viability activity was calculated by the following equation.

$$\% \text{ Cell viability} = [(\text{Abs (test sample)} - \text{Abs (blank)}) / (\text{Abs (control)} - \text{Abs (blank)})] \times 100$$

Where, Abs (test sample) = absorbance of test sample solution

Abs (control) = absorbance of DMSO solution

Abs (blank) = absorbance of MTT reagent

IC<sub>50</sub> (50 % inhibitory concentration) values were calculated by linear regressive excel program. The standard deviation was also calculated by the following equation.

$$\text{Standard Deviation (SD)} = \sqrt{\frac{(\bar{x}-x_1)^2 + (\bar{x}-x_2)^2 + \dots + (\bar{x}-x_n)^2}{(n-1)}}$$

Where,

$\bar{X}$  = average % inhibition

$x_1, x_2, \dots, x_n$  = % cell inhibition of test sample solution

n = number of times

## Results and Discussion

According to the preliminary phytochemical analysis of *H. integrifolia* showed the presence of alkaloids,  $\alpha$ -amino acids, carbohydrates, flavonoids, glycosides, organic acids, phenolic compounds, reducing sugars, saponins, starch, steroids, tannins and terpenoids in leaves, while  $\alpha$ -amino acids, carbohydrates, flavonoids, glycosides, organic acids, phenolic compounds, reducing sugars, saponins, steroids, tannins and terpenoids were found to be present in the barks. However, cyanogenic glycosides were not found in these samples. The main constituents such phenolic compounds, flavonoids, terpenoids and steroids, present in *H. integrifolia* may contribute to bioactivities such as antimicrobial, antioxidant and anticancer properties. Test reagents, observations and inferences for the analyses are summarized in Table 1.

**Table 1** Phytochemical Test Results of Leaves and Barks of *Holoptelea integrifolia* (Phyauk-seik)

Sr.No.	Tests	Extracts	Test Reagent	Observation	Leaves	Barks
1	Alkaloids	1% HCl	(i) Dragendorff's reagent	Orange ppt	+	-
			(ii) Sodium picrate solution	Yellow ppt	+	-
			(iii) Wagner's reagent	Brown ppt	+	-
			(iv) Mayer's reagent	White ppt	+	-
2	$\alpha$ -amino acids	H <sub>2</sub> O	Ninhydrin reagent	Purple colour	+	+
3	Carbohydrates	H <sub>2</sub> O	10% $\alpha$ -naphthol, conc:H <sub>2</sub> SO <sub>4</sub>	Red ring	+	+
4	Cyanogenic glycosides	H <sub>2</sub> O	Sodium picrate	No brick red colour	-	-
5	Flavonoids	EtOH	Mg turnings, conc : H <sub>2</sub> SO <sub>4</sub>	Pink colour	+	+
6	Glycosides	H <sub>2</sub> O	10% lead acetate	White ppt	+	+
7	Organic acids	H <sub>2</sub> O	Bromocresol green	Blue colour	+	+
8	Phenolic compounds	H <sub>2</sub> O	10% FeCl <sub>3</sub>	Deep blue	+	+
9	Reducing sugars	H <sub>2</sub> O	Benedict's solution	Brick-red ppt	+	+
10	Saponins	H <sub>2</sub> O	Distilled water	Frothing	+	+
11	Starch	H <sub>2</sub> O	I <sub>2</sub> solution	Deep blue	+	-
12	Steroids	PE	Acetic anhydride, conc:H <sub>2</sub> SO <sub>4</sub>	Green colour	+	+
13	Tannins	H <sub>2</sub> O	FeSO <sub>4</sub>	Deep blue	+	+
14	Terpenoids	CHCl <sub>3</sub>	Acetic anhydride, conc:H <sub>2</sub> SO <sub>4</sub>	Pink colour	+	+

(+) present      (-) absent      (ppt) precipitate

### Antioxidant activity of Leaves and Barks of *Holoptelea integrifolia* (Phyauk-seik)

The antioxidant activity of 70 % EtOH extract of leaves and barks of *H. integrifolia* was investigated with five different concentrations (100, 50, 25, 12.5 and 6.25  $\mu$ g/mL) by DPPH free radical scavenging assay. Their results are shown in Table 2 and Figure 2. The smaller IC<sub>50</sub> value indicates the higher the free radical scavenging activity. Here, the IC<sub>50</sub> values of 70 % EtOH extract of leaves and barks were found to be 32.75 and 77.97  $\mu$ g/mL. Therefore, 70 % EtOH extract of

leaves was more potent activity than barks. But, the 70 % EtOH extracts of both samples showed mild antioxidant activities by comparing with the IC<sub>50</sub> value 6.56 µg/mL of standard ascorbic acid.

**Table 2 % Radical Scavenger Activity and IC<sub>50</sub> Values of Crude Extracts of Leaves and Barks of *Holoptelea integrifolia* (Phyauk-seik)**

Test Samples	% RSA ± SD of Different Concentration (µg/mL)					IC <sub>50</sub> (µg/mL)
	6.25	12.5	25	50	100	
70 % EtOH (Leaves)	28.57 ±0.49	40.24 ±0.74	49.83 ±0.99	67.42 ±0.74	81.53 ±0.49	32.75
70 % EtOH (Barks)	26.12 ±0.49	27.88 ±0.99	33.45 ±0.49	41.82 ±0.49	56.45 ±0.99	77.97
Ascorbic Acid (Standard)	47.91 ±1.93	87.91 ±0.66	91.84 ±0.33	95.12 ±0.33	95.44 ±0.99	6.56

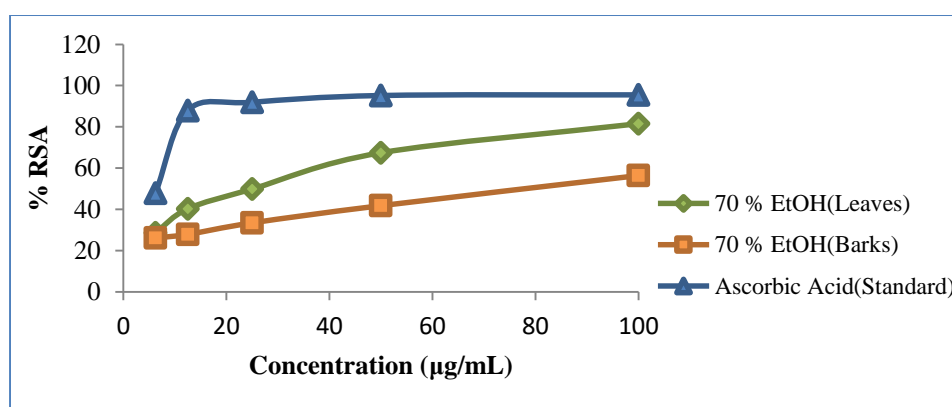


**Figure 2** % RSA of 70 % EtOH extracts of leaves and barks of *H. integrifolia* (Phyauk-seik)

**Antimicrobial activity of Leaves and Barks of *Holoptelea integrifolia* (Phyauk-seik)**

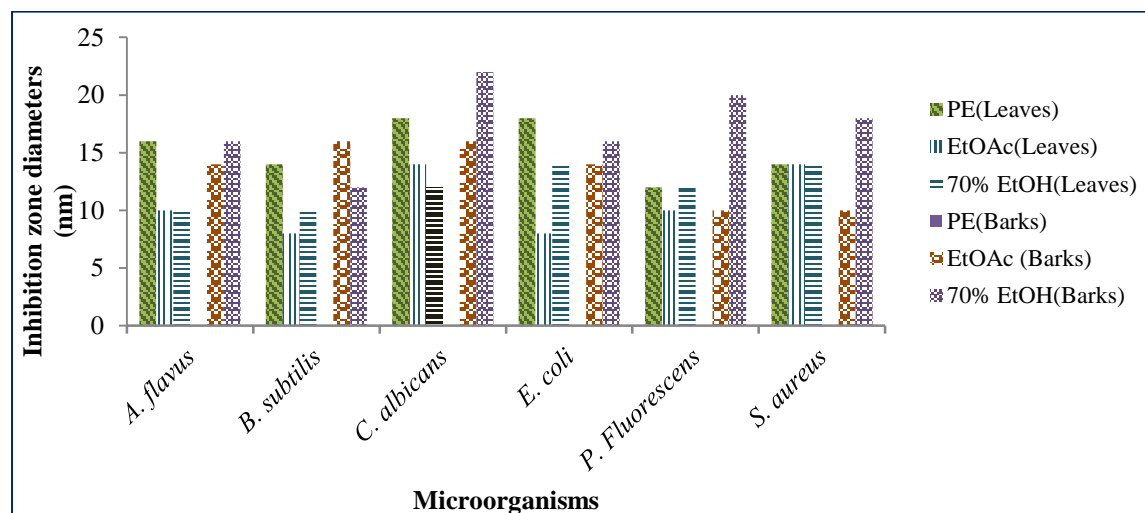
*In vitro* antimicrobial activity of PE, EtOAc and 70 % EtOH extracts of leaves and barks of *H. integrifolia* was studied by paper disc diffusion assay. Tested six microorganisms were *B. subtilis*, *S. aureus*, *P. fluorescens*, *A. flavus*, *C. albicans* and *E. coli*. It was carried out at Department of Botany, University of Yangon. The activities of the test extracts are expressed by measuring the zones (mm) of inhibition. Generally, the more susceptible the organism, the bigger is the zone of inhibition.

Among the extracts, the EtOAc and 70 % EtOH extracts of barks (10 ~ 22 mm) was found to be highly effective against six microorganisms than EtOAc and 70 % EtOH extracts of leaves (8 ~ 18 mm). And, the PE extract of leaves was observed to possess significant activity, but PE extract of barks did not show the activity against all tested microorganisms. The observed antimicrobial activity is expressed as the inhibition zone diameters as shown in Table 3 and Figure 3.

**Table 3** Inhibition Zone Diameters of Crude Extracts of Leaves and Barks of *Holoptelea integrifolia* (Phyauk-seik)

Microorganisms	Inhibition Zone Diameters (mm)					
	Leaves			Barks		
	PE	EtOAc	70 % EtOH	PE	EtOAc	70 % EtOH
<i>A. flavus</i>	16 (+++)	10 (+)	10 (+)	-	14 (++)	16 (+++)
<i>B. subtilis</i>	14 (++)	8 (+)	10 (+)	-	16 (+++)	12 (++)
<i>C. albicans</i>	18 (+++)	14 (++)	12 (++)	-	16 (+++)	22 (+++)
<i>E. coli</i>	18 (+++)	8 (+)	14 (++)	-	14 (++)	16 (+++)
<i>P. fluorescens</i>	12 (++)	10 (+)	12 (++)	-	10 (+)	20 (+++)
<i>S. aureus</i>	14 (++)	14 (++)	14 (++)	-	10 (+)	18 (+++)

Agar well = 6 mm  
 (+) = 6 -10 mm (low activity)  
 (++) = 11-15 mm (moderate activity)  
 (+++) = 16 mm & above (high activity)  
 (-) = no zone of inhibition

**Figure 3** A bar graph of inhibition zone diameters of PE, EtOAc and 70% EtOH extracts of leaves and barks of *H. integrifolia* against six tested microorganisms**Antiproliferative activity of Leaves and Barks of *Holoptelea integrifolia* (Phyauk-seik)**

In *in vitro* antiproliferative activity of PE, EtOAc and 70 % EtOH extracts of leaves and barks of *H. integrifolia* were determined by MTT assay with two human cancer cell lines such as A 549 (lung cancer) and HeLa (cervix cancer) cell lines. These tests were done at Department of Natural Products Chemistry, Institute of Natural Medicine, University of Toyama, Japan. The antiproliferative effect was expressed as IC<sub>50</sub> values.

The antiproliferative activities of the tested samples are summarized in Table 4. Since, the lower the IC<sub>50</sub> values exhibit the higher the antiproliferative activity. The PE and 70 % EtOH extracts of barks showed significant antiproliferative activity against A 549 and HeLa cell lines

with the IC<sub>50</sub> values less than 20 µg/mL. And also, the EtOAc extract of barks less than 20 µg/mL showed potent activity against A 549 lung cancer cell line. They possessed higher activity than standard 5 FU (IC<sub>50</sub> values is 19.06 ~ 35.84 µg/mL) against two tested cell lines. The remaining EtOAc extract of barks, PE, EtOAc and 70 % EtOH extracts of leaves exhibited mild antiproliferative activities against A 549 and HeLa cell lines because of their IC<sub>50</sub> values were greater than 100 µg/mL (Figures 4 and 5).

**Table 4 % Cell Viability IC<sub>50</sub> Values of Crude Extracts of Leaves and Barks of *Holoptelea integrifolia* (Phyauk-seik) Against Two Human Cancer Cell Lines**

Test Samples	50 % Inhibition (IC <sub>50</sub> µg/mL)			
	Leaves		Barks	
	Lung A 549	Cervix HeLa	Lung A 549	Cervix HeLa
PE extract	>200.00	>200.00	<20.00	<20.00
EtOAc extract	118.75	131.43	<20.00	141.20
70 % EtOH extract	100.56	118.84	<20.00	<20.00
5-Fluorouracil (Positive Control)	19.06	35.84	19.06	35.84

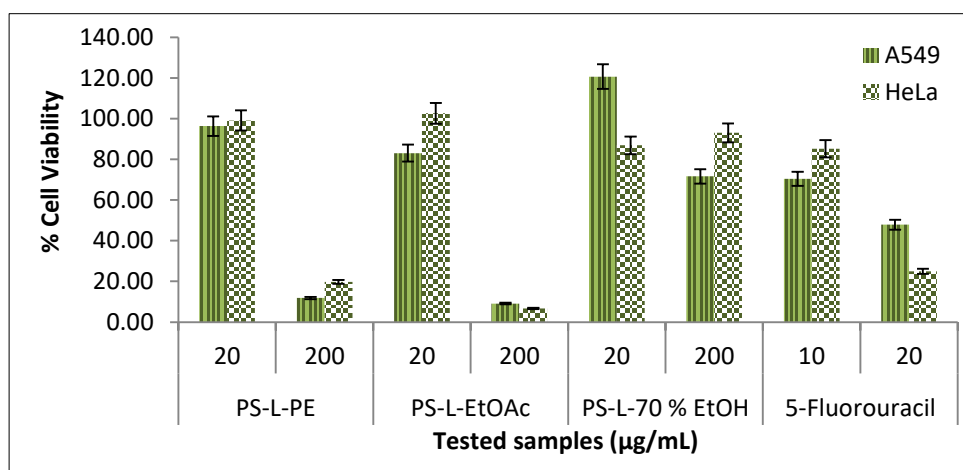


**Figure 4** A bar graph diagram for antiproliferative activity of crude extracts of leaves of *H. integrifolia* against human lung (A549) and cervix (HeLa) cancer cell lines

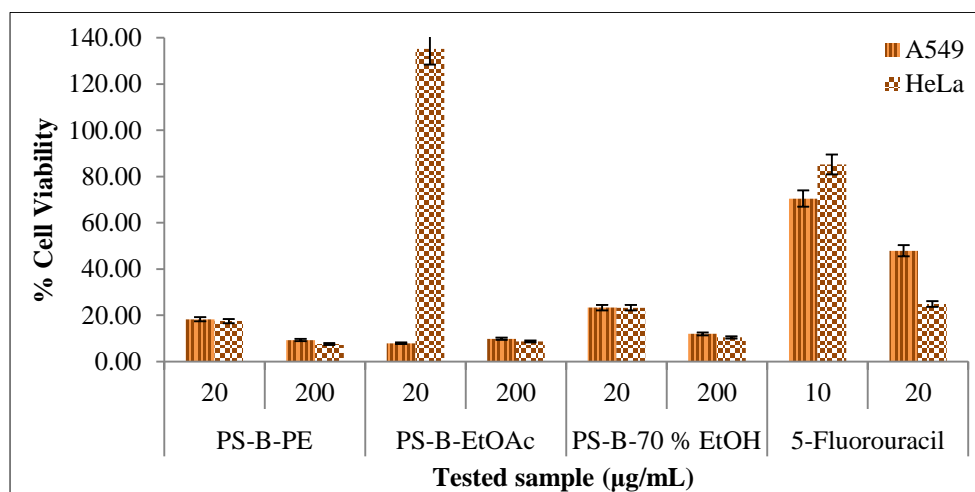


**Figure 5** A bar graph diagram for antiproliferative activity of crude extracts of barks of *H. integrifolia* against human lung (A549) and cervix (HeLa) cancer cell lines

## Conclusion

Based on preliminary phytochemical determination of leaves and barks of *H. integrifolia*, various types of bioactive organic constituents were found in both samples, except cyanogenic glycosides. The results of antioxidant activity suggested that the 70 % EtOH extracts of leaves and barks exhibited mild activity by comparing with the standard ascorbic acid. The antimicrobial activity results of EtOAc and 70 % EtOH extracts of both samples and PE extract of leaves showed significant antimicrobial activity on six tested microorganisms, except PE extract of barks. According to the antiproliferative activity determination, PE, EtOAc and 70 % EtOH extracts of barks were more potent activity than that of leaves extracts against two human cancer cell lines. According to the results, *H. integrifolia*, Phyauk-seik, leaves and barks contained many phytochemicals, mild antioxidant activities, and most of the extracts showed significant antimicrobial activities and had good news for cervix and lung cancer. However, this study is a preliminary step and further study is necessary to investigate the toxicology, detailed chemical characterization and other pharmacological profile of these plants constituents for the development of new drugs.

## Acknowledgement

The authors would like to express their profound gratitude to the Department of Higher Education (Lower Myanmar), Ministry of Education, Yangon, Myanmar, for provision of opportunity to do this research and Myanmar Academy of Arts and Science for allowing to present this paper.

## References

- Ashokkumar, R. and Ramaswamy, M. (2013) "Determination of DPPH Free Radical Scavenging Oxidation Effects of Methanolic Leaf Extracts of Some Indian Medicinal Plant Species". *Journal of Chemical, Biological and Physical Sciences*, vol. 3(2), pp. 1273 – 1278
- Brand-Williams, W., Cuvelier, M. E. and Berse, C. (1995). "Use of a Free Radical Method to Evaluate Antioxidant Activity". *Lebensm.-Wiss. u.-Technol* , vol. 28(1), pp. 25-30
- Danthala, V., Gottumukkula, K. M., Salla, D. R., Aramati, B. M. R. and Rani, S. (2017) "Comparison of Methanol Extracts of Leaf, Stem Bark and Stem of *Holoptelea integrifolia* Planch for Anticancer and Anti-angiogenic Activity". *International Journal of Research in Pharmacy and Pharmaceutical Sciences*, vol. 2(5), pp.44-51
- Harborne, J. B. (1984) *Phytochemical Method, A Guide to Modern Techniques of Plant Analysis*. 2<sup>nd</sup> Ed., New York: Chapman and Hall, pp. 120-126
- Marini-Bettolo, G. B., Nicolettice, H. M. and Patamia, M. (1981) "Plant Screening by Chemical and Chromatographic Procedure under Field Conditions". *J. Chromatog*, vol. 45, pp. 121 – 123
- Mondal, D. N., Barik, B. R., Dey, A. K., Patra, A. and Kundu, A. B. (2016) "Holoptelin A and B, Two New Triterpenoid Fatty Acids Esters from *Holoptelea integrifolia*". *Indian Drugs*, vol. 3(1), pp. 69-72
- M-Tin Wa. (1972) "Phytochemical Screening, Methods and Procedures". *Phytochemical Bulletin of Botanical Society of America, Inc.*, vol. 5(3), pp. 4-10
- Robinson, T. (1983) *The Organic Constituents of Higher Plants*. North Amherst: 5<sup>th</sup> Ed, Cordus Press, pp. 285-286
- Sandhar, H. K., Kaur, M., Tiwari, P., Salhan, M., Sharma, P., Prasher, S. and Kumar, B. (2011) "Chemistry and Medicinal Properties of *Holoptelea integrifolia*". *International Journal of Drug Development and Research*, vol. 3(1), pp. 6-11
- Sharma, P. C., Yelen, M. B., Dennis, T. J. and Joshi, A. (2009) *Database on Medicinal Plants Used in Ayurveda*. CCRAS, Dept. of ISM & H, Min. of Health & Family Welfare, Govt. of India, vol. 4, pp. 171-173
- Shastri, B. N. (2007) *The Wealth of India, Raw Material Series*. New Delhi: Council of Scientific and Industrial Research, vol. 5(H-K), pp. 109-110
- Shriner, R. L., Fuson, R. C., Curtin, D. Y. and Morrill, T. C. (1980) *The Systematic Identification of Organic Compounds, A Laboratory Manual*, New York: John Wiley and Sons, pp. 15-20
- Trease, G.E. and Evans, W.C. (1980) *Pharmacognosy*, London: Spottis Woode Ballantyne Ltd., pp. 108-529
- Win, N. N., Ito, T., Aimaiti, S., Imagawa, H., Ngwe, H., Abe, I. and Morita, H. (2015) "Kaempulchraols A–H, Diterpenoids from the Rhizomes of *Kaempferia pulchra* collected in Myanmar". *J. Nat. Prod.*, vol. 78, pp. 1113–1118

## EVALUATION OF SOME BIOLOGICAL ACTIVITIES OF TUBER OF *Gloriosa superba* L. (Si-mi-dauk)

Yu Nwe Moe<sup>1</sup>, Khin Hnin Mon<sup>2</sup>, Ni Ni Than<sup>3</sup>

### Abstract

*Gloriosa superba* L. is one of the important medicinal plants. It is used in diseases, like cancer, gout, purgative and so on. In this study, preliminary phytochemical investigation of *G. superba* revealed the presence of alkaloid, flavonoid, glycoside, carbohydrate, starch,  $\alpha$ -amino acid, terpenoid, steroid, saponin, tannin, phenolic compound, organic acid and reducing sugar. Cyanogenic glycoside was absent in *G. superba*. Total alkaloids content (1.11 %) of selected plant sample was determined by using gravimetric method of Harbone. The antimicrobial activities of different crude extracts such as pet-ether, ethyl acetate, ethanol, methanol and watery extracts from *G. superba* were determined against six microorganisms such as *Agrobacterium tumefaciens*, *Bacillus subtilis*, *Candida albicans*, *Escherichia coli*, *Salmonella typhia* and *staphylococcus aureus* by paper disc diffusion method. According to antimicrobial activity screening, pet-ether extract cannot against all strains of microorganisms. EtOAc and H<sub>2</sub>O extracts were observed to possess mild antimicrobial activity whereas EtOH and MeOH extracts have pronounced antimicrobial activity against all tested microorganisms. Antiproliferative activity of EtOH and H<sub>2</sub>O extracts of *G. superba* (tuber) against A 549 (lung cancer) and Hela (cervix cancer) was investigated by using (3-(4,5-dimethylthiazol-2-yl)-2,5-diphenyltetrazolium bromide or MTT Assay. Antiproliferative activities of all extracts showed strong activities (IC<sub>50</sub> < 20  $\mu$ g/ mL against two cancer cell lines.

**Keywords:** *Gloriosa superba* L. (Si-mi-dauk), phytochemical, total alkaloids, antimicrobial, antiproliferative activities

### Introduction

Medicinal plants have been used as sources of medicine in virtually all cultures. In recent years, there have been a gradual revival of interest in the use of medicinal plants in developing countries because herbal medicines have been reported safe and without any adverse side effect especially when compared with synthetic drugs (Parkin *et al.*, 2000). *G. superba* is an important medicinal plant belonging to the family Liliaceae which is one of the endangered species among the medicinal plants. (Senthilkumar, 2013) The genus *G. superba* is a native to tropical Africa and is found growing naturally in many countries of tropical Asia including India, Burma, Malaysia and Srilanka. (Nebapure, 2012). It is a semi-woody herbaceous branched climber reaching approximately 5 meters height, with brilliant wavy-edged yellow and red flowers that appears from November to March every year. Fruits are oblong, ellipsoid capsule. Seeds are numerous and rounded. One to four stems arise from a single V-shaped fleshy cylindrical tuber. It has large pharmacological value due to present of an important alkaloid, colchicine, gloriosine and also other biologically active compounds (Jason and Mohamad, 2014). The phytochemical from *G. superba* can act as anti-oxidant and anti-cancer by hormonal action, enzymes stimulators, physical action (contact within the cells) and interference with DNA replication. *G. superba* has the potentiality to inhibit the human carcinoma cell line growth. It is used for the treatment of leprosy, inflammations, skin problems, snake bites, insect bite, gout, asthma, paralysis, cancer, fever and blood disorder (Ravindra *et al.*, 2009). The tuberous root stocks of *G. superba* was boiled with sesame oil and was applied twice a day on the joints, affected with arthritis reduces pain. The rural women prefer *G. superba* plant for gynecological disorders like abortion, menstrual trouble, conception disorders, sterility, delivery problems (Simon *et al.*, 2016).

<sup>1</sup> Third Year PhD student, Department of Chemistry, University of Yangon

<sup>2</sup> Dr, Associate Professor, Department of Chemistry, Mandalay University of Distance Education

<sup>3</sup> Dr, Professor and head, Department of Chemistry, University of Yangon

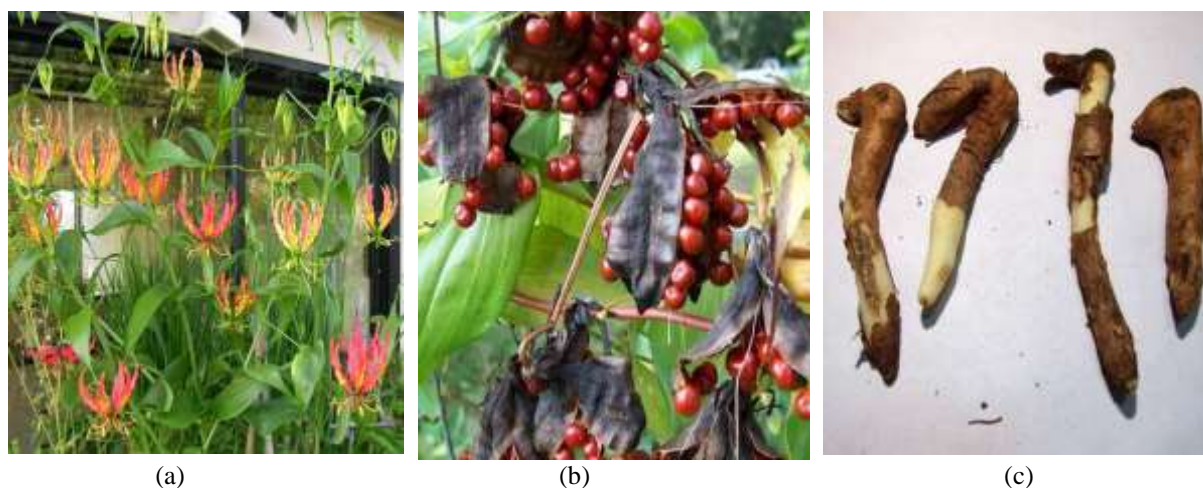


**Figure 1** The photographs of (a) plant of *G. superba*, (b) seed of *G. superba* (c) tuber of *G. superba*

#### Botanical Aspect of *Gloriosa superba* L.

Family	Liliaceae
Genus	Gloriosa
Species	<i>superba</i>
Botanical name	<i>Gloriosa superba</i> L.
Myanmar name	si-mi-dauk

### Materials and Methods

#### Collection and Preparation of Selected Medicinal Plant Sample

The tuber of *G. superba* (si-mi-dauk) was collected from Aunglan in Magway Region, during August, 2018. The collected sample was washed with water and air-dried at room temperature. The dried species were made into powder by using grinding machine.

#### Phytochemical Screening

Preliminary phytochemical tests such as alkaloids, glycosides, carbohydrates,  $\alpha$ -amino acids, flavonoids, terpenoids and steroids, saponins, tannins, phenolic compounds, reducing sugars, cyanogenic glycoside and organic acid were carried out according to the appropriate reported methods (Harborne, 1993).

#### Quantitative Analysis of Total Alkaloids

In tuber of *G. superba*, the total alkaloids content was determined by gravimetric method of Harbone. 5 g of powder sample was weighted into 250 mL conical flask and 200 mL of (20 %) acetic acid in ethanol added, covered and allowed to stand for 4 h and then filtered. The filtrate was concentrated on a water bath at 60 °C to one quarter of its original volume and concentrated aqueous ammonium hydroxide solution was added drop-wise to the extract in order to precipitate the alkaloid. The whole solution was centrifuged and the precipitate was collected and washed with 15 % ammonium hydroxide solution. The precipitate obtained as alkaloid was dried in an oven at 60 °C for 30 min and weighed. Alkaloid content was calculated and expressed as a percentage of the weight of sample analyzed. The percentage of total alkaloid content was calculated as:

$$\text{Percentage of total alkaloids (\%)} = \frac{\text{Weight of residue} \times 100}{\text{Weight of sample taken}}$$

(Harborne., 1993)

### Preparation of Various Crude Extracts

Dried powdered tuber sample of *G. superba* (25 g) was extracted with ethanol 50 mL, for 3 days at room temperature (3 times). The mixture was filtered with filter paper. The filtrate was concentrated by removal of the solvent to give the ethanol extract. Similarly, pet-ether, ethanol, methanol and watery extracts were prepared the above procedure.

Watery extract of dry powder sample (25 g) was prepared by boiling with 50 mL of distilled water for 6 h and filtered. The filtrate was concentrated by removal of the water to give the watery extract.

### Screening of Antimicrobial Activity of Crude Extracts of the *G. superba* L.Tuber

The screening of antimicrobial activity of the various crude extracts such as PE, EtOAc, EtOH, MeOH and H<sub>2</sub>O extracts of the tuber of *G. superba* were carried out by paper disc diffusion method at Department of Botany, University of Yangon. Six microorganisms namely *Agrobacterium tumefaciens*, *Bacillus subtilis*, *Candida albicans*, *Escherichia coli*, *Salmonella typhi*, and *Staphylococcus aureus* were used for this test. 10 µL of each crude extract was put on paper disc and air-dried at room temperature for 24 h. The test organisms were incubated in test broth medium containing glucose (0.5 g), polypeptone (0.2 g) and distilled water (100 mL) at appropriate temperature for 24 h. Assay medium containing glucose (1.0 g), polypeptone (0.2 g), agar (1.6 g) and distilled water (100 mL) were placed in beaker and the contents were heated for 10 min. The assay medium was put into sterilized conical flask and plugged with cotton wool and then autoclaved at 121 °C for 15 min. After cooling down to 40 °C, 0.1 mL of suspended strain was inoculated to the assay medium with the help of a sterilized disposable pipette near the burner. About 20 mL of medium was poured into the sterilized petri-dishes and allowed to set the medium. The dishes were cooled for 2 h at room temperature. After solidification, paper discs impregnated with samples (crude extracts) were applied on the agar plates and incubated at 27 °C for 24-36 h. Clear zones (inhibition zones) surrounding the paper discs indicate the presence of bioactive metabolites which inhibit the growth of test organisms. The diameter of clear zone around the well were measured with digital calipers in millimeter. The antimicrobial activity was determined by measuring the clear zone around the wells.

### Determination of Antiproliferative Activities of Ethanol and Watery Extracts of the *G. superba* by using MTT assay

In *in vitro* antiproliferative activities of EtOH and H<sub>2</sub>O extracts of the tuber of *G. superba* were determined against two human cancer cell lines such as A 549 (lung cancer) and Hela (cervix cancer) (Win *et al.*, 2015). These tests were done at Department of Natural Products Chemistry, Institute of Natural Medicine, University of Toyama, Japan.

### Preparation of medium for cell growth

500 mL of minimum Essential Medium ( $\alpha$  MEM) was added to 50 mL of fetal bovine serum (FBS) solution to prepare supplemented medium for all cell types.

From the above medium solution, 200 mL of this supplemented medium was taken and mixed with 2 mL of Non-Essential Amino Acid (NEAA) that was used for A549 cancer cell line.

From the above medium solution, only 100 mL of these supplemented medium was also used for Hela cell line.

### Preparation of phosphate buffer saline solution

The phosphate buffer saline (PBS) powder (4.8 g) was dissolved in 500 mL of ultra-pure water sterilized and kept in the refrigerator.

### Preparation of cell growth

The cell was taken from the stock and transferred into a 15 mL centrifuge tube followed by addition of respective medium (5 mL). The suspension cell was centrifuged in the refrigerated centrifuge machine (1000 rpm) for 3 min. After the centrifugation, the supernatant was carefully removed without disturbing the cell pellet. And then fresh medium (2 mL) was gently added to the side of the tube and slowly pipetted up and down 2 to 3 times to re-suspend the cell pellet. The suspension cell was centrifuged for 3 min. The supernatant was carefully removed without disturbing the cell pellet. The cell suspension was diluted with 6 mL of medium. Finally, the cells were transferred to the desired sterile container and the cells were incubated until 70-100 % cell confluences for 7 days at an incubator.

### Preparation of sample and control solutions by Serial Dilution Method

1 mL of each of the EtOH and H<sub>2</sub>O extracts of the tuber of *G. superba* was dissolved in each of 100 µL of DMSO solution to get 10000 µg/mL sample solution. The solution was necessary to vibrate at vibrator. The two eppendorff tubes for each sample were used for serial dilution. The fresh medium (686 µL) was added in the first eppendorff tube and then another fresh medium (540 µL) was put into the second tube. 14 µL of stock sample solution was added to the 686 µL fresh medium with first eppendorff tube and vibrated well for solubility. And then 60 µL from the first eppendorff tube was added to the 540 µL fresh medium with second eppendorff tube and slowly pipetted up and down 2 to 3 times. Finally, 200 and 20 µg/mL of serial solution were obtained and kept in the refrigerator.

The control solutions were serially prepared as described above procedure. Instead of sample extract, 5-fluorouracil (5FU) was used for the positive control. Only DMSO was used for negative control.

### Procedure for screening of antiproliferative activity by MTT Assay

After the cell growth, the 70-100 % cell in the medium was aspirated with aspirator. Cell was washed with PBS (5 mL) for two times. The cell was trypsinized with trypsin

(4 mL) and incubated for 2-3 min. And then the medium (1 mL) was added to stop trypsinization. The cell suspension was transferred to 15 mL centrifuge tube. The tube (cell suspension) was centrifuged in the refrigerated centrifuge machine (2000 rpm) with the same centrifuge tube for 3 min. After the centrifugation, the supernatant was carefully removed without disturbing the cell pellet and the cell was found at the bottom of the centrifuge tube. The cell in the centrifuge tube was added with fresh medium (3 mL) gently to the side of the tube and slowly pipetted up and down 2 to 3 times to re-suspend the cell pellet. The number of cell was counted with Haemocytometer.

The solution (10 mL) was mixed with the trypan blue (40 mL) in the chamber and the covered slip was cleaned with alcohol (70% EtOH). The chamber was dried and the cover slip was fixed in position. The cell was harvested and the (10 µL) of the cells added to the Haemocytometer (do not overfill). And then the chamber was placed in the inverted microscope under a 10 X objective and phase contrast was used to distinguish the cell. The cell was counted in the large, central gridded square (1 mm). The gridded square was circled and multiplied by 10<sup>4</sup> to estimate the number of cell per millimeter. The number of cell was counted by the following equation.

No. of cell in stock = counted cell/  $4 \times 10^4$   $\times$  dilution factor  $\times$  volume of stock cell solution

After the cell counting, the medium was added with (120 mL/  $120 \times 10^3$   $\mu$ L) of medium for 12 plates. 100  $\mu$ L medium of cell was filled in 96 well plates. The cell in 96 well plates was incubated in an incubator for 24 h.

After incubation, the medium was removed by absorption machine (very carefully) and washed with 100  $\mu$ L of the different concentrations of sample and control solution was added in the 96 well plates. The sample solutions in 96 well plates with cell was incubated in an incubator for 72 h.

The sample solution with cell and medium was added with 100  $\mu$ L MTT reagent. And then the 96 well plates were incubated in an incubator for 3 h. After incubation, the absorbance of each solution was measured at 450 nm by using UV-visible spectrophotometer for Hela cell line and for A 549 cell line, 96 well plates were added 100  $\mu$ L DMSO solution and then measured the absorbance at 570 nm by using UV-visible spectrophotometer. The percent cell viability activity was calculated by the following equation.

$$\% \text{ Cell viability} = [(\text{Abs (test sample)} - \text{Abs (blank)}) / (\text{Abs (control)} - \text{Abs (blank)})] \times 100$$

Where,

Abs (test sample) = absorbance of test sample solution

Abs (control) = absorbance of DMSO solution

Abs (blank) = absorbance of MTT reagent

IC<sub>50</sub> (50 % inhibition concentration) values were calculated by linear regressive excel program. The standard deviation was also calculated by the following equation.

$$\text{Standard Deviation (SD)} = \sqrt{\frac{(\bar{x}-x_1)^2 + (\bar{x}-x_2)^2 + \dots + (\bar{x}-x_n)^2}{(n-1)}}$$

Where,

$\bar{X}$  = average % inhibition

X<sub>1</sub>, X<sub>2</sub>, ..., X<sub>n</sub> = % cell inhibition of test sample solution

n = number of times

## Results and Discussion

### Types of Phytochemicals Present in *G. superba* L.

In order to find out the types of phytochemical constituents present in the tuber of *G. superba*, the phytochemical tests were preliminary carried out according to the reported procedure. From the data findings, it was observed that various secondary metabolites such as alkaloid, flavonoid, glycoside, carbohydrate, starch,  $\alpha$ -amino acid, terpenoid, steroid, saponin, tannin, phenolic compound, organic acid and reducing sugar were present, however cyanogenic glycoside was not detected in the sample (Table 1). According to the results, it can be seen that tuber of *G. superba* might contain potent bioactive secondary metabolites.

These secondary metabolites contribute significantly towards the biological activities of medicinal plants such as antimicrobial and antiproliferative activities.

**Table 1** Phytochemicals Present of *G.superba* L.

No	Types of compounds	Extract	Test reagents	Observation	<i>G. superba</i>
1	Alkaloid	1 % HCl	Mayer's reagent	ppt(white)	+
			Dragendorff's reagent	ppt(orange)	+
			Wagner's reagent	ppt(reddish brown)	+
2	Glycoside	H <sub>2</sub> O	10 % lead acetate	ppt (white)	+
3	Carbohydrate	H <sub>2</sub> O	10 % $\alpha$ -naphthol, H <sub>2</sub> SO <sub>4</sub>	red ring	+
4	$\alpha$ -amino acid	H <sub>2</sub> O	Ninhydrin reagent	purple color	+
5	Flavonoid	70 % EtOH	Mg turning and conc: HCl	pink color	+
6	Terpenoids	CHCl <sub>3</sub>	Acetic anhydride and conc: H <sub>2</sub> SO <sub>4</sub>	pink color	+
7	Steroid	PE	Acetic anhydride and conc: H <sub>2</sub> SO <sub>4</sub>	green color	+
8	Tannin	H <sub>2</sub> O	0.1 % FeCl <sub>3</sub>	brownish green	+
9	Phenolic compound	H <sub>2</sub> O	5% Ferric chloride	dark blue	+
10	Saponins	H <sub>2</sub> O	Distilled water	frothing	+
11	Reducing Sugars	H <sub>2</sub> SO <sub>4</sub> (dil)	Benedict's solution	brick red ppt	+
12	Organic acid	H <sub>2</sub> O	Bromocresol green	yellow color	+
13	Starch	H <sub>2</sub> O	Iodine solution	bluish black ppt	+
14	Cyanogenic glycoside	H <sub>2</sub> O	H <sub>2</sub> SO <sub>4</sub> , sodium picrate	No brick red	-

(+) present, (-) absent, ppt = precipitate.

### Quantitative Analysis of Total Alkaloids

In this study, the total alkaloid content of tuber of *G. superba* was estimated by Harbone method. According to this method, the total alkaloids content is found to be 1.11 % in selected sample. Alkaloid acts as a local anaesthetics, anti-tumor, anti-malarials, anti-bacterials agents and pain killer. The higher the total alkaloid contents, the more activity against the various diseases (Megale *et al.*, 2013).

### Antimicrobial Activities of Different Crude Extracts

Four crude extracts such as EtOAc, EtOH, MeOH and H<sub>2</sub>O extracts of the tuber of *G. superba* were subjected to screening of antimicrobial activity against six different pathogenic microbes such as *Agrobacterium tumefaciens*, *Bacillus subtilis*, *Candida albicans*, *Escherichia coli*, *Salmonella typhi*, and *Staphylococcus aureus* using ager disc diffusion method. This method is based on zone diameter including the disc diameter, in millimeter (mm). The larger the zone diameter, the higher the activity is. According to the results, PE extract was not against all tested microorganisms because the active constituents present in selected sample, it may not dissolve in non-polar solvent medium. EtOAc extract showed active against (16 – 30 mm) in *A. tumefaciens*,

*B. subtilis*, *C. albicans*, *E. coli* but does not show in *S. typhi* and *S. aureus*. H<sub>2</sub>O extract can inhibit five types of microbes (14 - 28 mm) except *B. subtilis*. Whereas EtOH and MeOH extracts were found to be high with diameter zones of inhibition ranged from 12 to 30 mm against all tested microorganisms as shown in Table 2. Among the extracts, EtOH and MeOH extracts can against six different pathogenic microbes. Therefore these extracts showed higher activity than other extracts, as shown in Figure 3.

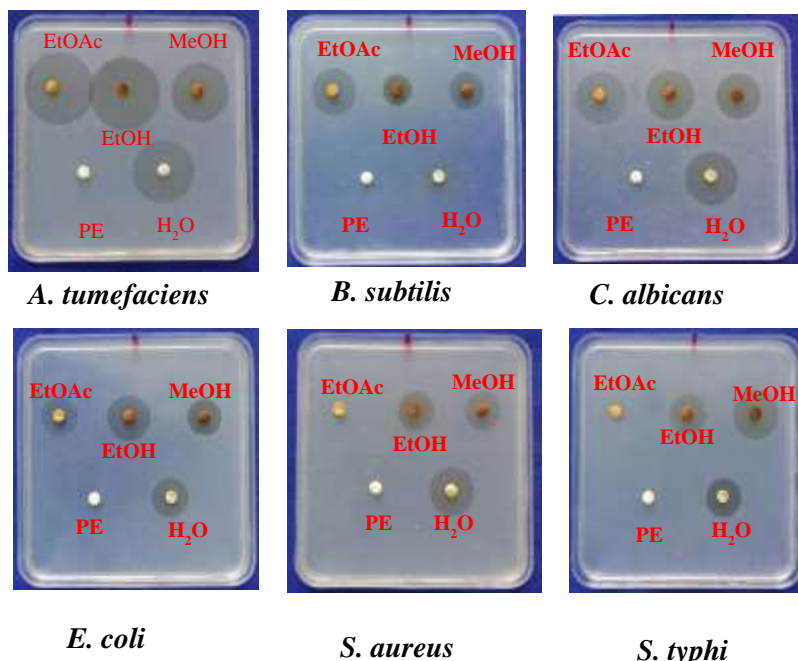


**Figure 2** The photographs of the antimicrobial activities of crude extracts of *G. superba* L.

**Table 2** Antimicrobial Activities of Crude Extracts of *G. superba* L.

No.	Microorganisms	Inhibition zones diameters(mm) of different crude extracts				
		PE	EtOAc	EtOH	MeOH	H <sub>2</sub> O
1	<i>A. tumefaciens</i>	-	30 (+++)	30 (+++)	26 (+++)	28 (+++)
2	<i>B. subtilis</i>	-	18 (+++)	12 (+)	16 (++)	-
3	<i>C. albicans</i>	-	30 (+++)	28 (+++)	26 (+++)	26 (+++)
4	<i>E. coli</i>	-	16 (++)	22 (+++)	16 (++)	16 (++)
5	<i>S. typhi</i>	-	-	14 (++)	18 (+++)	14 (++)
6	<i>S. aureus</i>	-	-	14 (++)	14 (++)	16 (++)

Disc size-6 mm

10-12 mm(+) =weak activity, 13-17(++) = high activity, > 18 mm(+++) = very high activity

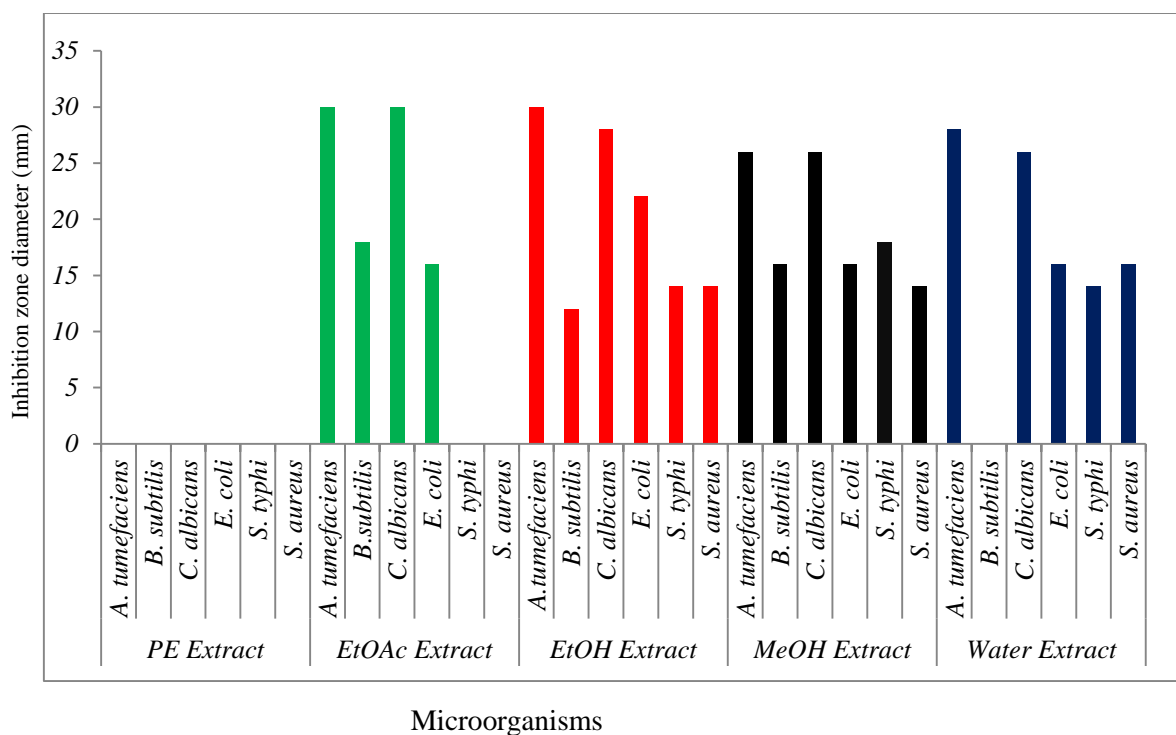


**Figure 3** A bar graph of antimicrobial crude extracts *G. superba* L.

### Antiproliferative Activity of the EtOH and H<sub>2</sub>O Extracts of the *G. superba* L.

The antiproliferative activity is the activity relating to a substance used to prevent or retard the spread of cells, especially malignant cells, into surrounding tissues. Antiproliferative activity of the sample was studied *in vitro* against human cancer cell lines. Screening of antiproliferative activities of ethanol and watery extracts from the tuber of *G. superba* was done against two human cancer cell lines such as A 549 (human lung cancer) and Hela (human cervix cancer). Antiproliferative activity was expressed as the IC<sub>50</sub> (50 % inhibitory concentration) value. 5-Fluorouracil was used as positive control. The antiproliferative activity of ethanol and watery extracts are summarized in table 3.

Since the lower the IC<sub>50</sub> values, the higher the antiproliferative activity. For both Hela and A 549 cell lines, the EtOH and H<sub>2</sub>O extracts of the tuber of *G. superba* showed potent activities (IC<sub>50</sub> <20 µg/ml). These results indicated that the tuber of *G. superba* could be regarded as an anti-cancer herbal medicine as well as a potential crude drug source for the development of anti-cancer compounds.

**Table 3** Antiproliferative Activities of Crude Extracts of *G. superba* Against Two Types of Cancer Cell Lines

Extracts	Hela (cell viability)			A 549 (cell viability)		
	20 µg/mL	200 µg/mL	IC <sub>50</sub> µg/mL	20 µg/mL	200 µg/mL	IC <sub>50</sub> µg/mL
EtOH	8.00	21.45	<20	11.62	25.35	<20
H <sub>2</sub> O	8.43	13.18	<20	14.73	17.39	<20

Hela = human cervix cancer

A 549 = human lung cancer

**Table 4 Antiproliferative Activities of Positive Control (5FU) Against Two Types of Cancer Cell Lines**

Cell lines	Concentrations ( $\mu\text{M}$ )	% Cell viability	IC <sub>50</sub> ( $\mu\text{M}$ )
Hela	2	91.44	
	10	85.22	15.84
	20	24.39	
A549	2	136.24	
	10	70.45	19.06
	20	47.89	

### Conclusion

From the overall assessment concerning with the investigation of phytochemicals and biological activities on the tuber of *G. superba* L., the following inferences can be deduced. Various types of secondary metabolites such as alkaloid, flavonoid, glycoside, carbohydrate, starch,  $\alpha$ -amino acid, terpenoid, steroid, saponin, tannin, phenolic compound, organic acid and reducing sugar were present, however cyanogenic glycoside was not detected in the sample. Total alkaloids content of the tuber of *G. superba* is 1.11 %. According to the screening of antimicrobial activity, PE extract was not against all tested microorganisms because the active constituents present in selected sample, it may not dissolve in non-polar solvent medium. EtOAc extract showed highly against (16 – 30 mm) in *A. tumefaciens*, *B. subtilis*, *C. albicans*, *E. coli* but does not showed in *S. typhi* and *S. aureus*. H<sub>2</sub>O extract can inhibit five types of microbes (14 - 28 mm) except *B. subtilis*. Whereas EtOH and MeOH extracts were found to be high with the zones of inhibition ranged from 12 to 30 mm against all tested microorganisms. Among the extracts, EtOH and MeOH extracts can inhibit against six different pathogenic microbes. Therefore, these extracts showed higher activity than other extracts. Moreover, the EtOH and H<sub>2</sub>O extracts of the tuber of *G. superba* showed highly antiproliferative activities (IC<sub>50</sub> <20  $\mu\text{g/ml}$ ). Therefore, selected sample can prevent human cervix cancer (Hela) and human lung cancer (A 549). With these results, the tested plant might be useful for the treatment of bacteria and fungus infected diseases and be used as anticancer agent.

### Acknowledgements

The authors would like to express their profound gratitude to the Department of Higher Education, Ministry of Education, Yangon, Myanmar, for provision of opportunity to do this research and Myanmar Academy of Arts and Science for allowing to present this paper. Grateful thanks are also to Professor

Dr Hiroyuki Morita, Institute of Natural Medicine, University of Toyama for his help and suggestions throughout course of antiproliferative activity.

## References

- Harborne, J. B. (1993). *Phytochemistry Dictionary: A Hand Book of Bioactive Compounds from Plants*, London.
- Jason, R. J. and Mohamed, I. M. (2014). "Quantification of Colchicine in Various Parts of *Gloriosa superba* by HPLC". *J. Chem and Pharm. Sci.*, vol. 2, pp. 53-55
- Megale, S. and Elango, R. (2013). "Antifungal Activities of Tubers and Seeds Extracts of *Gloriosa superba* L. Against in Human Pathogens". *Int. J. Sci. Res.*, vol. 2, pp. 12-24
- Nebapure, S. M. (2012). "Extraction and bioefficacy of *Gloriosa superba* L. Against *Spodoptera litura* (FABRICUS) and *Tribolium castaneum* (HERBST.)" *Division of Entomology India. Agri. Res. Inst.*, New Delhi.
- Parkin, D. M., Bray, F., Ferlay, J. and Pisani, P. (2000). The World Cancer: Globocan 2000". *Int. J. Cancer.*, vol. 94, pp. 153-156
- Ravindra, A. and Mahendra, K. R. (2009). "Review: Current Advances in *Gloriosa superba* L". *J. Biol. Diversity*, vol. 10 (4), pp. 210-214
- Senthilkumar, M. (2013). "Phytochemical Screening and Antibacterial Activity of *Gloriosa superba* L." *Int. J. Pharm. and Phytochem. Res.*, vol. 5(1), pp. 31-36
- Simon, S. E. and Jayakumar, F. A. (2016). "Anti-oxidant Activity and Anticancer Study on Phytochemicals Extract from Tubers of *Gloriosa superba* against Human Cancer Cell (Hep-G2)". *J. Pharm. And Phytochem.*, vol. 3, pp. 2332-2347
- Win, N. N., Ito, T., Aimaiti, S., Imagawa, H., Ngwe, H., Abe, I. and Morita, H. (2015). "Kaempulchraols A-H, Diterpenoids from the Rhizomes of *Kaempferia pulchra* collected in Myanmar". *J. Nat. Prod.*, vol. 78, pp. 1113-1118

## **ISOLATION, CHARACTERIZATION AND BIOACTIVITY OF CASEIN AND ALBUMIN FROM FRESH AND PACKED COW MILK SAMPLES**

Sandar Moe<sup>1</sup>, Pyone Kyi<sup>2</sup>

### **Abstract**

The aim of the study is to isolate and characterize the casein and albumin from selected fresh and packed cow milk samples as well as to determine the minerals and antioxidant activities. Preliminary milk quality tests of both milk samples showed that pH (6.8-6.5) were within normal range in the presence of carbohydrate and reducing sugar gave good quality with alcohol test. The main component of casein I and II (9.11 % and 7.36 %) from both samples were isolated by adjustment of isoelectric point (pH 4.6) with 10 % acetic acid. After removing of casein, 2.2 g of CaCO<sub>3</sub> was added to the filtrate (whey solution) to precipitate albumin I and II (2.18 % and 0.21 %). The isolated casein and albumin were characterized by FT IR spectroscopy, amino acid tests (such as Millon's test, Biuret test, Ninhydrin test, Xanthoproteic test) and protein precipitation tests (salt test, organic solvent test, acidic agent test, heat and acid test and heavy metal ions test) respectively. FT IR spectra of isolated casein I and II illustrate better fit with the reported spectra than those of albumin I and II. Atomic absorption spectroscopy (AAS) of isolated casein and albumin showed sufficient amount of minerals. The isolated casein possessed mild antioxidant activity whereas albumin possessed practically inactive by DPPH assay. Therefore, it may be better to use the fresh cow milk for the production of more nutritious dairy food.

**Keywords:** Fresh and packed cow milk, quality tests, casein, albumin, FT IR, protein tests, AAS, antioxidant activity

### **Introduction**

Milk is the most nutritionally complete food found in nature. All kinds of milk, human or animal, contain vitamins, minerals, proteins (most casein), carbohydrates (principally lactose), and lipids (fats). The amounts of these nutrients present in different types of milk differ greatly. However, cow's milk and goat's milk are almost identical in every respect (Seyhan Ege's Homepage, 1997). Milk contains three kinds of protein: caseins, lactalbumins and lactoglobulins, all of which are globular protein (Spurlock, 2014). Casein is a combination of phosphoproteins presenting in milk and cheese. It is the amount of 3 % in milk along with 4-5 % of lactose and 3-4 % of fats and the rest is water (Ahluwalia and Dhingra, 2005). Caseins exist in micelles which are composed of submicelles linked by the characteristic of hydrocolloid which are freely suspended in the aqueous phase of milk (Tarte, 2019). Casein can be electrophoretically fractioned into four major components: alpha-, beta-, gamma- and kappa- casein. Casein develops precipitation from milk at pH 4.6, which has negative charge by comparing the pH of the milk. Therefore, it can be precipitated as salt by adding acids (Miller, Jarvis and Mcbean, 2006). Casein can be used in glues, the coating of paper, and the binding of colours in paints and wallpaper. It is also used as a coating for fine leather, and is cured with rennet to produce a plastic material used for buttons. Casein is also employed in the manufacture of pharmaceutical and nutritional product (Seyhan Ege's Homepage, 1997). The aim of the study is to isolate and characterize the casein and albumin from fresh and packed cow milk samples as well as to determine the minerals and antioxidant activities.

---

<sup>1</sup> Dr, Associate Professor, Department of Chemistry, Taunggyi University

<sup>2</sup> Candidate, MSc, Department of Chemistry, Taunggyi University

## Materials and Methods

### Sample Collection

Packed cow milk was collected from Myoma Market, Taunggyi Township. Fresh cow milk was freshly collected from the cow farm at Panthakwar Village, Taunggyi Township, Southern Shan State and immediately operated after collection.

### Measuring of Milk Quality Test

#### Alcohol Test

The test was done by mixing equal amount of each milk sample (5 mL) and 68 % of ethanol solution (5 mL) in a test tube. If the tested milk is good quality, there will be no coagulation, clotting or precipitation. Presence of flakes or clots indicated poor quality milk.

#### Determination of pH Value

Milk sample (50 mL) was taken in a beaker and pH meter was put in a beaker for 5 min to determine milk quality. The result of pH value was obtained.

#### Test for Carbohydrates

Cow milk sample (2 mL) and 2 drops of 10 %  $\alpha$ -naphthol solution were added to the test tube. Concentrated  $H_2SO_4$  (1 mL) was carefully poured into dropwise using a dropper on the inner wall of the test tube. A red ring colour appeared at the junction between the two layers.

#### Test for Reducing Sugars

Cow milk sample (5 drops) and 2 mL of Benedict's solution were added to the test tube. The mixture was boiled into water bath for 5 min. The formation of green precipitation within 3 min indicated the presence of reducing sugars.

### Isolation of Casein and Albumin from Fresh and Packed Cow Milk Sample

Milk (100 mL) was warmed to 40 °C in water bath. After warming, 10 % acetic acid was added in a drop wise manner to adjust the pH to the isoelectric point of casein. At isoelectric point casein precipitated out along with butter fat leaving a liquid component called whey. The milky whey liquid becomes clear when casein separates out completely. Casein was separated from the whey by straining the precipitate through four layers of cheese cloth. The precipitated casein was washed with 20 mL of 95 % ethanol with vigorous stirring for 5 min. The suspension was then filtered and washed with 20 mL of ethanol: ether (1:1) mixture. Finally the precipitate was washed with 30 mL of ether. After the final wash the precipitate was transferred into porcelain basin and dried at 40-50 °C in an oven. After drying, the weight of casein I and II were recorded as 9.11 % and 7.36 %. All the milk samples were similarly treated.

After the casein filtration, 2.2 g of powdered calcium carbonate was added to the filtrate and the solution was mixed thoroughly. The mixture was boiled for about 10 min and stirred continuously. (Pamarthy, Bhat and Sukumaran, 2016). And then, the mixture was filtered on a filter paper to obtain precipitated albumin. The albumin was dried and weighed. The yield of albumin I and II from different milk samples were recorded as 2.18 % and 0.21 %

## **Identification of Isolated Casein and Albumin**

The FT IR spectra of isolated two caseins (I and II) and two albumins (I and II) from fresh and packed milk were recorded on FT IR- 8400, SHIMADZU, Japan, at the Department of Chemistry, University of Yangon.

## **Characterization of Isolated Casein and Albumin**

### **Amino Acid Tests for Casein**

#### **Millon's test**

Casein (1 g) was placed in a test tube. Millon's reagent (5 drops) was added and the tube was immersed in a boiling water bath for 5 min. Yellow precipitate indicated the presence of tyrosine residue which occurred in nearly all proteins.

#### **Ninhydrin test**

Three drops of 1 % solution of ninhydrin reagent was added to 1 g of Casein. The solution was heated for 5 min in a boiling water bath. They gave characteristic deep blue colour. It indicated the presence of  $\alpha$ -amino acid and proteins containing free amino groups.

#### **Biuret test**

Casein (1 g) and 3 M NaOH (2 mL) were mixed thoroughly in a test tube. Then, 0.5 %  $\text{CuSO}_4 \cdot 5\text{H}_2\text{O}$  solution was added drop by drop to the above mixture. The result was obtained as blue colour.

#### **Xanthoproteic test**

Casein (1 g) was added to conc:  $\text{HNO}_3$  (1 mL) in a test tube. A white precipitate was formed and then heated in water bath. They turned yellow with tyrosine and orange with the essential amino acid "tryptophan" indicating a high nutritive value.

### **Protein Precipitation Tests for Albumin**

#### **Precipitation by Salt**

Albumin (3 mL) was taken into a test tube. Equal volume of ammonium sulphate was added to it. The mixture was allowed to stand for about 5 min and filtered by using filter paper. The filtrate (3 mL) was taken into another test tube and the same volume of NaOH was added to it, then  $\text{CuSO}_4$  solution was added drop by drop to the filtrate. The white precipitate was obtained.

#### **Precipitation by Organic Solvents**

Albumin (1 mL) was added to 4 mL of EtOH in test tube. The solutions were mixed well and were allowed to stand until the white precipitate was obtained.

#### **Precipitation by Acid Agents**

Albumin (1 mL) was added to an equal volume of picric acid solution. The yellow precipitate was observed.

#### **Precipitation by Heavy Metal Ions**

Albumin (1 mL) was added to 10 drops of lead acetate solution in test tube. The formation of white precipitate was noted.

### Precipitation by Heat and Acid

Albumin (10 mL) was taken into a test tube and then a few drops of 1 % acetic acid were added to it. Coagulation was taken place and albumin was precipitated (Essay UK, 2018; Chemistry. mcmaster, 2014).

## Results and Discussion

### Preliminary Milk Test

Fresh and packed cow milk samples were collected from Taunggyi area. The alcohol test and pH measurement of milk are important to determine milk quality. Alcohol tests of fresh and packed cow milk samples showed the good quality from the absence of coagulation, clotting or precipitation. The measurement of pH of milk is important in testing for impurities, spoilage, and signs of mastitis infection. Fresh and packed cow milk samples indicated the pH 6.8 and 6.6 which are within the normal range (6.8). Red ring and green precipitate indicate the presence of carbohydrates and trace of reducing sugars. These data are shown in Table 1 and Figure 1.

**Table 1** Milk Quality of Fresh and Packed Cow Milk Samples

Test	Chemical Reagent	Observation	Results	
			I	II
Alcohol test	65 % ethanol	no coagulation	good quality	good quality
pH	pH meter	6.8-6.6	6.8	6.6
Carbohydrates	10 % $\alpha$ -naphthol, conc. $H_2SO_4$	red ring	+	+
Reducing sugars	Benedict's solution	green ppt.	+	+

(+) = positive test, I = fresh cow milk, II = packed cow milk, (ppt.) = precipitate

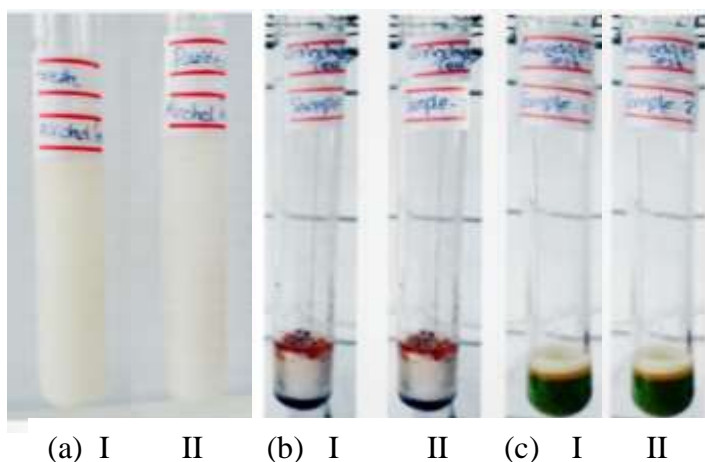


**Figure 1** Milk quality test of (a) alcohol (b) carbohydrates and (c) reducing sugars tests from fresh (I) and packed (II) cow milk samples

### Identification of Isolated Compounds

Caseins I and II (9.11 % and 7.36 %) and albumins I and II (2.18 % and 0.21 %) were obtained by precipitation with acid and  $CaCO_3$  (Figure 2). Yield percentage of casein I and albumin I of fresh cow milk are higher than casein II and albumin II of packed cow milk. Therefore, only

casein I and albumin I have been chosen for further study of mineral content by AAS and antioxidant activity by DPPH Assay.

The FTIR spectra of the isolated caseins I and II are very similar to the reported casein as described in Table 2 and Figure 3.

The bands around  $1600\text{ cm}^{-1}$  and  $1500\text{ cm}^{-1}$  assignable to amide I and II are prominent. The broad band about  $3500\text{-}2500\text{ cm}^{-1}$  shows O-H stretching band, the weak band around  $3100\text{ cm}^{-1}$  shows olefinic C-H stretching. Saturated  $sp^3$  C-H stretching bands also appear at just below  $3000\text{ cm}^{-1}$ . The comparison of the FT IR spectra of the isolated albumins I and II with the reported one for albumin in Figure 4 are not fitted as the case with the casein samples. Amide I and II bands appear to be very weak, so also is the band around  $3000\text{ cm}^{-1}$  for N-H and O-H stretching. The aliphatic  $sp^3$  C-H stretching bands below  $3000\text{ cm}^{-1}$  remains, but it appears to be very weak in albumin II.

In this experiment, chemical tests on isolated casein from both milk samples were done in order to determine the presence of specific amino acids in this type of protein. Millon's test is given by any compound containing phenolic hydroxy group. Consequently, any proteins containing tyrosine gives a positive test of a yellow precipitate. Ninhydrin test is used to detect the presence of  $\alpha$  - amino acid and proteins containing free amino groups. They gave characteristic deep blue colour. Biuret test is a chemical test used to determine the presence of peptide bond in a substance. A positive test indicated a deep blue colour due to copper ion complex with the amide group of the protein. Xanthoproteic test was used for the detection of aromatic amino acids. Appearance of yellow colour obtained was due to the nitration of aromatic ring as shown in Table 3 and Figure 5.

The results of precipitation tests such as salt test (white ppt.), organic solvent test (white ppt.), acidic agent test (yellow ppt.), heavy metal ion test (white ppt.) and heat and acid test (white ppt.) indicate the presence of protein in isolated albumin I and II as shown in Table 4 and Figure 6 (Essays UK, 2008).



**Figure 2** Isolation of casein I, II, albumin I and II from fresh and packed cow milk samples

**Table 2** Comparison of FT IR Spectra of Isolated Caseins I and II with Reported Casein\*

Wave number ( $\text{cm}^{-1}$ )			Assignment
Casein I	Casein II	Reported Casein*	
3279	3280	3500-2500	O-H and N-H stretching
2917, 2850	2919, 2851	2950- 2830	$\nu_{\text{as}}$ and $\nu_{\text{s}}$ C-H stretching of $\text{CH}_3$ , $\text{CH}_2$
1714	1742	1730	C=O stretching
1629, 1537	1639, 1533	1600-1500	amide I and amide II
1172, 1095	1172, 1094	1200-1000	C-O-C stretching
719	720	750	secondary amide N-H wagging

(\*Hewavitharana and Bram van Brakel, 1997)

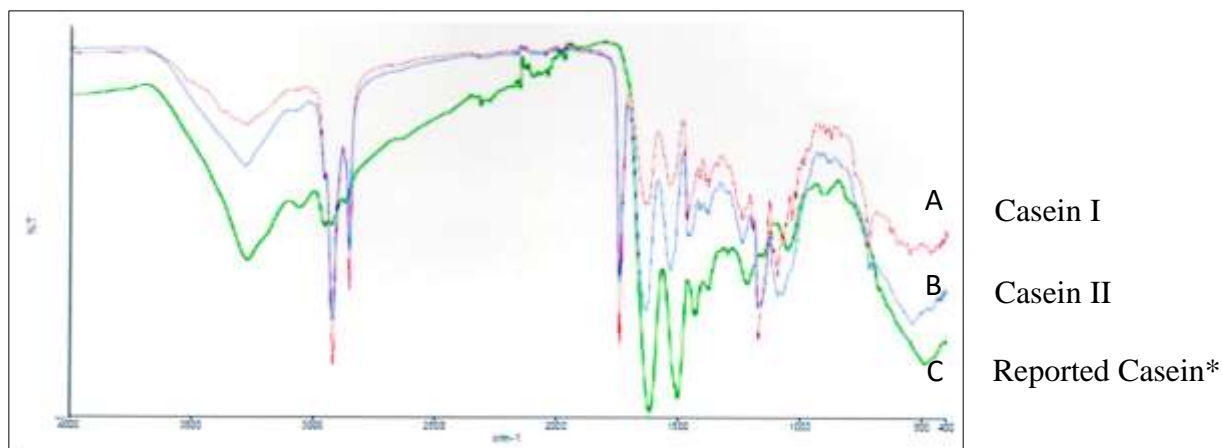


**Figure 3** Comparison of the FT IR spectra of the isolated casein I (A) and casein II (B) with that reported casein \*(C)

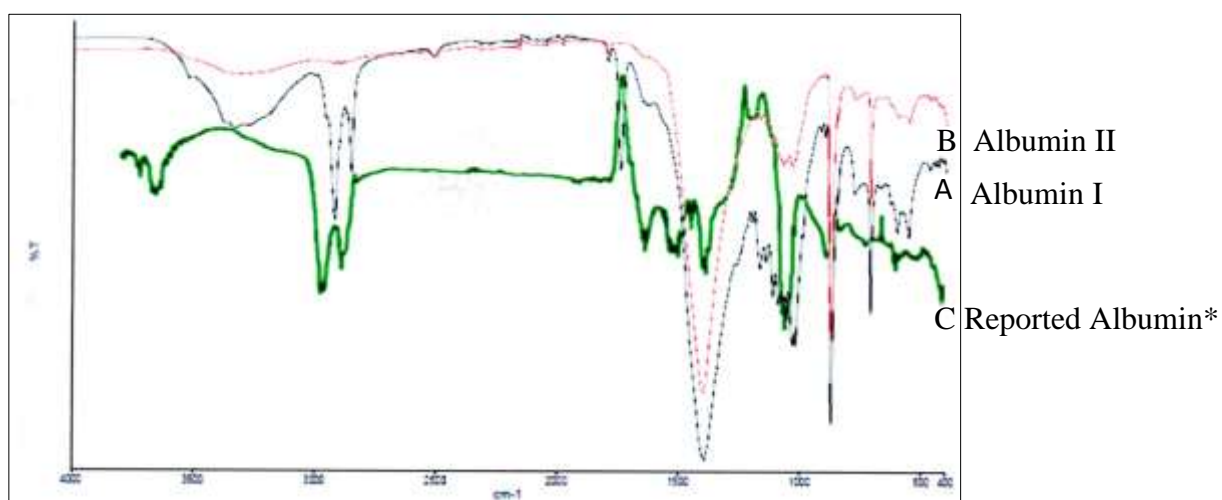


**Figure 4** Comparison of the FT IR spectra of the isolated albumin I (A) and albumin II (B) with that reported albumin \*(C)

**Table 3 Results of Some Chemical Tests for Isolated Caseins I and II**

Test	Chemical Reagent	Observation	Results	
			Casein I	Casein II
Millon's test	HgSO <sub>4</sub> , 15 % H <sub>2</sub> SO <sub>4</sub>	yellow ppt.	+	+
Ninhydrin test	Ninhydrin, ethanol, acetic acid	blue colour	+	+
Biuret test	3 M NaOH, 0.5 % CuSO <sub>4</sub> .5H <sub>2</sub> O	deep blue colour	+	+
Xanthoproteic test	Conc. HNO <sub>3</sub> , NH <sub>4</sub> OH	yellow colour	+	+

Millon    Ninhydrin    Biuret    Xanthoproteic    Millon    Ninhydrin    Biuret    Xanthoproteic

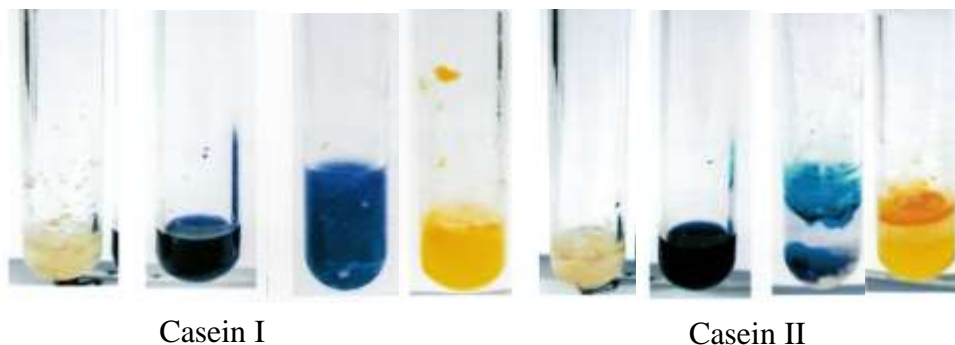


Figure 5 Some chemical tests of isolated caseins I and II

Table 4 Results of Some Chemical Tests of Isolated Albumins I and II

Test	Chemical Reagent	Observation	Results	
			Albumin I	Albumin II
Salt test	(NH <sub>4</sub> ) <sub>2</sub> SO <sub>4</sub> solution, NaOH, CuSO <sub>4</sub> .5H <sub>2</sub> O	white ppt.	+	+
Organic Solvent test	ethanol	white ppt.	+	+
Acidic Agent test	picric acid solution	yellow ppt.	+	+
Heavy Metal Ion test	1 % lead acetate	white ppt.	+	+
Heat and Acid test	1 % CH <sub>3</sub> COOH	white ppt.	+	+



Figure 6 Some chemical tests of isolated albumins I and II

**Some Heavy Metals Present in Isolated Casein I and Albumin I**

Atomic absorption spectroscopy (Perkin Elmer Analysis – 300 AAS, USA) was used for determination of some heavy metals present in the isolated casein I and albumin I. The isolated casein I and albumin I were found to contain, Fe (6.4616 and 6.5969 ppm), Mn (0.4721 and 0.5193 ppm), Zn (1.3661 and 0.8366 ppm) and Cu (0.3828 and 0.3723 ppm), respectively which indicate the presence of sufficient amounts of minerals. The results are shown in Table 4.

Table 4 Elemental Analysis of Isolated Casein I and Albumin I

Elements	Casein I (ppm)	Albumin I (ppm)
Fe	6.4616	6.5969
Mn	0.4721	0.5193
Zn	1.3661	0.8366
Cu	0.3828	0.3723

### Antioxidant Activity of Isolated Casein I and Albumin I

The value of percent inhibition in isolated casein I was very low and that in albumin I was not found. As a consequence, the isolated casein I gave low antioxidant activity and albumin I was no antioxidant activity (Table 5, Figure7).

**Table 5** *In Vitro* Antioxidant Activity of Casein I and Albumin I Against DPPH Radical Scavenging

Sample	Concentration ( $\mu\text{g/mL}$ )	% Inhibition	Method
Casein I	1000	$5.99 \pm 1.4$	DPPH Radical
Albumin I	1000	0	DPPH Radical
Ascorbic acid (standard)	500	$84.78 \pm 0.39$	DPPH Radical

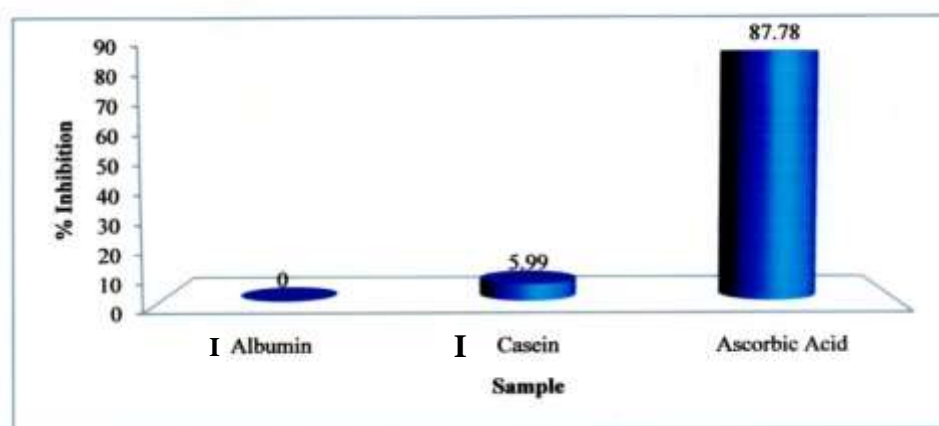


**Figure 7** Bar graph of isolated albumin I, casein I and standard ascorbic acid

### Conclusion

The alcohol test (no coagulation), pH (6.8- 6.5), carbohydrates test (red ring) and reducing sugars test (green precipitate) showed good quality for the fresh and packed cow milk samples. The yield of caseins I and II (9.11 % and 7.36 %) and albumins I and II (2.18 % and 0.21 %) by precipitation method indicated that the fresh cow milk was richer in these compounds than the packed milk. The FT IR spectral data showed that the isolated caseins I and II which were more agreeable with the reported spectra than those of the isolated albumins I and II. The isolated casein and albumin were also observed to give positive by amino acid test and protein precipitation tests. Furthermore, the isolated casein I and albumin I were also found to contain Fe (6.4616 and 6.5969 ppm), Zn (1.3661 and 0.8366 ppm), Mn (0.4721 and 0.5193 ppm), and Cu (0.3828 and 0.3723 ppm) by AAS. However, Albumin I exhibited no antioxidant property and casein I was very low antioxidant activity by DPPH method. Above all, it may be concluded that, fresh cow milk is a more nutritious food dairy product than packed cow milk.

### Acknowledgements

The author would like to thank the Myanmar Academy of Arts and Science for allowing to present this paper and Professor and Head Dr Ah Mar Yi and Professor Dr Kyae Mon Lwin, Department of Chemistry, Taunggyi University for their kind encouragement.

## References

- Ahluwalia, V. and Dhingra, S. (2005). *College Practical Chemistry*. Isolation of Casein (Accessed: 12 July, 2014)
- Chemistry. mcmaster. (2014). Chem 2006-1997/98- Experiment 11. <http://www.chemistry.mamaster.ca/chem206/lab manual/exp11/206exp11.html>. (Accessed: 15 July 2014)
- Essays, UK. (2018). Isolation of Casein from Milk and Powdered Milk. Retrieved from <https:// www.ukessays.com/essays/ biology/the-isolation-of-casein-from-milk> (Accessed: 26 April 2020)
- Hewavitharana, A. K. and Brakel, Bv. (1997). "Fourier Transform Infrared Spectrometric Method for the Rapid Determination of Casein in Raw Milk". *Analyst*, vol. 122, pp.701-704
- Miller, G., Jarvis, J. and Mc Bean, L. (2006). "Components of Milk". *Handbook of Dairy Foods and Nutrition*, National Dairy Council, Florida: 3<sup>rd</sup> Ed, CRC Press
- Pamarthy, J., Bhat,V. and Sukumaran, M.K. (2016). "A Comparative Study on Casein and Albumin Contents in Cow and Commercial Milk Samples". *Journal of Dental and Medical Sciences*, vol. 15(1), pp. 102-106
- SeyhanEge's Homepage (1997).Proteins and Carbohydrates.Isolation of Casein and Lactose from Milk. <http://www.chemistry.mcmaster.ca/chem206/labmanual/exp11/206 exp11.html> (Accessed: 14 July 2014)
- Spurlock, D. (2014). Isolation and Identification of Casein from Milk Course Notes <http://homepages.ius.edu/dspurloc/c122/casein.htm>. (Accessed: 14 July 2014)
- Tarte, R. (2009). Principle of Milk Protein: *Ingredients in Meat Products*. New York: Springer -Verlag pp 152-157

## PREPARATION OF BIOETHANOL FROM SORGHUM STARCH AND ITS CHARACTERIZATION

Mya Hnin Aye Khaing<sup>1</sup>, Thidar Win<sup>2</sup>, Ni Ni Sein<sup>3</sup>, Khin Moh Moh Hlaing<sup>4</sup>,  
Aung Kyaw Moe<sup>5</sup>, Ni Ni Aung<sup>6</sup>

### Abstract

Bioethanol was prepared from powder of sorghum (*Sorghum bicolor* L. Moench) grain by enzymatic hydrolysis.  $\alpha$ -Amylase from germinated wheat grains was used for liquefaction of starch and  $\alpha$ -glucosidase from ungerminated flint corn was used in saccharification step. After liquefaction and saccharification, the solution was tested for glucose by using Benedict solution and Fehling solution. During fermentation of liquid glucose by *Saccharomyces cerevisiae* yeast for 6 days, the changes of physicochemical properties such as pH (5.2 to 3.7), acid content (0.093 % to 0.423 %), glucose content (155 to 63 mg L<sup>-1</sup>) and specific gravity (0.994 to 0.975) during fermentation were determined. After distillation the yield percentage of alcohol in fermented solution is 10 % and the physicochemical properties such as specific gravity, refractive, colour, free acid, free base and alcohol content of the hydrated bioethanol and dehydrated bioethanol were comparatively studied with absolute ethanol. Moreover, the functional groups of bioethanol were analysed by FT IR spectroscopy.

**Keywords:** sorghum, bioethanol,  $\alpha$ -amylase,  $\alpha$ -glucosidase, *Saccharomyces cerevisiae*, glucose, physicochemical properties

### Introduction

Bioethanol is derived exclusively from the fermentation of plant starches such as sugar cane, grains, potato and corn and agricultural waste. Though ethanol can be extracted as a by-product from a chemical reaction with ethylene and other some products, these sources are not considered renewable. The interest for renewable biofuels has increased significant over the past few years. It is important to find an alternative to oil, due both to the limited supply and the effect from the greenhouse gases that are released from oil use. One possible biofuel is bioethanol. The world's leading manufacturers and industries are seeking to substitute petrochemical-based petroleum supplies continue to decline (Zhan *et al.*, 2003). Great attention has been given to ethanol production using various substrates which can be classified into three main types of materials, which are sugars from sugarcane, sugar beet, sweet sorghum, molasses and fruits), starches (from sweet sorghum grain, cassava, corn, potato and root crops) and cellulose materials (from agricultural residue, wood and paper mills) (Lin and Tanaka, 2006), because of the increase in demand for ethanol which is considered as an alternative biochemical source (Lynd *et al.*, 1991). Steps involved in enzymatic preparation of ethanol include starch liquefaction, starch saccharification, fermentation, distillation and dehydration. In liquefaction step, gelatinization is required to increase the rate of hydrolysis as the native starch is slowly degraded by  $\alpha$ -amylase (Nadir *et al.*, 2009). Liquefaction process is employed to loosen the structure of starch polymer and reduce the viscosity of the gelatinized starch and ease the next hydrolysis processing.  $\alpha$ -amylase is employed due to its active actions (1) degrade the long starch chains so that starch will not form a gel at lower temperature and, (2) produce more chain ends, as glucoamylase, the enzyme used in the saccharification step, will cleave glucose molecules only from the nonreducing ends of the chains. In liquefaction, pH is not allowed to drop below 4.5 otherwise the  $\alpha$ -amylase

---

<sup>1</sup> Dr, Lecturer, Department of Chemistry, Meiktila University

<sup>2</sup> Dr, Rector (Rtd), University of Mandalay

<sup>3</sup> Dr, Professor (Rtd), Department of Chemistry, University of Yangon

<sup>4</sup> Dr, Lecturer, Department of Chemistry, Meiktila University

<sup>5</sup> Lecturer, Department of Chemistry, Meiktila University

<sup>6</sup> Dr, Professor and Head, Department of Chemistry, Meiktila University

will be denatured (Nigam and Singh, 1995). Saccharification step is important to further hydrolyze the liquefied starch.  $\alpha$ -Glucosidase is used in the saccharification step. The glucosidase breaks the  $\alpha$ -(1,6) glycosidic bonds in the liquefied starch chains.



Fermentation step is to convert glucose to ethanol. *Saccharomyces cerevisiae* (yeast) is used for fermentation of sugar solution.



For the ethanol to be used as usable fuel, water must be removed. Most of the water is removed by distillation. The most widely used purification method is a physical absorption process using a molecular sieve. Another method, azeotropic distillation, is achieved by adding hydrocarbon benzene which also denatures ethanol. Last method involves use of calcium oxide as desiccant.

## Materials and Methods

### Sample Collection

Sorghum grains were collected from Meiktila Township, Mandalay Region. Wheat grains were collected from Butalin Township, Sagging Region, after harvesting crops. Flint corn was collected from Shan-Ywa Village, Kyaukse Township, Mandalay Region.

### Preparation of Bioethanol by Liquefaction and Saccharification

#### Substrate

Sorghum grains were blended into small size to enhance the hydrolysis process.

#### Enzymes

$\alpha$ -Amylase was extracted from germinated wheat grains and  $\alpha$ -glucosidase was extracted from ungerminated flint corn by ammonium sulphate precipitation method. The activities of  $\alpha$ -amylase and  $\alpha$ -glucosidase were determined by spectrophotometric method at 750 nm employing Nelson-Somogyi Method.

#### Yeast

*Saccharomyces cerevisiae* yeast was obtained from a local market in dry form. For inoculum, 100 mL of distilled water was heated to 40 °C. After that, 0.5 % (w/w) of *Saccharomyces cerevisiae* yeast was added into the warm water to activate the yeast. The mixture was left for 5-10 min at 150 rpm.

### Liquefaction and saccharification of sorghum starch

Sorghum (200 g) was added to a 1 L beaker and 900 mL of distilled water was then added into it. The mixture was heated while stirring for 1 h and then cooled down to 55 °C. After that 100 mL of 1 % (w/v)  $\alpha$ -amylase solution was added and stirred for 1 h. After 1 h liquefaction, the solution was cooled down to 50 °C and the pH of the solution was adjusted to 5 with hydrochloric acid. Next, 100 mL of 1 % (w/v)  $\alpha$ -glucosidase solution was added and the mixture was left for 2 h. After 2 h saccharification, the solution was filtered into a glass bottle with a thin layer cotton cloth. After liquefaction and saccharification, the solution was tested for glucose by using Benedict solution and Fehling solution.

## **Fermentation**

Into the liquid glucose solution 0.5 % (w/w) of urea and 0.05 % (w/w) potassium dihydrogen phosphate were added. After 10 min, the activated yeast solution was added. The mixture was mixed thoroughly to disperse uniformly. The bottle was loosely closed and fermented for 6 days at room temperature. After 6<sup>th</sup> day, the fermented solution was filtered into a glass bottle with a thin layer cotton cloth. The physicochemical properties such as pH, specific gravity, refractive index, colour, free acid content, free base content of the fermented solution were investigated during fermentation.

## **Distillation**

The fermented solution was filtered with a thin layer cotton cloth and then put into a 1L round-bottomed flask. During distillation the distillate at 78°C was collected as bioethanol in a receiver. The yield percentage of alcohol is 10% obtained from fermented solution.

## **Dehydration of bioethanol**

Bioethanol (100 mL) was put into a 1L beaker and then calcium oxide (15 g) was added into it. After constant stirring for 2 h, the mixture was transferred to a 1 L round-bottomed flask and heated. At 78 °C, dehydrated bioethanol was liberated and collected in a receiver.

## **Characterization of Prepared Bioethanol**

### **Qualitative test**

Ethanol obtained after distillation was tested by using Lucas test and iodoform test.

### **Determination of the physicochemical properties of hydrated Bioethanol, dehydrated bioethanol and absolute ethanol**

Specific gravity was determined by using a density bottle and refractive index was determined by a refractometer. Colour of bioethanol was determined by using Lovibond Tintometer. Free acid (as acetic acid) and free base (as ammonia) were determined by titrimetric method.

### **FT IR analysis of prepared bioethanol**

Attenuated total reflection Fourier transform infrared (ATR-FT IR) spectra of the prepared bioethanol (both hydrated and dehydrated) were recorded on a Perkin Elmer FT IR spectrometer in a range of wave number from 4000 to 550 cm<sup>-1</sup>. For comparison purpose the spectrum of absolute ethanol from Pure Chemical Industries, was also recorded.

## **Results and Discussion**

### **Calculation of Enzyme Activities**

$\alpha$ -Amylase was extracted from 5<sup>th</sup> day germinated wheat grains by ammonium sulphate precipitation method. Sorghum starch was degraded into maltose by  $\alpha$ -amylase. The amount of maltose liberated was determined by Nelson Somogyi method at 750 nm (Hatanaka and Kobara, 1980). The activity was calculated as the following:

$$\text{Activity} = \frac{\text{amount of maltose liberated}}{\text{volume of enzyme} \times \text{time}}$$

Moreover,  $\alpha$ -glucosidase was extracted from flint corn by ammonium sulphate precipitation method.  $\alpha$ -Glucosidase degraded maltose into glucose and the amount of glucose liberated was determined by Nelson-Somogyi method at 750 nm. The activities of  $\alpha$ -amylase and  $\alpha$ -glucosidase are shown in Table 1.

$$\text{Activity} = \frac{\text{amount of glucose liberated}}{\text{volume of enzyme} \times \text{time}}$$

**Table 1** Activities of  $\alpha$ -Amylase and  $\alpha$ -Glucosidase

No	Enzyme	Activity ( $\mu\text{mol mL}^{-1} \text{min}^{-1}$ )
1	$\alpha$ -Amylase	9.0
2	$\alpha$ -Glucosidase	54.03

### Liquefaction and Saccharification of Sorghum Starch Powder

In the liquefaction step, hydrolysis of starch was carried out by  $\alpha$ -amylase enzyme at 55 °C for 1 h. This condition was chosen because plant amylases were found to have optimum temperature of 55 °C (Nerkar, *et al.*, 2011). In the saccharification step  $\alpha$ -glucosidase breaks down starch to glucose. Saccharification temperature was chosen as 50 °C at pH 5 because the optimum temperature of sweet corn was reported to be 50 °C and the maximal activity was found in the range of pH 4.6 to 5 (Chaw Ei Phyu, 2010). The reported maximum saccharification was occurred at 45 °C (Aggarwal *et al.*, 2001). The glucose produced in the liquefaction and saccharification steps were confirmed by the Benedict test and Fehling test. Brick red precipitates were observed in these tests (Figure 1).

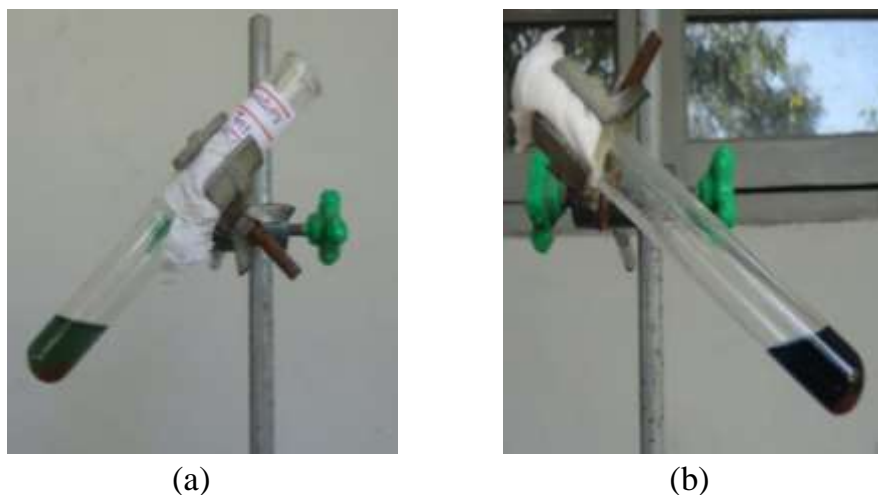


**Figure 1** Tests for glucose (a) Benedict (b) Fehling

### Fermentation of liquid glucose solution

In this step activated *Saccharomyces cerevisiae* was added to ferment the liquid glucose solution. After fermentation for 6 days the physicochemical properties of the fermented solution were determined. The results are shown in Table 2.

**Table 2 Physicochemical Properties of Fermented Solution During Fermentation**

No.	Parameters determined	Fermentation Time					
		1 <sup>st</sup> day	2 <sup>nd</sup> day	3 <sup>rd</sup> day	4 <sup>th</sup> day	5 <sup>th</sup> day	6 <sup>th</sup> day
1	pH	5.2	5.1	4.5	3.9	3.8	3.7
2	Specific gravity	0.994	0.990	0.986	0.980	0.978	0.975
3	Acid content (%)	0.093	0.177	0.252	0.327	0.399	0.423
4	Glucose (mg L <sup>-1</sup> )	155	140	130	125	112	63

### Distillation of Fermented Solution

After fermentation for 6 days, the fermented solution was distilled and the distillate was collected at 78 °C. The alcohol content of the hydrated bioethanol was 20 %. In the distillation process, the alcohol content was increased up to 95 % by repeat distillation (Table 3).

### Dehydration of Bioethanol

Since prepared bioethanol contained 5 % water, dehydration was carried out by using calcium oxide as desiccant. After dehydration the alcohol content increased up to 98 % (Table 3).

### Qualitative Tests for Bioethanol

Bioethanol was qualitatively examined by Lucas test and iodoform test. No oily layer was obtained when treated bioethanol with anhydrous zinc chloride and hydrochloric acid. When ethanol was treated with chloroform, iodine and sodium hydroxide in water bath, yellow precipitate of iodoform were obtained (Figure 2).

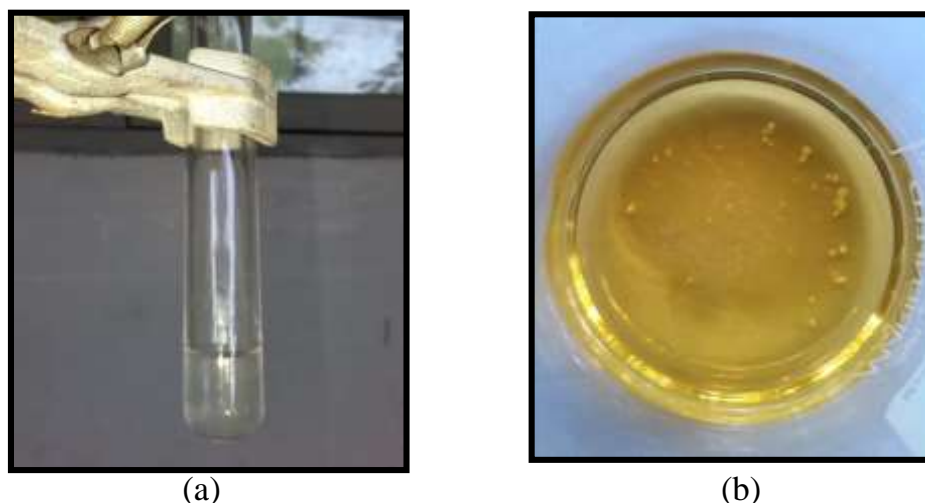


**Figure 2** Qualitative test for bioethanol (a) Lucas test (b) iodoform test

### Comparison of Some Physicochemical Properties of Hydrated, Dehydrated and Absolute Ethanol from Pure Chemical Industries

Physicochemical properties of hydrated, dehydrated and absolute ethanol from Pure Chemical Industries, were compared and the results are shown in (Table 3). The specific gravity of distilled water is, by definition, equal to one. Pure ethanol has a specific gravity of 0.79. Therefore, it follows that a mixture of water and ethanol must have a specific gravity that is less than one, the more alcohol the lower the specific gravity. Specific gravity of the fermented solution was found to be 0.994 after fermentation for 6 days. After distillation the specific gravity decreased

to 0.803 indicating that the increase in ethanol content. It means that yield of ethanol content after 6 days fermentation increased from 20 % to 95 % after distillation. After dehydration the ethanol content increased to 98 %. The specific gravity of absolute ethanol from Pure Chemical Industries was found to be 0.793 and ethanol content was 99 %. Refractive index is the ratio of velocity of light in air to that in the substance. Refractive index of the hydrated bioethanol was 1.382 while that of dehydrated one was 1.37. These values are slightly higher than that of absolute ethanol. Refractive index has been found to provide a reliable indication of the dry weight of the solids in the solution. All the colours of the hydrated and dehydrated bioethanol were colourless by measuring Lovibond tintometer as the absolute ethanol. Free acids and free base percentages were determined by titrimetric method. Free acid as acetic acid contents were found to be nearly the same, i.e., 0.006 % and 0.007 %. Free base as ammonia contents in hydrated ethanol (0.006 %) was higher than those of dehydrated ethanol (0.003 %) and absolute ethanol (0.0025 %).

**Table 3 Comparison of the Physicochemical Properties of Hydrated, Dehydrated and Absolute Ethanol**

No	Parameters	Hydrated bioethanol	Dehydrated bioethanol	Absolute ethanol
1	Specific gravity	0.803	0.801	0.793
2	Refractive index	1.382	1.371	1.361
3	Colour	colourless	colourless	colourless
4	Free acid (acetic acid) (%)	0.007	0.006	0.006
5	Free base (as ammonia) (%)	0.006	0.003	0.0025
6	Alcohol content (%)	95	98	99

### FT IR Spectral Data of Dehydrated Bioethanol, Hydrated Bioethanol and Absolute Ethanol

FT IR spectra of dehydrated bioethanol, hydrated bioethanol and absolute ethanol from Pure Chemical Industries were shown in (Figure 3) and the spectral data are shown in Table 4. All the spectra show –OH stretching vibration at between 3500-3300  $\text{cm}^{-1}$ . However, the intensity of –OH stretching peak for hydrated ethanol was found to be higher than those of dehydrated and absolute ethanol. It is due to the coalescent peak which is caused by the –OH peak from water and that from ethanol. All spectra show that the –CH stretching peaks were between 2983-2973  $\text{cm}^{-1}$ . The –OH bending and –CH bending vibrations were observed at  $\sim 1650 \text{ cm}^{-1}$  and  $1455 \text{ cm}^{-1}$  respectively. The C-C-O stretching vibrations were observed at  $\sim 1275$  and  $1087 \text{ cm}^{-1}$ . Among the spectra the spectrum of dehydrated bioethanol was similar to that of absolute ethanol.

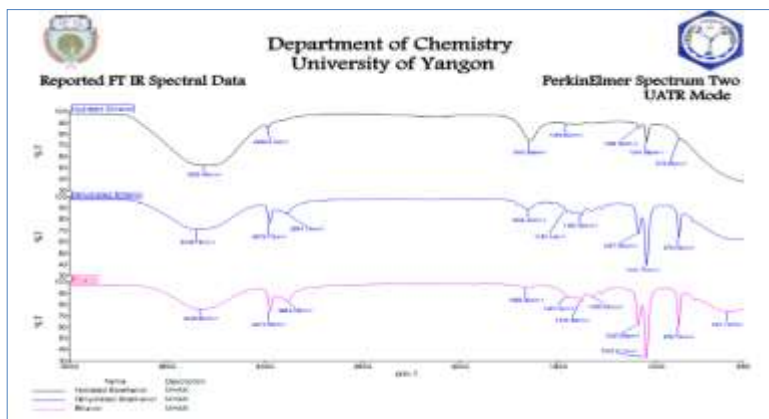


**Figure 3** FT IR spectra of dehydrated bioethanol, hydrated bioethanol and absolute ethanol from Pure Chemical Industries

**Table 4 FT IR Spectral Data for Dehydrated Bioethanol, Hydrated Bioethanol and Absolute Ethanol**

Sr No	Wave number (cm <sup>-1</sup> )			Remark
	Hydrated bioethanol	Dehydrated bioethanol	Absolute ethanol	
1	3306	3339	3325	O-H stretching
2	2983	2975, 2894	2973, 2883	C-H stretching of CH <sub>3</sub> and CH <sub>2</sub>
3	1455	1455	1455	-OH bending
4	1272	1275	1275	C-C-O bending
5	1085	1087	1087	C-O stretching

### Conclusion

Enzymatic hydrolysis of sorghum starch was carried out to prepare bioethanol in this study.  $\alpha$ -Amylase was extracted from germinated wheat grain having the activity of 9.0  $\mu\text{mol mL}^{-1} \text{min}^{-1}$  and  $\alpha$ -glucosidase was extracted from ungerminated flint corn having activity of 54.03  $\mu\text{mol mL}^{-1} \text{min}^{-1}$  were used for liquefaction and saccharification of sorghum starch. *Saccharomyces cerevisiae* yeast was used for the fermentation of glucose solution. After saccharification the obtained glucose solution was confirmed by using Benedict solution and Fehling solution which gave red precipitate. After fermentation the pH of the fermented solution was 3.7 and specific gravity was 0.975. Distillation of the fermented solution at 78°C gave hydrated bioethanol which contain the alcohol content (95%). After dehydration with calcium oxide the alcohol content increase to 98 % in dehydrated ethanol. The physicochemical properties of the hydrated bioethanol were specific gravity (0.803), refractive index (1.382), colour (colourless), free acid as acetic acid (0.007 %), free base as ammonia (0.006 %) and alcohol content (95 %). After dehydration, the physicochemical properties of dehydrated bioethanol were specific gravity (0.801), refractive index (1.371), colour (colourless), free acid as acetic acid (0.006 %), free base as ammonia (0.003 %) and alcohol content (98 %). FT IR spectra of dehydrated bioethanol, hydrated bioethanol and absolute ethanol from Pure Chemical Industries were comparatively studied. In hydrated bioethanol, the intensity of OH- stretching peak was found to be higher than those of dehydrated and absolute ethanol. This peak is a coalescent peak which is caused by OH- group from water and that from ethanol. All spectral data show the characteristic peaks of ethanol. Thus, the spectrum of dehydrated bioethanol was similar to that of absolute bioethanol.

### Acknowledgements

We would like to thank to the Department of Higher Education, Ministry of Education in Myanmar, for giving the opportunity to do this research. Our deepest gratitude is expressed to Dr Ba Han, Rector, Meiktila University, for his encouragement and kind help to do this research. Thanks, are also extended to all teachers Department of Chemistry, Meiktila University, for their helpful advice.

## References

- Aggarwal, N. K., Nigam, P., Singh, D. and Yadav, B. S. (2001). "Process Optimization for the Production of Sugar for the Bio-ethanol Industry from Sorghum, A Non-Conventional Source of Starch", *World Journal of Microbiology and Biotechnology*, vol. 17, pp 411-415
- Chaw Ei Phyu, (2010). "*Enzymatic Preparation of Bioethanol from Sweet Corn*", PhD Dissertation, Department of Chemistry, University of Yangon, Myanmar
- Hatanaka, C. and Kobara, Y. (1980), "Determination of Glucose by a Modification of Somogyi-Nelson Method", *Faculty of Applied Biological Science*, Department of Applied Biochemistry, Hiroshima University, vol. 44(12), pp 2943-2949
- Lin, Y. and Tanaka, S. (2006). "Ethanol Fermentation from Biomass Resources: Current State and Prospect", *Applied Microbiology and Biotechnology*, vol. 69, pp 627-642
- Lynd, L. R., Cushman, J. H., Nichols, R. J. and Wyman, C. E. (1991). "Fuel Ethanol from Cellulosic Biomass", *Science*, vol. 251, pp 1318-1323
- Nadir, N., Mel, M., Karim, M. I. A. and Yunus, R. M. (2009). "Process Improvement of Pharmaceutical Grade Ethanol Production using Sorghum", *Int.J.Sci.Eng., Tech.*, vol. 2(1), pp 55-60
- Nerkar, G. S., Chaudhari, Y. A., and Khutle, N. M. (2011). "Extraction and Characterization of Alpha Amylase from *Phaseolus aconitifolius*", *Current Pharma Research*, vol. 1(2), pp 115-122
- Nigam, P., and Singh, D. (1995). "Enzyme and Microbial Systems Involved in Starch Processing", *Enzyme Microb. Technol.* vol. 17, pp 770-778
- Zhan, X., Wang, D., Tuinstra, M. R., Bcan, S., Scib, P. A., and Sun, X. S. (2003). "Ethanol and Lactic Acid Production as Affected by Sorghum Genotype and Location", *Industrial Crops and Products*, vol. 18, pp 245-255

## STUDY ON RADON EXPLORATION IN THE BUILDING MATERIALS BY USING LR-115 DETECTOR

Win Ko<sup>1</sup>, Toe Toe Lwin<sup>2</sup>, Hnin Hnin Than<sup>3</sup>

### Abstract

Radon is an alpha emitting radioactive gas. It can exist in ground water, soil, building materials mines, caves and other underground places. In this study, radon concentration in old buildings and new buildings was measured by using LR-115 type II detector in a can mode. The preliminary study, the LR-115 detector was treated with alpha emitter Am-241 for standard. The tracks formed in LR-115 were etched with 2.5 M NaOH at 60 °C for 90 min. The etched tracks in irradiated LR-115 detector were found to be spherical shape by using optical microscope. And then, radon level in old buildings and new buildings was measured by LR-115 detector using the same procedure. The observed shape of track agrees with the preliminary study and it indicates that this is due to interaction between detector and alpha particles via radon present in old and new buildings. The average track density was found to be 133.5484 and 312.3674 track/cm<sup>2</sup>d in all detectors in Bagaya Monastery and Me Nu Oak Kyaung. According to the observed track density, the average radon activity was found to be 667.7418 and 1561.8369 Bq/m<sup>3</sup> in all detectors in Bagaya Monastery and Me Nu Oak Kyaung. The calculated radon exhalation rate mean values were 1.0755 and 2.5155 mBq/m<sup>2</sup>h in Bagaya Monastery and Me Nu Oak Kyaung. The average radon concentration was found to be 10.7548 and 25.1553 Bq/m<sup>3</sup> in Bagaya Monastery and Me Nu Oak Kyaung. The average track density was found to be 39.0459 and 84.8824 track/cm<sup>2</sup>d in all detectors in new buildings at Sagaing and Monywa. According to the observed track density, the average radon activity was found to be 185.9329 and 404.2021 Bq/m<sup>3</sup> in all detectors in new buildings at Sagaing and Monywa. The calculated radon exhalation rate mean values were 0.3095 and 0.6728 mBq/m<sup>2</sup>h in new buildings at Sagaing and Monywa. The average radon concentration was found to be 3.0949 and 6.7279 Bq/m<sup>3</sup> in new buildings at Sagaing and Monywa.

**Keywords:** LR-115, alpha, track density, exhalation rate, radon, Bagaya Monastery, Me Nu Oak Kyaung

### Introduction

Radon is a radioactive gas that has no colour, smell or taste. It is produced in the ground from uranium and diffuses into the atmosphere. It can also be found in groundwater supplies and can be released into the indoor air when taps and showers are turned on. For most people, radon is the largest source of radiation exposure throughout their lifetime. Radon is the second most important cause of lung cancer after smoking and the leading cause of cancer among non-smokers. The IAEA has published a safety guide (on Protection of the Public against Exposure Indoors due to Radon and Other Natural Sources of Radiation) to assist national authorities in reducing exposure to radon. This safety guide also includes guidance on how to prepare a radon action plan.

Solid State Nuclear Track Detectors (SSNTDs) in track etch technique has been used in the present study due to their simplicity, low cost, non-destructive, small size, and having integrating capability for large scale studies for the measurement of radon activity, and radon exhalation rates studies in various samples. The SSNTDs can also be used in radiobiological studies as the biological effectiveness of densely ionizing radiation. It is great interest for estimating the radiation risk for the public resulting from exposure to radon and its daughters (Dorschel *et al.*, 2003).

---

<sup>1</sup> 3PhD Candidate, Lecturer, Department of Chemistry, Monywa University

<sup>2</sup> Dr, Associate Professor, Department of Chemistry, West Yangon University

<sup>3</sup> Dr, Professor and Head, Department of Chemistry, Maubin University

### Applications of SSNTDs related to radon measurements:

1. Radon measurements in tap water, natural water and soil: This kind of measurements is useful in uranium and thorium prospecting. It is also important to identify the radon rich areas. Knowledge of the radon levels in soil is important for classifying different areas for construction purposes and for planning of new buildings.
2. Radon emanation and exhalation from soil and building materials: It is useful to characterize building materials and soils as radon sources.
3. Radon monitoring in mines and other underground places: This is an important issue for radiological protection of miners, as well as in epidemiological studies involving miners.
4. Separation of thoron from radon: This is usually achieved based on the distance, because thoron is relatively very short-lived and cannot diffuse too far from the place of origin.
5. Application in earth sciences and radon measurements in caves.
6. Earthquake predictions: Radon concentrations in underground water and deep wells have been observed to increase significantly before earthquake (Ng *et al.*, 2004).
7. Volcanic studies: The radon flux increases before volcanic eruption

Pristine LR-115 (cellulose nitrate, type II, strippable, procured from DOSIRAD, France) is alpha sensitive plastic track detector. It is a 12 $\mu\text{m}$  thick film of red dyed cellulose nitrate emulsion coated on inert polyester base of 100 $\mu\text{m}$  thickness as shown in Figure 1. It has maximum sensitivity for alpha particles, fission fragments and ionizing particles with high enough linear energy transfer (LET). It is widely used for detection and measurement of weak concentrations of ionizing particles, high-resolution neutron radiographic uses, alpha radiography, cosmic ray investigations etc. The passage of ionizing radiation through insulating solids creates narrow trails of intense damage on atomic scale. These trails are called 'Tracks' which can be made visible under an ordinary optical microscope on being treated with a suitable chemical etchant that preferentially attacks the damaged material and removes the surrounding but undamaged portion at a slow speed (Siems, 2001).

The tracks recorded by these films are not directly visible and must therefore be intensified by treatment in an alkaline solution. The etched tracks get enlarged and represent the sites of original damaged regions. The track etching mechanism of LR-115 has been studied at different temperatures ranging from 30 $^{\circ}\text{C}$  to 60 $^{\circ}\text{C}$  for different etching times. The recommended etch conditions given by the manufacturer are 10% NaOH, at 60  $^{\circ}\text{C}$ , 65 to 95min (without agitation) (Singh *et al.*, 1989).

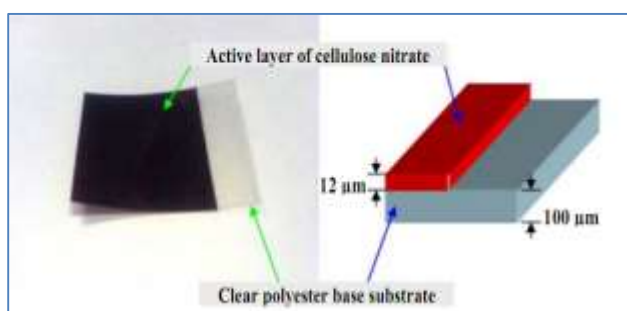


**Figure 1** Photo of LR-115 detector



**Figure 2** Interaction of LR-115 detectors with standard Am-241 source

## Materials and Methods

This section mainly consists of two parts. The first part is concerned with the interaction of LR-115 detector with standard alpha radiations. The second part is concerned with investigation of radon level from old buildings and new buildings by applying LR-115.

### Treatment of LR-115 Detector with Standard Am-241

LR-115 detectors were cut into small pieces of 1 cm × 1 cm. The samples were irradiated with alpha from Am-241 source with 12  $\mu\text{Ci}$  at 0.5 cm distance from source target for 15 min at Nuclear Physics Laboratory, University of Yangon (Figure 2). The LR-115 was removed from the alpha source and etched chemically in 2.5M NaOH solution at 60 °C for 90 min in an oven. The etched tracks on the detectors were scanned, using an optical microscope at 400x magnification.

### Treatment of LR-115 Detector with Alpha Particles from Radon in Old Buildings

The measurement of radon concentration in the Bagaya Monastery built in 1782 and the Me Nu Oak Kyaung built in 1822, Innwa district of Mandalay Region was done by using LR-115 type II detector (Figure 3 and 4). Each five detectors (1m×1cm) were placed under the bridge ladder of the Bagaya Monastery and basement of the Me Nu Oak Kyaung by using “Can” mode for recording the alpha particles emitted by radon-222 gas present in ambient air and also its short-lived daughters typically  $^{218}\text{Po}$  and  $^{214}\text{Po}$  which generally attached themselves to the aerosols. After the exposure period of three months (90 days), the detectors were etched for 90 min in 2.5M NaOH solution maintained at 60 °C in an oven. At the end of etching, the detectors were removed, washed with distilled water. After drying the detectors are ready to count under an optical microscope for track density measurements. The measured track density was converted in to  $\text{Bq/m}^3$  by using a calibration factor ( $0.2 \text{ tracks/cm}^2\text{d} = \text{Bq/m}^3$ ) determined by the National Institute of Radiological Science (NIRS), Vietnam (Nguyen Thi Thu Ha *et al.*, 2016).



**Figure 3** Detection of alpha particles from radon in Bagaya Monastery (1782)



**Figure 4** Detection of alpha particles from radon in Me Nu Oak Kyaung (1822)

### Treatment of LR-115 Detector with Alpha Particles from Radon in New Buildings

The measurement of radon concentration in two new buildings at Sagaing and Monywa, (built in 2017) was studied by using LR-115 type II detectors (Figure 5). Each five detectors (1m×1cm) were placed at the bathroom having only one small ventilation in the new building at Monywa and first floor in another new building at Sagaing by using ‘Can’ mode for recording the alpha particles emitted by radon-222 gas present in ambient air and also its short lived daughters typically  $^{218}\text{Po}$  and  $^{214}\text{Po}$  which generally attach themselves to the aerosols. After the exposure period of three months (90 days), the detectors were etched for 90 min in 2.5 M NaOH solution

maintained at 60 °C in an oven. At the end of etching, the detectors are removed, washed in distilled water. After drying the detectors are ready to count under an optical microscope for track density measurements (Figures 6 and 7). The measured track density was converted in to Bq/m<sup>3</sup> by using a calibration factor (0.2 tracks/cm<sup>2</sup>d = Bq/m<sup>3</sup>) determined by the National Institute of Radiological Science (NIRS), Vietnam (Nguyen Thi Thu Ha *et al.*, 2016).

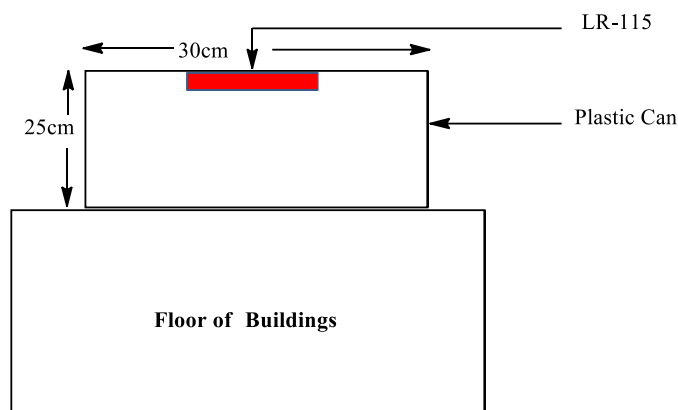


**Figure 5** Flow diagram for placing 'Can' mode detector



**Figure 6** Chemical etching of the detectors in an oven



**Figure 7** Microscope with digital camera (OLYMPUS BX-51)

### Radon Exhalation Rate ( $E_x$ )

The radon exposure inside the can was obtained from the track density of the detector by using calibration factor of 0.21 tracks/cm<sup>2</sup>d obtained from an earlier calibration experiment.

The exhalation rate is found from the expression (Eappen and Mayya, 2004).

$$E_x = \frac{CV\lambda}{A[t + \frac{1}{\lambda}(e^{-\lambda t} - 1)]}$$

Where,

- $E_x$  = radon exhalation rate (Bq/m<sup>2</sup>h)
- $C$  = radon activity as measured by LR-115 (Bq/m<sup>3</sup>)
- $t$  = exposure time (h)
- $V$  = volume of Can (m<sup>3</sup>)
- $A$  = area or sample surface (m<sup>2</sup>)
- $\lambda$  = decay constant for radon ( $7.56 \times 10^{-3} \text{ h}^{-1}$ ) (Sharma *et. al.*, 2014)

**Radon Concentration (C<sub>Rn</sub>)**

The risk of lung cancer from domestic exposure of <sup>222</sup>Rn and its daughters can be estimated directly from the inhalation exposure (radon) effective dose. The contribution of radon concentration from the samples can be calculated from the expression.

$$C_{Rn} = \frac{E_x \times A}{V \times \lambda_v}$$

Where,

- C<sub>Rn</sub> = radon concentration (Bq/m<sup>3</sup>)
- E<sub>x</sub> = radon exhalation rate (Bq/m<sup>2</sup>h)
- A = radon exhalation area (m<sup>2</sup>)
- V = volume (m<sup>3</sup>)
- λ<sub>v</sub> = air exchange rate (h<sup>-1</sup>) = 0.5 h<sup>-1</sup> (Saad *et al.*, 2010)

**Results and Discussion**

**Observation of Alpha Particles Emitting from Am-241 Source**

The characterization of nuclear tracks by alpha irradiation was found to be the formation of spots and the whole tracks on LR-115. It can be clearly seen in Figure 8. These formations of tracks agreed well with the literature (Dolleiser and Hashemi-Nezhad, 2002).



**Figure 8** Photomicrographs for the revelation of the alpha particle tracks in LR-115 detector for Am-241 source

**Observation of Radon via Alpha Particles Emitting from Old Buildings**

For this purpose, five pieces of LR-115 type II detectors (1cm×1cm) were used for detection of radon in the Bagaya Monastery which was built in 1782 and the Me Nu Oak Kyaung which was built in 1822 at Innwa (Figure 9 and 10).

Each LR-115 type II detector was fixed at the top of inside each ‘can’. And then, each ‘can’ was placed under the bridge ladder of the Bagaya Monastery and the basement of the Me Nu Oak Kyaung according to facing the detector and α-emitted via from radon in building materials. After the exposure period of three months, they were etched in 10% NaOH at 60 °C for 90 min. The resultant photomicrographs are shown in Figures 9 and 10 respectively. The radon activity, radon exhalation rate and radon concentration are computed as shown in Section. These values are presented in Tables 1 and 2.

From Table 1, the track densities in all detectors were found to be ranged between 124.4942 and 141.4707 track/cm<sup>2</sup> placed under the bridge ladder of the Bagaya Monastery. The average value of track density in ambient air was found to be 133.5484 track/cm<sup>2</sup>. According to the observed track density in all five detectors, the radon activity was found to be between 622.4712

and 707.3536 Bq/m<sup>3</sup>. The average value was 667.7419 Bq/m<sup>3</sup>. The calculated radon exhalation rate values in five detectors were between 1.0026 and 1.1393 mBq/m<sup>2</sup>h and the average value was 1.0755 mBq/m<sup>2</sup>h. Therefore, the radon concentration placed under the bridge ladder of this old monastery was found to be 10.7548 Bq/m<sup>3</sup>.

From the Table 2, the track density in all detectors was found to be between 305.5768 and 328.2121 track/cm<sup>2</sup> at the basement of Me Nu Oak Kyaung. The average value was found to be 312.3674 track/cm<sup>2</sup>. According to the observed track density in all five detectors, the radon activity was found to be between 1527.8839 and 1641.0605 Bq/m<sup>3</sup>. The average value was 1561.8369 Bq/m<sup>3</sup>. The calculated radon exhalation rate values were between 2.4608 and 2.6431 mBq/m<sup>2</sup>h and the mean value was 2.5155 mBq/m<sup>2</sup>h. Therefore, the radon concentration at basement of this old building was found to be 25.1553 Bq/m<sup>3</sup>.

It was observed that the radon concentration (25.1553 Bq/m<sup>3</sup>) at the basement of Me Nu Oak Kyaung was higher than that (10.7548 Bq/m<sup>3</sup>) placed under the bridge ladder of the Bagaya Monastery at Innwa. This may be due to the brick temple of the Me Nu Oak Kyaung. According to the literature, the principle routes of entry of radon into buildings pass through cracks in walls and foundations and gaps where service enter the building (for example, around waste/plumbing and electrical ducts). Other sources of radon in homes are: the building materials, including concrete, bricks, natural building stones, natural gypsum, and materials using industrial by-products such as phosphogypsum, blast furnace slag, and coal fly ash (Kovács *et al.*, 2017) and domestic and drinking water supply to the home. Therefore, radon could be more produced in the concrete and bricks at the Me Nu Oak Kyaung than wooden built in Bagaya Monastery.

Outdoor, radon is rarely a problem as it quickly dilutes to very low concentrations. Indoors, radon can build up to very high level. Therefore, decreases in radon concentrations are observed when windows and doors are opened, showing the importance of ventilation (Khan *et al.*, 2012).



**Figure 9** Photomicrographs for the revelation of the alpha particle tracks in LR-115 detector placed at the Bagaya Monastery

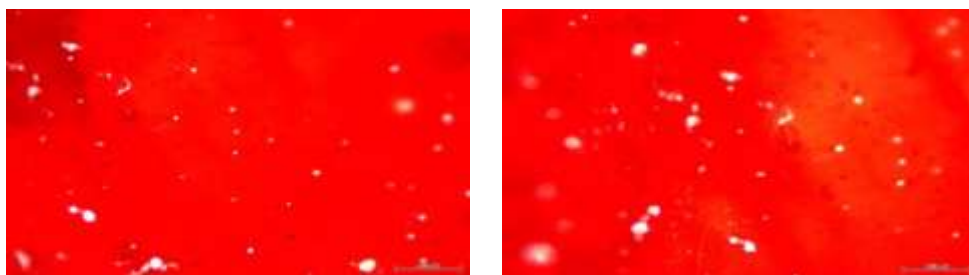


**Figure 10** Photomicrographs for the revelation of the alpha particle tracks in LR-115 detector placed at the Me Nu Oak Kyaung

**Table 1 Measurement of Track Density, Radon Activity, Radon Exhalation Rate and Radon Concentration at the Bagaya Monastery (1782)**

Detectors	Track Density (tracks/cm <sup>2</sup> d)	Radon Activity (Bq/m <sup>3</sup> )	Radon Exhalation Rate (mBq/m <sup>2</sup> h)	Radon Concentration (Bq/m <sup>3</sup> )
1	124.4942	622.4712	1.0481	10.4814
2	130.1531	650.7654	1.1393	11.3928
3	135.8119	679.0595	1.0937	10.9371
4	135.8119	679.0595	1.0026	10.0257
5	141.4707	707.3536	1.0937	10.9371
Mean Value	133.5484	667.7418	1.0755	10.7548

**Table 2 Measurement of Track Density, Radon Activity, Radon Exhalation Rate and Radon Concentration at the Me Nu Oak Kyaung (1822)**

Detectors	Track Density (tracks/cm <sup>2</sup> d)	Radon Activity (Bq/m <sup>3</sup> )	Radon Exhalation Rate (mBq/m <sup>2</sup> h)	Radon Concentration (Bq/m <sup>3</sup> )
1	305.5768	1527.8839	2.4608	24.6085
2	305.5768	1527.8839	2.4608	24.6085
3	311.2356	1556.1780	2.5064	25.0642
4	311.2356	1556.1780	2.5064	25.0642
5	328.2121	1641.0605	2.6431	26.4313
Mean Value	312.3674	1561.8369	2.5155	25.1553

**Observation of Radon via Alpha Particles Emitting from New Building**

For this purpose, five LR-115 type II detectors (1cm×1cm) were used for detection of radon in the bathroom of new bridge building which was built in Monywa, 2017 and in the first floor of new bridge building which was built in Sagaing in 2017.

Each LR-115 type II detector was fixed at the top of inside the each ‘can’. And then, each five can are placed at the bathroom of new bridge building in Monywa and at the first floor of new bridge building in Sagaing according to facing the detector and α-emitted via from radon in building materials. After the exposure period of two months, each LR-115 detectors were etched in 2.5 M NaOH at 60°C for 90 min. The resultant photomicrographs are shown in Figures 11 and 12, respectively. The radon activity, radon exhalation rate and radon concentration are computed as shown above in Section. These values are presented in Tables 3 and 4.

From the Table 3, the track density was found to be between 50.9295 and 101.8590 track/cm<sup>2</sup> in all detectors at the bathroom of new bridge building in Monywa. The average value was found to be 84.8824 track/cm<sup>2</sup>. According to the observed track density, the radon activity was found to be between 242.5213 and 485.0425 Bq/m<sup>3</sup>. The average was 404.2021 Bq/m<sup>3</sup>. The calculated radon exhalation rate values were between 0.4037 and 0.8074 mBq/m<sup>2</sup>h and the mean value was 0.6728 mBq/m<sup>2</sup>h. Therefore, the radon concentration in the bathroom of new building was found to be 6.7279 Bq/m<sup>3</sup>.

From the Table 4, the track density is found to be between 33.9530 and 42.4412 track/cm<sup>2</sup> in all detectors at the first floor of new bridge building in Sagaing. The average value is found to be 39.0459 track/cm<sup>2</sup>. According to the observed track density, the radon activity was found to be between 161.6808 and 202.101 Bq/m<sup>3</sup>. The average was 185.9329 Bq/m<sup>3</sup>. The calculated radon

exhalation rate values were between 0.2691 and 0.3364 mBq/m<sup>2</sup>h and the mean value was 0.3095mBq/m<sup>2</sup>h. Therefore, the radon concentration in the first floor of new bridge building was found to be 3.0949 Bq/m<sup>3</sup>.

It was observed that the radon concentration (6.72792 Bq/m<sup>3</sup>) in the bathroom of new bridge building at the Monywa was higher than that of (3.0949 Bq/m<sup>3</sup>) first floor of new bridge building at the Sagaing. This is due to the lesser ventilation which one of the factors on radon accumulation. Therefore, radon could be more produced in ground floor than in the upper floor.

According to the literature, radon is a known cause of lung cancer when it is inhaled. Living for one year in a house with radon concentration of 300 Bq/m<sup>3</sup> results in effective dose of the order of 10 mSv which is equivalent to: four head CT scan, 25 years of exposure to average external background radiation, or smoking 1 cigarette per day. The lung cancer increases by approximately 16% for every 100 Bq/m<sup>3</sup> of radon exposure in the home (Krewski *et al*, 2005). Fortunately, the observed radon concentrations in these new buildings are very low for risk of lung cancer.

The international commission on radiation protection (ICRP-65, 1993) has recommended that the action level for radon concentration in ambient air should be in the range 200-600Bq/m<sup>3</sup>. The measured radon concentration values are below the recommended action level.

Therefore, decreases in radon concentrations should be opened windows and doors and the room without window set up exhaust fan.

According to the experimental results from old building and new building, revealed that radon concentration in old building is higher than that of new building. This is due to route of entry of radon into buildings is through cracks in walls and foundations and gaps. Therefore, people stay in old building should put wallpaper on the wall to prevent the radon which causes lungs cancer.

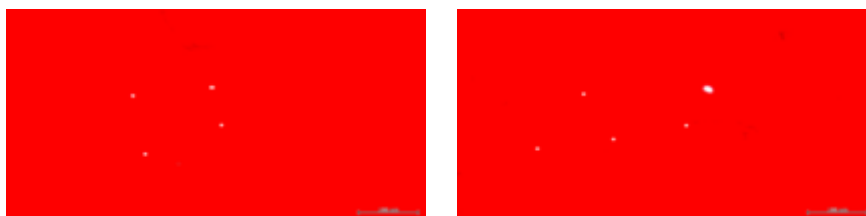


**Figure 11** Photomicrographs for the revelation of the alpha particle tracks in LR-115 detector placed at Sagaing, 2017



**Figure 12** Photomicrographs for the revelation of the alpha particle tracks in LR-115 detector placed at Monywa, 2017

**Table 3 Measurement of Track Density, Radon Activity, Radon Exhalation Rate and Radon Concentration at Monywa (2017)**

Detector	Track Density (tracks/cm <sup>2</sup> d)	Radon Activity (Bq/m <sup>3</sup> )	Radon Exhalation Rate (mBq/m <sup>2</sup> h)	Radon Concentration (Bq/m <sup>3</sup> )
1	50.9295	242.5213	0.4037	4.0368
2	84.8824	404.2021	0.6728	6.7279
3	93.3707	444.6223	0.7401	7.4007
4	93.3707	444.6223	0.7401	7.4007
5	101.8589	485.0425	0.8074	8.0735
Mean Value	84.8824	404.2021	0.6728	6.7279

**Table 4 Measurement of Track Density, Radon Activity, Radon Exhalation Rate and Radon Concentration at Sagaing (2017)**

Detector	Track Density (tracks/cm <sup>2</sup> d)	Radon Activity (Bq/m <sup>3</sup> )	Radon Exhalation Rate (mBq/m <sup>2</sup> h)	Radon Concentration (Bq/m <sup>3</sup> )
1	33.9530	161.6808	0.2691	2.6912
2	33.9530	161.6808	0.2691	2.6912
3	42.4412	202.1010	0.3364	3.3640
4	42.4412	202.1010	0.3364	3.3640
5	42.4412	202.1010	0.3364	3.3640
Mean Value	39.0459	185.9329	0.3095	3.0949

### Conclusion

In this study, it can be concluded that the concentration of radon was detected in all samples (Bagaya Monastery, Me Nu Oak Kyaung, the floor of a new building in Sagaing, and a bathroom of the new building in Monywa) as alpha emitted radioactive substance. According to the results, the radon concentration in the old building is higher than that of the new building. Therefore, people who stay in the old building should be noticed the health risk from radon.

Radon is a known cause of lung cancer when it is inhaled (Krewski *et al.*, 2005). Therefore, decreases in radon concentrations are observed, when windows and doors are opened showing the importance of ventilation.

### Acknowledgements

We would like to express our sincere gratitude to Dr Thuya Oo, Rector, Monywa University for his permission to do this research as well as invaluable suggestions. We are also deeply grateful to Professor Dr Than Than Win, Head of Chemistry Department, Monywa University, for her kind help and suggestion. We also greatly appreciated Professor Dr Ni Ni Than, Head of Chemistry Department, University of Yangon.

## References

- Dolleiser, M. and Hashemi-Nezhad, S. R. (2002). "A Fully Automated Optical Microscope for Analysis of Particle Tracks in Solids". *Nuclear Instruments and Methods in Physics Research Section B: Beam Interactions with Materials and Atoms*, vol. 198(1-2), pp. 98-107.
- Dörschel, B., Hermsdorf, D., Pieck, S., Starke, S., Thiele, H., & Weickert, F. (2003). "Studies of SSNTDs Made from LR-115 in View of Their Applicability in Radiobiological Experiments with Alpha Particles". *Nuclear Instruments and Methods in Physics Research Section B: Beam Interactions with Materials and Atoms*, vol. 207(2), pp.154-164.
- Eappen, K. P., and Mayya, Y. S. (2004). "Calibration Factors for LR-115 (type-II) Based Radon Thoron Discriminating Dosimeter". *Radiation Measurements*, vol. 38(1), pp.5-17.
- Kovács, T., Shahrokhi, A., Sas, Z., Vigh, T., and Somlai, J. (2017). "Radon Exhalation Study of Manganese Clay Residue and Usability in Brick Production". *Journal of Environmental Radioactivity*, vol.168, pp.15-20.
- Krewski, D., Lubin, J. H., Zielinski, J. M., Alavanja, M., Catalan, V. S., Field, R. W., and Wilcox, H. B. (2005). Residential Radon and Risk of Lung Cancer: a Combined Analysis of 7 North American Case-Control Studies. *Epidemiology*, pp.137-145.
- Ng, F. M. F., Yip, C. W. Y., Ho, J. P. Y., Nikezic, D., and Yu, K. N. (2004). "Non-destructive Measurement of Active-layer Thickness of LR 115 SSNTD". *Radiation Measurements*, vol. 38(1), 1-3.
- Nguyen, T. T. H., Giap T. V. and Cuong. L. D. (2016). "Technical Procedure Determination of Thoron Indoor Concentration by LR-115 Type II". *Journal of Environmental Science and Engineering*. vol. 5, pp.109-114.
- Nikezic, D., Ng, F. M. F., and Yu, K. N. (2004). "Sensitivity of LR 115 Detectors in Hemispherical Chambers for Radon Measurements." *Nuclear Instruments and Methods in Physics Research Section B: Beam Interactions with Materials and Atoms*, vol. b 217(4), pp.637-643.
- Saad, A. F., Abdalla, Y. K., Hussein, N. A., and Elyaseery, I. S. (2010). "Radon Exhalation Rate from Building Materials Used on the Garyounis University Campus, Benghazi, Libya". *Turkish Journal of Engineering and Environmental Sciences*, vol. b34 (1), pp.67-74.
- Sharma, J., Mahur, A. K., Kumar, R., Varshney, R., Sonkawade, R. G., Swarup, R., Singh, H. and Prasad.R. (2014). "Radon Exhalation in Some Building Construction Materials and Effect of Plastering and Paints on the Radon Exhalation Rate Using Fired Bricks". *Advances in Applied Science Research*, vol. 5(2), pp.382-386
- Siems, M., Freyer, K., Treutler, H. C., Jönsson, G., & Enge, W. (2001). "Experimental Study on the Aging Process of the LR 115 Cellulose Nitrate Radon Detector". *Radiation Measurements*, vol. 34(1-6), pp.81-84
- Singh, P., Singh, N., and Chakarvarti, S. K. (1989). "59Ni Ion Track Registration in Cellulose Nitrate CN-85." *Nuclear Instruments and Methods in Physics Research Section B: Beam Interactions with Materials and Atoms*, vol. 36(2), pp.211-215.
- Smith, K. P., Blunt, D. L., and Arnish, J. J. (1998). *Potential Radiological Doses Associated with The Disposal of Petroleum Industry NORM via Landspreading. Final Report, September 1998* (No. DOE/BC/W-31-109-ENG-38-5). Argonne National Lab., Lakewood, Co. (United States).
- Tse, K. C. C., Ng, F. M. F., Nikezic, D., & Yu, K. N. (2007). "Bulk Etch Characteristics of Colorless LR 115 SSNTD". *Nuclear Instruments and Methods in Physics Research Section B: Beam Interactions with Materials and Atoms*, vol. 263(1), pp.294-299.

## STUDIES ON SYNTHESIS AND CHARACTERIZATION OF NANOCARBON FROM RICE HUSK CHAR

Zaw Oo<sup>1</sup>, Yi Yi Myint<sup>2</sup>

### Abstract

In this research work, some physicochemical properties of rice husk raw and rice husk char were determined by AOAC method. The nanocarbons were prepared from rice husk char with  $\text{NaNO}_3$ ,  $\text{KMnO}_4$  and  $\text{H}_2\text{SO}_4$  by modified Hummer Method under different conditions. Similarly, nanocarbons were prepared from rice husk char with  $\text{H}_3\text{PO}_4$ ,  $\text{KMnO}_4$  and  $\text{H}_2\text{SO}_4$  by the same method under different conditions. The synthesized nanocarbons were also characterized by using X-ray diffraction analysis (XRD) and Scanning Electron Microscopy analysis (SEM) techniques.

**Keywords:** physicochemical, Nanocarbon, Hummer method, XRD, SEM

### Introduction

A carbon-based material whose constituents are of nanoscale dimensions, or which is produced by nanotechnology. Nanomaterials are currently on the cutting edge of material science research and are gradually finding applications in our daily life, including life science, energy, and environmental applications. Among many nanomaterials, carbon nanomaterials such as carbon nanotubes (CNTs), graphite, diamonds, fullerenes, and graphene, with their high specific surface areas and large pore volumes, have remained at the forefront of nanotechnology. In this study nanocarbons were synthesized from rice husk biochar (Figure 1).

#### (a) Rice husk

Rice husk are the hard protecting coverings of grains of rice and part of the chaff of the rice. Rice hulls are the coatings of seeds, or grains, of rice. The husk protects the seed during the growing season, since it is formed from hard materials, including opaline silica and lignin. Rice husk is used as building material, fertilizer, insulation material and fuel.

#### (b) Rice husk biochar

Biochar is a type of black carbon produced from a carbonaceous material through the application of heat or chemicals. Biochar is a carbon rich highly porous substance obtained after pyrolysis of organic biomass. Production of biochar is a sustainable option for waste and disease management. It contains 50 % of the original carbon which is highly recalcitrant in nature; therefore its production helps in carbon sequestration by locking the carbon present in the plant biomass. Biochar is used as a tool for waste management, as a soil conditioner, treatment of waste water, building sector, cosmetic industries, metallurgy, food industry and energy production.

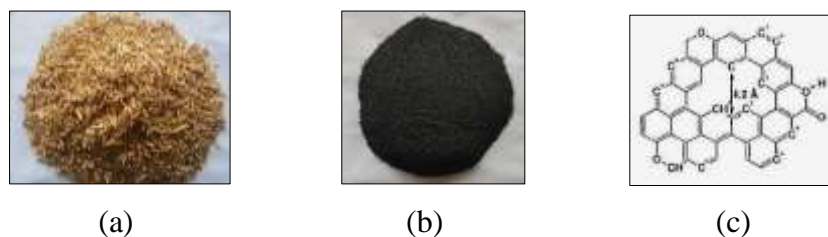


**Figure 1** (a) Rice husk (b) Rice husk biochar and (c) Composition of biochar

<sup>1</sup> 3PhD Candidate, Department of Chemistry, Mandalay University

<sup>2</sup> Dr, Professor and Head, Department of Chemistry, University of Mandalay

## (c) Nanocarbons

### (i) Fullerenes

Fullerene is a spherical carbon compound and is an allotrope of carbon such as diamond, graphite and carbon nanotubes. Fullerenes of C<sub>60</sub>, C<sub>70</sub> and C<sub>84</sub> are well known. They are isolable carbon compounds in a sole molecular species. Among them, the C<sub>60</sub> is a representative species. Kroto, Smalley and Curl first observed the C<sub>60</sub> in which the 60 carbon atoms consist of 12 five-membered rings and 20 six-membered rings and won their joint Nobel prizes in chemistry in 1996 for their contributions (Kroto *et al.*, 1985). Osawa predicted existence of fullerene in 1970, earlier than the first observation of fullerene.

### (ii) Carbon nanotubes

A carbon nanotube (CNT) has a cylindrical structure with a nanoscale diameter that is like a rolled graphene sheet. Iijima first observed a CNT in 1991. A CNT consists of only sp<sup>2</sup> carbons similar to fullerenes. There are diverse CNTs on the basis of their length, diameter of the nanotube, state of chirality, and number of the layer. The variety of these structures provides various band structures and metallic and semiconducting properties. A normal synthetic procedure gives a mixture of semiconducting CNTs in 2/3 and metallic CNTs in 1/3, because rolling a carbon sheet occurs randomly.

### (iii) Graphene/graphene oxides

Graphene, which is one of the nanocarbon materials, consists of all six-membered rings with sp<sup>2</sup> carbons having a twodimensional sheet structure. Graphene has been known for long time, since graphite is formed by combination of graphenes with van der Waals force. However, details of the properties were unclear until late years, because an isolation procedure of graphene from graphite was not well developed for long time. Geim and Novoselov *et al.* in 2004 successfully isolated a thinflake graphene by a simple procedure. They used a tape to peel off a graphene layer from highly oriented pyrolytic graphite (HOPG) and then the peeled graphene layer is stuck on a substrate. After this observation, studies of graphene have proved the particular characteristics of electronic, mechanical, and chemical properties. Geim and Novoselov won their joint Nobel prizes in physics in 2010 for their contributions (Geim, 2009; Novoselov, 2005).

### (iv) Nanodiamonds

Diamond, an allotrope of carbon, has excellent hardness, coefficient of friction, thermal conductivity, insulation characteristics, and refractive index. Large and highly pure diamond is good for use as jewelry. Furthermore, the major industrial application of diamond is for cutting and polishing tools, because it is the hardest of natural products. However, diamond is not workable enough because of its hardness so there is a limitation for industrial use of a large diamond. Nanodiamond (ND) is a nanoparticle having the crystal structure of diamond, and it has excellent properties of normal diamond. ND is artificially synthesized for additives of engine oil.

### (v) Nanocarbon unit structures

#### Cycloparaphenylenes (CPP)

Carbon nanotubes (CNT) have advanced chemistry, material science, life science and other research fields. CNTs can be prepared by physical methods such as arc discharge, laser furnace, and chemical vapor deposition techniques. One disadvantage of these physical methods is forming several kinds of CNTs with various diameters, thus uniform CNTs do not form. Cycloparaphenylenes (CPP), the so-called carbon nanoring, have a cyclic structure formed by

linkages of *p*-substituted benzenes. The CPP attracted researchers in fundamental chemistry and material science, because it is a unit structure of CNT.

#### (d) Characterization of nanoparticle

##### 1. XRD measurement

X-ray diffraction analysis of nanoparticle was conducted using X-ray diffractometer equipment with a Cu K $\alpha$  radiation at an accelerating voltage 40 kV and emission current 30 mA in the range of diffraction angle  $2\theta = 10 - 80^\circ$ . The XRD analysis was conducted to investigate the interlayer spacing of the prepared sample.

##### 2. SEM measurement

The Scanning Electron Microscopy analysis was conducted to study the changes in surface morphology such as smoothness and roughness of sample. Samples were coated with gold prior to recording of images for rendering the same conductivity.

##### 3. Debye-Scherrer's Equation

The average particles of prepared powders were calculated by "Debye-Scheerer Equation" using XRD line broadening method.

$$D = \frac{K\lambda}{\beta \cos \theta}$$

Where, D = the mean size of crystallites (nm)

K= crystallite shape factor

$\lambda$  = the wavelength of incident X-ray

$\beta$  = full width at high maximum in radians of the X-ray diffraction peak

$\theta$  = Bragg's angle

##### 4. Bragg's Law Equation

The interplanar spacing in nm of prepared powders was calculated by "Bragg's Law Equation" using XRD line broadening method.

$$n\lambda = 2d \sin \theta$$

Where, d = interplanar spacing nm

## Materials and Methods

### Sampling

The rice husk raw was collected from Nabekan Village, Wundwin Township, Mandalay Region (Figure 2). The sample was first cleaned and washed with water. And then, the collected samples were kept in air to dry at room temperature for a few weeks. Biochar was prepared from rice husk by AOAC method (A.O.A.C, 2000).

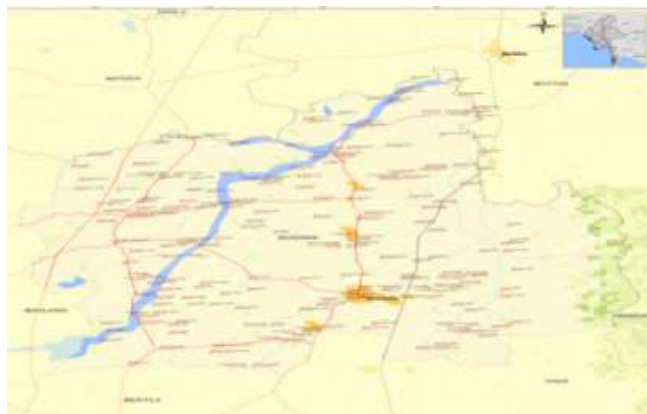


**Figure 2** Nabekan Village, Wundwin Township, Mandalay Region.

Some physicochemical properties of rice husk raw and rice husk char such as ash content, pH values and moisture content were determined by the A.O.A.C method (A.O.A.C, 2000).

### **Preparation of nanocarbons NC-1 from rice husk char with NaNO<sub>3</sub>, KMnO<sub>4</sub> and H<sub>2</sub>SO<sub>4</sub> (6 h stirring time)**

#### **Procedure**

0.5 g of rice husk char was mixed with 0.25 g of sodium nitrate and was stirred in ice bath. After that, 20 mL of concentrated sulphuric acid was added (drop by drop along to the wall of the beaker) to the above mixture and then, 2 g of potassium permanganate was slowly added and was stirred in ice bath for 1 h. Then, the whole mixture was stirred at room temperature for 3 h. After that, 50 mL of water was added to the mixture and stirred for 1 h. Then, 50 mL of hot water and 7.5 mL of 30 % H<sub>2</sub>O<sub>2</sub> solution were added drop by drop to the mixture and it was stirred for 1 h. Finally, the mixture was filtered and the filtered powder by washing with 5 % HCl solution and washed with distilled water till neutral to get NC-1 powder.

Similarly, NC-2(stirring time 8 h), NC-3(using double amount of NaNO<sub>3</sub>, KMnO<sub>4</sub> and H<sub>2</sub>SO<sub>4</sub>), NC-4(stirring time 3 h and sonication time 3 h), NC-5(stirring time 3.5 h and sonication time 4.5 h), NC-6(using double amount of NaNO<sub>3</sub>, KMnO<sub>4</sub> and H<sub>2</sub>SO<sub>4</sub>, stirring time 3 h and sonication time 3 h) were prepared using the same procedure as described for NC-1.

### **Preparation of nanocarbon NC-7 from rice husk char with H<sub>3</sub>PO<sub>4</sub>, KMnO<sub>4</sub> and H<sub>2</sub>SO<sub>4</sub> (6.5 h stirring time)**

#### **Procedure**

0.5 g of rice husk char was mixed with 3mL of phosphoric acid and was stirred in ice bath. After that, 27 mL of concentrated sulphuric acid was added (drop by drop along to the wall of the beaker) to the above mixture and then, 1.32 g of potassium permanganate was slowly added and was stirred in ice bath for 1.5 h. Then, the whole mixture was stirred for 4.5 h. After that, 1 mL of concentrated H<sub>2</sub>O<sub>2</sub> solution was added drop by drop to the mixture and was stirred for 0.5 h. Then 10 mL of concentrated HCl was added drop by drop and 30 mL of water was added to the mixture. Finally, the mixture was filtered and the filtered powder was washed with distilled water till neutral to get NC-7 powder.

Similarly, NC-8(stirring time 10 h), NC-9(using double amount of phosphoric acid, KMnO<sub>4</sub> and H<sub>2</sub>SO<sub>4</sub>) and NC-10(stirring time 3 h and sonication time 7 h) were prepared using the same procedure as described for NC-7.

## Characterization of synthesized nanocarbons from rice husk char

### XRD analysis

Powder X-ray diffraction (XRD) patterns were performed using a RIGAKU Multiplex 2k W, X-ray diffractometer with Cu K $\alpha$  radiation of wavelength 1.54056 Å

### SEM Analysis

The samples were examined by Scanning Electron Microscope (SEM) for a visual inspection of external porosity, and morphology.

## Results and Discussion

### Determination of ash content, pH values and moisture content

The ash content, pH values and moisture content of rice husk raw and rice husk charcoal were determined by AOAC method. The results are shown in Table 1.

**Table 1 Determination of ash content, pH values, and moisture content of rice husk raw and rice husk char**

No	Properties	Rice husk raw	Rice husk char	Apparatus used
1	Ash (%)	16.14	32.59	Muffle furnace
2	pH	7.82	7.84	pH meter
3	Moisture (%)	8.76	4.09	Oven

From the results, the pH values of the two samples are nearly the same, but the ash content of rice husk charcoal is twice of the ash content of rice husk raw and the moisture content of rice husk charcoal is half of the moisture content of rice husk raw. Among these two samples, rice husk char was selected for the study.

### XRD Analysis of Synthesized Nanocarbon NC-1 from Rice Husk Char

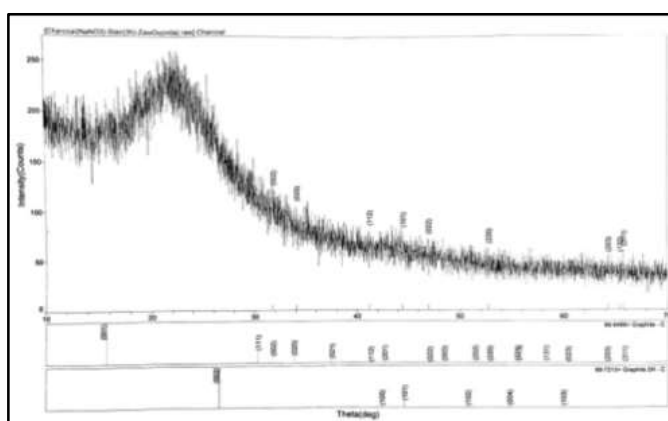


**Figure 3** XRD diffraction pattern of nanocarbon NC-1 from rice husk char

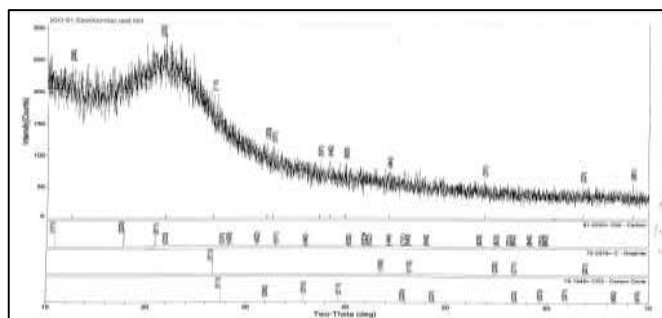
The crystallite size and crystal structure of nanocarbon NC-1 from the rice husk char was determined from the XRD study.

**Table 2 The average particle size of nanocarbon NC-1 from rice husk char**

Peak No.	Bragg angle ( $2\theta$ )	Miller indices (h k l)	FWHM of peak ( $\beta$ ) radians	Particle size, D (nm)
1	31.741	(0 0 2)	0.0083	17.174
2	34.024	(0 2 0)	0.0027	53.105
3	41.183	(1 1 2)	0.0014	104.620
4	44.464	(1 0 1)	0.0063	23.511
5	46.953	(0 2 2)	0.0023	64.993
6	52.752	(2 2 0)	0.0046	33.270

The localized peaks at  $2\theta = 31.741^\circ$ ,  $34.024^\circ$ ,  $41.183^\circ$ ,  $44.464^\circ$ ,  $46.953^\circ$  and  $52.752^\circ$  that referred to plane reflections of (002), (020), (112), (101), (022) and (220), respectively. According to Table 5, the range of particle size of synthesized nanocarbon NC-1 from rice husk char was found to be 17.174nm-104.620 nm and average particle size is 44.232 nm.

### XRD Analysis of Synthesized Nanocarbon NC-2 from Rice Husk Char

**Figure 4** XRD diffraction pattern of nanocarbon NC-2 from rice husk char

The crystallite size and crystal structure of nanocarbon NC-2 from the rice husk char was determined from the XRD study.

**Table 3 The average particle size of nanocarbon NC-2 from rice husk char**

Peak No.	Bragg angle ( $2\theta$ )	Miller indices (h k l)	FWHM of peak ( $\beta$ ) radians	Particle size, D (nm)
1	12.497	(2 0 0)	0.0094	14.673
2	21.792	(2 2 2)	0.0039	35.802
3	26.604	(1 1 1)	0.0044	32.020
4	53.930	(3 1 1)	0.0027	56.976
5	63.568	(2 2 1)	0.0071	22.718
6	68.460	(9 5 1)	0.0027	61.420

The localized peaks at  $2\theta = 12.497^\circ$ ,  $21.792^\circ$ ,  $26.604^\circ$ ,  $53.930^\circ$ ,  $63.568^\circ$  and  $68.460^\circ$  that referred to plane reflections of (200), (222), (111), (311), (221) and (951), respectively. The broad peak at around  $26^\circ$  confirms the presence of amorphous nanocarbon material. According to Table 3, the range of particle size of synthesized nanocarbon NC-2 from rice husk char was found to be 14.673nm-61.420 nm and average particle size is 32.5489 nm.

**XRD Analysis of Synthesized Nanocarbon NC-3 from Rice Husk Char**

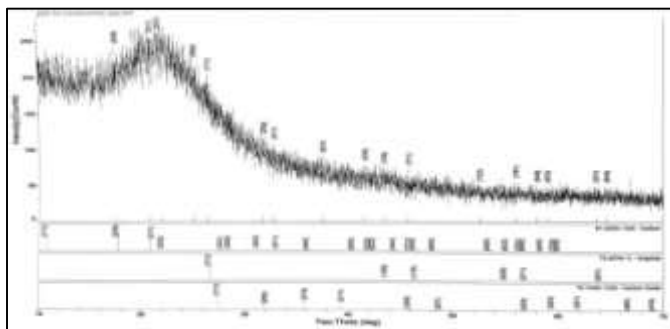


**Figure 5** XRD diffraction pattern of nanocarbon NC-3 from rice husk char

The crystallite size and crystal structure of nanocarbon NC-3 from the rice husk char was determined from the XRD study.

**Table 4** The average particle size of nanocarbon NC-3 from rice husk char

Peak No.	Bragg angle (2θ)	Miller indices (h k l)	FWHM of peak (β) radians	Particle size, D (nm)
1	17.438	(2 2 0)	0.0047	29.513
2	20.840	(3 1 1)	0.0062	22.485
3	21.901	(2 2 2)	0.0092	15.180
4	43.511	(1 0 0)	0.0095	15.539
5	45.935	(7 1 1)	0.0027	50.850
6	56.143	(7 5 1)	0.0017	91.406

The localized peaks at  $2\theta = 17.438^\circ, 20.840^\circ, 21.901^\circ, 43.511^\circ, 45.935^\circ$  and  $56.143^\circ$  that referred to plane reflections of (220), (311), (222), (100), (711) and (751), respectively. The broad peak at around  $26^\circ$  confirms the presence of amorphous nanocarbon material. According to Table 4, the range of particle size of synthesized nanocarbon NC-3 from rice husk char was found to be 15.180nm-91.406 nm and average particle size is 34.7114 nm.

**XRD Analysis of Synthesized Nanocarbon NC-4 from Rice Husk Char**

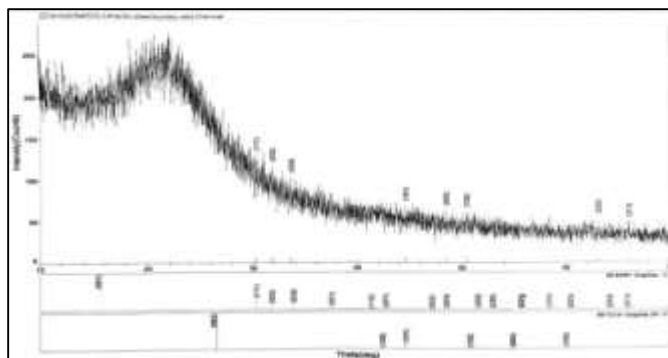


**Figure 6** XRD diffraction pattern of nanocarbon NC-4 from rice husk char

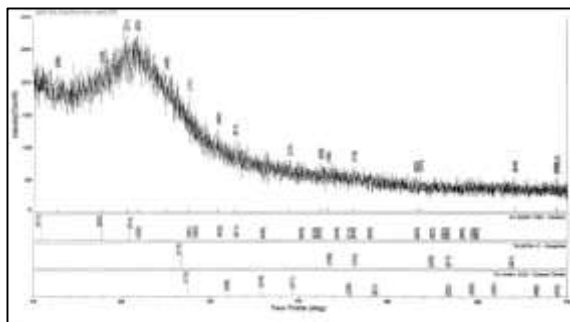
The crystallite size and crystal structure of nanocarbon NC-4 from the rice husk char was determined from the XRD study.

**Table 5 The average particle size of nanocarbon NC-4 from rice husk char**

Peak No.	Bragg angle (2 $\theta$ )	Miller indices (h k l)	FWHM of peak ( $\beta$ ) radians	Particle size, D (nm)
1	30.247	(1 1 1)	0.0016	88.768
2	31.776	(0 0 2)	0.0040	35.639
3	33.582	(0 2 0)	0.0063	22.733
4	44.615	(1 0 1)	0.0027	54.889
5	48.509	(0 0 3)	0.0075	20.051
6	63.101	(2 2 2)	0.0018	89.385

The localized peaks at  $2\theta = 30.247^\circ$ ,  $31.776^\circ$ ,  $33.582^\circ$ ,  $44.615^\circ$ ,  $48.509^\circ$  and  $63.101^\circ$  that referred to plane reflections of (111), (002), (020), (101), (003) and (222), respectively. According to Table 5, the range of particle size of synthesized nanocarbon NC-4 from rice husk char was found to be 20.051nm-89.385nm and average particle size is 47.163 nm.

### XRD Analysis of Synthesized Nanocarbon NC-5 from Rice Husk Char

**Figure 7** XRD diffraction pattern of nanocarbon NC-5 from rice

The crystallite size and crystal structure of husk char nanocarbon NC-5 from the rice husk char was determined from the XRD study.

**Table 6 The average particle size of nanocarbon NC-5 from rice husk char**

Peak No.	Bragg angle (2 $\theta$ )	Miller indices (h k l)	FWHM of peak ( $\beta$ ) radians	Particle size, D (nm)
1	12.684	(2 0 0)	0.0063	21.898
2	17.666	(2 2 0)	0.0049	28.317
3	20.531	(3 1 1)	0.0050	27.868
4	21.717	(2 2 2)	0.0072	19.390
5	24.911	(4 0 0)	0.0050	28.083
6	27.462	(1 1 1)	0.0014	100.816
7	64.179	(8 4 4)	0.0015	107.890

The localized peaks at  $2\theta = 12.684^\circ$ ,  $17.666^\circ$ ,  $20.531^\circ$ ,  $21.717^\circ$ ,  $24.911^\circ$ ,  $27.462^\circ$  and  $64.179^\circ$  that referred to plane reflections of (200), (220), (311), (222), (400), (111) and (844), respectively. The broad peak at around  $26^\circ$  confirms the presence of amorphous nanocarbon material. According to Table 6, the range of particle size of synthesized nanocarbon NC-5 from rice husk char was found to be 19.390nm-107.890 nm and average particle size is 42.2241 nm.

### XRD Analysis of Synthesized Nanocarbon NC-6 from Rice Husk Char

The crystallite size and crystal structure of nanocarbon NC-6 from the rice husk char was determined from the XRD study.

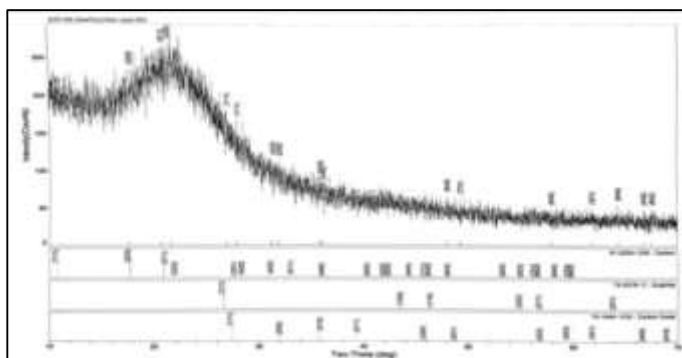


**Figure 8** XRD diffraction pattern of nanocarbon NC-6 from rice husk char

**Table 7** The average particle size of nanocarbon NC-6 from rice husk char

Peak No.	Bragg angle ( $2\theta$ )	Miller indices (h k l)	FWHM of peak ( $\beta$ ) radians	Particle size, D (nm)
1	17.579	(2 2 0)	0.0064	21.678
2	20.587	(3 1 1)	0.0059	23.619
3	21.521	(2 2 2)	0.0072	19.384
4	26.733	(1 1 1)	0.0048	29.360
5	27.710	(1 1 1)	0.0029	48.696
6	67.582	(8 6 2)	0.0024	68.724

The localized peaks at  $2\theta = 17.579^\circ, 20.587^\circ, 21.521^\circ, 26.733^\circ, 27.710^\circ$  and  $67.582^\circ$  that referred to plane reflections of (220), (311), (222), (111), (111) and (862), respectively. The broad peak at around  $26^\circ$  confirms the presence of amorphous nanocarbon material. According to Table 7, the range of particle size of synthesized nanocarbon NC-6 from rice husk char was found to be 19.384nm-68.742 nm and average particle size is 35.2175 nm.

### XRD Analysis of Synthesized Nanocarbon NC-7 from Rice Husk Char

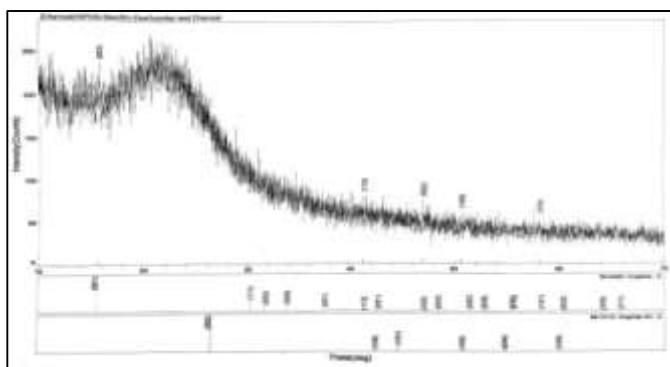


**Figure 9** XRD diffraction pattern of nanocarbon NC-7 from rice husk char

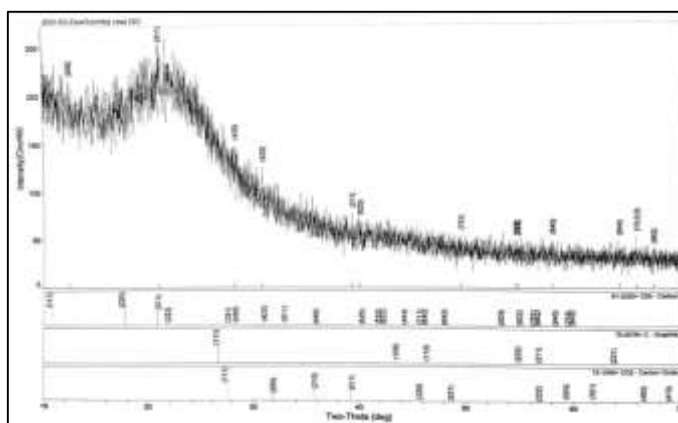
The crystallite size and crystal structure of nanocarbon NC-7 from the rice husk char was determined from the XRD study.

**Table 8 The average particle size of nanocarbon NC-7 from rice husk char**

Peak No.	Bragg angle ( $2\theta$ )	Miller indices (h k l)	FWHM of peak ( $\beta$ ) radians	Particle size, D (nm)
1	15.697	(0 0 1)	0.0054	25.630
2	41.226	(1 1 2)	0.0053	27.639
3	46.990	(0 2 2)	0.0046	32.501
4	50.693	(1 0 2)	0.0047	32.280
5	58.155	(1 3 1)	0.0038	41.285

The localized peaks at  $2\theta = 15.697^\circ$ ,  $41.226^\circ$ ,  $46.990^\circ$ ,  $50.693^\circ$  and  $58.155^\circ$  that referred to plane reflections of (001), (112), (022), (102) and (131), respectively. According to Table 8, the range of particle size of synthesized nanocarbon NC-7 from rice husk char was found to be 25.630nm-41.285 nm and average particle size is 31.867 nm.

### XRD Analysis of Synthesized Nanocarbon NC-8 from Rice Husk Char

**Figure 10** XRD diffraction pattern of nanocarbon NC-8 from rice husk char

The crystallite size and crystal structure of nanocarbon NC-8 from the rice husk char was determined from the XRD study.

**Table 9 The average particle size of nanocarbon NC-8 from rice husk char**

Peak No.	Bragg angle ( $2\theta$ )	Miller indices (h k l)	FWHM of peak ( $\beta$ ) radians	Particle size, D (nm)
1	12.482	(2 0 0)	0.0080	17.241
2	20.908	(3 1 1)	0.0056	24.897
3	28.089	(4 2 0)	0.0055	25.697
4	30.738	(4 2 2)	0.0029	49.033
5	39.339	(2 1 1)	0.0052	28.006
6	54.783	(2 2 2)	0.0027	57.194

The localized peaks at  $2\theta = 12.482^\circ$ ,  $20.908^\circ$ ,  $28.089^\circ$ ,  $30.738^\circ$ ,  $39.339^\circ$  and  $54.783^\circ$  that referred to plane reflections of (200), (311), (420), (422), (211) and (222), respectively. The broad peak at around  $26^\circ$  confirms the presence of amorphous nanocarbon material. According to Table 9, the range of particle size of synthesized nanocarbon NC-8 from rice husk char was found to be 17.241nm-57.194 nm and average particle size is 36.8098 nm.

**XRD Analysis of Synthesized Nanocarbon NC-9 from Rice Husk Char**

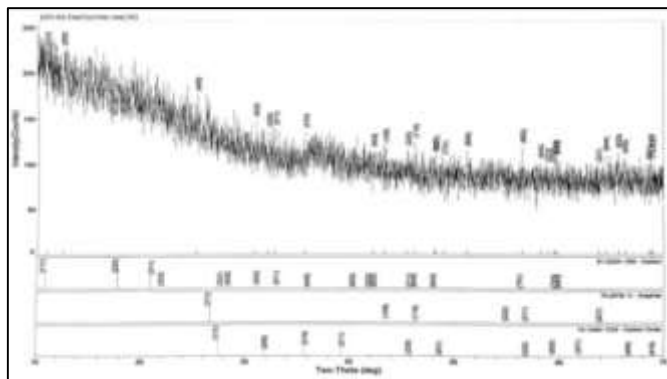


**Figure 11** XRD diffraction pattern of nanocarbon NC-9 from rice husk char

The crystallite size and crystal structure of nanocarbon NC-9 from the rice husk char was determined from the XRD study.

**Table 10** The average particle size of nanocarbon NC-9 from rice husk char

Peak No.	Bragg angle (2θ)	Miller indices (h k l)	FWHM of peak (β) radians	Particle size, D (nm)
1	10.887	(1 1 1)	0.0049	28.108
2	12.489	(2 0 0)	0.0042	32.840
3	25.191	(4 0 0)	0.0020	70.246
4	58.944	(0 2 3)	0.0134	11.753
5	59.480	(7 5 3)	0.0080	19.739
6	59.643	(7 5 3)	0.0010	158.037

The localized peaks at  $2\theta = 10.887^\circ, 12.489^\circ, 25.191^\circ, 58.944^\circ, 59.480^\circ$  and  $59.643^\circ$  that referred to plane reflections of (111), (200), (400), (023), (753) and (753), respectively. The broad peak at around  $26^\circ$  confirms the presence of amorphous nanocarbon material. According to Table 10, the range of particle size of synthesized nanocarbon NC-9 from rice husk char was found to be 11.753nm-158.037 nm and average particle size is 44.1708 nm.

**XRD Analysis of Synthesized Nanocarbon NC-10 from Rice Husk Char**

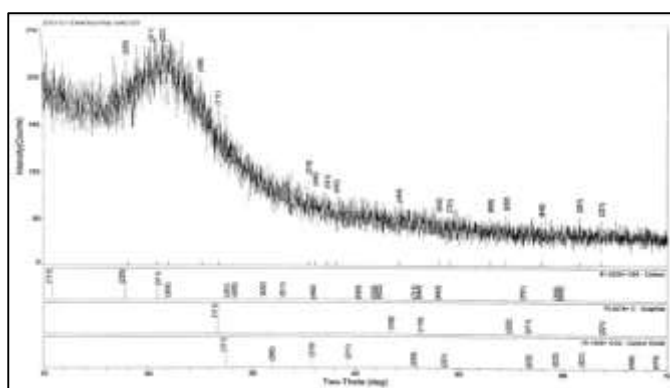


**Figure 12** XRD diffraction pattern of nanocarbon NC-10 from rice husk char

The crystallite size and crystal structure of nanocarbon NC-10 from the rice husk char was determined from the XRD study.

**Table 11 The average particle size of nanocarbon NC-10 from rice husk char**

Peak No.	Bragg angle ( $2\theta$ )	Miller indices (h k l)	FWHM of peak ( $\beta$ ) radians	Particle size, D (nm)
1	17.952	(2 2 0)	0.0042	33.050
2	20.773	(3 1 1)	0.0088	15.840
3	21.858	(2 2 2)	0.0081	17.240
4	37.280	(5 3 1)	0.0109	13.275
5	38.154	(4 4 2)	0.0026	55.799
6	63.707	(2 2 1)	0.0019	84.958

The localized peaks at  $2\theta = 17.952^\circ$ ,  $20.773^\circ$ ,  $21.858^\circ$ ,  $37.280^\circ$ ,  $38.154^\circ$  and  $63.707^\circ$  that referred to plane reflections of (220), (311), (222), (531), (442) and (221), respectively. The broad peak at around  $26^\circ$  confirms the presence of amorphous nanocarbon material. According to Table 11, the range of particle size of synthesized nanocarbon NC-10 from rice husk char was found to be 13.275nm-84.958 nm and average particle size is 37.220 nm.

**Table 12 The average crystalize sizes and lattice crystal nature for all nanocarbons**

No	Nanocarbon	Average crystalize size	Lattice crystal nature
1	NC-1	44.2320	Hexagonal
2	NC-2	32.5489	Cubic
3	NC-3	34.7114	Cubic
4	NC-4	41.1630	Hexagonal
5	NC-5	42.2241	Cubic
6	NC-6	35.2175	Cubic
7	NC-7	31.8670	Hexagonal
8	NC-8	36.8098	Cubic
9	NC-9	44.1708	Cubic
10	NC-10	37.2200	Cubic

In this table, the lattice crystal natures of synthesized nanocarbons are cubic and hexagonal. According to the XRD patterns, the average crystalize sizes and lattice crystal nature for all nanocarbons are 32.5489 nm, 34.7114 nm, 41.1630 nm, 42.2241 nm, 35.2175 nm, 31.8670 nm, 36.8098 nm, 44.1708 nm and 37.2200 nm are respectively. Thus, all the data are in the range of nanoparticle scale 1 nm to 100 nm.

### SEM Analysis

The morphologies of prepared nanocarbons are investigated by SEM microscopy. Figure 13 (a) and (b) shows the morphologies of nanocarbon NC-8 and nanocarbon NC-10.

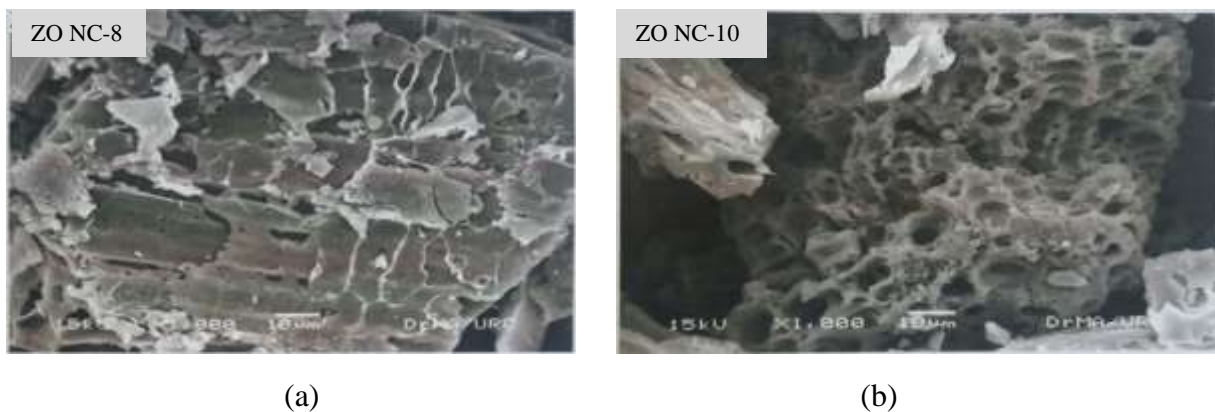


**Figure 13** SEM micrographs of (a) nanocarbon NC-8 and (b) nanocarbon NC-10

The SEM micrographs suggest that the material has non regular compacted surface with cavities. This could be due to breakdown of the lignocellulosic material and evaporation of volatile compounds that leave the nanocarbons with well developed pores.

### Conclusion

In this research work, the preparation of nanocarbons (NC-1 to NC-6) was carried out from rice husk char by  $\text{NaNO}_3$ ,  $\text{KMnO}_4$  and  $\text{H}_2\text{SO}_4$  by Modified Hummer Method with various conditions. Similarly, the preparation of nanocarbons (NC-7 to NC-11) was carried out from rice husk char by  $\text{H}_3\text{PO}_4$ ,  $\text{KMnO}_4$  and  $\text{H}_2\text{SO}_4$  with various conditions. Moreover, studying on the X-ray diffraction (XRD) analysis, the lattice crystal nature of the synthesized nanocarbon was observed as cubic and hexagonal. The average crystalize sizes of synthesized nanocarbon are 44.232 nm, 32.549 nm, 34.711 nm, 47.163 nm, 42.224 nm, 35.218 nm, 31.867 nm, 36.8098 nm, 44.171 nm, 37.220 nm and 57.645 nm respectively. Finally, the morphology of the synthesized nanocarbon NC-8 and NC-10 are investigated by Scanning Electron Microscopy (SEM) micrograph indicate the non regular compacted surface with cavities and protuberances. Nanocarbons can be prepared from the waste rice husks for application in electrochemical energy storage, biogenetic and organic solar cells.

### Acknowledgements

I would like to express my gratitude to Dr Yi Yi Myint, Professor and Head, Department of Chemistry, University of Mandalay, for her guidance to do this research work. I also thank to all of my teachers from whom I have learned and to all my friends for their patience and understanding during my research work.

## References

- AOAC (2000). "Official Methods of Analysis". 17th Edition, The Association of Official Analytical Chemists, USA. Methods 925.10, 65.17, 974.24, 992.16.
- Ajayan, P. M., Ebbesen, T. W., Ichihashi, T., Iijima, S., Tanigaki, K., and Hiura, H. (1993). Opening Carbon Nanotubes with Oxygen and Implications for Filling. *Nature*, 362(6420), 522-525.
- Balasubramanian, K., Lee, E. J., Weitz, R. T., Burghard, M., & Kern, K. (2008). Carbon Nanotube Transistors—Chemical Functionalization and Device Characterization. *Physica Status Solid (a)*, 205(3), 633-646.
- Bolotin, K. I., Sikes, K. J., Jiang, Z., Klima, M., Fudenberg, G., Hone, J. E., and Stormer, H. L. (2008). Ultrahigh Electron Mobility in Suspended Graphene. *Solid State Communications*, 146(9-10), 351-355.
- Ganin, A. Y., Takabayashi, Y., Khimyak, Y. Z., Margadonna, S., Tamai, A., Rosseinsky, M. J., & Prassides, K. (2008). Bulk Superconductivity at 38 K in a Molecular System. *Nature Materials*, 7(5), 367-371.
- Geim, A. K. (2009). Graphene: Status and Prospects. *Science*, 324(5934), 1530-1534.
- Kim, J., Page, A. J., Irlle, S., and Morokuma, K. (2012). Dynamics of Local Chirality during SWCNT Growth: Armchair versus Zigzag Nanotubes. *Journal of the American Chemical Society*, 134(22), 9311-9319.
- Kroto, H. W., Heath, J. R., O'Brien, S. C., Curl, R. F., and Smalley, R. E. (1985). C<sub>60</sub>: Buckminsterfullerene. *Nature*, 318 (6042), pp. 162-163.
- Kybert, N. J., Lerner, M. B., Yodh, J. S., Preti, G., and Johnson, A. C. (2013). Differentiation of Complex Vapor Mixtures using Versatile DNA-carbon Nanotube Chemical Sensor Arrays. *ACS Nano*, 7(3), 2800-2807.
- Miyato, Y. (2011). Basics of Carbon Nanotube and Its Applications. *Journal of MMIJ*, 127(2), 61-68.
- Novoselov, K. S., Geim, A. K., Morozov, S. V., Jiang, D., Zhang, Y., Dubonos, S. V., and Firsov, A. A. (2004). Electric Field Effect in Atomically Thin Carbon Films. *Science*, 306(5696), 666-669.
- Novoselov, K. S., Geim, A. K., Morozov, S. V., Jiang, D., Katsnelson, M. I., Grigorieva, and Firsov, A. A. (2005). Two-dimensional Gas of Massless Dirac Fermions in Graphene. *Nature*, 438(7065), 197-200.
- Omachi, H., Nakayama, T., Takahashi, E., Segawa, Y., & Itami, K. (2013). Initiation of Carbon Nanotube Growth by well-defined Carbon Nanorings. *Nature Chemistry*, 5(7), 572-576.
- Park, J., Kim, Y., Kim, G. T., and Ha, J. S. (2011). Facile Fabrication of SWCNT/SnO<sub>2</sub> Nanowire Heterojunction Devices on Flexible Polyimide substrate. *Advanced Functional Materials*, 21(21), 4159-4165.
- Pesin, D., and MacDonald, A. H. (2012). Spintronics and Pseudospintronics in Graphene and Topological Insulators. *Nature materials*, 11(5), 409-416.
- Tanigaki, K., Ebbesen, T. W., Saito, S., Mizuki, J., Tsai, J. S., Kubo, Y., and Kuroshima, S. (1991). Superconductivity at 33 K in CsxRbyC<sub>60</sub>. *Nature*, 352(6332), 222-223.
- Zhang, Y., Tan, Y. W., Stormer, H. L., & Kim, P. (2005). Experimental observation of the quantum Hall effect and Berry's phase in graphene. *nature*, 438(7065), 201-204.

## **PREPARATION AND APPLICATION OF ORGANIC FERTILIZERS FROM VEGETABLE WASTES, COW DUNG, SESAME MEAL CAKE AND EFFECTIVE MICROORGANISM SOLUTIONS**

Tin Tin Sein,<sup>1</sup> Kyu Kyu Maw,<sup>2</sup> Soe Tun Myaing<sup>3</sup>

### **Abstract**

Organic fertilizers were prepared from the selected materials such as wastes of vegetables, cow dung, sesame meal cake, rice straw and the prepared EM solution under aerobic and anaerobic conditions. To know the effect of lime on the prepared fertilizers, quick lime powder was used. The aerobic digesters (4' × 6' × 0.75') were used in aerobic conditions. The anaerobic digesters (11.5" × 13.5") were used in anaerobic conditions. The successive layers of selected materials were done and prepared EM solution was added over the layers. Organic fertilizers were performed by composting. The elemental contents of prepared organic fertilizers were determined by Energy Dispersive X-Ray Fluorescence (EDXRF) spectroscopic method. The physical properties, the moisture contents and pH values of prepared organic fertilizers were determined. The total nitrogen, total phosphorus and total potassium contents of the prepared organic fertilizers were determined by instrumental methods. The amount of organic carbon and organic matter of the prepared organic fertilizers were also determined. The properties of prepared aerobic organic fertilizers were compared with anaerobic organic fertilizers. To show the effect of the prepared organic fertilizers, the plantations on those of vegetables such as Chinese cabbage, lettuce and radish were carried out by using four kinds of prepared organic fertilizers and the plant growth was compared.

**Keywords:** organic fertilizer, effective microorganism solution, vegetable wastes, sesame meal cake, aerobic condition

### **Introduction**

Generally, both organic and inorganic fertilizers are used for the cultivation of vegetables. With the escalating interest in organic vegetable cultivation due to its health and environmental benefits both locally and globally, intensified research on all aspects of organic farming is timely and urgent (Vimala *et al.*, 2010).

One of the main goals of every organic farmer is to build long-term soil fertility and tilth by feeding the soil with a variety of natural amendments. The regular addition of compost is one of the best ways to enhance soil organic and humic content, which helps to build a fertile soil structure. Such as soil structure makes better use of water and nutrients. It is easier to till and, overall, is better able to achieve optimum yields on a long-term basis (Baldwin and Jackie, 2006).

Compost, as a product of recycling processes, can be a very appropriate input material for organic farming, provided the composting process is well-managed, the input materials are free of contaminants, and the resulting product is applied according to the system's ecological needs (Streminska and Raviv, 2016).

High-quality compost is one of the essential organic matter inputs, along with green manures, used to manage soil health in organic farming and gardening systems (Miles, 2015).

Compost “happens” either aerobically (with oxygen) or an aerobically (without oxygen) when organic materials are mixed and piled together (Cooperband, 2002).

---

<sup>1</sup> Dr, Lecturer, Department of Chemistry, University of Magway

<sup>2</sup> Dr, Lecturer, Department of Chemistry, University of Magway

<sup>3</sup> Dr, Lecturer, Department of Chemistry, University of Magway

Composting is a natural process in which fresh organic matter (animal manure, food wastes, green wastes, agricultural residues, etc.) is transformed into more stable humus-like substances, nutrients are being recycled and energy is being produced (Streminska and Raviv, 2016).

EM has a great potential to be used in accelerating the composting process and increased nutrient in compost. Microorganisms (EM) is a mixture of organisms that has a reviving action on humans, animals, and the natural environment. (Mayer *et al.*, 2010). Application of EM in composting of organic matter showed positive result in the decomposition process and the mineralization. EM controls the temperature and reduces pathogens in the compost to produce good quality of compost (Saravanan *et al.*, 2013). EM compost had fast decomposition rate, rich in nutrients, more microbial activities, good germination and more yields compared with compost without EM (Khan and Ishaq, 2011). The aim of this research is to prepare the organic fertilizers from vegetable wastes cow dung, sesame meal cake and EM solutions under different conditions and to apply the prepared organic fertilizers on cultivation of some vegetables.

## Materials and Methods

### Sample Collection

Vegetable waste was collected from local market, Chanmyatharsi Township, Mandalay Region. Cow dung and rice straw were collected from Taung Pyone Village, Madaya Township, Mandalay Region. Sesame meal cake was collected from Local market, Mandalay Region. Slaked lime solution (pH 9.5) was prepared and added into vegetable waste (Figure1).

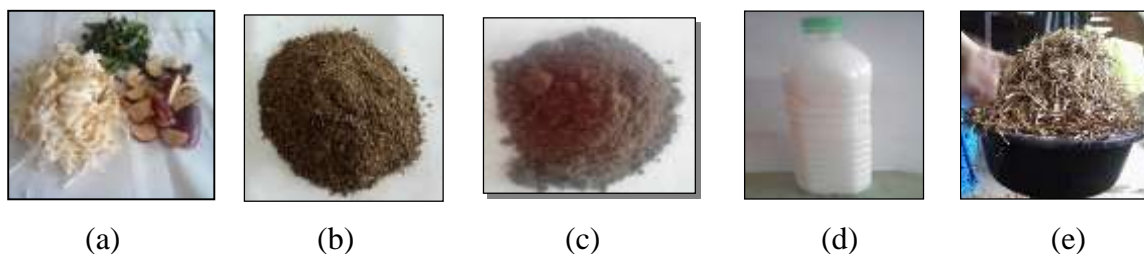


**Figure 1** (a) Vegetable waste, (b) Cow dung powder, (c) Sesame meal cake, (d) Slaked lime solution and (e) Rice straw

### Preparation of Effective Microorganism Solutions

1 kg of fresh small pieces of vegetable waste, 1 kg of cow dung and 1 kg of sesame meal cake were put into the anaerobic digester by successive layers and one liter of purified water was added into the anaerobic digester. The neck of the digester was entwined with teflon. It was tightly sealed with the lid connecting delivery tube (pipe). While the preparation of effective microorganism solutions, biogas was evolved. After the production of biogas for 5 days, the anaerobic digester was tightly sealed and kept for one month (Figure 2). After one month, the mixture in the anaerobic digester can be used as EM solution.



**Figure 2** Preparation of EM solution by anaerobic digester

**Preparation of Organic Fertilizers**

**Sampling**

Vegetable waste samples were cut into small pieces about one inch. Sesame meal cake were ground to get powder samples. The cow dung sample was pounded and sieved with 60 mesh sieve to get powder. Rice straw samples were cut into small pieces.

**Preparation of organic fertilizers under aerobic conditions**

2 kg of rice straw, 2 kg of sesame meal cake, 500 mL of effective microorganism (EM) solution, 2 kg of vegetable wastes, and 2 kg of cow dung were put layer by layer and this layering process was done for two times. It was put into aerobic digester (4' × 6' × 0.75 ') and stored for two months (Figure 3)



Preparation of layer by mixing waste with EM

Layering process

**Figure 3** Procedure of organic fertilizers under aerobic condition

**Turning over the sample under aerobic conditions**

During decomposition the layers were turned over regularly, in order that it remains well aerated and all the materials were converted into compost. The first turning over was done after two weeks. The second turning over took place after two weeks. Then each turning over was done after one week. If necessary, water was sprinkled over the container during the process. After two months, decomposition was complete because the plant materials were changed into an unrecognizable crumbly dry mass. However, some stalks do not decompose completely and can still be seen (Figure 4).



After two weeks

After four weeks

After six weeks

After eight weeks

**Figure 4** Changes of prepared organic fertilizers during eight weeks

### Preparation of organic fertilizer under anaerobic condition

For anaerobic condition, 11.5" inches diameter and 13.5" height of plastic container with lid having same capacity was used in aerobic condition and tightly closed (Figure 5). 1 kg of rice straw, 1 kg of sesame meal cake, 500 mL of EM solution, 1 kg of vegetable wastes and 1 kg of cow dung were weighed and put layer by layer into anaerobic digester with lid and highly sealed to get compost for two months.

Four organic fertilizers were prepared under different conditions.

- (i) aerobic conditions by the use of lime and without lime (prepared organic fertilizers, POF A1 and A2).
- (ii) anaerobic conditions by the use of lime and without lime (prepared organic fertilizers POF An1 and An2).



**Figure 5** Preparation of anaerobic organic fertilizers

### Some Parameters of Prepared Organic Fertilizers

#### Determination of pH

About 25 g of sample was weighed accurately and placed into a bottle and 100mL of distilled water was added and then the pH of prepared organic fertilizers was measured by pH meter.

#### Determination of moisture content

Accurately weighed 10 g of sample powder was added into a Petri dish previously dried and cooled in a desiccator. The dish containing the sample was placed in an oven and dried for 30 min at  $101^{\circ}\text{C} \pm 1^{\circ}\text{C}$ . The dish was then removed from the oven and cooled in a desiccator at room temperature and weighed. It was repeated until constant weight was obtained.

#### Determination of nutrients, organic carbon and organic matter

Total nitrogen, total  $\text{P}_2\text{O}_5$ , total  $\text{K}_2\text{O}$ , organic carbon and organic matter of the prepared organic fertilizers were determined at Department of Agriculture (Land Use), Mandalay by using Atomic Absorption Spectroscopic method and Walkey and Polack's Methods.

#### Determination of Elemental Analysis of Prepared Organic Fertilizer

Elemental analysis of prepared organic fertilizers was measured at Department of Chemistry, Monywa University by applying EDXRF (Energy Dispersive X-Ray Fluorescence Spectroscopy) Method.

#### Determination of Plant Height of Three Vegetables by Using Prepared Organic Fertilizers

Organic farming was carried out by using prepared organic fertilizer (POF A1, POF A2, POF An1, POF An2) for selected vegetable such as Chinese cabbage, lettuce and radish. To evaluate

the effect of prepared organic fertilizers on the plants, plant heights of 10 plants for each were recorded and mean heights of those were determined after 45 days plantation.

## Results and Discussion

### Preparation of Organic Fertilizers Under Different Conditions

Under aerobic condition and anaerobic conditions; vegetable wastes, cow dung, sesame meal cake, rice straw and the prepared EM solution with lime and without lime were used to prepare organic fertilizers (POFA1, POFA2, POFAn1 and POFAn 2).

### Some Parameters of Prepared Organic Fertilizers Under Different Conditions

According to the results as shown in Table 1, all prepared organic fertilizers were alkaline. The moisture content was the highest 7.5% in POF A1. The moisture contents of fertilizers in anaerobic condition were found to be lower than aerobic conditions.

**Table 1 The pH Values and Moisture Contents of Prepared Organic Fertilizers with and without Lime Under Aerobic and Anaerobic Conditions**

Organic fertilizer	pH	Moisture (%)
POF A1	9.0	7.45
POF A2	8.5	6.38
POF An1	8.5	5.41
POF An2	8.0	5.37

POF A1 = Prepared organic fertilizer with lime under aerobic condition  
 POF A2 = Prepared organic fertilizer without lime under aerobic condition  
 POF An1 = Prepared organic fertilizer with lime under anaerobic condition  
 POF An2 = Prepared organic fertilizer without lime under anaerobic condition

### Nutrient Parameters of Prepared Organic Fertilizers

Total nitrogen content in POFAn1 and POFAn2 were greater than those in POF A1 and POFA2. Nitrogen content is effective to promote plant growth especially stem and leaf. The highest content of total  $P_2O_5$  (4.91%) were coincidentally same in POFAn1 and POFAn2 whereas the content of  $K_2O$  (%) in all fertilizers were found to be ranged between 1.31-1.99%. Organic carbon (27.23%) and matter (49.64%) of POFAn1 were found to be the highest out of four different organic fertilizers. The results are shown in Table 2 and Figures 6 and 7.

**Table 2 Nutritional Values of Prepared Organic Fertilizers**

Nutrient	Aerobic Organic Fertilizer		Anaerobic Organic Fertilizer	
	POF A1	POF A2	POF An1	POF An2
Total Nitrogen (%)	2.01	1.64	2.44	2.52
Total $P_2O_5$ (%)	2.44	1.85	4.91	4.91
Total $K_2O$ (%)	1.78	1.99	1.31	1.89
Organic carbon (%)	17.28	16.58	27.23	25.08
Organic matter (%)	29.80	28.59	49.64	43.24

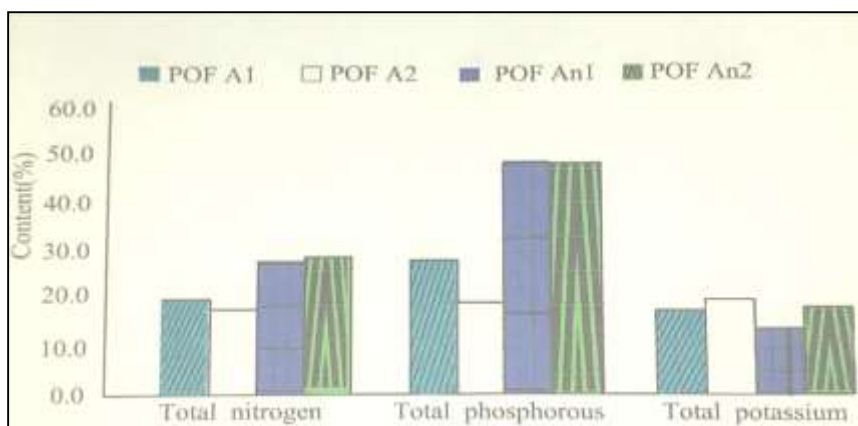


**Figure 6** Total ( NPK ) content of prepared organic fertilizers

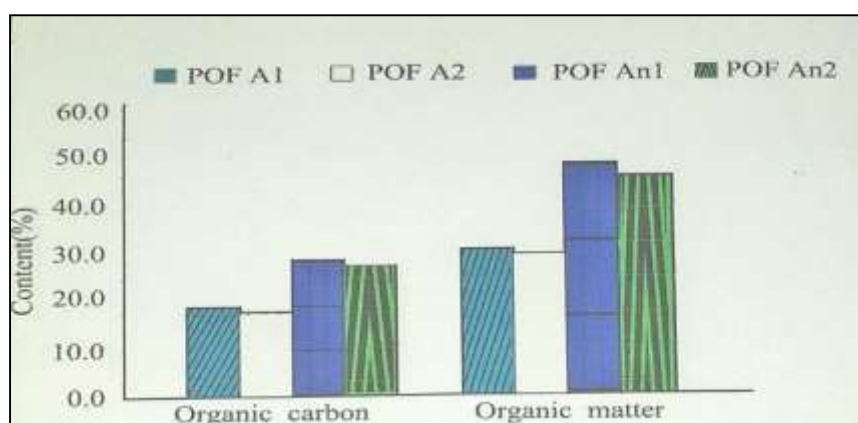


**Figure 7** Organic carbon and organic matter content of prepared organic fertilizers

**Elemental Analysis of Prepared Organic Fertilizers**

Elemental composition of prepared organic fertilizers analyzed by EDXRF are presented in Table 3 and shown in Figure 8. Silicon was found to be the highest followed by calcium, potassium and manganese in all prepared organic fertilizers. The essential elements for plant growth such as P, S, Fe, Mn and Cu were also detected in prepared organic fertilizers.

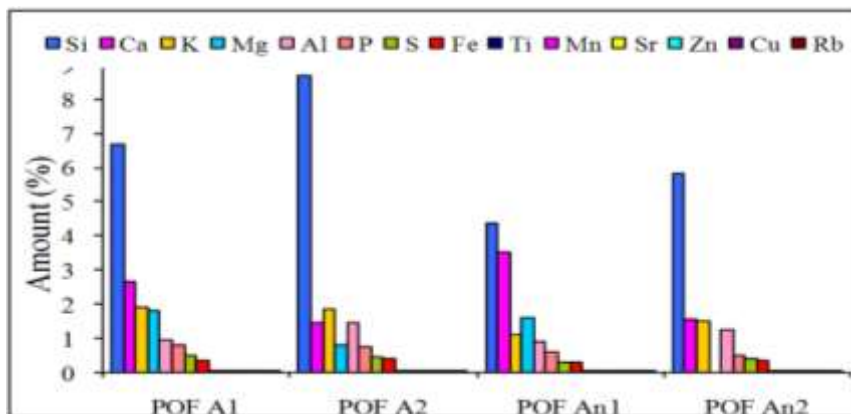


**Figure 8** Elemental contents of different prepared organic fertilizers

**Table 3 Relative Abundance of Elements in Different Organic Fertilizers by EDXRF**

No.	Elements	Relative Abundance (%)			
		POF A1	POF A2	POF An1	POF An2
1	Si	6.685	8.677	4.351	5.828
2	Ca	2.675	1.441	3.532	1.537
3	K	1.892	1.883	1.120	1.505
4	Mg	1.820	0.810	1.589	-
5	Al	0.969	1.457	0.910	1.279
6	P	0.829	0.756	0.610	0.521
7	S	0.510	0.450	0.319	0.402
8	Fe	0.370	0.397	0.311	0.350
9	Ti	0.035	0.048	0.045	0.056
10	Mn	0.026	0.026	0.020	0.019
11	Sr	0.007	-	0.007	0.007
12	Zn	0.006	0.005	0.006	0.005
13	Cu	0.004	0.004	0.004	0.003
14	Rb	0.004	-	-	-
15	Zr	-	0.006	0.005	0.005
16	Cr	-	0.004	-	0.003

**Plant Height of Three Vegetables by Using Different Organic Fertilizers**

This data was recorded from 10 Chinese cabbage planted by prepared organic fertilizers after 45 days. In Table 4, the plant height of chinese cabbage grown on POFAn1 was found to be the highest. The control under same condition was comparatively studied.

**Table 4 Plant Height of Chinese Cabbage after 45 days Plantation by Different Organic Fertilizers**

Sample	Plant Height (inches)				
	POFA1	POFA2	POFAn1	POFAn2	Control
1	10.50	9.50	10.00	11.00	9.50
2	11.00	10.00	10.00	11.00	9.50
3	11.00	10.50	11.50	11.50	9.50
4	11.00	10.50	12.00	11.50	10.00
5	12.00	10.50	12.00	12.00	11.00
6	12.00	10.50	12.00	12.00	11.00
7	12.00	10.50	12.00	12.00	11.50
8	12.00	10.50	12.00	12.00	11.50
9	12.00	11.50	12.00	12.00	11.50
10	13.00	12.00	12.00	12.00	12.00
Mean ± SD	11.65 ± 1.17	10.60 ± 0.72	11.80 ± 0.69	11.70 ± 0.42	10.75 ± 0.39

This data was recorded from 10 plants of lettuce. According to Table 5, plant height of lettuce cultivated by using POFAn1 was found to be the highest followed by POF A2.

**Table 5 Plant Height of Lettuce after 45 days Plantation by Different Organic Fertilizers**

Sample	Plant Height (inches)				
	POFA1	POFA2	POFAn1	POFAn2	Control
1	6.50	7.50	7.00	7.00	5.00
2	7.50	8.00	7.00	7.50	6.00
3	8.00	8.00	7.50	8.00	7.00
4	8.00	8.00	7.50	8.00	7.00
5	8.00	8.00	8.00	8.00	7.50
6	8.50	8.50	8.50	8.50	7.50
7	8.50	8.50	8.50	8.50	7.50
8	9.00	9.00	8.50	8.50	8.00
9	9.00	9.00	9.00	9.00	8.00
10	9.00	10.00	9.00	9.00	8.00
Mean ± SD	8.20 ± 0.40	8.45 ± 0.74	8.50 ± 0.68	8.20 ± 0.63	7.15 ± 0.89

This data was recorded from 10 plants of radish. According to Table 6, plant height of radish by using POFAn1 was found to be the highest and control was found to be the lowest.

**Table 6 Plant Height of Radish after 45 days Plantation by Different Organic Fertilizers**

Sample	Plant height (inches)				
	POFA1	POFA2	POFAn1	POFAn2	Control
1	13.00	10.50	12.00	11.50	9.00
2	13.00	11.00	12.50	12.00	9.50
3	13.00	11.50	13.00	12.00	9.50
4	13.00	11.00	13.00	12.50	10.00
5	13.00	12.00	13.00	13.00	10.00
6	13.00	12.00	13.50	13.00	10.50
7	13.00	13.00	13.50	14.00	11.00
8	13.00	14.00	13.50	14.00	11.00
9	13.50	15.00	14.00	14.50	11.50
10	14.00	16.00	15.00	15.00	12.00
Mean ± SD	12.95 ± 0.40	13.00 ± 1.9	13.30 ± 0.82	13.15 ± 1.31	10.40 ± 1.05

Plant heights of vegetables: Chinese cabbage, lettuce and radish with control were comparatively recorded after 45 days cultivation. Among these, POFAn1 prepared from organic fertilizer with lime under anaerobic condition was found to have the maximum plant height 11.80inches (Chinese cabbage), 8.5inches (lettuce) and 13.30inches (radish), respectively (Figures 9, 10 and 11). Plot sites of three vegetable cultivation using different organic fertilizers after 45 days were also presented in Figures 12, 13 and 14.

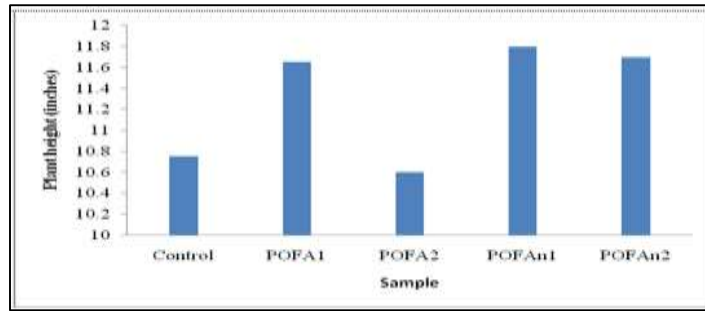


**Figure 9** Comparison of plant height on different organic fertilizers (Chinese cabbage)

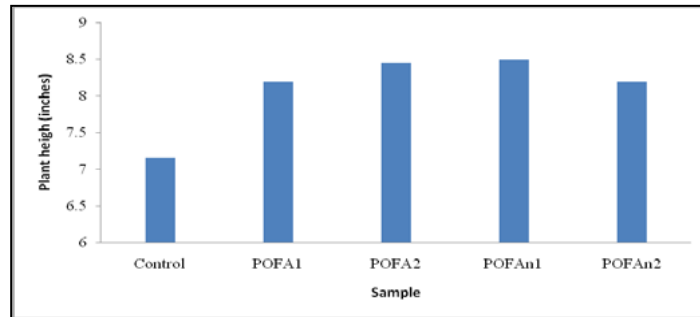


**Figure 10** Comparison of plant height on different organic fertilizers (lettuce)

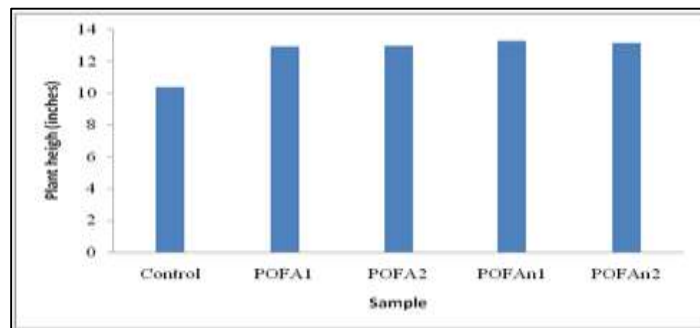


**Figure 11** Comparison of plant height on different organic fertilizers (radish)



**Figure 12** Plots of Chinese cabbage cultivation by using (I) POFA1, (II) POFA2, (III) POFAn1 and (IV) POFAn2

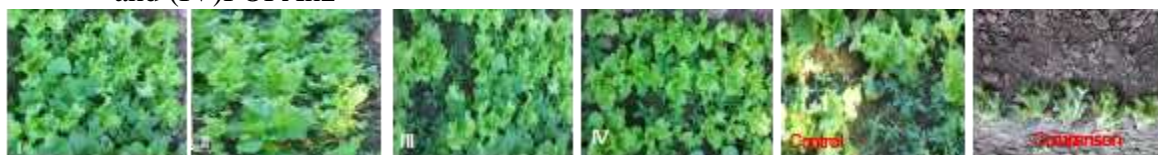


**Figure 13** Plots of lettuce cultivation by using (I) POFA1, (II) POFA2, (III) POFAn1 and (IV) POFAn2



**Figure 14** Plots of radish cultivation by using (I) POFA1, (II) POFA2, (III) POFAn1 and (IV) POFAn2

## Conclusion

Four different organic fertilizers (POFA1, POFA2, POFAn1 and POFAn2) were prepared from the wastes of vegetables, cow dung, sesame meal cake, the prepared EM solution and rice straw with lime and without lime under aerobic condition and anaerobic condition. From the elemental analysis, the essential trace elements such as silicon, calcium, potassium, aluminium, phosphorous, sulfur, iron, titanium, manganese, zinc and copper were found in all prepared organic fertilizers. The pH of the organic fertilizers were found to be alkaline (8.0-9.0). The moisture contents of the fertilizers were the range of 5.37-7.45 %. The total nitrogen contents of the prepared organic fertilizers were found to be the range of 1.64-2.01 % for aerobic condition and 2.44-2.52 % for anaerobic condition. The total phosphorus contents of the prepared organic fertilizers were found to be the range of 1.85-2.44 % for aerobic condition and 4.91 % for anaerobic condition. The total potassium contents of the prepared organic fertilizers were found to be the range of 1.78-1.99 % for aerobic condition and 1.31-1.89 % for anaerobic condition. The amount of organic carbon and organic matter were the range of 16.58-17.28 %, 25.08-27.73 % for aerobic condition and 28.59-29.80 %, 43.24-49.64 % for anaerobic condition. All prepared organic fertilizers contain adequate amount of nutritional values and should be applied for organic farming. The plantation of vegetables such as Chinese cabbage, lettuce and radish by using prepared organic fertilizers was carried out and the plant growth were compared after 45 days of plantation. It was found that plant heights of Chinese cabbage (11.8 inches), lettuce (8.5 inches) and radish (13.3 inches) in plot 4 by using POF An1 are higher than other plots. From the observation, using POFAn1 can support more plant growth than others for selected vegetables. POFAn1 can supply more organic carbon (27.73%) and organic matter (49.64%) than that of others to the soil and plants.

Therefore, anaerobic condition should be selected for the mass production of organic fertilizer. The organic fertilizer should be used widely in agriculture instead of /mixed with chemical fertilizer because of their low cost, good fertility of the soil and supplying more trace elements. The obvious advantages of the prepared organic fertilizer are economically viable, convenient and effective. Therefore, prepared organic fertilizer has great potential for applications.

## Acknowledgements

The authors would like to thank the Myanmar Academy of Arts and Science for allowing to present this paper and Professor and Head Dr Thidar Aung, Department of Chemistry, Magway University for her kind encouragement.

## References

- Baldwin, K. R. and Jackie, T. (2002). "Composing on Organic Farm", *The Family Streptomycetaceae, Part I: Taxonomy, In Dworkin, Martin; Falkow, Stanley; Rosenbergy, Eugene; Schleifer, Karl-Heins; Stackebrandt, Erko. The Prokaryotes*, pp.538-604.
- Cooperband, L. (2002). *The Art and Science of Composting*, Center for Integrated Agricultural Systems, University of Wisconsin-Madison, United State, pp.1-17
- Khan, A and F. Ishaq. (2011.) "Chemical Nutrient Analysis of Different Composts (Vermicompost and Pitcompost) and Their Effect on the Growth of a Vegetative Crop Pisumsativum", *Asian Journal of Plant Science and Research*, vol.1 (1), pp. 116-130.
- Mayer, J., S. Scheid., F. Widmer., A. Fliebach and H. R. Oberholzer. (2010). How effective are Effective Microorganisms (EM) , Results from a Field Study in Temperate Climate, *Applied Soil Ecology*, 46(2), pp. 230-239.
- Miles, A. (2015). *Making and Using Compost, A Project for the Center of Agroecology & Sustainable Food Systems (CASFS)*, University of California, United State
- Saravanan, P., S. S. Kumar and C. Ajithan. (2013). "Eco-friendly Practice of Utilization of Food Wastes". *International Journal of Pharmaceutical Sciences Innovation*, pp.14-17
- Streminska, M.A. and Raviv, M. (2016)."Handbook for Composting and Compost Use in Organic Horticulture". *BioGreenhouse COST Action FA 1105*. ISBN: 978-94-6257-749-7, pp. 45-51.
- Vimala, P. Roff, M.N.M., Shokri, O.A. and Lim, A.H. (2010). "Effect of Organic Fertilizer on the Yield and Nutrient Content of Leaf-mustard (*Brassica juncea*) Organically Grown under Shelter, *J.Trop.Agric.and Fd.Sc.*vol. 38(2). pp. 153-160

## SYNTHESIS AND CHARACTERIZATION OF FULLERENE FROM GRAPHITE ORE

Chit Chit Maw<sup>1</sup>, Yi Yi Myint<sup>2</sup>

### Abstract

This research work concerned with synthesis and characterization of fullerene from graphite ore. The graphite ore was collected from Thabeikkyin Township, Mandalay Region. The synthesis of fullerene was carried out by Modified Hummer's method in which graphite powder was oxidized with the help of oxidizing agent H<sub>2</sub>SO<sub>4</sub> and KMnO<sub>4</sub>. Moreover, the various amounts of NaNO<sub>3</sub>, H<sub>3</sub>PO<sub>4</sub>, KMnO<sub>4</sub> and H<sub>2</sub>SO<sub>4</sub> were used to produce fullerene. The crystal lattice size of graphite and fullerene were characterized by X-ray diffraction (XRD). The prepared fullerenes were analysed by Thermo gravimetric analysis (TG-DTA). The morphology of the graphite and the synthesized fullerene were investigated by scanning electron microscope (SEM).

**Keywords:** Graphite, Fullerene, Hummer's method, XRD, TG-DTA, SEM

### Introduction

The prefix "nano" has found in last decade on ever-increasing application to different fields of the knowledge. Nanoscience, nanotechnology, nanomaterials or nanochemistry are only a few of the new nano-containing terms. The nanosized world is typically measured in nanometers (1 nm=10<sup>-9</sup> m) (Hahens *et al.*, 2007).

Nowadays, nanotechnology research is developed as a cutting-edge interdisciplinary technology involving chemistry, physics, material science, biology and medicine (Roco, 2004). Nanomaterials and nanoparticles exhibit high strength, high thermal stability, low permeability and high conductivity properties, among other unique properties which stimulate the scientific commonly to focus their research on developing new applications and products related to nanotechnology. Nanoparticles are 1 nm to 100 nm in size. They have very small sizes and large surface area to volume ratios. Their atoms may also be arranged into tubes or rings. Carbon can form nanoparticle stimulates with a variety of shapes (Fears *et al.*, 2011).

Graphite is a crystalline form of carbon, a native element mineral and one of the allotropes of carbon. Graphite is the most stable form of carbon under standard conditions. Graphite occurs in metamorphic rocks. Minerals associated with graphite include quartz, calcite, micas and tourmaline (Anthony *et al.*, 1990).

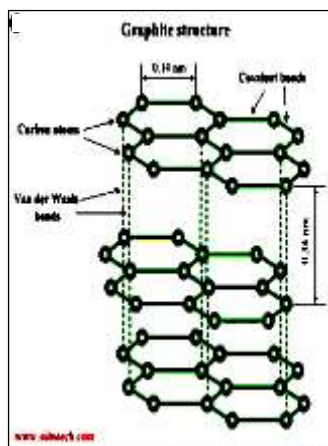
The fullerenes are the third allotrope of carbon after graphite and diamond. Each molecule of fullerene family (C<sub>n</sub>) consists of 12 pentagons and m number of hexagons conforming to the relation  $m = (n-20/2)$  (Euler's theorem). C<sub>60</sub> fullerene was produced from a graphite (Dietz *et al.*, 1981). The most abundant form of fullerenes is Buckminster fullerene (C<sub>60</sub>) with 60 carbon atoms arranged in a spherical structure (Kratschmer *et al.*, 1990). It contains 12 pentagons and 20 hexagons. The pentagonal rings contain only single bonds (Hawkins *et al.*, 1991).

Fullerenes are used in a wide range of applications such as in optical and electronic devices (polymer additives, solar cells, photovoltaic) (Kronholm and Hummelen, 2007), in commercial cosmetic products (Xiao *et al.*, 2005), and in biomedicine (antiviral, anti-cancer, and antioxidant agents, in drug delivery systems) (Tagmatarchis and Shinohara, 2001). The aim of this research work is to synthesize and characterize fullerene from graphite ore.

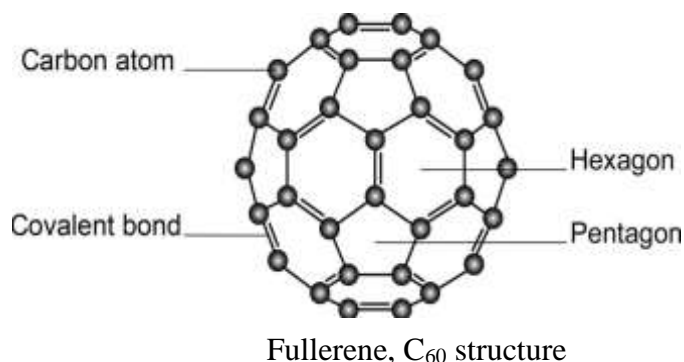
---

<sup>1</sup> Lecturer, Department of Chemistry, Meiktila University

<sup>2</sup> Dr, Professor and Head, Department of Chemistry, University of Mandalay



Graphite structure

Fullerene, C<sub>60</sub> structure

## Materials and Methods

### Sample Collection

The graphite ore was collected from Thabeikkyin Township, Mandalay Region. The graphite ore was ground to get the powder. The graphite powder samples were stored in a well-stoppered bottle and used through out this research and presented in Figure 1.

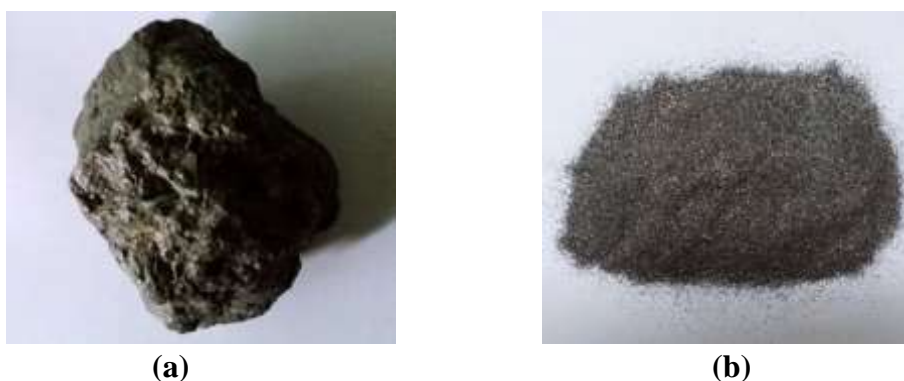


**Figure 1** (a) Graphite ore (b) Graphite powder

### Preparation of Fullerene from Graphite with NaNO<sub>3</sub>, KMnO<sub>4</sub> and H<sub>2</sub>SO<sub>4</sub> by Modified Hummer's Method under Different Conditions

#### Preparation of fullerenes (C-1) and (C-2) from graphite with NaNO<sub>3</sub>, KMnO<sub>4</sub> and H<sub>2</sub>SO<sub>4</sub>

A 0.5 g of graphite powder sample and 0.25 g of sodium nitrate were mixed and stirred in ice bath by using magnetic stirrer. 20 mL of concentrated sulphuric acid and 2.0 g of potassium permanganate were added into the solution. The solution was stirred for 1 h. After stirring 1 h, this solution was removed from ice bath and again stirred for 3 h at room temperature. Then, 50 mL of distilled water was added into the solution and stirred for another 1 h at room temperature. 50 mL of hot water and 7.5 mL of 30 % hydrogen peroxide were added into the solution. The solution was stirred for 1 h at room temperature. Bright yellow color solution was obtained. This solution was centrifuged and the precipitate was collected and washed with 5 % hydrochloric acid and then with distilled water until it became neutral. Fullerene (C-1) was obtained.

The fullerene (C-2) was also prepared according to the same procedure as (C-1) preparation. However, the stirring time 3 h and sonication time 3 h were taken for preparation of C-2.

### Preparation of Fullerene from Graphite with H<sub>3</sub>PO<sub>4</sub>, KMnO<sub>4</sub> and H<sub>2</sub>SO<sub>4</sub> by Modified Hummer's Method under Different Conditions

#### Preparation of fullerenes (C-3) and (C-4) from graphite with H<sub>3</sub>PO<sub>4</sub>, KMnO<sub>4</sub> and H<sub>2</sub>SO<sub>4</sub>

A 0.25 g of graphite powder sample and 27 mL of concentrated sulphuric acid and 3 mL of phosphoric acid were mixed and stirred in ice bath by using magnetic stirrer. 1.32 g of potassium permanganate was slowly added to this solution and stirred for 1 h. After stirring 1 h, this solution was removed from ice bath and again stirred for 5 h at room temperature. Then dark green solution was obtained. 1 mL of hydrogen peroxide was added drop by drop and stirred for 0.5 h at room temperature. 10 mL of concentrated HCl and 30 mL of deionized water were added into the solution. This solution was centrifuged. The resultant precipitate was washed with 5 % HCl and distilled water until neutral. Finally, fullerene was obtained.

The fullerene (C-4) was prepared according to the same procedure of (C-3). However, the stirring time 9.5 h was taken for preparation of C-4.

## Results and Discussion

Fullerene nanoparticles were synthesized from graphite ore by modified Hummer's method. The preparation of fullerene nanoparticles were performed under four different conditions. And the graphite ore powder and prepared fullerene nanoparticles were characterized by advanced methods such as XRD, TG DTA and SEM.

### Characterization of Graphite Ore and Prepared Fullerene by XRD

The graphite ore powder was characterized by XRD and the chromatogram and results are presented in Figure 2 and Table 1-2. According to the results, the graphite sample shows a sharp peak ( $2\theta = 26.141^\circ$ ) which corresponds to the diffraction line (002) with the intercellular spacing in the crystal (d) respectively is 3.4061. The range of particle size of graphite were found to be 152.76-855.98 nm and average particle size is 490.47 nm. Phase ID reported that graphite sample was graphite 2H. According to graphite grading HB scale, the collected graphite ore sample was found to be hard

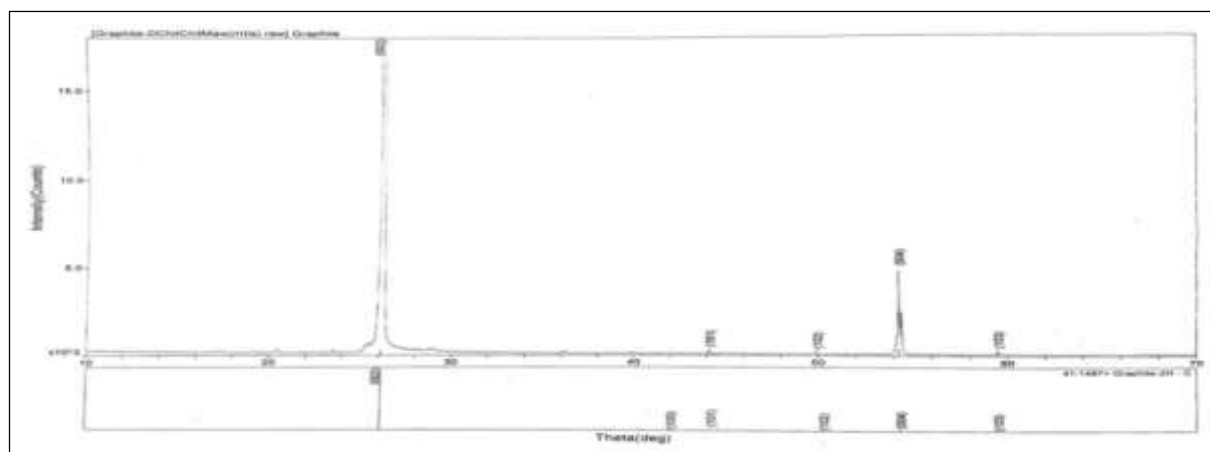


**Table 1 The Results from XRD Pattern of Graphite Ore**

Peak No.	Bragg angle ( $2\theta$ )	Miller indices (h k l)	FWHM of peak ( $\beta$ ) radians	Inter cellular spacing d (nm)	Particle size, D (nm)
1.	26.141	002	0.0018	3.4061	761.74
2.	44.129	101	0.0034	2.0505	435.12
3.	49.930	102	0.0099	1.8250	152.76
4.	54.270	004	0.0018	1.6889	855.98
5.	59.461	103	0.0064	1.5532	246.73

**Table 2 The Peak ID Report of Graphite Ore**

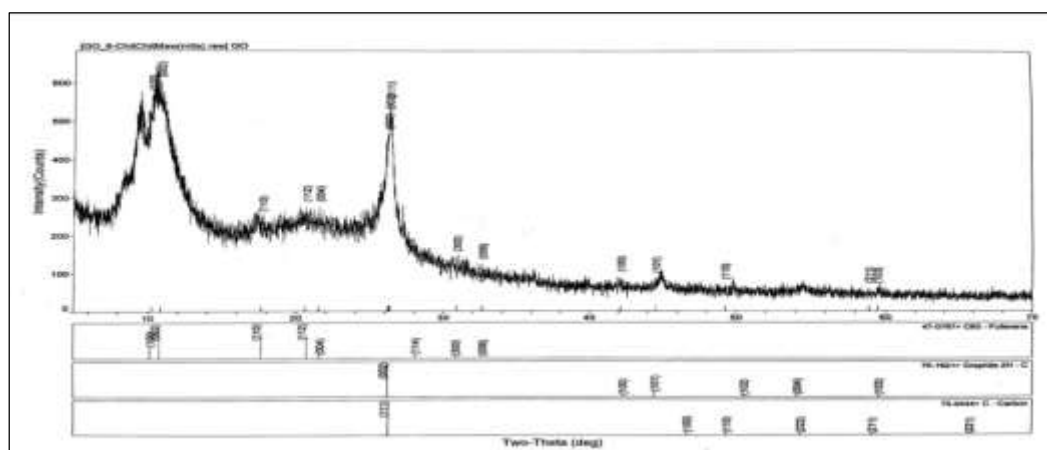
Peak No.	Bragg angle ( $2\theta$ )	Miller indices (h k l)	Area (%)	Phase ID
1.	26.141	002	100.0	Graphite 2H
2.	44.129	101	6.0	Graphite 2H
3.	49.930	102	1.0	Graphite 2H
4.	54.270	004	4.0	Graphite 2H
5.	59.461	103	1.0	Graphite 2H

Fullerene nanoparticles were synthesized by using  $H_2SO_4$ ,  $NaNO_3$ ,  $KMnO_4$ ,  $H_2O_2$ ,  $HCl$  and  $H_3PO_4$  under four different stirring times and shaking time. The highest yield of C-4 was 88.40 % followed by C-2, C-3 and C-1 as shown in Table 3.

**Table 3 Yield Percent of Fullerene (C-1 to C-4)**

No	Fullerene	Yield (%)
1	C-1	73.02
2	C-2	76.08
3	C-3	74.52
4	C-4	88.40

The prepared fullene (C-1 to C-4) were characterized by XRD and the results are presented in Figure 3-6 and Table 4-12.

**Figure 3 XRD diffraction pattern of fullerene (C-1)**

**Table 4 The Results from XRD Diffractogram of Fullerene (C-1)**

Peak No.	Bragg angle (2θ)	Miller indices (h k l)	FWHM of peak (β) radians	Particle size D (nm)
1.	10.218	(1 0 0)	0.0060	23.735
2.	10.840	(0 0 2)	0.0152	9.061
3.	17.651	(1 1 0)	0.0093	14.921
4.	20.621	(1 1 2)	0.0098	14.220
5.	21.530	(0 0 4)	0.0034	41.049
6.	30.888	(3 0 0)	0.0027	52.683
7.	32.650	(0 0 6)	0.0044	32.470

According to Table 4, the range of particle size of prepared fullerene (C-1) were found to be 9.061-52.683 nm and average particle size is 26.877 nm.

**Table 5 The Peak ID Report of Fullerene (C-1)**

Peak No.	Bragg angle (2θ)	Miller indices (h k l)	Area (%)	Phase ID
1.	10.218	(1 0 0)	20.6	C <sub>60</sub>
2.	10.840	(0 0 2)	97.5	C <sub>60</sub>
3.	17.651	(1 1 0)	14.5	C <sub>60</sub>
4.	20.621	(1 1 2)	18.7	C <sub>60</sub>
5.	21.530	(0 0 4)	6.6	C <sub>60</sub>
6.	30.888	(3 0 0)	3.2	C <sub>60</sub>
7.	32.650	(0 0 6)	5.5	C <sub>60</sub>

For C<sub>60</sub>, the localized peaks at 2θ = 10.218°, 10.840°, 17.651°, 20.621°, 21.530°, 30.888° and 32.650° that referred to plane reflections of (100), (002), (110), (112), (004), (300) and (006), respectively. According to Table 5, phase ID of prepared C-1 was confirmed as C<sub>60</sub> and should be fullerene.

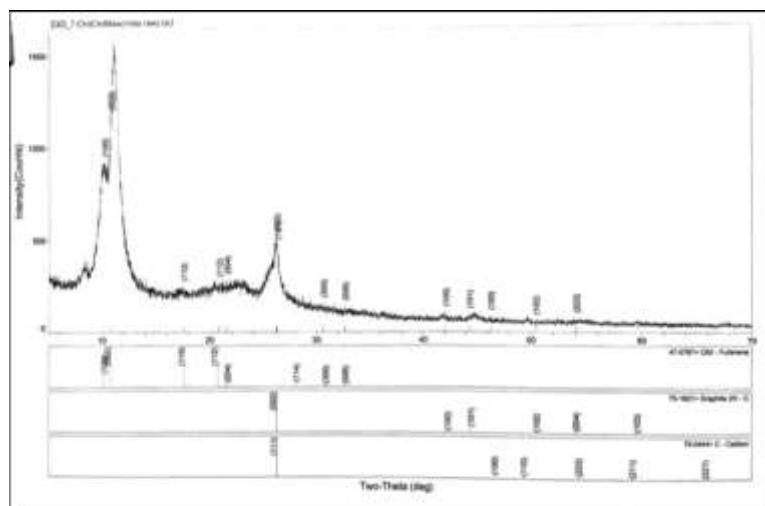


**Figure 4 XRD diffraction pattern of fullerene (C-2)**

**Table 6 The Results from XRD Diffractogram of Fullerene (C-2)**

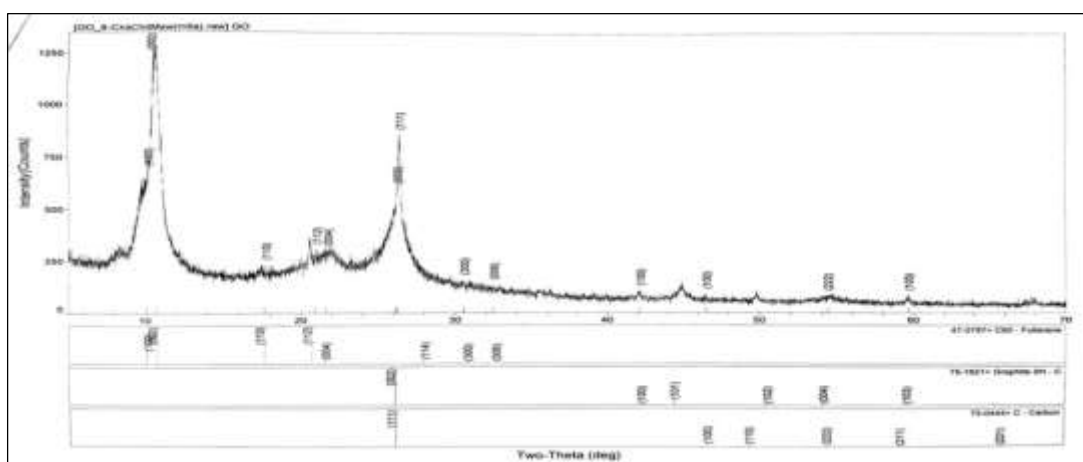
Peak No.	Bragg angle ( $2\theta$ )	Miller indices (h k l)	FWHM of peak ( $\beta$ ) radians	Particle size D (nm)
1.	10.220	(1 0 0)	0.0122	29.025
2.	10.841	(0 0 2)	0.0116	18.162
3.	17.550	(1 1 0)	0.0071	19.542
4.	20.831	(1 1 2)	0.0114	12.054
5.	30.638	(3 0 0)	0.0066	21.539
6.	32.668	(0 0 6)	0.0040	35.721

According to Figure 4 and Table 6, the range of particle size of prepared fullerene (C-2) were found to be 12.054-35.721 nm and average particle size is 27.829 nm.

**Table 7 The Peak ID Report of Fullerene (C-2)**

Peak No	Bragg angle ( $2\theta$ )	Miller indices (h k l)	Area (%)	Phase ID
1.	10.220	(1 0 0)	100.0	C <sub>60</sub>
2.	10.841	(0 0 2)	88.1	C <sub>60</sub>
3.	17.550	(1 1 0)	5.9	C <sub>60</sub>
4.	20.831	(1 1 2)	10.6	C <sub>60</sub>
5.	30.638	(3 0 0)	4.0	C <sub>60</sub>
6.	32.668	(0 0 6)	2.3	C <sub>60</sub>

For C<sub>60</sub>, the localized peaks at  $2\theta = 10.220^\circ$ ,  $10.841^\circ$ ,  $17.550^\circ$ ,  $20.831^\circ$ ,  $30.638^\circ$  and  $32.668^\circ$  that referred to plane reflections of (100), (002), (110), (112), (300) and (006), respectively. According to Table 7, prepared C-2 was confirmed as C<sub>60</sub> and should be fullerene.

**Figure 5 XRD diffraction pattern of fullerene (C-3)**

**Table 8 The Results from XRD Diffractogram of Fullerene (C-3)**

Peak No.	Bragg angle (2θ)	Miller indices (h k l)	FWHM of peak (β) radians	Particle size D (nm)
1.	10.150	(1 0 0)	0.0167	8.242
2.	10.750	(0 0 2)	0.0095	14.496
3.	17.655	(1 1 0)	0.0054	25.694
4.	20.906	(1 1 2)	0.0027	51.638
5.	21.632	(0 0 4)	0.0131	10.656
6.	30.533	(3 0 0)	0.0038	37.402
7.	32.470	(0 0 6)	0.0063	22.668

According to Figure 5 and Table 8, the range of particle size of prepared fullerene (C-3) were found to be 8.242-51.638 nm and average particle size is 24.399 nm.

**Table 9 The Peak ID Report of Fullerene (C-3)**

Peak No	Bragg angle (2θ)	Miller indices (h k l)	Area (%)	Phase ID
1.	10.150	(1 0 0)	51.4	C <sub>60</sub>
2.	10.750	(0 0 2)	100.0	C <sub>60</sub>
3.	17.655	(1 1 0)	3.8	C <sub>60</sub>
4.	20.906	(1 1 2)	2.2	C <sub>60</sub>
5.	21.632	(0 0 4)	9.5	C <sub>60</sub>
6.	30.533	(3 0 0)	1.8	C <sub>60</sub>
7.	32.470	(0 0 6)	3.0	C <sub>60</sub>

For C<sub>60</sub>, the localized peaks at 2θ = 10.150°, 10.750°, 17.655°, 20.906°, 21.632°, 30.533° and 32.470° that referred to plane reflections of (100), (002), (110), (112), (004), (300) and (006), respectively. According to Table 9, the phase purity of prepared C-3 was confirmed as C<sub>60</sub> and should be fullerene.

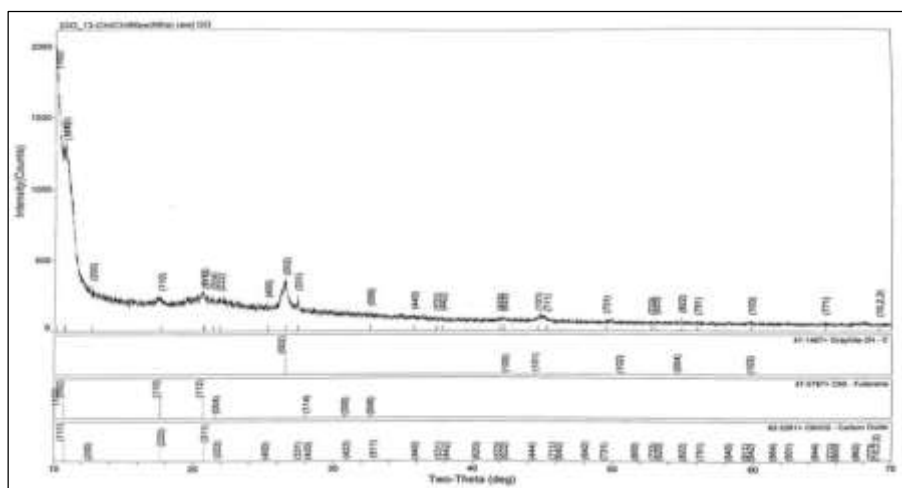


**Figure 6 XRD diffraction pattern of fullerene (C-4)**

**Table 10 The Results from XRD Diffractogram of Fullerene (C-4)**

Peak No.	Bragg angle ( $2\theta$ )	Miller indices (h k l)	FWHM of peak ( $\beta$ ) radians	Particle size D (nm)
1	10.180	1 0 0	0.0065	21.206
2	10.730	0 0 2	0.0099	13.910
5	17.606	1 1 0	0.0078	17.788
6	20.640	1 1 2	0.0086	16.205
8	21.332	0 0 4	0.0069	20.220
9	32.570	0 0 6	0.0068	21.007

According to Table 10, the range of particle size of prepared fullerene (C-4) were found to be 13.910-21.206 nm and average particle size is 18.389 nm.

**Table 11 The Peak ID Report of Fullerene (C-4)**

Peak No.	Bragg angle ( $2\theta$ )	Miller indices (h k l)	Area (%)	Phase ID
1	10.180	1 0 0	65.7	C <sub>60</sub>
2	10.730	0 0 2	99.8	C <sub>60</sub>
3	17.606	1 1 0	5.2	C <sub>60</sub>
4	20.640	1 1 2	7.4	C <sub>60</sub>
5	21.332	0 0 4	4.1	C <sub>60</sub>
6	32.570	0 0 6	2.6	C <sub>60</sub>

For C<sub>60</sub>, the localized peaks at  $2\theta = 10.180^\circ$ ,  $10.730^\circ$ ,  $17.606^\circ$ ,  $20.640^\circ$ ,  $21.332^\circ$ , and  $32.570^\circ$  that referred to plane reflections of (100), (002), (110), (112), (004) and (006), respectively. According to Table 11, prepared C-4 was confirmed as C<sub>60</sub> and should be fullerene. Average particle size for four prepared fullerenes (C-1 to C-4) are listed in Table 12. From these data the average particle size of prepared fullerene were nano.

**Table 12 Average Particle Size for Fullerene (C-1 to C-4)**

No.	Fullerene	Average Particle Size (nm)
1.	C-1	26.877
2.	C-2	27.829
3.	C-3	24.399
4.	C-4	18.389

**Thermal Stabilities of Prepared Fullerene by TG -DTA**

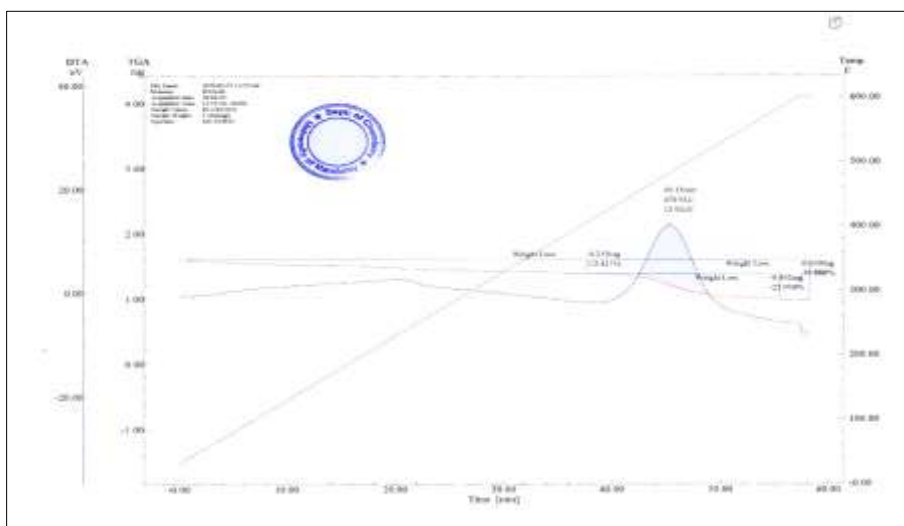
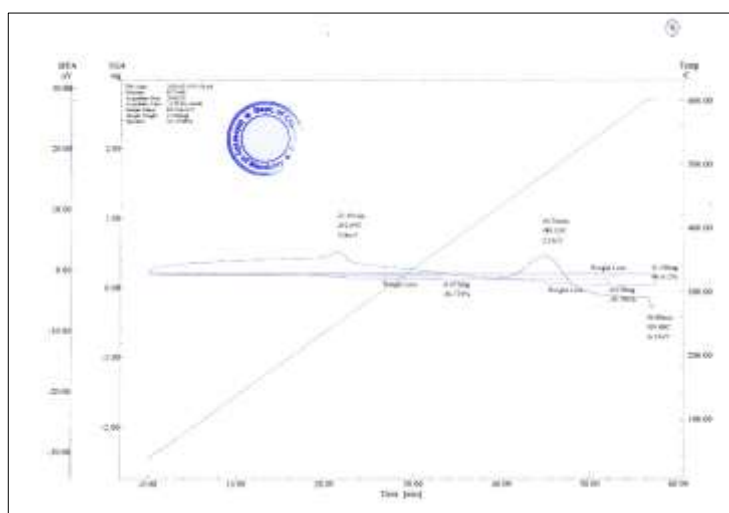


**Figure 7** TG-DTA thermogram of fullerene C-1

**Table 13** TG-DTA Analysis of Fullerene C-1

No.	Temperature (°C)	Weight loss (%)	Type of peak	Remark
1.	229.42	13.421	exothermic	Due to the loss of moisture and impurity
2.	479.91	39.888	exothermic	Break down of some bonds and degradation occur

According to Figure 7 and Table 13, the maximum degradation was found to be 479.91°C and the weight loss is 39.888 %. The thermal analysis of C-1 shows basically two mass loss steps (TG) with corresponding thermal events in the DTA curves. The first steps up to 229.42 °C show mass losses 13.421 % due to the physically adsorbed water on the material and impurity, probably occurred during storage. The second mass loss step (479.91 °C) may be the break down of some bonds and degradation of carbon skeleton.

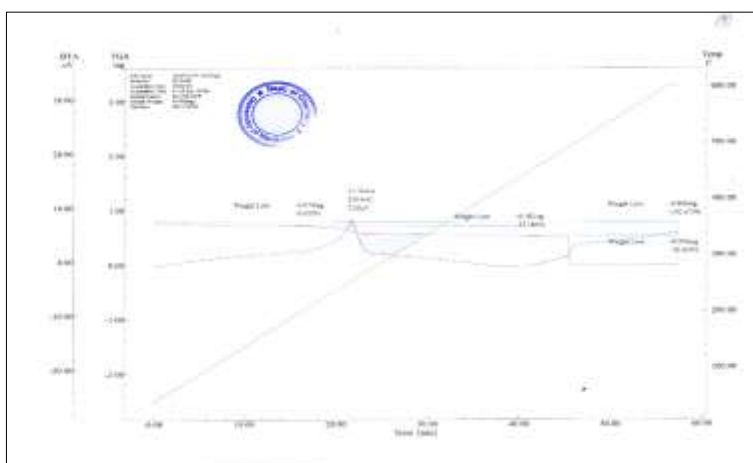


**Figure 8** TG-DTA thermogram of fullerene C-2

**Table 14 TG-DTA Data Analysis of Fullerene C-2**

No.	Temperature (°C)	Weight loss (%)	Type of peak	Remark
1.	252.09	36.735	exothermic	due to the loss of moisture and impurity
2.	484.05	39.796	exothermic	break down some bonds and degradation occurs
3.	599.80	80.612	exothermic	break down some bonds and degradation occurs

According to Table 14, the maximum degradation was found to be 599.80 °C and the weight loss is 80.612 %. The thermal analysis of C-2 (Figure 8) shows three mass loss steps (TG) with corresponding thermal events in the DTA curves. The first steps up to 252.09 °C show mass losses 36.735 % due to the physically adsorbed water on the material and impurity. The second mass loss step (484.05 °C) and the third mass loss step (599.80 °C) can be assigned to the break down of some bonds and degradation of carbon skeleton.

**Figure 9 TG-DTA thermogram of fullerene C-3****Table 15 TG-DTA Analysis of Fullerene C-3**

No.	Temperature (°C)	Weight loss (%)	Type of peak	Remark
1.	253.44	23.185	exothermic	Due to the loss of moisture and degradation occur in some extent
2.	300.20	100.00	exothermic	Complete degradation occur

According to Table 15, the maximum degradation was found to be 300.20 °C and the weight loss is 100.00 %. The thermal analysis of C-3 (Figure 9) shows two mass loss steps (TG) with corresponding thermal events in the DTA curves. The first step up to 253.44 °C show mass losses 23.185 % due to the physically adsorbed water on the material and impurity. The second step at 300.20 °C can be assigned to occur complete degradation (100% mass loss).

### Morphology of Prepared Fullerenes by SEM

The morphology of graphite, prepared C-1 and C-3 were analysed by SEM microscopy (Figures 10).

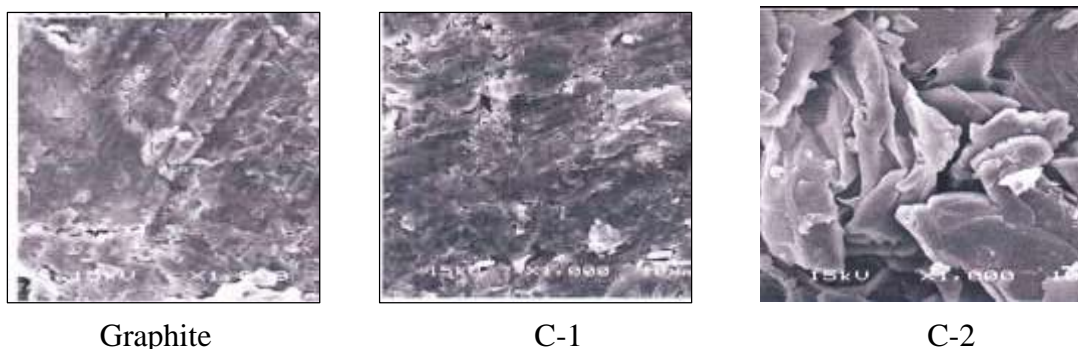


**Figure 10** SEM image of graphite and prepared fullerenes (C-1) (C-2)

According to SEM microscopy, in graphite, graphene sheets are packaged with a distance between sheets. The SEM image of C-2 shows disorganization of material and a greater distance between sheets that indicates there was an expansion and change of graphite due to the aspect of crumpled and exfoliated.

### Conclusion

In this research, the preparation of fullerene (C-1 to C-4) was carried out from graphite by the changing amount of  $\text{NaNO}_3$ ,  $\text{H}_3\text{PO}_4$ ,  $\text{KMnO}_4$  and  $\text{H}_2\text{SO}_4$  with various time intervals such as stirring times and sonication times, respectively. The yield percent of fullerene were found to be 73.02 % for C-1, 76.08 % for C-2, 74.52 % for C-3 and 88.40 % for C-4. The crystalline size and crystal nature of graphite and fullerene were investigated by XRD spectra. From the XRD result, the particle size of graphite was found to be 152.76-855.98 nm. The average particle size of graphite was found 490.47 nm. The average particle size of prepared fullerene were found to be 26.877 nm in C-1, 27.829 nm in C-2, 24.399 nm in C-3 and 18.389 nm in C-4 respectively. From the XRD data, the prepared fullerene C-1 to C-4 were confirmed according to  $2\theta$  value and ID phase. Furthermore, the thermal stability of fullerene was determined using thermo-gravimetric analysis (TG-DTA). From the TGA data, the fullerene started to degrade at 229.42 °C (13.421%) in C-1, 252.09 °C (36.735 %) in C-2 and 253 °C (23.185 %) in C-3. The maximum degradations were found to be 479.91 °C (39.888 %) in C-1, 599.80 °C (80.612 %) in C-2 and 300.20 °C, (100.0 %) in C-3. Among them, C-3 was completely decomposed at 300.2 °C. Finally, the surface morphology of graphite and prepared fullerene were analyzed by SEM microscopy. According to SEM microscopy, the morphology of graphite was found as packaged sheets. The SEM image of C-2 shows disorganization of graphite.

### Acknowledgements

The authors would like to thank the Department of Higher Education (Lower Myanmar), Ministry of Education, Yangon, Myanmar, for allowing us to carry out this research programme. Thanks are also extended to the Myanmar Academy of Arts and Science and Professor Dr Ni Ni Aung, Head of Department of Chemistry, Meiktila University for allowing to carry out this research programme.

## References

- Anthony, J.W., Bideaux, R. A., Bladh, K.W and Nichols, M.C. (eds). (1990). "Graphite"., Hand Book of Mineralogy. I (Elements, Sulfides, Sulfosalts). Chantilly, VA; US: Mineralogical Society of America.
- Deitz, T.G., Duncan, M.A., Powers, D.E. and Smalley, R.E. (1981). "Laser Production of Supersonic Metal Cluster Beams", *J. Chem. Phys.*, vol. 74, pp. 6500-6511.
- Fears, R, Kenneth, D., Krug, H., Aebi, K, Stamm, H. and Anklam, E. (2011). "Impact of Engineered Nanomaterials on Health Consideration for Benefit-Risk Assessment Joint Research Centre Corporate Activities", Publications Office of the European Union.
- Hahens W.I., Oomen A.G., Dejong W.H. and Cassee, F.R. (2007). What Do We Know about the Kinetic Properties of Nanoparticles in the Body? *Regulatory Toxicology and Pharmacology*, vol. 49, pp.217- 229.
- Hawkins, J.M., Meyor, A., Lewis, L.A., Loren, S. and Hollander, P.J. (1991). "Crystal Structure of Osmylated C<sub>60</sub>: Confirmation of the Soccer Ball Framework", *Science*, vol. 252, pp. 312-313.
- Kratschmer, W., Lamb, L., Fostiopoulos, K. and Hoffman, D.R. (1990). "Solid C<sub>60</sub>- a New Form of Carbon", *Nature*, vol. 347, pp.354-358.
- Kronholm, D. and Hummelen, J.C. (2007). "Fullerene-based n-type Semiconductors in Organic Electronic", *Mater. Metters*, vol. 2, pp.16-19.
- Roco, M.C., (2004)." Nanoscale Science and Eengineering. Unifying and Transforming Tools", *AIChE J.* vol.50, pp.890-897.
- Tagmatarchis, N. and Shin Ohara, H. (2001). "Fullerenes in Medicinal Chemistry and their Biological Application", *Mini-Rew. Med Chem-1*, pp.339-348.
- Xiao, L., Takada, H., Maeda, K., Haramoto, M. and Miwa, N. (2005). "Antioxidant Effects of Water-soluble Fullerene Derivatives against Ultraviolet Ray or Peroxylipid through their Action of Scavenging the Reactive Oxygen". *Species in Human Skin Keratinocytes, Biomed, Pharmacotherapy*, vol. 59, pp.351- 358.

## PREPARATION AND CHARACTERIZATION OF CARBOXYMETHYL CELLULOSE (CMC) FROM PINEAPPLE LEAVES

Htet Htet Than Sein<sup>1</sup>, Thinzar Nu<sup>2</sup>, Myo Maung Maung<sup>3</sup>

### Abstract

Pineapple leaves are one of the abundantly available waste materials and used for production natural fibres. Cellulose was isolated from pineapple leaf fibres (PALF) by mechanical and chemical treatments using alkaline, inorganic salts and acids. Cellulose was then converted to carboxymethyl cellulose by an alkalization and etherification process, using various concentrations of sodium hydroxide (10 %, 20 %, 30 % and 40 % w/v) and sodium monochloroacetate (SMCA), in isopropyl alcohol medium. All the carboxymethyl cellulose (CMC) obtained from various concentrations of NaOH were investigated on yield percent, solubility of water and degree of substitution to get the optimum CMC. These results indicate that the optimum reaction of alkalization was reached at 30 % NaOH. The physicochemical properties of optimum CMC such as moisture content, pH and solubility were also determined. Characterization of raw sample, bleached sample, cellulose and CMC were carried out by analyzing the XRD pattern, spectra of FT IR and SEM photomicrographs. The XRD analysis showed that the native cellulose was transformed into an amorphous phase, as evidenced from the characteristic peaks that had almost disappeared. FT IR analysis indicated that, in addition to the main characteristic bands of cellulose, CMC showed new characteristic absorption bands at 1591 and 1413  $\text{cm}^{-1}$ , which are associated with the anti-symmetric and symmetric stretching vibrations of  $\text{COO}^-$ , respectively. In SEM analysis, it can be seen the significantly changes from cellulose to CMC. These results confirmed the carboxymethylation process from cellulose.

**Keywords:** Pineapple leaf fibres, cellulose, carboxymethyl cellulose, alkalization, etherification

### Introduction

Plant fibres are mainly composed of cellulose, hemicellulose and lignin (Moran *et al.*, 2008). There are many plant fibres available which has potential to be applied in industries as raw materials such as pineapple leaf, coir, abaca, sisal, cotton, jute, bamboo, banana, hemp and talipot. Among them pineapple leaf fibres (PALF) is one of the waste materials in agriculture sector, which is widely grown in India as well as Asia.

Commercially pineapple fruits are very important and leaves are considered as waste materials of fruit which is being used for producing natural fibres. Fresh leaves yield about 2 to 3 % of fibres. Fibers has white in colour, smooth, glossy as silk, medium length fibres with high tensile strength. It has a softer surface than other natural fibres and it absorbs and maintains a food colour. The chemical composition of PALF constitute holocellulose (70-80 %), lignin (5-12 %) and ash (1.1 %) (Yogesh and Hari, 2017).

Cellulose is an organic compound with the formula  $(\text{C}_6\text{H}_{10}\text{O}_5)_n$ , a polysaccharide consisting of a linear chain of several hundred to many thousands of  $\beta$  (1 $\rightarrow$ 4 ) and is the most abundant renewable material resources on earth. Ligin and hemicellulose are amorphous in structure while cellulose is semicrystalline (Yang *et al.*, 2007).

In general, cellulose extraction can be divided into immersion method, chemical method and biological method. Natural cellulose was extracted from pineapple leaf (PAL) by using chemical method with steaming process (Fu *et al.*, 2013). To obtain pure cellulose, the raw material is treated with alkali and bleached. The chemical treatment breaks intermolecular and intramolecular hydrogen bonding between the hydrogen group of cellulose and hemicellulose and

---

<sup>1</sup> PhD Candidate, Department of Chemistry, University of Yangon

<sup>2</sup> Dr, Associate Professor, Department of Chemistry, University of Yangon

<sup>3</sup> Dr, Lecturer, Department of Chemistry, Dagon University

can increase the hydrophilicity (Abraham *et al.*, 2011). However, alkali treatment and bleaching do not significantly increase the crystallinity of cellulose fibres. Subsequently, acid hydrolysis can increase crystallinity and reduce the diameter of fibres (Mahardika *et al.*, 2018).

The steam process results in a hydrolysis of glycosidic bonds in the hemicelluloses and to a lesser extent in the cellulose. It also leads to a cleavage of hemicellulose-lignin bonds. The reactions result in an increased water solubilization of hemicelluloses and in an increased solubility of lignin in alkaline or organic solvents, leaving the cellulose as a solid residue (Cherian *et al.*, 2011).

Cellulose must be converted into its derivatives. One of the most common derivatives is carboxymethyl cellulose (CMC). CMC is manmade modified cellulose, a linear, long chain, water soluble and anionic polysaccharide (Mondal *et al.*, 2015). The preparation of CMC involves two reaction steps, which are alkalization and etherification process. In the alkalization process, the cellulose is treated with NaOH, often in the presence of inert solvent (ethanol or isopropanol), which acts both as a swelling agent and as a dilutant which facilitates good penetration to the crystalline structure of cellulose. In etherification step the alkali cellulose is reacted with monochloroacetic acid (MCA) or sodium monochloroacetate (SMCA) to form carboxymethyl cellulose ethers (Tasaso, 2015).

The aim of the research work is to prepare and characterize carboxymethyl cellulose via extracted cellulose from pineapple leaf fibres. The obtained CMC will be used as composite films for packaging application in next phase of the research work.

## Materials and Methods

### Sample Collection

Pineapple leaf was collected from farm of Shaw Pyar Village, Patheingyi Township, Ayeyarwady Region. Other required chemicals were purchased from chemical store. Distilled water was used as the solvent in all analyses.

### Extraction of Pineapple Leaf Fibres

The pineapple leaf fibres (PALF) from the pineapple leaves can be extracted by manual or mechanical methods. The most common and effective way of the extraction of PALF was the manual method, and it was used in this research work. Firstly, pineapple leaves were washed with water. Then, a plate was used to scratch and remove skin of the leaf from the surface. The fibres were detached after skin removal. After that, the fibres were washed with distilled water and dried in sunlight. Dry fibres were cut into small pieces.

### Isolation of Cellulose from Pineapple Leaf Fibres

Cellulose was isolated from PALF by steam explosion process along with mild chemical treatment including alkaline extraction, bleaching and acid hydrolysis. PALF were treated with 2 % NaOH (with fibres to liquor ratio of 1:10) in an autoclave and kept at 120 °C temperature and 138 kPa pressure for a period of one hour. Pressure was then released immediately. The fibres were washed in distilled water until the alkaline solution was completely free from the fibres.

The steam exploded fibres were bleached using a mixture solution of 0.65 M NaOH and 1.30 M glacial CH<sub>3</sub>COOH, mixed with 12 % NaClO solution in 1:3 ratio. The bleaching was repeated six times. After that, the bleached fibres were treated with 11% H<sub>2</sub>C<sub>2</sub>O<sub>4</sub> acid in an autoclave at 120 °C temperature and 138 kPa pressure. The pressure was then released

immediately. The autoclave was again set to reach 138 kPa and the fibres were kept under that pressure for 15 min. The pressure was released and the process repeated eight times.

The fibres were then taken out and washed until the fibres were free from acid. The processed cellulose fibre was suspended in distilled water and kept stirring with a mechanical stirrer for about 4 h until the fibrils were dispersed uniformly. Finally, the cellulose fibre was sonicated for 30 min at room temperature. The fibres were then filtered using a filter paper and dried in an oven at 60 °C.

### **Preparation of Carboxymethyl Cellulose via Cellulose Isolated from Pineapple Leaf Fibres**

Carboxymethyl cellulose was prepared from cellulose according to the procedure. First of all, 5 g of cellulose powder was weighed and added to 150 mL of isopropanol with continuous stirring for an hour. Then, 15 mL of (10 %, 20 %, 30 % and 40 % w/v) NaOH was added dropwise into the mixture and further stirred for an hour at room temperature. The carboxymethylation was started when 6 g of MCA (monochloroacetate) was added with continuous stirring for another 1.5 h. The mixture was covered with aluminum foil and placed into the hot air oven at 60 °C for 3.5 h.

The slurry was subsequently soaked in 100 mL of methanol for overnight. On the next day, the slurry was neutralized with 90 % of acetic acid to pH 7 and then filtered. The final product was washed for three times by soaking in 50 mL of ethanol for 10 min to remove undesirable by-products, and then it was washed again with 100 mL of absolute methanol for the last time. The obtained CMC from cellulose pineapple leaf fibre (CPALF) was filtered and dried at 60 °C to constant weight and kept in a dry place.

### **Determination of degree of substitution (DS) of CMC**

Sodium carboxymethyl cellulose was converted to the acid form (H-CMC) by adding an aqueous solution of 6 mL of 6 N HCl per 2 g of the sample, with continued stirring for 30 min. The dispersion was filtered in order to remove the excess acid. The precipitate was washed with methanol. Then the precipitate was again dispersed in acetone, filtered, dried and ground.

The obtained H-CMC was used for the DS determination. About 0.5 g of the H-CMC sample was dissolved in 20 mL of 0.2 N NaOH and 50 mL of distilled water was also added. The solution was transferred to a 100 mL volumetric flask, which was then filled up to the mark with distilled water. 25 mL of the solution was transferred to an Erlenmeyer flask and diluted by addition of 50-100 mL of bi-distilled water. The excess of NaOH was back-titrated with standard 0.05 N HCl using phenolphthalein indicator. The titration was repeated three times and the average value of the HCl volume was used for the calculations. The milli-equivalents of consumed acid per gram of the sample were calculated as the following equation.

$$A = \frac{(B \times C) - (D \times E)}{F}$$

Where,

A = milli-equivalents of consumed acid per gram of specimen

B = milliliters of added sodium hydroxide

C = normality of sodium hydroxide

D = milliliters of consumed hydrochloric acid

E = normality of hydrochloric acid

F = specimen grams used

The degree of substitution (DS) was then calculated as follows:

$$DS = \frac{(0.162) \times A}{1 - (0.058 \times A)}$$

Where:

162g/mol is the molar mass of an anhydroglucose unit (AGU),

58 is the net increase in the mass of an AGU for each carboxymethyl group substituted.

### Characterization of the Prepared Samples

The physicochemical properties (moisture, pH and solubility) of cellulose and carboxymethyl cellulose were determined by analytical method. The crystallinity index was calculated by using XRD analysis. The structural characterization of CPALF and CMC were characterized by using FT IR. The morphological structure of prepared samples was characterized by SEM.

X-ray diffraction (XRD) analysis was carried out using Rigaku X-ray Diffractometer, RINI 2000/PC software, Cat. No 9240 J 101, Japan. Copper tube with nickel filter was used. The diffraction pattern was recorded in terms of  $2\theta$  in the range of 10-70 °.

FT IR spectrum was recorded in the range of 4000-400  $\text{cm}^{-1}$  by using 8400 SHIMADZU, Japan FT IR spectrophotometer.

The scanning electron microscopy (SEM) images were recorded by using JSM-5610 Model SEM, JEOL-Ltd., Japan.

## Results and Discussion

### Physicochemical Properties of CMC

The degree of substitution (DS) of CMC obtained in this research work was in the range of 2.0705-2.1303, as present in Table 1. The DS and yield percent of CMC increased with increasing in concentration of NaOH from 10 % to 40 % and attained a maximum DS of 2.1303 with yield (182 %) in 30 % NaOH concentration. Above 30 % NaOH, the DS and yield percent were found to be decreased. It can be seen that the CMC obtained by using 30 % NaOH was more soluble in water than other CMC. According to the results, CMC obtained by using 30% NaOH concentration was selected as the optimum CMC. The physicochemical properties of optimum CMC are shown in Table 2. Moisture content analysis was conducted to calculate the total solid in the sample. The moisture content of CMC obtained from PAL is 7.4329 %. According to the standard procedure, the moisture content of CMC should not be higher than 12 %. So, CMC obtained by using 30 % NaOH was considered as pure CMC because it was within the moisture content (%) of standard CMC. The pH of the 1 % (w/v) CMC solution was in the range of 6 to 8. This CMC was soluble in water and forms viscous solution with water but insoluble in ethanol and methanol. These tests can be confirmed that the optimum CMC is obtained.

**Table 1 Yield Percent and Degree of Substitution of CMC Samples with Various Concentrations of NaOH**

Concentration of NaOH (%)	Solubility in water	Yield (%)	Degree of Substitution (DS)	pH
10	slightly soluble	133	2.1019	6.64
20	slightly soluble	158	2.1103	6.70
30	soluble	182	2.1303	7.14
40	slightly soluble	165	2.0705	6.77

**Table 2 Physicochemical Properties of Optimum CMC (30% NaOH )**

Test	CMC
moisture content (%)	7.4329
pH	7.14
viscosity (cP)	40.39
water	+
ethanol	-
methanol	-
DS	2.1303

(+) soluble, (-) insoluble

### XRD Analysis

XRD diffractometer was used to determine the index of crystallinity ( $C_1$ ) of PALF at each stage in the process (raw, bleaching, acid hydrolysis and carboxymethylation). The crystallinity index percent was calculated by using the following equation, by measuring the peak height of the crystalline region ( $I_{200}$ ) and the amorphous region ( $I_{am}$ ).

$$C_1 (\%) = \frac{I_{200} - I_{am}}{I_{200}} \times 100 \%$$

Where,  $I_{200}$  is the maximum intensity of the peak for cellulose I ( $2\theta = 22^\circ - 23^\circ$ ) and cellulose II ( $2\theta = 18^\circ - 22^\circ$ ).  $I_{am}$  represent the minimum intensity of diffraction attributed to amorphous cellulose I ( $2\theta = 16^\circ - 19^\circ$ ) and cellulose II ( $2\theta = 13^\circ - 15^\circ$ ). Figures 1(a), (b), (c) and (d) show the XRD patterns of the raw pineapple leaf fibres (RPALF), bleached pineapple leaf fibres (BPALF), cellulose pineapple leaf fibres (CPALF) and carboxymethyl cellulose (CMC), respectively. Among them, the peak of Figure 1 (d) appears at  $2\theta = 20.51^\circ$  and  $2\theta = 14^\circ$ , suggesting the characteristic of cellulose II. The characteristic diffraction peaks of the rest were observed at the values of  $2\theta = 22.67^\circ$  and  $18.5^\circ$ . Therefore, the structure of RPALF, BPALF and CPALF was considered to be typical cellulose I because they have the characteristics of amorphous and crystalline regions.

The crystallinity index percent for all samples was calculated by peak height method and represented as shown in Table 3. The  $C_1$  of the RPALF was calculated as 60.5 % and increase in case of BPALF to 75.2 % (due to the removal of hemicellulose and lignin as amorphous part), and 89.05 % in case of CPALF in which remaining amorphous part was removed during acid hydrolysis. It was found that the  $C_1$  of CMC decreased as 51.4 %. The decreased of crystallinity on the alkalization and carboxymethylation process of cellulose were due to the cleavage of hydrogen bonds and this also results in the extending the distance between cellulose molecules. Therefore, all characteristic peaks of cellulose have been disappeared and transformed into an amorphous phase.

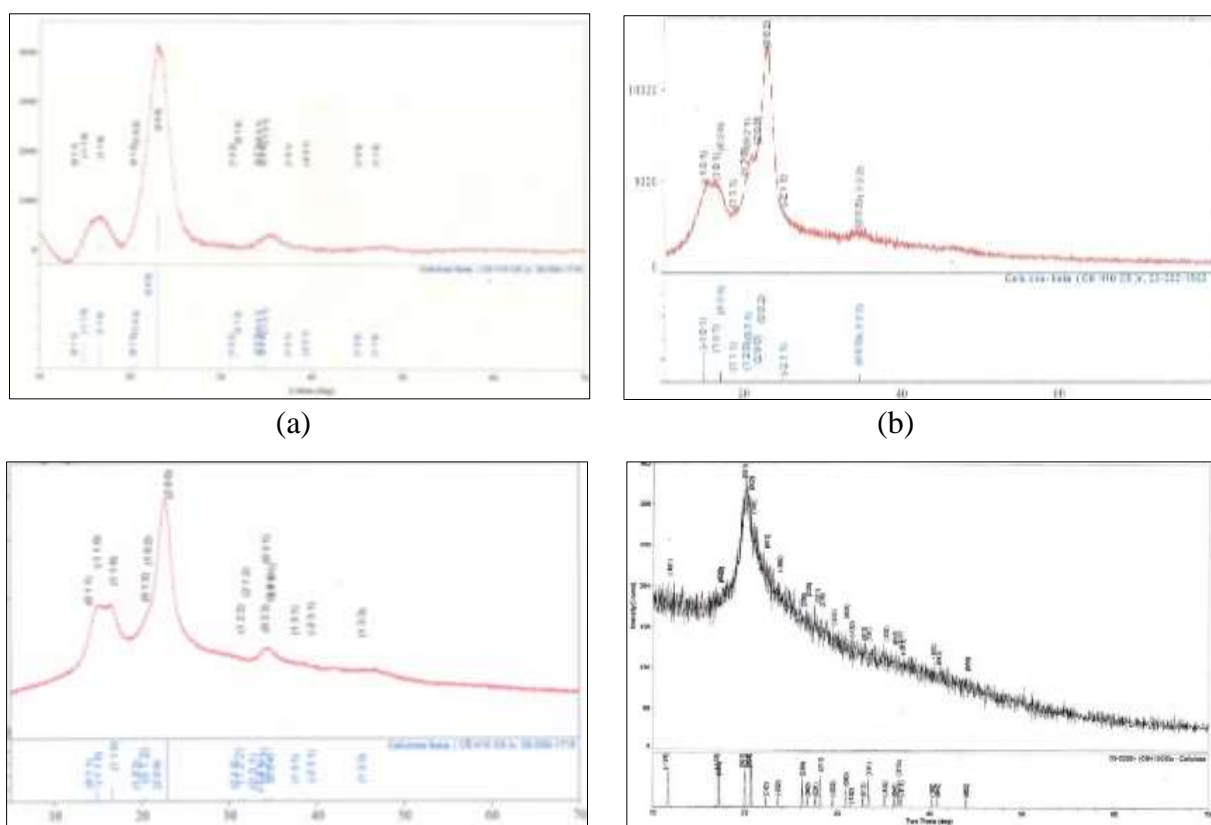


**Figure 1** XRD diffractograms of (a) raw pineapple leaf fibres RPALF (b) bleached pineapple leaf fibres BPALF (c) cellulose pineapple leaf fibres CPALF and (d) carboxymethyl cellulose CMC

**Table 3** Crystallinity Index Percent of all Samples

Samples	Crystallinity Index (%)
RPALF	60.50
BPALF	75.12
CPALF	89.05
CMC	51.40



**Table 4 FT IR Band Assignments of RPALF, BPALF, CPALF and CMC**

Observed wavenumber (cm <sup>-1</sup> )				Literature * wavenumber (cm <sup>-1</sup> )	Band Assignment
RPALF	BPALF	CPALF	CMC		
3431	3338	3334	3263	3600-3200	O-H stretching
2918	2917	2890	2876	2980-2850	C-H stretching (ketone and carbonyl)
1729	-	-	-	1765-1715	C=O stretching of ester
1641	1644	1638	-	1665-1620	O-H bending
-	-	-	1591	1650-1550	COO <sup>-</sup> stretching (anti-symmetric)
1514	-	-	-	1600-1500	C=C stretching (aromatic ring in lignin)
-	-	-	1413	1440-1435	COO <sup>-</sup> stretching (symmetric)
1427	1425	1428	-	1430-1420	CH <sub>2</sub> scissoring motion in cellulose
1314	1315	1315	1321	1390-1319	C-O-H bending
1244	-	-	-	1310-1210	C-O stretching (aryl group in lignin)
1158 } 1031 }	1160 } 1032 }	1160 } 1054 }	1052 }	1200-1000	C-O-C stretching (symmetric)
897	897	897	898	937-897	β (1-4) glycosidic linkage between the glucose unit in cellulose

\* Silverstein *et al.*, 2003

### SEM Analysis

In order to further investigate the structural changes in the fibres, SEM micrographs of the RPALF, BPALF, CPALF and CMC are shown in Figure 3 (a), (b), (c) and (d). According to the SEM images, the surface morphology of all samples except CMC is composed of several microfibrils. These images visually suggest the partial removal of hemicellulose, lignin and pectin after high pressure chemical treatment, which are the cementing materials around the fibres bundles. The raw PALF was found to be aggregate and microfibrils are still bound to one another due to the presence of lignin and hemicellulose components. After bleaching treatment, the bonding between lignin and hemicellulose had been broken due to the removal of the amorphous content in microfibril bundle. The CPALF image shows a reduction in fiber size after acid hydrolysis. The CPALF sizes are much smaller than the other fibres samples before treatments. This explanation is also supported by XRD crystallinity index data. It can be seen from SEM micrographs that high pressure steam treatment helps in fibres separation and fibrillation.

The surface morphology of prepared CMC can be clearly seen that the obtained products are rod like structure and surfaces are more extended than the cellulose. It had long and narrow strand characteristics. This image clearly showed that the conversion of cellulose to CMC leads to changes in its ribbon shape.

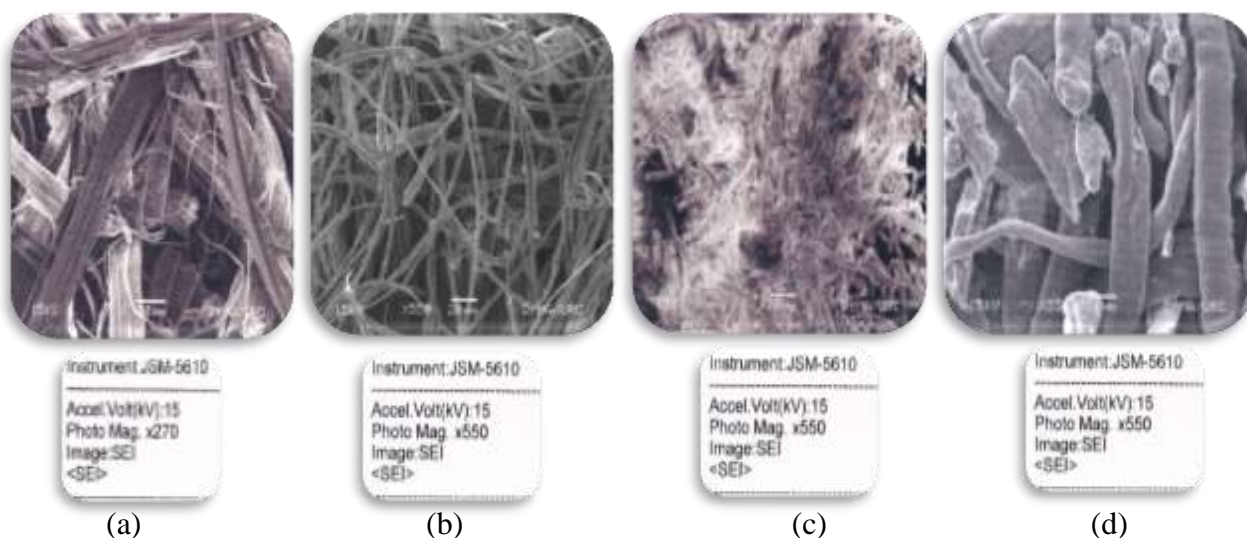


**Figure 3** SEM micrographs of (a) raw pineapple leaf fibres RPALF (b) bleached pineapple leaf fibres BPALF (c) cellulose pineapple leaf fibres CPALF and (d) carboxymethyl cellulose CMC

### Conclusion

Cellulose fibres were isolated from pineapple leaf fibres through alkali treatment, bleached and acid hydrolysis. Furthermore, isolated cellulose successfully converted to carboxymethyl cellulose (CMC) using various concentration of NaOH in the range from 10 % to 40 % and etherified with sodium monchloroacetate (SMCA) in isopropanol medium. To get the optimum condition of CMC from isolated cellulose, this cellulose was treated by using 15 mL of 30 % NaOH, 6 g of SMCA in 150 mL of isopropanol solvent at room temperature. In this research work, the highest DS and yield percent of CMC obtained by using 30 % NaOH concentration were 2.1303 and (182 %). So, this concentration regarded the optimum concentration of CMC. Each step from the raw sample to the CMC were characterized by XRD, FT IR and SEM. XRD analysis confirmed that the crystallinity index percent of CMC decreased in comparison with that of cellulose and other samples due to the cleavage of hydrogen bonds and this also results in the extending the distance between cellulose molecules. FT IR analysis showed that, in addition to the main characteristic bands of cellulose, new characteristic absorption bands for CMC at  $1519\text{ cm}^{-1}$  and  $1413\text{ cm}^{-1}$ , which related to the anti-symmetric and symmetric stretching vibration of  $\text{COO}^-$ . According to the SEM analysis, the significantly changes from raw sample to CMC were clearly observed in each chemical reaction.

This investigation showed that the chemical process was more efficient and effective process for the preparation of CMC from cellulose. Prepared CMC is suitable for developing biopolymer composite film at the second part of the study.

## Acknowledgements

The authors would like to express their profound gratitude to the Department of Higher Education, Ministry of Education, Yangon, Myanmar, for provision of opportunity to do this research and Myanmar Academy of Arts and Science for allowing to present this paper.

## References

- Abraham, E., Deepa, B., Pothan, L. A., Jacob, M., Tomas, S. and Cvelbar, U. (2011). "Extraction of Nanocellulose Fibrils from Lignocellulosic Fibres: A Novel Approach". *Carbohydrate Polymer*, vol. 86, pp. 1468-1475
- Cherian, B. M., Leao, A. L., Souza, S. F. D., Costa, L. M. M., Olyveira, G. M. D., Kottaisamy, M., Nagaragin, E. R. and Thomas, S. (2011). "Cellulose Nanocomposites with Nanofibres Isolated from Pineapple Leaf Fibers for Medical Applications". *Carbohydrate Polymer*, vol. 86, pp. 1790-1798
- Fu, T., Li, J., Wang, Q., Huang, H., Wei, X., Cui, L., Wang, Y. and Wang, F. (2013). "Structure and Properties of Natural Cellulose Extracted from Pineapple Leaf". *Advanced Materials Research*, vol. 815, pp. 379-385
- Lavanya, D., Kulkarni, P. K., Dixit, M., Raavi, P. K. and Krishna, L. N. V. (2011). "Sources of Cellulose and Their Application – A Review". *International Journal of Drug Formulation and Research*, vol. 2(6), pp. 19-34
- Mahardika, M., Abral, H., Kasim, A., Arief, S. and Asrofi, M. (2018). "Production of Nanocellulose from Pineapple Leaf Fibres via High-Shear Homogenization and Ultrasonication". *Fibres*, vol. 6 (28), pp. 1-12
- Mondal, M. I. H., Yeasmin, M. S. and Rahman, M. S. (2015). "Preparation of Food Grade Carboxymethyl Cellulose from Corn Husk Agrowaste". *International Journal of Biological Macromolecules*, vol.79, pp. 144-150
- Moran, J. I., Alvarez, V. A., Cyras, V. P. and Vazquez, A. (2008). "Extraction of Cellulose and Preparation of Nanocellulose from Sisal Fibers". *Cellulose*, vol. 10, pp. 149-159
- Silverstein, R. M., Webster, F. X. and Kiemle, D. J. (2003). *Spectrometric Identification of Organic Compounds*. New York: 7<sup>th</sup> Edition, John Wiley and Sons, Inc.
- Tasaso, P. (2015). "Optimization of Reaction Conditions for Synthesis of Carboxymethyl Cellulose from Oil Palm Fronds". *International Journal of Chemical Engineering and Applications*, vol. 6 (2), pp. 101-104
- Yang, H., Yan, R., Chen, H., Lee, D. H. and Zheng, C. (2007). "Characteristics of Hemicellulose, Cellulose and Lignin Pyrolysis". *Fuel*, vol. 86, pp. 1781-1788
- Yogesh, M. and Hari, R. A. N. (2017). "Study on Pineapple Leaves Fibre and its Polymer Based Composite: A Review". *International Journal of Science and Research*, vol. 6 (1), pp. 799-807

## USING SLOW SAND FILTRATION METHOD WITH DOMESTIC CHARCOAL TO TREAT DISTILLERY WASTEWATER IN AUNGLAN TOWNSHIP

Thandar<sup>1</sup>, Thwe War Aung<sup>2</sup>, Kyi Kyi Thein<sup>3</sup>

### Abstract

Distilleries generate large volume of wastewater which poses a considerable environmental impact by polluting the natural environment. This study focused to evaluate the feasibility of slow sand filtration integrated with domestic charcoal layer as a promising treatment method for the distillery wastewater effluent. Distillery wastewater was collected from Aunglan Township, Thayet District in Magway Region. Before and after treatment for two weeks, selected parameters of effluent were analyzed. All of the effluent parameters (pH, conductivity, total alkalinity, COD, DO, BOD, and chloride, calcium, magnesium and bicarbonate) of treated distillery wastewater sample were within the allowable limits of USEPA standard except turbidity, total hardness, TDS, total phosphate, ammonia nitrogen. After treatment, pH value of the acidic wastewater changed from 3.67 to 6.10 and total alkalinity and total hardness values were found to be 70 ppm and 550 ppm, respectively. *E.coli* in the distillery wastewater was reduced significantly than the initial value but higher than USEPA limit. The slower sand filtration treatment can be taken as an alternative and economical method for treatment of wastewater.

**Keywords:** distillery wastewater, slow sand filtration method, charcoal, *E.coli*

### Introduction

Water pollution occurs when unwanted materials enter in to water, changes the quality of water and harmful to environment and human health. Metal ions are often present in wastewater from industries, and sometimes there is the need to reduce their concentrations to certain minimum (Hassena *et al.*, 2017). Clean water is essential for health and the living in general for humans. For some people the access of clean and fresh water is a simplicity but for others, the lack of clean water, especially in rural areas creates one of the biggest humanitarian problems in the world today (Williams, 2015). Due to increased human population, industrialization, use of fertilizers and man-made activity water is highly polluted with different harmful contaminants. The use of current wastewater treatment technologies for such reclamation is progressively failing to meet required treatment levels. Industrial wastewater is one of the major sources of aquatic pollution which could significantly endanger surrounding environments and ecosystems (Agyemang *et al.*, 2013).

Advanced wastewater treatment technologies are essential for the treatment of industrial wastewater to protect public health and to meet water quality criteria for the aquatic environment and for water recycling and reuse. The protection of receiving waters is essential to prevent eutrophication and oxygen depletion in order to sustain fish and other aquatic life (Agyemang *et al.*, 2015).

The best approach to working out an effective and efficient method of industrial wastewater treatment is to understand how substances are dissolved or suspended in water and then to deduce plausible chemical or physical actions that would reverse those processes (Gutierrez, 2018). Slow sand filtration plays a key role in rural water treatment (Skat, 1996). Slow sand filtration is a type of centralized or semi-centralized water purification system (Bruni and Spuhler, 2020). Filter operation neither requires sophisticated mechanical parts nor the use of chemicals. Since slow sand filters reduce the number of microorganisms present in the water, they improve the bacteriological

---

<sup>1</sup> Dr, Lecturer, Department of Chemistry, University of Magway

<sup>2</sup> Dr, Lecturer, Department of Chemistry, University of Magway

<sup>3</sup> Lecturer, Department of Chemistry, University of Magway

water quality. In addition, fine organic and inorganic matter is separated, and the organic compounds dissolved in the water are oxidized (Skat, 1996). A well-designed and properly maintained slow sand filter (SFF) effectively removes turbidity and pathogenic organisms through various biological, physical and chemical process in a single treatment step (Bruni and Spuhler, 2020). Good quality of water resources depends on a large number of physico-chemical parameters and biological characteristics (Sharma *et al.*, 2016). In this study, some physicochemical parameters such as pH, turbidity, conductivity, total alkalinity, total hardness, total dissolved solids, chloride, DO, BOD and COD, etc. were analyzed for testing water quality, after treatment of distillery wastewater by slow sand filtration method.

## Material and Methods

### Sample Collection

A total of about 40 L of wastewater was collected from Aunglan Township, Thayet District in Magway Region (Figure 1). Aunglan Township is far away 81.39 miles from Magway Township. The collection was carried out the periods of January in 2019. The distillery wastewater was stored in 20 L sterilized prewashed polyethylene containers, rinsing each container three times with the wastewater sample before collection. The sampling containers were sealed and stored in clean, dry and dust free environment at room temperature until further analysis in the laboratory.



Figure 1 Location map of study area

### Treatment of Distillery Wastewater by Slow Sand Filtration System

The design of slow sand filtration system was applied for the distillery wastewater treatment (Bryant *et al.*, 2015).

### Preparation of sand, gravel and charcoal

The collected sand was sieved through a 100 mesh sieve to get coarse sand and fine sand. Then, the different size gravels, coarse sand, fine sand and charcoal (domestic charcoal) were washed with pure water and dried in an air at room temperature for 72 h. After that, they were

washed with 0.01 M HCl and once again with distilled water. Then, they were also washed with ammonia solution 0.1 M and once again with distilled water.

### Pre-treatment tank

The slow sand filtration system was designed, using a 100 L plastic container. A green thread socket covered with a mesh was fitted through a hole created at the base of the container. The mesh was used to prevent particles (e.g., fine sand) from clogging the effluent outlet. Connected to the socket was a PVC tube which served as effluent outlet. The plastic lid was used to cover the set-up during treatment to prevent foreign particles from dropping into the treatment system. It was used as filter for treatment. Another container was prepared in the same way. Design of pre-treatment tank was shown in Figure 2.



**Figure 2** The overall set-up of the slow-sand filtration system used for the treatment

### Treatment of distillery wastewater with pre-treatment tank

Firstly, the filter bed was made of a bottom layer of stones (average of 5 mm in diameter) to a depth of 10 cm. The strata were covered with a mesh to prevent mixing of the gravels and the coarse sand. The coarse sand with depth of 12 cm occupied the second layer. The final layer of the filter bed was activated charcoal (from domestic charcoal) of a depth of about 8 cm. The whole filter high occupied 60 cm of the plastic container. Then, another filter bed was also made up of bottom layer of 10 cm depth of gravels (average of 2 mm in diameter). After that, second layer was followed by fine sand of about a depth of 15 cm. The high depth of fine sand was so to increase retention time in order to ensure efficient treatment. The final layer of the filter bed was also domestic charcoal of a depth of about 8 cm. Then 20 L of distillery wastewater sample was added into the first treatment tank. After one week treatment, this sample was also added to another treatment tank for one week. The components of the slow sand filtration bed used in this study are shown in the Figures 3, 4, 5 and 6. After two weeks treatment, some physicochemical parameters of distillery wastewater were measured.



**Figure 3** Different size gravel (average 5 mm and 2 mm in diameter) used in slow sand filtration system



**Figure 4** Fine sand and coarse sand used in slow sand filtration system



**Figure 5** Charcoal used in slow sand filtration system **Figure 6** Mesh to prevent mixing of the gravels and the coarse sand

### Analysis of Distillery Wastewater Quality

Some physicochemical parameters and *E. coli* count of distillery wastewater before and after treatment were analysed by the methods and instruments as listed in Table 1.

**Table 1** Methods and Instruments Used for Wastewater Quality Analysis

Parameters	Method used	Instrument used
pH	ISO 10523:2008	Robot Mentech
Turbidity	ISO 7027:1999	Robot Mentech
Conductivity	NS-ISO 7888:1993	Robot Mentech
Total alkalinity	ISO 9963:1996	Robot Mentech
Total hardness	Titrimetric Method	Titration
TDS	Gravimetric Method	HANNA (HI-9145), Italy
COD	Titrimetric Method	-
DO, BOD	Manual Method	DO Probe
Cl, Ca, Mg,	ISO 14911:1998, ISO 10304 1:2009	Ion Chromatography (IC)
Bicarbonate	Titrimetric Method	Continuous Flow Analyzer (Skalar)
Total phosphate	Spectrophotometric Method	UV-1800 Spectrophotometer
Ammonia-Nitrogen	Titrimetric method	Micro Kjeldhal method
Fe, Cu	Spectrophotometric Method	Atomic Absorption Spectrophotometer, nov AA 400,
<i>E. coli</i>	Plate Count Method	Analytikjena, Gram staining and UV detection with UV Lamp

### Determination of Some Physicochemical Parameters of Distillery Wastewater

In this experiment, some physicochemical parameters such as pH, turbidity, conductivity, total alkalinity, total hardness, total dissolved solids, chemical oxygen demand, dissolved oxygen, biochemical oxygen demand, chloride, calcium, magnesium, bicarbonate, total phosphate, ammonia-nitrogen, Fe, Cu and *E. coli* of distillery wastewater sample before and after treatment using slow sand filtration method were analyzed.

### **Determination of pH in the distillery wastewater sample**

The pH value of wastewater sample was measured with ISO 10523:2008 method by Robot Mentech machine at Ministry of Agricultural Research (MAR), Yezin, Naypyitaw.

### **Determination of turbidity in the distillery wastewater sample**

The turbidity value of wastewater sample was also measured with ISO 7027:1999 method by Robot Mentech machine at Ministry of Agricultural Research (MAR), Yezin, Naypyitaw.

### **Determination of conductivity in the distillery wastewater sample**

The conductivity value of wastewater sample was also measured with NS-ISO 7888:1993 method by Robot Mentech machine at Ministry of Agricultural Research (MAR), Yezin, Naypyitaw.

### **Determination of total alkalinity in the distillery wastewater sample**

The total alkalinity value of wastewater sample was determined by ISO 9963:1996 method using Robot Mentech machine at Ministry of Agricultural Research (MAR), Yezin, Naypyitaw.

### **Determination of total hardness in the distillery wastewater sample**

The distillery wastewater (50 mL) was poured into the beaker and total hardness value was recorded directly from Titrator display at Ministry of Agricultural Research (MAR), Yezin, Naypyitaw.

### **Determination of total dissolved solids in the distillery wastewater sample**

Distillery wastewater (100 mL) was accurately measured and filtered with the preweighed filter paper. The filtrate was evaporated to dryness in a preweighed porcelain crucible on oven. Then the crucible with residue was cooled in a desiccator for half an hour and weighed. The process of heating in the oven and cooling in the desiccator until a constant weight was obtained (Vogel, 1968).

### **Determination of chemical oxygen demand in the distillery wastewater sample**

COD was measured by the permanganate oxidation method. 25 mL of wastewater sample was placed in a conical flask. A 2.5 mL of potassium permanganate solution was added to the sample and the flask was placed on a boiling water bath for 1 hour. After that, the sample was cooled for 10 minutes. Then, 2.5 mL of potassium iodide was added to the sample and followed by 5 mL of sulphuric acid solution. The solution was titrated with standard sodium thiosulphate solution until a pale yellow color was obtained. The starch solution (1 mL) was added to the above solution to get a blue color. The titration was continued until the blue color disappeared completely. The whole above procedure was repeated for another two times. A blank test in the manner using distilled water instead of the sample was also carried out (Government of India and Government of the Netherlands, 1999).

### **Determination of dissolved oxygen in the distillery wastewater sample**

Distillery wastewater was filled into the glass bottle so that bubbling did not occur and initially dissolved oxygen content was determined by manual method. Dissolved oxygen contents was recorded directly from DO probe display at Ministry of Agricultural Research (MAR), Yezin, Naypyitaw.

### **Determination of biochemical oxygen demand in the distillery wastewater sample**

The distillery wastewater was filled in the glass bottle without bubbling. The initially dissolved oxygen (DO) content was determined by a dissolved oxygen meter at Ministry of Agricultural Research (MAR), Yezin, Naypyitaw. Solutions of 1 mL of 0.05 % urea and 1 mL of phosphate buffer was added to the bottle. The bottle was incubated at 20 °C for 5 days. After incubation, the concentration of oxygen was determined by the dissolved oxygen meter. The difference between the initial DO content and DO content after 5 days incubation was the 5 days biochemical oxygen demand (BOD) in ppm.

### **Determination of chloride content in the distillery wastewater sample**

The chloride value of wastewater sample was measured with ISO 14911:1998 method by Ion Chromatography (IC) machine at Ministry of Agricultural Research (MAR), Yezin, Naypyitaw.

### **Determination of calcium and magnesium contents in the distillery wastewater sample**

The metal ions content (Ca, Mg) of distillery wastewater sample were determined with ISO 14911:1998 and ISO 10304 1:2009 methods by Ion Chromatography (IC) machine at Ministry of Agricultural Research (MAR), Yezin, Naypyitaw.

### **Determination of bicarbonate in the distillery wastewater sample**

Bicarbonate was measured by Titrimetric Method using Continuous Flow Analyzer (Skalar) at Ministry of Agricultural Research (MAR), Yezin, Naypyitaw. It was also measured by titration with standardized hydrochloric acid using methyl orange as indicator. Methyl orange turns yellow below pH 4.0. At this pH, the carbonic acid decomposes to give carbon dioxide and water.

### **Determination of total phosphate in the distillery wastewater sample**

The content of total phosphate in the distillery wastewater was determined by the colorimetric molybdenum blue method. The 25 mL of wastewater was placed in a conical flask. A 1 mL of ammonium molybdate solution and 3 drops of chlorostannous acid solution were added and allowed to stand for 15 min. The solution was placed in a glass cell and the absorbance was measured in a UV-visible double-beam spectrophotometer at 690 nm. Prior to this, a standard calibration curve (absorbance vs. concentration) was made with phosphate concentration of 0.0, 0.2, 0.4, 0.6, 0.8, 1.0 and 1.2 ppm, and the absorbance were measured by spectrophotometric method using UV-1800 Spectrophotometer. It was measured at Ministry of Agricultural Research (MAR), Yezin, Naypyitaw.

### **Determination of ammonia nitrogen content in the distillery wastewater sample**

The wastewater sample (5 mL) was introduced into a dried Pyrex Kjeldahl flask. The catalyst mixture composed of (3.5 g) anhydrous potassium sulphate, (0.4 g) copper sulphate and concentrated sulphuric acid (15 mL) were added. The flask was partially closed by means of a funnel and the contents were digested by heating the flask in an inclined position in the digester. The mixture was heated gently for about 30 minutes and heating was continued vigorously for about 1 h until the solution become clear. Then the flask was allowed to cool and about 10 mL of distilled water and a few sodium thiosulphates were added and Kjeldahl distillation apparatus was set up. Sodium hydroxide 30 % solution (80 mL) was poured through the side arm into the flask together with 100 mL of distilled water. The contents were distilled by direct heating. The ammonia evolved was allowed to absorb in 100 mL of 4 % boric acid solution contained in the receiver flask.

The ammonia distillate was titrated with 0.1 M hydrochloric acid, using the mixed indicator solution until the color changed from green to pinkish. Blank and standard determinations were also carried out as described above except that distilled water and standard ammonia solution were used in lieu of the sample solution. The amounts of total nitrogen and subsequently protein content in the sample was calculated as described in general formula (Government of India and Government of the Netherlands, 1999).

$$\text{Total protein} = (\text{total N} - \text{non-protein N}) \times 6.25$$

### **Determination of iron and copper contents in the distillery wastewater sample**

The contents of Fe and Cu were determined by spectrophotometric method using atomic absorption spectrophotometer (Nov AA 400) at Ministry of Agricultural Research (MAR), Yezin, Naypyitaw.

### **Determination of *E. coli* in the Distillery Wastewater by Plate Count Method**

Resolic acid 0.1 g, sodium hydroxide 0.7998 g and distilled water 10 mL were mixed into the reagent bottle. Then, the solution was stored in the refrigerator for one week. After cooling the refrigerator, resolic acid solution 0.1 mL, Defco agar 5.2 g and distilled water 250 mL were boiled on the stove for 15 min. Then, the mixture solution 6 mL was poured into the petri dish. It was shaken on the shaker for 18 h. It was used for control to compare with *E.coli* counting in wastewater. Moreover, wastewater sample 1 mL and the mixture solution 5 mL were added into another petri dish. The petri dish was also shaken on the shaker for 18 h. And then, wastewater containing petri dish was compared with the control using UV detection method to count *E.coli* bacteria. *E.coli* count in the distillery wastewater sample was measured at Ministry of Agricultural Research (MAR), Yezin, Naypyitaw.

## **Results and Discussion**

### **Some Physicochemical Parameters of Untreated and Treated of Distillery Wastewater Sample**

Some physico-chemical parameters such as pH, turbidity, conductivity, total alkalinity, total hardness, total dissolved solids (TDS), chemical oxygen demand (COD), dissolved oxygen (DO) and biochemical oxygen demand (BOD), chloride, calcium, magnesium, bicarbonate, total phosphate, ammonia nitrogen, iron, copper and *E.coli* of distillery wastewater sample before and after treatment by using slow sand filtration technique were determined and the results are comparatively shown in Table 2.

#### **pH**

The pH values of water are very important in determination of water quality since it effects other chemical reactions such as solubility and metal toxicity. In this study, the pH value of untreated wastewater sample was 3.67. Lower the pH value higher is the corrosive nature of water. After treatment with slow sand filter, the pH value of wastewater sample was increased to 6.10. The value of treated wastewater was within the range of USEPA standard value 6-9.

#### **Biochemical oxygen demand**

Before treatment, the biochemical oxygen demand value of wastewater sample was 71.70 ppm. The biochemical oxygen demand value of treated wastewater sample was found to be 30.50 ppm. The value of treated wastewater sample was within the permissible level of USEPA

standard 50 ppm. If the BOD concentration is higher, the water is polluted. According to the results of BOD, the wastewater was none polluted.

### **Chloride content**

Before treatment, the chloride value of wastewater sample was 3.38 ppm. After treatment, the chloride value was reduced to 2.02 ppm. USEPA standard value of chloride is 142 ppm. Therefore, the chloride value of treated wastewater sample was satisfied with the USEPA value 142 ppm. The presence of a low salt content may render the wastewater suitable for domestic, agricultural and industrial uses.

### **Calcium and magnesium contents**

The content of calcium and magnesium value of untreated wastewater sample were 20 ppm and 16.25 ppm. After treatment, the content of calcium and magnesium values of treated wastewater sample were found to reduced 7.75 ppm and 7.26 ppm. USEPA standard of calcium and magnesium values were 230 ppm and 100 ppm. These values were satisfied the USEPA standard.

### **Bicarbonate**

The bicarbonate value of untreated wastewater sample was 5.45 ppm. After treatment, the dissolved oxygen value of wastewater sample was increased to 6.5 ppm. Therefore, the resulted value of treated wastewater was within the permissible level of USEPA standard (6.5-8.4 ppm) and they were suitable for domestic purposes.

### **Total phosphate**

Before treatment, the total phosphate value of wastewater sample was 2598 ppm. After treatment, the phosphate value was reduced to 198.40 ppm. USEPA standard value of phosphate is 30 ppm. Phosphate is an essential nutrient for living organisms in water bodies. The total phosphate value was not satisfied USEPA standard. High concentrations of phosphate can indicate the presence of pollution due to decomposition of organic matters.

### **Ammonia nitrogen**

Ammonia nitrogen value of untreated wastewater sample was 8.60 ppm. After treatment, ammonia nitrogen value decreased to 3.10 ppm. From result obtained, the treated ammonia nitrogen value of wastewater sample was deviated from the USEPA standard 2 ppm and the analyzed wastewater was not suitable for domestic purposes.

### **Iron and copper contents**

Before treatment, the values of iron and copper concentrations in the wastewater sample were 10.46 ppm and 1.99 ppm respectively. After treatment, the value of iron and copper concentrations in the wastewater sample were 4.45 ppm and 0.45 ppm respectively. Therefore, the values of iron and copper in the treated wastewater sample were not consistent with the USEPA standard value 0.3 ppm and 0.2 ppm. The contents of iron and copper in the wastewater were not suitable for domestic, agricultural and industrial uses.

***E. coli* count**

Before treatment, the number of *E. coli* in the wastewater sample was 2500 CFU/100 mL. After treatment, the number of *E. coli* in the wastewater sample was reduced to 300 CFU/100 mL. USEPA standard value of *E. coli* is 100 CFU/100 mL. Therefore, the treated value of wastewater sample was not consistent with the USEPA standard. But, *E. coli* in the distillery wastewater was reduced significantly than initial wastewater.

**Table 2 Comparative Data of some Physicochemical Parameters in Distillery Wastewater before Treatment and after Treatment with Slow Sand Filter**

Parameters	Unit	Before treatment	After treatment	USPA Standard
pH	-	3.67	6.10	6-9
Turbidity	NTU	459	44.50	10
Conductivity	$\mu\text{Scm}^{-1}$	5059.25	1619.25	2000
Total alkalinity	ppm	120	70	500
Total hardness	ppm	1240	550	500
Total dissolved solids	ppm	3500	1250	1200
Chemical oxygen demand	Ppm	171.40	75.20	100
Dissolved oxygen	ppm	3.70	5.55	4-6
Biochemical oxygen demand	ppm	71.70	30.50	50
Chloride	ppm	3.38	2.02	142
Calcium	ppm	20	7.75	230
Magnesium	ppm	16.25	7.26	100
Bicarbonate	ppm	5.45	6.50	6.5-8.4
Total phosphate	ppm	2598	198.40	30
Ammonia - nitrogen	ppm	8.60	2.56	2
Iron	ppm	10.46	4.45	0.50
Copper	ppm	1.99	0.45	0.20
<i>E. coli</i>	CFU/100 mL	2500	300	100

### Conclusion

Distillery effluent released to the environment prior to any treatment poses a threat to the natural environment. Many advanced technologies are developed for wastewater treatment but most of them are not cost effective. In this study, slow sand filtration treatment technique was used as filter using locally available materials such as coarse sand, fine sand, gravels and domestic charcoal. The results of current study show that it is possible to reduce pollution from distillery wastewater. The application of slow sand filtration method can also be considered as an alternative and economical method for reducing water pollution in rural areas. This research using slower sand filtration method was found to be handy to prepare, beneficial and cost effective for reducing water contamination in rural areas.

### Acknowledgement

The authors would like to thank the Myanmar Academy of Arts and Science for allowing to present this paper and Professor and Head Dr Thida Aung, Department of Chemistry, Magway University for her kind encouragement.

### References

- Agyemang, E.O., Awuah, E., Darkwah, L., Arthur, R. and Osei, G. (2013). "Water Quality Assessment of a Wastewater Treatment Plant in a Ghanaian Beverage Industry", *International Journal of Water Resources and Environmental Engineering*, vol.5(5), pp. 272-279
- Bryant, M. and Narh, R.T. (2015). "Using Slow Sand Filtration System with Activated Charcoal Layer to Treat Salon Waste Water in a Selected Community in Cape Coast", *Ghana Journal of Advanced Chemical Engineering*, vol.5(4), pp.1-8
- Burni, M.A. and Spuhler, D. (2020). *Slow Sand Filtration*, <https://sswm.info/sswm-university-course/module-6-disaster-situations-planning-and-preparedness/further-resources-0/slow-sand-filtration> Accessed, 27, March, 2020
- Government of India and Government of the Netherlands. (1999). *Standard Analytical Procedures for Water Analysis, Hydrology Project*, New Delhi
- Gutierrez, M. (2018). "Biogas Production from Different Lignocellulosic Biomass Sources: Advances and Perspectives," *Europ PMC Tunder's Group*. vol. 8(5), pp.1-5
- Hassena, M., Malik, A., Javed, M. F., Arshad, S., Asif, N., Zulfiqar, S. and Hanif, J. (2017). "Water Pollution and Human Health". *Environ Risk Assess Remediat*, vol. 3(1), pp. 1-19
- PSSCO. (2010). *Water Quality Field Guide*. Roseville CA: PASCO Scientific, United States, America, pp.27-89
- Sharma, V., Walia, Y.K and Kumar, K. (2016). " Assessment of Physico Chemical Parameters for Analysing Water: A Review", *J. Biol. Chem. Chron*, vol.2(1), pp. 25-33
- Skat,S. (1996). *Surface Water Treatment by Roughing Filters*, A Design, Construction and Operation Manual, (3<sup>th</sup> Ed.), London, pp.1-180
- Vogel, A.L. (1968). *A Text Book of Qualitative Inorganic Analysis: (3<sup>rd</sup> Ed.)*, London: Longman, Co. Ltd
- Williams, H. (2015). *Slow Sand Filtration as a Water Treatment Method, an Inventorying Study of Slow Sand Filters Purification Rates in Rural Areas in Colombia*, Bachelor Thesis 30 ECTS Credits Bachelor of Science in Environmental and Energy Engineering, pp. 1-95

## **INVESTIGATION ON CONTAMINATION OF HEAVY METALS IN ROADSIDE SOIL AT KALI-TOLLGATE AND BAYINTNAUNG- QUARTER BETWEEN BAGO-MAWLAMYINE HIGHWAY**

San San Kyu<sup>1</sup>, Kyaw Naing<sup>2</sup>, Win Aung<sup>3</sup>

### **Abstract**

The research work intend to study the heavy metal contamination, originating from motor vehicle traffic in roadside soils near the Kali-Tollgate and Bayintnaung- Quarter on the highway road of Bago to Mawlamyine. Twenty one soil samples were collected from (Kali-Tollgate) according to the distances. Five soil samples were collected from Bayintnaung-Quarter according to the depth profile. Semi-quantitative analyses of the soil samples were done using EDXRF technique. Atomic absorption spectrophotometric method was used for the determinations of heavy metals in soil samples. Changes of concentrations of heavy metals (Pb, Zn, Cu and Cd) with distance from the highway road were studied by using single exponential decay model equation. The data were compared with maximum allowable limit of soil of highway road. The Lead content of the roadside soil range from 12.1 to 102.5 ppm, the Zinc content of the roadside soil range from 8.8 to 206.5 ppm, the copper content of the roadside soil range from 14.1 to 111.5 ppm and the cadmium content of the roadside soil range from 1.3 to 7.9 ppm according to the distance. In general heavy metal concentration decreased with increased distance from the highway road. In all soil samples measured according to the depth profile, Zn concentration was highest, whereas Cd concentration was lowest. In the depth profile of 0.5, 20- 30 cm, Pb concentration were in the range of 55.10 ppm to 20 ppm, Zn concentration were in the range of 264.20 to 56.60 ppm ,Cu concentrations were in the range of 48.0 ppm to 9.2 ppm, Cd concentrations were in the range of 2.1 ppm to 1.3ppm. The maximum heavy metal concentration was observed at 0-5 cm depth and the concentration decreased with an increase. The data obtained that measured according to the distances except Cd, were within the maximum allowable limit. They slowly find entry into food chain leading to serious health hazards. Therefore, there is an urgent need for policy regulations to minimize indiscriminate disposal of oil contaminated residues, vehicular emissions, road transport and traffic emissions and the wear and tear of mechanical parts in vehicles beside.

**Keywords:** Highway Contamination, Heavy Metal, Bago-Mawlamyine Highway Road, Kali-Tollgate, Cadmium

### **Introduction**

The term heavy metals, which is in common use, refers to metals with a density greater than a certain value, usually  $5 \text{ g cm}^{-3}$  or having atomic number greater than iron (atomic number 26). Heavy metal pollution in urban street dust has become a growing concern in recent years. Street dust is one major way through which heavy metals may find their way into soils and subsequently living tissues of plants and human being. In monitoring urban pollution, there is need to consider the material that cause the occurrence of pollutants. The main processes by which vehicles spread heavy metals (Pb, Zn, Cu, Cd) from roadside dust into the environment are combustion processes, the wear of cars (tires, brakes) refers to metals with a density greater than a certain value (brakes, engine), leaking of oil and corrosion. Lead is released in combustion of leaded petrol, zinc is derived from tire dust, copper is derived from brake abrasion and corrosion of radiators, the other heavy metals has mixed origins. Heavy metals are also released due to weathering of road surface asphalt and corrosion at crash barriers and road signs. The source of cadmium in the urban areas are much less well defined than those of lead, but metal plating and tire reinforced with metals were considered the likely common anthropogenic sources of cadmium in street dust through burning of tires and bad roads. Other sources of cadmium and zinc are found

---

<sup>1</sup> Associate professor, Department of Engineering Chemistry, Technological University (Hpa-an)

<sup>2</sup> Deputy Permanent Secretary

<sup>3</sup> Associate professor Department of Chemistry, Pakokku University

in lubricating oils as part of many activities. Environment is the basis of all forms of life. All life on earth depend on life-support systems such as pure water, fresh air and good soil (Leke, 1999). The environment impacts of toxic heavy metals are very important. This research is investigation on contamination of heavy metals in roadside soil due to the highway effects. The effect of toxic heavy are the heavy metals on roadside environment is very important to know, what metals that contained in the roadside soils, plants and how much they are contained and how much is their effects on roadside soils and plants. The aim at this research work is to study the heavy metal contamination in roadside soils near the Kali-Tollgate on the highway road of Bago to Mawlamyine.

### **Materials and Methods**

Soil samples were collected from Kali-Tollgate and Bayintnaung- Quarter on the highway road of Bago to Mawlamyine. All the samples were dried in air to drive out moisture. Each air dried samples were sieved through a nylon sieve of 250  $\mu\text{m}$  diameter. The following instruments used for the determination of heavy metals; Energy Dispersive X-ray Fluorescence Spectrometer (EDXRF- 700), Atomic Absorption Spectrophotometer (Perkin Elmer Analyst-300 AAS USA).

#### **Elemental Analysis of Soil by EDXRF Technique**

EDXRF measurements were made in accordance with the procedure mentioned with the catalogue. Before measurements samples were prepared as pellets. Thus using air as reference, EDXRE spectra of the pellets were recorded.

#### **Determination of Heavy Metal Contents in Soil by Atomic Absorption Spectrophotometric Method**

A 1g of air dried roadside soil samples were accurately weighed and place in a 250 ml beaker and them treated with 10 ml aliquots of concentrated nitric acid and the mixture was heated until dry on a sand both and then cooled. This procedure was repeated with another 10 ml concentrated hydrochloric acid. The digested soil samples were then warmed in 20 ml of 2 M hydrochloric acid to rediscover the metal salts. Extracts were filtered and the volume was then adjusted to 40 ml, with deionized water. The hydrochloric acid concentrations in the solution was determined by atomic absorption spectrophotometer.

### **Results and Discussion**

Seven soil samples from Kali-Tollgate and five soil samples from Bayintnaung-Quarter on Bago-Mawlamyiine highway road were collected according to the distances and the depth profile.

#### **Qualitative Analysis of soil samples by EDXRF Technique**

Element contents in soil samples were shown in Table 3, Fig 1, and Fig 2. All soil samples contain Si, Fe, Ca, K, Ti, Sr, Zn and Mn.

**Table 1 Roadside Soil Samples from Kali Tollgate according to the Distances**

Distances From Road (m)	Samples No.		
	Summer	Rainy	Winter
Edge	1	8	15
30	2	9	16
60	3	10	17
90	4	11	18
120	5	12	19
240	6	13	20
300	7	14	21

**Table 2 Roadside Soil Samples from Bayintnaung-Quarter according to the Depth Profile**

Depth Profile ( m)	Sample No.
0 -5	22
5-10	23
10-15	24
15-20	25
20-30	26

**Table 3 Elemental Contents in the Soil Samples (as determined by EDXRF)**

Samples	Relative abundance (%)										
	Si	Fe	Ca	K	Zn	Pb	Cu	Ti	Sr	Zr	Mn
1	74.3	2.5	5.7	9.6	-	4.7	-	0.2	2.3	0.7	-
2	81.5	10.1	2.7	3.4	0.1	0.2	-	1.3	0.1	0.2	-
3	73.6	13.3	7.6	-	-	-	-	0.8	4.4	0.3	-
4	85.9	7.9	1.2	3.2	-	0.3	-	1.1	0.1	0.2	0.2
5	88.9	5.6	0.8	3.2	-	-	-	1.1	0.1	0.2	0.2
6	87.4	6.7	1.1	2.5	0.9	0.4	0.2	1.2	0.1	0.2	0.1
7	76.7	13.4	4.1	3.1	0.2	0.6	0.2	1.1	0.1	0.2	0.2

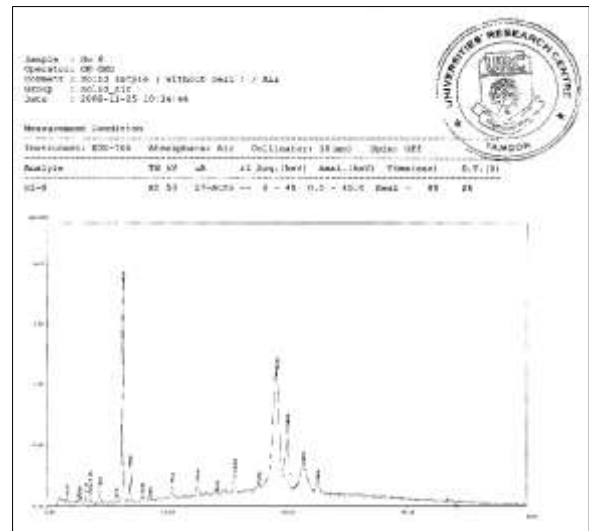
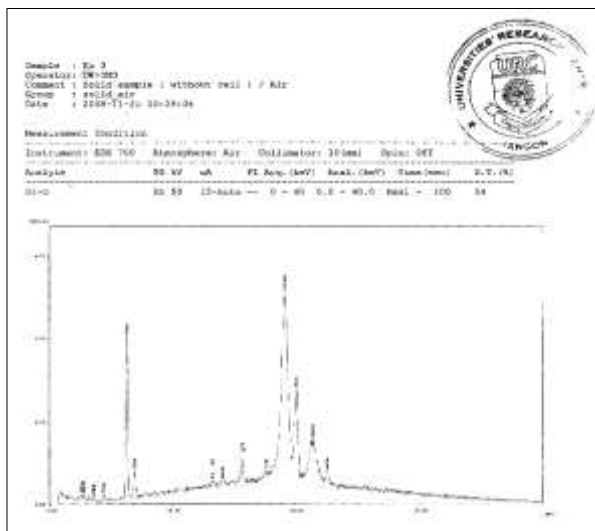


**Figure 1** EDXRF spectrum for soil sample No.3 **Figure 2** EDXRF spectrum for soil sample No.6

**Determination of heavy metal (Pb, Zn, Cu, Cd) concentrations in the soil samples were determined by AAS Technique**

The heavy metal contents in soil measured in summer season at Kali-Tollgate according to the distances were shown in table 4. The decrease of elemental concentrations with distance from the highway would indicate aerial deposition of metal particulates in the roadside environment from extraneous sources.

**Table 4 Heavy Metal Contents in Soil Measured in Summer Season at Kali-Tollgate according to the Distances**

Samples	Distances from road (m)	Pb(ppm)	Zn(ppm)	Cu(ppm)	Cd(ppm)
1	Edge	102.5	206.5	111.5	7.9
2	30	91.6	107.4	100.4	3.8
3	60	87.9	103.9	66.2	3.7
4	90	66.3	77.8	45.0	3.6
5	120	64.2	72.5	43.2	3.5
6	240	45.2	14.1	21.5	3.4
7	300	12.1	8.8	14.1	1.3
Maximum Allowable Limit		100	300	100	5

According to table, concentrations of all metals decreased with an increased in distance from the Bago-Mawlamyine highway road at Kali-Tollgate. Pb concentrations were in the range of 102.5 ppm at edge to 12.1ppm (300 m distance). Zn concentrations were in the ange of 206.5 ppm at edge to 8.8 ppm (300 m distance).Cu concentrations were in the range of 111.5 ppm at edge to 14.1 ppm (300 m distance).Cd concentrations were in the range of 7.9 ppm at edge to 1.3 ppm (300 m distance).

$$Y = ae^{-bx} \text{ (sigma plot, 2004)}$$

Where x = concentration of the studied metal

Y = the distance from the highway road

a,b = parameters of the exponential equation

(Sigma plot, 2004)

By using Microsoft excel, changes of the concentrations of heavy metals (Pb, Zn, Cu and Cd) with distance from roadside were plotted as single exponential decay model equation. The plot of Pb contents measured at Kali Tollgate in summer season was shown in Figure 3. The plot of Zn contents measured at Kali Tollgate in summer season was shown in Figure 4. The plot of Cu contents measured at Kali Tollgate in summer season was shown in Figure 5. The plot of Cd contents measured at Kali Tollgate in summer season was shown in Figure 6. From these Figures, the values of R<sup>2</sup> are equal one. So, decrease of metal concentrations from highway road were considered as single exponential decay model equation.

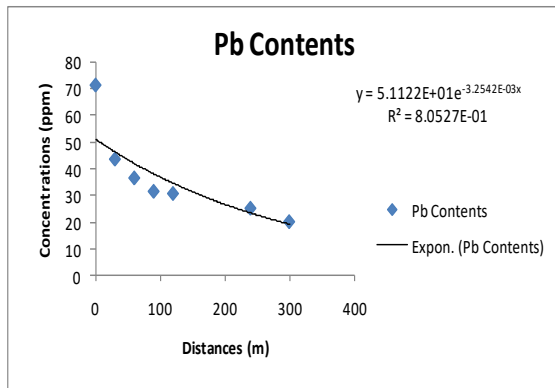


**Figure 3** Plot of Pb contents as a function of distance from highway road at Kali- Tollgate in summer season

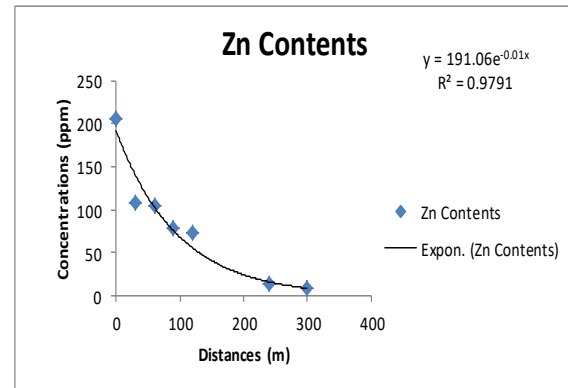


**Figure 4** Plot of Zn contents as a function of distance from highway road at Kali-Tollgate in summer season

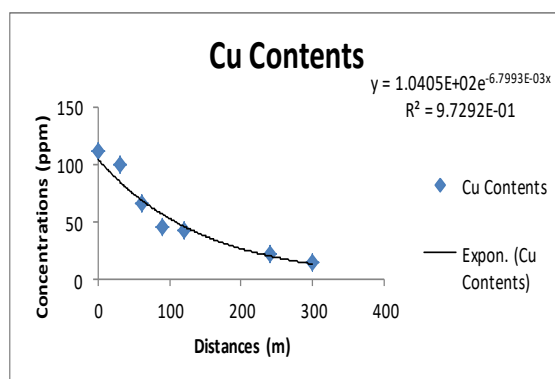


**Figure 5** Plot of Cu contents as a function of distance from highway road at Kali-Tollgate in summer season

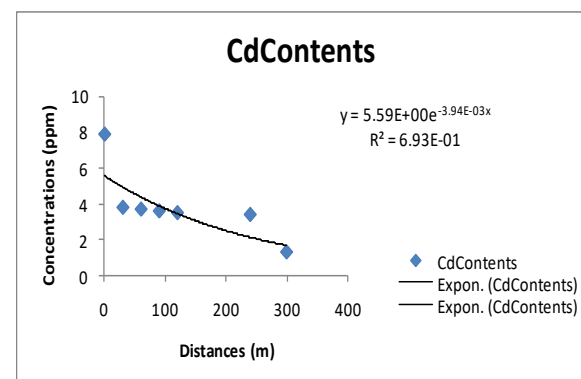


**Figure 6** Plot of Cd contents as a function of distance from highway road at Kali-Tollgate in summer season

The heavy metal contents in soil measured in rainy season at Kali-Tollgate according to the distances were shown in Table 5. According to table, concentrations of all metals decreased with an increased in distance from the Bago-Mawlamyine highway road at Kali-Tollgate because the rainfalls washed out the heavy metals in soil and carried away or permeate into the soil. Pb concentrations were in the range of 60.3 ppm at edge to 2.1 ppm (300 m distance). Zn concentrations were in the range of 158.4 ppm at edge to 4.1 ppm (300 m distance).Cu concentrations were in the range of 55.7 ppm at edge to 2.6 ppm (300 m distance).Cd concentrations were in the range of 6.1 ppm at edge to 0.5 ppm (300 m distance). The plot of Pb contents measured at Kali Tollgate in rainy season was shown in Figure 7. The plot of Zn contents measured at Kali Tollgate in rainy season was shown in Figure 8. The plot of Cu contents measured at Kali Tollgate in rainy season was shown in Figure 9. The plot of Cd contents measured at Kali Tollgate in rainy season was shown in Figure 10. Their respective exponential equation was shown in the figures.

The heavy metal contents in soil measured in winter season at Kali-Tollgate according to the distances were shown in table 6. The contaminated dust particles were carried away by the wind. The father from the edge of the road were lower the concentration of heavy metals. According to table, concentrations of all metals decreased with an increased in distance from the Bago-Mawlamyine highway road at Kali-Tollgate. Pb concentrations were in the range of 71.4 ppm at edge to 6.5 ppm (300 m distance). Zn concentrations were in the range of 173.2 ppm at edge to 5.9 ppm (300 m distance).Cu concentrations were in the range of 120.4 ppm at edge to 5.3 ppm (300 m distance).Cd concentrations were in the range of 6.8 ppm at edge to

0.9 ppm (300 m distance). Decreased of metal concentrations from highway road was considered as single exponential decay model equation. The plot of Pb contents measured at Kali Tollgate in winter season was shown in Figure 11. The plot of Zn contents measured at Kali Tollgate in winter season was shown in Figure 12. The plot of Cu contents measured at Kali Tollgate in winter season was shown in Figure 13. The plot of Cd contents measured at Kali Tollgate in winter season was shown in Figure 14. Their respective exponential equations was shown in the figures.

**Table 5 Heavy Metal Contents in Soil Measured at Kali Tollgate in Rainy Season according to the Distances**

Samples	Distances from road (m)	Pb(ppm)	Zn(ppm)	Cu(ppm)	Cd(ppm)
8	Edge	60.3	158.4	55.7	6.1
9	30	54.6	80.1	48.0	5.2
10	60	52.5	62.5	47.6	4.8
11	90	48.1	60.5	41.1	4.5
12	120	40.3	58.1	31.1	4.1
13	240	20.8	12.3	10.0	3.8
14	300	2.1	4.1	2.6	0.5
Maximum Allowable Limit		100	300	100	5

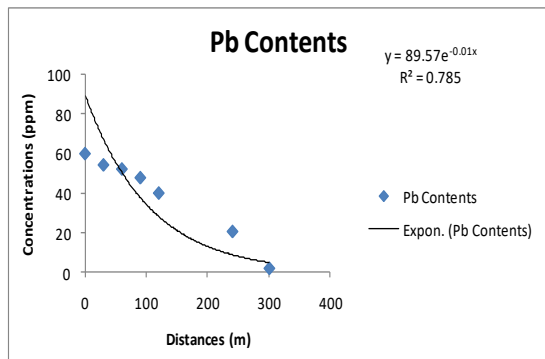


**Figure 7** Plot of Pb contents as a function of distance from highway road at Kali- Tollgate in rainy season

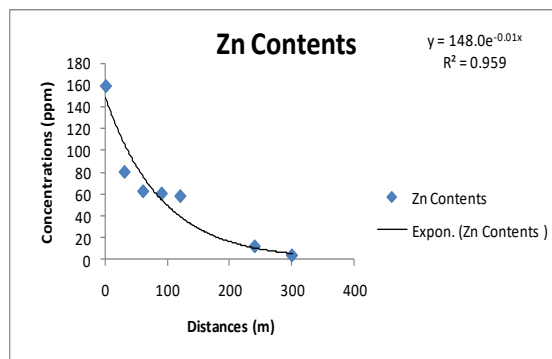


**Figure 8** Plot of Zn contents as a function of distance from highway road at Kali-Tollgate in rainy season

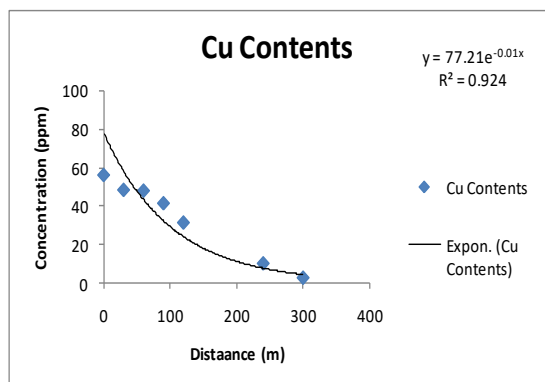


**Figure 9** Plot of Cu contents as a function of distance from highway road at Kali-Tollgate in rainy season

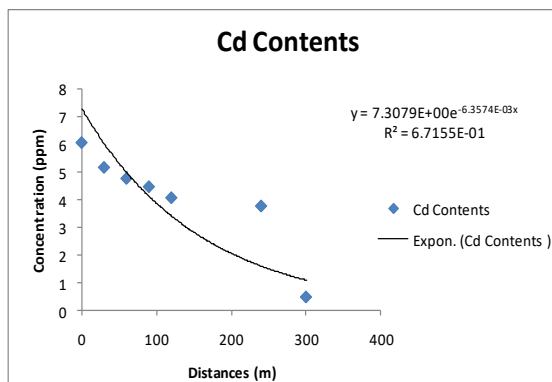


**Figure 10** Plot of Cd contents as a function of distance from highway road at Kali-Tollgate in rainy season

**Table 6 Heavy Metal Contents in Soil Measured at Kali Tollgate in Winter Season according to the Distances**

Samples	Distances from road (m)	Pb(ppm)	Zn(ppm)	Cu(ppm)	Cd(ppm)
15	Edge	71.4	173.2	120.4	6.8
16	30	43.8	159.8	102.6	6.3
17	60	36.8	142.4	92.8	5.2
18	90	31.8	138.5	16.3	4.8
19	120	31.0	94.8	5.7	4.0
20	240	20.5	70.2	5.6	3.6
21	300	6.5	5.9	5.3	0.9
Maximum Allowable Limit		100	300	100	5

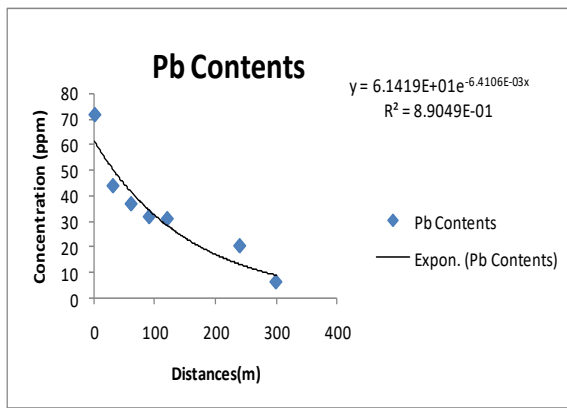


**Figure 11** Plot of Pb contents as a function of distance from highway road at Kali-Tollgate in winter season

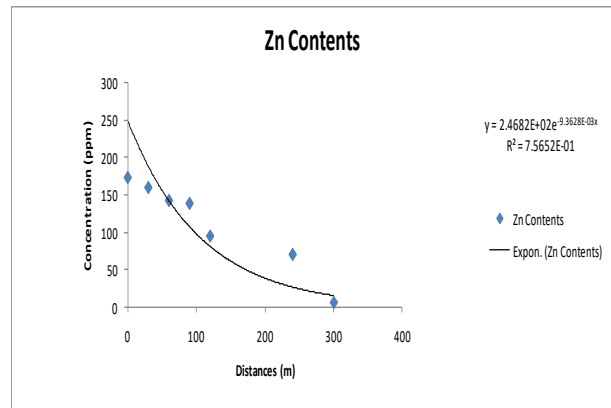


**Figure 12** Plot of Zn contents as a function of distance from highway road at Kali-Tollgate in winter season

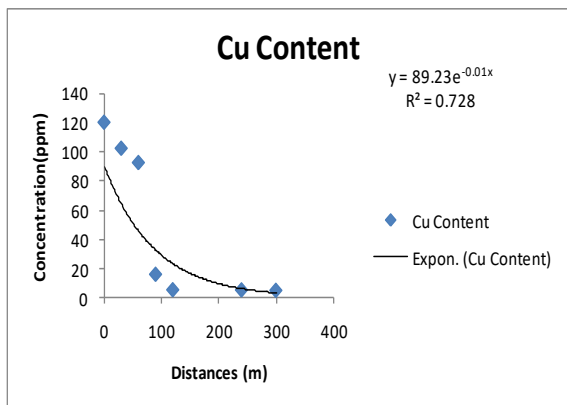


**Figure 13** Plot of Pb contents as a function of distance from highway road at Kali-Tollgate in winter season

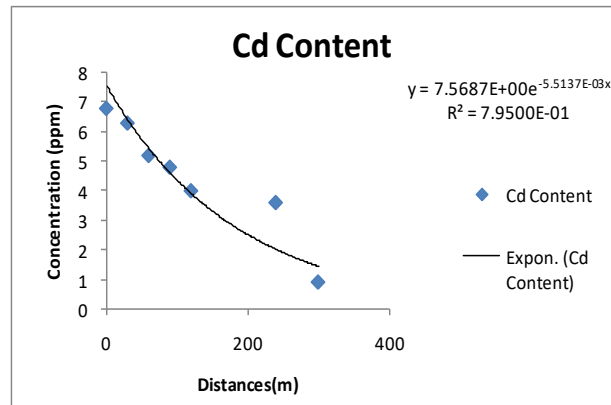


**Figure 14** Plot of Cu contents as a function of distance from highway road at Kali-Tollgate in winter season

**Table 7 The Regression Equation for the Heavy Metals Contents with Respect to Distance (X) from the Highway Road**

No.	Metals	Kali -Tollgate	
		Regression Equation	R <sup>2</sup>
1	Pb (Summer)	$Y=1.1827E+02e^{-6.1035E-03x}$	8.4599E-01
2	Zn (Summer)	$Y=191.0e^{-0.01x}$	0.979
3	Cu (Summer)	$Y=1.0405E+02e^{-6.7993E-03x}$	9.7292E-01
4	Cd (Summer)	$Y=5.59E+00 e^{-3.94E-03x}$	6.93E-01
5	Pb (Rainy )	$Y=89.57e^{-0.01x}$	0.785
6	Zn (Rainy )	$Y=148.0e^{-0.01x}$	0.959
7	Cu (Rainy )	$Y=77.21e^{-0.01x}$	0.924
8	Cd (Rainy )	$Y=7.3079E+00 e^{-6.3574E-03x}$	6.7155E-01
9	Pb (Winter )	$Y=6.1419E+01e^{-6.4106E-03x}$	8.9049E-01
10	Zn (Winter )	$Y=2.4682E+02e^{-9.3628E-03x}$	7.5652E-01
11	Cu (Winter )	$Y=89.23e^{-0.01x}$	0.728
12	Cd (Winter )	$Y=7.5687E+00e^{-5.5137E-03x}$	7.9500E-01

**Heavy Metal Concentrations Changes with the Depth Profile**

Changes of heavy metal contents with the depth profile at Bayintnaung-Quarter at the edge of Bago Mawlamyine highway road was shown in Table 8.

**Table 8 Changes of Heavy Metal Contents in Soil Samples with Depth Profile at Bayintnaung-Quarter**

Samples	Depth profile(cm)	Pb(ppm)	Zn(ppm)	Cu(ppm)	Cd(ppm)
22	0-5	55.10	264.20	48.00	2.10
23	5-10	54.90	229.50	31.40	1.90
24	10-15	53.30	175.40	27.20	1.70
25	15-20	22.90	144.20	10.60	1.70
26	20-30	20.00	56.60	9.20	1.30

From this table, in all soil samples, Zn concentrations were highest whereas Cd concentrations were lowest. In the depth profile of 0 - 5 cm and 20-30 cm, Pb concentrations were in the range of, 55.10 ppm to 20 ppm ,Zn concentration were in the range of 264.2 ppm to 56.60 ppm ,Cu concentrations were in the range of 48.0 to 9.2 ppm, Cd concentrations were in the range of 2.1 to 1.3 ppm . The maximum heavy metal concentrations were observed at 0-5 cm depth and the concentration decreased with an increase in depth.

The histogram of changes of Pb contents with depth Bayitnaung-Quarter was shown in Figure 15. The histogram of changes of Zn contents with depth Bayitnaung-Quarter was hown in Figure 16. The histogram of changes of Cu contents with depth Bayitnaung-Quarter was shown in Figure 17. The histogram of changes of Cd contents with depth Bayitnaung-Quarter was shown in Figure 18.

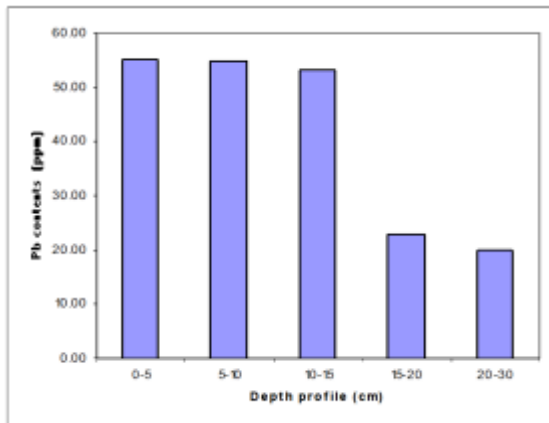


**Figure 15** Changes of Pb contents with Depth profile at Bayintnaung Quarter

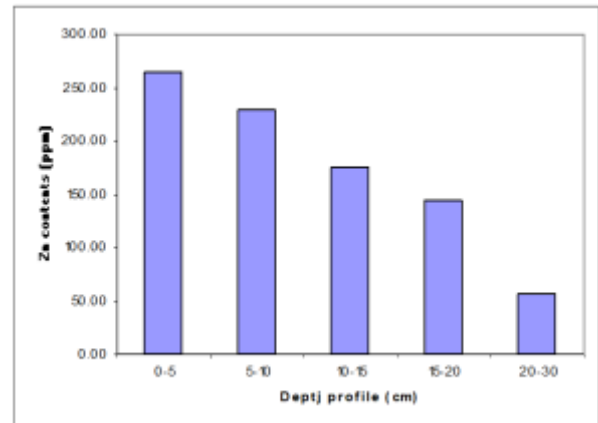


**Figure 16** Changes of Zn contents with depth profile at Bayintnaung Quarter

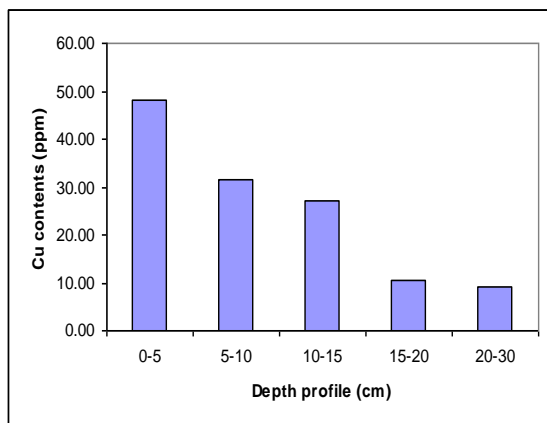


**Figure 17** Changes of Cu contents with depth profile at Bayintnaung-Quarter

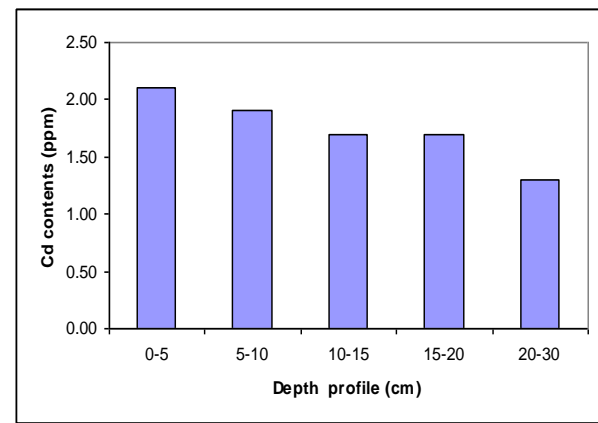


**Figure 18** Changes of Cd contents with depth profile at Bayintnaung Quarter

### Conclusion

The research work intends to study the heavy metal contamination, originating from motor vehicle traffic in roadside soils near the Kali-Tollgate on the high way road of Bago to Mawlamyine. From this research, all soil samples contain Si, Fe, Cd, K, Ti, Sr, Zn and Mn. The Lead content of the roadside soil range from 12.1 to 102.5 ppm in summer, 2.1 to 60.3 ppm in rainy, 6.5 to 71.4 ppm in winter season at Kali-Tollgate according to the distance. The Zinc content of the roadside soil range from 8.8 to 206.5 ppm in summer, 4.1 to 158.4 ppm in rainy, 5.9 to 173.2 ppm in winter season at Kali-Tollgate according to the distance. The copper content of the roadside soil range from 14.1 to 111.5 ppm in summer, 10.0 to 55.7 ppm in rainy, 5.3 to 120.4 ppm in winter season at Kali-Tollgate according to the distance. Cadmium content of the roadside soil range from 1.3 to 7.9 ppm in summer, 0.5 to 6.1 ppm in rainy, 0.9 to 6.8 ppm in winter season at Kali-Tollgate according to the distance.

In all soil samples measured according to the depth profile, Zn concentration was highest, whereas Cd concentration was lowest. In the depth profile of 20 to 30 cm to 0.5 cm. Pb concentration were in the range of, 20 ppm to 55.10 ppm, Zn concentration were in the range of 56.60 to 264.20, Cu concentrations were in the range of 9.2 to 48.0 ppm, Cd concentrations were in the range of 1.30 to 2.1 ppm. The maximum heavy metal concentrations were observed at 0-5 cm depth and the concentration decreased with an increase in depth.

The data obtained that measured according to the distances except Cd, were within the maximum allowable limit. Cd concentration was higher than that of maximum allowable limit. So, the resultant Cd contamination might be due to different sources as well as their sinks in the soil profile. The findings of present study would be helpful for understanding soil contamination in the surface soil near national highway influenced by road transportation. If the heavy metals leak into adjacent agricultural fields. They slowly find entry into food chain leading to serious health hazards. Therefore, there is an urgent need for policy regulations to minimize indiscriminate disposal of oil contaminated residues, vehicular emissions, road transport and traffic emissions and the wear and tear of mechanical parts in vehicles beside urban highways.

### Acknowledgments

The author would like to express their profound gratitude to the Department of Higher Education, Ministry of Education, Yangon, Myanmar for permitting this grant to carry out the research programme and thanks are extended to Myanmar Academy of Arts and Science, Yangon. And also thanks to Dr. Kyaw Naing, Deputy Permanent Secretary and Dr. Win Aung, Associate professor, Department of Chemistry, Pakokku University for their kind encouragement.

### References

- Ales, A.P. and Nina Zupancic, N.Z., (2009), "Heavy Metal Contamination of Roadside Soil along Ljubljana-Obrezja Highway", *RMZ-Materials and Geoenvironment*, 52, 403-418
- Ayodele, J.T., (1998), "Chromium, Zinc and Manganese in Kano Municipality Street Dust", *Chem, Soc. Nig*, 23, 24-31
- Alistair, D. and Willam H.G., (2006), "Heavy metal contamination of Roadside Soils of Northern England". Northern England", *Soil and Water Research Journal*, 1, 158-163
- Chong C. (1986), "Determination of Silver, Bismuth, Cadmium, Copper, Iron, Nickel and Zinc in Lead and Tin Base Solder and White Metal Bearing Alloys by Atomic Absorption Spectrophotometer," *Talanta*, 33, 91- 94
- Jaradat, Q.M. (1999), "Contamination of Roadside Soil, plants and Air with Heavy metals in Jordan" Jordan, A Comparative Study", *Turk J. Chem*, 23, 313-318
- Kabata, A. (1986), "*Trace Elements in Soils and Plants*", Boca Raton press, 313-318
- Leke, T.T., (1999), "*Environmental Health*", Adeka Press and Publishing Co. ltd, Markudi., 16-24
- Pendias K.A., and Pendias, H., (1992), "*Trace Elements in Soil and Plants*", 2<sup>nd</sup> Edition, Boca Raton: CRC Press, Florida, U.S.A. 305-313
- Van Bohemen, H.D. and Van De Laak, W.H.J., (2003), "The Influence of Road. Infrastructure and Traffic on Soil, Water, and Air Quality", *Environmental Management*, 31, 50-68

# AN INVESTIGATION INTO THE EFFICACY OF GRAPHENE OXIDES AS AN ADSORBENT FOR THE REMOVAL OF LEAD FROM AQUEOUS SOLUTION

Nwe Nwe Win<sup>1</sup>, Thazin Nyo<sup>2</sup>, Ohn Ohn Soe<sup>3</sup>

## Abstract

Heavy metals are a concern in the environment as they accumulate and are non-biodegradable and thus bio-toxic. Many technologies have been employed for the removal of heavy metals in the environment. However, adsorption process is arguably the most promising and effective fundamental approach for the removal of heavy metals in wastewater treatment processes. An effective and facial method for removal of Pb<sup>2+</sup> ion from aqueous solution is based on the prepared graphene oxides. The oxygenous functional groups on the surface of graphene oxides were primarily responsible for the sorption of metal ions. The graphene oxides were prepared from different graphite sources using modified Hummer's method. The prepared graphene oxides (LGO, CGO, FGO) were used as adsorbent for removal of heavy metal ion (Pb<sup>2+</sup> ion). The different graphite varieties (LGP, CGP, FGP) and the prepared graphene oxides (LGO, CGO, FGO) were characterized by XRD, UV-vis, FT IR and SEM. To obtain the optimum parameters for the removal of Pb<sup>2+</sup> ion from model aqueous solution, adsorbent dosage, Pb<sup>2+</sup> ion concentration and contact time were examined by complexometric titration method. The maximum removal capacity of Pb<sup>2+</sup> ion using LGO, CGO and FGO were found to be 94.60 %, 95.66 % and 87.32 % at their optimal conditions. The removal capacity of Pb<sup>2+</sup> ion on CGO and LGO was not quite different but FGO was lower than the other two. The obtained results demonstrated that the prepared graphene oxides can be used as an effective adsorbent for Pb<sup>2+</sup> ion removal from water.

**Keywords:** Graphite, graphene oxide, modified Hummer's method, heavy metal and adsorption capacity

## Introduction

Water pollution due to the indiscriminate disposal of metal ions and organic contaminants has been a rising worldwide environmental concern (Madadrang *et al.*, 2012). Heavy metals are among the most common pollutants found in wastewater and can be accumulated in the environmental and living tissues, causing various diseases and disordering of living organisms even at a trace level (Chen *et al.*, 2016). Pb (II) is one of the most toxic heavy metals, which is generated by mining, electroplating, dyeing, battery, textile, explosive, and other industries. Lead poisoning can bring serious risks to kidney, liver, blood, nerve, and reproductive systems, causing symptoms as anemia, chronic headache, dysentery, amentia, etc (Guo *et al.*, 2018). For environmental protection, it is necessary to remove these metal contaminants from the wastewater before releasing into the environment. Entire removal of heavy metals and organic contaminants in natural water resources can not only protect the environment itself, but also stop the toxic contaminant transfer in food chains (Madadrang *et al.*, 2012). Many technologies and methods for heavy metals ions removal from waste waters have been developed, such as ion-exchange, evaporation and concentration, chemical precipitation, reverse osmosis, adsorption, and electro dialysis (Mi *et al.*, 2012). Adsorption is the most extensively used method due to its simplicity, flexibility, insensitivity to toxic substances, high efficiency in large scale applications and low cost (Shaaban *et al.*, 2019). Graphene oxide (GO) offers interesting properties such as hydrophilicity due to the presence of carboxylic functional groups and epoxy groups essential for high sorption capacity. This material has gained importance in portable and wastewater treatment due to its

---

<sup>1</sup> 3 PhD-Chem-8, Department of Chemistry, University of Yangon

<sup>2</sup> Dr, Lecturer, Department of Chemistry, Dagon University

<sup>3</sup> Dr, Associate Professor, Department of Chemistry, Loikaw University

extraordinary properties such as its high adsorption capacity and catalysis efficiency (Khumalo *et al.*, 2017).

In this paper, the optimal conditions of  $\text{Pb}^{2+}$  ion adsorption by GO were determined such as dosage, concentration and contact time.

## Materials and Methods

### Materials

In this research, local graphite (LGP) was collected from Lin-yaung-chi mine, Mogok Township. Commercial graphite (CGP) was purchased from local chemical shop and flake graphite (FGP) was also purchased from Alfa Aesar Company, Japan. They were used without further purification. All chemicals used were of analytical reagent grade.

### Preparation of Stock and Standard Solutions of Lead (II) nitrate Solution

1.615 g of 99 %  $\text{Pb}(\text{NO}_3)_2$  was dissolved in distilled water in 1 L volumetric flask up to the mark to obtain 1000 ppm of lead stock solution. By serial dilution, the  $\text{Pb}^{2+}$  solution 200 ppm was prepared.

### Preparation of Graphene Oxides

Each graphene oxide was prepared according to the modified Hummer's method (Song *et al.*, 2014). 5 g of graphite and 2.5 g of  $\text{NaNO}_3$  were mixed with 108 mL  $\text{H}_2\text{SO}_4$  and 12 mL  $\text{H}_3\text{PO}_4$  and stirred in an ice bath for 10 min. Next, 15 g of  $\text{KMnO}_4$  was slowly added and the temperature of the mixture remained below 5 °C. The suspension was then reacted for 2 h in an ice bath and stirred for 60 min before again being stirred in a 40 °C water bath for 60 min. The temperature of the mixture was adjusted to a constant 98 °C for 60 min while water was added continuously. Deionized water was further added so that the volume of the suspension was 400 mL. After 5 min, 15 mL of  $\text{H}_2\text{O}_2$  was added to stop oxidation reaction and to reduce excess  $\text{KMnO}_4$  and the colour of mixture changed to brilliant yellow. The reaction product was washed with deionized water to remove the acid and with 5 % HCl solution repeatedly to remove metal ions. The GO gel-like layer starts appearing when the pH of the supernatant is neutralized, after several centrifugation rounds. Finally, the product was dried at 60 °C.

### Characterization of Different Graphite and the Prepared Graphene Oxides by XRD, UV-Vis, FT IR and SEM

The different graphite varieties (LGP, CGP and FGP) and prepared graphene oxides (LGO, CGO and FGO) were characterized by XRD, UV-Vis, FT IR and SEM.

### Batch Adsorption Experiments

The adsorption experiments were conducted using batch technique. In all, 1.615 g of 99 %  $\text{Pb}(\text{NO}_3)_2$  was dissolved in 1000 mL distilled water to obtain a solution with  $\text{Pb}^{2+}$  concentration of 1000  $\text{mgL}^{-1}$ . Experimental solutions of the desired concentration were obtained by further dilution. Measurements of the lead ion solutions with known concentrations of 50 to 350 ppm were conducted to optimize dosage and contact time. A certain dosage of LGO, CGO and FGO was added into the  $\text{Pb}^{2+}$  solution, then the flask was shaking under a room temperature and a fixed rotation speed of 150 rpm in a shaker. After completing a certain contact time, the prepared graphene oxides were separated from  $\text{Pb}^{2+}$  solution by filtration. The resultant filtrates were

analyzed by complexometric titration. All of the samples were tested by triplicated and all the experiments were also performed at room temperature. The removal efficiency was calculated by the following equation:

$$R \% = C_0 - C_e / C_0 \times 100$$

Where,  $C_0$  and  $C_e$  are the initial and equilibrium metal ion concentration (ppm) in the aliquots, respectively (Shaaban *et al.*, 2019).

### Titration Procedure

200 ppm of  $Pb^{2+}$  ion solution, 10 cm<sup>3</sup> of 9 % hexamethylenetetramine and 4 cm<sup>3</sup> of 0.01 % (w/v) xylenol orange indicator solution were added. The pH of this mixed solution was adjusted with a 0.01 M NaOH or 0.01 M HNO<sub>3</sub> (pH 5.6). The mixed solution was titrated with 0.01 M EDTA solution.

## Results and Discussion

### XRD Analysis

The crystalline structures of different graphite varieties and prepared graphene oxides were characterized by XRD. The X-ray Diffraction patterns (XRD) of LGP, CGP, FGP and prepared graphene oxides (LGO, CGO, FGO) were shown in Figure 1 and Table 1. The sharp peaks of graphite LGP, CGP, FGP at  $2\theta=27.44^\circ$  ( $d=0.3248$  nm),  $2\theta=26.609^\circ$  ( $d=0.3347$  nm),  $2\theta=26.485^\circ$  ( $d=0.3362$  nm) corresponding to the plane (002), that shifts to  $2\theta=10.104^\circ$  ( $d=0.8747$  nm),  $2\theta=10.557^\circ$  ( $d=0.8373$  nm),  $2\theta=10.394^\circ$  ( $d=0.8504$  nm) on chemical oxidation, confirming the formation of prepared graphene oxides (LGO, CGO, FGO). The crystallite sizes 5.13 nm, 4.05 nm and 5.33 nm can be assigned to the LGO, CGO and FGO, respectively. The increase in interlayer spacing from different graphite varieties to prepared graphene oxides is due to the introduction of the various functional groups that have been introduced by the oxidation of graphite.

### UV-Visible Analysis

The UV-vis spectroscopic measurement was carried out in the range of (200 – 400) nm to monitor the graphite samples and the degree of oxidation for the graphene oxide samples. The UV-visible spectra were shown in Figures 2 (a, b, c). The maximum  $\pi-\pi^*$  transition of C = C, C - C peaks of LGP, CGP and FGP were found ( $\lambda=258.0$  nm,  $\lambda=267.3$  nm and  $\lambda=296.1$  nm). From UV-vis spectroscopic studies, Figure 2 (d, e, f), it can be inferred that the optical absorption of LGO, CGO, FGO were dominated by the  $\pi-\pi^*$  plasmon peak near (201.6 nm, 204.2 nm, 200.8 nm). The shoulder peak at (311.2 nm, 307.6 nm, 307.8 nm) revealed for n -  $\pi^*$  transitions of C = O bond from oxidized carbon of LGO, CGO and FGO. The  $\pi-\pi^*$  plasmon peak depends on two kinds of conjugative effect: one is related to nanometer-scale  $sp^2$  clusters, and the other arises from linking chromophore units such as C = C, C = O and C - O bonds. This result clearly indicated in Table 2.

### FT IR Analysis

The FT IR analysis can be one of the direct evidences for the different graphite varieties and prepared graphene oxides as it provides information about the functional groups that present in the samples. The spectra of LGP, CGP and FGP showed typical peaks of broad band at 3624 cm<sup>-1</sup>, 3703 cm<sup>-1</sup>, 3726 cm<sup>-1</sup> related to the O-H (free and carboxylic), while the peaks at 1639 cm<sup>-1</sup>, (1479, 1037, 1033, 941, 912) cm<sup>-1</sup> and (794, 690, 540, 528, 468, 466, 414) cm<sup>-1</sup> arise from the stretching vibration of C=C, C-H in plane bending and C-H out of plane deformation of benzene. The spectra of the prepared graphene oxides illustrated absorption peaks at (3347, 3692,

3443)  $\text{cm}^{-1}$  assigned to hydroxyl groups, (3242, 3053)  $\text{cm}^{-1}$  attributed to C-H stretching vibration, (1726, 1581, 1609)  $\text{cm}^{-1}$  corresponded to C=O stretching vibrations in the carbonyl. The peak at 1548  $\text{cm}^{-1}$  is due to C=C in aromatic ring while 1377  $\text{cm}^{-1}$  corresponded to C-O stretching of carboxylic acid. 1242  $\text{cm}^{-1}$  and 1315  $\text{cm}^{-1}$  are for C-O-C stretching vibration of epoxide, 1128  $\text{cm}^{-1}$  are C-O stretching of alcohol group. The peaks at (1030, 1003, 925, 912)  $\text{cm}^{-1}$  are C-H in plane bending and (680, 584)  $\text{cm}^{-1}$  are C-H out of plane deformation of benzene, respectively. These results were shown in Figure 3 and Table 3.

### SEM Analysis

Surface morphologies of the different graphite varieties and the prepared graphene oxides were determined by using SEM and the micrographs were shown in Figure 4. Figure 4 (a, b, c) are platelet like crystalline form of carbon. Figure 4 (d) showed the SEM image of LGO which resembled randomly aggregated, thin crumpled sheets closely associated with each other and forming a disordered solid. Figure 4 (e) shows that CGO image revealed the crumpled and ripple structure which was the result of deformation upon the exfoliation and restacking processes. Figure 4 (f) shows SEM image of FGO. The morphology of FGO appears as a tightly packed layer with a corrugate surface that sometimes is wrinkled.

### Batch Adsorption Study

The batch experiments were done by studying different parameters.

#### Effect of dosage of adsorbent

The effect of dosages on the adsorption properties was investigated in the range 0.02 g to 0.14 g. Table 4 shows the corresponding data in terms of percent removal with respect to adsorbent doses. The optimal dosages were occurred at 0.08 g for (LGO, FGO), and 0.06 g for (CGO). The maximum removal percent were occurred at 92.57 % for LGO, 93.60 % for CGO and 84.30 % for FGO, respectively. Figure 5 shows the number of active sites available for adsorption increase as the adsorbent dosage increase, providing  $\text{Pb}^{2+}$  ion more probabilities to be adsorbed, consequently leading to increase of the adsorption percent. The higher the adsorbent dose is attributed to the particle interactions such as aggregation. This aggregation would lead to a decrease in the total surface area of the adsorbent. The increase of the adsorbent dosage, the adsorption percent increase, while the adsorption quantity decreased, respectively.

#### Effect of initial concentration of $\text{Pb}^{2+}$ ion

The removal of  $\text{Pb}^{2+}$  ion was performed using various initial concentrations from 50 ppm to 350 ppm at 30 min. Table 5 and Figure 6 show the removal of  $\text{Pb}^{2+}$  ion from aqueous solution. The maximum removal efficiencies were occurred at 250 ppm for all samples. The results indicate that the equilibrium sorption capacities of the sorbent increase with increasing the initial  $\text{Pb}^{2+}$  ion concentration due to the strong driving force of the concentration gradient at solid-liquid interface which causes an increase of the amount of metal ions adsorbed on the adsorbent. At low concentration of initial metal ions sufficient adsorption sites are available for the heavy metal ions and as the initial concentration of metal ions increases, more and more surface sites are covered and at high concentration of the metal ions, the capacity of the adsorbent get exhausted due to the non-availability of the surface sites.

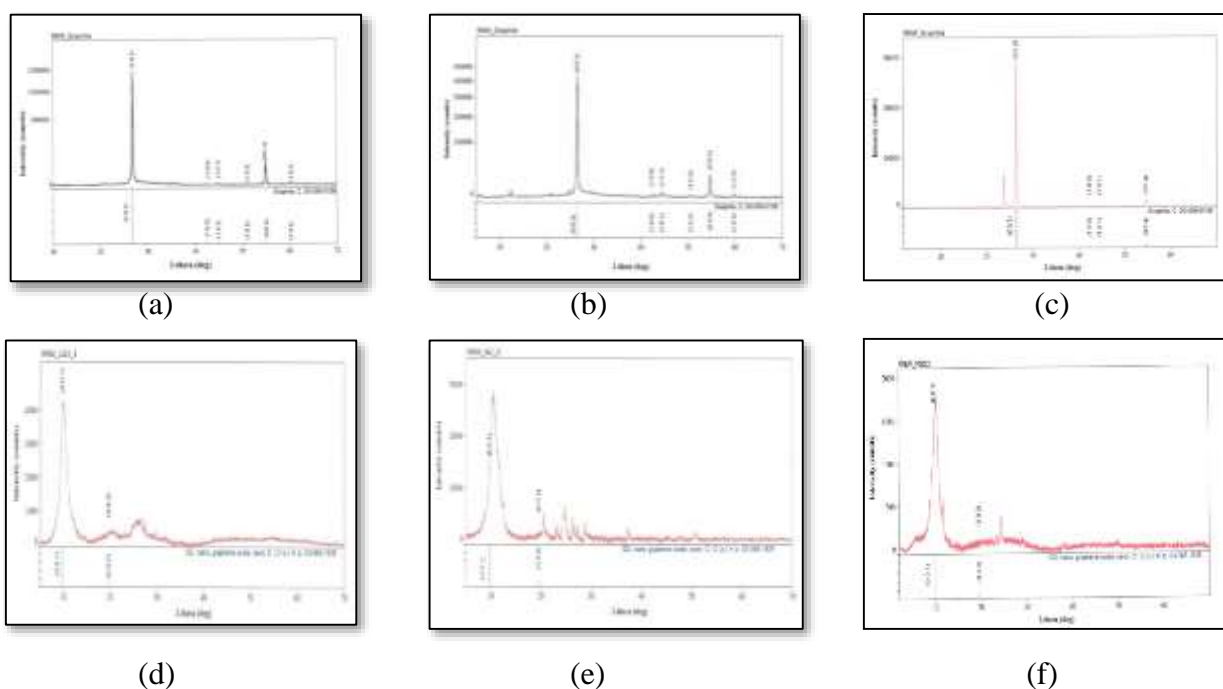
#### Effect of contact time

The influence of adsorption time intervals on the uptake capacities of the prepared graphene oxides was investigated. The contact time was varied between 15 min to 105 min. The time required to achieve the adsorption equilibrium were 60 min for LGO, 30 min for CGO and 75 min

for FGO, respectively. This can be attributed to the large surface area the sufficient exposure of active sites and the high surface reactivity of the graphene oxides. This data was shown in Table 6 and Figure 7.

**Effect of optimal parameters on Pb<sup>2+</sup> ion removal**

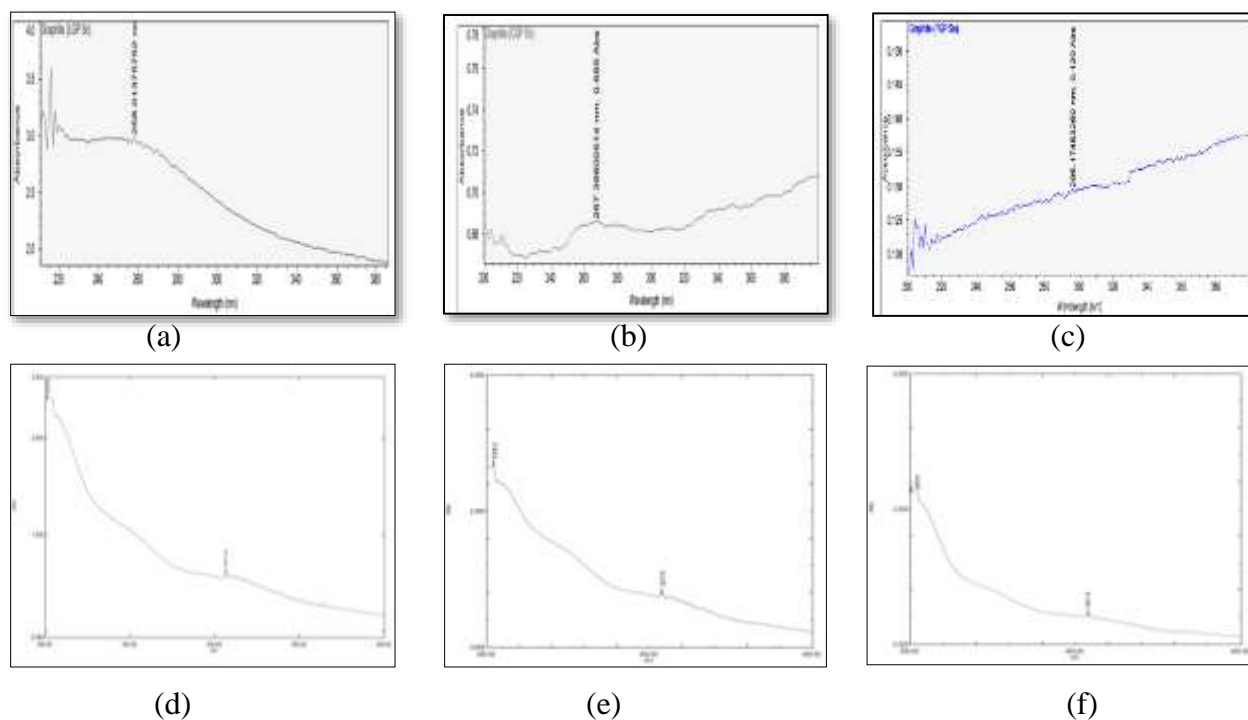
Ability of graphene oxides as adsorbent was influenced by optimal parameters. Maximum adsorption experiments were carried out at optimal condition, including adsorbent dosage, concentration of metal ion and contact time. Table 7 and Figure 8 show the maximum removal percent of Pb<sup>2+</sup> ion under comparable conditions. The maximum removal percent efficiency of Pb<sup>2+</sup> ion 94.60 %, 95.66 % and 87.32 % were found by using 0.08 g of LGO, 0.06 g of CGO and 0.08 g of FGO in 250 ppm of Pb<sup>2+</sup> ion. The optimal contact times of LGO, CGO and FGO were 60 min, 30 min and 75 min. So, CGO had a high potential for heavy metal removing compared with LGO and FGO adsorbents. Results show that the adsorption equilibrium, the removal efficiencies were nearly 96 %. Among graphene oxide samples, CGO is an excellent adsorbent for removal of heavy metal ions.



**Figure 1** XRD diffractograms of (a) LGP (b) CGP (c) FGP (d) LGO (e) CGO and (f) FGO

**Table 1** Phase Identification of LGP, CGP, FGP, LGO, CGO and FGO

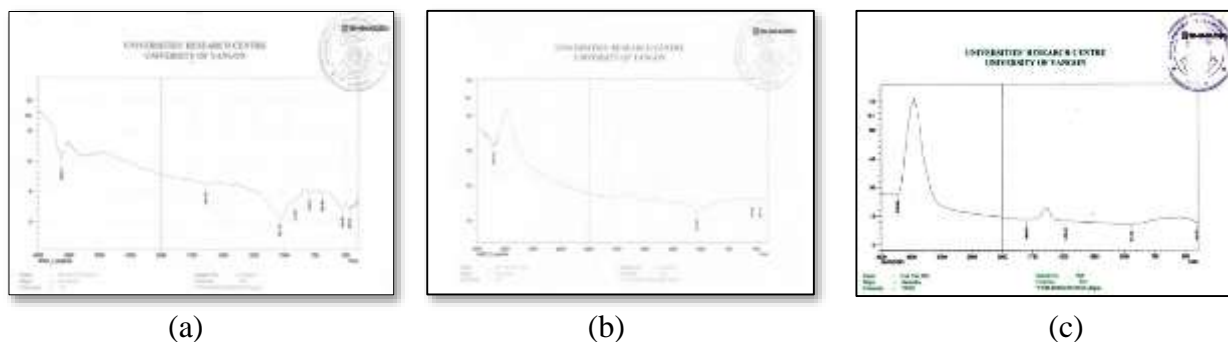
Samples	Miller Indies (h k l)	Bragg angle (2θ) Degree	Interplannar spacing d (nm)	Phase Identification	Crystallite size (nm)
LGP	0 0 2	27.44	0.3248	Graphite	56.0
CGP	0 0 2	26.609	0.3347	Graphite	40.3
FGP	0 0 2	26.485	0.3362	Graphite	33.43
LGO	0 0 1	10.104	0.8747	Graphene oxide	5.13
CGO	0 0 1	10.557	0.8373	Graphene oxide	4.05
FGO	0 0 1	10.394	0.8504	Graphene oxide	5.33



**Figure 2** UV-Vis spectra of (a) LGP (b) CGP (c) FGP, (d) LGO, (e) CGO and (f) FGO

**Table 2** UV-Vis Analysis of LGP, CGP, FGP, LGO, CGO and FGO

Samples	Wavelength (nm)	Band Assignment
LGP	258.0	$\pi$ - $\pi^*$ transition of C = C , C - C
CGP	267.3	$\pi$ - $\pi^*$ transition of C = C , C - C
FGP	296.1	$\pi$ - $\pi^*$ transition of C = C , C - C
LGO	201.6	$\pi$ - $\pi^*$ transition of C = C , C - C
	311.2	n- $\pi^*$ transition of C = O
CGO	204.2	$\pi$ - $\pi^*$ transition of C = C , C - C
	307.6	n- $\pi^*$ transition of C = O
FGO	200.8	$\pi$ - $\pi^*$ transition of C = C , C - C
	307.8	n- $\pi^*$ transition of C = O



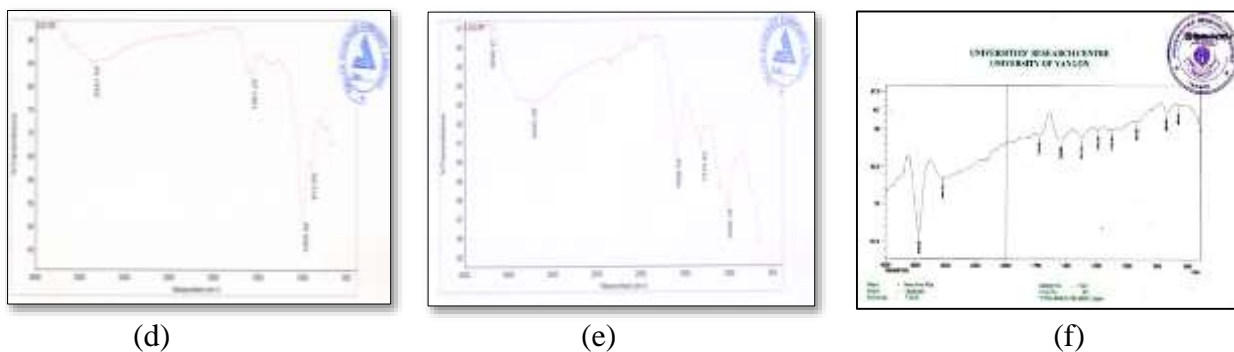
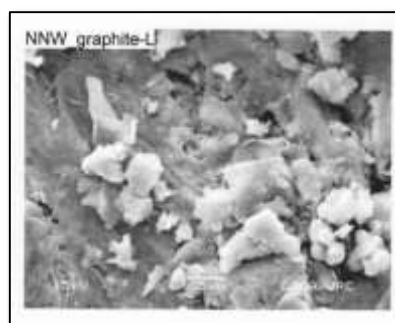


Figure 3 FT IR spectra of (a) LGP (b) CGP (c) FGP, (d) LGO (e) CGO and (f) FGO

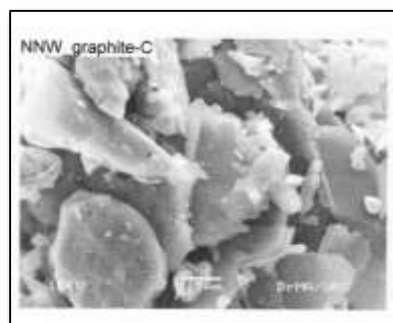
Table 3 Assignment of FT IR Spectra Data of LGP, CGP, FGP, LGO, CGO and FGO

No.	Observed value (cm <sup>-1</sup> )						Literature values* (cm <sup>-1</sup> )	Band Assignment
	LGP	CGP	FGP	LGO	CGO	FGO		
1	3624	3703	3726	3347	3692	3443	3200-3600	OH stretching vibration
2					3243			
3	-	-	-	-	-	3053	3000-3100	C-H stretching vibration
4	1639	-	-	-	-	-	1600-1750	C=C stretching vibration
5	-	-	-	1581	1609	1726	1540-1870	C=O stretching in carbonyl
6	-	-	-	-	-	1548	1500-1600	C=C stretching vibration
7	-	-	-	-	-	1377	1385	C-O stretching of carboxylic acid
8	-	-	-	-	1315	1242	1230-1320	C-O-C stretching vibration of epoxide
9	-	-	-	-	-	1128	1087-1124	C-O stretching of alcohol group
10	1037	1033	1479	1003	1030	-925	990-1790	C-H in plane bending
11	912							
12	794	540	414	-	-	680	450-750	C-H out of plane deformation (benzene)
13	690							
14	528							
15	468							
	466							

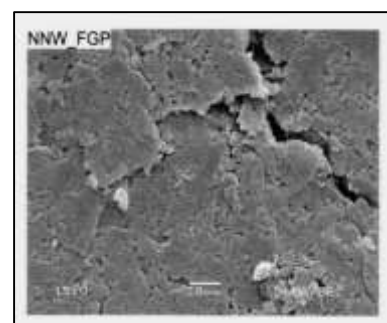
\*Sun *et al.*, 2011



(a)



(b)



(c)

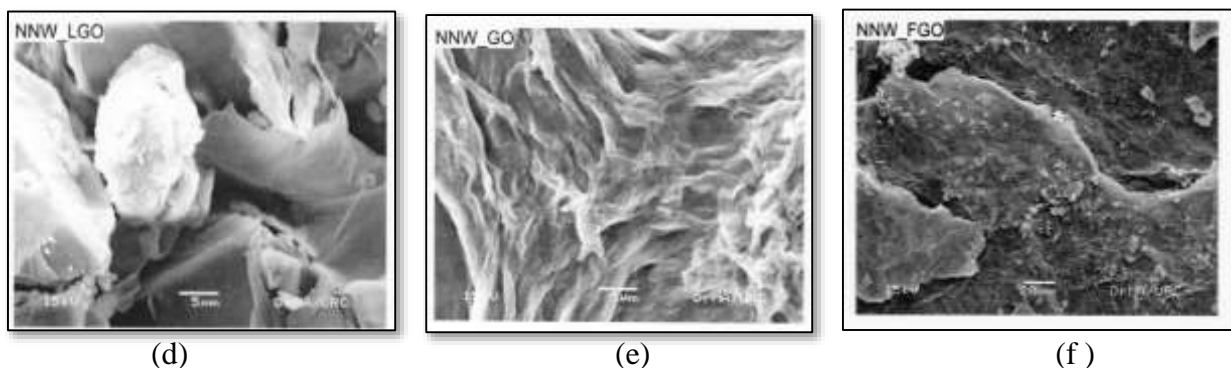
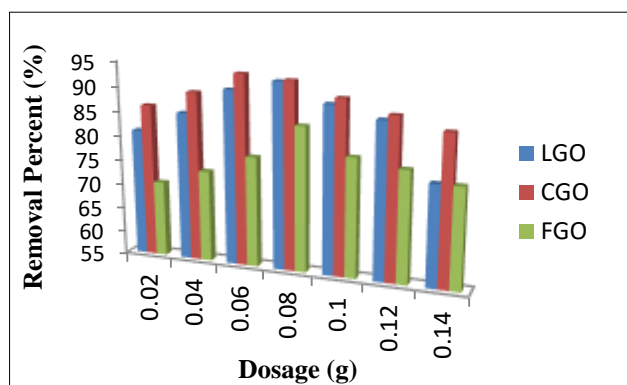


Figure 4 SEM micrographs of (a) LGP (b) CGP (c) FGP (d) LGO (e) CGO and (f) FGO

Table 4 Removal Percent of Pb<sup>2+</sup> Ion by Using Different Graphene Oxides (LGO, CGO, FGO) as a Function of Dosages

No.	Weight of Dosage (g)	Removal Percent (%)		
		LGO	CGO	FGO
1	0.02	80.85 ± 2.82	86.12 ± 4.24	70.36 ± 2.82
2	0.04	85.09 ± 1.41	89.40 ± 5.65	73.57 ± 1.41
3	0.06	90.35 ± 1.41	93.60 ± 1.41	77.35 ± 1.41
4	0.08	92.57 ± 2.82	92.85 ± 4.24	84.30 ± 1.41
5	0.10	88.82 ± 1.41	90.09 ± 2.82	79.03 ± 2.82
6	0.12	86.54 ± 2.82	87.57 ± 1.41	77.57 ± 1.41
7	0.14	75.37 ± 0.70	85.20 ± 0.70	75.37 ± 7.37



Experimental condition  
 Contact time = 30 min  
 Temperature = RT  
 Pb<sup>2+</sup> ion Concentration = 200 ppm  
 Stirring rate = 150 rpm  
 Volume of solution = 50 mL

Figure 5 Removal percent of Pb<sup>2+</sup> ion solution by different graphene oxides as a function of dosages

Table 5 Removal Percent of Pb<sup>2+</sup> Ion by Using Different Graphene Oxides (LGO, CGO, FGO) as a Function of Concentrations

No.	Concentration of Pb <sup>2+</sup> ion solution (ppm)	Removal Percent (%)		
		LGO	CGO	FGO
1	50	79.82 ± 6.25	83.08 ± 4.41	71.87 ± 4.42
2	100	81.79 ± 9.51	85.02 ± 6.34	73.12 ± 3.17
3	150	85.92 ± 3.45	91.54 ± 1.67	79.46 ± 1.72
4	200	92.81 ± 4.24	93.12 ± 1.42	84.76 ± 2.82
5	250	93.52 ± 3.13	95.08 ± 5.19	85.03 ± 3.11
6	300	86.58 ± 3.06	89.02 ± 6.16	84.58 ± 3.35
7	350	83.03 ± 4.15	86.54 ± 1.22	81.03 ± 2.34

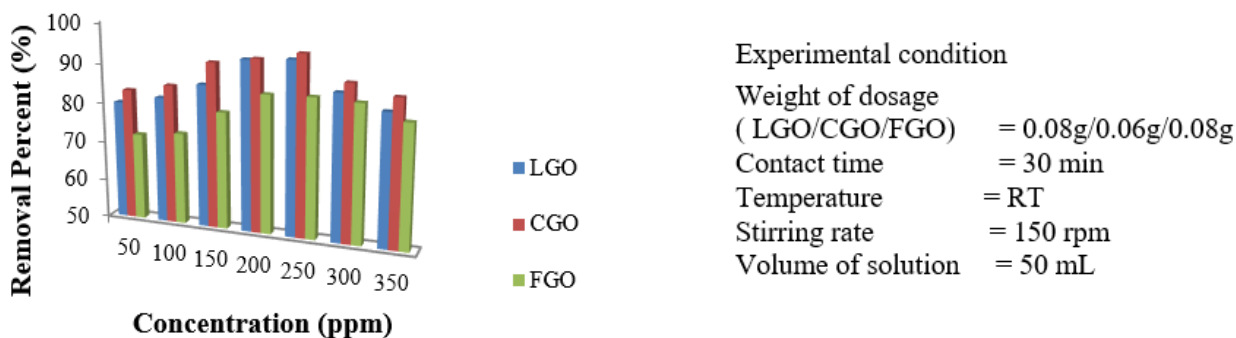


**Figure 6** Removal percent of Pb<sup>2+</sup> ion solution by different graphene oxides as a function of concentrations

**Table 6** Removal Percent of Pb<sup>2+</sup> Ion Solution by Using Different Graphene Oxides (LGO, CGO, FGO) as a Function of Contact Times

No.	Contact Time (min)	Removal Percent (%)		
		LGO	CGO	FGO
1	15	84.05 ± 1.50	88.18 ± 12.72	79.19 ± 8.17
2	30	92.85 ± 4.48	95.21 ± 2.82	84.92 ± 4.24
3	45	93.84 ± 2.82	93.16 ± 1.41	85.49 ± 5.65
4	60	94.12 ± 3.10	92.61 ± 9.89	86.51 ± 1.41
5	75	82.32 ± 2.82	89.68 ± 4.24	87.15 ± 1.41
6	90	80.36 ± 7.07	88.35 ± 1.41	84.21 ± 5.65
7	105	79.12 ± 2.82	87.46 ± 2.82	82.70 ± 7.07

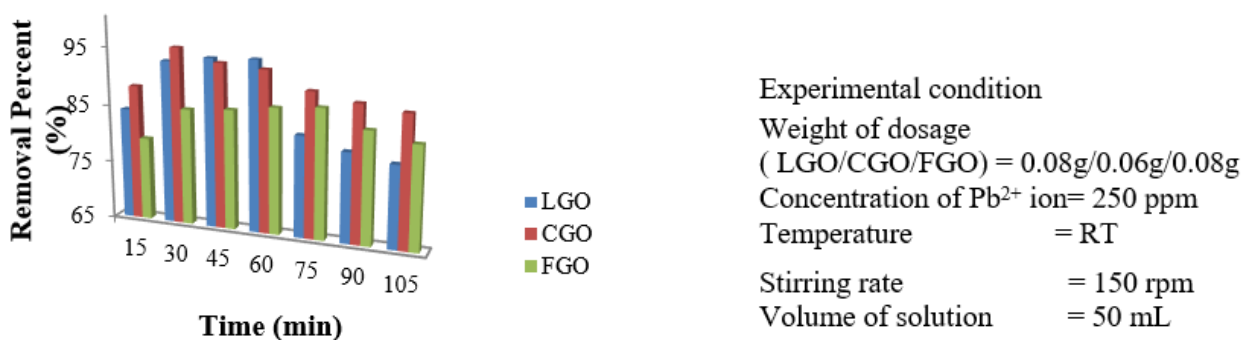


**Figure 7** Removal percent of Pb<sup>2+</sup> ion solution by graphene oxides (LGO, CGO, FGO) as a function of contact times

**Table 7** Removal of Pb<sup>2+</sup> Ion by Prepared Graphene Oxides (LGO, CGO, FGO) at Optimal Conditions

Sample	Dosage (g)	Pb <sup>2+</sup> Ion Concentration (ppm)	Time (min)	Removal Percent (%)
LGO	0.08	250	60	94.60 ± 0.16
CGO	0.06	250	30	95.66 ± 0.41
FGO	0.08	250	75	87.32 ± 0.15

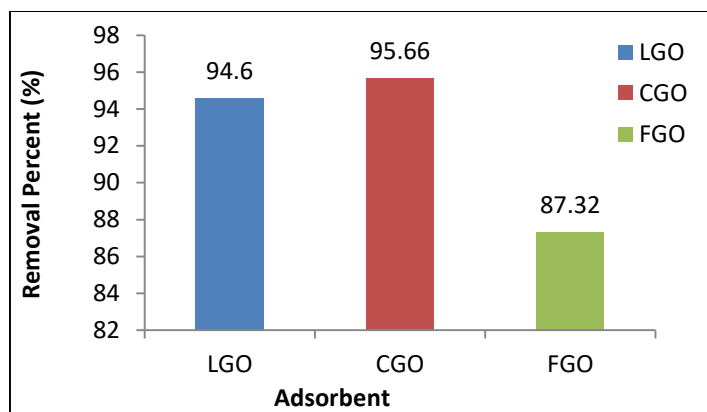


**Figure 8** The optimal parameters of prepared graphene oxides (LGO, CGO, FGO) for removal of  $Pb^{2+}$  ion

### Conclusion

The result of graphene oxide materials in adsorption indicates that it has a great future in the decontamination of water. The efficiency of these materials on the removal of heavy metals ( $Pb^{2+}$ ) from contaminated water will be depending on factors such as dosage, initial concentration of metal ion, and contact time. The presence of oxygen-containing groups and characteristic peaks in FT-IR and XRD analysis indicated the successful preparation of GO sheets. Among the prepared graphene oxides, CGO showed successfully removed nearly 95.66 % of heavy metal ion ( $Pb^{2+}$  ion) from aqueous solution under optimum experimental conditions of 250 ppm of  $Pb^{2+}$ , adsorbent dosage of 0.06 g and contact time of 30 min. CGO is highly recommended to be used in water treatment for its high adsorption capacity followed by LGO and FGO. So, CGO is an excellent adsorbent for removal of heavy metal ions. Thus, CGO can be considered the most effective adsorbent on the removal of  $Pb^{2+}$  ion from aqueous solution.

### Acknowledgements

The authors would like to thank the Myanmar Academy of Art and Science for allowing to present this paper and Professor and Head Dr Ni Ni Than, Department of Chemistry, University of Yangon, for her kind encouragement.

### References

- Chen, X., Zhou, S., Zhang, L., You, T. and Xu, F. (2016). "Adsorption of Heavy Metals by Graphene Oxide/Cellulose Hydrogel Prepared from NaOH/Urea Aqueous Solution". *Materials*, vol. 9(582), pp.1-15.
- Guo, T., Bulin, C., Li, B., Zhao, Z., Yu, H., Sun, He., Ge, X., Xing, R. and Zhang, B. (2018). "Efficient Removal of Aqueous Pb (II) Using Partially Reduced Graphene Oxide- $Fe_3O_4$ ". *Adsorption Science & Technology*, vol. 36(3-4), pp. 1031-1048.
- Khumalo, N. P., Mhlanga, S. D., Kuvarega, A. T., Vilakati, G. D., Mamba, B. B. and Dlamini, D. S. (2017). "Adsorptive Removal of Heavy Metals from Aqueous Solution by Graphene Oxide Modified Membranes". *International Journal of Scientific & Engineering Research*, vol. 8(4), pp. 1184-1194.
- Madadrang, C. J., Kim, H. Y., Gao, G., Wang, N., Zhu, J., Feng, H., Gorrington, M., Kasner, M. L. and Hou, S. (2012). "Adsorption Behavior of EDTA-Graphene Oxide for Pb (II) Removal". *ACS Applied Materials & Interfaces*, vol. 4, pp. 1186-1193.
- Mi, X., Huang, G., Xie, W., Wang, W., Liu, Y. and Gao, J. (2012). "Preparation of Graphene Oxide Aerogel and Its Adsorption for  $Cu^{2+}$  Ions". *Carbon*, vol. 50, pp. 4856-4864.
- Shaaban, A. F., Khalil, A. A., Elewa, B. S., Ismail, M. N. and Eldemerdash, U. M. (2019). "A New Modified Exfoliated Graphene Oxide for Removal of Copper (II), Lead (II) and Nickel (II) Ions from Aqueous Solutions". *Egyptian Journal of Chemistry*, vol. 62(10), pp. 1823-1849.
- Song, J., Wang, X. and Chang, C. T. (2014). "Preparation and Characterization of Graphene Oxide". *Journal of Materials*, vol. 2014, pp. 1-6.
- Sun, H., Yang, Y. and Huang, Q. (2011). "Preparation and Structural Variation of Graphite Oxide and Graphene Oxide". *Integrated Ferroelectrics an International Journal*, vol. 128, pp. 163-170.

## PREPARATION AND CHARACTERIZATION OF MAGNETITE Fe<sub>3</sub>O<sub>4</sub> NANOPARTICLES

Kyawt Kyawt<sup>1,2</sup>, Khin Mar Cho<sup>3</sup>, Myat Kyaw Thu<sup>4</sup>

### Abstract

Magnetite Fe<sub>3</sub>O<sub>4</sub> nanoparticles were prepared by a chemical co-precipitation method using FeSO<sub>4</sub>·7H<sub>2</sub>O and FeCl<sub>3</sub> as precursors. The prepared Fe<sub>3</sub>O<sub>4</sub> nanoparticles were characterized by X-ray Diffraction Analysis (XRD), Scanning Electron Microscopy (SEM), Raman Spectroscopy, Fourier Transform Infrared Spectroscopy (FT IR), Thermo gravimetric Differential Thermal Analysis (TG-DTA) and UV-Visible Spectroscopy. The XRD patterns showed the formation of the single phase for Fe<sub>3</sub>O<sub>4</sub> nanoparticles. The crystallite size of Fe<sub>3</sub>O<sub>4</sub> nanoparticles was 16.91 nm when calculated by Scherrer equation. Fe<sub>3</sub>O<sub>4</sub> nanoparticles showed face-centered cubic structure with a = 8.4099 Å. The SEM image of Fe<sub>3</sub>O<sub>4</sub> nanoparticles revealed the agglomeration of the particles. In Raman spectrum the dominant peaks were observed at 211, 274, 380, 472, 584 and 653 when using the laser 532 nm excitation source. FT IR spectral data indicated the characteristic Fe-O stretching vibration at 540 cm<sup>-1</sup>. TG-DTA thermogram showed the thermal stability of Fe<sub>3</sub>O<sub>4</sub> nanoparticles beyond 300 °C. The wavelength of maximum absorption of Fe<sub>3</sub>O<sub>4</sub> nanoparticles was observed at 322 nm.

**Keywords:** Fe<sub>3</sub>O<sub>4</sub> nanoparticles, magnetite, co-precipitation method, face-centered cubic

### Introduction

Nano is a prefix used in front of a macroscopic unit to change its value by orders of magnitude. Nano means one billionth, or 10<sup>-9</sup>. Thus, one nanometer is one billionth of a meter (Balzani, 2005). Nanoparticles are tiny materials with their sizes range from 1 to 100 nm. They can be classified into different classes according to their properties, shapes or sizes. Fullerenes, metal nanoparticles, ceramic nanoparticles, and polymeric nanoparticles are examples of different classes. Nanoparticles possess unique physical and chemical properties due to their high surface area and volume ratio. Their reactivity, toughness and other properties also depend on their unique size, shape and structure. Nanoparticles have found widespread applications in water treatment, energy production and contaminant sensing. In addition, an increasing number of literatures also describe how novel nanoparticles can be used to address major environmental challenges (Perreault *et al.*, 2015).

Metal elements are able to form different types of oxide compounds. They adopt a number of structural geometries with an electronic structure with metallic, semiconductor or insulator character such as optical, optoelectronic, magnetic, electrical, thermal, electrochemical, photo- electrochemical, mechanical, and catalytic properties (Vayssieres, 2004). The efficiency of the aforesaid properties of metal oxides largely varies with the reduction of particle size into nanoscale and which is either enhanced or completely novel properties compared to their bulk materials (Zhang, 2008). Iron oxide nanoparticles have been attracting much attention of researchers for its environmental benignity, multivalent oxidation states, abundant polymorphism, mutual polymorphous changes in nanophase, nontoxicity and low cost (Zhu *et al.*, 2014). The magnetic properties in the photocatalytic system make photocatalysts very easy to be separated and recycled from wastewater after using an external magnet (Nikazar *et al.*, 2014).

---

<sup>1</sup> PhD Candidate, Department of Chemistry, University of Yangon

<sup>2</sup> Lecturer, Department of Chemistry, Bago University

<sup>3</sup> Associate Professor, Department of Chemistry, University of Yangon

<sup>4</sup> Professor, Department of Chemistry, University of Yangon

In addition, super paramagnetic Fe<sub>3</sub>O<sub>4</sub> nanoparticles possess a promising adsorption capacity for contaminants along with optimal magnetic properties, showing rapid separation of the adsorbent from solution via a magnetic field (Chen *et al.*, 2011). Among different phases of iron oxide, the magnetite (Fe<sub>3</sub>O<sub>4</sub>), the maghemite ( $\gamma$ -Fe<sub>2</sub>O<sub>3</sub>), and the hematite ( $\alpha$ -Fe<sub>2</sub>O<sub>3</sub>) are probably the most common for fundamental study and also very important in technologically. Magnetite (Fe<sub>3</sub>O<sub>4</sub>) assumes inverse cubic spinel structure in which iron cation exists in two oxidation states of Fe<sup>2+</sup> and Fe<sup>3+</sup> and hence shows very interesting properties. Magnetic properties of magnetite nanoparticles have been widely studied because of their relevance to magnetic recording, biomedical applications and so on (Daou *et al.*, 2006). Co-precipitation is probably the simplest and most efficient synthetic route to obtain magnetic particles. In co-precipitation, a stoichiometric mixture of ferrous and ferric precursors in aqueous medium are used as an iron source, which under alkaline conditions yield super paramagnetic nanoparticles. The size distribution in co-precipitation is relatively broad because in the precipitation process, nucleation and particle growth are both present and in competition. Nevertheless, co-precipitation is most widely used because it has the potential for industrialization (Pereira *et al.*, 2012).

The aim of the present study is to prepare Fe<sub>3</sub>O<sub>4</sub> nanoparticles by chemical co-precipitation method and to study its structural, morphological and thermal properties.

## Materials and Methods

### Preparation of Fe<sub>3</sub>O<sub>4</sub> Nanoparticles

Magnetite iron (III) oxide nanoparticles were prepared by using the route of chemical co-precipitation. In brief, 50 mL of 0.02 M of aqueous iron (II) sulphate hexahydrate (FeSO<sub>4</sub>.7H<sub>2</sub>O) solution was mixed thoroughly with 50 mL of 0.04 M of aqueous iron (III) chloride (FeCl<sub>3</sub>) solution and heated to 80°C with a vigorous magnetic stirring. While stirring, ammonium hydroxide solution was added until pH 11. The dark blackish brown precipitate obtained was filtered and washed thoroughly with deionized water for several times and dried at 100°C for 12 h.

### Characterization of Fe<sub>3</sub>O<sub>4</sub> Nanoparticles

X-ray diffraction pattern of Fe<sub>3</sub>O<sub>4</sub> nanoparticles were recorded on XRD diffractometer (MultiFlex 2kW Type, Rigaku. D/max 220, Japan) at Universities' Research Center, Yangon. X-ray patterns were recorded with CuK $\alpha$  radiation ( $\lambda=1.54056 \text{ \AA}$ ) at 40 kV and 50 mA and the diffraction angle ranged from 10° to 70° of 2 $\theta$ . Crystallite size of Fe<sub>3</sub>O<sub>4</sub> nanoparticles was calculated by Scherrer's equation. Surface morphology of the prepared sample was studied by scanning electron microscope (JSM-5610LV, JEOL, Japan) at Universities' Research Center, Yangon. Molecular structure of the prepared sample was studied by Raman Spectrometer (Lab RAM HR 800, HORIBA, Japan) at Universities' Research Center, Yangon. Raman analysis was carried out with a laser at 532 nm excitation source. Fourier transform infrared (FT IR) Spectrum of the sample was recorded on FT IR spectrometer (FT-IR 8400, SHIMADZU, Japan) at Universities of Yangon. FT IR analysis was carried out in a range of wavenumber from 4000 to 400 cm<sup>-1</sup>. Thermogravimetric-Differential Analysis (TG-TDA) was performed at Universities' Research Center, Yangon. TG-TDA thermogram was obtained by using Al<sub>2</sub>O<sub>3</sub> as reference. The measurement was carried out at a heating rate of 20.0 k J min<sup>-1</sup> and scanned from 40°C to 600°C with a scanning rate of 20°C min<sup>-1</sup>, under nitrogen atmosphere of 20 psi. UV-Visible absorption spectrum of the sample was recorded in a range of 200 nm to 800 by UV-Visible (SHIMADZU UV-2600), Japan at Bago University.

## Results and Discussion

### XRD Analysis of Prepared Fe<sub>3</sub>O<sub>4</sub> Nanoparticles

The characterization of the resulting Fe<sub>3</sub>O<sub>4</sub> particles after heat treatment was performed by means of X-ray diffraction (XRD) for confirming the presence of nanoparticles and analyzing its structure. The XRD pattern of Fe<sub>3</sub>O<sub>4</sub> nanoparticles is illustrated in Figure 1. Six diffraction peaks were observed at 2θ values of 30.099°, 35.391°, 43.248°, 53.322°, 56.909° and 62.540° corresponding to Miller indices (220), (311), (400), (422), (511), and (440), respectively and a single phase of Fe<sub>3</sub>O<sub>4</sub> nanoparticles was observed (Table 1). These peaks were in well agreement with the standard Fe<sub>3</sub>O<sub>4</sub> (72-2303 > Magnetite Fe<sub>3</sub>O<sub>4</sub>). Since the Miller indices were all odd and all even Fe<sub>3</sub>O<sub>4</sub> nanoparticles were indexed as face-centered cubic with a = 8.4099 Å. The average crystallite size of Fe<sub>3</sub>O<sub>4</sub> nanoparticles was 16.91 nm using Sherrer's equation (Table 2).

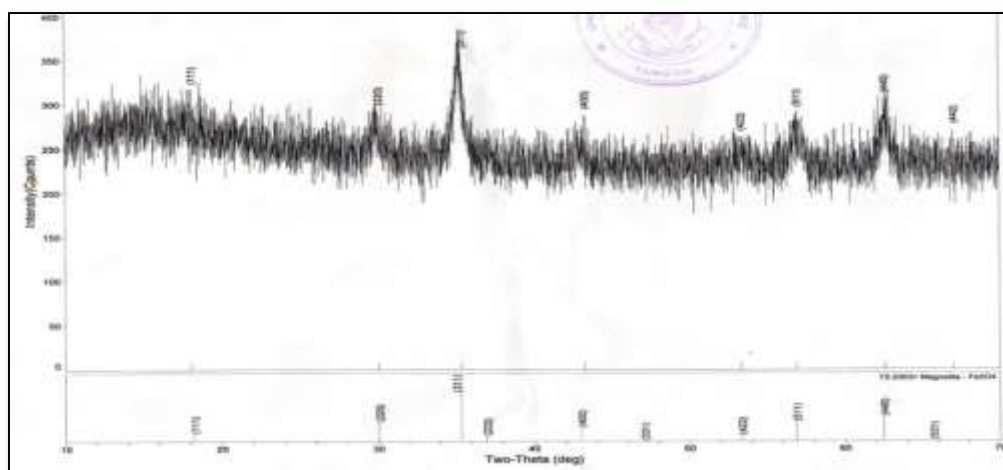


Figure 1 XRD diffractogram of Fe<sub>3</sub>O<sub>4</sub> nanoparticles

Table 1 Phase Identification of Fe<sub>3</sub>O<sub>4</sub> Nanoparticles

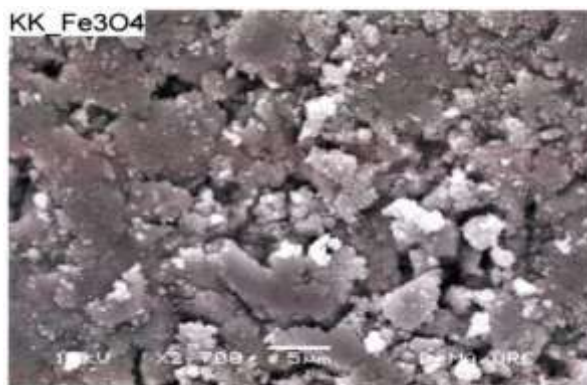
No.	Diffraction Angle '2θ' (°)	Interplanar Spacing 'd' (Å)	Miller Indices (hkl)	Phase ID
1	30.099	2.9665	220	Fe <sub>3</sub> O <sub>4</sub>
2	35.391	2.5341	311	Fe <sub>3</sub> O <sub>4</sub>
3	43.248	2.0902	400	Fe <sub>3</sub> O <sub>4</sub>
4	53.322	1.7167	422	Fe <sub>3</sub> O <sub>4</sub>
5	56.909	1.6167	511	Fe <sub>3</sub> O <sub>4</sub>
6	62.540	1.4840	440	Fe <sub>3</sub> O <sub>4</sub>

Table 2 Lattice Parameter, Crystal Structures and Average Crystallite Size of Fe<sub>3</sub>O<sub>4</sub> nanoparticles

Sample	Lattice Parameters						Crystal Structures	Average Crystallite Size (nm)
	Axial Length (Å)			Interaxial Angle (°)				
Fe <sub>3</sub> O <sub>4</sub> nanoparticles	a	b	c	α	β	γ		
	8.4099	8.4099	8.4099	90	90	90	Cubic	16.91

### SEM Analysis of Prepared Fe<sub>3</sub>O<sub>4</sub> Nanoparticles

The morphological study was done by using SEM. The SEM micrograph (Figure 2) shows the formation of large agglomerates of nanoscale particles. It can be attributed to the growth by coalescence of nuclei, resulting in particles that tend to aggregate.



**Figure 2** SEM micrograph of Fe<sub>3</sub>O<sub>4</sub> nanoparticles

### Raman Characterization

The Raman spectrum of Fe<sub>3</sub>O<sub>4</sub> nanoparticles having six Raman active modes of ( $A_{1g} + 2E_g + 3T_{2g}$ ) is illustrated in Figure 3. The vibrational frequencies at 211 cm<sup>-1</sup> ( $T_{2g(1)}$ ), 274 cm<sup>-1</sup> ( $E_g$ ), 380 cm<sup>-1</sup> ( $E_g$ ), 472 cm<sup>-1</sup> ( $T_{2g(2)}$ ), 584 cm<sup>-1</sup> ( $T_{2g(3)}$ ) and 653 cm<sup>-1</sup> ( $A_{1g}$ ), respectively, when using the laser 532 nm.  $A_{1g}$  band is due to the symmetric stretching of oxygen atoms ('breathing motion') in the tetrahedral FeO<sub>4</sub> group, along the (111) direction (Iliev *et al.*, 2011). Vibrational modes of  $E_g$  and  $T_{2g(2)}$  were attributed to the symmetric and asymmetric bending of oxygen with respect to iron in the tetrahedral void respectively. The remaining two Raman modes were due to the motion of both oxygen and iron cations at the tetrahedral sites: the  $T_{2g(3)}$  mode through an asymmetric stretching of iron and oxygen, and the  $T_{2g(1)}$  mode through the complete translation of the FeO<sub>4</sub> unit within the spinel unit cell. Reported values in the literature for these vibrations are 193 ( $T_{2g(1)}$ ), 306 ( $E_g$ ), 450–490 ( $T_{2g(2)}$ ), 538 ( $T_{2g(3)}$ ) and 668 cm<sup>-1</sup> ( $A_{1g}$ ) for the magnetite case (Shebanova and Lazor, 2003).

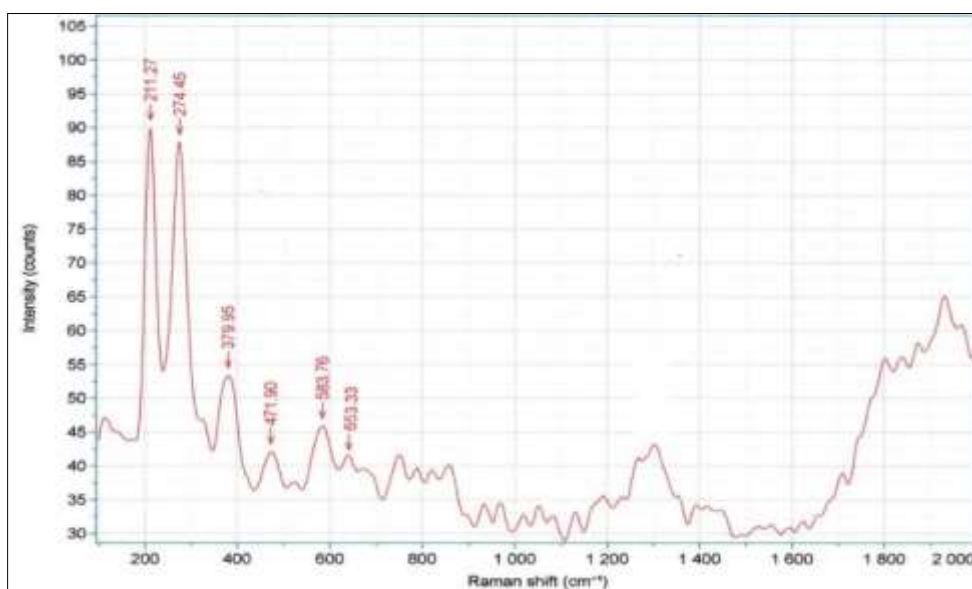


**Figure 3** Raman spectrum of Fe<sub>3</sub>O<sub>4</sub> nanoparticles

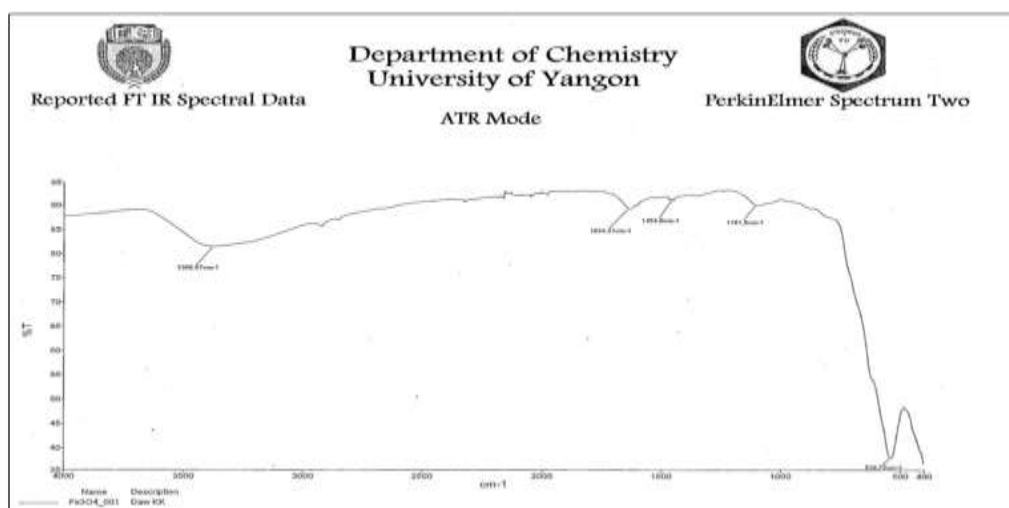
**Table 3 Raman Spectral Data Interpretation of Fe<sub>3</sub>O<sub>4</sub> Nanoparticles**

No.	Raman shift ( cm <sup>-1</sup> )		Peak Assignment
	Observed values	Reported values*	
1	211	193	T <sub>2g</sub> (1) translatory movement of the whole Fe <sub>3</sub> O <sub>4</sub>
2	274	306	E <sub>g</sub> symmetric bend of oxygen with respect to Fe
3	380	336	E <sub>g</sub> symmetric bend of oxygen with respect to Fe
4	472	450-490	T <sub>2g</sub> (2) asymmetric stretch of Fe and O
5	584	538	T <sub>2g</sub> (3) asymmetric bend of oxygen with respect to Fe
6	653	668	A <sub>1g</sub> symmetric stretch of oxygen atoms along Fe–O bonds

\*Shebanova and Lazor , 2003

### FT IR Analysis

The prepared Fe<sub>3</sub>O<sub>4</sub> nanoparticles were analyzed by FTIR spectroscopy technique in order to find out the functional groups present in the particles. FT IR spectrum of Fe<sub>3</sub>O<sub>4</sub> nanoparticles is shown in Figure 4 and the corresponding spectral data were presented in Table 4. From FT IR spectral data, the characteristic Fe-O stretching vibration was observed at 580 cm<sup>-1</sup>. The abroad band at 3369 cm<sup>-1</sup> was due to O-H stretching vibration and O-H bending vibration was also observed at 1455 cm<sup>-1</sup>.

**Figure 4** FT IR spectrum of Fe<sub>3</sub>O<sub>4</sub> nanoparticles**Table 4** FT IR Spectral Data Interpretation of Fe<sub>3</sub>O<sub>4</sub> Nanoparticles

No.	Wavenumber ( cm <sup>-1</sup> )		Band Assignment
	Observed values	Reported values	
1	3369	3000 - 3600*	O-H stretching vibration
2	1455	1200 - 1450*	O-H bending Vibration
3	580	577**	Fe-O stretching vibration

\* Willard *et al.*, 1965\*\* Farrokhi *et al.*, 2014

## TG-DTA Analysis

TG-DTA is based on the changes in physical and chemical properties of material, when the temperature is increasing, measuring the difference in the weight and providing information about the composition and the purity of the sample. The sample is usually in the solid state and the changes that occur on heating include melting, phase transition, sublimation and decomposition. The decomposition temperature for the three different precursors was determined in order to know the influence of the precursor design on the structure and morphology of the obtained nanoparticles (Shriver, 2006).

TG-DTA analysis is performed for  $\text{Fe}_3\text{O}_4$  nanoparticles between 40 °C to 600 °C. TG-DTA thermogram of  $\text{Fe}_3\text{O}_4$  nanoparticles is shown in Figure 5 and the corresponding thermal data are presented in Table 5. From TG-DTA thermogram, two endothermic peaks were observed. Between the temperatures 30 °C to 120 °C the weight loss was about 7.07 % due to removal of adsorbed water molecules on the surface. Between 110 °C to 250 °C the weight loss was about 2.2 % due to removal of residual water molecules. Beyond 300 °C,  $\text{Fe}_3\text{O}_4$  nanoparticles were thermally stable. The total weight loss for  $\text{Fe}_3\text{O}_4$  nanoparticles was 11.05 %.

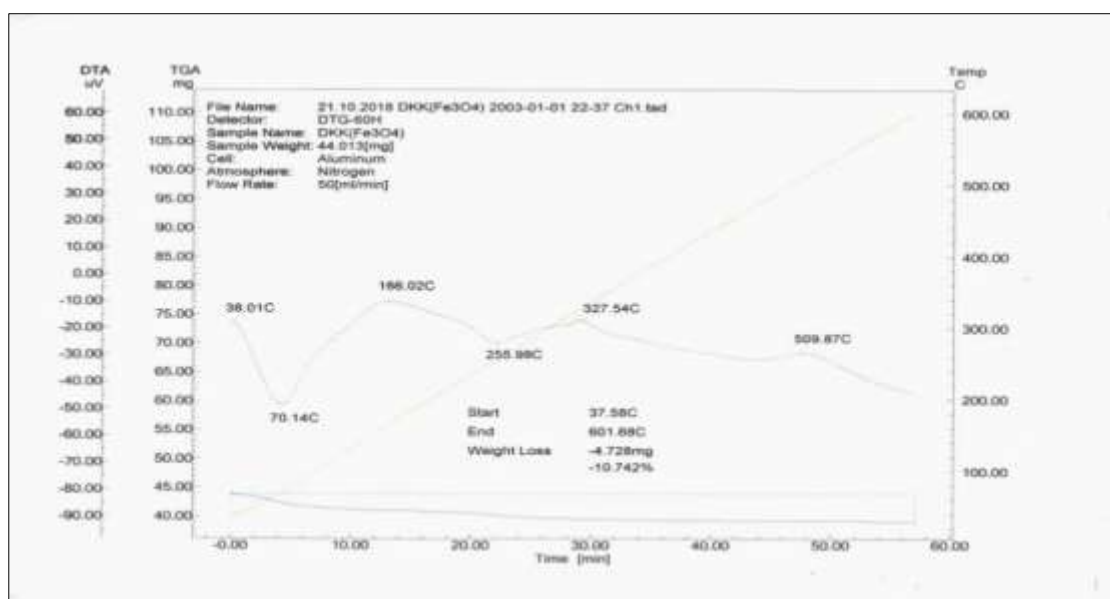


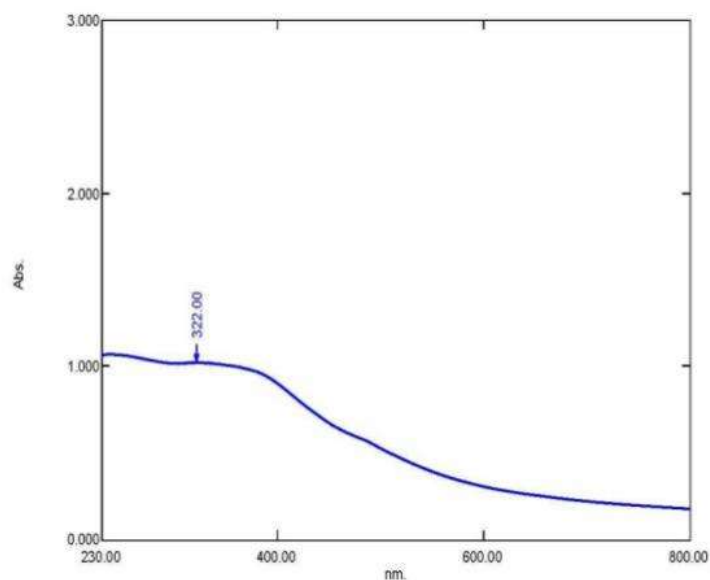
Figure 5 TG-DTA thermogram of  $\text{Fe}_3\text{O}_4$  nanoparticles

Table 5 TG-DTA Data of  $\text{Fe}_3\text{O}_4$  Nanoparticles

No.	Temperature Range (°C)	Break in Temperature(°C)	Weight loss (%)	Nature of peak	Remark
1	37.58 - 120	70.14	7.07	Endothermic peak	Removal of adsorbed water
2	120 - 310	255.98	2.2	Endothermic peak (very small)	Removal of residual water
3	310 - 601.68	-	1.78	-	Thermally stable

## UV-Visible Spectroscopy

UV-Visible spectrophotometer was used to study the optical absorption. The optical absorption spectrum for Fe<sub>3</sub>O<sub>4</sub> nanoparticles is shown in Figure 6. From UV-Visible absorption spectrum, it was observed that the maximum absorption peak of Fe<sub>3</sub>O<sub>4</sub> nanoparticles was 322 nm. This could be due to the excitation of nanoparticles from ground state to excited state (Rajendran and Sengodan, 2017).



**Figure 6** UV-Visible absorption spectrum of Fe<sub>3</sub>O<sub>4</sub> nanoparticles

## Conclusion

From the overall assessment of the present research work, the following inferences would be drawn. In this research, magnetic iron oxide (Fe<sub>3</sub>O<sub>4</sub>) nanoparticles were prepared by coprecipitation of Fe<sup>2+</sup> and Fe<sup>3+</sup> salts solution with ammonium hydroxide solution. Resulting sample was analyzed utilizing XRD, SEM, Raman spectroscopy, FT IR, TG-TDA, and UV-Visible methods. The Fe<sub>3</sub>O<sub>4</sub> nanoparticles were indexed as cubic with a crystallite size of 16.91 nm. SEM image of Fe<sub>3</sub>O<sub>4</sub> nanoparticles were generally spherical in shape and that they tend to form agglomerates and connect tightly to one another to form groups. From Raman spectroscopy, Fe<sub>3</sub>O<sub>4</sub> nanoparticles had six Raman active modes including the characteristic peak of Fe<sub>3</sub>O<sub>4</sub> at 653 cm<sup>-1</sup>. It revealed the main phase of magnetite. From FT IR spectral data, Fe-O stretching vibration was observed at 580 cm<sup>-1</sup>. TG-TDA analysis revealed the thermally stable of Fe<sub>3</sub>O<sub>4</sub> nanoparticles beyond 300 °C. From UV-Visible absorption spectrum, the wavelength of maximum absorption of Fe<sub>3</sub>O<sub>4</sub> nanoparticles was found at 322 nm. This result suggests that the Fe<sub>3</sub>O<sub>4</sub> nanoparticles had strong light absorption properties in the ultraviolet and visible light range and can degrade organic pollutants in the wide spectral range.

## Acknowledgements

The authors would like to acknowledge to Dr Ni Ni Than, Professor and Head, Department of Chemistry, University of Yangon for providing to do this research work. The authors would also like to express our gratitude to the Myanmar Academy of Arts and Science for allowing to submit this paper.

## References

- Balzani, V. (2005). "Nanoscience and Nanotechnology: A Personal View of a Chemist". *Small*, vol. 1(3), pp.278-283
- Chen, C., Gunawan, P. and Xu, R. (2011). "Self-Assembled Fe<sub>3</sub>O<sub>4</sub>-Layered Double Hydroxide Colloidal Nanohybrids with Excellent Performance for Treatment of Organic Dyes in Water". *Journal of Materials Chemistry*, vol. 21, pp. 1218-1225
- Daou, T., Pourroy, J., Bégin-Colin, G., Greneche, S., Ulhaq-Bouillet, J. M., Legare, C., Bernhardt, P., Leuvrey, P. and Rogez, G. (2006). "Hydrothermal Synthesis of Monodisperse Magnetite Nanoparticles". *Chem Mater.*, vol. 18, pp. 4399-4404
- Farrokhi, M., Seyydeh-Cobra, H., Jae-Kyu, Y. and Shirzard-Siboni, M. (2014). "Application of Fe<sub>3</sub>O<sub>4</sub>-ZnO Nanocomposite on the Removal of Azo Dye from Aqueous Solution: Kinetics and Equilibrium Studies". *J. Water Air Soil Pollute*, vol. 325 (211), pp.1-12
- Iliev, M. N., Mazumdar, D., Ma, J. X., Gupta, A., Rigato, F. and Fontcuberta, J. (2011). "Monitoring B-site Ordering and Strain Relaxation in NiFe<sub>2</sub>O<sub>4</sub> Epitaxial Films by Polarized Raman Spectroscopy". *Phys Rev. B*, vol. 83, pp. 014108
- Nikazar, M., Alizadeh M., Lalavi R. and Rostami, M.H. (2014). "The Optimum Conditions for Synthesis of Fe<sub>3</sub>O<sub>4</sub>/ZnO Core/Shell Magnetic Nanoparticles for Photodegradation of Phenol". *Iranian J. Environ. Health Sci. Eng.*, vol. 12 (21), pp.3-6
- Pereira, C., Pereira, A. M., Fernandes, C., Rocha, M., Mendes, R., Fernandez-Garcia, M. P., Guedes, A., Tavares, P. B., Greneche, J. M., Jo, J. P. A. and Freire, C. (2012). "Superparamagnetic MFe<sub>2</sub>O<sub>4</sub> (M = Fe, Co, Mn) Nanoparticles: Tuning the Particle Size and Magnetic Properties through a Novel One-Step Coprecipitation Route". *Chem. Mater.*, vol. 24, pp.1496-1504
- Perreault, F., de Faria, A. F. and Elimelech, M. (2015). "Environmental Applications of Graphene-Based Nanomaterials". *Chem. Soc. Rev.*, pp. 390
- Rajendran, S.P. and Sengodan, K. (2017). "Synthesis and Characterization of Zinc Oxide and Iron Oxide Nanoparticles Using Sesbania Grandiflora Leaf Extract as Reducing Agent". *Journal of Nanoscience* vol.2017, pp.1-11
- Shebanova, O.N. and Lazor, P. (2003). "Raman Spectroscopic Study of Magnetite (FeFe<sub>2</sub>O<sub>4</sub>): A New Assignment for the Vibrational Spectrum". *Journal of Solid State Chemistry*, vol.174, pp. 424-430
- Shriver, D.F. and Atkins, P.W. (2006). *Inorganic Chemistry*. Oxford: 4<sup>th</sup>Ed. Oxford University Press, pp.189-190
- Vayssieres, L. (2004). "On the Design of Advanced Metal Oxide Nanomaterials," *Int. J. of Nanotechnology*, vol.1, pp. 1-40
- Willard, H.H., Merritt, L.L. and Dean, J.A. (1965). *Instrumental Method of Analysis*. New York: 4<sup>th</sup> Edition, D. Van Nostrand Co., Inc., pp. 142-143
- Zhang, M. (2008). *Nonaqueous Synthesis of Metal Oxide Nanoparticles and Their Surface Coating*. Ph.D., University of New Orleans
- Zhu, J., Simon Ng, K. Y. and Deng, D. (2014). "Micro Single Crystals of Hematite with Nearly 100% Exposed {104} Facets: Preferred Etching and Lithium Storage". *Cryst.Growth Des.*, vol. 14,

## PREPARATION OF Fe<sub>3</sub>O<sub>4</sub>-ZnO-CuO NANOCOMPOSITES WITH DIFFERENT MOLE RATIOS AND THEIR CHARACTERIZATIONS

Ei Ei Phyto Cin<sup>1</sup>, Khin Mar Cho<sup>2</sup>, Yee Mun Than<sup>3</sup>

### Abstract

Magnetically separable Fe<sub>3</sub>O<sub>4</sub>-ZnO-CuO nanocomposites were prepared by sol-gel method. The XRD pattern of Fe<sub>3</sub>O<sub>4</sub>- ZnO- CuO nanocomposite showed the presence of Fe<sub>3</sub>O<sub>4</sub>, ZnO and CuO peaks. The crystallite sizes of Fe<sub>3</sub>O<sub>4</sub>- ZnO-0.5CuO, Fe<sub>3</sub>O<sub>4</sub>- ZnO- 1CuO, Fe<sub>3</sub>O<sub>4</sub>- ZnO- 2.5CuO and Fe<sub>3</sub>O<sub>4</sub>- ZnO- 5CuO nanocomposites were also calculated as 34.1 nm, 23.4 nm, 25.1 nm and 24.4 nm respectively. Characteristic peaks of Fe-O, Zn-O and Cu-O were found in the FT IR spectra. SEM images of Fe<sub>3</sub>O<sub>4</sub>- ZnO- CuO nanocomposite showed both spherical and clew like shaped particles. EDS showed the presence of Fe, Zn, Cu and O elements in Fe<sub>3</sub>O<sub>4</sub>- ZnO- CuO nanocomposite. Fe<sub>3</sub>O<sub>4</sub>- ZnO- CuO nanocomposites with different mole ratios were found to have cubic structure and TEM image of Fe<sub>3</sub>O<sub>4</sub>-ZnO-CuO nanocomposite also showed the cubic morphology. By TG-DTA weight loss less than 7 % were indicated thermal stability of the prepared of Fe<sub>3</sub>O<sub>4</sub>- ZnO- CuO nanocomposite.

**Keywords:** nanocomposite, sol-gel method, cubic morphology, thermal stability

### Introduction

Nanomaterial is a material with the size of nanoscale (1-100 nm). This material has a unique properties and high value for commercial applications. The key factors of nanoparticles are small particle size, narrow size distribution, low agglomeration and high dispersion. Nanomaterial can be applied in various fields such as cosmetics, paints, displays, batteries, medicine, catalysis, gas sensor, food engineering (production, processing, safety and packaging), agriculture, energy (storage and conversion) and construction (Akir *et al.*, 2016).

The semiconductor zinc oxide (ZnO) is one of the most efficient and environmentally-friendly catalysts because of its non-toxicity, low cost, good catalytic performance and high stability. However, ZnO having direct wide band-gap (~3.24 eV) is only responsive to ultraviolet (UV) light and reduces its efficiency in visible light. ZnO causes a high recombination rate of electron and hole which are produced due to the irradiation of light (Hou *et al.*, 2015; Akir *et al.*, 2016). Therefore, to overcome these limitations, methods like doping, coupled with another semiconductor and deposition of noble metal can be used for the modification of ZnO (Mageshwari *et al.*, 2016). Combining ZnO with CuO helps in separating photogenerated electron-hole pairs, which is crucial for effective photocatalysis and thus, increasing the degradation efficiency of organic dye (Taufik and Saleh, 2017).

In general, after the completion of the photocatalytic reaction it is difficult to recover the photocatalyst from the mixture. Since Fe<sub>3</sub>O<sub>4</sub> has not only the good adsorption capacity but also possesses magnetic property it can magnetically separate the catalyst from organic dye solution easier.

Thus, a magnetic material such as Fe<sub>3</sub>O<sub>4</sub> coupled with the ZnO-CuO nanocomposite can be used for the removal of dye and to be reused the composite by magnetic isolation (Heravi *et al.*, 2015). Magnetic separation is an easy and time saving method for separating and recycling materials used as photocatalysts under a suitable magnetic field. This method can reduce the extent of agglomeration during recovery and can improve the reusability of the catalyst (Xuan *et al.*, 2008).

---

<sup>1</sup> Lecturer, Department of Chemistry, Taunggoke Degree College

<sup>2</sup> Associate Professor, Department of Chemistry, University of Yangon

<sup>3</sup> Lecturer, Department of Chemistry, University of Yangon

The main aim of this research is to synthesize the magnetically separable Fe<sub>3</sub>O<sub>4</sub>-ZnO- CuO nanocomposites with different mole ratios by sol-gel method and structurally characterize.

## Materials and Methods

### Preparation of CuO Nanoparticles

CuO nanoparticles were prepared by sol-gel method as described by Taufik *et al.*, (2015) with some modifications.

Briefly, 150 mL of 0.33 M sodium hydroxide solution was added drop-wise into 100 mL of 0.25 M Cu (NO<sub>3</sub>)<sub>2</sub>. 3H<sub>2</sub>O solution (0.25 mol) in a 500 mL beaker with constant stirring in one direction until pH 12 was reached. Then, it was kept at 80 °C under magnetically stirring for 3 h to form a gel. After drying the gel at 80 °C for 4 h, it was annealed at 125 °C for 5 h to get black powder of CuO. The gel was then annealed at 600 °C for 5 h in a muffle furnace.

In similar way, the procedure was carried out using 0.125 M, 0.625 M and 1.25 M of Cu(NO<sub>3</sub>)<sub>2</sub>.3H<sub>2</sub>O solutions were used to get different mole ratios of the nanocomposites.

### Preparation of Fe<sub>3</sub>O<sub>4</sub> Nanoparticles

Fe<sub>3</sub>O<sub>4</sub> nanoparticles were prepared by sol-gel method as described by Taufik *et al.*, (2015) with some modifications.

Firstly, 5 mL of glacial acetic acid (CH<sub>3</sub>COOH) and 30 mL of ethylene glycol (CH<sub>2</sub>OH)<sub>2</sub> were added into 100 mL of 0.25 M FeSO<sub>4</sub>.7H<sub>2</sub>O solution (0.025 mol) in a 500 mL beaker while stirring continuously until pH value of 3 was reached. After that, 150 mL of 0.33 M of sodium hydroxide solution was added drop-wise into the above solution with constant stirring in one direction until pH 3 was reached. The final solution was kept at 80 °C under magnetically stirring for 3h to form a gel. After drying the gel at 80 °C for 4 h, it was annealed at 125 °C for 3 h to get black powder of Fe<sub>3</sub>O<sub>4</sub>.

### Preparation of Different Mole Ratios of Fe<sub>3</sub>O<sub>4</sub>-ZnO-CuO Nanocomposite

Fe<sub>3</sub>O<sub>4</sub>-ZnO-CuO nanocomposite was prepared by sol-gel method as described by Taufik *et al.*, (2015) with some modifications.

Firstly, 50 mL of 0.5 M of NaOH solution (0.025 mol) was added drop-wise into 100 mL of 0.25 M ZnSO<sub>4</sub>.7H<sub>2</sub>O solution (0.125 mol). This solution is designated as solution A and it was stirred and heated at 80 °C. Meanwhile, the above synthesized Fe<sub>3</sub>O<sub>4</sub> and CuO nanoparticles were dispersed in 30 mL each of ethanol and were designated as solutions B and C, respectively. After that, solutions B and C were added into solution A and the mixtures were continuously stirred at 80 °C for 2 h. Then, the mixtures were centrifuged and washed for several times with ethanol and distilled water. The final product was allowed to stand overnight at room temperature and then heated at 125 °C for 5 h under vacuum condition. In this way Fe<sub>3</sub>O<sub>4</sub>- ZnO- CuO nanocomposite was obtained. The following mole ratios of metal oxides were used as described in Table 1 to get other mole ratios of nanocomposites.

**Table 1 Mole Ratios of Metal Oxides for Fe<sub>3</sub>O<sub>4</sub>-ZnO-CuO Nanocomposites**

No	Sample	Mole of Metal Oxide (mol)		
		ZnO	Fe <sub>3</sub> O <sub>4</sub>	CuO
1	Fe <sub>3</sub> O <sub>4</sub> -ZnO-0.5 CuO	0.025	0.025	0.0125
2	Fe <sub>3</sub> O <sub>4</sub> -ZnO-1.0 CuO	0.025	0.025	0.0250
3	Fe <sub>3</sub> O <sub>4</sub> -ZnO-2.5 CuO	0.025	0.025	0.0625
4	Fe <sub>3</sub> O <sub>4</sub> -ZnO-5.0 CuO	0.025	0.025	0.1250

### Characterization Techniques

The phase purity was examined by using Rigaku X-ray diffractometer (Rigaku Co., Japan) with Cu K $\alpha$  ( $\lambda=1.54056$  Å) radiation over a range of  $2\theta$  angles from  $10^\circ$  to  $70^\circ$ . The average crystallite size was also calculated using the data obtained from diffractogram by Scherer's formula. Fourier transform infrared (FT IR) spectra of the samples were recorded on a FT IR spectrometer (FT IR-8400 SHIMADZU, Japan) in a range of wavenumber from  $4000$  to  $500$  cm $^{-1}$ . Surface morphology of each of the prepared samples was studied by scanning electron microscope and energy dispersive X-ray spectroscopy (SEM-EDS) (Phenom PROX, Netherlands) Pyin Oo Lwin. Samples were also investigated by transmission electron microscope (TEM, JEOL TEM-3010 with an accelerating voltage of  $100$  kV at State Key Laboratory, College of Science, Beijing University of Chemical Technology, China. Thermo gravimetric - Differential Analysis (TG-DTA) was performed at Universities' Research Center, Yangon. TG-DTA thermogram was obtained by using Al<sub>2</sub>O<sub>3</sub> as reference. The measurements were carried out at a heating rate of  $20.0$  kJ min $^{-1}$  and scanning from  $40^\circ$  C to  $600^\circ$  C with a scanning rate of  $20^\circ$  C min $^{-1}$ , under nitrogen atmosphere of  $20$  psi.

## Results and Discussion

### Characterization by X-Ray Diffraction Analysis

The phase purity, crystallite sizes and crystal structures of Fe<sub>3</sub>O<sub>4</sub>, CuO and Fe<sub>3</sub>O<sub>4</sub>- ZnO- CuO nanocomposite were investigated by X-ray diffraction analysis. Figure 1(a) shows the X-ray diffraction pattern of Fe<sub>3</sub>O<sub>4</sub> nanoparticles. All the peaks of the (111), (220), (311), (222), (400), (422), (511) and (440) in XRD pattern were well - matched with standard diffraction pattern of Fe<sub>3</sub>O<sub>4</sub>(88-0315 > Magnetite). Only single phase of Fe<sub>3</sub>O<sub>4</sub> with no other phase was found in this XRD pattern. It indicates the purity of the Fe<sub>3</sub>O<sub>4</sub> sample. Figure 1(b) shows the X-ray diffraction pattern of CuO nanoparticles. Similarly, in the XRD pattern of CuO, all peaks were well - matched with standard diffraction pattern of CuO (85-5889 > CuO). No other impurity peaks were observed. The X-ray diffraction patterns of Fe<sub>3</sub>O<sub>4</sub>- ZnO- CuO nanocomposites with different mole ratios are depicted in Figures 2 (a), 2(b), 2(c) and 2(e). It was seen that additional peaks other than Fe<sub>3</sub>O<sub>4</sub> peaks and CuO peaks appeared in the X-ray diffractogram due to the presence of ZnO NPs. In these diffractogram of the composites the Fe<sub>3</sub>O<sub>4</sub> peaks and CuO peaks were observed to be slightly shifted from their peak positions. Furthermore, the diffractogram showed only Fe<sub>3</sub>O<sub>4</sub>, ZnO and CuO phases and it indicated the absence of impurities.

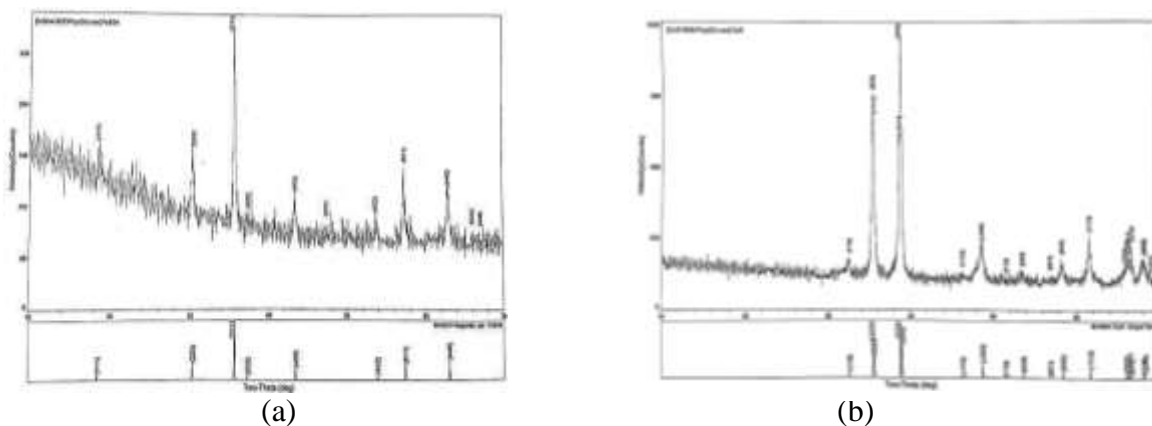


**Figure 1** X-ray diffraction patterns of (a)  $\text{Fe}_3\text{O}_4$  and (b)  $\text{CuO}$

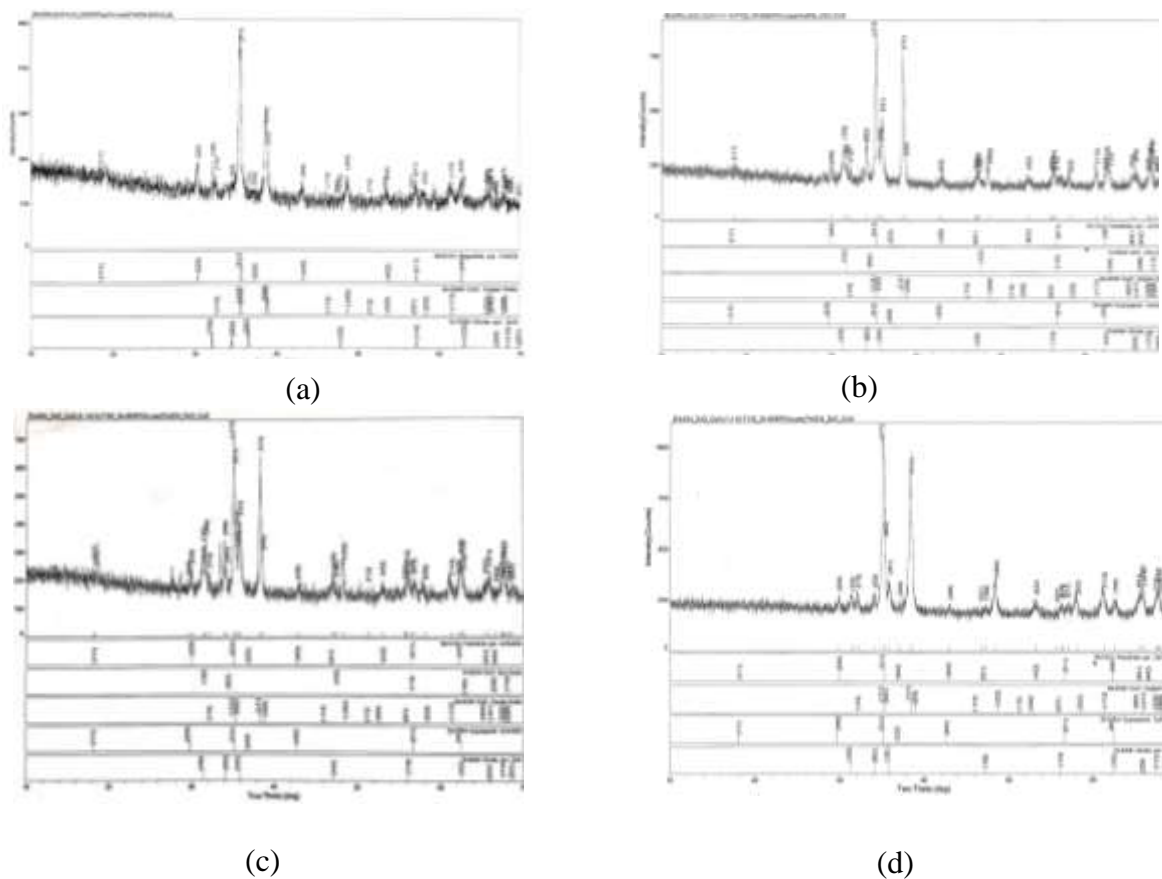


**Figure 2** X-ray diffraction patterns of (a)  $\text{Fe}_3\text{O}_4$ -  $\text{ZnO}$ - $0.5\text{CuO}$  (b)  $\text{Fe}_3\text{O}_4$ -  $\text{ZnO}$ - $1\text{CuO}$  (c)  $\text{Fe}_3\text{O}_4$ - $\text{ZnO}$ - $2.5\text{CuO}$  (d)  $\text{Fe}_3\text{O}_4$ -  $\text{ZnO}$ - $5\text{CuO}$  nanocomposites

The average crystallite sizes of samples were calculated from the dominant peaks of X-ray line broadening planes using Scherrer equation,  $\tau = \frac{0.9\lambda}{\beta \cos\theta}$  in which  $\tau$  is the crystallite size (nm),  $\lambda$  is the diffraction wavelength (0.154059 nm for  $\text{Cu K}\alpha$  radiation),  $\theta$  is the diffraction angle (degree) and ' $\beta$ ' is the full width at half maximum (FWHM) for the diffraction peak (radian). Table 2 shows the crystallite sizes of  $\text{Fe}_3\text{O}_4$  nanoparticles,  $\text{CuO}$  nanoparticles and  $\text{Fe}_3\text{O}_4$ - $\text{ZnO}$ - $\text{CuO}$  nanocomposites with different mole ratios. Crystallite sizes of  $\text{Fe}_3\text{O}_4$ - $\text{ZnO}$ - $\text{CuO}$  nanocomposites were larger than  $\text{CuO}$  nanoparticles (21.5 nm) and the crystallite sizes of the nanocomposites were not much different except  $\text{Fe}_3\text{O}_4$ - $\text{ZnO}$ - $0.5\text{CuO}$  nanocomposites which was 34.1 nm.

Table 3 shows the lattice constants of Fe<sub>3</sub>O<sub>4</sub> nanoparticles, CuO nanoparticles and Fe<sub>3</sub>O<sub>4</sub>-ZnO-CuO nanocomposites. CuO was indexed as monoclinic with ‘a’ (4.6843 Å) and ‘b’ (3.4261 Å) and longer ‘c’ (5.1254 Å) whereas Fe<sub>3</sub>O<sub>4</sub> and the composites were cubic with equal lengths.

**Table 2 Crystallite Sizes of Fe<sub>3</sub>O<sub>4</sub> -ZnO -CuO Nanocomposites with Different Mole Ratios**

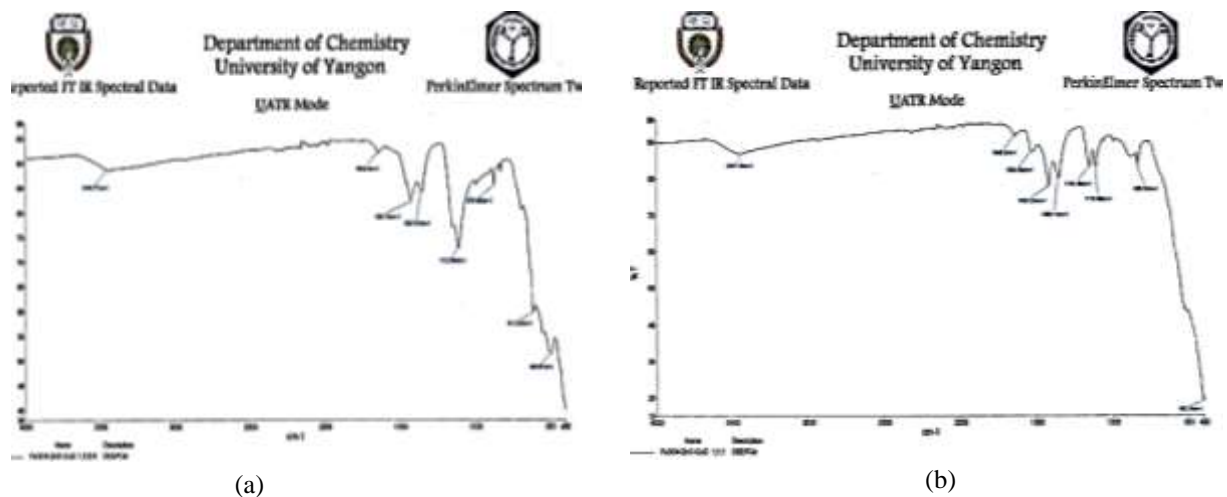
No	Sample	Calculated Crystallite Size (nm)
1	Fe <sub>3</sub> O <sub>4</sub> nanoparticles	29.6
2	CuO nanoparticles	21.5
3	Fe <sub>3</sub> O <sub>4</sub> -ZnO - 0.5CuO nanocomposites	34.1
4	Fe <sub>3</sub> O <sub>4</sub> -ZnO -1 CuO nanocomposites	23.4
5	Fe <sub>3</sub> O <sub>4</sub> -ZnO - 2.5CuO nanocomposites	25.1
6	Fe <sub>3</sub> O <sub>4</sub> -ZnO - 5CuO nanocomposites	24.4

**Table 3 Lattice Constants of Fe<sub>3</sub>O<sub>4</sub>-ZnO-CuO Nanocomposites with Different Mole Ratios**

No	Sample	Axial length (Å)			Interaxial angle(°)			Crystal structure
		a	b	c	α	β	γ	
1	Fe <sub>3</sub> O <sub>4</sub>	8.3482	8.3482	8.3482	90	90	90	Cubic
2	CuO	4.6843	3.4281	5.1254	90	99.27	90	Monoclinic
3	Fe <sub>3</sub> O <sub>4</sub> -ZnO-0.5CuO	6.2226	6.2226	6.2225	90	90	90	Cubic
4	Fe <sub>3</sub> O <sub>4</sub> -ZnO -1.0CuO	6.2167	6.2167	6.2167	90	90	90	Cubic
5	Fe <sub>3</sub> O <sub>4</sub> -ZnO-2.5CuO	6.2480	6.2480	6.2480	90	90	90	Cubic
6	Fe <sub>3</sub> O <sub>4</sub> -ZnO-5.0CuO	6.2361	6.2361	6.2361	90	90	90	Cubic

**Characterization by FT IR**

Figure 3 shows the FT IR spectra of Fe<sub>3</sub>O<sub>4</sub>-ZnO-CuO nanocomposites and interpretation of the spectral data are described in Table 4. Characteristic vibration peaks of Fe-O appeared between 570-580 cm<sup>-1</sup>, Cu-O between 830-875 cm<sup>-1</sup> and Zn-O peaks between 615-623 cm<sup>-1</sup> in the Fe<sub>3</sub>O<sub>4</sub>-ZnO-CuO nanocomposites.



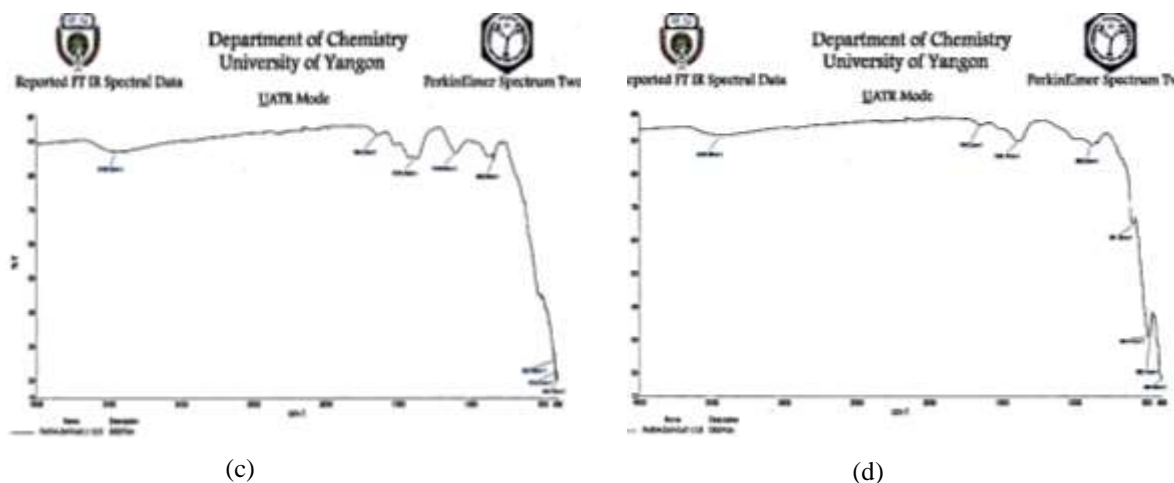


**Figure 3** FT-IR spectra of (a) Fe<sub>3</sub>O<sub>4</sub>- ZnO- 0.5CuO (b) Fe<sub>3</sub>O<sub>4</sub>- ZnO- CuO (c) Fe<sub>3</sub>O<sub>4</sub>- ZnO- 2.5CuO (d) Fe<sub>3</sub>O<sub>4</sub>-ZnO-5CuO nanocomposites

**Table 4** FT IR Spectral Data of Fe<sub>3</sub>O<sub>4</sub>-ZnO-CuO Nanocomposites with Different Mole Ratios

No	Observed wavenumber ( cm <sup>-1</sup> )				Reported value (cm <sup>-1</sup> )	Remark
	Fe <sub>3</sub> O <sub>4</sub> -ZnO-0.5CuO	Fe <sub>3</sub> O <sub>4</sub> -ZnO-1CuO	Fe <sub>3</sub> O <sub>4</sub> -ZnO-2.5CuO	Fe <sub>3</sub> O <sub>4</sub> -ZnO-5CuO		
1	3443	3447	3439	3435	3447*	O-H stretching vibration
2	875	839	839	830	850**	Cu-O stretching
3	612	620	615	618	610*	Zn-O stretching
4	580	570	527	591	585*	Fe-O stretching vibration
6	490	406	422,415 403	484,456 406	400- 500***	Cu-O and Zn-O stretching

\* Kulkarni *et al.*, 2017 \*\* Muhamad *et al.*, 2007 \*\*\* Vanaja *et al.*, 2016

### Characterization by SEM-EDS

SEM is a scanning electron microscope that illustrates the sample surface by scanning with a beam of high-energy electrons. X-ray in the SEM can be used to identify the elemental composition of a sample by a technique known as energy dispersive x-ray (EDS). (Abd Mutalib *et al.*, 2017). Figure 4 shows the SEM images of the nanocomposites. The surface morphology of Fe<sub>3</sub>O<sub>4</sub>- ZnO- 0.5CuO nanocomposite was found to have quasi spherical shape particles. When the mole ratio of CuO increased both spherical and clew like shape particles were also observed in Fe<sub>3</sub>O<sub>4</sub>-ZnO - 1CuO, Fe<sub>3</sub>O<sub>4</sub>- ZnO- 2.5 CuO and Fe<sub>3</sub>O<sub>4</sub>-ZnO- 5 CuO nanocomposites.

Figure 5 depicts EDS spectra of nanocomposites with different mole ratios. The peaks corresponding to Fe, Zn, Cu and O confirmed the formation of Fe<sub>3</sub>O<sub>4</sub>- ZnO- CuO nanocomposites. Three peaks each for Fe, Zn and Cu were observed. A peak less than 1 keV is O peak. Table 5 shows the weight percents of elements found in Fe<sub>3</sub>O<sub>4</sub>-ZnO-CuO nanocomposites with different mole ratios. It was found that as mole of CuO was increased from the weight of Cu also increased. Some impurity peaks were observed. Among them Fe<sub>3</sub>O<sub>4</sub>-ZnO- 5CuO was found to have the lowest impurity.

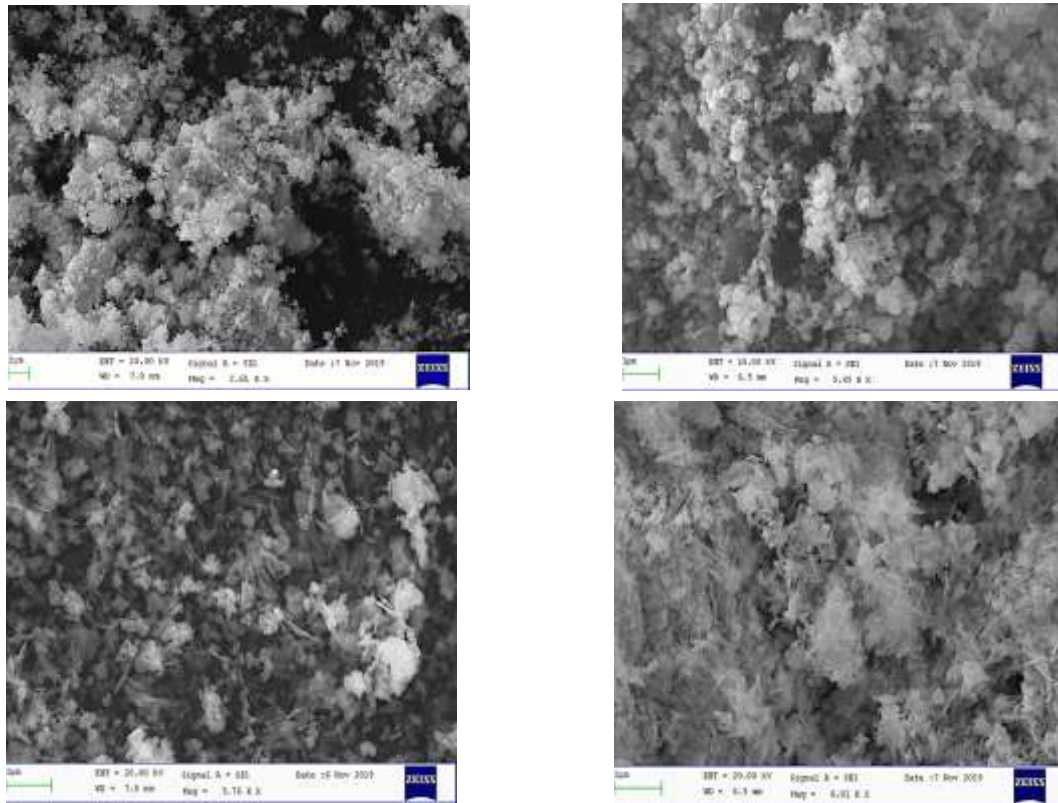


**Figure 4** SEM images of (a)  $\text{Fe}_3\text{O}_4\text{-ZnO-0.5CuO}$  (b)  $\text{Fe}_3\text{O}_4\text{-ZnO-CuO}$  (c)  $\text{Fe}_3\text{O}_4\text{-ZnO-2.5CuO}$  (d)  $\text{Fe}_3\text{O}_4\text{-ZnO-5CuO}$  nanocomposites

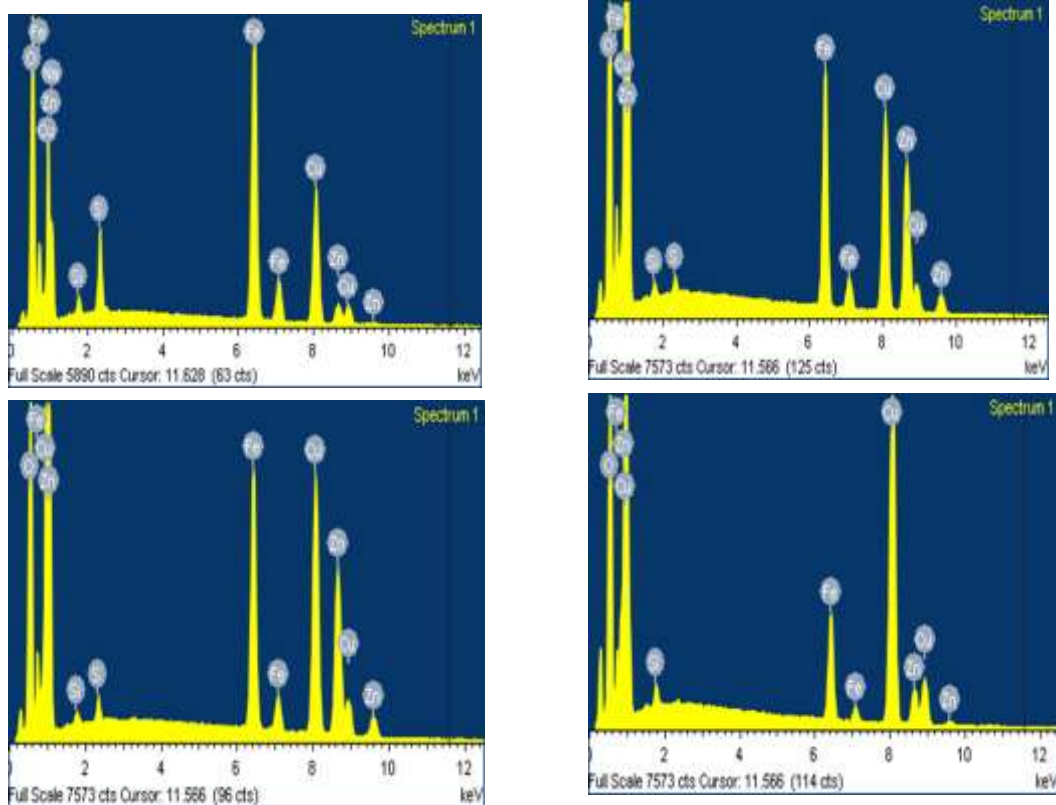


**Figure 5** EDS images of (a)  $\text{Fe}_3\text{O}_4\text{-ZnO-0.5CuO}$  (b)  $\text{Fe}_3\text{O}_4\text{-ZnO-CuO}$  (c)  $\text{Fe}_3\text{O}_4\text{-ZnO-2.5CuO}$  (d)  $\text{Fe}_3\text{O}_4\text{-ZnO-5CuO}$  nanocomposites

**Table 5 Weight Percent of Fe<sub>3</sub>O<sub>4</sub>-ZnO-CuO Nanocomposites with Different Mole Ratios**

No	Sample	Weight Percent (%)						
		Fe	Cu	Zn	O	Na	S	Si
1	Fe <sub>3</sub> O <sub>4</sub> -ZnO-0.5CuO	15.94	27.79	24.72	27.85	1.27	1.78	0.65
2	Fe <sub>3</sub> O <sub>4</sub> -ZnO-1 CuO	15.89	28.31	27.44	27.46	-	0.46	0.44
3	Fe <sub>3</sub> O <sub>4</sub> -ZnO-2.5CuO	15.79	33.18	26.96	23.022	-	0.55	0.30
4	Fe <sub>3</sub> O <sub>4</sub> -ZnO-5CuO	15.73	38.16	23.34	22.52	-	-	0.25

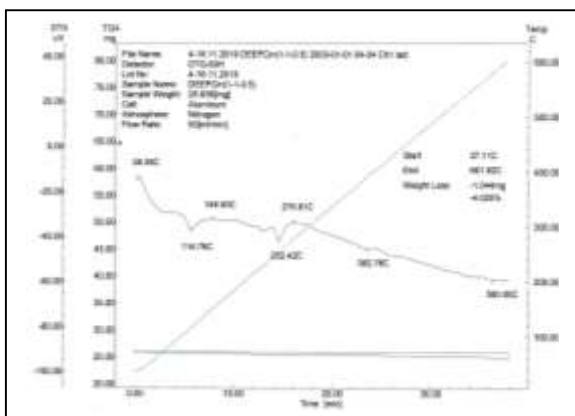
### Characterization by TEM

Figure 6 is the TEM image of Fe<sub>3</sub>O<sub>4</sub> -ZnO - CuO nanocomposite. TEM image of the magnetic Fe<sub>3</sub>O<sub>4</sub>-ZnO-CuO nanocomposite shows the cubic morphology and the crystallite size obtained by TEM was not much different from the data obtained by XRD.

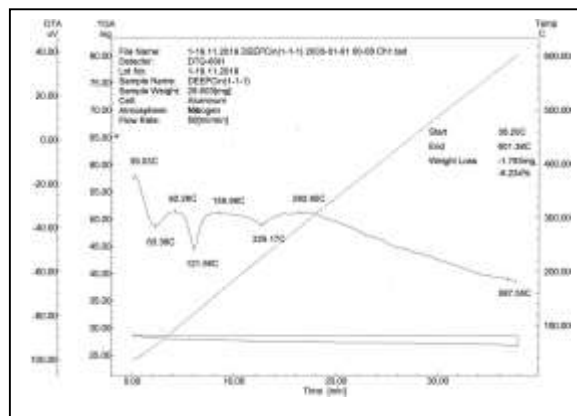
**Figure 6** TEM image of Fe<sub>3</sub>O<sub>4</sub>-ZnO-CuO nanocomposites

### Thermal Analysis by TG-DTA

Figure 7 shows the TG-DAT thermograms of Fe<sub>3</sub>O<sub>4</sub>-ZnO- CuO nanocomposites with different mole ratios. In all the thermograms, small endothermic peaks were observed due to removal of physically sorbed water. In the heating temperature range of 40 °C to 600 °C, small weight losses of less than 7% were observed in all nanocomposites indicating the thermal stability of the prepared nanocomposites. In Fe<sub>3</sub>O<sub>4</sub>-ZnO- 5CuO the smallest weight loss of 3% was observed compared to other nanocomposites with different mole ratios Table 6.



(a)



(b)

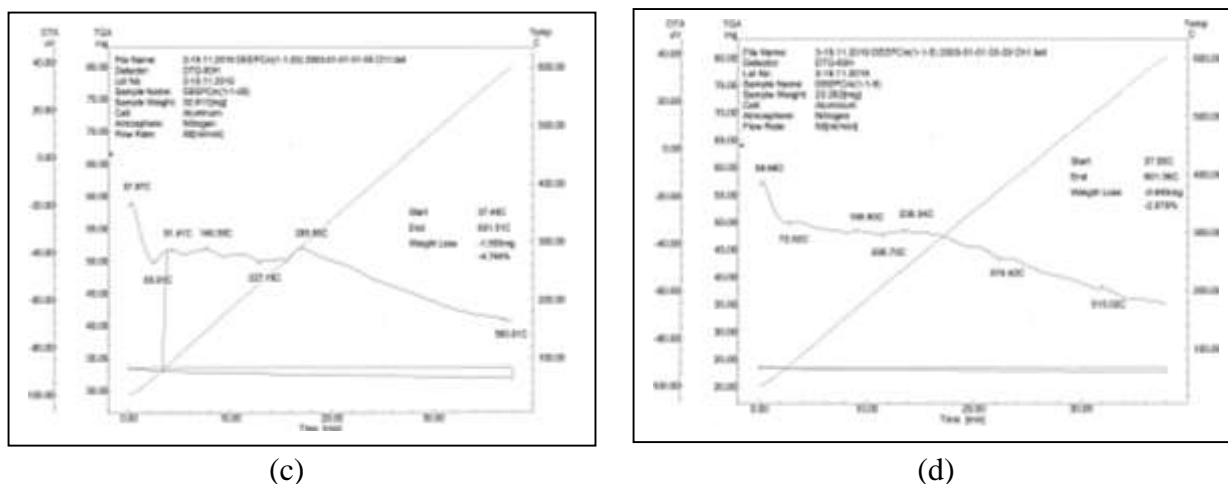


**Figure 7** TG-DTA Thermograms of (a) Fe<sub>3</sub>O<sub>4</sub>- ZnO- 0.5CuO (b) Fe<sub>3</sub>O<sub>4</sub>- ZnO- CuO (c) Fe<sub>3</sub>O<sub>4</sub>- ZnO- 2.5CuO (d) Fe<sub>3</sub>O<sub>4</sub>-ZnO-5CuO nanocomposites

**Table 6** Weight Loss Percent of Fe<sub>3</sub>O<sub>4</sub>-ZnO-CuO Nanocomposites with Different Mole Ratios

No	Samples	Weight loss (%)
1	Fe <sub>3</sub> O <sub>4</sub> -ZnO-0.5CuO	4.025
2	Fe <sub>3</sub> O <sub>4</sub> -ZnO- 1CuO	6.234
3	Fe <sub>3</sub> O <sub>4</sub> -ZnO-2.5 CuO	4.764
4	Fe <sub>3</sub> O <sub>4</sub> -ZnO-5 CuO	2.979

**Magnetic Property of Fe<sub>3</sub>O<sub>4</sub>-ZnO-CuO Nanocomposites**

Figure 8 depicts a visual confirmation of the magnetic activity of Fe<sub>3</sub>O<sub>4</sub>-ZnO-5CuO nanocomposite. The heterogeneous nanocomposites suspended in solution were attracted towards a magnet. This showed that the Fe<sub>3</sub>O<sub>4</sub>-ZnO-5CuO nanocomposite used as a photocatalyst can be separated out from the suspension using a magnet on completion of the reaction suggesting its potential use in large scale water treatment.



**Figure 8** magnetic properties of prepared Fe<sub>3</sub>O<sub>4</sub>-ZnO-5CuO nanocomposites

**Conclusion**

Magnetic Fe<sub>3</sub>O<sub>4</sub>- ZnO- CuO nanocomposites with different mole ratios have been prepared using sol-gel method. X-ray diffraction analysis showed the cubic structure of composites and the crystallite sizes of 34.1 nm, 23.4 nm, 25.1 nm and 23.2 nm were observed for Fe<sub>3</sub>O<sub>4</sub>-ZnO- CuO nanocomposites with different mole ratios. FT IR spectra revealed the presence of the characteristic

peaks of Fe-O, Zn-O and Cu-O in the nanocomposites. Spherical and clew like shape particles were observed in Fe<sub>3</sub>O<sub>4</sub>-ZnO-5CuO nanocomposites by SEM images. EDS showed the presence of Fe, Zn, Cu and O atoms. Among them Fe<sub>3</sub>O<sub>4</sub>- ZnO- 5CuO nanocomposites showed having lowest impurity. TEM image of Fe<sub>3</sub>O<sub>4</sub>-ZnO- CuO nanocomposites showed the cubic morphology. According to TG-DTA thermograms, small weight losses of less than 7 % were observed in all nanocomposites indicating the thermal stability of the nanocomposites. Magnetic property of the photocatalyst Fe<sub>3</sub>O<sub>4</sub>-ZnO-CuO nanocomposites can improve the reusability of the for water treatment.

### Acknowledgements

The authors would like to thank to Dr Cho Cho Than, Professor and Head, Department of Chemistry, Taunggoke Degree College, for her provision of the research facilities. We also would like to express our profound gratitude to Myanmar Academy of Arts and Science for allowing to present this paper.

### References

- Abd Mutalib, M., Rahman, M.A., Othman, M.H.D., Ismail, A.F and Jaafar, J. (2007). "Membrane Characterization", vol.5 (3), pp.161-179
- Akir, S., Barrs, A., Coffinier, Y., Bououdina, M., Boukherroub, R. and Dakhlaoui-Omrani, A. (2016). "Eco-friendly Synthesis of ZnO Nanoparticles with Different Morphologies and their Visible Light Photocatalytic Performance for the Degradation of Rhodamine B", *Ceram. Int.* vol. 42(8), pp. 10259-10265
- Heravi, M.M., Beheshtiha S.Y.S., Dehghani, M. and Hosseintash, N. (2015). "Using Magnetic Nanoparticles Fe<sub>3</sub>O<sub>4</sub> as a Reusable Catalyst for the Synthesis of Pyran and Pyridine Derivatives via One-pot Multicomponent Reaction", *Journal of the Iranian Chemical Society*, vol.2(11), pp. 2075-2081
- Hou, X., Wang, L., Li, F., He, G. and Li, L. (2016). "Controlled Loading of Gold Nanoparticles on ZnO Nanorods and their High Photocatalytic Activity. *Mater.Lett.*, vol. 159, pp.502-505
- Kulkarni,S.D., Kumbar, S. M., Menon, S. G., Choudhari, K. S. and Santhosh. C. (2017). "Novel Magnetically Separable Fe<sub>3</sub> O<sub>4</sub> @ZnO Core-Shell Nanocomposite for UV and Visible Light Photocatalysis". *Advanced Science Letters*, vol. 23, pp.1724-1729
- Magneshwari, K., Nataraj, D., Pal, T., Sathyamoorthy, R. and J. Park, J. (2015). "Improved Photocatalytic Acitivity of ZnO Coupled CuO Nanocomposites Synthesized by Reflux Condensation Method". *J. Alloys Compd*, vol.625, pp. 362-370
- Muhamad, E.N., Irmawati, R. and Abdullah. A.H. (2007). "Effect of Number of Washing on the Characteristics of Copper Oxide Nanopowders". *The Malaysian Journal of Analytical Sciences*, vol.11, pp. 294-301
- Taufik, A., Kalim,I. and R. Saleh.(2015). "Preparation, Characterization and Photocatalytic Activity of Multifunctional Fe<sub>3</sub>O<sub>4</sub>/ZnO/CuO Hybrid Nanoparticles". *Materials Science Forum*, vol.827, 37-42
- Taufik, A. and Saleh. R. (2017). "Adsorption and Sonocatalytic Performance of Magnetite ZnO/CuO with NGP Variation". *Ceramics International*, vol.43, pp. 3510-3520
- Vanaja, A. and Rao. K. S. (2016). "Precursors and Medium Effect on Zinc Oxide Nanoparticles Synthesized by Sol-Gel Process". *International Journal of Applied and Natural Sciences*, vol .5(1), pp. 53-62
- Xuan, S., Jiang, W., Gong, X., Hu, Y. and Chen, Z. (2008). "Magnetically Separable Fe<sub>3</sub>O<sub>4</sub> / TiO<sub>2</sub> Hollow Spheres: Fabrication and Photocatalytic Activity". *The Journal of Physical Chemistry C*, vol.113 (2 ), pp.553-558

## SYNTHESIS AND APPLICATION OF RAYON ZINC OXIDE NANOCOMPOSITE

Khin Mya Than Sein<sup>1</sup>, Myat Lay Nwe<sup>2</sup>, Khaing Khaing Kyu<sup>3</sup>

### Abstract

The mean of composite are combination of two or more materials present as separate phases and combined to form desired structures so as to take advantage of certain desirable properties of each component. The constituents can be organic, inorganic or metallic in the form of particles, rods, fibers and plates. In this research work, the matrix material (rayon) was prepared from waste paper (A4 printed paper) by using viscose method. The rayon-ZnO nanocomposite fiber was synthesized from zinc chloride and rayon by using melt compounding technique. The synthesized rayon-ZnO nanocomposite was characterized by using EDXRF, FT-IR, SEM and TG-DTA analysis. Synthesized rayon-ZnO nanocomposite was applied in wastewater treatment process. Coagulation and filtration methods were also used to treat the textile wastewater sample. According to the results, rayon-ZnO nanocomposite has good removal efficiency of organic and inorganic pollutant from wastewater. Furthermore, the efficiency of rayon-ZnO nanocomposite was examined by calculation of percent removal efficiency and water quality index (WQI).

**Keywords:** Viscose, Rayon, Nanocomposite, Textile Wastewater, Water Quality Index

### Introduction

Metal oxide nanoparticles and composite materials are widely applied in the field of research development and diverse applications in industries including surface coatings optoelectronic, bioengineering, biodiagnostics and agriculture. Their intrinsic properties are mainly determined by size, shape, composition, crystallinity and morphology (Soosen, *et al.* 2009). The mean of “composite” is when two or more different materials are combined together to create a superior and unique material. This is an extremely broad definition that holds true for all composites however, more recently the term “composite” describes reinforced plastics. Composites materials can be made organic and inorganic substances by using different methods. The main types of composite are polymer matrix composite, metal matrix composite and ceramic matrix composite (Soosen, and *et al.* 2009). Polymer matrix composite with discontinuous fillers are widely used for the application like die attachment, electrically and thermally conductive, adhesives encapsulations and thermal interface materials. It is well known that polymers are easily process able and need low processing temperatures. However, compared to ceramics they have lower electrical and thermal of the most popular areas for current research and development. At present, easily availability of nanomaterials offers the promise of developing polymer matrix nanocomposites with tailored thermal mechanical and electric properties for a particular application. Polymer matrix nanocomposites are polymer matrix containing fillers with at least one dimension in the range of 1 nm to 100 nm (Divij and Goyal, 2014). Nanocomposite fibers have attracted attention in recent years because improved mechanical, thermal, solvent resistance and fire retardant properties compare to the pure or conventional composite fibers. Therefore, much work has focused on developing nanocomposite fibers using various polymers (Kato, Usuki, and Okada, 1997). In this research, rayon-ZnO nanocomposite was synthesized from zinc chloride and rayon by using melt compounding process. The synthesized rayon-ZnO nanocomposite was applied as superior adsorbent material in wastewater treatment process. Moreover, the efficiency of synthesized rayon-ZnO nanocomposite has been studied.

---

<sup>1</sup> Lecturer, Department of Chemistry, Mandalay University of Distance Education

<sup>2</sup> Dr, Associate Professor, Department of Literature, Technology University (Kyaing Tong)

<sup>3</sup> Dr, Professor, Department of Chemistry, University of Mandalay

## Materials and Methods

### Elimination of ink from the waste paper

In this research, waste papers (A4 printed papers) were collected.

**Aging:** For aging step, the collected samples were placed in an oven for accelerated aging at 60° C for 24 hours. Accelerated ageing of the samples is necessary because the storage of the recovered papers can influence their deinkability.

**Defibration:** Second step is defibration step. The pieces of sample 50 g were placed in a 1 liter glass vessel 150 mL of sodium complex solution was added into it and the heated dilution water was filled up to a total volume of 500 mL. Then, it was stirred, 38 mL of solution and 10 mL of EDTA solution was added and it was stirred again to obtain the disintegrated sample pulp. At the end of pulping the pH of pulp was measured by pH meter.

**Storage:** The disintegrated sample for subsequent treatment was stored for 60 minutes in a water bath at 45°C.

**Homogenization:** After storage, the stock pulp was stirred for homogenization. Then, it was diluted with the warm water to terminate any chemical reaction.

**Floation:** The glass bottle (1 L) containing some hot dilution water was heated for some minutes. Disintegrated samples were added into the bottle and it was filled up with dilution water. Then, the floation process was done by stirring with stirrer and giving air supply with air- pumper. The starting point is for the floating time, when the air supply is started. During the entire floating process, the froth was removed by using scraper as possible. The skimmed-off floation rejects was collected in a tank. The dilution water was continually added to maintain for the drainage during the floation. This process was run for 15 minutes. Finally, the solution containing the pulp in a bottle was filtered and the deinked pulp was collected. The resulting deinked pulp was dried in oven at 30°C until it was dried moderately. Then, the recycle pulp was obtained.

### Preparation of Viscose Rayon from Recycle pulp

Cellulose (recycle pulp from waste paper) was immersed in 20% aqueous sodium hydroxide (NaOH) at a temperature in the range of 18 to 25°C in order to swell the cellulose fiber and to convert cellulose to alkali cellulose. The swollen alkali cellulose mass is pressed to a wet weight equivalent of 2.5 to 3.0 times the original pulp weight to obtain an accurate ratio of alkali to cellulose. These alkali cellulose placed in beaker are allowed to react with 25 mL of (100 %) carbondisulphide, CS<sub>2</sub> at room temperature to form cellulosexanthate. The orange cellulosexanthate is dissolved in 5% sodium hydroxide to obtain a viscous orange coloured solution called viscose. The viscose solution was passed at 40% sulphuric acid solution. The fibers were getting formed in the acid bath. The freshly regenerated rayon contains many salts and other water soluble impurities which need to be removed. Therefore the prepared rayon washed with distilled water, until the neutralization occurs. Finally, the rayon product was obtained.

### Preparation of Rayon-ZnO Nanocomposite

Rayon (15) g was completely dissolved in 100 mL of 65% ZnCl<sub>2</sub> aqueous solution at 80°C with 500 r/min constant stirring. Then, 15% NaOH aqueous solution was added drop-wise to the rayon-zinc chloride aqueous solution and heated with 500 r/min constant stirring to achieve a final pH value of 8.4. After the composite was aged for 30 min with constant stirring at 80°C, the rayon-ZnO nanocomposite was obtained (Jinxia, Wenhua, Yajun, and Zhiguo, 2016).

## Characterization of Synthesized Rayon and Rayon-ZnO Nanocomposite

### Energy Dispersive X-ray Fluorescence Analysis

The relative abundances of the prepared samples were determined by EDXRF (EDX-700 Spectrometer) at the Universities' Research Center, Yangon University.

### FT-IR Analysis

The functional groups present in prepared samples were investigated by FT-IR (SHIMADZU-8400, Spectrometer) at the Universities' Research Center, Yangon University.

### Scanning Electron Microscopy Analysis

The surface morphology of prepared samples were examined by SEM (JSM 5610 LV, JEOL, Ltd) at the West Universities' Research Center, Yangon.

### Thermal Stability (TG-DTA) Analysis

Thermal stability of rayon-ZnO nanocomposite was investigated by thermogravimetric differential analysis (TG-DTA) employing Shimadzu DTG 60H differential thermal analyzer at Universities' Research Center, Yangon University.

## Wastewater Treatment Process

### Sample collection

In this research, the wastewater sample was collected from Textile Dyeing Area (weaving zone) of Inn Baw Khone Village, Inlay Lake, Nyaung Shwe Township, Taunggyi District, Southern Shan State.

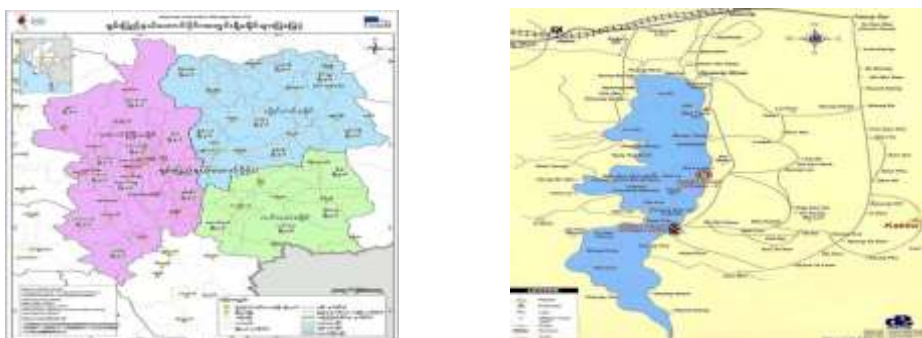


**Figure 1** Location map of the wastewater sampling area (Khurtsia, 2015)

## Wastewater Characteristics

### Physical Characteristics

The important physical characteristics of wastewater such as total solids content, suspended solids, colour, odour, dissolved oxygen (DO), temperature and turbidity were determined (Korey, C. PASCO Scientific, 2010).

### Chemical Characteristics

The chemical characteristics of wastewater sample such as chemical oxygen demand (COD), pH, alkalinity, total dissolved solids (TDS) and total hardness were determined (Korey, C. PASCO Scientific, 2010).

## Determination of Elemental Contents in Water Samples

The contents of some element and trace heavy metals were determined by using EDXRF analysis.

## Bacteriological Examination of Water Samples

*E. Coli* was determined at water and soil examination laboratory, Yangon.

## Examination the Efficiency of Synthesized Rayon-ZnO Nanocomposite

Wastewater sample was treated with rayon-ZnO nanocomposite by using coagulation and filtration methods. The experimental conditions, different contact times (5, 10, 15, 60 min and overnight) and different coagulant weight (0.1, 0.2, 0.5, 1 and 2 g) were used for the process of removal impurities from wastewater sample. According to results, the optimum conditions were selected. Therefore, coagulant weight (0.1 g), contact time (15 min) adsorbent dosage (0.1 g) and volume of wastewater (100 mL) were used for three times in this treatment process. Moreover, the efficiency of rayon-ZnO nanocomposite was examined by Percent Removal Efficiency and Water Quality Index (Korey, C. PASCO Scientific, 2010).

## Results and Discussion

### Characterization of Rayon-ZnO Nanocomposite

#### EDXRF Analysis

The characteristic peaks for different element in the functional layer are presented in EDXRF spectra, which were obtained for the surface of sample shown in Figure (2). It can be seen that the ZnO was found to be present on the surface of rayon samples as 46%.



**Figure 2** EDXRF spectrum of synthesized rayon- ZnO nanocomposite

#### FT-IR Analysis

FT-IR studies were carried out to confirm the identification and bond structure of associated functional groups of synthesized rayon-ZnO nanocomposite using optimized parameters. The FT-IR spectra of synthesized rayon, nano ZnO and rayon-ZnO nanocomposite were shown in Figure (3). In comparison of rayon, nano ZnO and rayon-ZnO nanocomposite of spectra resulted data are found to the intermolecular hydrogen bonds in rayon may be weaker than those in the rayon-ZnO and the low crystallinity and intermolecular hydrogen bonds in rayon make it more reactive component when participating in chemical reaction (Moosavi-Nasab, and Yousefi, 2011). Rayon has the characteristic peak at 893 and 1012  $\text{cm}^{-1}$  while the correlated bands of rayon-ZnO centered at around 904 and 1047  $\text{cm}^{-1}$ , respectively. In the FT-IR spectrum of rayon, the broad band appears

at  $3541\text{ cm}^{-1}$  (OH group of rayon) and this value was found to be  $3452\text{ cm}^{-1}$  for rayon-ZnO. This broadening might be due to intermolecular hydrogen bonding between ZnO nanoparticles and cellulose rayon fabric.

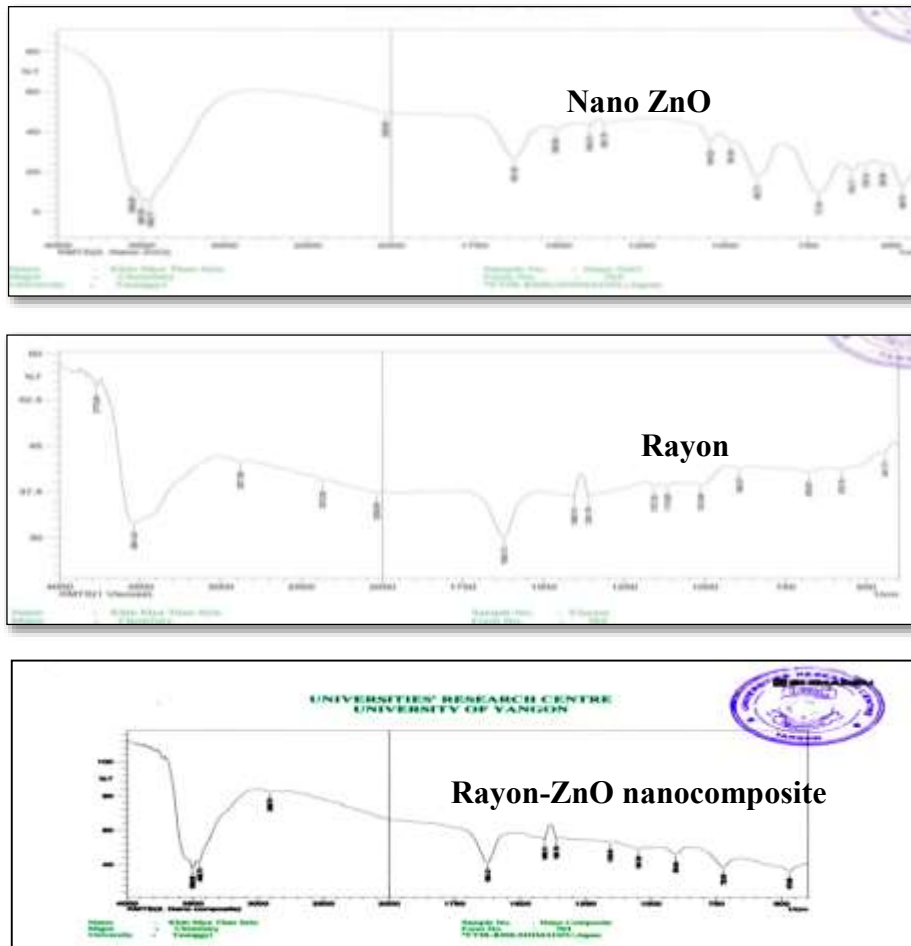


**Figure 3** FT-IR spectrum of synthesized rayon, nano ZnO and rayon-ZnO nanocomposite

FT-IR spectrum shows the presence of ZnO stretching vibration at  $3452$  and  $470\text{ cm}^{-1}$ . In the initial nucleation state the O-H functional groups on the rayon could bind to the surface of the ZnO particles. This clearly indicates the FT-IR spectrum of rayon-ZnO nanocomposite as compared to that the FT-IR spectrum of prepared rayon and ZnO nanoparticles. The proposed structure of rayon-ZnO nanocomposite might be as follows.

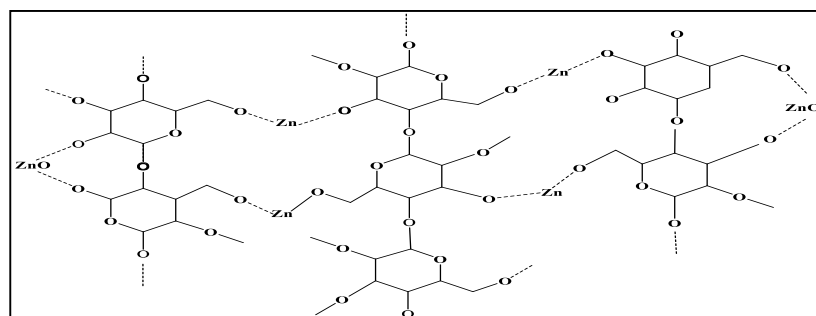


**Figure 4** Proposed structure of synthesized rayon-ZnO nanocomposite

## SEM Analysis

Figure (5) shows the SEM micrographs of synthesized rayon-ZnO nanocomposite. It can be seen, the SEM photograph of rayon-ZnO nanocomposite as compared to that SEM image of prepared rayon.

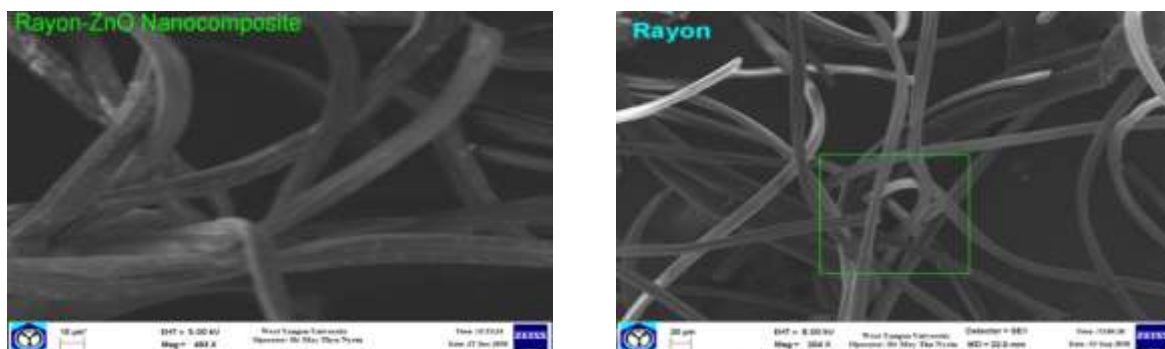


**Figure 5** SEM micrographs of synthesized rayon and rayon-ZnO nanocomposite

This figures can be seen that good dispersion of ZnO nanoparticles into the rayon matrix. It is clear from many references that the ZnO nanoparticles show spherical morphology. Due to the large specific surface area and high surface energy, some nanoparticles are aggregated. The aggregation occurred probably during the process of drying (Attarad, *et al* 2016). The particle size distribution of the zinc oxide is uniform with diameters of approximately 60- 90 nm in nanocomposite.

## Thermal Analysis

The TG-DTA thermogram of synthesized rayon-ZnO nanocomposite was showed in Figure (6). TG-DTA curve showed the nature of decomposition such as the release of free water as well as the liberation of volatile materials and combustion between 38°C and 600°C was presented. Thermal analysis data of synthesized rayon-ZnO nanocomposite were listed in Table (1).

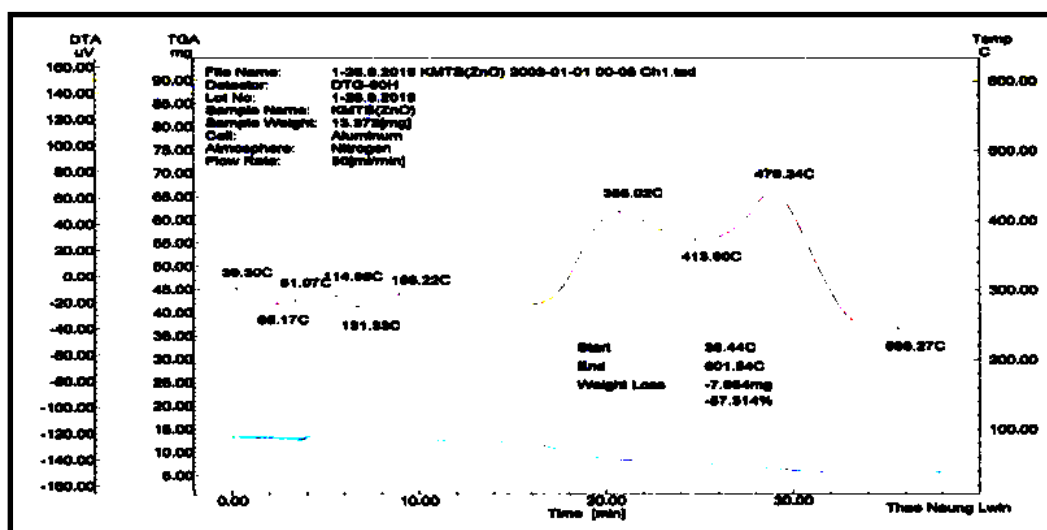


**Figure 6** TG-DTA thermogram of synthesized rayon-ZnO nanocomposite

**Table 1 Thermal Analysis Data of Synthesized Rayon-ZnO Nanocomposite**

No.	TG		DTA		Remark
	Beak in Temp (°C)	Weight loss (%)	Peak Temp (°C)	Nature of reaction	
1	39-131	17	81	Endo	Dehydration
2	168-356	57	356	Exo	Cleavage of the glycosidic linkages
3	413-479	20	413	Exo	Degradation of composite
4	-	-	479	Exo	Decomposition of polymer fiber matrix

### Wastewater Treatment Process

#### Examination the Efficiency of Synthesized Rayon-ZnO Nanocomposite

The observed data for some physicochemical parameters of samples (wastewater, treated water and removal efficiency of rayon-ZnO nanocomposite) were shown in Table (2).

**Table 2 Some Physicochemical Parameters of Water Samples**

No.	Parameter	Units	Resulted Data			*Guide Line* USA (2015)	
			Waste water	Treated water	Removal Efficiency (%)	Aquatic life	EPA
1	pH	-	3.06	8.75	-	6.5-9.0	6.5-9.0
2	Colour	-	358.5	-	<b>99.99</b>	<40	5-50
3	Temperature	°C	34.8	0.62	-	0-40	-
4	Turbidity	NTU	0.42	-	<b>99.99</b>	<80	5-25
5	Conductivity	ms/cm	5160.5	-	<b>99.99</b>	100-2000	750
6	Total hardness	mg/L	202.49	71.25	64.81	50-150	9-100
7	Total alkalinity	mg/L	470.0	-	<b>99.99</b>	50-150	30.5
8	Total solid (TS)	mg/L	28950	3030	89.53	<80	600
9	Total dissolved solid (TDS)	mg/L	27030	3030	88.79	-	500
10	Total suspended solid (TSS)	mg/L	1950	-	<b>99.99</b>	-	-
11	Nitrate	mg/L	16.74	0.75	95.51	0-2	0.015
12	Sulphate	mg/L	20.74	14.23	31.38	<1000	4.8
13	Chloride	mg/L	6.73	3.77	43.98	>60	3.9
14	Phosphate	mg/L	10.52	0.41	96.10	0.02	0.012

The results of before treatment and after treatment using rayon-ZnO nanocomposite exceed the limit of public use compared with guide line (Aquatic life and EPA, USA 2015). According to the results, wastewater sample gave unsatisfactory remarks.

#### Some organic pollutant parameters in water samples

The observed data for some organic parameters of samples (wastewater, treated water and removal efficiency of rayon-ZnO nanocomposite) were shown in Table (3).

**Table 3 Some Organic Pollutant Parameter in Water Samples**

No.	Parameter	Unit	Resulted Data			*Guide Line* USA (2015)	
			Wastewater	Treated water	Removal Efficiency (%)	Aquatic life	EPA
1	COD	mg/L	47	4.78	88.82	-	<40
2	DO	mg/L	2.0	4.5	-	>6	4-6
3	BOD	mg/L	98.7	0	<b>99.99</b>	-	<15

As described above Table (3), the results of before treatment and after treatment by using rayon-ZnO nanocomposite exceed the limit of public use compared with guide line (Aquatic life and EPA, USA 2015). These results indicate that the wastewater sample is highly polluted. DO value of water sample was very low and oxygen dissolved insufficiently. So, pretreatment of dyeing wastewater is required for the control of water quality to achieve minimal impact on the receiving ecosystems.

#### Determination of elemental contents in water samples

Elemental contents of samples (wastewater, treated water and removal efficiency of rayon-ZnO nanocomposite) were expressed in Table (4).

**Table 4 Elemental Contents in Water Samples by EDXRF**

No.	Element	Unit	Resulted Data			*Guide Line* USA (2015)	
			Waste water	Treated water	Removal Efficiency (%)	Aquatic life	EPA
1	Magnesium	ppm	363	0.148	99.95	-	-
2	Aluminum	ppm	182	0.0541	99.99	-	-
3	Silicon	ppm	185	0.0141	99.23	-	-
4	Phosphorus	ppm	15.1	0.0736	99.51	-	-
5	Sulphur	ppm	1310	0.0730	99.44	30-150	30-150
6	Chlorine	ppm	274	1.51	99.44	-	-
7	Potassium	ppm	39.4	0.0052	99.99	10-12	10-12
8	Calcium	ppm	275	0.0945	99.96	75-200	75-200
9	Titanium	ppm	4.88	0.0005	99.98	-	-
10.	Chromium	ppm	1.76	<b>ND</b>	<b>99.99</b>	-	0.01- 0.1
11	Iron	ppm	6.39	<b>ND</b>	<b>99.99</b>	<10	0.05-0.5
12	Copper	ppm	2.26	<b>ND</b>	<b>99.99</b>	0.05-1.5	0.05-1.5
13	Zinc	ppm	10.2	1.31	87.15	-	-
14	Tin	ppm	12.7	0.0015	99.98	-	-

According to the results, adsorption is viewed as successful, productive and economic strategy for the removal of various contaminations from wastewater. The resulted percent yield of wastewater sample gave satisfactory remarks.

#### Bacteriological examination of wastewater sample

By microbial examination, E.coli was absent in wastewater. On the other hand according to the analysis results, the wastewater was found to be harmful for aquatic plants and animals on the dyeing area zone flow down into lake. Therefore, dyeing wastewater is required for the control

of water quality to its suitability for a particular purpose such as drinking water source, recreation and health, aquatic lives and agricultural use etc. and to achieve minimal impact on the receiving ecosystems.

**Calculation of the water quality index**

In the present study, the attempt has been made to apply the WQI as useful method in assessing the suitability of water for various uses. Water Quality Index of wastewater was shown in Table (5).

**Table 5 Water Quality Index of Wastewater**

No.	Parameter	Results	Q-value	Weighting Factor	Parameter Index
1	BOD	98.7	2	0.11	0.22
2	Dissolved Oxygen	2.0	8	0.17	1.36
3	Fecal Coliform	ND	98	0.16	15.68
4	Nitrates	16.74	37	0.10	3.70
5	pH	3.06	4	0.11	0.44
6	Temperature	34.8	10	0.10	1.00
7	Total Dissolved Solids	27030	20	0.07	1.40
8	Total Phosphate	10.52	2	0.10	0.20
9	Turbidity	0.42	84	0.09	7.56
<b>Water Quality Index: WQI</b>					<b>31.56</b>
<b>Quality Rating</b>					<b>Bad</b>

According to W.Q.I value, water quality level of wastewater sample was found to be bad (Korey, C. PASCO Scientific, 2010). Moreover, Water Quality Index of after treatment by using rayon-ZnO nanocomposite was shown in Table (6).

**Table 6 Water Quality Index of Treated Water Sample**

No.	Parameter	Results	Q-value	Weighting Factor	Parameter Index
1	BOD	0	96	0.11	10.56
2	Dissolved Oxygen	4.5	8	0.17	1.36
3	Fecal Coliform	ND	98	0.16	15.68
4	Nitrates	0.75	95	0.10	9.5
5	pH	8.75	67	0.11	7.37
6	Temperature	0.62	89	0.10	8.90
7	Total Dissolved Solids	3030	20	0.07	1.40
8	Total Phosphate	0.41	78	0.10	7.8
9	Turbidity	0	97	0.09	8.73
<b>Water Quality Index: WQI</b>					<b>71.3</b>
<b>Quality Rating</b>					<b>Good</b>

W.Q.I values (quality rating) of water sample level were found to change from bad to good (Korey, C. PASCO Scientific, 2010). Therefore, synthesized Rayon-ZnO nanocomposite has strong absorption and adsorption abilities for a series of organic and inorganic contaminants.

## Conclusion

In this research, the synthesis of rayon-ZnO nanocomposite was achieved from rayon and zinc chloride in alkaline condition by using melt compounding process. The synthesized rayon-ZnO nanocomposite could be applied in the wastewater treatment for removal of organic and inorganic pollutant. The removal efficiency of rayon- ZnO nanocomposite was deeply investigated for possible application of textile wastewater treatment. According to the results, rayon-ZnO nanocomposite can remove organic and inorganic pollutant from wastewater. WQI values of water samples were used to indicate the removal efficiency of synthesized rayon-ZnO nanocomposite. According to W.Q.I values (quality rating) of after treatment, treated water can be used in domestic use, specialized industrial application and agriculture. Furthermore, it is suitable for optimizing growth and survival of fish and other aquatic life. So, the composite material as commercial product could be prepared from using raw materials such as ZnO and cellulose (recycle pulp), easy preparation method with low cost and dose.

## Acknowledgements

The authors would like to express the deepest thanks to Dr, Aung Naing Soe and Dr,Thida, Pro-rectors, Mandalay University of Distance Education of for their permission to write the research journal. We deeply express our gratitude Dr, Aye Aye Myint, Professor and Head and Dr, Moe Moe, Professor, Department of Chemistry, Mandalay University of Distance Education, for their excellent advices and good guidance to do this research.

## References

- Attarad, A., Sidra, A., Qaisar, Maqbool, S.N., Muhammad, F.S., Madiha, A., Rehman, P. and Muhammad, Z. (2016). "Zinc Impregnated Cellulose Nanocomposites: Synthesis, characterization and applications". *Journal of Physical and Chemistry of Solids*, pp.1-22.
- Divij, D.V. and Goyal, R.K. (2014). *Thermal and Dielectric Properties of High Performance polymer/ZnO Nanocomposites*. 2<sup>nd</sup> Ed., International conference on structural Nano Composites (NANOSTRUC), pp.1-10.
- Jinxia, M., Wenhua, Z., Yajun, T. and Zhiguo, W., (2016), "Preparation of Zinc oxide-Starch Nanocomposite and Its Application on Coating" Springer; pp.2-26.
- Kato, M., Usuki, A. and Okada, A. (1997). "*J. Appl. Polym. Sci.*", vol. 66. pp. 1781-1785.
- Kumar, D. and Alappat, B. (2009). "NSF- Water Quality Index: Does It Represent the Experts' Opinion?", *Pract. Period. Hazard. Toxic Radioact. Waste Manage.*, vol.13(1), pp.75-79.
- Korey, C. PASCO Scientific, (2010), *Water Quality Field Guide*, United States of America, pp.2-121.
- Kolodziejczak-Radzimska, A. and Jesionowski, T. (2014), "Zinc oxide- From Synthesis to Application", *Material*, vol. 7, pp. 2833-2881.
- Khurtsia, K. (2015). "*Inle Lake Conser Vation and Rehabilitation Stories from Mymmar*". United Nations Development Programme, UNDP, pp.1-2.
- Laleh, M.A., Saeed, R. and Alizadeh, G. (2015), "Preparation and Characterization of Nylon 6/Silver Nanocomposite Fibers for Permanents Antibacterial Effect", *ORIENTAL JOURNAL OF CHEMISTRY*, vol.31 (1) pp. 257-262.
- Navale, G.R., Thripuranthaka M., Late,D.J., Shinde S.S., (2015), "Antimicrobial Activity of ZnO Nanoparticles Against Pathogenic Bateria and Fungi" *JSM Nanotechnol Nanomed 3 (!)* : pp.1033.
- Moosavi-Nasab, M. and Yousefi, A. (2011). "Biotechnological Production of Cellulose by Gluconacetobacter Xylinus from Agricultural Waste", *Iran J Biotechnol*, vol.9 (2), pp.94-101.
- Supri, A. G., Salmah, H. and Hazvan, K. (2008), *Malaysian Polymer*, vol. 2, pp. 39-53.
- Soosen, S. M., Bose L. and George, K. C. (2009), "Optical Properties of ZnO Nanoparticles", *SB Academic*, vol. 105, pp.57-65.
- Ravishankar, R. V. and Jamuna, B. A. (2011), "Nanoparticles and their Potential Application as Antimicrobials", Mysore: Formatex. pp. 197-209.
- Teli, M. D. and Sheikh, J., (2013), "Study of Grafted Silver Nanoparticles Containing Durable Antibacterial Bamboo Rayon", *Cellulose Chemistry and Technology*, vol.47, (1-2), pp.69-75.
- Teli, M. D. and Sheikh, J., (2014), "Bamboo Rayon-Copper Nanoparticles Composites as Durable Antibacterial Textile Materials," *Composites Interfaces*, vol.21, (2), pp.161-171.

## PHYTOCHEMICAL SCREENING, NUTRITIVE VALUES AND SOME BIOLOGICAL ACTIVITIES OF SEED (KERNEL) OF *ZIZIPHUS MAURITIANA* LAM. (ZEE)

Thet Thet Mon<sup>1</sup>, Khin Chaw Win<sup>2</sup>, Ni Ni Than<sup>3</sup>

### Abstract

The main aim of the present work is to study phytochemical screening, nutritive values and some biological activities of seed (kernel) of *Z. mauritiana* Lam. (Zee). For preliminary phytochemical test, alkaloids,  $\alpha$ -amino acids, carbohydrates, flavonoids, glycosides, phenolic compounds, saponins, starch, tannins, steroids and terpenoids were determined but cyanogenic glycosides and reducing sugars were absent in the Zee seed. The nutritive values such as crude proteins, ash, fibers, moisture, carbohydrates and fats were found to be 39.91 %, 4.27 %, 15.29 %, 7.23 %, 12.97 % and 27.56 % respectively. Moreover, methanol, ethyl acetate, ethanol extracts were revealed antimicrobial activity (inhibition zone diameters = 11~18 mm) against all tested microorganisms while pet-ether and watery extracts did not show activity. Ethanol extract was possessed potent antimicrobial activity than methanol and ethyl acetate extracts. Antiproliferative activity of ethanol and watery extracts of *Z. mauritiana* Lam. against Hela (Cervix) and A 549 (Lung) cancer cell lines were screened by MTT assay. The IC<sub>50</sub> value of watery extract was found to be 170.36  $\mu$ g/mL against cervix cancer. Both ethanol and watery extracts did not show anti-inflammatory activity and cytotoxicity effect.

**Keywords:** antimicrobial, antiproliferative, Hela, A549, MTT assay, anti-inflammatory, cytotoxicity

### Introduction

Plants are valuable gift of nature. Especially, medicinal plants have been used as traditional remedies since ancient time. Medicinal plants have a great importance in the field of research because they are safe to use for the communities. There are so many herb plants which produce a variety of bioactive constituents of known therapeutic values (Ghasham *et al.*, 2017)

A medicinal plant, *Ziziphus mauritiana* Lam belongs to the family Rhamnaceae and genus is *Ziziphus*. It is a tropical and subtropical fruit tree widely distributed in many Asian countries such Afghanistan, Bhutan, India, Indonesia, Malaysia, Myanmar, Nepal, Sri Lanka, Vietnam, Thailand, Africa and Australia (Mahajan *et al.*, 2009). It is wild plant as well as ber seeds are spread by birds, native animals and humans who eat the fruit and expel the seeds. Till now, around 40 species of *Ziziphus* are in record and out of which *Z. mauritiana* Lam. is very common, especially in dry places (Ghasham *et al.*, 2017).

*Z. mauritiana* Lam. is a spiny, every green shrub or small tree up to 15 m high, with trunk 40 cm or more in diameter, spreading crown, stipular spines and many dropping branches (Sukirti *et al.*, 2012). The seeds of *Z. mauritiana*, a species close to *Z. Jujuba*, used to treat insomnia and reduce the body temperature and sweat. *Z. mauritiana* seeds have been also used as sedative and hypnotic drugs in many Asian countries. According to Literature, the seeds contain large amounts of fatty oil and proteins, sterols, and triterpenoid compounds (betulin and betulinic acid) and also contain a large amount of vitamin C (Sena *et al.*, 1998)

In literature, many studies reported that *Z. mauritiana* have some medical benefits such as antioxidant, anti-microbial, anti-diarrheal, anti-diabetic, hepto protective and anti-cancer

---

<sup>1</sup> Assistant Lecturer, <sup>2</sup> PhD, Department of Chemistry, Dagon University

<sup>2</sup> Dr, Lecturer, Department of Chemistry, University of Yangon

<sup>3</sup> Dr, Professor and Head, Department of Chemistry, University of Yangon

(Abdallah *et al.*, 2016). The current study aimed to evaluate nutritional value, anti-microbial, in-vitro anti-proliferative and anti-inflammatory activities of seed extracts.

## Materials and Methods

### Collection and Preparation of Plant material

Seeds of *Z. mauritiana* Lam. were collected from Kyauk Pantaung Township, Mandalay Region in March, 2018. The sample was identified by Department of Botany, University of Yangon. The seed were dried in shade for up to one week and the dried seeds were crushed to fine powder using electronic mill. And then this powdered sample was kept in air tight container protected from moisture until used.

### Preliminary Phytochemical Test

The dried powder samples were used to determine the major phytochemical constituents such as alkaloids,  $\alpha$ -amino acids, carbohydrates, cyanogenic glycosides, flavonoids, glycosides, phenolic compound, reducing sugar, saponins, starch, tannins, steroids and terpenoids by using standard procedures (M-Tin Wa, 1972, Marini-Bettolo *et al.*, 1981).

### Analysis of Nutritional Values

Nutritional values such as proteins, ash, fibers, moisture, carbohydrates and fats of *Ziziphus mauritiana* Lam. were examined by using procedures (AOAC, 1990) at Small Scale Industries Department, Yangon, Myanmar.

### Determination of moisture content

Sample (2 g) was placed in the moisture dish, which had previously been dried and cooled in air-tight desiccators, and accurately weighed. The dish with the sample was placed in an oven and dried for 30 min at 100 °C. Then, they were removed from the oven and cooled in the air-tight desiccators at room, temperature and weighed. The procedure was repeated until the loss in weight had not been changed. The moisture content can be calculated by the following formula.

$$\text{Moisture (\%)} = \frac{\text{loss in weight (g)}}{\text{weight of sample (g)}} \times 100$$

### Determination of ash content

Sample (2 g) was introduced into a predried and cooled porcelain crucible and accurately weighed. Then, it was heated gently over a burner until the sample was thoroughly charred. The crucible and content were then transferred to the muffle furnace at 600 °C for two hours until the residue was free from carbon. Then the crucible containing residue was cooled in a desiccators and weighed. Heating, cooling and weighing were repeated until constant weight was attained. The ash content of the sample was calculated using the following equation.

$$\text{Ash (\%)} = \frac{\text{weight of residue (g)}}{\text{weight of sample (g)}} \times 100$$

### Determination of fats content

About (10 g) of sample was weighed, placed in a cloth bag and the bag was then placed in a soxhlet extractor. Petroleum ether (b.pt. 60-80 °C) was poured into the extractor until some of it overflowed into the flask. The flask was heated on a water bath. The extraction was assumed to be

completed when a small amount of extract placed on a watch glass did not leave any residue on evaporation of solvent. A duration of about 8 h was required for complete extraction. The pet-ether was removed by simple distilled until the volume of the pet-ether was remained to about 10 mL. The last tract of the solvent was then removed by placing the content in an oven at about 100 °C) until the constant weight was obtained. The fats content of sampled was calculated by the following equation.

$$\text{Fat (\%)} = \frac{\text{weight of fat (g)}}{\text{weight of sample (g)}} \times 100$$

### Determination of fibers content

About (2 g) of samples were accurately weighed and introduced into 500 mL round bottomed flask. Then, 1.25 % sulphuric acid (200 mL) was poured into the flask. The flask was connected with reflux condenser and digested for about 30 min. The flask was connected was rotated with hand every few minutes in order to mix the contents and remove particles from the sides. The contents in the flask were filtered through a linen filter supported in a Buchner funnel with water suction pump and washed to free from acid with boiling distilled water. The residue was then washed down into the flask with 1.25 % sodium hydroxide (200 mL) and boiled for about 30 min, rotating the flask in 5 min intervals. After boiling, the flask was removed and filtered through the same linen filter used in acid hydrolysis. The residue was washed thoroughly with hot distilled water until free from alkali. Then, the residue was heated in an oven at 100 °C until the constant weight was obtained. The crucible and content were then ignited in a muffle furnace at a dull-red heat (approx., 600 °C) until all organic matter had been destroyed (approx., 20 minutes). The contents of the crucible were cooled and weighed. Heating, cooling and weighing were repeated until a constant of sample was calculated by the following equation.

$$\text{Fiber (\%)} = \frac{\text{weight of fiber (g)}}{\text{weight of sample (g)}} \times 100$$

### Determination of protein content

Accurately weighed sample (0.5 g) was introduced in the dry Kjeldahl's digestion flask. Potassium sulphate (0.2 g) and copper sulphate (0.05 g) were added to the flask. Concentrated sulphuric acid (10 mL) was then poured into the flask in such a way as to wash down any solid adhering to the neck and the contents were shaken until well mixed. The flask was placed in the neck of the flask. The contents were digested and heated over a small flame so that the liquid boiled gently. Digesting was contained until the mixture become clear and almost pale green color. Then, the flask completely to the steam distillation for about 30 min. 40 % NaOH (100 mL) was also added in it to make the mixture strongly alkaline. Before 40 % NaOH was poured into the apparatus, the tip of the condenser dipped beneath the surface of 0.005 M sulphuric acid (50 mL) of a conical flask (receiver-flask). The steam liberated from boiling water in flask was passed through the mixture in apparatus. When ammonia evolved was carried by steam and condensed was assumed to be completed 15 min after boiling of the solution. Then, the receiver flask was removed and the tip the condenser was washed with distilled water by means of washing bottle into the receiver.

The excess acid remained unreacted with ammonia was titrated with standard sodium hydroxide solution. The percentage of protein content can be calculated by using the following calculation.

$$\text{Protein (\%)} = \frac{0.014 \times 100 \times (v_1 - v_2) M_B \times 6.25}{W}$$

Where,

$v_1$	=	Volume (mL) of NaOH solution used in blank
$v_2$	=	Volume (mL) of NaOH solution used in test
$M_B$	=	Molarity of NaOH solution
$W$	=	Weight (g) of the sample
0.014	=	Milliequivalent weight of the nitrogen

### Determination of carbohydrate content

The carbohydrate present in foods include, starch (glycogen in animal tissue), dextrin, mono and disaccharides. The total carbohydrate content of any food can be obtained as the difference between 100 and the sum of the percentage of moisture, protein, fat, ash and fiber. Although individual carbohydrates can, if necessary, be estimated separately by chemical methods, the described above is sufficiently accurately for practical nutrition work.

### Determination of energy values

The energy value of the samples was calculated by the following equation.

$$\text{Energy value (kcal/100g)} = (4 \times \text{protein}) + (4 \times \text{carbohydrate}) + (9 \times \text{fat})$$

### Antimicrobial Activity

The antimicrobial activity of different crude extracts such as watery, ethanol, ethyl acetate, petroleum ether and methanol extracts were determined against six strains of microorganisms, *Bacillus subtilis*, *Bacillus pumilus*, *Staphylococcus aureus*, *Pseudomonas aeruginosa*, *Candida albicans* and *Escherichia coli*, by employing agar well diffusion method at Pharmaceutical Research Department (PRD), Ministry of Industry, Yangon, Myanmar. (Abalaka *et al.*, 2010)

#### (a) Preparation of Nutrient Agar Medium

To a mixture of 1 g of meat extract, 1 g of peptone, 0.5 g of NaCl and 1.5 g of agar powdered were placed in a sterilized 250 mL conical flask, 100 mL of sterile distilled water were added to obtain nutrient agar medium. The resulting mixture was heat to dissolve the contents. Then the pH of the resulting solution was adjusted to 7.2 with 0.1 M NaOH solution. It was sterilized in an autoclave at 121 °C for 15 min.

#### (b) Screening by Agar Well Diffusion Method

About 20-25 mL of agar medium contained test organisms poured into the sterile petri-dishes under aseptic condition near the flame of the spirit burner and left the agar solid, the cork bower about 10 mm in diameter was sterilized and made a well in the agar plate previously described. Then the extract samples were introduced into the well (about 0.2 mL). They were then incubated at 36 °C for 24 h. The formation of inhibition zone around the well was observed. This observation indicates the presence of antimicrobial active compounds in the extract.

### Screening of Antiproliferative activity by using MTT assays

In *in vitro* antiproliferative activity of ethanol and watery extracts of the fruits of *Z. mauritiana* Lam. was determined against two human cancer cell lines such as A 549 (lung cancer)

and Hela (human cervix cancer). These tests were done by the procedure described by Win *et al.*, (2015) at Department of Natural Products Chemistry, Institute of Natural Medicine, and University of Toyama, Japan.

After the cell growth, the 70-100 % cell in the medium was aspirated with aspirator. The cell was washed with PBS (5 mL) for 2 times. The cells are trypsinased with trypsin (4 mL) and incubated for 2–3 minutes. And then the medium (1 mL) was added to stop trypsinization. The cell suspension was transferred to 15 mL centrifuge tube. The tube (cell suspension) was centrifuged in the refrigerated centrifuge machine (3000 rpm) with the same centrifuge tube for 3 minutes. After the centrifugation, the supernatant was carefully removed without disturbing the cell pellet and the cell was found at the bottom of the centrifuge tube. The cell in the centrifuge tube was added with fresh medium (3 mL) gently to the side of the tube and slowly pipetted up and down 2 to 3 time to re-suspend the cell pellet. The number of cell was counted with Haemocytometer.

The cell solution (10  $\mu\text{L}$ ) was mixed in the Tryphan blue (40  $\mu\text{L}$ ). The chamber and the covered slip were cleaned with alcohol (70 % EtOH). The chamber was dried and the overslip was fixed in position. The cell was harvested and the 10  $\mu\text{L}$  of the cell was added to the Haemocytometer (do not overfill). And then the chamber was placed in the inverted microscope under a 10X objective and phase contrast was used to distinguish the cell. The cell was counted in the large, central gridded square (1  $\text{mm}^2$ ). The gridded square was circled and multiplied by  $10^4$  to estimate the number of cell per millimeter. The number of cell was counted by the following equation,

$$\text{No. of cell in stock} = \text{counted cell}/4 \times 10^4 \times \text{dilution factor} \times \text{volume of stock cell solution}$$

After the cell counting, the cell was added with 120 mL ( $120 \times 10^3 \mu\text{L}$ ) of medium for 12 plates. 10 mL (100  $\mu\text{L}$ ) medium of cell was filled in 96 well plates. The cell in 96 well plates was incubated in an incubator for 24 hours.

After the incubation, the medium was removed by absorption machine (very carefully) and washed with 100  $\mu\text{L}$  PBS solution. And then 100  $\mu\text{L}$  of the different concentrations of sample and control solution was added in the 96 well plates. The sample solutions in 96 well plates with cells were incubated in an incubator for 72 hours. The sample solution with cell and medium was added with 100  $\mu\text{L}$  MTT reagent. And then the 96 well plates were incubated in an incubator for 3 hours. After the incubation, the absorbance of each solution was measured at 570 nm by using UV-visible spectrophotometer. The percent cell viability activity was calculated by the following equation.

$$\% \text{ Cell viability} = \frac{(\text{Abs (test sample)} - \text{Abs (blank)})}{(\text{Abs (control)} - \text{Abs (blank)})} \times 100$$

Where,

Abs (test sample) = absorbance of test sample solution

Abs (control) = absorbance of DMSO solution

Abs (blank) = absorbance of MTT reagent

IC<sub>50</sub> (50 % inhibitory concentration) values were calculated by linear regressive excel program. The standard deviation was also calculated by the following equation.

$$\text{Standard Deviation (SD)} = \sqrt{\frac{(\bar{x} - x_1)^2 + (\bar{x} - x_2)^2 + \dots + (\bar{x} - x_n)^2}{(n - 1)}}$$

Where,

X = average % inhibition

$x_1, x_2, \dots, x_n$  = % cell inhibition of test sample solution

n = number of times

### Anti-inflammatory and cell viability activity

Anti-inflammatory activity of the samples was evaluated by NO inhibition assay according to the method of Jin *et al.*, (2012) with some modifications. The RAW264.7 cells was cultured in  $\alpha$ -MEM supplemented with 10 % heat incubated fetal bovine serum, and 1 % penicillin (10,000 U/mL)-streptomycin (10 mg/L). When the cell proliferation reaches about 70 % confluency, the cells were harvested using cell scraper and diluted to a suspended in fresh medium. The 100  $\mu$ L of cells ( $4 \times 10^4$ /well) were seeded in the 96-well plates and incubated for 24 h at 37 °C in a humidified atmospheric containing 5 % CO<sub>2</sub>. The cells were then treated with 50  $\mu$ L each of LPS (100 mg/mL) and different doses of samples for 24 h. NO production was monitored by measuring the accumulation of nitrite in the culture supernatant using Griess reagent (Schmidt *et al.*, 1996). In brief, 100  $\mu$ L each of the supernatant from 96-wells was mixed with equal volume of Griess reagent (0.5 % sulfanilamide and 0.05 % naphthylenediamide dihydrochloride in 2.5 % H<sub>3</sub>PO<sub>4</sub>) in the new 96 well plates and allowed to stand for 10 min at room temperature. The absorbance at 540 nm was measured using microplate reader. L-NMMA monoacetate was used as a positive control. On the other hand, the effect of the samples on the cell proliferation was evaluated by MTT solution (5 mg/mL) in the medium was added. After 3 h incubation, the medium was discarded and 100  $\mu$ L each of DMSO was added to dissolve the formazan crystals and the absorbance at 570 nm was recorded by microplate reader. The percentage of NO inhibition and that of cell viability was calculated as follows:

$$\text{NO inhibition (\%)} = \frac{\text{Abs}_{(\text{control})} - \text{Abs}_{(\text{sample})}}{\text{Abs}_{(\text{control})}} \times 100$$

Where, Abs<sub>(control)</sub> and Abs<sub>(blank)</sub> are the absorbance of the control group treated by LPS alone and the absorbance of the samples

$$\text{Cell viability (\%)} = \frac{\text{Abs}_{(\text{test sample})} - \text{Abs}_{(\text{blank})}}{\text{Abs}_{(\text{control})} - \text{Abs}_{(\text{blank})}}$$

## Results and Discussion

### Phytochemical constituents of *Z. mauritiana* Lam. (Zee)

Preliminary phytochemical investigation was carried out to know the secondary metabolites present in the seed (kernel) of *Z. mauritiana* Lam. The results are summarized in Table 1.

According to the results, it was observed that alkaloids,  $\alpha$ -amino acids, carbohydrates, flavonoids, glycosides, phenolic compounds, saponins, starch, tannins and steroids were present while cyanogenic glycosides and reducing sugars were not detected in seed sample. Therefore, It can be seen that the seed of Zee sample might contain potent secondary metabolites.

**Table 1 Results of Phytochemical Investigation on *Z. mauritiana* Lam. (Zee)**

No	Tests	Extracts	Test reagents	Observations	Results
1.	Alkaloids	1 % HCl	Wagner's reagent Mayer's reagent	Reddish brown ppt White ppt	+ +
2.	$\alpha$ -amino acids	H <sub>2</sub> O	Ninhydrin reagent	Pink spot	+
3.	Carbohydrates	H <sub>2</sub> O	10 % $\alpha$ - naphthol, Conc : H <sub>2</sub> SO <sub>4</sub>	Red ring	+
4.	Cyanogenic Glycosides	H <sub>2</sub> O	Sodium picrate paper, Conc: H <sub>2</sub> SO <sub>4</sub>	No change in color	-
5.	Flavonoids	EtOH	Conc: HCl, Mg ribbon	Pink colour	+
6.	Glycosides	H <sub>2</sub> O	10 % lead acetate	White ppt	+
7.	Phenolic Compounds	H <sub>2</sub> O	10 % FeCl <sub>3</sub>	Deep blue	+
8.	Reducing sugars	H <sub>2</sub> O	Benedict's solution	No brick-red color	-
9.	Saponins	H <sub>2</sub> O	Distilled water	Frothing	+
10.	Starch	H <sub>2</sub> O	I <sub>2</sub> solution	Blue	+
11.	Tannins	EtOH	1 % FeCl <sub>3</sub>	Greenish yellow	+
12.	Steroids	PE	Acetic anhydride, Conc: H <sub>2</sub> SO <sub>4</sub>	Greenish yellow	+
13.	Terpenoids	CHCl <sub>3</sub>	Acetic anhydride, Conc: H <sub>2</sub> SO <sub>4</sub>	Pink color	+

(+) = Present, (-) = Absence, ppt = precipitate

#### Some Nutritional Values of *Z. mauritiana* Lam. (Zee)

The nutritional values of Zee were investigated by AOAC methods. Moisture content was determined by oven drying method and found to be 7.23 %. Larger the moisture content, the shorter the shelf-life. Proteins content was measured by micro-Kjeldahl method and it was observed 39.91%. The ash content was 4.27 % and measured by ashing in the muffle furnace. Fibers was determined by acid-alkali treatment and found to be 15.29%. Fats content was measured by Soxhlet extraction method using PE (b.pt. 60-80 °C) that was determined 27.56%. The total carbohydrate and energy value can be calculated and found to be 12.97 % and 459.56 (kcal/100 g) respectively.

The result are summarized in Table 2 and from these data, it can be clearly seen that the protein contents is very high. Protein is important building block of bones, muscles, cartilage skin and blood. Therefore, the seed could be used as protein supplement for low protein legumes such as cereals. Next is fats content that fats from vegetable sources can help lower risk of heart attack, stroke and other major health problem. So, it was determined high nutritive values in the Zee seed sample.

**Table 2 Results of Nutritional values on *Z. mauritiana* Lam.**

No.	Parameters	Contents (%)
1	Proteins	39.91
2	Ash	4.27
3	Fibers	15.29
4	Moisture	7.23
5	Carbohydrates	12.97
6	Fats	27.56
7	Energy value	459.56 (kcal/100 g)

### Screening of Antimicrobial Activity

The antimicrobial activity of ethyl acetate, ethanol, methanol, pet-ether and watery extracts from *Z. mauritiana* Lam. were screened by agar well diffusion method. The resultant inhibition zone diameters are described in Table 3. A larger inhibition zone diameter usually means that the antimicrobial is more potent.

According to the result, ethanol, ethyl acetate and methanol extracts were revealed antimicrobial activity against all tested microorganisms (inhibition zone diameters = 11~18 mm) but pet-ether and watery extracts did not show the activity.

**Table 3 Inhibition zone diameter of different crude extracts of *Z. mauritiana* Lam. against different strains of microorganism**

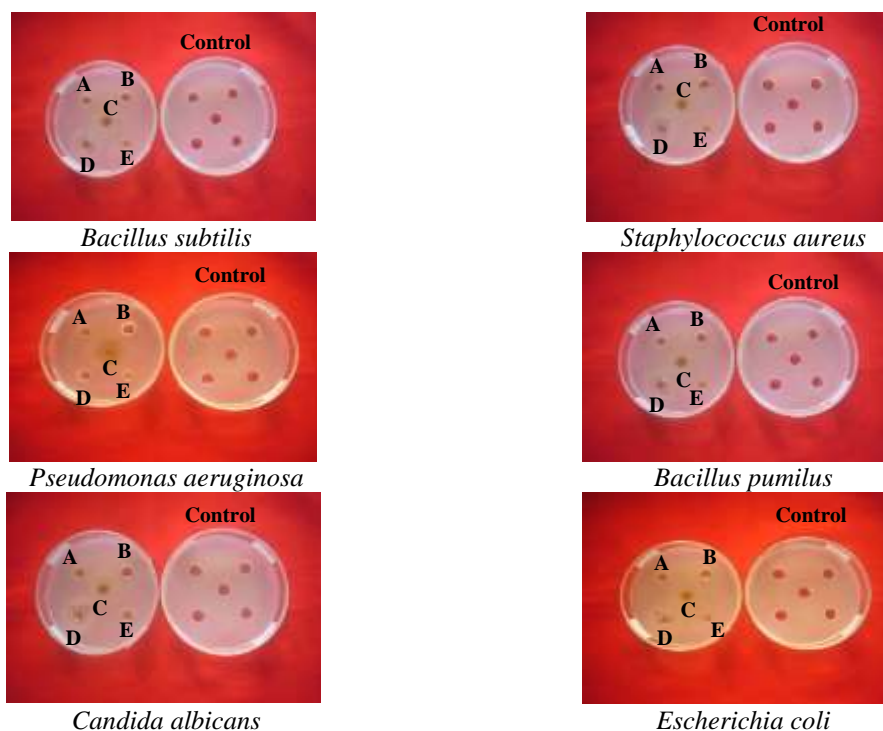
Sample	Extracts	<i>B. subtilis</i> (mm)	<i>S. aureus</i> (mm)	<i>P. aeruginosa</i> (mm)	<i>B. pumilus</i> (mm)	<i>Candida albicans</i> (mm)	<i>E-coli</i> (mm)
<i>Ziziphus mauritiana</i> Lam. (Zee)	Pet-ether	-	-	-	-	-	-
	MeOH	15 (++)	15 (++)	14 (++)	15 (++)	15 (++)	15 (++)
	EtOAc	11 (+)	12 (+)	12 (+)	12 (+)	11 (+)	12 (+)
	EtOH	15 (++)	16 (++)	14 (++)	16 (++)	18 (++)	17 (++)
	H <sub>2</sub> O	-	-	-	-	-	-

Agar well-10 mm

10 mm ~14 mm (+)

15 mm ~ 19 mm (++)

20 mm above (++++)



- A = PE Extract
- B = MeOH Extract
- C = H<sub>2</sub>O Extract
- D = EtOH Extract
- E = EtOAc Extract

**Figure 1** Inhibition zones of various crude extracts against microorganisms

### Investigation of Antiproliferative Activity

In vitro antiproliferative activity of ethanol and watery extracts of *Z. mauritiana* Lam. (seed) was determined against two cancer cell lines, Hela (Human cervix) and A 549 (Lung). In this activity 5-Fluorouracil is used as a positive control. Antiproliferative agent is the ability of a compound to stop the growth of cells that means not allowing the cancer cells to multiply rapidly. The result was shown in Table 4. According to result, the watery extract of Zee was found to possess activity against Hela cell line ( $IC_{50}$  value = 170.36  $\mu\text{g/mL}$ ). However, ethanol extract did not show activity.

**Table 4 Anti-proliferative Activity of Crude Extracts of *Z. mauritiana* Lam.**

Sample	Hela			A549			
	20 $\mu\text{g/mL}$	200 $\mu\text{g/mL}$	$IC_{50}$	20 $\mu\text{g/mL}$	200 $\mu\text{g/mL}$	$IC_{50}$	
EtOH (seed)	57.60 $\pm$ 1.48	90.66 $\pm$ 4.88	>200	69.70 $\pm$ 8.41	70.00 $\pm$ 3.50	>200	
	86.24 $\pm$ 1.98	42.86 $\pm$ 1.77	170.36	77.88 $\pm$ 4.17	55.17 $\pm$ 0.35	>200	
H <sub>2</sub> O (seed)	2 $\mu\text{g/mL}$	10 $\mu\text{g/mL}$	20 $\mu\text{g/mL}$	$IC_{50}$	2 $\mu\text{g/mL}$	10 $\mu\text{g/mL}$	20 $\mu\text{g/mL}$
	91.44 $\pm$ 4.95	85.22 $\pm$ 0.28	24.93 $\pm$ 6.22	15.84	136.23 $\pm$ 12.94	70.45 $\pm$ 5.59	47.89 $\pm$ 8.21

\* 5-FU (5-Fluorouracil) = Positive control

A549 = Lung cancer cell line

Hela = Cervix cancer cell line

### Screening of anti-inflammatory and Cell viability activity

Anti-inflammatory and cell viability activity of ethanol and watery extracts was investigated by MTT assay and L-NMMA is used as a positive control. Anti-inflammatory agents block some substances in the body that can cause cancer. The % NO inhibition result is inversely proportional to % cell viability. It can be clearly seen that in Table 4. The greater  $IC_{50}$  values of % cell viability than the % NO inhibition that the sample was possessed anti-inflammatory effect. Less  $IC_{50}$  value of % cell viability means that it was cytotoxicity effect. According to result, Zee seed sample did not possess anti-inflammatory activity and cytotoxicity effect.

**Table 5 Anti-inflammatory Activity of *Ziziphus mauritiana* Lam. (Zee)**

Sample	%NO inhibition			% Cell Viability		
	10 $\mu\text{g/mL}$	100 $\mu\text{g/mL}$	$IC_{50}$	10 $\mu\text{g/mL}$	100 $\mu\text{g/mL}$	$IC_{50}$
EtOH (seed)	6.01 $\pm$ 0.79	45.36 $\pm$ 1.04	>100	84.09 $\pm$ 1.29	85.63 $\pm$ 3.81	>100
H <sub>2</sub> O (seed)	3.83 $\pm$ 0.46	27.87 $\pm$ 0.3	>100	72.35 $\pm$ 2.33	50.54 $\pm$ 2.55	>100
*L-NMMA	18.49 $\pm$ 0.10	50.35 $\pm$ 0.10	98.25	100.32 $\pm$ 12.41	92.01 $\pm$ 1.02	>100

\* L-NMMA (L-N monomethyl-L-arginine) = Positive control

■ Can be concluded as extract that has anti-inflammatory effect

## Conclusion

From the overall assessment, the following inferences could be deduced. There were rich phytochemical constituents in Zee seed sample. It was found that high nutritional values among them proteins content was observed in highest amount (39.91%). So, the plant source of protein could be explored for better supplement in food. For antimicrobial activity, ethanol extract showed potent antimicrobial activity with inhibition zone diameter ranges between 14-18 mm against all tested organism.

Nowadays, there are so many popular anti-cancer agent in medicinal plants. So, most of the people are interested in investigation of antiproliferative activity. Watery extract of Zee seed showed mild antiproliferative activity against Hela cell line ( $IC_{50} = 170.36 \mu\text{g/mL}$ ). It was neither anti-inflammatory activity nor cytotoxicity effect in Zee sample. Therefore, the present study will contribute that seed of *Z. mauritiana* Lam. can be used as traditional medicine for some diseases.

## Acknowledgements

The authors would like to thank the Department of Higher Education, Ministry of Education, Yangon, Myanmar, for the permission of doing this research and Myanmar Academy of Arts and Science for allowing to present this paper. Special thanks to Dr Nwet Nwet Win, Department of Natural Products Chemistry, Institute of Natural Medicine, and University of Toyama, Japan for her help and suggestion for antiproliferative and anti-inflammatory activities.

## References

- Abalakai, M. E., Daniyanl, S. Y. and Mann, A. (2010). "Evaluation of the antimicrobial activities of two *Ziziphus* species (*Ziziphus mauritiana* L. and *Ziziphus spinachristi* L.) on some microbial pathogens". *Afr. J. Pharm. Pharmacol.*, vol. 4 (4), pp. 135-139.
- Abdallah, E. M., Elsharkawy, E. R. and Aldelaziz, E. (2016). "Biological activities of methanolic leaf extract of *Ziziphus mauritiana*". *A Society of Nature Publication*, vol. 9 (4), pp. 605-614.
- AOAC. (1990). *Official Method of Analysis of the Association of Official Analytical Chemists*. Ed. K. Helrich, Virginia; 15<sup>th</sup> Ed. 1, AOAC Inc.
- Ghasham, A. A., Muzaini, M. A., Kamal, A. Q., Gamal, O. E., Riyaz A. K., Syeda, A. F., Sana, H., Agamy, E. E. and Abdallah, W. E. (2017). "Phytochemical Screening, Antioxidant and Antimicrobial Activities of Methanolic Extract of *Ziziphus mauritiana* Lam. Leaves Collected from Unaizah, Saudi Arabia". *Intl. J. of Pharmaceutical Research & Allied Sciences*, vol. 6 (3), pp. 33-46.
- Jin, S. E., Son, Y. K., Min, B. S., Jung, H. A. and Choi, J. S. (2012). "Anti-inflammatory and antioxidant activities of constituents isolated from *Pueraria lobata* roots". *Archives of Pharmacol Research*, vol. 35 (5), pp. 823-837.
- M-Tin Wa. (1972). "Phytochemical Screening Methods and procedures". *Phytochemical Bulletin of Botanical Society of America Inc.*, vol. 5 (3), pp. 4-10.
- Mahajan, R. T. and Chopda, M. Z. (2009). "Phyto-pharmacology of *Ziziphus jujube* mill—a plant review". *Pharmacognosy Reviews*, vol. 3 (6), pp. 320-329.
- Marini-Bettolo, G. B., Nicoletti, M. and Patamia, M. (1981). "Plant Screening by Chemical and Chromatographic Procedure under Field Conditions". *J. Chromatography*, vol. 213, pp. 113-127.
- Schmidt, S., Annemarie, D., Prtra, A. and Uwe, F. (1996). "Identification of Interleukin 1-induced Apoptosis in Rat Islets Using in the Specific Labelling of Fragmented DNA". *J. of autoimmunity*, vol. 9 (3), pp. 309-313.
- Sena, L. P., Vanderjagt, D. J. and Rivera, C. (1998). "Analysis of nutritional components of eight famine foods of Republic of Niger". *Plant Foods for Human Nutrition*, vol. 52 (4), pp. 17-30.
- Sukirti, U., Prashant, U., Ghosh, A.K. and Vijender, S. (2012). "A Review on Pharmacological Potential of This Underutilized Plant". *Intl. J. of Current Research and Review*, vol. 4 (3), pp. 141-144.
- Win, N. N., Ito, T., Aimaiti, S., Imagawa, H., Ngwe, H., Abe, I. and Morita, H. (2015). "Kaempferols A-H, Diterpenoids from the rhizomes of *Kaempferia pulchra* collected in Myanmar". *J. Nat. Prod.*, vol. 78, pp. 1113-1118.

# PREPARATION AND CHARACTERIZATION OF SILVER DOPED BISMUTH FERRITE NANOPARTICLES BY CO-PRECIPIATION METHOD

Thuzar Nyein<sup>1</sup>, Zaw Naing<sup>2</sup>, Cho Cho<sup>3</sup>

## Abstract

The main aim of the research work is to study the preparation and characterization of silver doped bismuth ferrite, Ag-BiFeO<sub>3</sub> by co-precipitation method. In this method, Ag-BiFeO<sub>3</sub> nanoparticles were prepared by using bismuth nitrate, ferrite nitrate and silver nitrate as starting materials with different ratios (1:1:0.125, 1:1:0.25, 1:1:0.5 and 1:1:1) and the prepared silver doped samples were noted as S-1, S-2, S-3, S-4 respectively. The precursor powder was calcined at 500 °C for 4 h. The prepared samples were characterized by XRD, SEM and EDXRF techniques. The ratio (1:1:1) of bismuth nitrate, ferrite nitrate and silver nitrate was selected as optimum ratio due to its high crystallinity and average crystallite size. Some physicochemical properties and optical properties of prepared Ag-BiFeO<sub>3</sub> powder samples were also determined.

**Keywords:** Ag-BiFeO<sub>3</sub> powder, Co-precipitation method, XRD, SEM, EDXRF techniques

## Introduction

Among all the perovskite materials with ABO<sub>3</sub> structure studied, BiFeO<sub>3</sub> shows ferroelectric properties with a high Curie temperature ( $T_C \sim 830$  °C) and G-type antiferromagnetic properties below the Neel temperature ( $T_N \sim 370$  °C) (Selbach *et al.*, 2007). Therefore, it has been widely used in magnetic and ferroelectric devices. Apart from ferroelectric properties, BiFeO<sub>3</sub> is one of the materials with the largest known electric polarizations and has a small ( $\approx 3$  eV) band gap for which it is likely applied in conducting domain walls, catalyst and fuel and/or solar cells (Fischer and Polomska, 1980). BiFeO<sub>3</sub> exhibits photocatalytic activities under visible light irradiation for water splitting and degradation of pollutants because of its narrow band gap and excellent chemical stability (Erenstein *et al.*, 2007). In fact, doping of BiFeO<sub>3</sub> with a foreign atom at either A or B site of the ABO<sub>3</sub> lattice has been proven to be a valuable route to enhancing its properties. Demonstrated substitution of Bi<sup>3+</sup> with Ag resulted in remarkable improvement of the photocatalytic activity of BiFeO<sub>3</sub> under visible light (Freitas, 2013).

Many researches have attempted to synthesis nanostructured BiFeO<sub>3</sub>, such as spherical, nanorods, nanowires and plates with different methods. Several techniques have been utilized to prepare BiFeO<sub>3</sub> nanostructures, ball-milling technique, co-precipitation, polymeric assisted route, hydrothermal, reverse micelles etc. Choosing proper synthesis techniques play an important role in controlling the size and surface area and hence the properties of materials (Johari, 2011). Among all used techniques, the co-precipitation method has many advantages such as the use of low temperature, low cost, simplicity, energy saving, relatively low impurity content resulting from the easy formation of bismutite phase during calcination and uniform-sized BiFeO<sub>3</sub> nanoparticles (Muneeswaran *et al.*, 2013).

In this present work, BiFeO<sub>3</sub> nanoparticles were synthesized using co-precipitation method. The effect of calcination temperature on its structural, morphological, optical and electrical properties has been studied.

---

<sup>1</sup> PhD Candidate, Department of Chemistry, University of Yangon

<sup>2</sup> Dr, Associate Professor, Department of Chemistry, Dagon University

<sup>3</sup> Dr, Professor, Department of Chemistry, University of Yangon

## Materials and Methods

### Materials and Methods

Ferric nitrate nanohydrate ( $\text{Fe}(\text{NO}_3)_3 \cdot 9\text{H}_2\text{O}$ ) with 98 % purity, bismuth nitrate pentahydrate ( $\text{Bi}(\text{NO}_3)_3 \cdot 5\text{H}_2\text{O}$ ) with 98 % purity, silver nitrate with 98 % purity and other reagents were purchased from commercial sources with analytical purity and used as received. Laboratory equipment was used at Chemistry Laboratory of Yangon University and also at the Maubin University and Universities' Research Center, Lower Myanmar, Yangon Region. Instruments employed were hot plate, magnetic stirrer, oven, furnace and spectrophotometer. The methodologies and techniques used were carried out according to the procedures given in the recommended texts and literatures.

### Preparation of Silver Doped Bismuth Ferrite Nanoparticles

Bismuth nitrate pentahydrate [ $\text{Bi}(\text{NO}_3)_3 \cdot 5\text{H}_2\text{O}$ ], ferric nitrate nanohydrate [ $\text{Fe}(\text{NO}_3)_3 \cdot 9\text{H}_2\text{O}$ ] and silver nitrate [ $\text{AgNO}_3$ ] were mixed with different mole ratios (1:1:0.125, 1:1:0.25, 1:1:0.5 and 1:1:1) respectively and dissolved in distilled water and stirred for about 20 min at room temperature to form a clear solution. The mixture of 10 mL of 2.5 M ammonia and 10 mL of distilled water were added in this clear solution to get the reaction product. These precipitates were kept at room temperature for about 24 h and were washed several times with distilled water to remove unreacted products and then filtered. Final products were dried in the oven at 100 °C for about 5 h. The obtained powder was calcined at 500 °C for 4 h.

### Characterization

The average crystallite sizes of prepared silver doped bismuth ferrite ( $\text{Ag-BiFeO}_3$ ) nanoparticles were calculated from XRD pattern by using Scherrer equation. XRD model was Regaku, X-ray Diffractometer, RINT 2000 P/C software at no. 9240 J 101, Japan. The surface morphology of prepared silver doped bismuth ferrite ( $\text{Ag-BiFeO}_3$ ) nanoparticles was examined by a JSM 5610 LV scanning microscope, JEOL Ltd., Japan. The relative abundance of elements of silver doped bismuth ferrite ( $\text{Ag-BiFeO}_3$ ) nanoparticles were analyzed by using EDXRF (Energy Dispersive X-ray Fluorescence) Spectrometer Shimadzu EDX-700, Japan. The optical properties of the prepared silver doped bismuth ferrite ( $\text{Ag-BiFeO}_3$ ) nanoparticles were determined by using UV-1800 SHIMADZU UV spectrophotometer (Amtt Customer Support & Analytical Laboratory).

### Determination of Some Physicochemical Properties

#### pH

1 g of ( $\text{Ag-BiFeO}_3$ ) sample was placed into a Pyrex 200 mL beaker and 100 mL of distilled water was added. The content of the beaker was heated at 80 °C for 10 min. The beaker and content were gently shaken and the sample was filtered. The filtrate was cooled at room temperature and pH of the sample was determined by using a pH meter.

#### Moisture content

Moisture content (%) was determined by the oven method at  $110 \pm 5$  °C. An accurately weighed sample (about 1 g) was added to a pre-dried and cooled dish with a cover. The uncovered dish is placed in the electric oven, and dried at  $110 \pm 5$  °C for 2 h. After heating, the cover was placed in position and in desiccator for cooling. And weighing which was repeated until a constant weight was obtained. The moisture percent is represented by the loss in weight.

### Bulk density

A clean dry 10 mL graduated cylinder was weighed. It was then filled with the dry sample to the 10 mL mark and reweighed. The graduated cylinder was placed in a tapping box and the cylinder was gently tapped until there was no more reduction in volume. The minimum volume was recorded and the bulk density was calculated.

### Porosity

The porosity of sample was measured by dry-wet method. About 1 g of the dry sample was placed in a beaker and 0.8 mL of distilled water was added. The sample was equilibrated with distilled water for 24 h and then was determined by dividing the amount of water adsorbed (mL) with the amount of the dry sample (mL).

### Surface area by methylene blue adsorption test

A stock solution of methylene blue was prepared by dissolving 0.1 g of methylene blue in 1 L distilled water. By serial dilution, the methylene blue solutions within the concentration ranges from 10 ppm to 100 ppm were prepared. Analyses were carried out spectrometrically by using Cary 60 UV-Visible spectrophotometer. Different concentrations of dye solutions and 0.1 g of sample were determined and the surface area was calculated.

## Results and Discussion

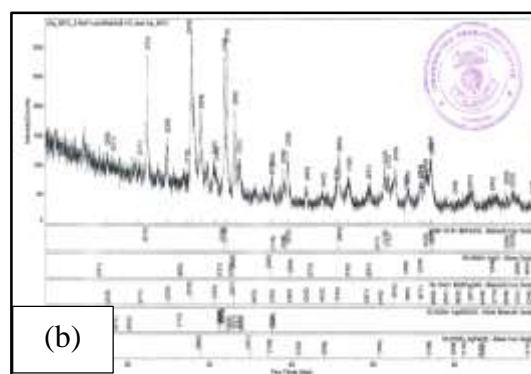
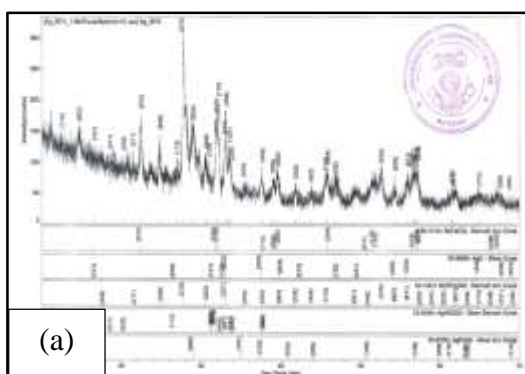
### Preparation of Silver Doped Bismuth Ferrite (Ag-BiFeO<sub>3</sub>) Nanoparticles

Different molar ratios (1:1:0.125, 1:1:0.25, 1:1:0.5 and 1:1:1) of bismuth nitrate pentahydrate, ferrite nitrate nanohydrate and silver nitrate were mixed respectively and dissolved in distilled water, and then stirred for about 20 min at room temperature to obtain a clear solution. Various pH levels were obtained by dropping of the mixture of 10 mL of 2.5 M ammonia and 10 mL of distilled water. This solution was kept at room temperature for about 24 h. The resulting precipitates were washed several times with distilled water and then filtered. Final products (precipitates) were dried in the oven at 100 °C for about 5 h and calcined at 500 °C for 4 h.

### Characterization

#### XRD Analysis

The average crystallite sizes of prepared samples (S-1, S-2, S-3, S-4) were calculated by using Debye-Scherrer equation. It was observed that the crystallite size increases with increasing silver doping levels which may be due to the growth of particles size. Among them, the sample S-4 has high crystallinity and average crystallite size was found to be 33.06 nm from calculating. Based on the XRD results, S-4 was chosen for selected sample.



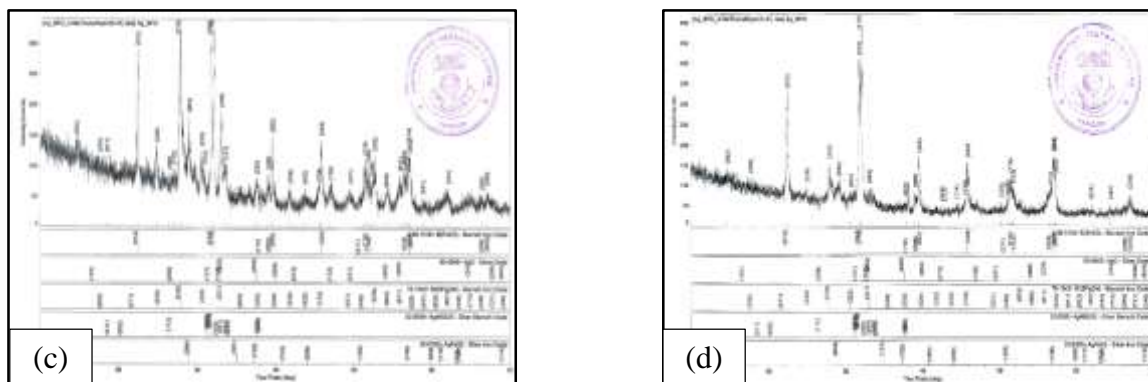


Figure 1 XRD diffractograms of (a) S-1 (b) S-2 (c) S-3 (d) S-4 nanoparticles

Table 1 Average Crystallite Sizes of Prepared Ag-BiFeO<sub>3</sub> Nanoparticles

Samples	Average crystallite sizes (nm)		Lattice Parameters (Å°)			Crystal system
	XRD data	using Debye Scherrer equation	a	b	c	
S-1	31.72	23.29	9.9546	9.9546	9.9546	Cubic
S-2	31.48	26.44	10.0292	10.0292	10.0292	Cubic
S-3	39.20	30.88	9.7967	9.7967	9.7967	Cubic
S-4	39.44	33.06	9.5300	9.5300	12.2496	Hexagonal

SEM Analysis

SEM micrographs of prepared silver doped bismuth ferrite (S-1 to S-4) were indicated in Figures 2 (a) to 2 (d). Figure 2 (d) showed the SEM image of selected sample S-4 and it can be seen that the spherical shape and agglomeration nature increases with increasing silver doping levels.

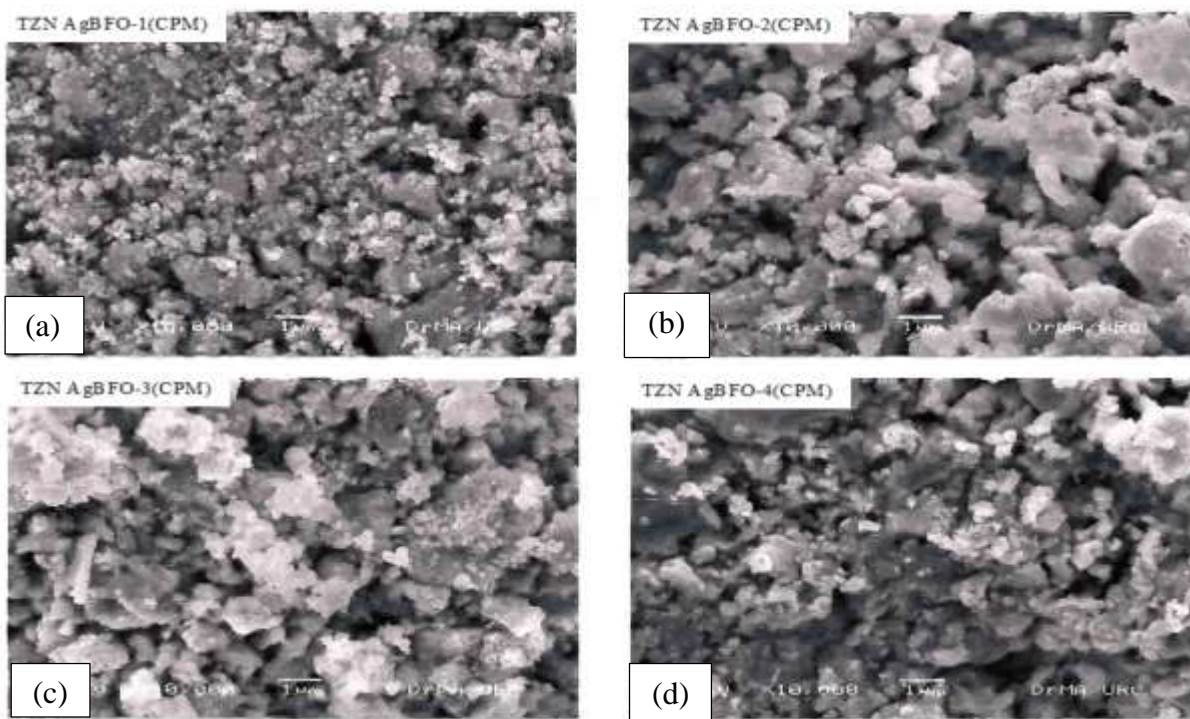
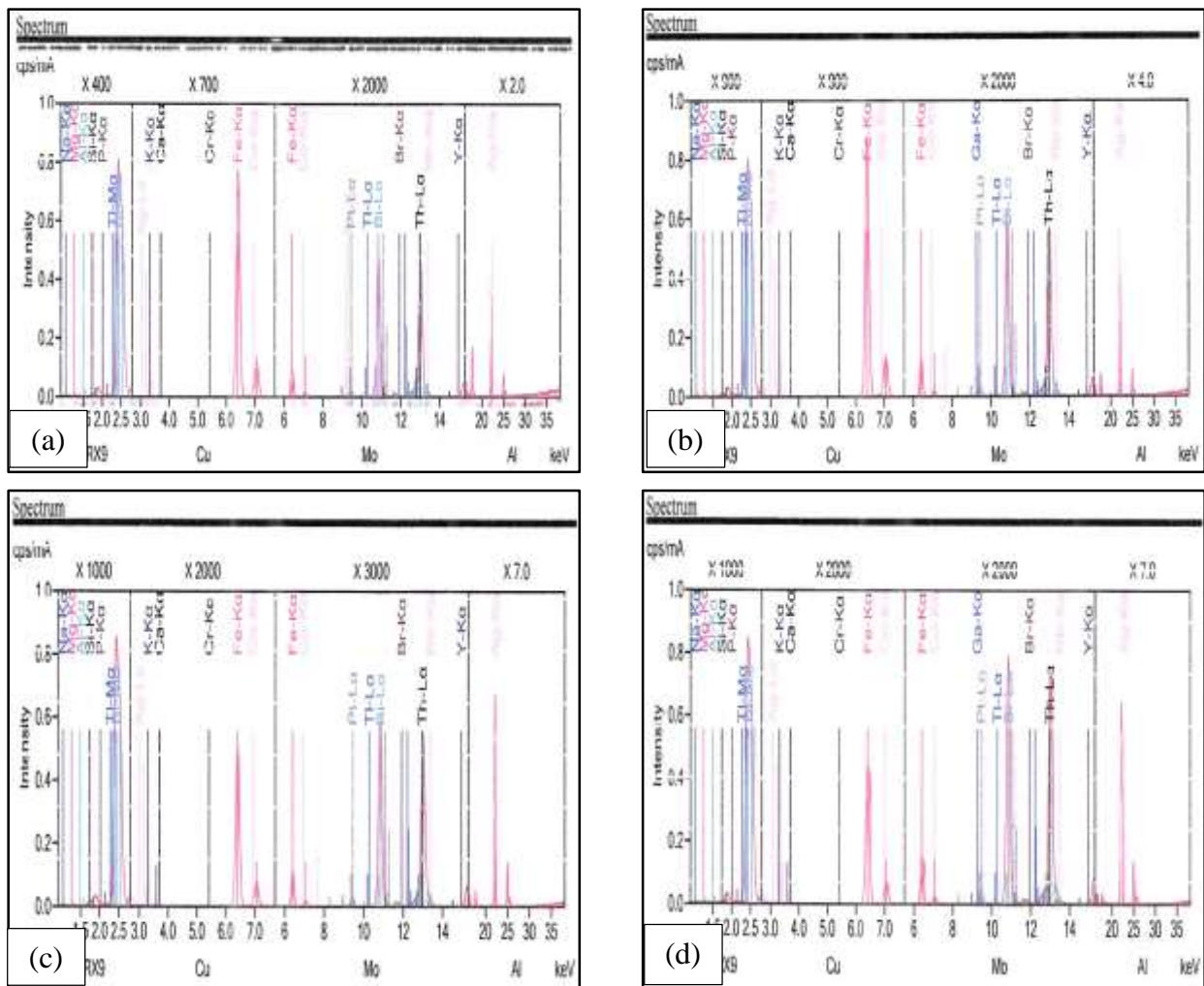


Figure 2 SEM micrographs of (a) S-1 (b) S-2 (c) S-3 (d) S-4 nanoparticles

**EDXRF Analysis**

The EDXRF spectra of prepared samples with different ratios showed that the silver content was increased with increasing the silver doping levels. Therefore, the sample S-4 was chosen for selected sample due to the silver doping percent.



**Figure 3** EDXRF spectra of (a) S-1 (b) S-2 (c) S-3 (d) S-4 nanoparticles

**Table 2** Relative Abundance of Elements in Prepared Ag-BiFeO<sub>3</sub> Nanoparticles

Samples	Relative Abundance of Elements (%)		
	Bi	Fe	Ag
S-1	22.1	8.29	0.631
S-2	30.9	11.8	1.68
S-3	26.9	9.98	2.74
S-4	29.0	10.9	3.26

**Physicochemical Properties**

The physicochemical properties of selected sample (S-4) by co-precipitation method were such as pH, moisture, bulk density, porosity and surface area. The sample showed neutral (pH-7) and the moisture percent and bulk density were 0.11 % and 1.25 g cm<sup>-3</sup> respectively. Therefore, it was found that the lesser the moisture percent the better the crystallinity. The porosity and surface area of the sample indicated 80 % and 571 m<sup>2</sup> g<sup>-1</sup>. Thus, the large surface area and porosity revealed

the good nanoparticles for photodegradation, electrical application (semiconductors), optical devices and electrochemical cells.

**Table 3 Physicochemical Properties of S-4 Nanoparticles**

Sample	pH	Moisture (%)	Bulk density (g cm <sup>-3</sup> )	Porosity (%)	Surface area (m <sup>2</sup> g <sup>-1</sup> )
S-4	7.0	0.11	1.25	80	571

### Optical Properties

The optical properties of selected sample (S-4) were studied by UV-visible absorption spectroscopy in the spectral range (200-400 nm). The absorption coefficient ( $\alpha$ ) was calculated from the observed absorption spectra and the optical band gap of S-4 sample was calculated from the Tauc's plot of  $(\alpha h\nu)^2$  vs  $h\nu$ . The optical band gap of S-4 sample was found to be 2.25 eV. According to the band gap value, the perovskite S-4 sample found within the semiconductor band-gap range.

### Tauc's plot

$$(\alpha h\nu)^n = K (h\nu - E_g)$$

Where  $\alpha$  = absorption coefficient  
 $h\nu$  = incident photon energy  
 $K$  = constant  
 $E_g$  = optical band gap energy  
 $n$  = nature of transition

**Table 4 Band Gap Value of Prepared Silver Doped Bismuth Ferrite (S-4) Nanoparticles**

Sample	Band gap value (eV)
S-4	2.25

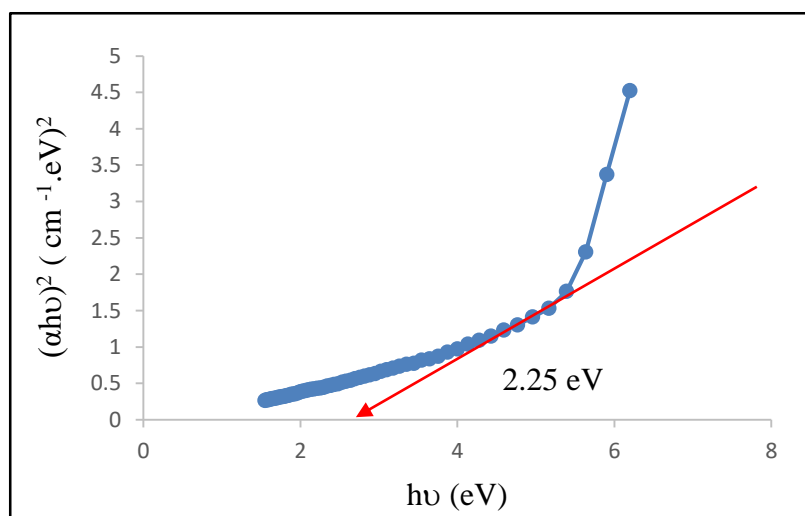


**Figure 4** Plot of  $(\alpha h\nu)^2$  against  $h\nu$  for prepared silver doped bismuth ferrite (S-4) nanoparticles

## Conclusion

Silver doped bismuth ferrite (Ag-BiFeO<sub>3</sub>) nanoparticles were successfully prepared by co-precipitation method at different ratios. The resulting nanoparticles were characterized by XRD, SEM and EDXRF techniques. According to physicochemical properties (porosity and surface area), optical properties (Band Gap Value) and other characterization studies (XRD, SEM, EDXRF), the selected S-4 nanoparticles may be used as good adsorbent for photo degradation, semiconductor for electrical application and sensor for optical properties.

## Acknowledgements

The authors would like to thank the Department of Higher Education, Yangon, Myanmar for allowing to carry out this research work. Profound gratitude is especially thankful to Ministry of Education, Myanmar and Professor Dr Ni Ni Than, Head of Department of Chemistry, University of Yangon for providing all the departmental facilities.

## References

- Erenstein, W., Mathur, N.D. and Scott, J.F. (2007). "Multiferroic and Magnetoelectric Materials". *Nature*, vol. 442(7104), pp. 759-765
- Freitas, V. F. (2013). "Structural Phase Relations in Perovskite-structured BiFeO<sub>3</sub> Based Multiferroic Compounds". *J. Adv. Ceram.*, vol. 2(2), pp.103–111
- Fischer, P., Polomska, M. (1980). "Temperature Dependence of the Crystal and Magnetic Structures of BiFeO<sub>3</sub>". *J. Physics C*, vol. 13(10), pp. 1931-1940
- Johari, A. (2011). "Synthesis and Characterization of Bismuth Ferrite Nanoparticles". *AKGEC. J. Technol.*, vol. 2(2), pp.17-20
- Muneeswaran, M., Jegatheesan, P. and Giridharan, N.V. (2013). "Synthesis of Nanosized BiFeO<sub>3</sub> Powders by Co-precipitation Method". *J. Experimental Nanoscience*, vol. 8(3), PP. 341-346
- Selbach, S.M., Tybell, T., Einarsud, M.A. and Grande, T. (2007). "Size Dependent Properties of Multiferroic Bismuth Ferrite Nanoparticles". *Chem. Mater.*, vol. 19(26), pp.6478-6484